Routes to Novel Azo Compounds

Paul M. Iannarelli, MChem

Thesis presented for the degree of

Doctor of Philosophy,

The University of Edinburgh

May 2008

Declaration

I declare that this thesis is my own composition, that the work which is described has been carried out by myself, unless otherwise stated, and that it has not been submitted in any previous application for a higher degree.

This thesis describes the results of research carried out in the Department of Chemistry, University of Edinburgh, under the supervision of Prof. Hamish McNab.

Paul Michael Iannarelli
University of Edinburgh
February 2008

Signed:-

Date:-

Acknowledgements

I would like to thank Professor Hamish McNab for his invaluable support, encouragement and advice throughout my PhD. I would also like to thank Dr Clive Foster, Dr Lilian Monahan and Mr Alan Dickinson of Fujifilm Imaging Colorants for their help and advice.

My thanks also go to the technical staff at the University of Edinburgh, especially John Millar for his training on the running of NMR spectra, and Robert Smith for LC-MS training.

My thanks also go to my parents who have supported me throughout my university studies.

Thanks also to all those in the McNab group, past and present, who have helped.

Lecture Courses Attended

Organic Research Seminars, University of Edinburgh, School of Chemistry (3 years attendance).

Organic Colloquia, University of Edinburgh, School of Chemistry (3 years attendance).

Royal Society of Chemistry, Perkin Division, Annual Scottish Meeting (3 years attendance).

Fujifilm Imaging Colorants Colour Course, Stephen Westland (5 lectures).

Postgraduate NMR Course, Dr Dusan Uhrin (5 lectures).

SCI Conference, University of Glasgow, April 2005.

ISRIUM International Conference, University of Edinburgh, July 2005.

WestChem Organon Meeting, University of Glasgow, September 2005.

RSC Symposium, University of Edinburgh, October 2005, (4 lectures).

Supramolecular Chemistry Symposium, University of Edinburgh, (4 lectures).

EPSRC Mass Spectrometry Summer School, University of Swansea, September 2006.

Process Chemistry Course, Pfizer, Sandwich, November 2006.

Abstract

Routes to novel heterocyclic azo compounds and components of use as potential inkjet dyes were investigated.

A new route to fluorenones from biphenyl acid chlorides using FVP (Flash Vacuum Pyrolysis) has been discovered. Fluorenone and 4-methylfluoren-9-one were prepared by FVP of 2-phenylbenzoyl chloride and 2-methylbiphenyl-2-carbonyl chloride respectively. Xanthen-9-one and thioxanthen-9-one were also prepared by FVP from the corresponding acid chlorides.

9-Phenanthrol could also be prepared *via* the FVP of biphenylacetyl choride and the application of this method to a heterocylic thiophene system afforded naphtho[1,2-*b*]thiophen-4-ol. Naphtho[2,1-*b*]thiophen-4-ol and naphtho[1,2-*b*]furan-4-ol could be obtained in low yields by the FVP of (2-thiophen-3-ylphenyl)acetic acid methyl ester and (2-furan-2-ylphenyl) acetic acid methyl ester over a tungsten trioxide catalyst. Coupling of these systems with the diazonium salt of Acid Yellow 9 afforded the corresponding azo compounds.

New heterocyclic dyes were also prepared from the condensation of heterocyclic hydrazines with 4,9-disulfophenanthrenequinone. Pyridine, pyridazine, phthalazine, isoquinoline and 2-quinoline disulfophenanthrene quinone metallised 2:1 nickel complexed magenta dyes were prepared. Industrial tests by standard methods revealed the pyridazine dye has a particularly impressive balance of light and ozone fastness over similar magenta dyes.

The reaction of an arylnitro compound with 2-aminopyridine appeared to be an attractive and high yielding route to 2-(phenylazo)pyridine. However, application of this reaction to substituted and naphthalene systems failed. This afforded by-products due to nucleophilic substitution of groups such as methoxy and the relatively uncommon nucleophilic substitution of hydrogen with none of the required azo products obtained. Therefore it appeared that the reaction of a nitro and amine was not a robust and versatile route to heterocyclic azo compounds.

An alternate route to heterocyclic azo compounds involved the use of the Mills reaction by the condensation *o*-anisidine, *p*-chloroaniline, 2-aminophenol, 3-aminophenol, naphthylamine, 8-amnioquinoline and 2-acetylamino-5-amino-benzenesulfonic acid with 2-nitrosopyridine afforded the heterocyclic azo products in moderate to high yields. The Mills reaction does appear to be the favored route to heterocyclic azo compounds.

Several factors were identified which affect the process of bisazo coupling of chromotropic acid and products obtained. Reaction at the *ipso* position of monoPACAs (2-phenylazochromotropic acid) leading to increased yields of the *ipso* substitution monoPACA by-product as opposed to the expected bisazo coupling position was a major problem. Studies indicated reactivity at the *ipso* position was greatly reduced by the presence of electron withdrawing groups around the phenyl ring of the monoPACA.

Further study indicated reaction at the bisazo coupling position increased with the strength of the diazonium salt used in bisazo coupling. Therefore the electronic nature of the monoPACA starting material and the diazonium salt used in bisazo coupling greatly affected the products obtained.

Reaction pH studies also revealed attack at the bisazo coupling position increases with pH and at lower pH (5.0 – 8.0) attack at the *ipso* position dominated. Reactivity of the monoPACA starting material also increased with pH.

The influence of steric effects upon bisazo coupling revealed, in the cases where *ortho* sulfonic acid groups were present in the monoPACA, a reduction in attack at the *ipso* position. Hence the reaction appeared to be directed towards the required bisazo coupling position.

Contents

1.0: Introduction

Preamble

The design and manufacture of new dyes for inkjet printing is one of the fastest growing areas of the modern dyestuff industry. This is due to the increased use in digital photography and home printing which require photo print quality and longevity to be achieved with the use of home inkjet printers. Suitable dyes are therefore required that exhibit intense colour, thermal stability and high ozone and light fastness.

The aim of this thesis was to study traditional and non-traditional routes to azo compounds. The use of these synthetic routes to prepare novel azo compounds which could be used as potential inkjet dyes with the required colour, thermal and fastness properties is also of interest.

1.1: Inkjet Printing

Lord Rayleigh first discovered the mechanism by which a liquid stream breaks up into droplets as far back as 1878 which is now the basis for modern non-impact inkjet technology.[1]

Impact printing such as typewriters, daisy wheel and dot matrix printers dominated office and home printing until 25 years ago. However there were many drawbacks of this technology. These printers were slow, noisy and were restricted to text and monochrome. This lead to the development of non-impact technologies which were quicker, more cost effective and able to produce full colour, high quality prints.

Inkjet printing can be described as today's leading non-impact printing technology in which droplets of ink are ejected from a nozzle either by continuous or drop-on-demand technology mechanisms. There are a wide range of commercial applications such as simple home and office use, to printing onto cardboard and colour filters for flat screen displays resulting from the fact that inkjet can be used for printing on a variety of substrates including paper, fabric, glass and metal.[2]

1.2: History and Concept

Inkjet devices were first used in the 1930s,[1,3] but it took until 1951 for Seimens to produce and patent the Minograph which was the first successful product. This was the first practical Rayleigh break-up device used as a commercial inkjet chart recorder, and was able to print characters or images.[3,4]

Further research in the 50s and 60s lead to a breakthrough in 1965 when Sweet developed a continuous inkjet technology printer which was faster and quieter.[5,6] Hertz then modified this system in 1967 to allow access to greyscale and commercial high quality colour images.[4] This system allowed the control of the number of drops of ink used in the formation of each pixel and hence control of the shades of grey printed.

Modern advances then lead to drop on demand inkjet printing with the first method applying the piezoelectric effect developed by Zoltan in 1972.[3,6] A further development by IBM in the 1970s lead to the first near letter quality inkjet product with clear advantages over continuous methods. The system was simpler, more reliable and less expensive, however, nozzles were still prone to clogging and the images were inconsistent. [5]

Another landmark discovery was thermal or bubble inkjet printing technology developed independently by Canon and Hewlett-Packard (HP) in 1979.[1,3,4,6] This method used the growth and collapse of a bubble to force out droplets of ink on demand. HP marketed the first low cost thermal inkjet printer in 1984, which used disposable printheads. This lead to a low cost, simple, full colour and high quality printing system making thermal inkjet technology dominant in the market and ending the use of continuous printers in the office.[4]

However, inkjet technology is still developing and problems remain such as ink drying time and throughput speeds. There are also significant problems associated with the development of the colorant, in particular longevity of prints on photographic papers and optical density of black dyes.

1.3: Continuous Technology

The continuous technology mechanism involves the application of a pressure wave to an orifice causing the inkjet stream to be broken into droplets of uniform size. An electrical charge can then be applied onto the droplets selectively. The drops then pass through a high voltage electric field, where upon they are deflected by either binary or multiple deflection techniques (Figures1.3.1 and 1.3.2).[4]

In binary deflection only certain drops are charged. The charged ink is then directed through an electrostatic field onto the medium with uncharged ink falling into the gutter for recirculation.

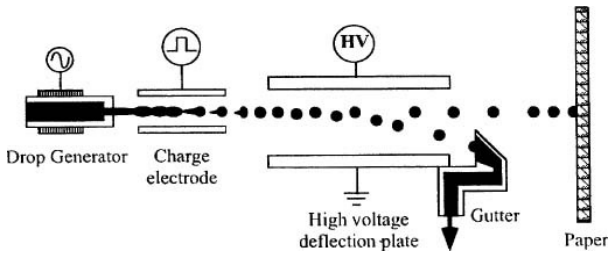

Figure 1.3.1: Binary deflection methods used in continuous inkjet printing.[4]

In multiple deflection systems, all drops are provided with a varying charge and deflected onto the paper at different levels. Again uncharged drops are passed into the gutter.

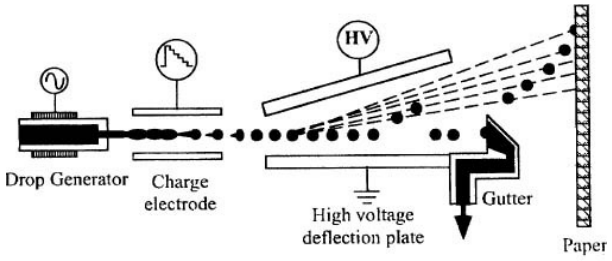

Figure 1.3.2: Multiple deflection methods used in continuous inkjet printing.[4]

Continuous inkjet technology is effective however, the wasted ink impacts upon the economy of the system. This can be overcome by recycling the unused ink although can lead to issues with the problem of solvent evaporation. Today,

continuous inkjet technology is used in industrial packaging or large format printing. The high drop production capability of these printers is particularly suited to writing on irregular surfaces at high speeds on the production line.

1.4: Drop on Demand Technology

Drop on demand technology is comprised of four main methods, thermal, piezoelectric, acoustic and electrostatic, although acoustic and electrostatic are still in the early stages of development.[4] Thermal printers contain an ink chamber with a heater and a nozzle nearby. A short pulse of current is passed through the heater causing a rapid temperature rise and a tiny steam bubble forms in water based inks. The bubble then exerts pressure causing an ultra fine droplet of ink to be ejected from the nozzle (Figure 1.4.1). A vacuum is created as a result of the bubble collapsing after the droplet is ejected, drawing new ink in to replace the ejected ink.

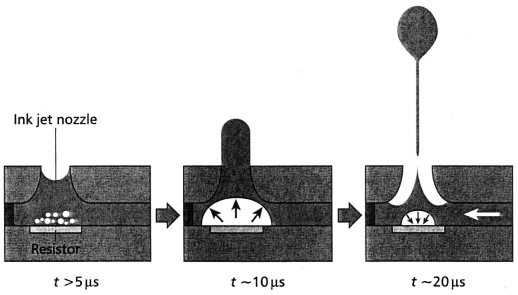

Figure 1.4.1: Thermal drop on demand inkjet technique.[4]

Piezoelectric printers convert a pulse of electrical energy into a mechanical pressure pulse causing ejection of a droplet of ink. The ejection is controlled by this electrical signal that produces a deformation in the piezoelectric crystal. This results in a pressure wave in the ink, which subsequently forces a droplet out through an orifice (Figure 1.4.2).

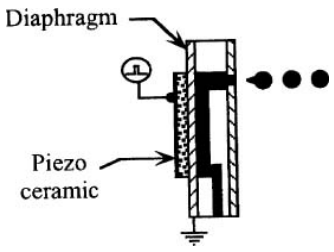

Figure 1.4.2: Piezoelectric inkjet printing.[4]

Despite the current dominance of thermal inkjet printers (HP, Canon and Lexmark), the piezoelectric method is used in Seiko Epson (SEC) printers and can compete commercially with thermal printers.

Drop on demand technology has several advantages over continuous as drops are only ejected when required and therefore every drop produced is used in forming the image hence, this approach is more efficient resulting in lower cost. Also no deflection methods are involved, therefore the complexities of charging droplets, the deflection hardware and the unreliability of ink circulation are eliminated.

1.5 Inks Used in Inkjet Printing

Three common types of inks used in inkjet printing are aqueous, solvent and hot melt inks.[6,7] Drop on demand printers generally use aqueous inks, whereas continuous printers tend to use solvent or hot melt inks.[4]

1.5.1: Aqueous Inks

Aqueous dyes are mainly used in drop on demand inkjet printing, especially in the home environment where odour and toxicity are of great concern. These were mainly sourced from existing dyes in the food and textile industry which tended to be highly water soluble resulting in water based inkjet dyes. Aqueous dyes also have the advantage of containing a safe solvent and being relatively cheap. However, water can promote the growth of bacteria and fungi and cause corrosion. These problems can be minimised by the use of additives (Section 1.6).

1.5.2: Solvent Inks

Solvent based inks are usually chosen with printing on hydrophobic substrates such as plastics or metals, or when fast drying times are required. Large character printing in an industrial environment is the main application of solvent inks or when one colour is required such as black. Methyl ethyl ketone is a common solvent, however, there has been a shift to less hazardous materials such as alcohol based inks. Toxicity problems also exist with some ink solvents. Generally, solvent based inks are used in continuous inkjet printing for industrial applications, but have little use in the home or office market.[6]

1.5.3: Hot Melt Inks

Hot melt inks can be used in thermal drop on demand printers. They are solid at ambient temperatures and become liquid due to heating in the ink chamber before ejection from the print head. Hot melt inks melt in the range of 60 - 125 ºC and have the potential to produce good quality results, but are still limited in application.

1.6: Composition of the Ink

There are several components used in a typical aqueous ink formulation. The major solvent component in drop on demand inks is water as it is excellent for anionic water soluble dyes. It is also the best solvent for bubble formation and is safe and of low cost. However, the drawbacks with using water are that it is a good medium for the growth of bacteria and fungi, leading to nozzle clogging, and is a good corrosion promoter.[3,6]

Table 1.6: The various components involved in a typical ink.[1]

Component	%
Dye (Water soluble)	~ 2-6%
Water	~ 70-80%
Humectant	~ 5-10%
Surfactant	~ 1%
Penetrant	~ 2-10%

Humecants are added to control water evaporation from the ink, preventing the ink from drying out and the dye crystallising and blocking the nozzle. Typical high boiling solvents used are diethylene glycol and 2-pyrrolidone.

Surfactants are added to lower the viscosity of the ink and allow droplet formation while the penetrant lowers the surface tension and effects rapid penetration into the medium. A typical surfactant would be Surfynol 465 and a penetrant pentane-1,5-diol.[2]

Chelating agents (EDTA) and pH control can also be important to prevent the formation of metal precipitates which can block the print nozzle in addition to controlling dye solubility and stability.

1.7: The Origin of Colour

The colorant (dye) is the key element of the inks used in inkjet printing, producing a bright, well defined image. The two main classes of colorant are dyes and pigments. Dyes have traditionally been preferred in inkjet printing as pigments are insoluble and tend to clog the nozzle. Pigments also tend to be duller.[6]

In basic colour theory there are three additive primary colours (red, green and blue) and three subtractive primary colours (yellow, cyan and magenta). The mixing of different wavelengths of energy to create white light is known as the additive colour process, such as used in a colour television, using the three colours red, green and blue. On the other hand, the subtractive colour process is used in the printing industry. Any material containing dyes or pigments will reflect, absorb or transmit light energy. This results in a colour being produced according to the subtractive colour theory, using the colours cyan, yellow and magenta. A cyan colorant will absorb red energy (ie. subtract red light from white incident light), and reflect the remaining light which appears cyan (combination of all other non-red wavelengths). In a similar manner, yellow results from subtraction of blue light from white light, while magenta results from subtraction of green light from white light (Figure 1.7.1). A black image is seen when all wavelengths are absorbed.

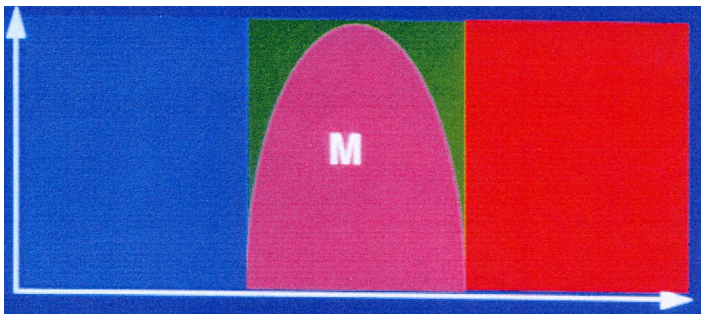

Figure 1.7.1: The idealised absorption spectrum for magenta showing the absorbance of green light, and reflectance of all other wavelengths, to give magenta.[14]

Cyan, yellow and magenta in addition to black are used in ink-jet printing to obtain any desired colour by various combinations of these three colours.[2] A 2-D representation of colour shows yellow, cyan and magenta at the extremities (Figure 1.7.2).

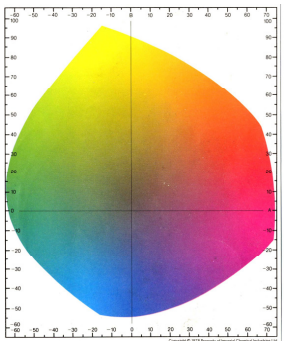

Figure 1.7.2: Colour map showing yellow, magenta and cyan.[22]

1.8: The Origin of Colour in Dyes

In general, the colour of a material is due to absorption of light which results in the promotion of electrons from the ground state orbitals (HOMO) to a higher unoccupied orbital (LUMO). The wavelength (λ) of light absorbed depends upon the difference in energy (ΔE) between the orbitals as expressed by equation 1. The colour observed is a result of the absorption of certain wavelengths of visible light by the dye and reflectance of the remaining wavelengths. Differences in dye structure leads to differences in energy levels and therefore the colour observed.[8,9]

Equation 1: $\Delta E = E_{LUMO} - E_{HOMO} = h\upsilon = hc/\lambda$

1.9: UV–Vis Spectra

All coloured substances give characteristic absorption curves or spectra, in which the degree of absorption is plotted against wavelength or frequency (Figure 1.9.1). An ultra-violet (~200-380 nm) or visible (~380 nm-760 nm) absorption curve is obtained which gives an accurate indication of the shade of the dye. The key parameters which are obtained from any UV-vis curve are the absorption maxima or peak wavelength (λ_{max}), which describes the colour of the dye, and the shape of the absorption curve. A symmetrical curve with no extra absorption areas evident is desirable, especially at high wavelengths. These "high wavelength tails" are observed when the curve does not fall directly to the baseline, but "tails" off at a much shallower gradient. This can contribute to an undesirable hue. Another important characteristic of the UV-vis spectra is the width of the curve at half the maximum absorption (half-band width, $W_{1/2}$). Bright dyes exhibit narrow absorption curves ($W_{1/2} < 100$ nm) and sharp peaks. On the other hand, dull dyes have much broader and less well defined peaks due to unwanted absorptions outside the desired range.[6,9]

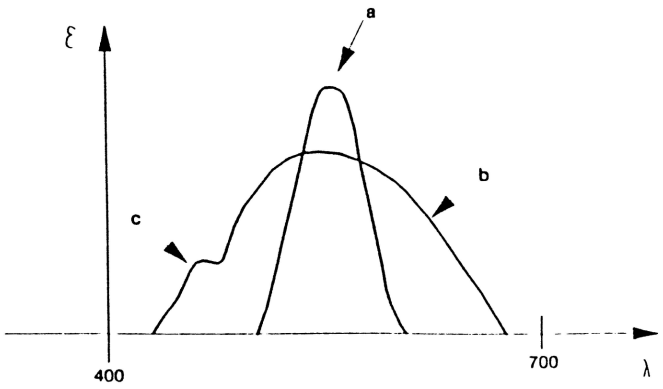

Figure 1.9.1: a) Idealised absorption curve obtained for a bright ideal magenta dye and b) a duller, non ideal magenta dye with unwanted secondary absorptions at c).[6]

If the substitution of one group for another causes absorbance at a higher wavelength in the UV-vis spectrum this is known as a bathochromic shift. The opposite is true for a hypsochromic shift.[9,10] The colour of a dye can also be gauged from the UV-vis spectrum with typical absorbances for ideal yellow, magenta and cyan dyes would be observed at approximately 410 nm, 540 nm and 640 nm respectively.

1.10: Colour Measurement

The perception of colour by individuals is highly subjective, and as such it is necessary to define an objective framework around which colours can be judged. The artist Albert H Munsell originated a colour ordering system in 1905 which is still used today. This system was based upon human perception and was devised before instrumentation was available for measuring and specifying colour. Many types of colour space are based upon Munsell's arising from the need to provide a uniform method to spread colours relative to their visual differences and to describe colour in numerical terms.[12,13,14]

1.10.1: The CIE System

Following extensive research into human colour perception and the generation of a "standard observer" the CIE (Commission Internationale de l'Eclairage) system was

developed in 1931. The CIE standards utilised three coordinates to locate a colour in space that are device and observer independent. Every measurement was related to a standard observer, which described how an average human sees colour.

The CIELab system was based on the fact that a colour cannot be both green and red at the same time nor blue and yellow. This resulted in a system that allowed a colour to be described in terms of three angular coordinates:

L - a measure of the lightness of an object (0 black to 100 white)
a - a measure of redness (positive a) or greeness (negative a)
b - a measure of yellowness (positive b) or blueness (negative b)
C - a measure of brightness

For neutral colours (white, grey and black) a and b values approach zero, while a higher a and b value represents a more saturated colour (Figure 1.10.2).

An alternative colour space measures colour in terms of lightness, chroma and hue (CIELCh). This system is based on CIELab but describes the location of a colour in space by use of polar coordinates rather than rectangular coordinates. Hue (colour) is the way in which someone would distinguish red from green, chroma is the saturation/intensity of a particular colour, *ie.* red and pink would have a similar hue value but a different chroma (Equations 2 and 3). Lightness distinguishes between dark and light colours on a scale of 0 – 100 from black to white as in the CIELab system.[14]

Equation 2: chroma (C) = $\sqrt{(a^2 + b^2)}$

Equation 3: hue (h) = $\tan^{-1}(b/a)$

Lightness, as with the Lab system, is the central axis, chroma (C) is the horizontal distance from the lightness axis and the hue (h) is an angle at which the chroma axis is rotated from red which is given an arbitrary hue of 0º. Magenta, yellow and cyan dyes have typical hue values of around 350º, 90º and 240º respectively.[11,13,14]

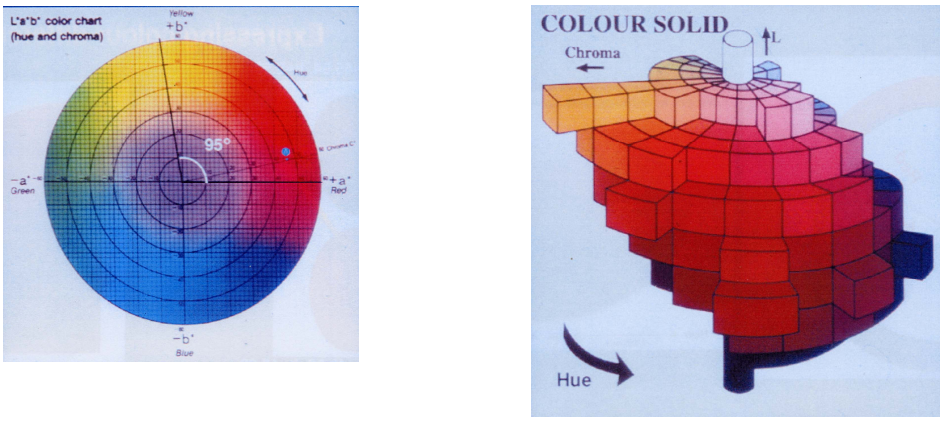

Figure 1.10.2: Two representations of CIE colour systems, showing L, a, b, C and h.[22]

1.11: Dye Requirements

Dyes used in inkjet printing must meet many requirements which include the prints displaying the same shade across a range of substrates. This is difficult due to a huge variety of substrate properties, different textures and absorption characteristics. Ideally a dye which is insensitive to such factors is required.[11] Other important factors include colour (hue), chroma (vividness), good light fastness, wet fastness and ozone fastness (Section 1.15). The ability of dyes to resist fading upon exposure to light and ozone is a major problem resulting in much research activity.

High aqueous solubility is required to minimise crystallisation and nozzle blockage. This can be achieved by the presence of functional groups that dissociate to give an ionic compound with the most common used being sulfonic acid groups. Dyes with these solubilising groups are rarely present as the free acid but rather as the metal salt. Sodium is the most common cation used, although other metals such as lithium and non metals such as ammonium ions have been used.[6]

Dyes must also be thermally stable up to temperatures of 300 ºC due to the mechanism involved in bubble formation. Another problem is the build up of insoluble impurities (kogation) on the heating element which have the potential to act as an insulating barrier causing the element to overheat. Good kogation (low concentration of impurities) can be achieved by the presence of sulfonic acid groups

on each fragment of the dye and hence each decomposition fragment is water soluble, and does not accumulate.

Other impurities such as bacteria and fungi must also be minimised with the use of biocides. The presence of metals are also undesirable as they promote corrosion and divalent metals such as Cu^{2+} can precipitate at low concentrations potentially blocking orifice printheads.[8] Chelating agents such as EDTA can be added to remove these ions as soluble complexes in addition to removal of impurities by ultrafiltration or dialysis (processes used to remove salts) through membranes impervious to higher molecular weights.[8]

1.12: Papers

The print media used with inkjet applications is also important to the quality of the image. The interaction of the inkjet dye with plain paper is one of the most important for product success and also the most difficult to control due to the inhomogeneous surface properties of different papers with widely different chemical properties. The structure of plain paper consists of a matted tangle of cellulose fibers of different lengths and cross sections as opposed to a smooth surface. Generally inkjet dyes do not perform well on plain papers, however, special coated media (swellable polymer or microporous) can be used to achieve higher quality images and control fastness problems.

These coatings result in the dye being held close to the surface providing maximum optical density and since the dye is not dispersed in the fibrous paper structure high quality glossy images can be achieved. Interaction of these coatings with the ink also promotes rapid ink absorption and generates the required spot diameter/shape by controlling the spread of ink on the paper. This provides high water and light fastness. However, all these additions adds to the expense and a large portion of the inkjet market requires plain papers.[11,15] The ideal situation is for the inkjet printhead/ink supplier to specify the optimised media.[11] An ink is often designed/tailored to a specific printer and medium to achieve the best results.

1.13: Structure of Dyes

A typical organic colorant has conjugation existing over a number of bonds. The chromophore, generally electron withdrawing groups such as azo, nitro or carbonyl containing group is principally responsible for the colour observed. The addition of groups conjugatively linked to the chromophore called auxochromes (generally electron donating groups containing atoms such as nitrogen, oxygen and halogens) cause a bathochromic shift providing a more intense colour.[6,11] A general rule is that the longer the conjugated system, a more bathochromic shift will be observed.[11]

The majority of dyes manufactured today are the product of an azo coupling reaction, in which the target molecule contains the azo group linking the two fragments together **1**. The most stable conformation of the azo group is trans in which both nitrogen atoms are sp^2 hybridised giving carbon-nitrogen-nitrogen bond angles of 120º.[8]

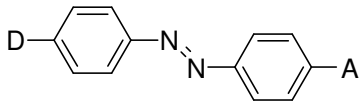

1

Most azo dyes are based on the above structure where the colour of the dye is influenced by the push/pull interaction of the electron donating (D) and electron withdrawing groups (A) in reference to the π electrons. Increasing the strength of the electron donating (D) or withdrawing groups (A) causes a bathochromic shift to be observed.

1.14: Azo/Hydrazone Tautomerism

Zincke and Binderwald first proposed in 1884 that an azo compound (with an OH present either *o*rtho or *para*) can exist in the azo or hydrazone form. This was realised from the observation that diazo coupling between aniline **2** and 1-naphthol **3** gave rise to the same product (4-phenylazo-1-naphthol **4**) as the condensation reaction between phenylhydrazine **5** and 1,4-naphthoquinone **6** (Scheme 1.14.1). It was therefore suggested that a tautomeric equilibrium between the azo **4** and hydrazone **7** products must exist.[8]

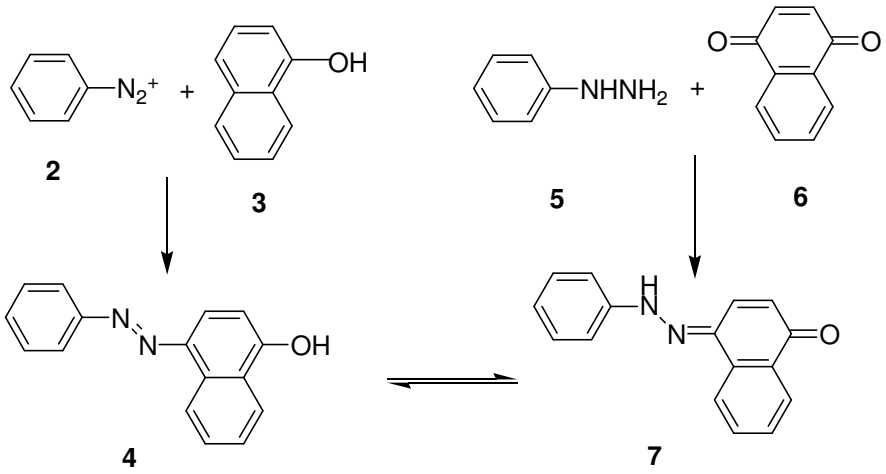

Scheme 1.14.1: Tautomeric equilibrium between azo and hydrazone forms.

A dye will have different colour and fastness properties depending upon the position of the tautomeric equilibrium. This tautomerism depends primarily upon the relative energies of the two tautomers but is also influenced by several other factors such as solvent, pH and the substituents present in the dye molecule.

In general more polar solvents such as water, formamide and acetic acid favour the hydrazone form, whereas less polar solvents such as pyridine, alcohols or hydrocarbons favour the azo form.[16] If the dye has an *ortho* substituent capable of intramolecular hydrogen bonding then the hydrazone form will dominate due to increased stability of its hydrogen bonded form over that of the azo. In comparison with the azo form, the hydrazone form will also exhibit a bathochromic shift and increase in extinction coefficient, both of which are desirable properties. This makes *ortho* substituted azo dyes highly attractive as commercial colourants as their properties are generally stable and predictable.[17]

1.15: Fastness Properties of Dyes

Dye fastness refers to the ability of a dye to resist fading or degradation of the chromophore due to exposure to light or pollutants.[17] Dyes fade to varying degrees when in contact with the atmosphere, the media and components within the ink. A dye that fades quickly is obviously unsatisfactory and therefore dyes are required that produce high quality colour images and have excellent stability. [8] The problem of

fastness on prolonged exposure to light remains a major issue in the design of inkjet dyes. Although the understanding of fading mechanisms is somewhat limited, guidelines have been helpful in developing correlations with dye structure.

1.15.1: Wet Fastness

Water fastness refers to the ability of a dye not to smudge if the paper becomes wet or is handled by a person with wet hands. One method of improving water fastness levels was by utilising the smelling salts (ammonium carbonate) principle (Scheme 1.15.1).

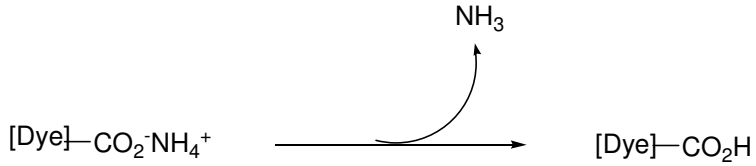

Scheme 1.15.1: Ammonium carbonate method of increasing wet fastness.

The ammonium salt of a carboxylic acid is unstable and decomposes to give gaseous ammonia. This confers a degree of water fastness to the dye by changing the dye from an ammonium salt to the insoluble free acid form of the dye on evaporation.[1,3,6]

These principles are used to produce the black dye **8** (Figure 1.15.1), which can be found in many printers. The number of sulfonic acid groups has been reduced and replaced with carboxylic acid groups to improve the water fastness.[7]

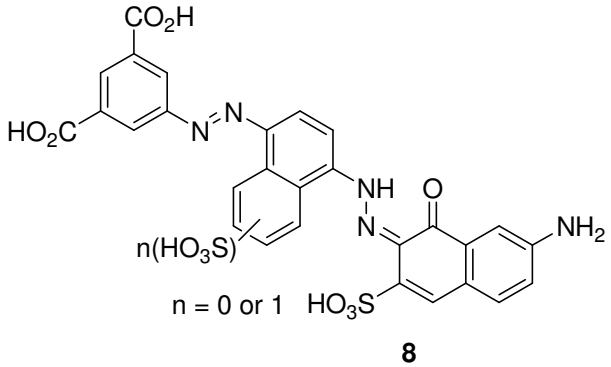

8

Figure 1.15.1: Black dye **8**.

1.15.2: Light Fastness

Light fastness is one of the main priorities of dye chemists. It is generally accepted that the chromophore is the most susceptible part of the molecule to aging upon prolonged exposure to light. The nature and position of substituents on the dye affect degradation processes. By varying the substituent and keeping the chromophore constant, differences in relative light stabilities are observed. Generally, electron withdrawing groups improve light stability, whereas electron donating groups cause deterioration. However, too many electron withdrawing groups also has a negative effect.[18]

When a molecule absorbs a photon of light energy, it is raised to an excited level, where photochemical reactions can occur. The capacity of coloured substances to store of the absorbed energy is limited and the excited molecule can lose its energy and return to the ground state by a variety of processes, such as fluorescence or phosphorescence (Figure 1.15.2). It can also decompose or react with another molecule.[8,9] In general, the longer the lifetime of the excited state, the more chance there is for it to react. Other factors such as the absorption characteristics of the dye, the nature of the solvent and substrate and the presence of air or moisture can play a part in photochemical reactions.[8]

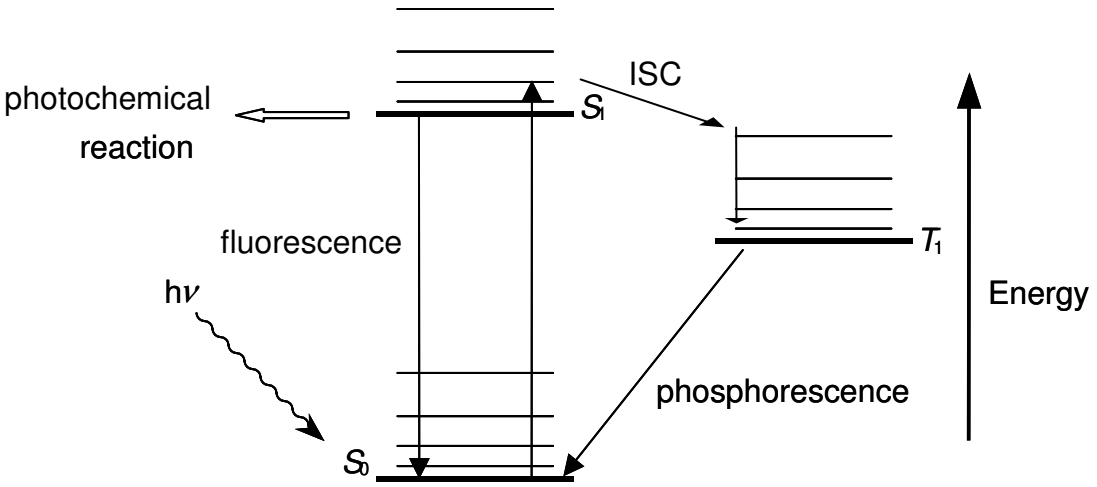

Figure 1.15.2: Processes by which an excited molecule can return to the ground state.

The two recognised pathways by which azo dyes can fade are by photo-reduction or photo-oxidation. These reactions depend on the chemical environment of the dye as determined by the media, components in the ink and the surrounding atmosphere. The understanding of the chemical environment is critical in protection against these mechanisms.[11]

Under anaerobic conditions an azo dye can be reduced to its amines by abstracting hydrogens atom from a hydrogen donor. Such decomposition is accelerated when the hydrogen donor or the dye is photoexcited. Common hydrogen donor groups include alcohols, amines, ketones, carboxylic acids, ethers and esters.[10]

Oxidative fading mechanisms can be caused by direct photoreactions of the dye, *i.e.* from the excited state, or indirect, caused by another photoexcited molecule *e.g.* singlet oxygen. The fading process is believed to be a consequence of the hydrazone form rather than the azo.[8] Magenta dyes that are in the hydrazone form, typically show poorer light fastness than those in the azo form.[19] The mechanism firstly involves the attack of singlet oxygen on the hydrazone tautomer **9** in the ground state, by a 6-π electron thermally allowed process (Ene reaction). This forms an unstable peroxide **10** which then decomposes to products (Scheme 1.15.2). Singlet oxygen sensitisers such as anthraquinones promote this reaction by transferring their energy to the oxygen upon excitation. A molecule locked in the azo form is thought to be more resistant to attack.[8,11]

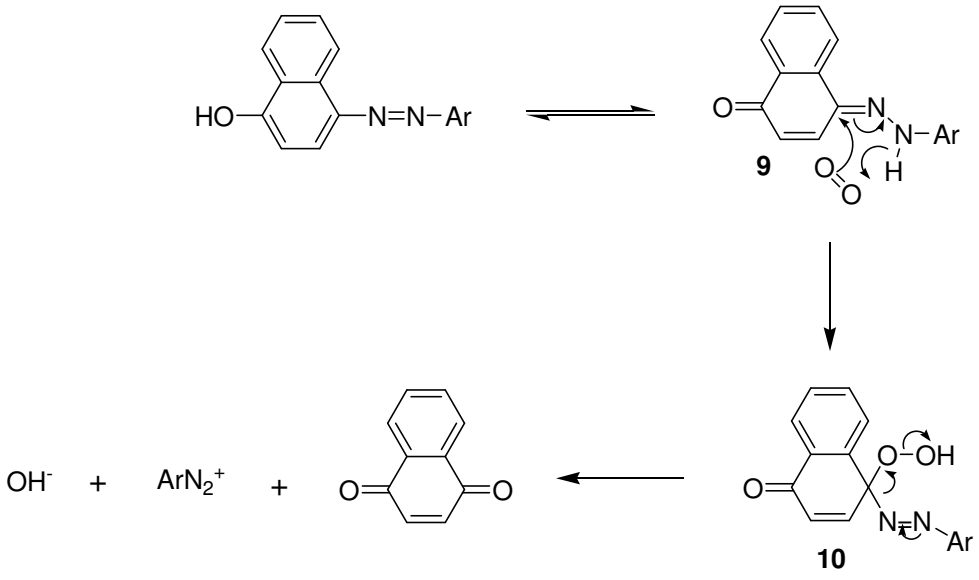

Scheme 1.15.2: Oxidative fading mechanism of an azo dye.

Both the reduction and oxidation degradation reactions are affected by the substituents in the dye and hydrogen donor. Singlet oxygen is electrophilic and attacks areas of high electron density, promoted by electron donating substituents. For this reason, metallised dyes with their electron withdrawing metal atom are particularly stable (Section 1.16).[11]

Recent work has shown that it is possible to incorporate substrates into a dye that act to scavenge reactive oxygen species or absorb UV light without affecting the chromophore.[20] The dyes tested were naphthalene based aromatic esters which acted as both UV and singlet oxygen quenchers. Each showed improved fastness properties over the parent dye.

1.15.3: Ozone Fastness

The fading of dyes on exposure to atmospheric pollutants such as ozone has also been identified as a problem. Studies into the mechanistic aspects suggest that in the case of azo dyes it is the hydrazone tautomer which is involved in the degradation, similar to the photoxidation reaction (Scheme 1.15.3).

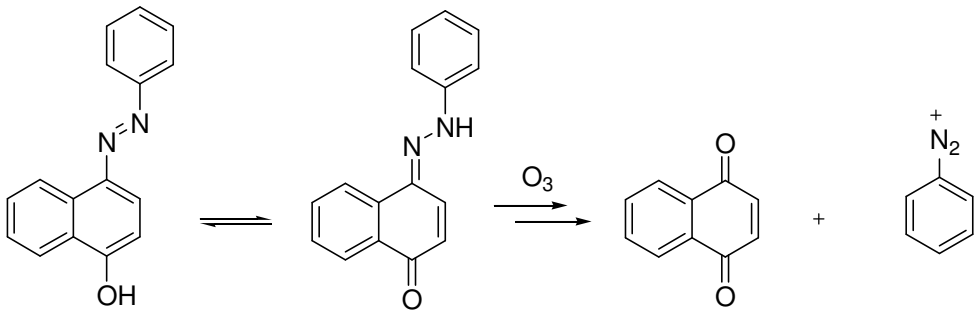

Scheme 1.15.3: Photoxidation of azo dyes due to ozone exposure.

It was found in the above system that the ozonolysis of 1,4-naphthoquinone resulted in simple aryl structures *via* possible decomposition of the diazonium salt intermediate and the quinone. However, the exact nature of this mechanism is still unclear.

1.16: Metallisation

In recent years progress towards the key technical requirement of high light fastness has been achieved by using metal-complexed dyes. Dyes which are metallised complexes often have excellent light fastness, but this tends to be at the expense of brightness, assumed to be due to the formation of aggregates.[1,8,21] Of the stable metal complexes required it is found that only meridional [5,5] complexes exhibit the required bright shades (Figure 1.16.1).

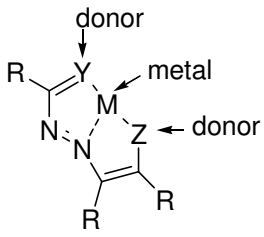

Figure 1.16.1: An example of a metallised complex (R = Ar).

The properties of the metallised complexes of the dye are different to those of the free ligand. Generally upon complexation a bathochromic shift is observed and the light fastness is increased. However the dyes do become duller and of lower solubility.[8] The impact of metallisation upon ozone fastness is less predictable.

The colour change is caused by chelation of the metal to elements of the dye bearing lone pairs of electrons such as the azo or hydroxyl. Upon chelation there is a perturbation of the π electron distribution *e.g.* co-ordination of the metal with a hydroxyl group which alters the ease of donation of the lone pair into the conjugated system, leading to an intense π-π^* transition (ligand to metal charge transfer), not present in the free ligand.[8] There is a greater effect for a more electropositive metal. However, this is a problem as predicting the shade then becomes more difficult. An ideal situation would be that upon formation of the complex there was no change in the λ_{max} value from the free ligand, but still the desired increase in absorption and narrowing of the curve resulted.

The improvement in light fastness of metallised complexes is also due to the perturbation of the π electron system. The electron deficient metal attracts electrons from the ionised hydroxyl group, and also from the azo group, so that electron

density at the azo group is reduced. Photochemical oxidation can also be reduced in metallised complexes by the metal acting as a barrier. This results in less surface area of the dye molecule being available to attack by singlet oxygen. However metallised complexes may have reduced solubility due to the formation of sheet like aggregates.[8]

However, some metal ions have undesirable toxicological profiles and so their use commercially is limited.

1.17: Electron Deficient Azo Dyes

In order to improve ozone fastness the synthesis of electron deficient heterocyclic azo dyes has also been studied. These dyes are expected to have increased resistance to photo-oxidation due to the electron deficient environment around the azo chromophore caused by the presence of the adjacent heterocycle.

The presence of electron withdrawing heteroatoms (*eg.* nitrogen) within the heterocycle is also expected to enhance the push/pull mechanism resulting in the desired bathochromic shift. Electron donating groups (D) on the corresponding aryl group could also enhance this mechanism as is seen in structure **11**.

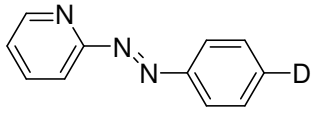

11

1.18: 1st Generation Dyes

The three types of dye originally used in inkjet printing, were acid, direct and food dyes, as they were readily available and provided vivid colours.[22]

Early yellow dyes were based upon 1,3,5-triazine systems such as C.I. Direct Yellow 86 **12**. Similar 1,3,5-triazine dyes were initially used as reactive dyes in textiles and exhibited good fastness properties when modified for use as inkjet dyes.

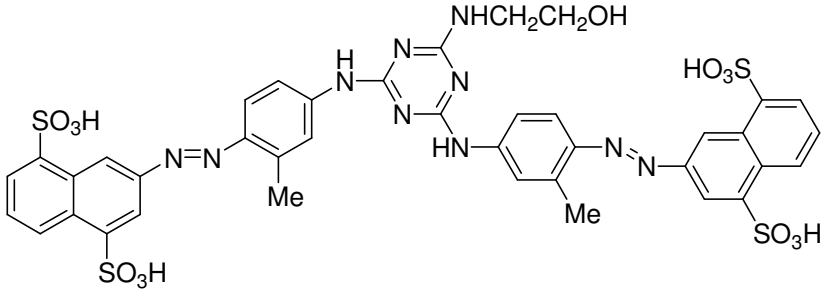

12

Early magenta dyes were based on xanthene structures such as C.I. Acid Red 52 **13**, giving excellent brightness with narrow absorption curves but had very poor fastness properties. Dyes such as these gave bluish shades of magenta, as reflected in a high λ_{max} value.[3]

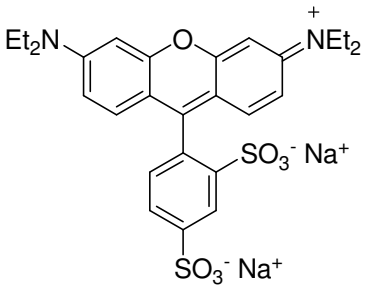

13

The first cyan dyes used were based on triphenylmethane structures, such as the very bright C.I. Acid Blue 9 **14**, but again this displayed very poor fastness properties.[1,23]

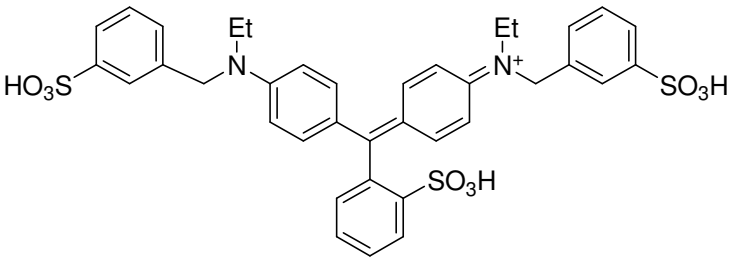

14

The first generation black dye was C.I. Food Black 2 **15** which was chosen for its high water solubility, attractive neutral shades of black and toxicological safety.[3] However, this high solubility also gave it poor water fastness on paper.

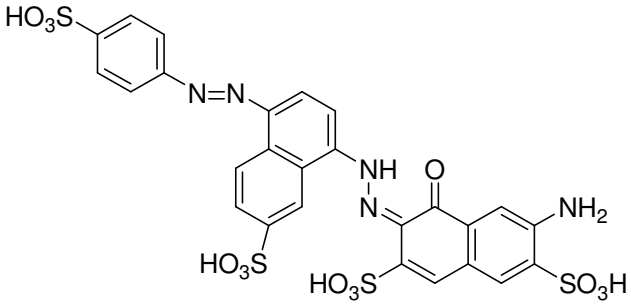

15

1.19: 2nd Generation Dyes

In developing the second generation of yellow, magenta, cyan and black dyes, simple modifications of the first generation dyes shown above were introduced. The replacement of sulfonic acid groups with carboxylic acid groups and treatment with ammonium carbonate resulted in improved water fastness (section 1.15.1). This lead to the development of modified 1st generation dyes with improved fastness properties and to the production of the black dye **8**, which can be found in many printers.[1,3,6]

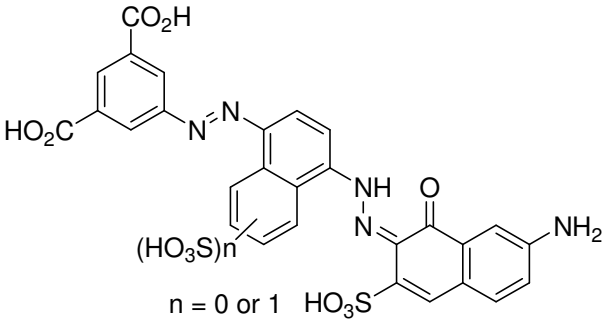

8

1.20: Current Trends

1.20.1: Yellow Dyes

Modern yellow dyes are based on azopyrazolones **16** or azopyridone **17** structures. These compounds can be made by a simple azo coupling reaction from the respective pyrazolone and pyridone, and exist in the hydrazone form. The yellow dyes discussed in Section 1.18 such as C.I. Direct Yellow 86 **12** are also still used today.

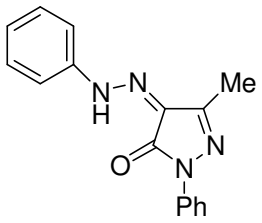

16

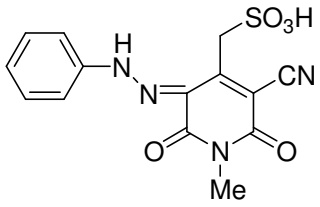

17

1.20.2: Magenta Dyes

Magenta dyes have at best moderate light fastness and fade before yellow dyes. The fading of dyes at unequal rates are most noticeable, and therefore the aim is to produce dyes with low and equal fade rates.[1] It has proved particularly difficult to design magenta dyes that exhibit optimal hue and brightness, high light and water fastness.[11,19]

Current magenta dyes are based on mono aminoazobenzenes and azonaphthol structures. Several different naphthols are used with the majority of magenta dyes derived from diazonium salt coupling with H-acid **18**. Dyes such as **19** are then obtained which give good shades of magenta. This is reflected in the number of patent applications for dyes of this type.[6,19] In the diazonium coupling reaction the question of regiochemistry arises. The coupling can occur *ortho* to either donating group and varying the pH of the reaction mixture can be used to control the site of azo coupling. This pH dependence is a consequence of two factors. Firstly below pH 7, only the free amine is available for coupling since the naphtholate is not present in solution ($pK_a > pH$). At a higher pH, both the free amine and naphtholate are present, but the naphtholate couples much faster than the amine. This means that monoazo and bisazo compounds can be selectively prepared.[8]

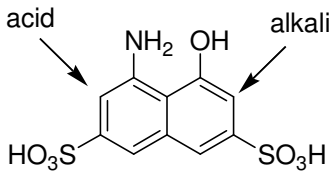

18

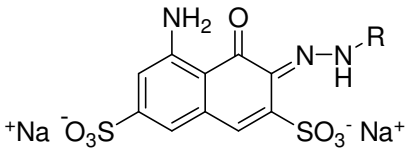

19

These dyes exhibit enhanced light fastness over early magenta dyes such as the xanthenes **13**, high brightness and moderate wet fastness. Another naphthol derivative, gamma acid, is also commonly used. Improvements in light fastness can also be achieved by dyes derived from gamma acid that exist in the azo form such as the acid red dye **20**.

Increased fastness can also be achieved by metallised complexes such as the reactive red dye **21**, but at the expense of brightness. Compounds **20** and **21** are easily synthesised by azo coupling reactions from the appropriate naphthol derivative and a diazotised aromatic amine. Despite these advances made in the synthesis of superior magenta dyes, all the targets have still not been met.[19,23]

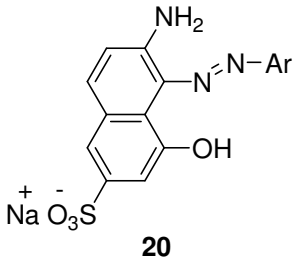

20

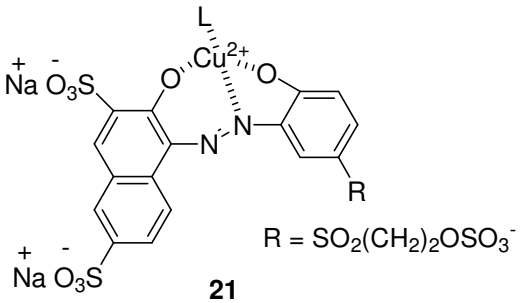

21

1.20.3: Cyan Dyes

Modern cyan dyes are based upon copper phthalocyanines, such as CI Direct Blue 199 **22**. These feature an extended conjugated system which allows a large number of resonance structures to be drawn, and are probably the strongest, brightest and most stable of all colorants used today.[6]

These dyes are made by the reaction of readily available sulfonated copper phthalocyanine and chlorosulfonic acid, followed by amidation. Several other copper phthalocyanines are also available with various numbers and positions of sulfonic acid groups. Despite the excellent properties shown by these dyes, there is still room for improvement with solubility issues due to aggregation.

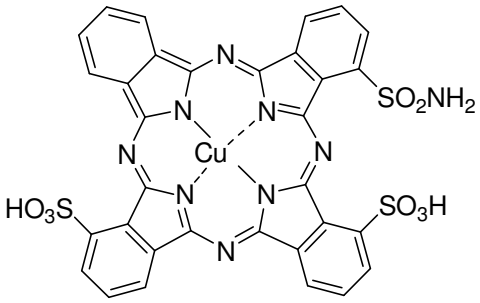

22

1.21: Conclusions

In conclusion, the design of dyes for inkjet printing is a growing industry with a large potential for future research. The technology is still rapidly developing in this field and in particular the synthetic methods towards new dyes. Many factors contribute to the success of a dye with the major problem still the stability to light and ozone.

The aims of this thesis are firstly to investigate traditional routes to novel heterocyclic phenanthrol system dyes and their colour, stability and fastness properties (Section 2.0). Also of interest is the investigation and development of non-traditional routes to heterocylic azo compounds, which includes the Mills reaction (Section 3.0). Finally a detailed study of the bisazo coupling reactions of chromotropic acid will be carried out to identify conditions required to maximise yields of bisazo product and reduce by-products due to *ipso* substitution (Section 4.0).

2.0: Routes to Heterocyclic Phenanthrol System Dyes

As mentioned in the introduction, current research targets involve the synthesis of electron deficient azo compounds **24** due to their improved dyeing properties. Dyes based on phenanthrol systems are of particular interest.

Two main routes to phenanthrol system azo compounds **24** exist. The first of these involves condensation of a quinone system **23** with an aromatic hydrazine to afford the azo product **24** (Scheme 2.0.1).

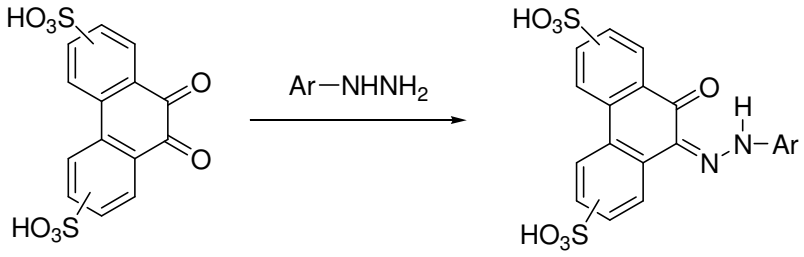

23 **24**

Scheme 2.0.1: Condensation of a quinone and hydrazine.

Another route to phenanthrol type azo compounds **24** is by the coupling of diazonium salts with 9-phenanthrol systems **25** (Scheme 2.0.2). This gives the same product **24** as in the case of condensation of a hydrazine with the quinone system **23**.

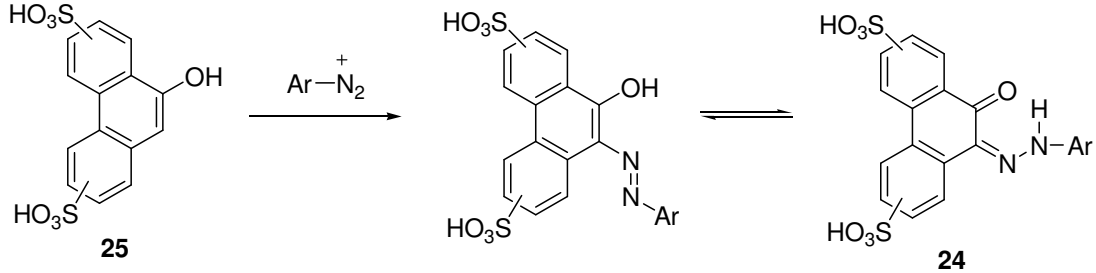

25 **24**

Scheme 2.0.2: Diazonium salt coupling with 9-phenanthrol systems **25**.

There are advantages in the preparation of azo compounds from the coupling of a diazonium salt to 9-phenanthrol systems **25** in that the regiochemistry of the reaction can be controlled due to only one coupling site. However, in the case of condensation of a hydrazine with a quinone **23** regiochemistry problems exist due to two possible condensation sites and the possibility of multiple substitution products **26** (Scheme 2.0.3).

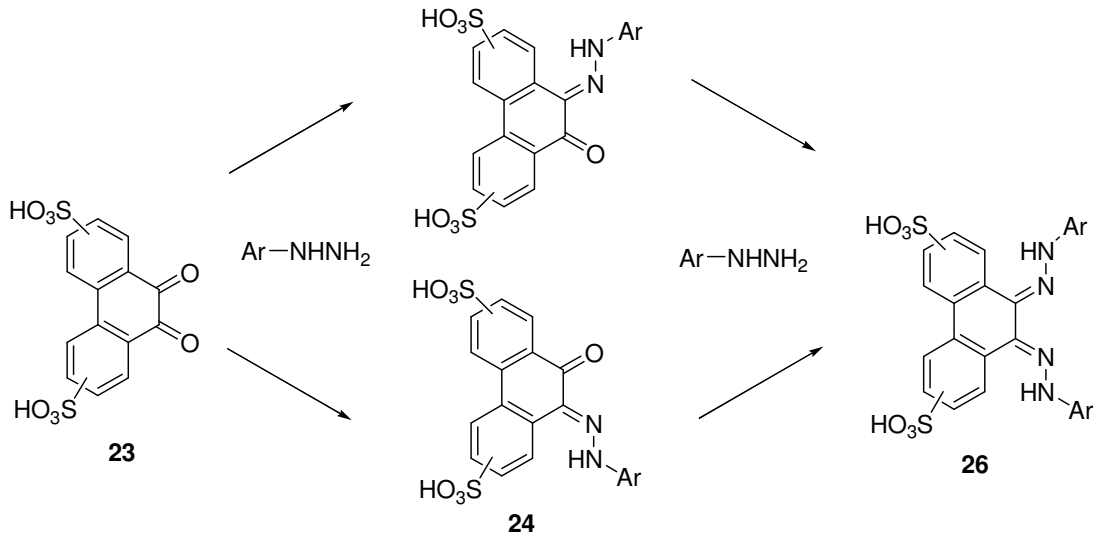

Scheme 2.0.3: Multiple substitution of quinone systems.

Therefore there is much interest in new routes to 9-phenanthrol **29** and related systems which may be of use as couplers in azo dye synthesis. One possible new route to 9-phenanthrol **29** is *via* cyclisation of a ketene **28** under flash vacuum pyrolysis (FVP) conditions (Scheme 2.0.4). In principle, ketenes might be generated under these conditions from the corresponding acid chlorides **27**.

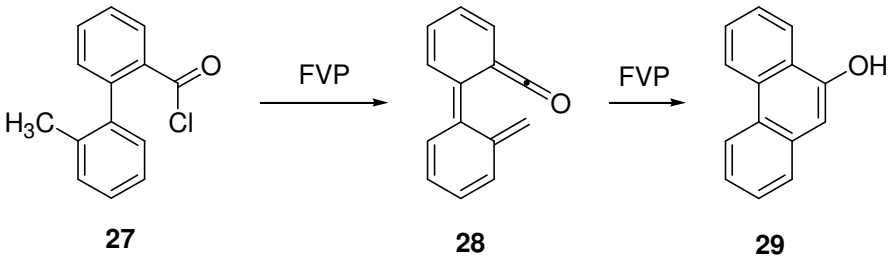

Scheme 2.0.4: Cyclisation of ketenes under FVP conditions.

The hydrazine route has its own advantages, in particular, applicability to heterocyclic azo dye synthesis due to pyridine-2-diazonium salts (and related heterocyclic diazonium salts) being unstable under aqueous conditions. There is also the possibility of extending the hydrazine route to phenanthrol systems **24** to afford new heterocyclic dyes and examine their properties.

2.1: Introduction to Acid Chloride Pyrolysis

The aim of this introduction is to discuss the known mechanisms of acid chloride pyrolysis. Such reactions were used to obtain cyclised targets such as 9-phenanthrol **29** which could then be used to prepare the required azo dyes.

There is very little known in the literature regarding the pyrolytic chemistry of acid chlorides and the mechanisms involved in this process. Pyrolysis reactions of acid chlorides proceed by several routes, namely *via* ketenes, *via* carbenes and by decarbonylation.

2.1.1: *Via* Ketenes

Pyrolysis of acid chlorides can generate ketene intermediates by hydrogen chloride elimination. These ketenes can then undergo various kinds of rearrangement to give different products of which cyclised systems are common.

An early example of the pyrolysis of acid chlorides *via* ketenes was published by Schiess and Heitzmann in 1977.[24,25] Pyrolysis of *o*-toluoyl chloride **30a** at 630 °C gave benzocyclobutenone **32a** in 97% yield (Table 2.1). The formation is by a primary loss of HCl *via* a six-membered transition state, this subsequently leads to a ketene intermediate **31a** which then cyclises to the product **32a** (Scheme 2.1.1). There was also extension of this method to include a variety of substituted examples (**a–j**) (Table 2.1).

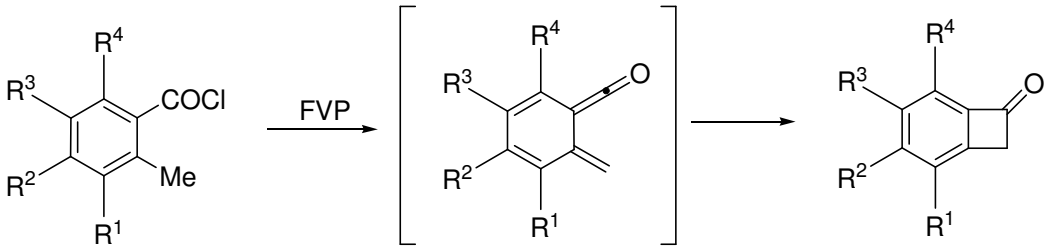

30 **31** **32**

Scheme 2.1.1: Pyrolysis of *o*-toluoyl chlorides gave benzocyclobutenones *via* a ketene.

This method was considered to be an efficient route to benzocyclobutenones **32a** since the strained bicyclic ring system can be prepared by this simple method from inexpensive precursors.

Table 2.1: Pyrolysis of substituted *o*-toluoyl chlorides **30** to give benzocyclobutenones **32** *via* a ketene **31**.

	R^1	R^2	R^3	R^4	**Furnace Temp °C**	**Yield**
a)	H	H	H	H	630	97%
b)	H	Me	H	Me	560	65%
c)	Me	Me	Me	Me	550	83%
d)	H	OMe	H	Me	590	67%
e)	H	H	H	OMe	590	63%
f)	OMe	H	H	OMe	590	63%
g)	H	OMe	OMe	H	530	37%
h)	H	H	CH=CH-CH=CH		550	73%
i)	Me	H	H	Me	630	27%
j)	H	H	Me	Me	630	61%

There have also been examples of heterocyclic acid chlorides undergoing similar cyclisations with the pyridine analogue **33** pyrolysed at 575 °C (1×10^{-4} Torr) to give the corresponding bicyclic product **35** *via* the pyridyl ketene **34** (Scheme 2.1.2).[26]

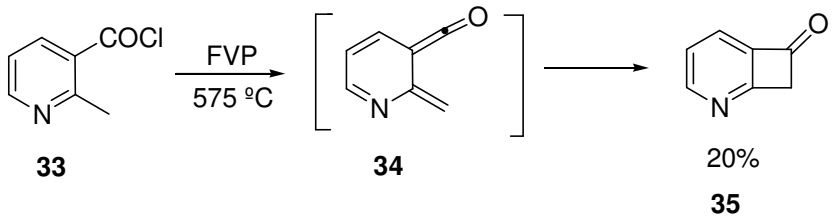

33 **34** **35**

Scheme 2.1.2: Pyrolysis of 3-chloroformyl-2-methylpyridine **33** to give pyrido[*b*]cyclobutene-5-one **35** *via* the ketene **34**.[26]

Further examples of the behaviour of substituted aromatic acid chlorides under pyrolysis conditions have also been reported.[27] Substituted 2-trimethylsilylbenzocyclobutenones were prepared by FVP from substituted acid chlorides **36** *via* the silyl ketene **37** (Scheme 2.1.3). However, when the *ortho* substituent was $CH(SiMe_3)_2$, pyrolysis of the compound between 590 °C and 610 °C gave a benzocyclobutenone derivative **38** in good yield (73%) by the loss of trimethylsilyl chloride as opposed to exclusively hydrogen chloride in the elimination step.[27] The bis(trimethylsilyl)methylbenzocyclobutenone **39** was obtained as a minor by-product in 7% yield. However, it appeared the thermal loss of trimethylsilyl chloride was favoured relative to the loss of hydrogen chloride in this case.

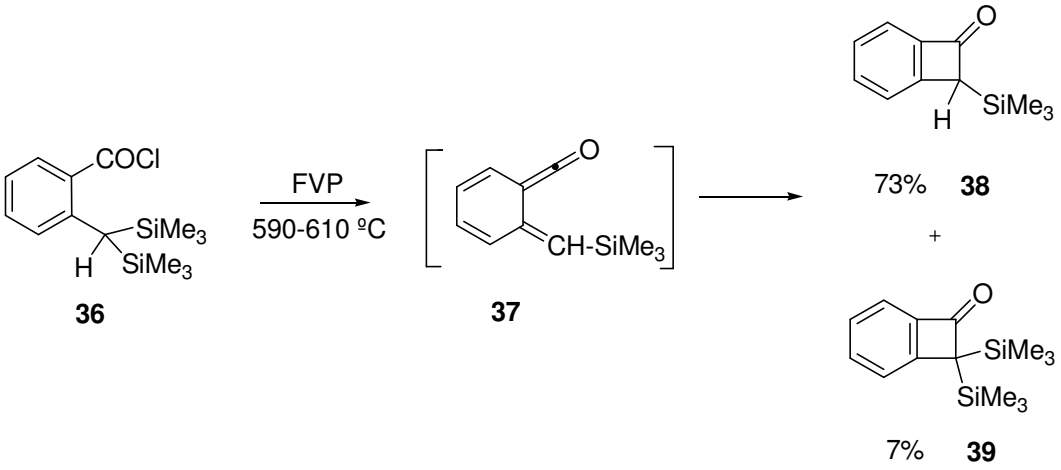

Scheme 2.1.3: Pyrolysis of *o*-substituted aroyl chloride **36** gave the benzocyclobutene derivative **38** *via* ketene **37**.[27]

This was also true of a number of substituted *o*-bis(trimethylsilyl)benzoyl chlorides although with varying ratios of products depending upon the type of thermal elimination favoured in each case (Scheme 2.1.4).[27]

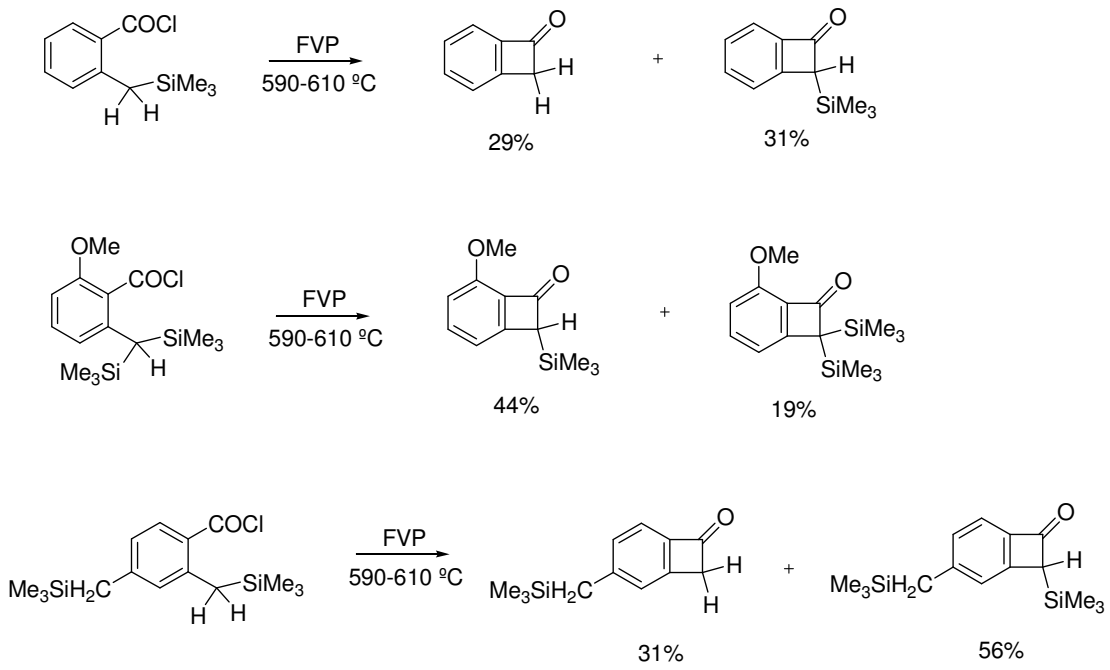

Scheme 2.1.4: FVP of variety of substituted trimethylsilylbenzoyl chlorides.[27]

The thermolysis of *o*-propylbenzoyl chloride **40** also leads to the formation of a ketene intermediate **41** (Scheme 2.1.5).[28] However, unlike the previous examples the corresponding substituted benzocyclobutenone **42** did not form, the ketene intermediate **41** underwent a [1,5]-hydrogen-shift to give the aldehyde product **43**.

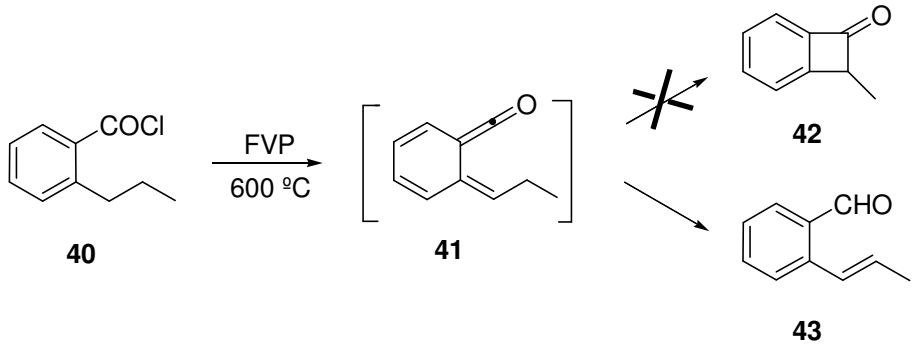

Scheme 2.1.5: Pyrolysis of *o*-propylbenzoyl chloride **40** gave aromatic aldehyde **43** *via* ketene **41**.[28]

2.1.2: *Via* Carbenes

The second type of acid chloride pyrolytic chemistry is *via* carbenes, which can be commonly generated by the elimination of hydrogen chloride to give a ketene. The subsequent loss of carbon monoxide gives the corresponding carbene.

The first example of this chemistry reported was the pyrolysis of norcarane carboxylic acid chloride **44** which leads to a ketene intermediate **45** by HCl elimination, which in turn lost CO to generate the carbene **46**. The carbene then rearranged and formed 1,2-cycloheptadiene **47** which dimerised to afford *trans*-tricyclotetradeca-7,9-diene **48** in 25% yield (Scheme 2.1.6).[29]

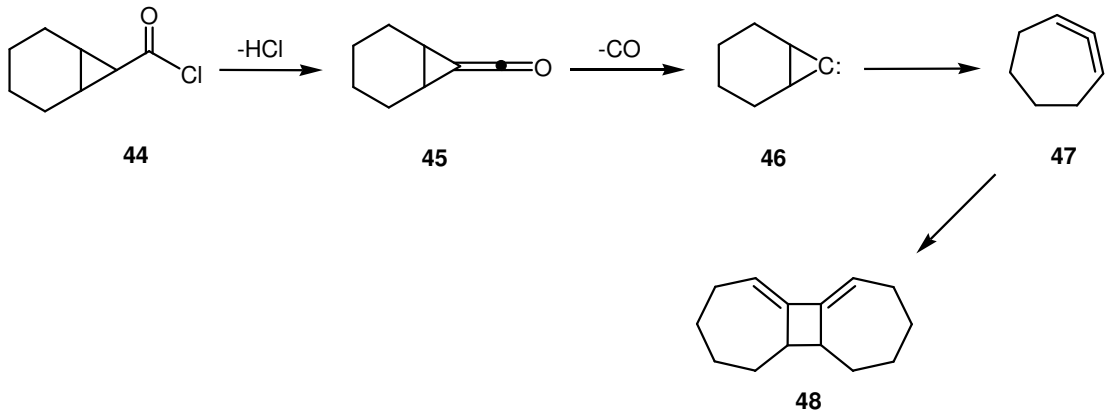

Scheme 2.1.6: Pyrolysis of norcarane carboxylic acid chloride **44** gave *trans*-tricyclotetradeca-7,9-diene **48** *via* carbene rearrangement.[29]

It was also found that in one of the examples discussed in the ketene section, the ketene intermediate from 3-chloroformyl-2-methylpyridine **34** (Scheme 2.1.2) could further eliminate CO to produce a carbene intermediate **49** if the pyrolysis was carried out under higher pressure conditions (1×10^{-2} Torr). The resulting carbene could either ring-contract to give 1-azafulvenallene **50** at 575 °C, or at 800 °C undergo rearrangement to give 1-cyanocyclopentadiene **51** (Scheme 2.1.7).[26]

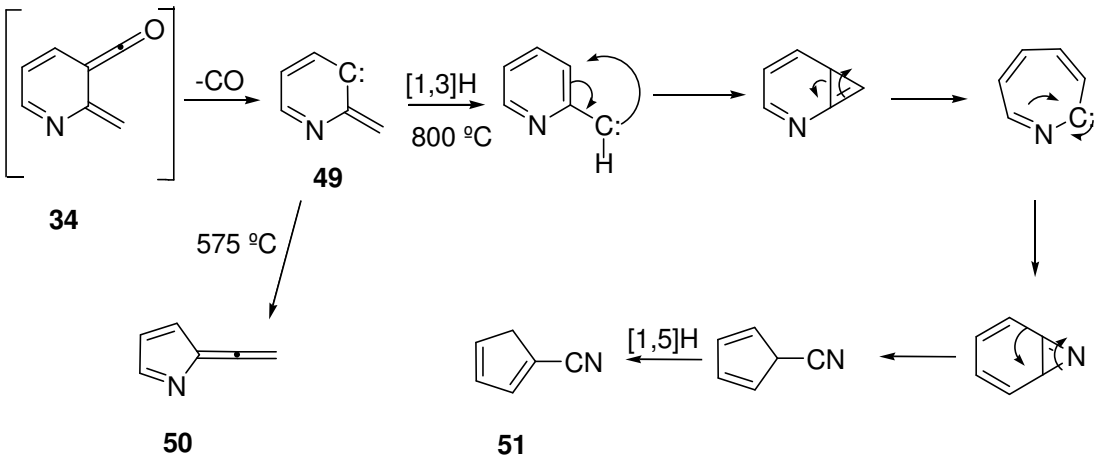

Scheme 2.1.7: Pyrolysis of 3-chloroformyl-2-methylpyridine **33** at higher pressure.[26]

In a further example of the acid chloride pyrolysis *via* carbenes, the FVP of 2-phenylcinnamoyl chloride **52** gave three major products namely the acetylene **55**, phenanthrene **57** and the benzazulene **56**. The methylenecarbene intermediate **54** was generated by loss of HCl and CO from the ketene intermediate **53**.[30] The proposed mechanism is that it then could either undergo insertion to afford phenanthrene **57** or addition to afford benzazulene **56**. The yields vary with furnace temperature (Scheme 2.1.8).[30] This product distribution is also found by the generation of the methylenecarbene **54** by an alternative method.[31] At low pyrolysis temperatures the position of equilibrium between the methylenecarbene intermediate **54** and acetylene **55** was largely to the right and hence acetylene **55** was the main product. However, as the temperature of the pyrolysis was increased the position of equilibrium moved towards the methylenecarbene intermediate **54** and increased yields of phenanthrene **57** and benzazulene **56** were obtained.[30]

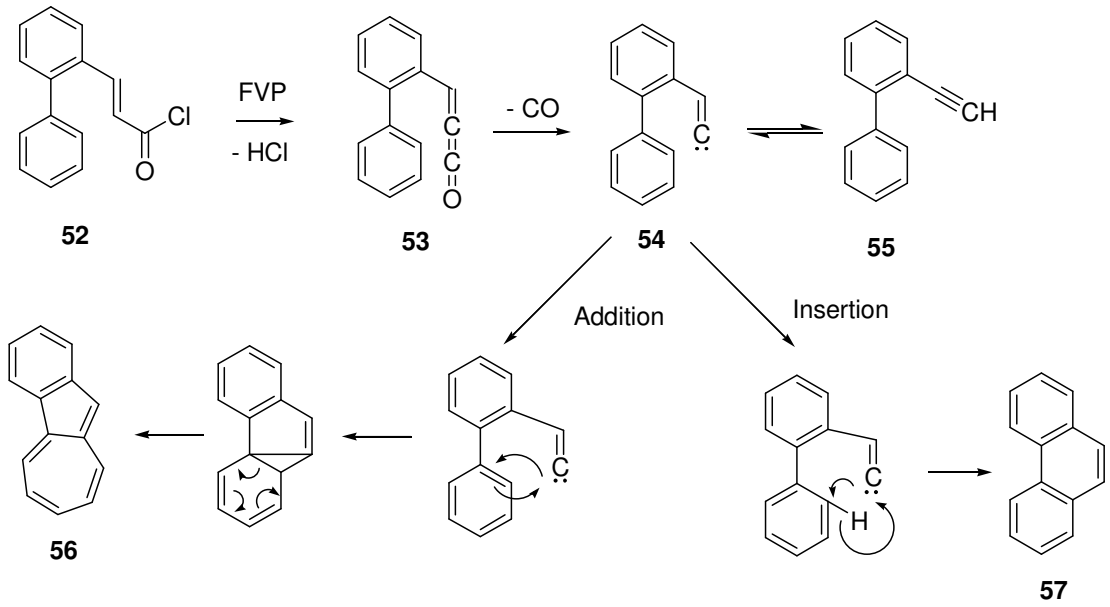

Scheme 2.1.8: FVP of 2-phenylcinnamoyl chloride **52** gave rise to three major products *via* methylenecarbene intermediate **54**.[30]

In addition to the above examples involving carbenes generated by the loss of CO from the ketene intermediate, carbenes may also be obtained by rearrangement of the ketene without decarbonylation.[32]

Pyrrole-2-carboxylic acid chloride **58** was pyrolysed at 650 °C and gave 2-carbonyl-2*H*-pyrrole **59** which is thought to undergo ring expansion to lead to the α-oxocarbene **60**. This was followed-up by ring opening to the (isocyanovinyl)ketenes **61, 62** (Scheme 2.1.9).

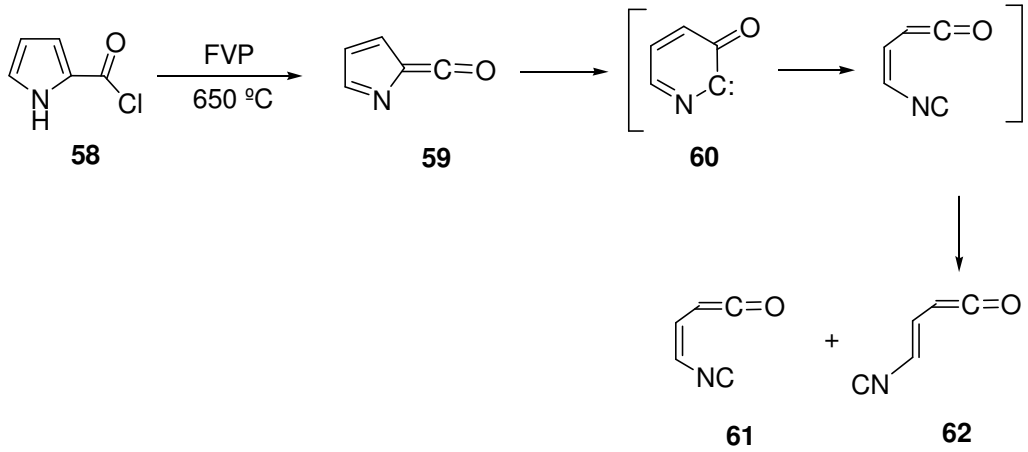

Scheme 2.1.9: Pyrolysis of pyrrole-2-carboxylic acid chloride **58** gave ketene **59** which undergoes ring expansion to form carbene **60**.[32]

2.1.3: *Via* Decarbonylation

Decarbonylation is often seen in acid chloride pyrolysis, as already encountered in section 2.1.2, where carbene intermediates are commonly obtained by the decomposition of ketenes following loss of the carbonyl group. However, examples in which decarbonylation occurs to give chlorine containing products, but not *via* a ketene can be also found in the literature.

The pyrolysis of triphenylacetyl chloride **63**, where elimination of HCl is not possible, afforded triphenylchloromethane **64** with the evolution of CO (Scheme 2.1.10). The pyrolysis started at the melting point of the acid chloride and was completed at 180 °C.[33]

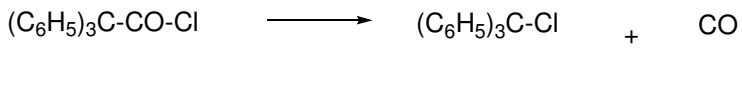

63 **64**

Scheme 2.1.10: Decarbonylation occurred in triphenylacetyl chloride **63** pyrolysis.[33]

Another example of an unusual decarbonylation which may possibly involve radical rearrangement has also been reported. Dehydroabietyl chloride **65** was pyrolysed at temperatures ranging from 290 to 500 °C in order to study the temperature dependence of pyrolysate composition. Four major olefin products **66, 67, 68** and **69** were identified by comparison of their gas liquid chromatography retention times with those of authentic samples (scheme 2.1.11).[34]

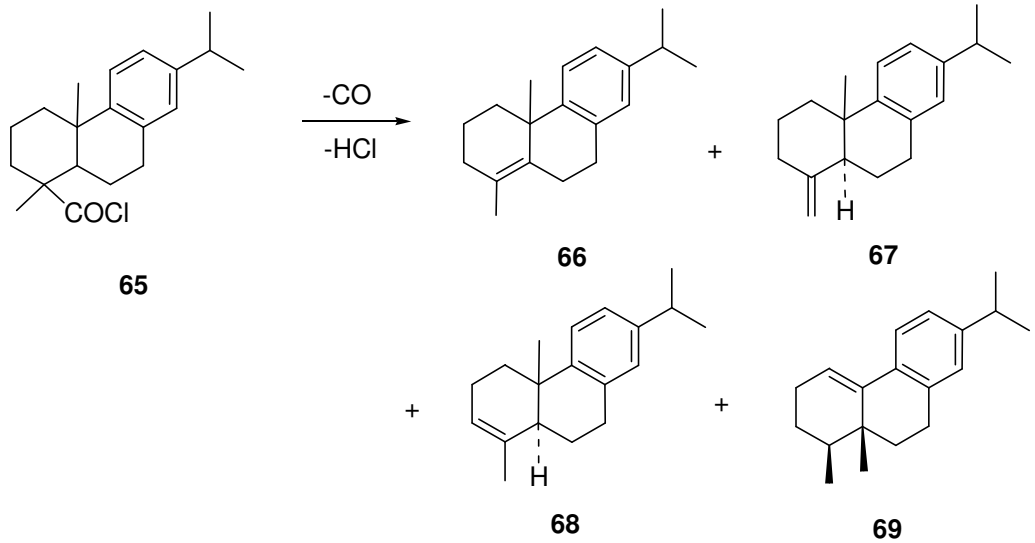

65 **66** **67** **68** **69**

Scheme 2.1.11: Pyrolysis of dehydroabietyl chloride **65** at 290-500 °C.[34]

Above 400 °C, almost all the acid chloride decomposed to give products. As the temperature increased further, product **69** started suffering a decrease in yield from 46% at 290 °C to 7% at 500 °C, whereas the yield of the other three products appeared less influenced by the furnace temperature. The proposed mechanism explaining this observation is shown in Scheme 2.1.12.[34]

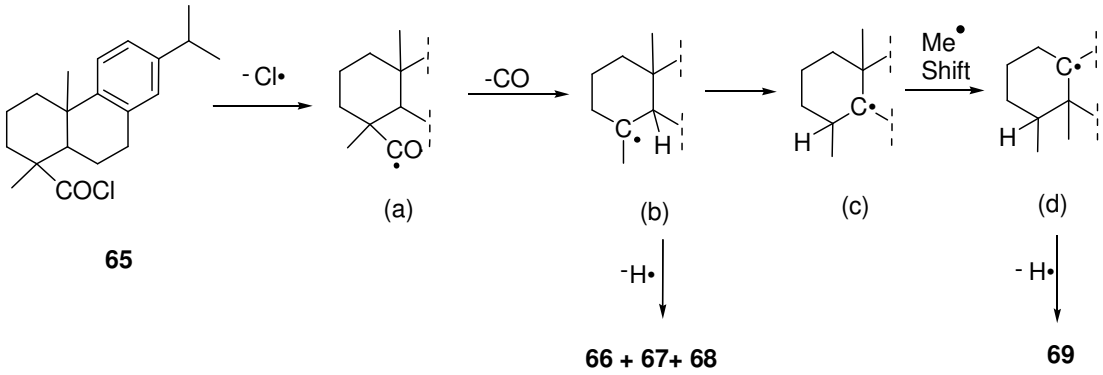

Scheme 2.1.12: Proposed mechanism of dehydroabietyl chloride pyrolysis.[34]

The authors suggested that the first step was the loss the chlorine atom which was followed by decarbonylation to give intermediate (b) (Scheme 2.1.12). Since the lower temperatures favoured rearrangement to the most stable radical (d) the formation of **69** was increased. As the temperature increased, so did the concentration of radicals and loss of a hydrogen atom became more probable. This consequently made radical stability less important, therefore the increasing the yield of products **66, 67** and **68**.

2.1.4: Conclusions

There is little known in the literature regarding the detail of the pyrolytic chemistry of acid chlorides. However initial studies indicate FVP may be a useful route to previously unknown cyclised targets of use in azo dye synthesis.

2.2: FVP Route to Phenanthrol Based Dyes

There is an interest in phenanthrene derivatives based on structure **70**. This section describes the preparation of 9-phenanthrol **29** and investigation of its subsequent coupling reactions with suitable diazonium salts at the 10 position of the phenanthrene ring to give heterocyclic azo compounds **70** of interest (Scheme 2.2.1). It may also be possible to prepare heterocyclic azo dyes of this type with a suitable environment to form a metallised complex **71** hence resulting in improved fastness properties. Therefore the initial aim is to develop a new synthetic route to 9-phenanthrol **29**.

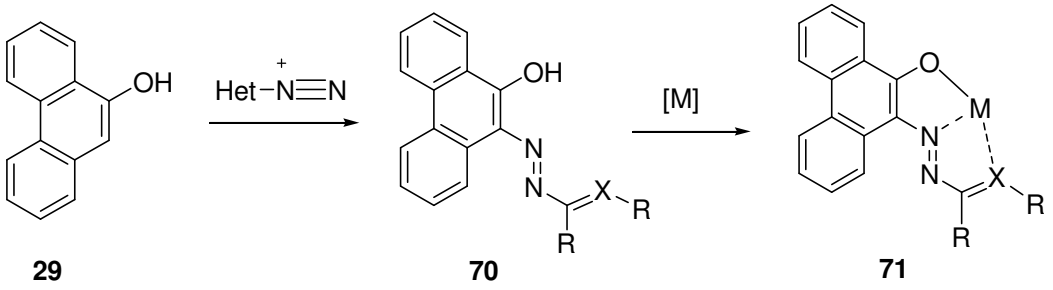

29 **70** **71**

Scheme 2.2.1: Azo coupling of 9-phenanthrol **29** and metallisation (R = Ar, X = donor)

A proposed route to 9-phenanthrol **29** was based on previous examples of the preparation of benzocyclobutenone **32** by pyrolysis of *o*-toluoyl chloride **30** at 630 ºC after loss of hydrogen chloride in 97% yield (Scheme 2.2.2).[25]

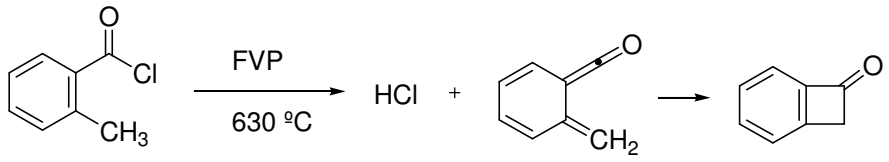

30 **31** **32**

97%

Scheme 2.2.2: Pyrolysis of *o*-toluoyl chloride **30**.[25]

The aim here is to adapt this to a biphenyl system to give 9-phenanthrol **29** from a biphenyl acid chloride **27** *via* a ketene **28** (Scheme 2.2.3). 9-Phenanthrol **29**

can then undergo diazonium salt coupling to give the required heterocyclic azo compounds **70**.

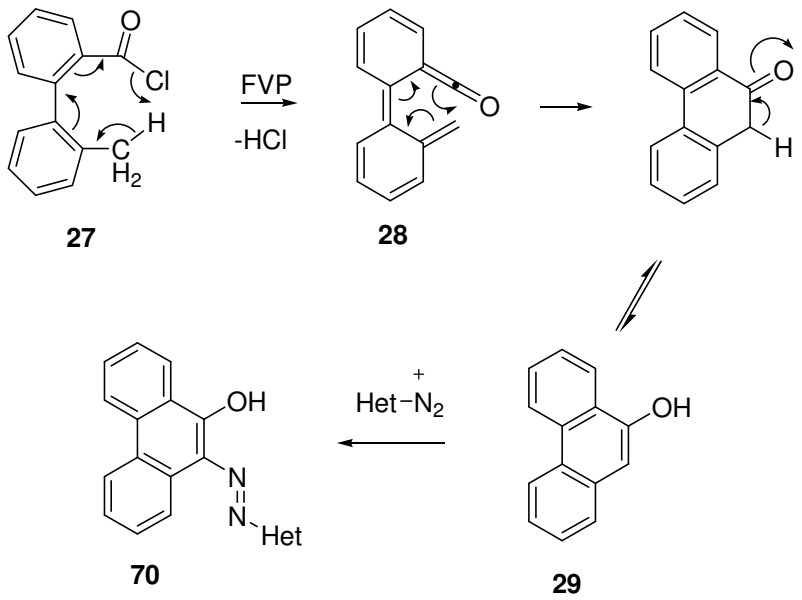

Scheme 2.2.3: Proposed route to phenanthrene based targets.

In order to synthesise the biphenyl acid chloride **27** firstly the appropriate biphenylcarboxylic acid **74** was prepared by Suzuki coupling of *o*-tolylboronic acid **72** with *o*-iodobenzoic acid **73** using palladium tetrakis(triphenylphosphine) as the catalyst (Scheme 2.2.4). This gave the biphenylcarboxylic acid **74** in 25% yield which was identified by comparison with literature ^{1}H NMR spectra and a characteristic carbonyl absorption in the IR spectrum.[35] However this reaction was not optimised.

The biphenylcarboxylic acid **74** was then treated with thionyl chloride to give the required acid chloride **27** in 97% yield which was identified by ^{1}H and ^{13}C NMR spectra and the observation of a shift in the carbonyl absorption peak in the IR spectrum from 1690 cm^{-1} characteristic of a carboxylic acid to 1770 cm^{-1} characteristic of an acid chloride (Scheme 2.2.4).

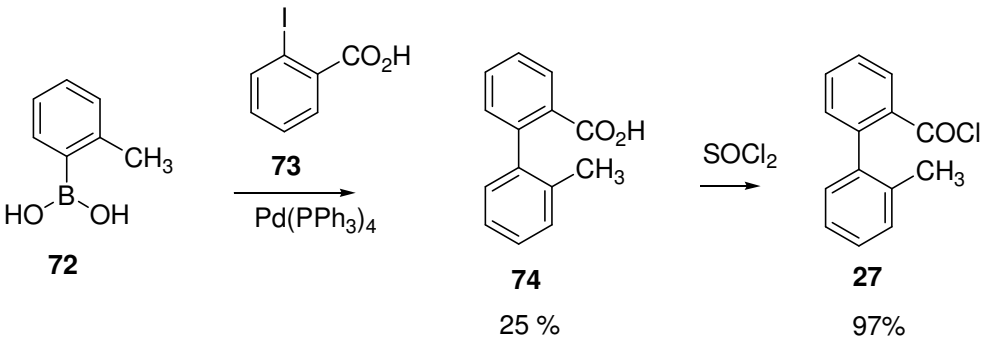

Scheme 2.2.4: Preparation of biphenyl acid chloride **27**.

The acid chloride **27** was subjected to FVP conditions at furnace temperatures 650 ºC, 750 ºC, 800 ºC, 850 ºC and 900 ºC. Analysis of the pyrolysis products revealed transformation of the acid chloride **27** to a single component over the temperature range studied. The percentage of the acid chloride **27** and product present at each pyrolysis temperature was represented graphically in a temperature profile by analysis of the integrals of the methyl signals corresponding to each product (Figure 2.2.1).

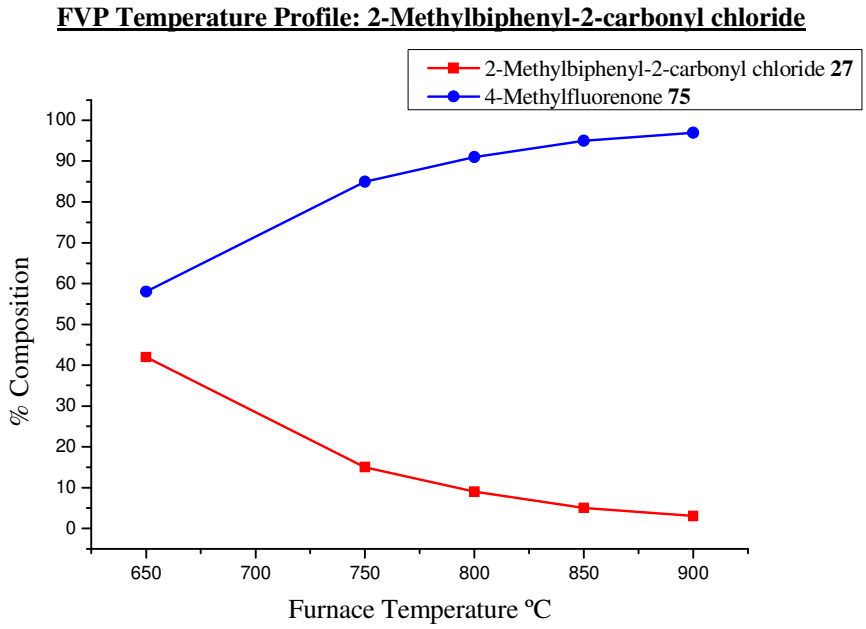

Figure 2.2.1: Temperature profile of pyrolysis of biphenyl acid chloride **27**.

By analysis of the ^{1}H and ^{13}C NMR spectra of the pyrolysis product it was immediately clear that 9-phenanthrol **29** was not present due to the characteristic methyl peak present in the ^{1}H NMR spectrum at δ = 2.60 and in the ^{13}C NMR spectrum at δ = 20.11. Further analysis by electron impact mass spectrometry revealed the product had a molecular ion peak at 194 indicating this product had the same mass as 9-phenanthrol **29**. The IR spectrum of the product contained a characteristic carbonyl absorption peak in the ketone region at ≈ 1710 cm^{-1}. By combining the data from these analyses the structure of 4-methylfluoren-9-one **75** was proposed. 4-Methylfluoren-9-one **75** was then positively identified as the unknown product of this reaction by comparison with the literature ^{1}H and ^{13}C NMR spectra.[36,37] Pyrolysis of the biphenyl acid chloride **27** at a furnace temperature of 900 ºC gave 4-methylfluoren-9-one **75** in 58% yield after purification by dry flash column chromatography (Scheme 2.2.5).

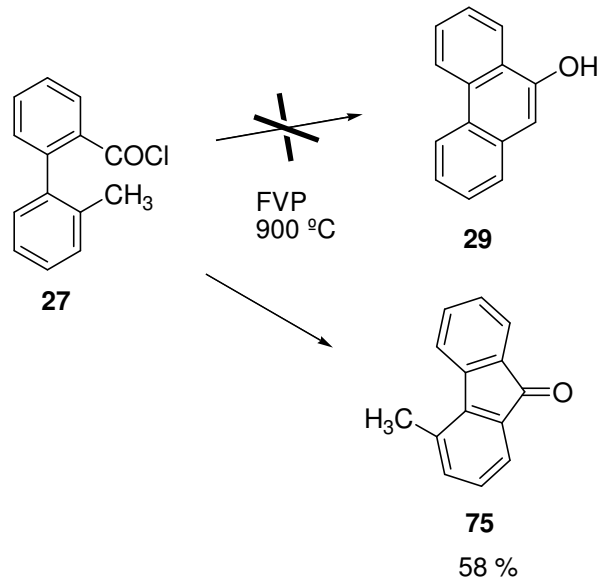

Scheme 2.2.5: Preparation of 4-methyfluoren-9-one **75** from the biphenyl acid chloride **27**.

The observation that 4-methylfluoren-9-one **75** was formed rather than 9-phenanthrol **29** indicated that the mechanism of cyclisation did not involve the *ortho* methyl group on the adjacent ring of the biphenyl acid chloride **27** but involved

attack at the alternative *ortho* CH on the opposite side of the ring. The cyclisation appeared to proceed *via* a thermal Friedel-Crafts-type acylation with overall loss of HCl and not formation of the expected ketene **28**. Hence this reaction appears to give a good new route to fluorenones although the exact mechanism of this cyclisation is unclear and will be continued in the next section. However, an alternative route to 9-phenanthrol **29** is required (Section 2.4).

2.3: Study of the Mechanism of Acid Chloride Pyrolysis

Due to the unusual behaviour of acid chlorides under pyrolysis conditions (Section 2.1) a number of different mechanisms can be proposed for the transformation of the biphenyl acid chloride to 4-methylfluorenone. These include a radical process, intramolecular attack or the involvement of carbene intermediates.

In order to investigate the mechanism of cylisation further several similar acid chlorides were prepared and their behaviour examined when exposed to similar FVP conditions. A final year project student, K. Huang, carried out various model reactions under supervision of the author, to clarify the mechanism.[39]

2.3.1: Radical Formation

The first possible mechanism included a radical cyclisation in which a ketyl radical **76** is generated by the loss of a chlorine atom by homolysis of the C-Cl bond. This then forms a carbon to carbon bond with the aromatic ring to give the delocalised radical **77** which subsequently collapses to the fluorenone **75** (Scheme 2.3.1).

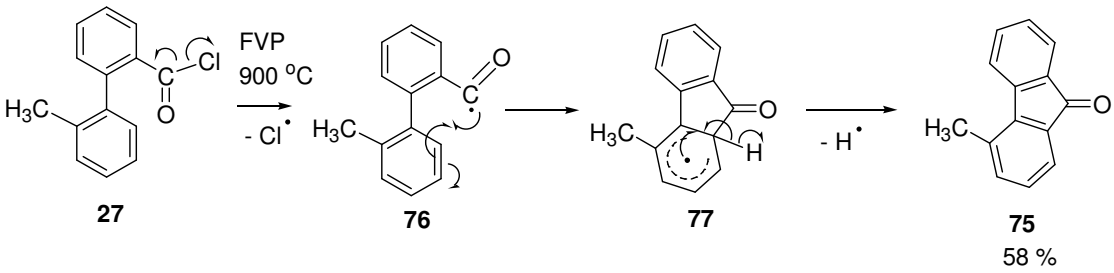

27 **76** **77** **75**
58 %

Scheme 2.3.1: Cyclisation *via* a radical process.

Ketyl radicals as the key intermediate **76** in the proposed mechanism are known to decarbonylate at much lower temperatures than 900 ºC under FVP conditions. As one example, the azocarbonyl compound **78** rapidly lost CO by pyrolysis at 750 °C after homolysis of the C-N bond and gave rise to 2-methoxyphenyl radical **79**, which rearranged to benzaldehyde **80** (Scheme 2.3.2). This is a well known property of 2-methoxyphenyl radicals.[38] Therefore, a mechanism involving a ketyl radical as key intermediate is unlikely.

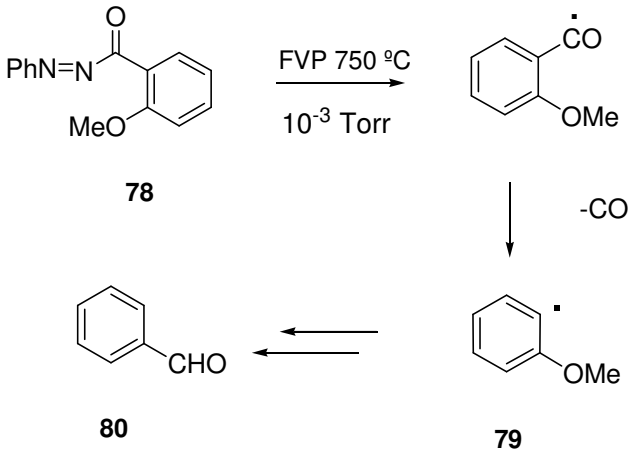

78 80 79

Scheme 2.3.2: Azo compound **78** rapidly decarbonylated at 750 °C.[38]

This mechanism was further discounted by the observation that the FVP of 2-methoxybenzoyl chloride **81** at temperatures between 700 °C and 800 °C did not afford benzaldehyde **80**.[39] Under the proposed radical mechanism this acid chloride **81** would be expected to lose the chlorine atom which would result in decarbonylation to give the phenyl radical **79** (Scheme 2.3.3). This would then rearrange to give benzaldehyde **80** as in the case of azocarbonyl **78** (Scheme 2.3.2). Therefore due to these observations a radical mechanism involving the carbonyl radical could be discounted.

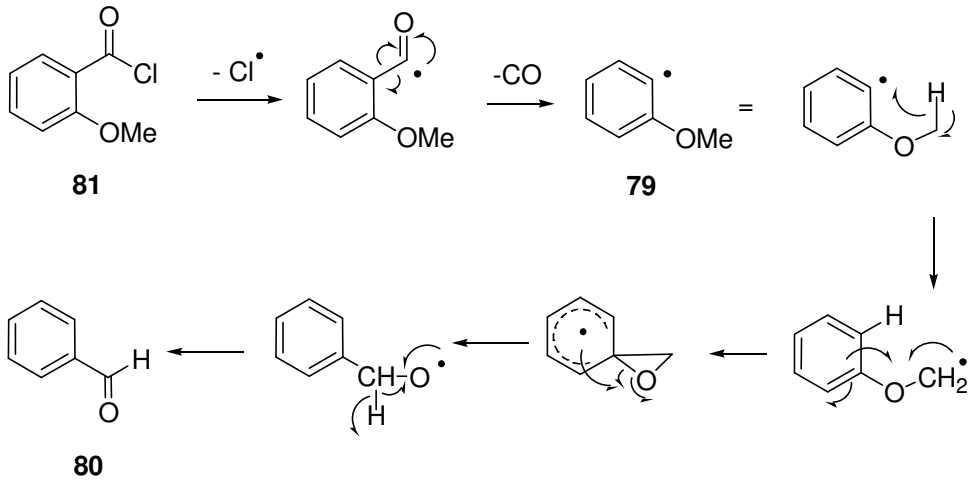

81 79 80

Scheme 2.3.3: Proposed FVP of 2-methoxybenzoyl chloride **81** in the event of a radical mechanism.

2.3.2: Other Examples of Acid Chloride Pyrolysis

In order to investigate this mechanism further, the behaviour of several similar acid chlorides under FVP conditions was examined by K. Huang.[39] FVP of *o*-phenylbenzoyl chloride **82** at various furnace temperatures from 550 ºC to 900 ºC resulted in transformation of the acid chloride to fluorenone **83** (Figure 2.3.1). Complete conversion of the acid chloride **82** was achieved at 900 ºC to give the fluorenone **83** in 96% yield (Scheme 2.3.4).[37]

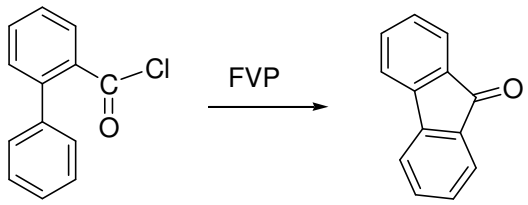

82 **83**

96%

2.3.4: FVP of *o*-phenylbenzoyl chloride **82** to afford fluorenone **83**.[37]

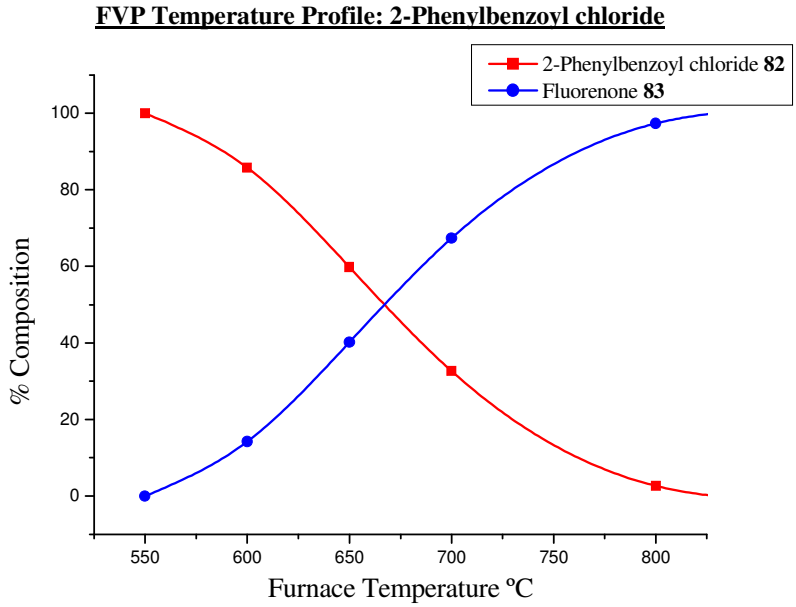

Figure 2.3.1: FVP temperature profile of 2-phenylbenzoyl chloride **82**.

The pyrolysis of 2-(phenylthio)benzoyl chloride **86** was also of interest. Firstly 2-(phenylthio)benzoic acid **85** was prepared using known literature methods from the treatment thiophenol **84** with the anthranilic acid diazonium salt **83** (Scheme 2.3.5).[40] This afforded 2-(phenylthio)benzoic acid **85** in 39% yield. The required acid chloride **86** was prepared in good yield by treatment of the carboxylic acid **85** with thionyl chloride (Scheme 2.3.5).[39]

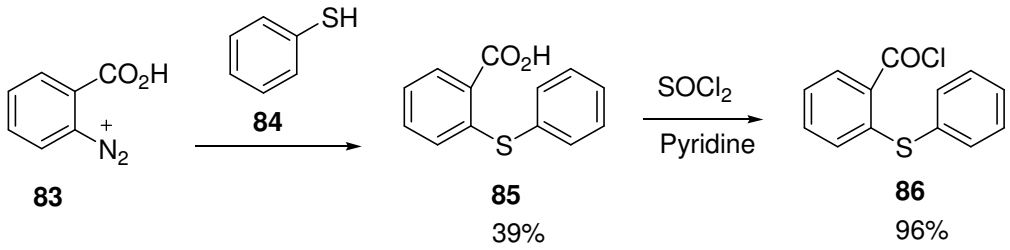

83 **85** 39% **86** 96%

Scheme 2.3.5: Synthesis of 2-(phenylthio)benzoic acid **85**.

The acid chloride **86** was then exposed to FVP conditions at a variety of furnace temperatures ranging from 700 °C to 900 °C to obtain a temperature profile of the conversion of the acid chloride **86** to the cyclised system (Figure 2.3.2).[39] Maximum conversion of 2-(phenylthio)benzoyl chloride **86** to thioxanthen-9-one **87** occurred at 900 °C to give the product in 91% yield (Scheme 2.3.6).

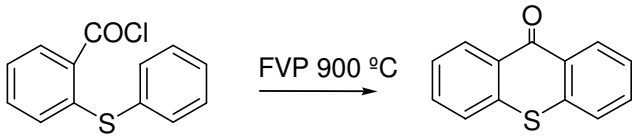

86 **87** 91%

Scheme 2.3.6: Synthesis of thioxanthen-9-one **87**.

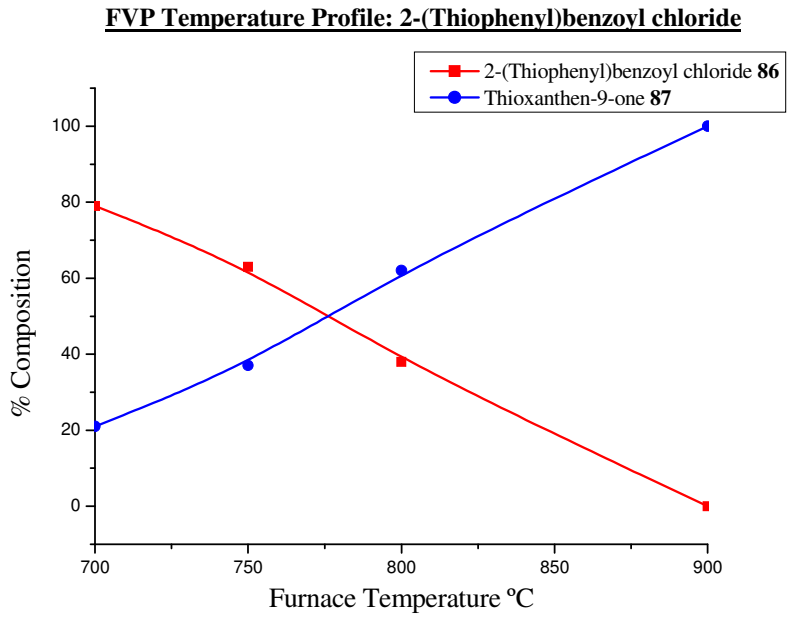

Figure 2.3.2: FVP temperature profile of 2-(thiophenyl)benzoyl chloride **86**.

This investigation was also extended to a related oxygen system. Firstly 2-phenoxybenzoyl chloride **89** was prepared in excellent yield from 2-phenoxybenzoic acid **88** by reaction with thionyl chloride in the presence of pyridine in dry ether (Scheme 2.3.7).

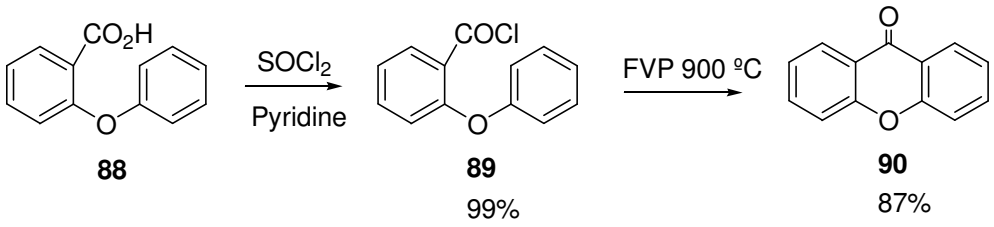

88 **89** 99% **90** 87%

Scheme 2.3.7: Synthesis of 2-phenoxybenzoyl chloride **89**.

The acid chloride **89** was then exposed to FVP conditions at varying furnace temperatures to obtain a temperature profile of the conversion of the acid chloride to xanthen-9-one **90** (Figure 2.3.3). Complete conversion of the acid chloride **89** to the cyclised product occurs at a furnace temperature of 900 °C to afford xanthen-9-one **90** in 87% yield.

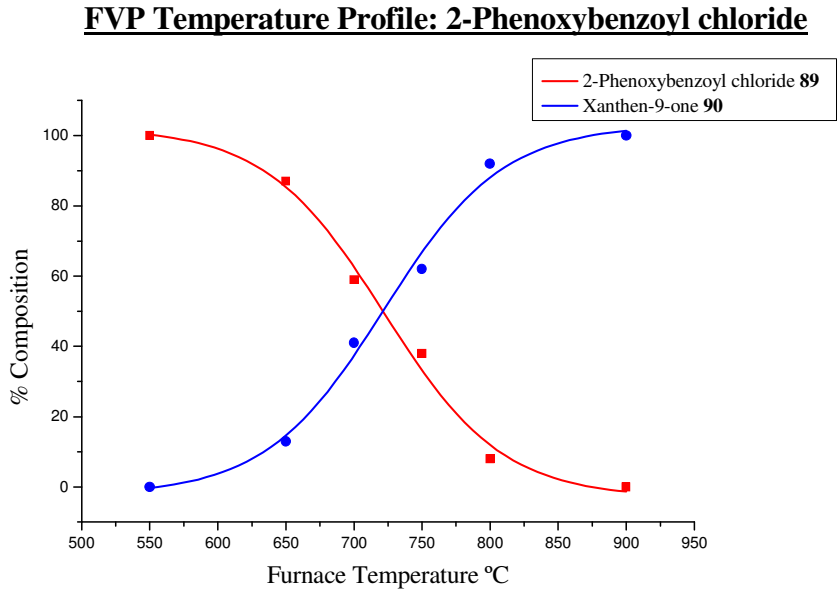

Figure 2.3.3: FVP temperature profile of 2-phenoxybenzoyl chloride **89**.

2.3.3: Comparison of Temperature Profiles

FVP of 2-phenylbenzoyl chloride **82**, 2-(thiophenyl)benzoyl chloride **86** and 2-phenoxybenzoyl chloride **89** lead to fluorenone **83**, thioxanthen-9-one **87** and xanthen-9-one **90** respectively in good yields. All examples appeared to undergo a thermal Friedel-Crafts-type acylation with overall loss of HCl involving ring closure.

Comparison of the temperature profiles of 2-(thiophenyl)benzoyl chloride **86** and 2-phenoxybenzoyl chloride **89** shows that similar furnace temperatures are needed to obtain complete conversion. The furnace temperature required to obtain 50% conversion of the acid chloride to the cyclised system is lower for 2-phenoxybenzoyl chloride **89** (at 725 °C) than that of 2-(thiophenyl)benzoyl chloride **86** (at 775 °C) (Figure 2.3.4). Hence more energy is required for conversion of the sulfur containing acid chloride to the cyclised product than in the case of the oxygen analogue.

FVP Temperature Profile: Xanthenone, Thioxanthenone

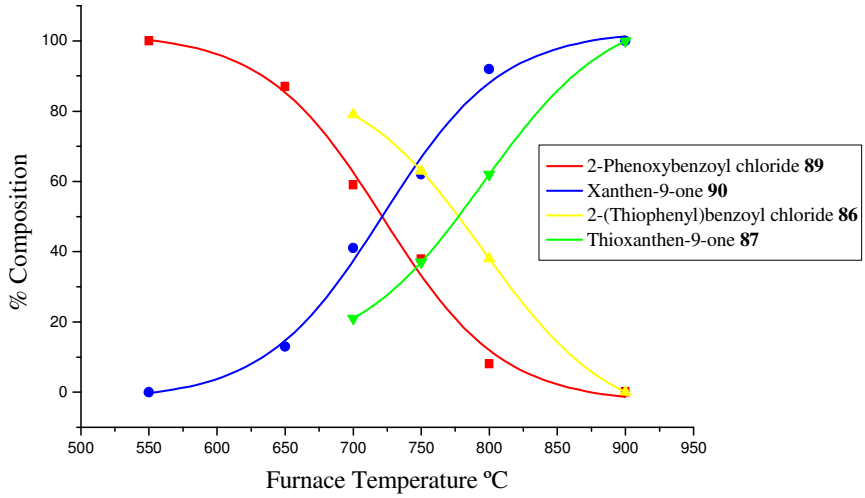

Figure 2.3.4: Comparison of temperature profiles of 2-(thiophenyl)benzoyl chloride **86** and 2-phenoxybenzoyl chloride **89**.

Comparison of the temperature profiles of the FVP of 2-phenylbenzoyl chloride **82**, 2-phenoxybenzoyl chloride **89** and 2-(thiophenyl)benzoyl chloride **86** showed cyclisation of 2-phenoxybenzoyl **89** and 2-(thiophenyl)benzoyl **86** chlorides required more energy than in the case of the 2-phenylbenzoyl chloride **82** (Figure 2.3.5). The furnace temperatures required to obtain 50% conversion of the acid chloride to the cyclised system were 650 °C, 725 °C and 775 °C for the biphenyl, phenoxy and thiophenyl acid chlorides respectively.

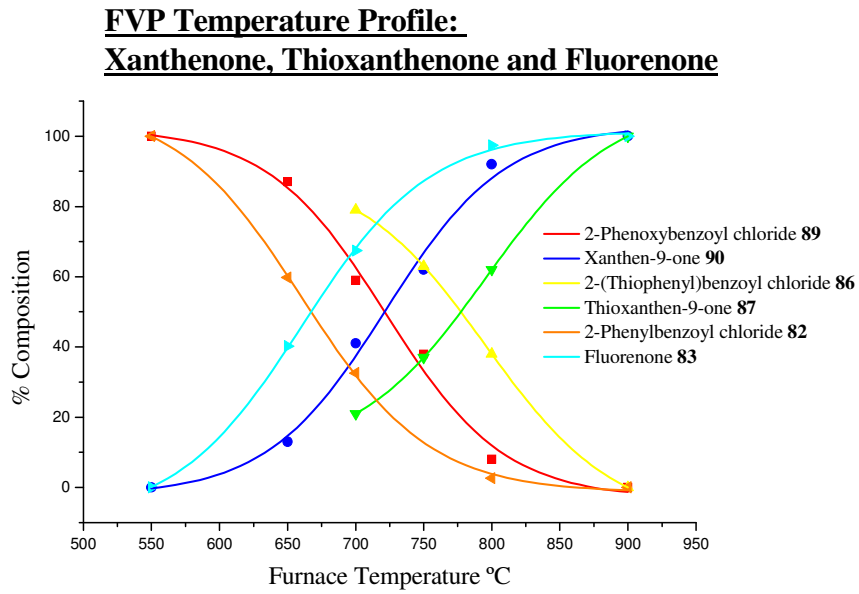

Figure 2.3.5: Comparison of temperature profiles of 2-phenylbenzoyl chloride **82**, 2-phenoxybenzoyl chloride **89** and 2-(thiophenyl)benzoyl chloride **86**.

2.3.4: Proposed Mechanisms

Under FVP conditions radical formation and pericyclic processes are the most usual mechanisms in the gas phase. Bond cleavage by heterolysis to form ionic intermediates can be ruled out due to the high ionisation energy required in the absence of solvation. Although the exact mechanism of the acid chloride cyclisation is unclear several mechanisms can be proposed or discounted based upon current experimental results.

2.3.4.1: Intramolecular Attack

One possible mechanism of cyclisation involves intramolecular attack of the carbonyl group leading to intermediate **91** which then loses HCl to afford thioxanthen-9-one **87** (Scheme 2.3.8).

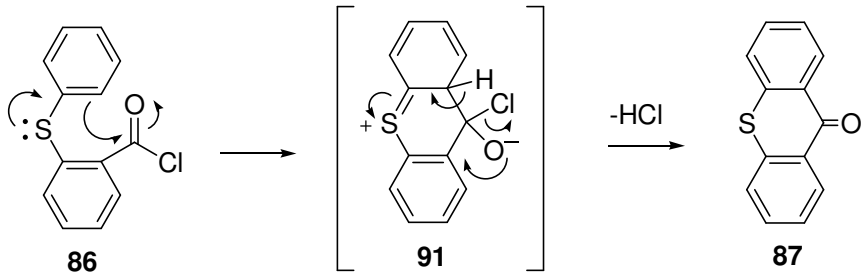

Scheme 2.3.8: Proposed mechanism *via* intramolecular attack.

However, the FVP temperature profile in Scheme 2.3.4 is unexpected as more energy is required to achieve conversion of the 2-phenoxy- and 2-(thiophenyl)-benzoyl acid chlorides **89** and **86** into the cyclic products than 2-phenylbenzoyl chloride **82**. Intuitively, the presence of a sulfur or oxygen atom in the molecule is anticipated to enhance the nucleophilicity of the benzene ring, hence the sigmoid curves for 2-(thiophenyl)benzoyl chloride **86** and 2-phenoxybenzoyl chloride **89** should be shifted to the left with conversion occurring at a lower temperature if the mechanism above is correct (Scheme 2.3.8). In practice, the opposite result is observed and implies a nucleophilic component of the attack is unlikely for aryl chloride pyrolysis.

2.3.4.2: Carbene Intermediates

Whereas nucleophilic component attack and radical formation are unlikely as the mechanistic pathway, cyclisation *via* pericyclic process could also be considered. Two proposed mechanisms might explain these observations. Both mechanisms involve carbene intermediates.

In the first type of proposed mechanism the substrate undergoes a [1,5]-chloro-shift to yield a ketene intermediate **92** which subsequently loses HCl to generate carbene, electrocyclisation of the carbene-ketene species **93** gives the required product (Scheme 2.3.9).

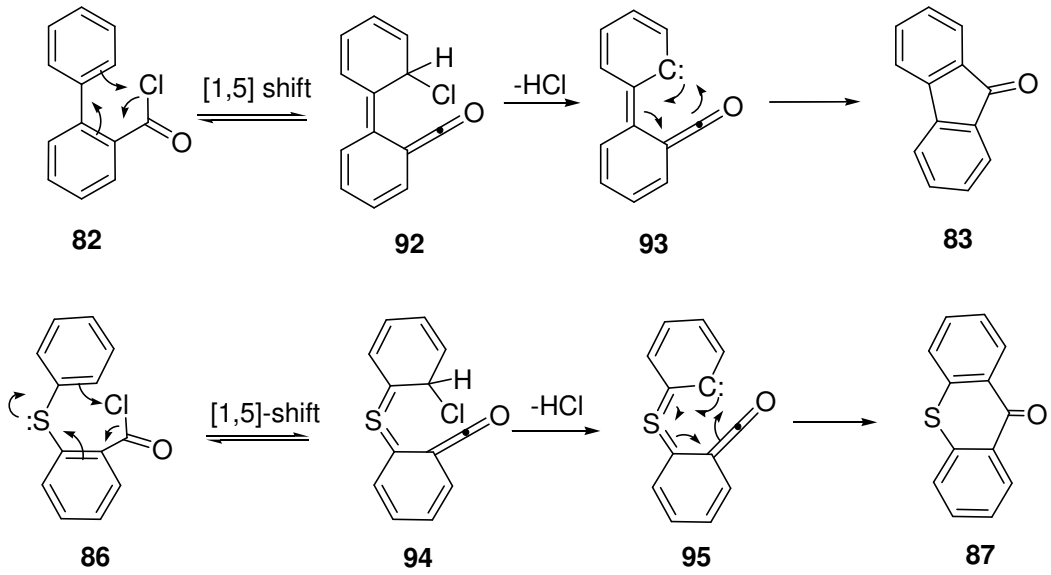

Scheme 2.3.9: Proposed mechanism to generate carbenes *via* [1,5]-chloro-shift.

For the biphenyl case this mechanism is viable with the generation of a carbene intermediate **93** by α-elimination of HCl possible and supported by previous literature examples.[41] However, this mechanism appears to be unlikely for the thio case. Thus, the first intermediate **94** obtained *via* [1,5]-chloro-shift involves valence shell expansion of sulfur which requires high energy and also the intermediate **95** has no benzene rings in the molecule with the lack of aromaticity further disfavoring this pathway. Furthermore, valence shell expansion is extremely unlikely in the case of 2-phenoxybenzoyl chloride **89** which discounts this pathway.

Another carbene intermediate mechanism *via* electrocyclisation can also be proposed. The first two steps provide the dibenzopyran **97** as an intermediate, which is obtained by electrocyclisation of acid chloride **82** giving intermediate **96** that undergoes [1,5]-hydrogen-shift. The dibenzopyran intermediate **97** further loses HCl to give the carbene species **98** which rearranges to fluorenone **83** in the suggested mechanism (Scheme 2.3.10).

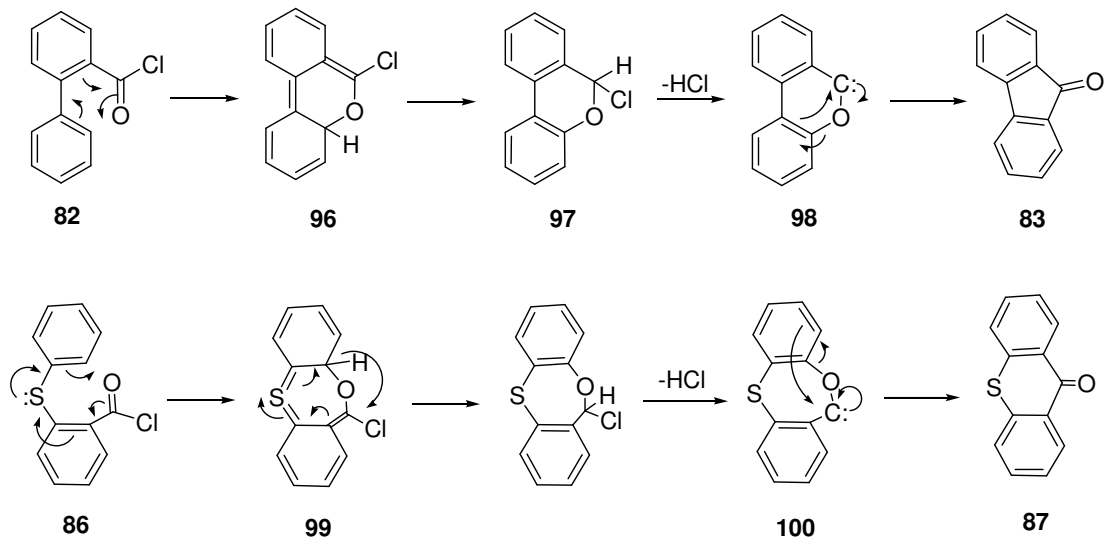

Scheme 2.3.10: Proposed mechanism to generate carbene intermediate *via* electrocyclisation.

In the thio-containing analogue, however, the proposed mechanism is less likely than for the biphenyl case. Prior to the formation of carbene intermediate **100**, electrocyclisation forces the molecule to adopt a seven-membered transition state **99** which is inevitably more ring-strained. The mechanism also involves valence shell expansion of sulfur requiring high energy and is thus unfavourable (Scheme 2.3.10). The requirement of valence shell expansion also discounts this mechanism as a possibility in the case of 2-phenoxybenzoyl chloride **89** which happens at a lower temperature than the sulfur analogue.

2.3.4.3: Concerted Radical Mechanism

Experimental observations have discounted all of the above proposed mechanisms. Therefore, the most likely mechanism remaining is a radical mechanism involving the breaking of the carbon-chlorine bond and the formation of the carbon-carbon bond in a concerted manner (Scheme 2.3.11). This avoids the formation of a ketyl radical which could undergo the expected decarbonylation under these conditions. However further investigation is required to confirm the exact nature of the acid chloride pyrolysis mechanism.

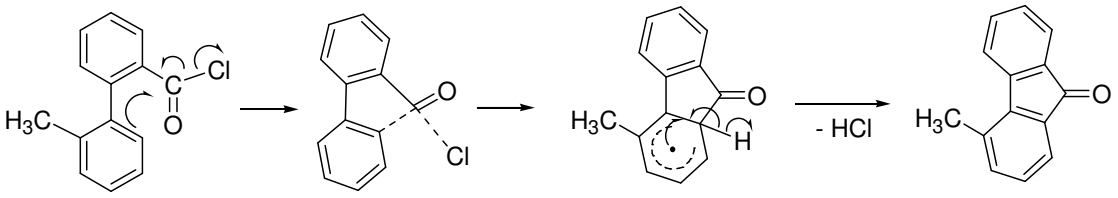

27 **75** 58%

Scheme 2.3.11: Proposed mechanism for acid chloride cyclisation.

2.4: Revised Route to 9-Phenanthrol

Following the failure of the initial FVP route to 9-phenanthrol **29** a revised synthesis was required. A new synthetic route was then proposed involving the pyrolysis of biphenyl-2-acetyl chloride **101** which would provide the extra carbon atom required for formation of the 6-membered aromatic ring and would overcome the problems in the attempted cyclisation onto a methyl group which lead to fluorenones. FVP of this acid chloride **101** would give 9-phenanthrol **29** *via* a ketene **102** (Scheme 2.4.1).

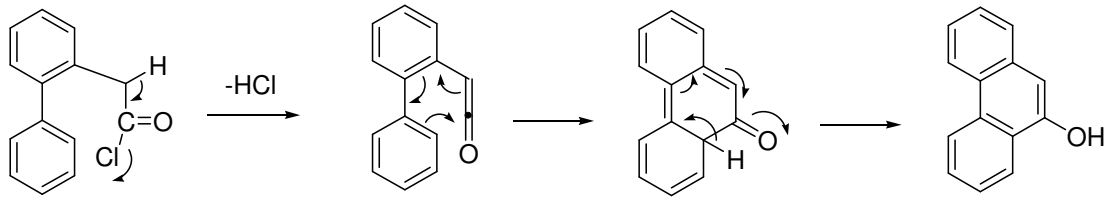

101 **102** **29**

Scheme 2.4.1: Proposed mechanism of cyclisation *via* the ketene **102**.

The first step in this synthesis was the Suzuki reaction of 2-bromophenylacetic acid **103** and phenylboronic acid **104** to give biphenylacetic acid **105** in high yield (Scheme 2.4.2).

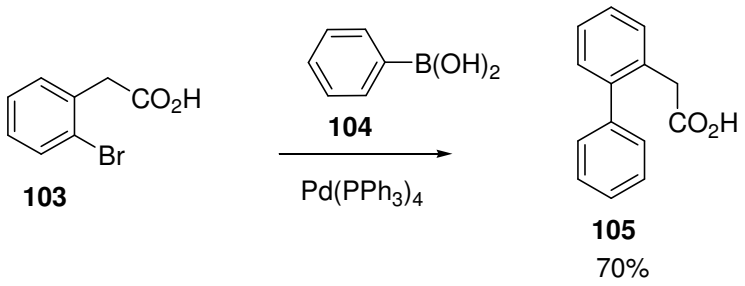

Scheme 2.4.2: Synthesis of biphenylacetic acid **105**.

Preparation of the corresponding acid chloride **106** using previous conditions of thionyl chloride in the presence of pyridine in dry ether failed. However, treatment of the carboxylic acid **105** with oxalyl chloride in dry chloroform containing one drop of DMF afforded the required acid chloride **106** in high yield (Scheme 2.4.3).[42] The product was positively identified by its NMR spectra including the presence of a new CH_2 signal in the ^1H NMR spectrum at $\delta_H = 4.05$ and a shift in the carbonyl absorption signal in the IR spectrum from the carboxylic acid region at 1711 cm^{-1} to the acid chloride region at 1798 cm^{-1}.

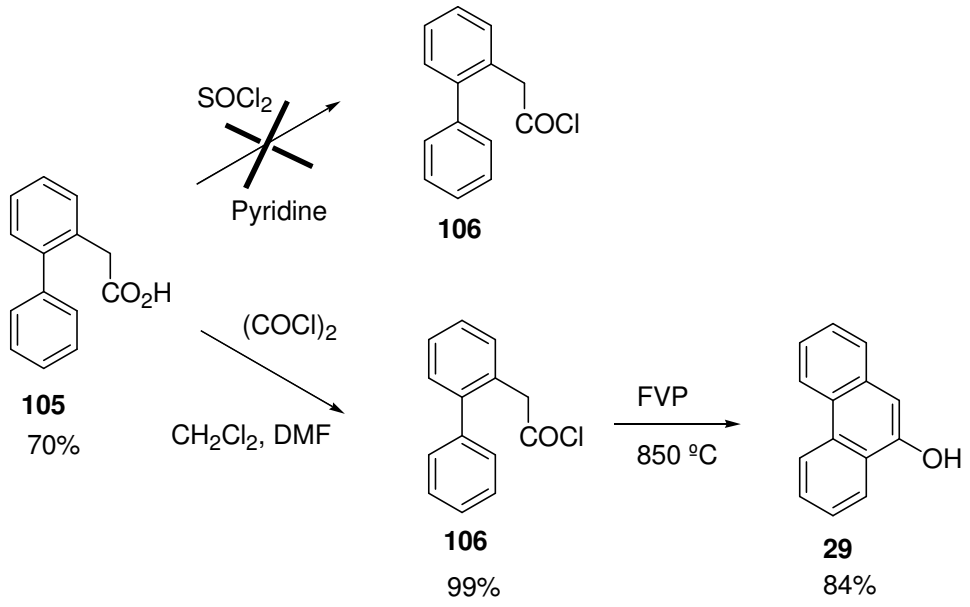

Scheme 2.4.3: Preparation of biphenyl-2-yl chloride **106**.

Exposure of the acid chloride **106** to FVP conditions at a furnace temperature of 850 °C afforded 9-phenanthrol **29** in 84% yield. A temperature profile of the transformation of biphenyl-2-ylacetyl chloride **106** to 9-phenanthrol **29** was then prepared. Comparison of the integral heights of the characteristic aromatic singlet in 9-phenanthrol at δ_H = 7.02 with the CH_2 signal corresponding to the acid chloride in the crude pyrolysates at furnace temperature ranges of 450 °C to 850 °C showed complete conversion at the relatively low furnace temperature of 650 °C (Figure 2.4.1).

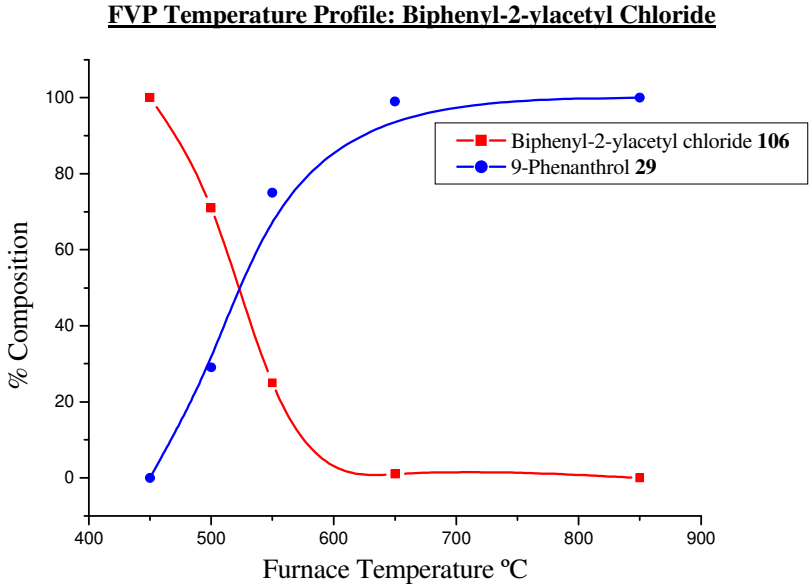

Figure 2.4.1: FVP temperature profile of biphenyl-2-yl acetyl chloride **106**.

2.5: Substituted Example

Also of interest was the expansion of this FVP route to substituted phenanthrol systems such as a *para* cyano example. Firstly (4-cyanobiphenyl-2-yl)acetic acid **109** was prepared by the Suzuki reaction of 2-iodophenylacetic acid **107** and 4-cyanophenylboronic acid **108** (Scheme 2.5.1). However, this only gave the Suzuki product 32% due to problems with self coupling of 2-iodophenylacetic acid **107** under these conditions to afford (2'-carboxymethylbiphenyl-2-yl)acetic acid **110.**

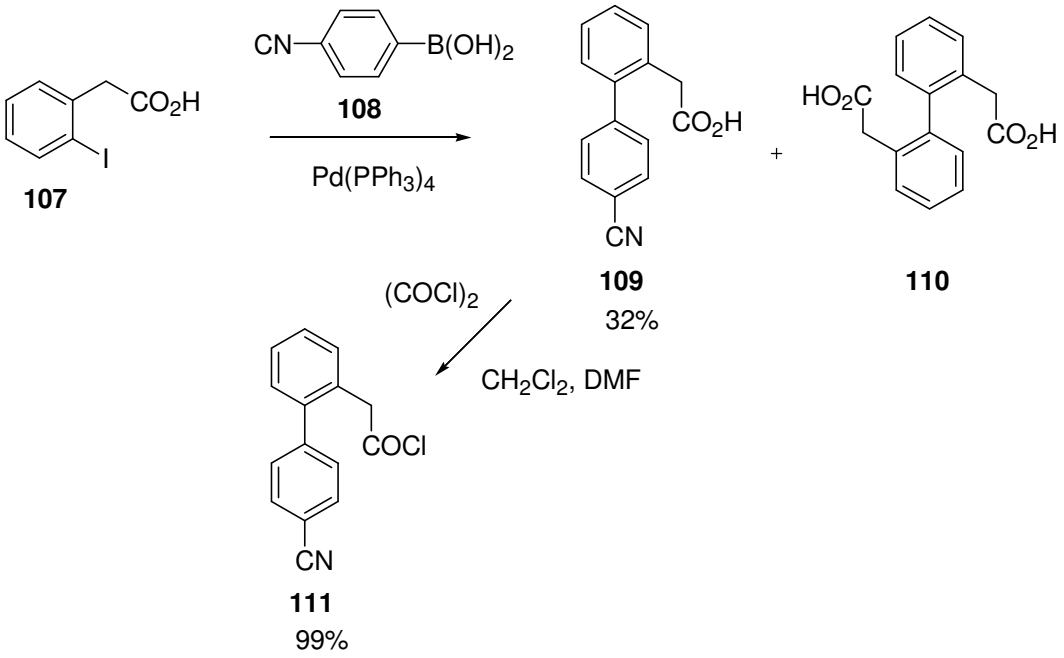

Scheme 2.5.1: Preparation of (4-cyanobiphenyl-2-yl)acetyl chloride **111**.

Treatment of the carboxylic acid **109** with oxalyl chloride in the presence of DMF afforded (4-cyanobiphenyl-2-yl)acetyl chloride **111** (ν_{max} 1796 cm^{-1}) in good yield (Scheme 2.5.1). The acid chloride **111** was then exposed to FVP conditions at a furnace temperature of 850 °C. However, under these conditions none of the required 10-hydroxyphenanthrene-2-carbonitrile **112** was recovered (Scheme 2.5.2). It appeared that the acid chloride must have decomposed/hydrolysed under storage conditions prior to FVP.

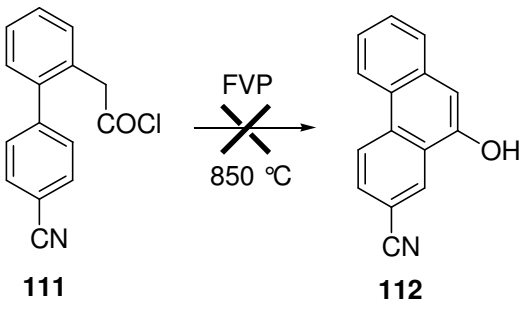

Scheme 2.5.2: FVP of (4-cyanobiphenyl-2-yl)acetyl chloride **111**.

2.6: Alternate Tungsten Trioxide FVP Routes to 9-Phenanthrol

In view of the problems encountered in the previous section with acid chloride stability an alternate route to 9-phenanthrol **29** was proposed. This is based on previous examples of the FVP of methyl esters similar to methyl biphenyl-2-ylacetate **113** over tungsten trioxide to afford cyclised systems.[43] This route would avoid problems due to decomposition or hydrolysis of the acid chloride.

Additionally, it may also be possible to avoid problems due to the self coupling of 2-iodophenylacetic acid **107** in the initial Suzuki reaction by the preparation of the ester **114**. The ester group has more electron withdrawing properties than the potentially electron donating carboxylic acid anion group present under the basic Suzuki reaction conditions. Suzuki coupling of methyl (2-iodophenyl)acetate **114** and phenyl boronic acid **104** or another appropriate boronic acid such as 4-cyanophenyl boronic acid **108** may then afford the coupled product in higher yield.

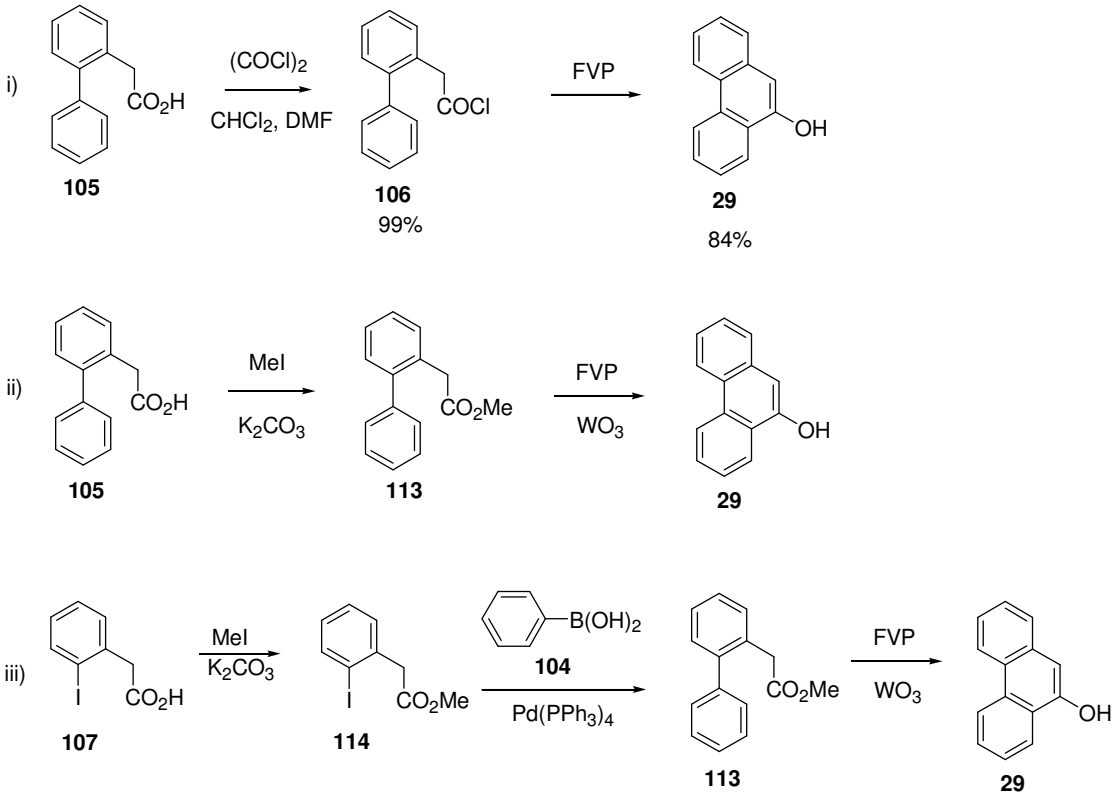

Scheme 2.6.1: Various FVP routes to 9-phenanthrol **29**.

In previous research the pyrolysis of cyclohexanol **115** over tungsten trioxide packed in a furnace tube resulted in the loss of water to give cyclohexene **116** (Scheme 2.6.2). Similarly the pyrolysis of methoxycyclohexane **117** resulted in loss of methanol to afford cyclohexene **116** (Scheme 2.6.2).[43]

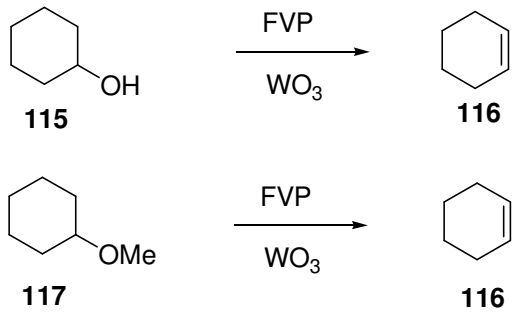

Scheme 2.6.2: FVP of initial precursors over tungsten trioxide.[43]

The extension of this pyrolysis to an ester system **118** gave the corresponding 2-cyanopyrrolizin-3-one **119** in good yield with loss of methanol (Scheme 2.6.3).

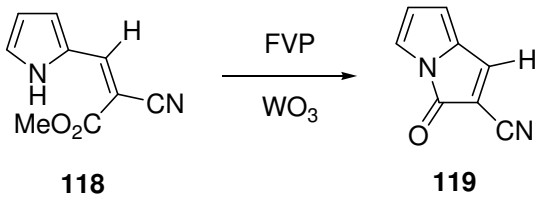

Scheme 2.6.3: FVP of an ester over tungsten trioxide.[43]

It may be possible to apply this method to give 9-phenanthrol **29** and related heterocyclic systems from the FVP of the corresponding esters. The synthesis of the esters could be achieved by the Suzuki reaction of methyl (2-iodophenyl)acetate **114** with the appropriate heterocyclic boronic acid (Scheme 2.6.4).

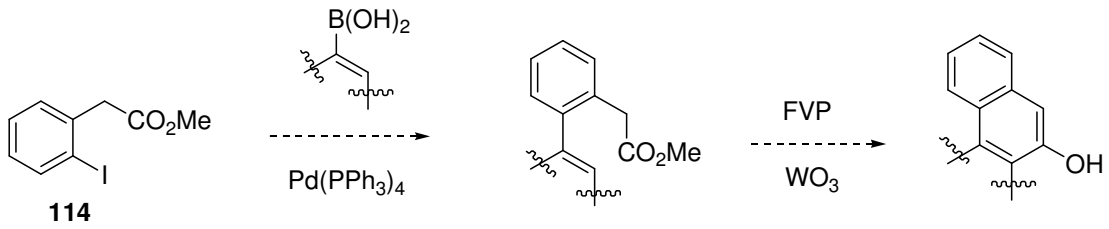

Scheme 2.6.4: Possible tungsten trioxide route to cyclised systems.

2.6.1: Pyrolysis of Methyl biphenyl-2-ylacetate

FVP of methyl biphenyl-2-ylacetate **113** over tungsten trioxide was carried out to establish if the required cyclisation to 9-phenanthrol **29** occurred. Methyl biphenyl-2-ylacetate **113** was prepared by methylation of biphenylacetic acid **105** with iodomethane in quantitative yield (Scheme 2.6.5).

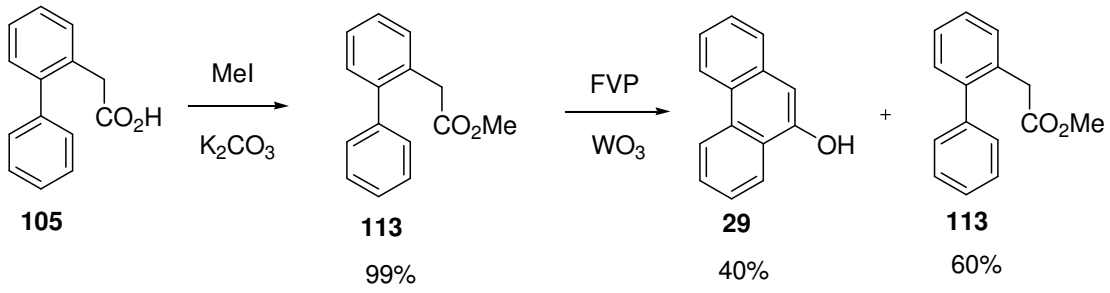

Scheme 2.6.5: FVP of methyl biphenyl-2-ylacetate **113**.

The ester was then exposed to FVP conditions over tungsten trioxide packed in a furnace tube at 600 ºC to afford the crude product 9-phenanthrol **29** in 40% yield with a 60% recovery of the ester starting material **113** (Scheme 2.6.5).

An attempt to increase the conversion of the ester **113** to 9-phenanthrol **29** by repeating the pyrolysis with an increased furnace temperature of 800 ºC only lead to decomposition of the ester with no product recovered. The pyrolysis was also repeated at a furnace temperature of 600 ºC with an additional packing of tungsten trioxide, however, these conditions gave a similar conversion.

In conclusion it was established it was possible to pyrolyse biphenyl esters over tungsten trioxide to afford phenanthrol type systems in a moderate yield. However, attempts to increase the conversion of the product by increased furnace temperature or increased catalyst lead to decomposition or similar product yields respectively. Nevertheless, this appeared to be a viable route to achieve 9-phenanthrol **29** and possibly related heterocyclic phenanthrol systems.

2.7: Heterocyclic Examples

The increased availability of a variety of heterocyclic boronic acids leads to the possible employment of this synthesis to prepare unknown heterocyclic phenanthrol analogues which may be of particular interest as potential coupling components in the preparation of heterocyclic azo compounds.

2.7.1: 2-Thiophene Systems

The synthesis of a 2-thiophene system was examined using the initial acid chloride route to phenanthrol systems. 2-(Thiophen-2-yl)phenylacetic acid **121** was prepared by a standard Suzuki reaction of 2-iodophenylacetic acid **107** and 2-thiopheneboronic acid **120** in high yield (Scheme 2.7.1).

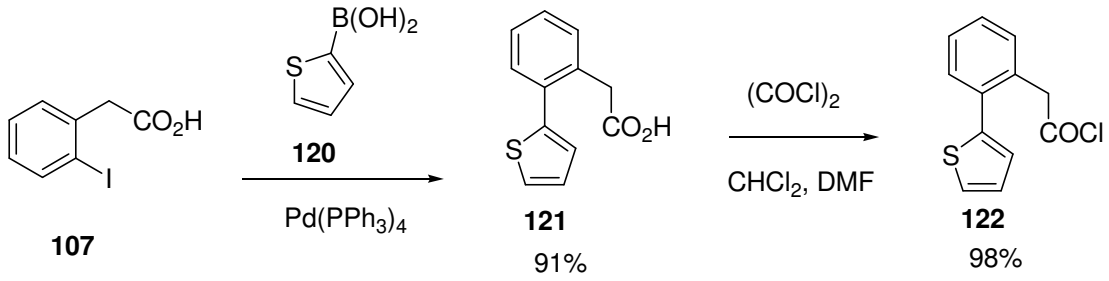

107 **121** 91% **122** 98%

Scheme 2.7.1: Preparation of 2-(thiophen-2-yl)phenylacetyl chloride **122**.

The corresponding acid chloride **122** was prepared by treatment of the acid **121** with oxalyl chloride in the presence of DMF to give 2-(thiophen-2-yl)phenylacetyl chloride **122** (ν_{max} 1796 cm^{-1}) (Scheme 2.7.1).

FVP of the acid chloride **122** at an furnace temperature of 850 ºC afforded naphtho[1,2-*b*]thiophen-4-ol **123** in 61% yield which was identified by characteristic ^{1}H and ^{13}C NMR spectra with the lack of a CH_2 signal in addition to the loss of a carbonyl absorption in the IR spectra and the presence of a hydroxyl absorption peak at 3304 cm^{-1} (Scheme 2.7.2). Therefore, it was possible to prepare previously unknown heterocylic phenanthrol systems *via* this new synthetic route.

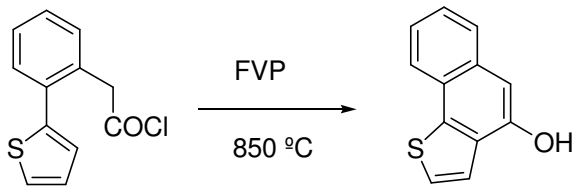

Scheme 2.7.2: FVP of 2-(thiophen-2-yl)phenylacetyl chloride **122**.

2.7.2: 3-Thiophene Systems

This synthesis was applied to the 3-thiopheneboronic acid **124** in order to prepare the alternative naphtho[2,1-*b*]thiophen-4-ol **126** isomer (Scheme 2.7.3). It would then be possible to establish any effect of the difference in the position of the heteroatom upon dye properties.

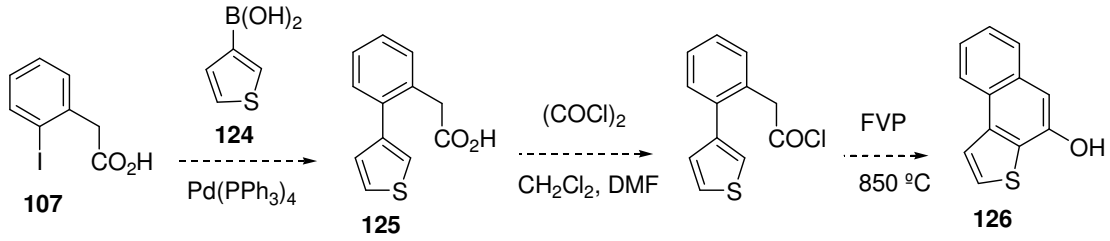

Scheme 2.7.3: Proposed synthesis of 3 naphtho[2,1-*b*]thiophen-4-ol **126**.

Unfortunately the Suzuki reaction of 2-iodophenylacetic acid **107** and 3-thiopheneboronic acid **124** failed. The iodo starting material **107** and a by-product **110** due to self coupling of the iodo starting material were recovered from the reaction (Scheme 2.7.4). No product **125** or 3-thiopheneboronic acid **124** was isolated from the reaction mixture.

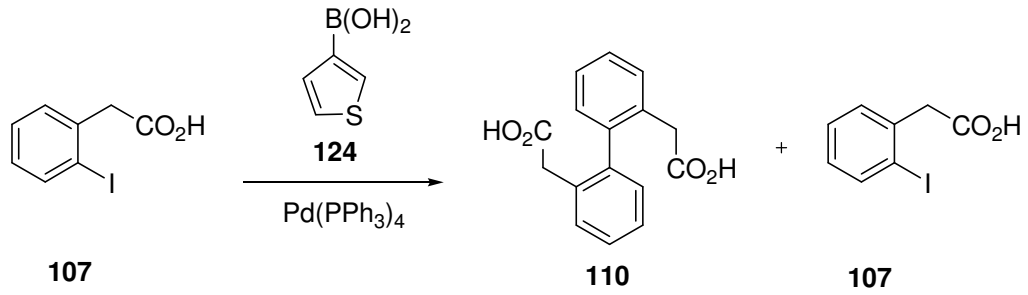

Scheme 2.7.4: Attempted synthesis of 2-(thiophen-3-yl)phenylacetic acid **125**.

An alternative route to naphtho[2,1-*b*]thiophen-4-ol **126** was possible. Firstly methyl(2-iodophenyl)acetate **114** was prepared in high yield by treatment of 2-iodophenylacetic acid **107** with iodomethane (Scheme 2.7.5). The Suzuki reaction of methyl 2-(iodophenyl)acetate **114** with 3-thiophene boronic acid afforded methyl 2-(thiophen-3-yl)phenylacetate **127** in high yield (Scheme 2.7.5). The product was identified by its characteristic NMR spectra and carbonyl absorption in the ester region (ν_{max} 1735 cm^{-1}).

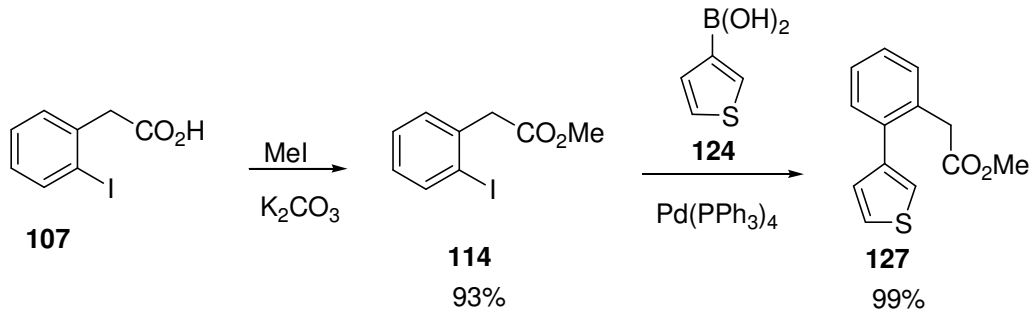

107 **114** 93% **127** 99%

Scheme 2.7.5: Preparation of methyl 2-(thiophen-3-yl)phenylacetate **127**.

Methyl 2-(thiophen-3-yl)phenylacetate **127** was then pyrolysed over tungsten trioxide at 600 ºC to afford a crude pyrolysate consisting of a mixture of the required cyclised product **126** and the ester starting material **127** in an approximately 2:3 ratio by comparison the integral height of characteristic peaks in the ^{1}H NMR spectra. Purification and isolation by column chromatography afforded naphtho[2,1-*b*]thiophen-4-ol **126** in 8% yield and recovered **127** in 24% yield (Scheme 2.7.6).

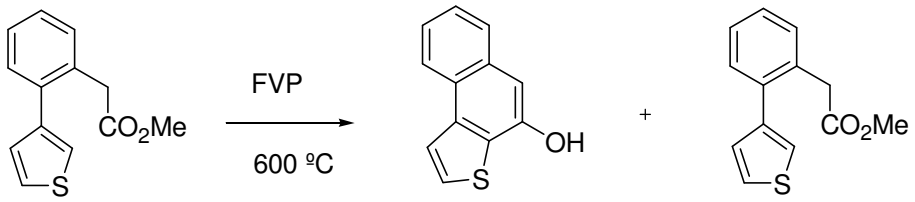

127 **126** 8% **127** 24%

Scheme 2.7.6: FVP of methyl 2-(thiophen-3-yl)phenylacetate **127**.

The cyclised product **126** was identified by the loss of the CH_2 and CH_3 signals in the ^1H and ^{13}C NMR spectra in addition to the presence of a characteristic singlet at δ_H = 7.02 corresponding to the aromatic proton adjacent to the hydroxyl group and the presence of a broad singlet of the hydroxyl group at δ_H = 5.76. This is comparable to the singlet observed in 9-phenanthrol **29** and naphtho[1,2-*b*]thiophen-4-ol **123** at δ_H = 7.02 and 6.80 respectively, corresponding to the aromatic proton adjacent to the hydroxyl group (Figure 2.7.1). There was also a loss of the carbonyl absorption in the ester region of the IR spectra and the presence of a broad absorption corresponding to the hydroxyl group at 3505 cm^{-1}.

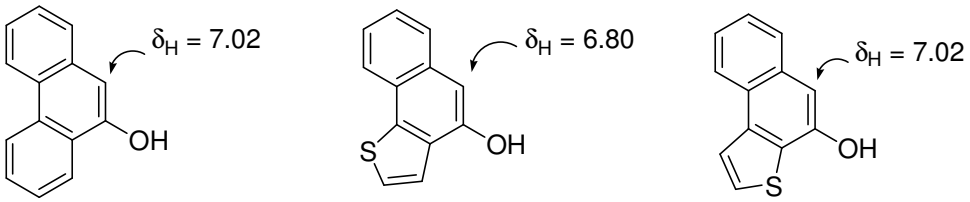

29 **123** **126**

Figure 2.7.1: Chemical shift of characteristic signals of **29**, **123** and **126**.

2.7.3: Furan Systems

The synthetic routes described were extended to the 2- and 3-furan systems. Due to problems with self coupling in the reaction of 2-iodophenylacetic acid **107** and 3-thiopheneboronic acid **124** the ester route to furan systems was chosen.

However in the case of reaction of methyl (2-iodophenyl)acetate **114** with 2- and 3-furanboronic acids **128** and **129**, the required Suzuki coupled esters **130** and **131** were not obtained. No methyl ester signal was present in either NMR spectrum. Mass spectrometry analysis indicated the products were the carboxylic acids **132** and **133** unexpectedly, which was confirmed by accurate mass evidence. Hence, it appeared the required esters were hydrolysed under the basic Suzuki reaction conditions to afford the acids (Scheme 2.7.7).

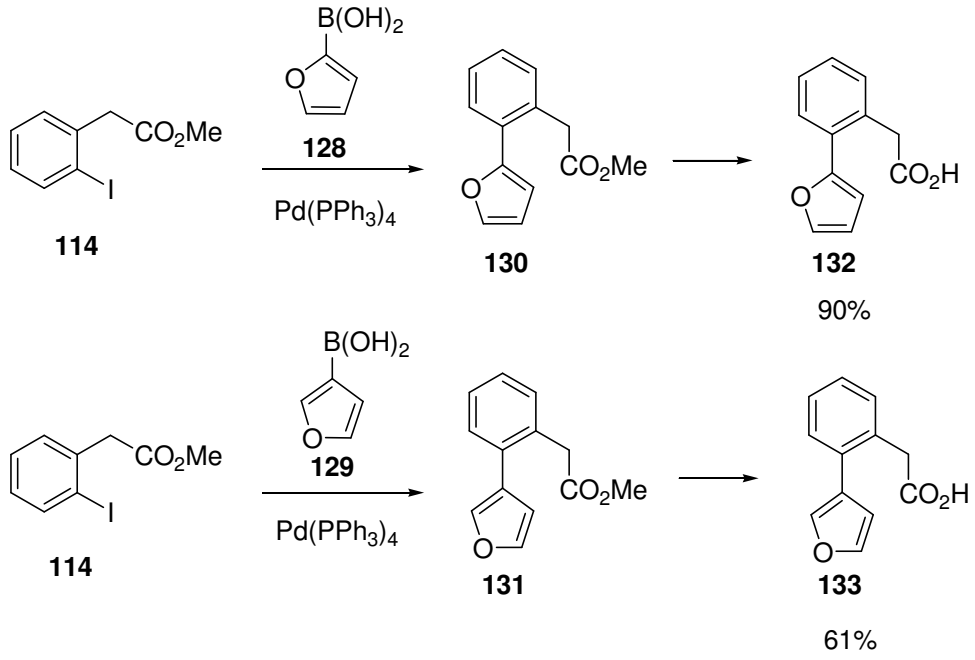

Scheme 2.7.7: Synthesis of 2- and 3-furancarboxylic acids **132** and **133**.

The required esters **130** and **131** for FVP were prepared by methylation of the 2- and 3-furancarboxylic acids **132** and **133** under standard conditions with iodomethane in good yield (Scheme 2.7.8).

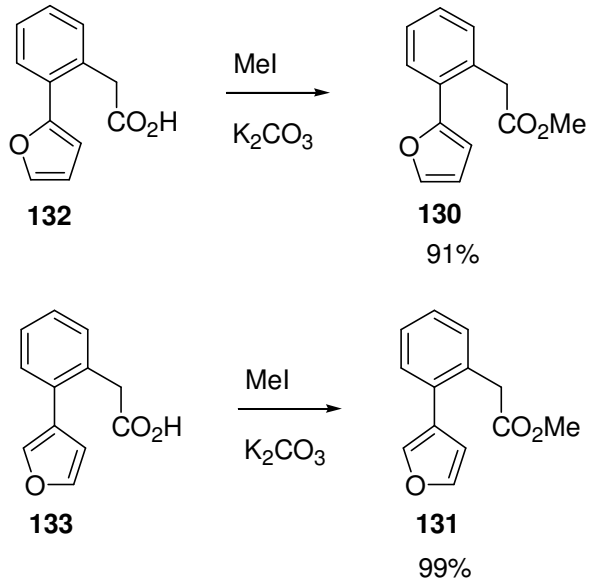

Scheme 2.7.8: Methylation of 2- and 3-furancarboxylic acids **132** and **133**.

The 2- and 3-furan esters **130** and **131** were pyrolysed over tungsten trioxide at 600 ºC to afford crude pyrolysates which were purified by chromatography. Naphtho[1,2-*b*]furan-4-ol **134** was obtained in 20% yield and identified by its characteristic ^{1}H and ^{13}C NMR spectra with the loss of the aliphatic CH_2 and CH_3 signals corresponding to the ester starting material (Scheme 2.7.9).

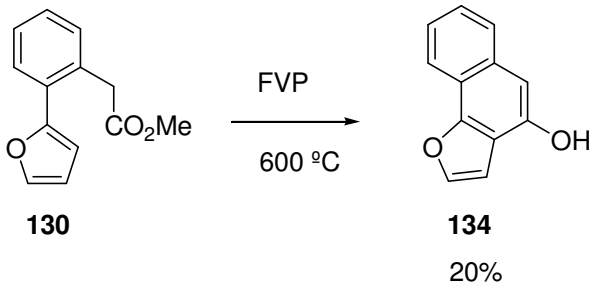

Scheme 2.7.9: FVP of methyl 2-(furan-2-yl)phenylacetate **130**.

However, in the case of the 3-furan ester **131** none of the required product **135** could be isolated or detected in the pyrolysate either by NMR or mass spectrometry analysis (Scheme 2.7.10). This may be due to the small scale of the pyrolysis and loss of material. Further scale up and study towards these heterocyclic cyclised systems is required.

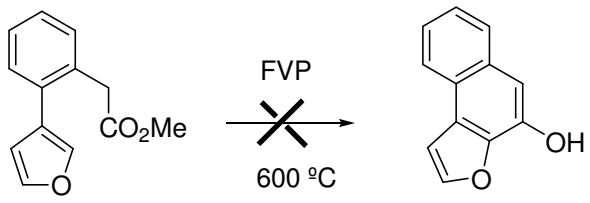

131 **135**

Scheme 2.7.10: FVP of methyl 2-(furan-3-yl)phenylacetate **131**.

2.7.4: Acid Chloride Route to Furan Systems

An attempt was made to prepare the furan cyclised systems **134** and **135** from the corresponding acid chlorides **136** and **137**. Treatment of the carboxylic acids **132** and **133** with oxalyl chloride under anhydrous conditions afforded crude products which could not be positively identified. Due to the instability of previous acid chlorides no purification techniques were carried out and the crude products pyrolysed at 850 ºC without isolation (Scheme 2.7.11). The pyrolysates were then analysed by ^{1}H NMR, however, none of the required system **134** and **135** could be detected in either case.

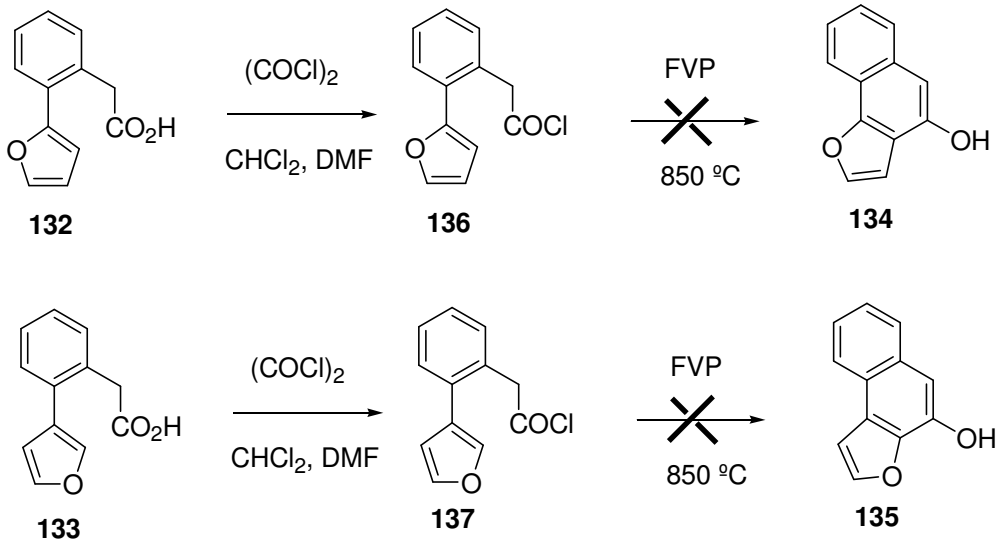

Scheme 2.7.11: Acid Chloride route to cyclised systems.

2.7.5: Conclusions

It is possible to prepare 9-phenanthrol **29** and heterocyclic phenanthrol systems by FVP of the acetic esters over tungsten trioxide to give the required product. However optimisation is required as the 3-thiophene **126** and 2-furan **134** examples were obtained in low yields with relatively poor conversion.

2.8: Preparation of Phenanthrol Azo Dyes

9-Phenanthrol **126** and the 2- and 3-thiophene phenanthrol systems **123** and **126** were coupled with appropriate diazonium salts to give azo compounds of interest. To achieve the required water solubility a diazonium salt with sulfonic acid groups present was used. This avoided problems associated with the harsh conditions required for sulfonation of the phenanthrol ring and avoided an extra step in the synthesis. A diazonium salt based on an amine supplied by Fujifilm, C. I. Acid Yellow 9 **136**, which had been involved in previous dye synthesis was used (Figure 2.8.1).

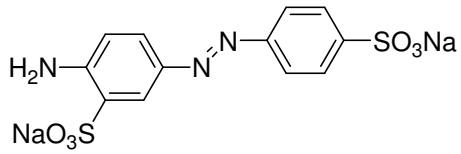

136

Figure 2.8.1: 2-Amino-5-(4-sulfophenylazo)-benzenesulfonic acid disodium salt **136** (C. I. Acid Yellow 9).

Throughout the remainder of this chapter water soluble dyes were obtained which were isolated from solution by the addition of sodium chloride (≈ 10% w/w). This resulted in the dye precipitating which was recovered by filtration. The resulting azo dye contained significant salt impurities, the majority of which could be removed by dialysis. An estimate of the percentage organic strength of the product quoted based on the percentage of carbon and nitrogen in the sample over the expected percentage of each element could then be made from CHN analysis. This was then taken into account to calculate the overall percentage yields of the reaction products. Water soluble azo products were particularly suited to detection by electrospray ionisation mass spectrometry due to the presence of sulfonic acid groups.

2.8.1: Azo Coupling to Phenanthrol Systems

The diazonium salt was prepared by treatment of Acid Yellow 9 **136** with sodium nitrite under acidic conditions and used immediately to prepare the azo compound of 9-phenanthrol **137** recovered as the sodium salt in 77% recovery by weight (Scheme 2.8.1). CHN analysis of the isolated product **137** revealed the strength to be 20% due to salt impurities therefore the overall yield of product recovered was 15% (see experimental section). This poor yield was mainly due to the poor recovery as a result of small scale filtration problems. The product was positively identified by ^{1}H and ^{13}C NMR spectra in addition to ESI mass spectrometry evidence showing $[MNa]^-$ at m/z = 583 where M was the mass of the organic component of the azo compound with the sulfonic acid groups in the absence of the sodium cation (SO_3^-). Hence azo compound **137** would be shown as MNa_2.

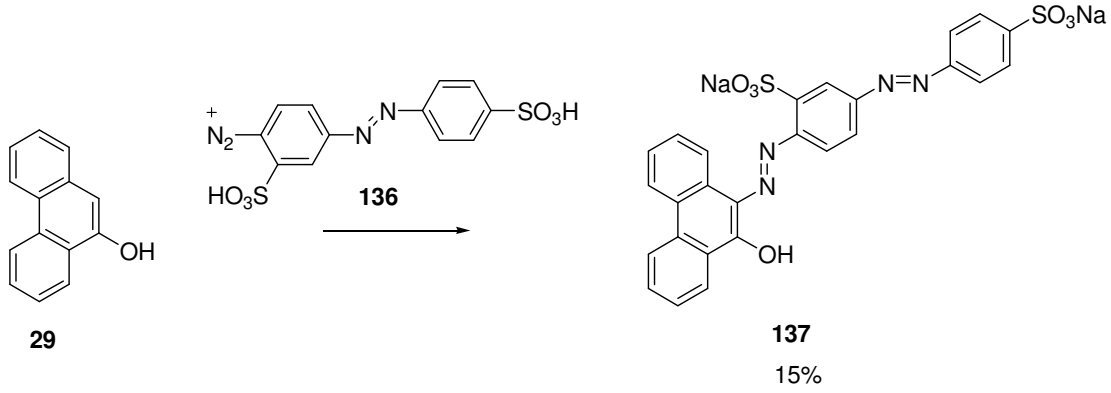

Scheme 2.8.1: Preparation of phenanthrol azo compound.

.

This synthesis was then extended to the 2- and 3-thiophene phenanthrol analogues **123** and **126** to afford the azo compounds **138** and **139** as the sodium salts. CHN analysis revealed the strength of the azos **138** and **139** to be 73% and 58% due to salt impurities with recovery of the products in 29% and 28% yields respectively after accounting for strength (see experimental section) (Scheme 2.8.2).

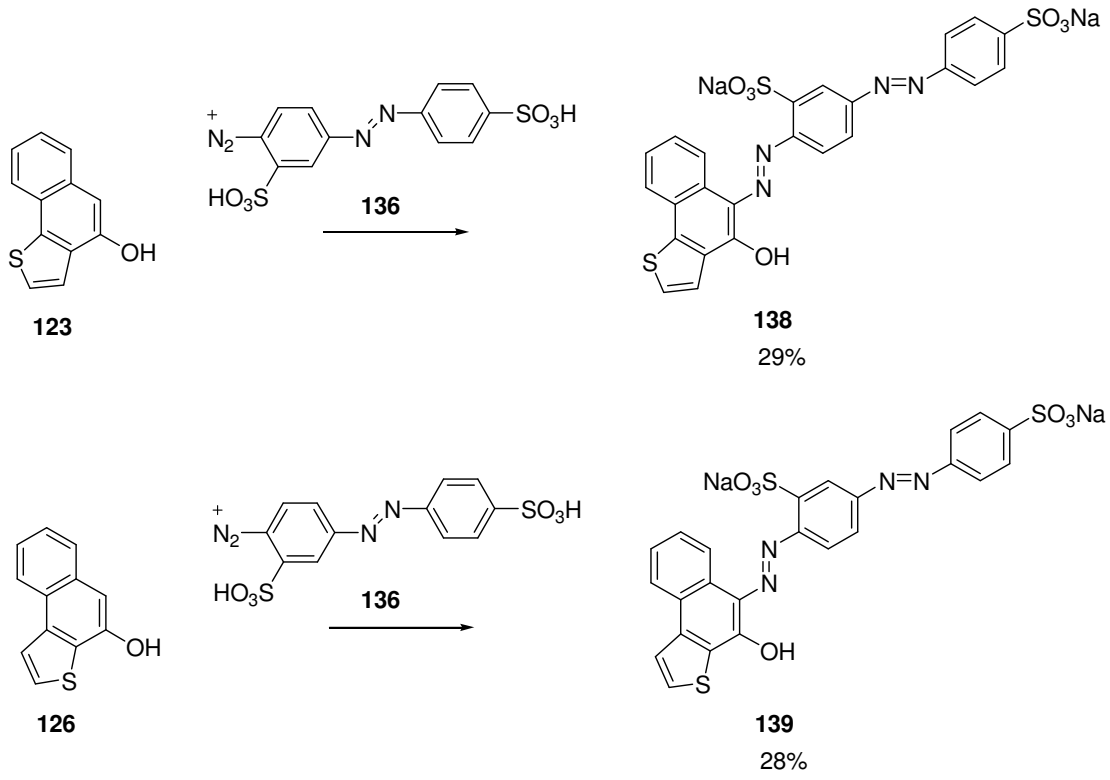

Scheme 2.8.2: Synthesis of 2- and 3-thiophene phenanthrol azos **138** and **139**.

2.8.2: Effect of Heteroatom upon Dye Properties

By analysis of the UV-vis spectra of the phenanthrol **137** and thiophene azo compounds **138** and **139** the effect of the heteroatom upon dye properties could be investigated (Figures 2.8.2, 2.8.3, 2.8.4, Table 2.8).

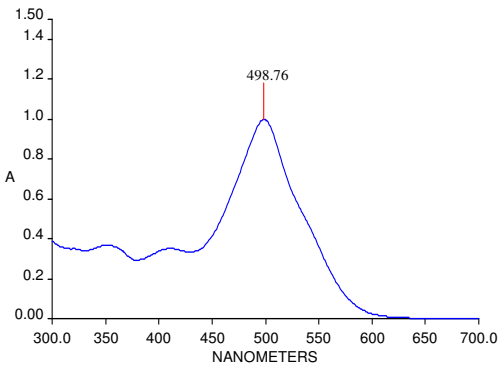

Figure 2.8.2: UV-vis spectra of dye phenanthrol **137**.

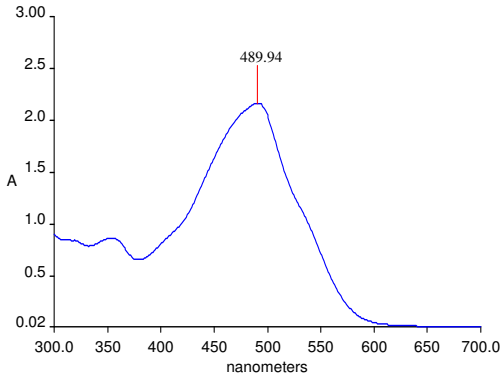

Figure 2.8.3: UV-vis spectra of dye **138**.

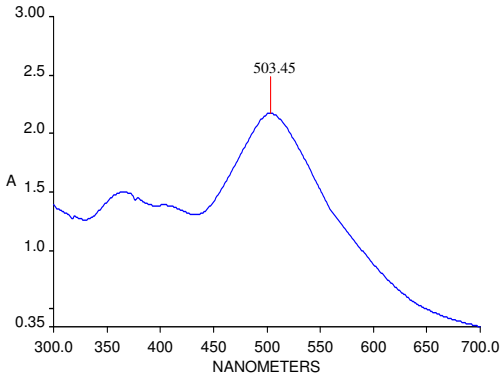

Figure 2.8.4: UV-vis spectra of dye **139**.

Table 2.8: Phenanthrol type dye properties.

Dye Structure	λ_{max}	$W_{1/2}$	ε / dm^{-3} mol^{-1} cm^{-1}
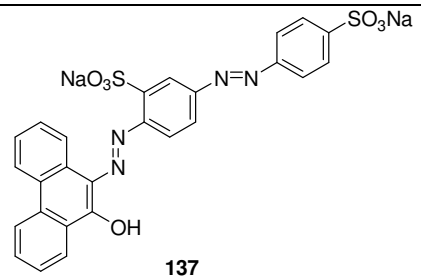 **137**	499 nm	78 nm	53000
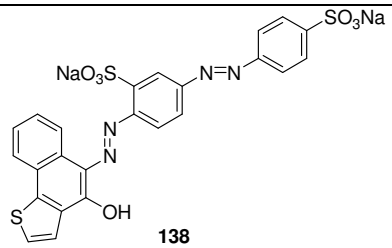 **138**	490 nm	108 nm	31000
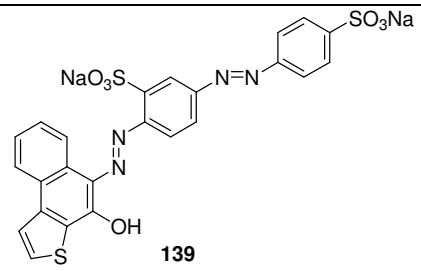 **139**	503 nm	> 200 nm	21800

The UV-vis spectra of the phenanthrol dye **137** showed a narrow absorption range with a λ_{max} of 499 nm and half width ($W_{1/2}$) of 78 nm resulting in a bright red dye. The extinction coefficient (ε) was 53000 dm^{-3} mol^{-1} cm^{-1} indicating an intense red dye.

In the case of the 2-thiophene phenanthrol dye **138** the presence of a sulfur heteroatom in the ring resulted in only a slight change in the λ_{max} of the dye, however, the dye was duller with an increased $W_{1/2}$ of 108 nm and less intense with an extinction coefficient $\varepsilon = 31000$ dm^{-3} mol^{-1} cm^{-1}.

The 3-thiophene azo dye **139** showed a slight shift in the absorption to a higher λ_{max} of 503 nm and as with dye **138** was much duller and less intense than the phenanthrol dye **137** due to a wide half width ($W_{1/2} > 200$ nm) with a low extinction coefficient of $\varepsilon = 21800$ dm^{-3} mol^{-1} cm^{-1}.

Therefore initial UV-vis spectral results indicated that the presence of a 5-membered thiophene ring rather than a phenyl ring resulted in little significant change in the spectral properties of the dyes. Scale up of this synthesis would be required for further testing of the properties of these dyes to establish the effect of the heteroatom upon light, ozone and water fastness.

2.9: Introduction to Hydrazine Routes to Azo Compounds

2.9.1: Literature Examples

Although the coupling of diazonium salts is one of the main routes to azo compounds another is the condensation of a hydrazine with a carbonyl group. The first example of this was reported by Fierz-David and co-workers in 1946 and from the observation that the same azo product **142** could be obtained from the coupling of the diazonium salt of 4-aminobenzenesulfonate **140** with 1-naphthol **141** as with the reaction of 4-hydrazinobenzene sulfonic acid **143** with 1,4-naphthoquinone **144** (Scheme 2.9.1).[44]

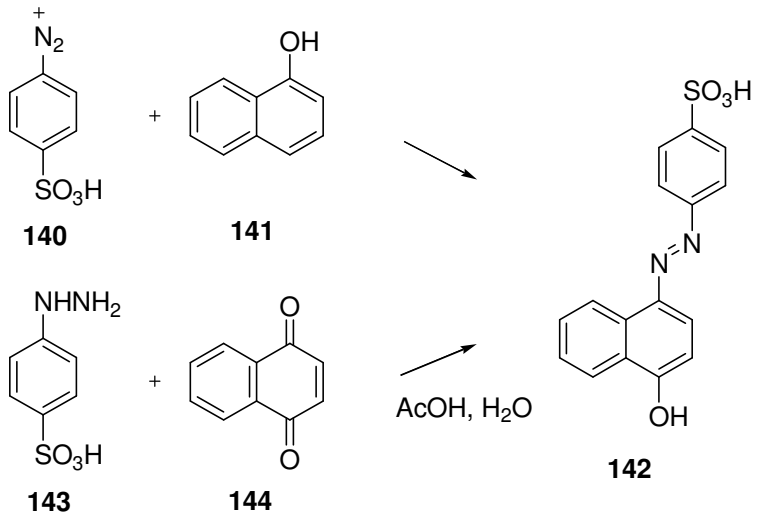

140 **141** **142** **143** **144**

Scheme 2.9.1: Initial hydrazine route to azo compounds.[44]

Related examples of the condensation of hydrazines and carbonyl groups have also been reported in similar systems (Scheme 2.9.2).[45]

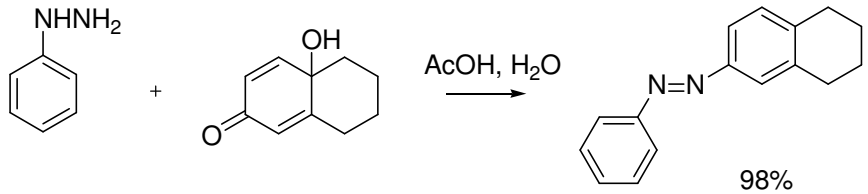

Scheme 2.9.2: Condensation to give azo compound.[45]

The reaction of hydrazines with quinone systems to prepare azo compounds with an *ortho* hydroxyl substitutent has also been reported. 4-*N*-Butylamino-5-ethyl-1,2-benzoquinone **145** was treated with phenylhydrazine **146a** and 4-nitrophenylhydrazine **146b** to give the corresponding azo compounds **147** although in low yields (Scheme 2.9.3).[46]

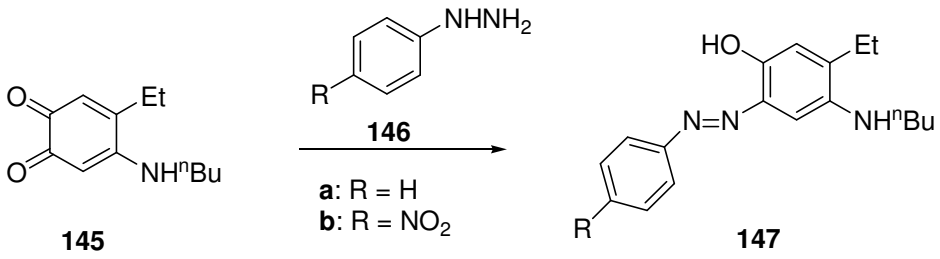

Scheme 2.9.3: Reaction of hydrazines with quinone systems (a: R = H (21% yield), b: R = NO_2 (30% yield)).[46]

2.9.2 Heterocyclic Systems

The applicability of this reaction to more complex heterocyclic systems has also been examined and is a common route to heterocyclic azo compounds. An early example involved the preparation of a variety of azo isoxazolones **149** *via* the condensation of phenylhydrazine with a carbonyl group on the azo **148** (Scheme 2.9.4).[47]

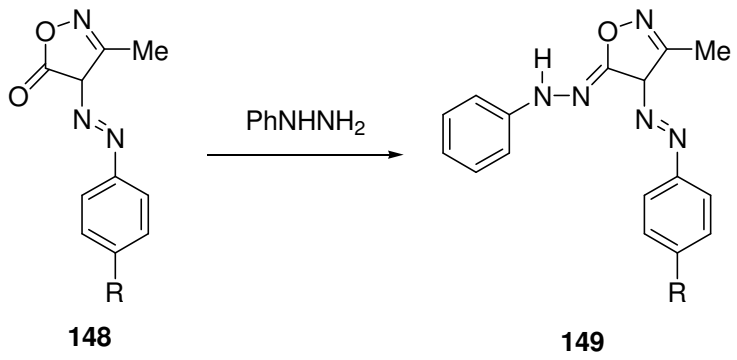

Scheme 2.9.4: Preparation of azo isoxazolones **149** (R = H (80% yield), Me (75% yield), Cl (80% yield)).[47]

There have also been a number of examples of the preparation of heterocyclic azo systems by the condensation of a carbonyl and hydrazine group in an acidic environment. Many of these examples are reported in industrial patents as a general route to hydrazo dyestuffs. Imperial Chemical Industries Ltd filed one of the initial patents of this type in 1979.[48] A variety of hydrazines **151** were condensed with 2,3,6-trioxotetrahydropyridine systems **150** to give the corresponding heterocylic azo systems **152** (Scheme 2.9.5).

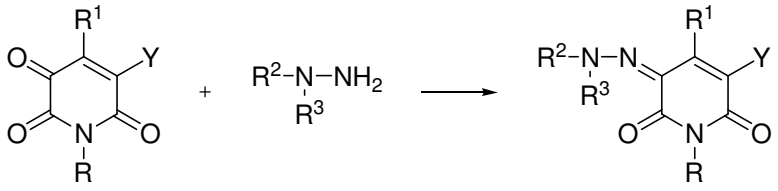

150 **151** **152**

R = hydrogen, alkyl, aralkyl, phenyl or substituted phenyl

R^1 = methyl, phenyl or substituted phenyl

R^2 = substituted aryl group

R^3 = hydrogen, alkyl or aryl

Y = carbamoyl or acetylamino

Scheme 2.9.5: Condensation of variety of acyl hydrazines with pyridine systems.[48]

This was reported to be a particularly attractive route to azo dyestuffs derived from pyridines as the use of a two stage diazotisation and coupling was avoided and previously unobtainable heterocyclic azo compounds could be prepared.

Patents have also been filed by several other companies involving the preparation of heterocyclic azo compounds for use as metallised dyes in ink jet printing. Kodak reported the synthesis of a dimorpholinophenol azo dye from the condensation of 4,5-dimorpholino-*o*-benzoquinone **153** and a substituted pyridine hydrazine **154** to give the corresponding azo **155** in 42% yield. This azo dye was then metallised with ferrous chloride tetrahydrate to afford the dye as a 2:1 complex **156** which contained two ligands around one Fe metal centre (Scheme 2.9.6).[49]

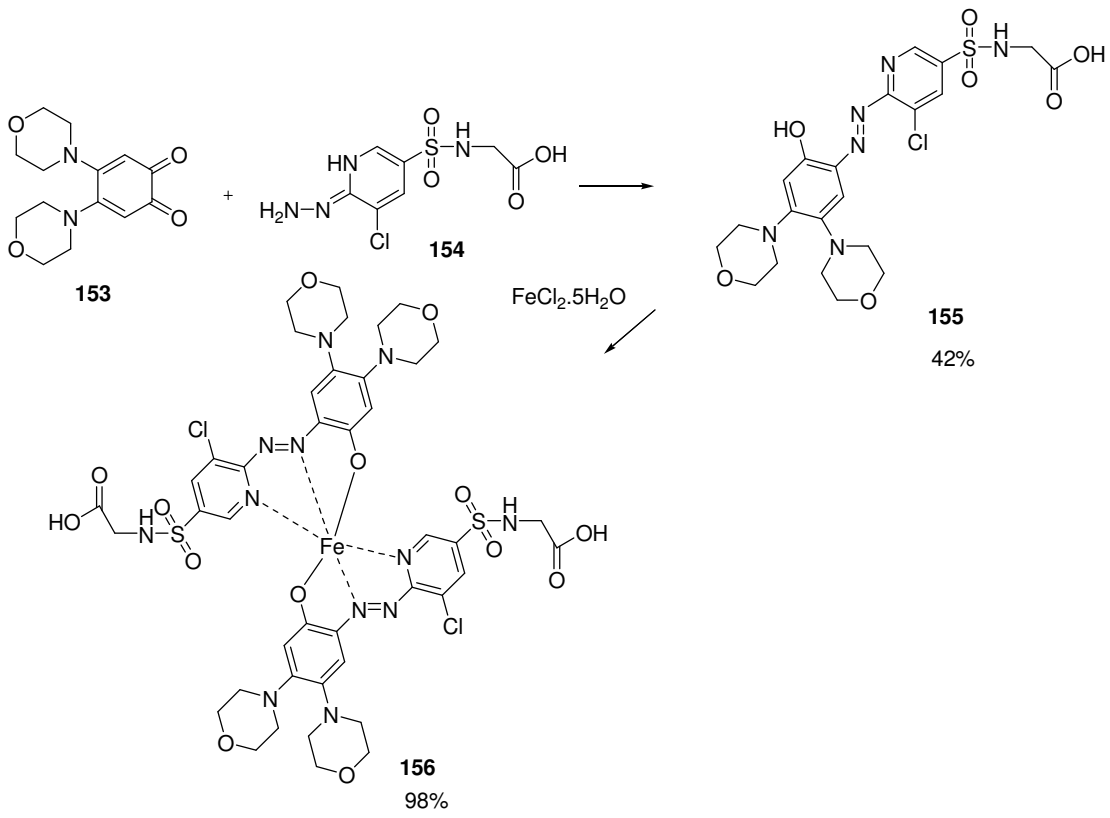

Scheme 2.9.6: Synthesis of heterocyclic metallised dye **156**.[49]

Several other examples of the condensation of a heterocyclic hydrazine system with quinones to give azo compounds have been reported. Ivashchenko and co-workers showed the condensation of substituted hydrazinopyrimidines **157** with phenanthrenequinone **158**, indole-2,3-dione **159** and α-naphthoquinone **160** gave the corresponding azo derivatives in 67%, 72% and 65% yields respectively (Scheme 2.9.7).[50]

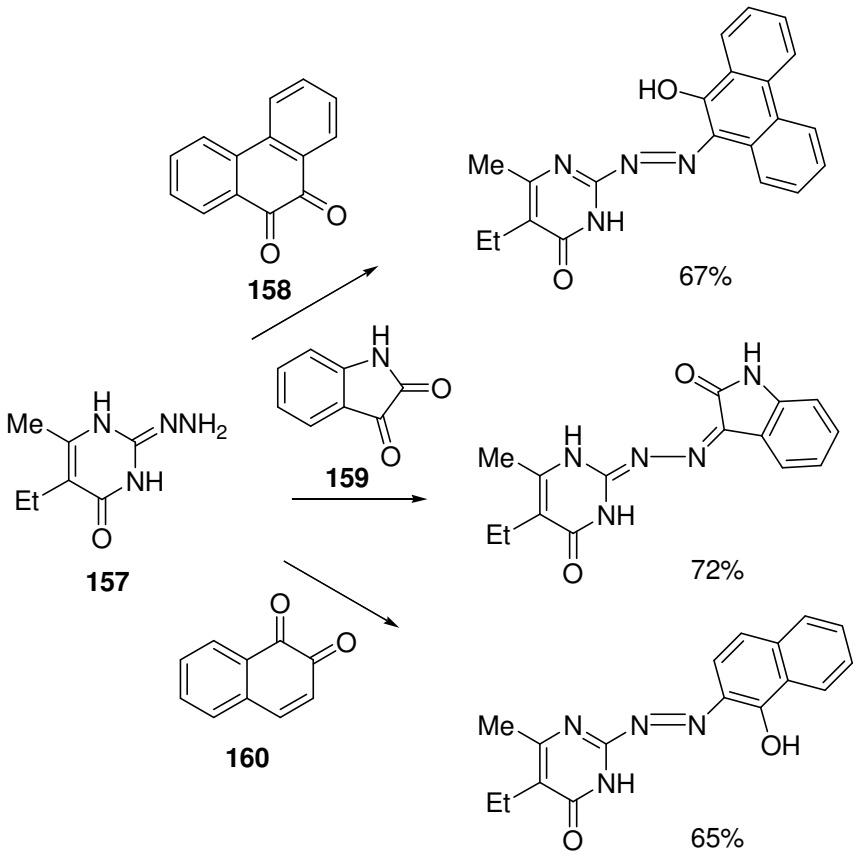

Scheme 2.9.7: Synthesis of a variety of pyrimidine azo products.[50]

The applicability of this reaction to substituted pyrimidines was then studied. A substituted arylpyrimidine **161** was prepared and condensed with 2-hydroxybenzaldehyde **162** and indole-2,3-dione **163** to give the corresponding azo compounds in 32% and 75% yields respectively (Scheme 2.9.8).[50] The tautomeric form of these azo products could not be confirmed.

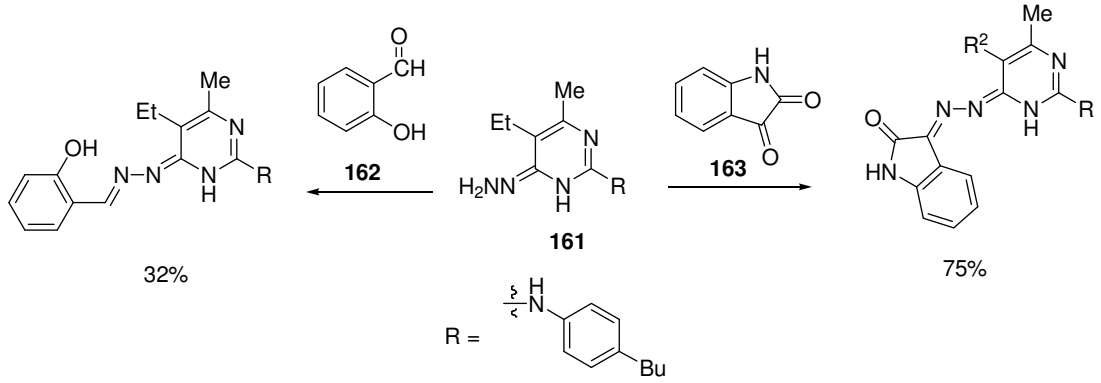

Scheme 2.9.8: Synthesis of substituted pyrimidines.[50]

The reaction of a pyrazole substituted hydrazinopyrimidine **164** with phenanthenequinone **165**, indole-2,3-dione **166** and 2-hydroxybenzaldehyde **167** similarly gave the corresponding azo compounds (Scheme 2.9.9).

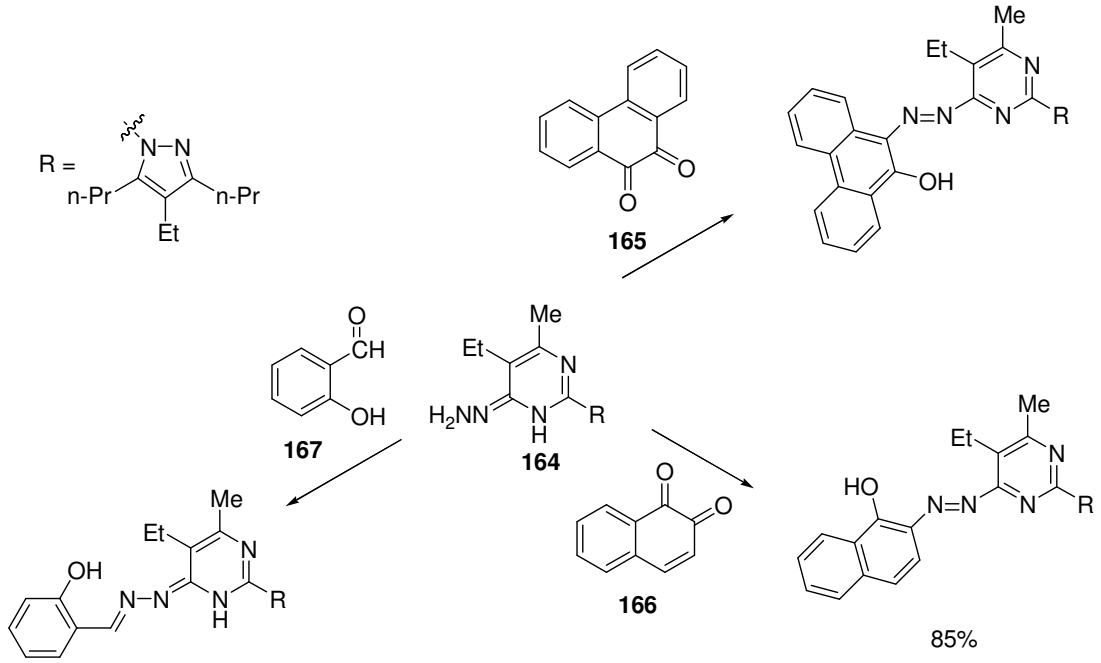

Scheme 2.9.9: Synthesis of substituted pyrimidine azo compounds.[50]

A further example of the reaction of heterocyclic hydrazines with a quinone was reported recently in the condensation of two equivalents of quinone **169** with a 2,6-dihydrazinopyridine **168** to give a bisazo dye **170**. The proposed use for this dye was as a sensitive chromogenic reagent for the detection of copper, cobalt, zinc and cadmium (Scheme 2.9.10).[51]

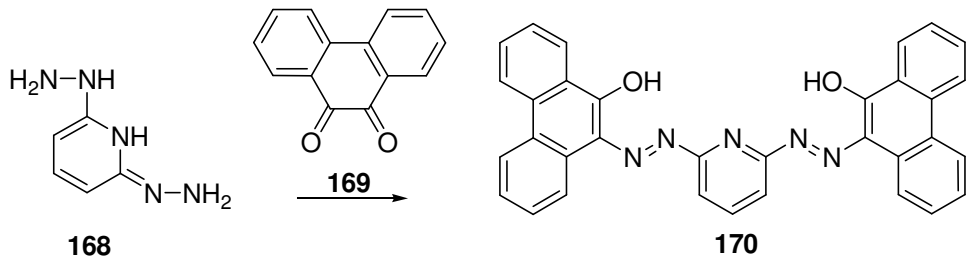

Scheme 2.9.10: Preparation of pyridine bis azo compounds.[51]

2.9.3: Conclusions

The condensation of a hydrazine and a carbonyl group to afford azo compounds has been known for 60 years with a large number examples of this chemistry reported, in particular over the past 25 years. This reaction appears to be versatile and is applicable to a number of complicated structural systems to give azo compounds in good yields. Reports have also highlighted the use of this condensation to form previously unobtainable heterocyclic azo compounds of particular interest in the dyestuffs industry. There appears to be much scope for the development of this route to achieve potentially interesting dye targets.

2.10: Routes to New Heterocyclic Quinone Dyes

Of particular interest are heterocyclic electron deficient dyes in which the presence of an electron withdrawing atom (eg. a nitrogen atom) within the heterocycle will enhance the push/pull mechanism resulting in the desired bathochromic shift. These dyes are also expected to have increased resistance to photo-oxidation due to the electron deficient environment around the azo chromophore caused by the presence of the adjacent heterocycle.

There has been much interest in azo dyes **172** from the coupling of heterocyclic hydrazines with 4,9-disulfophenanthrenequinone **171**. These dyes are water soluble due to the presence of two sulfonic acid groups in the phenanthrene ring and contain the correct environment for subsequent metallisation to achieve additional fastness properties (Scheme 2.10.1). Therefore routes to heterocyclic hydrazine systems are required.

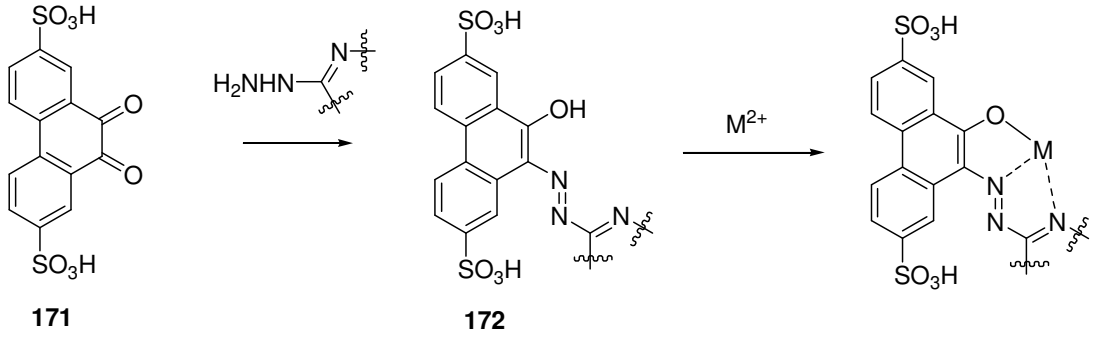

171 **172**

Scheme 2.10.1: Proposed general synthesis.

2.10.1: Synthesis of Hydrazinopyridazine

In consultation with industrial sponsors the following synthesis was proposed towards targets such as 3-hydrazinopyridazine **175** (Scheme 2.10.1). The hydrazine could be prepared from 3-chloropyridazine **174** which could be prepared from pyridazin-3-one **173**.

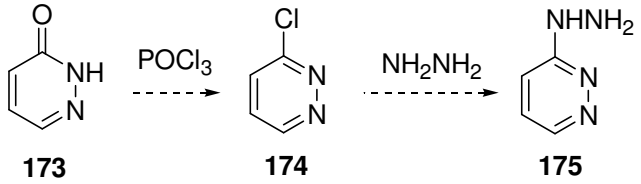

Scheme 2.10.1: Proposed synthesis of 3-hydrazinopyridazine **175**.

Pyridazin-3-one **173** was obtained by the high pressure hydrogenolysis of 4,5-dichloro-*2H*-pyridazin-3-one **177** over palladium on charcoal in high yield following a literature method (Scheme 2.10.2).[52] The 4,5-dichloro-*2H*-pyridazin-3-one **177** precursor was prepared by the condensation of mucochloric acid **176** and hydrazine monohydrate.[52]

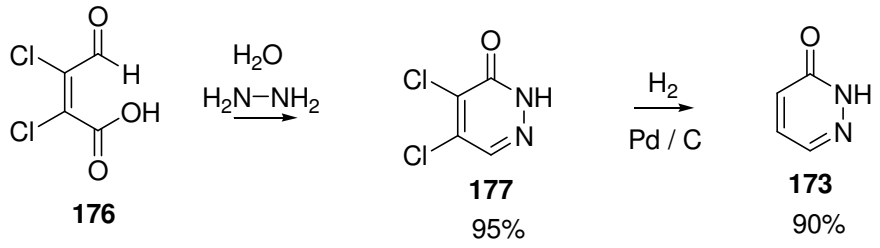

Scheme 2.10.2: Synthesis of pyridazin-3-one **173**.

3-Chloropyridazine **174** could then be prepared by treatment of pyridazin-3-one **173** with phosphorus oxychloride by a literature method to give 3-chloropyridazine **174** in a 98% crude yield (Scheme 2.10.3).[53] However, previous problems with the stability of this compound upon purification by distillation had been reported, therefore no further purification was carried out.[53]

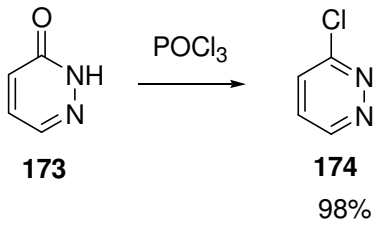

2.10.3: Synthesis of 3-chloropyridazine **174**.

The final step in this synthesis was the treatment of 3-chloropyridazine **174** with hydrazine to afford 3-hydrazinopyridazine **175**. After several attempts based upon the synthesis of similar hydrazinopyridazines in the literature, the most robust route to 3-hydrazinopyridazine **175** appeared to be the isolation of the product as its hydrochloride salt.[54,55] The crude reaction mixture was treated with hydrochloric acid and filtered to remove excess hydrazine as the hydrochloride salt. The remaining filtrates containing the pyridazine product were then slurried in ethanol and filtered to afford the precipitate containing 3-hydrazinopyridazine **175** as its dihydrochloride salt (Scheme 2.10.4). This product appeared stable as the salt and could be positively identified by characteristic NMR spectra which included three aromatic signals at δ_H = 8.80, 7.88 and 7.68 corresponding to the three pyridazine aromatic protons. An electrospray mass sprectrum also contained further evidence with the molecular ion MH^+ at m/z = 111. Further CHN analysis revealed the strength of the product to be 72% due to hydrochloride impurities giving an overall reaction yield of 51%.

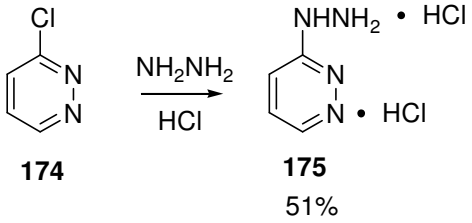

174 **175** 51%

Scheme 2.10.4: Synthesis of 3-hydrazinopyridazine dihydrochloride **175**.

Earlier attempts to isolate free hydrazine were generally unsuccessful leading to reaction of the crude product with acetone upon purification and resulting in an acetone by-product **178**.[54,55] This by-product was positively identified by characteristic NMR spectra including three aromatic signals at δ_H = 8.58, 8.21 and 7.84. There were also two methyl signals at δ_H = 2.04 and 2.08 in addition to accurate mass spectrometry evidence (Scheme 2.10.5).

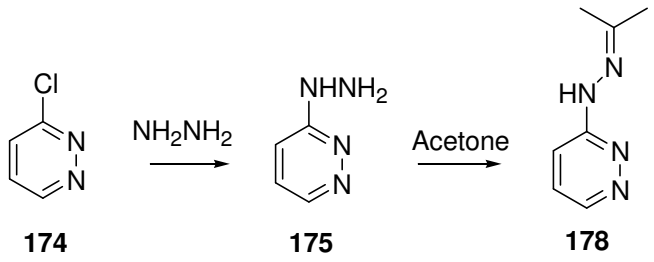

174 **175** **178**

Scheme 2.10.5: Attempts to prepare 3-hydrazinopyridazine **175**.

It was therefore possible to isolate 3-hydrazinopyridazine **175** as its stable hydrochloride salt which overcame previous problems encountered in earlier repeats of literature syntheses. Purification by this method also avoided reaction of the crude hydrazine to form its acetone by-product.

2.10.2: Synthesis of Hydrazinoquinolines

Other heterocyclic hydrazines of interest of interest could also be prepared such as 1-hydrazinoisoquinoline **180** and 2-hydrazinoquinoline **182** from 1-chloroisoquinoline **179** and 2-chloroquinoline **181** respectively by treatment with hydrazine hydrate in ethanol *via* a literature method (Scheme 2.10.6).[56] This gave 1-hydrazinoisoquinoline **180** and 2-hydrazinoquinoline **182** in high yields.

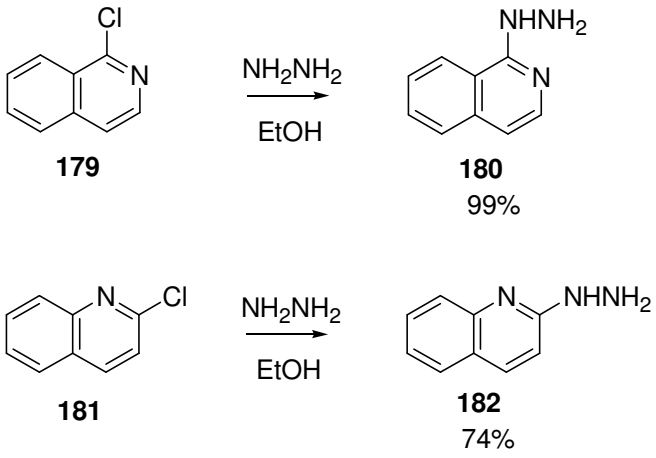

179 **180** 99%

181 **182** 74%

Scheme 2.10.6: Synthesis of hydrazinoquinolines **180** and **182**.

Recovery and purification of these hydrazines did not appear to be a problem in this case with both purified by recrystallisation and stable under standard conditions. Therefore it was possible to prepare hydrazinoquinolines of interest as potential heterocyclic dye components which were stable and could be purified easily with none of the problems encountered with stability previously associated with the synthesis of 3-hydrazinopyridazine **175**.

2.11: Synthesis of New Heterocyclic Azo Compounds

The heterocyclic hydrazines prepared earlier in addition to commercially available hydrazines such as phenylhydrazine **183**, 2-hydrazinopyridine **185** and 1-hydrazinophthalazine dihydrochloride salt **185** were then used to prepare a variety of 4,9-disulfophenanthrenequinone based azo compounds **186** - **191** by condensation of the hydrazines in dilute hydrochloric acid with the quinone **171** (Scheme 2.11.1). Reactions were followed by HPLC.

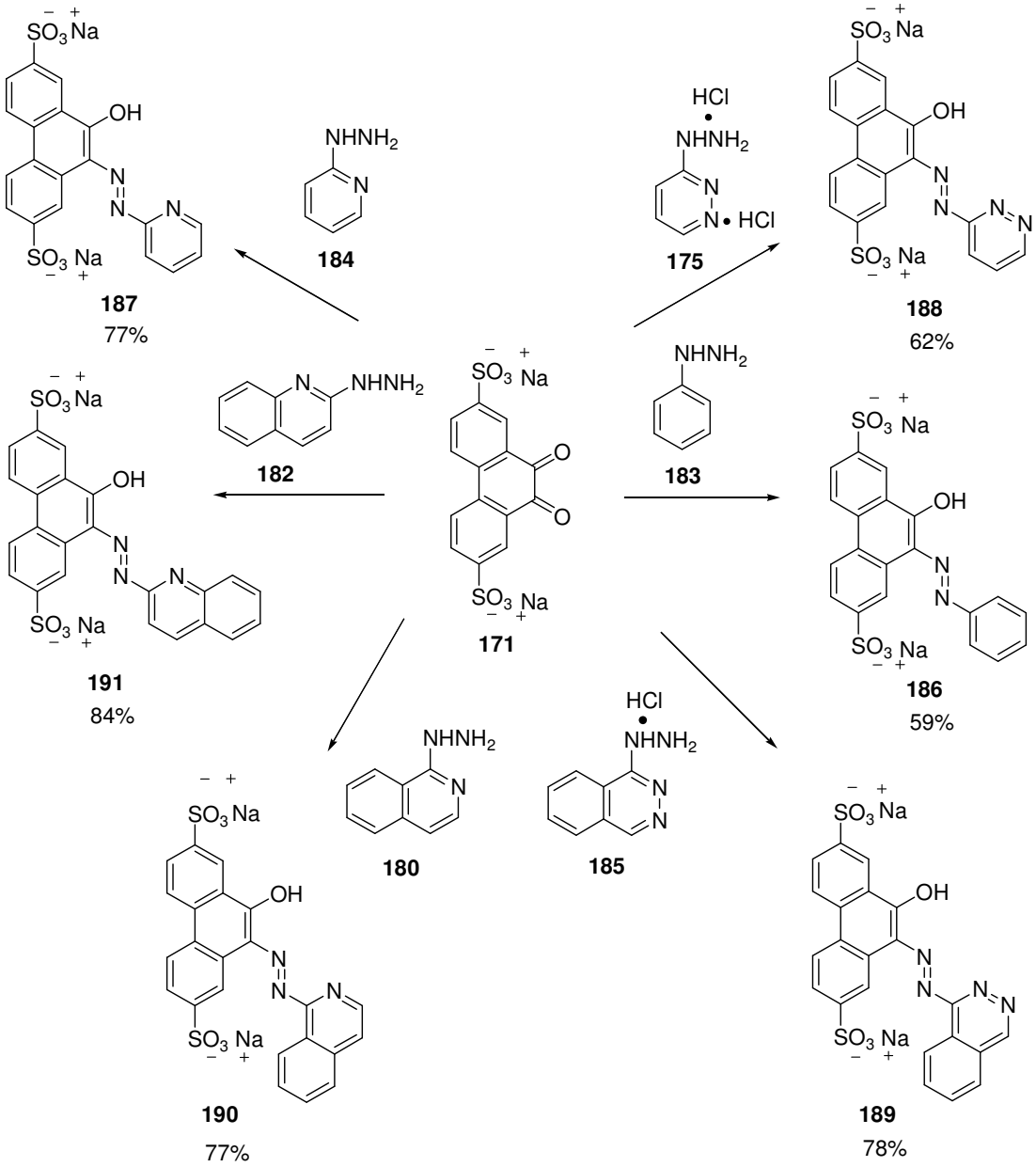

Scheme 2.11.1: Synthesis of quinone dyes.

The azo compounds **187 – 191** were recovered as the disodium salts complex by the method of salting the azo compounds out of solution followed by filtration as described in section 2.8. Excess salt impurities were then removed by dissolving the recovered precipitate paste in water at neutral pH and dialysis of the solution through dialysis membrane tubing which allows molecules of low molecular weight such as inorganic salts to pass through while retaining higher molecular weight compounds such as the azo products. Evaporation of the dialysis solution then afforded the largely desalinated azo product as the disodium salt.

All reactions proceeded in moderate to high yields with the products identified by characteristic ^{1}H and ^{13}C NMR spectra in addition to electrospray mass spectrometry in which the negative molecular ions such as $[M]^{2-}$ could be observed. In this case M was the mass of the organic component of the azo compound with the sulfonic acid groups in the absence of the sodium cation (SO_3^-). The molecular ions could also more commonly be detected as the single negative ions $[MH]^-$ and $[MNa]^-$ with single cations of H^+ or Na^+ around one of the sulfonic acid groups.

Dyes were present as the disodium salt ($SO_3^-Na^+$) in the solid form upon isolation of the precipitate. The organic strength of the azo compounds accounting for any remaining salt impurities could also be estimated by CHN analysis (see details in experimental section).

The dyes were also drawn throughout this chapter in the azo form as opposed to the hydrazine form due to this being the standard form dyes of this type are reported in industry. However many dyes exhibit tautomerism. The ^{1}H and ^{13}C NMR spectra of the isolated dyes indicate they are present in the hydrazone form in DMSO. Hence ^{1}H and ^{13}C NMR spectra of these dyes in D_2O are required to determine the tautomeric form under aqueous conditions.

In conclusion it was possible to prepare a variety of new heterocyclic azo compounds by reaction of heterocyclic hydrazines, some of which were commercially available, with 4,9-disulfophenanthrenequinone **171**. These azo compounds also had suitable environments in which to form metallised complexes which would lead to a bathochromic shift and increased light fastness.

2.12: Metallisation of Azo Compounds

As mentioned in the introduction, in recent years there has been interest in metal-complexed dyes due to their excellent light fastness properties. A suitable environment in which to coordinate a metal giving a meridional [5,5] complex which exhibits bright shades is required. Metallisation of the quinone dyes prepared in the previous section is possible to achieve the required light fastness.

2.12.1: Preparation of 2:1 Metallised Complexes

The heterocyclic azo compounds **187** - **191** prepared in the previous section were metallised with half an equivalent of nickel acetate tetrahydrate compared with the azo component to give the 2:1 nickel complexs **192** - **196** (Scheme 2.12.1).

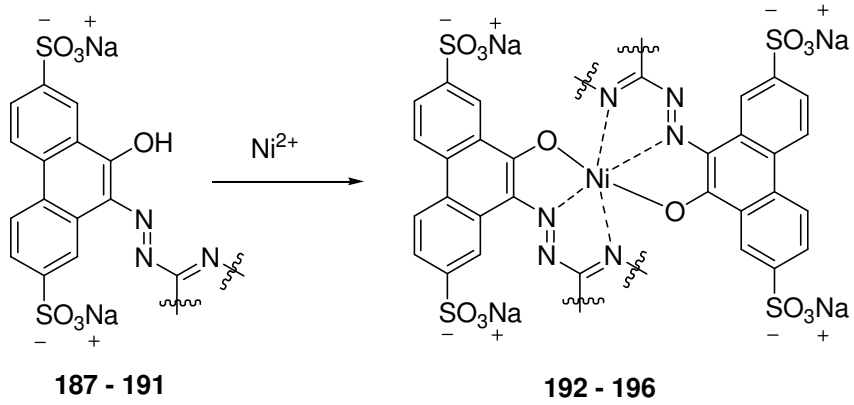

Scheme 2.12.1: Metallisation of heterocyclic azo dyes.

This was achieved by stirring the azo compounds **187 - 191** in a basic aqueous solution with addition of nickel acetate which lead to an immediate colour change from orange/red to magenta for these azo compounds. The reaction progress could be monitored by UV-vis spectroscopy due to the bathochromic shift in λ_{max} associated with metallisation. There was also a change in the extinction coefficient (ε) and half width ($W_{1/2}$) of the peak in the spectra which varied depending upon the azo compound (Table 2.12). The extinction coefficient was calculated from the isolated metallised product and quoted per mole of chromophore in the sample, thus the 2:1 metallised complex has two moles of chromophore per mole of the dye as two azo ligands are coordinated around the metal centre.

The metallised dyes **192 - 196** were recovered from the aqueous solution in a similar manner to the ligands by salting the precipitate out of solution, filtration, dialysis and evaporation to afford the largely desalinated metallised dye. Strengths of the dyes could be determined by CHN analysis, however, characterisation and identification of the metallised dyes was not possible by standard NMR techniques due to the presence of a metal centre. Therefore the presence of the required metallised complexes was confirmed by UV-vis spectroscopy and electrospray mass spectrometry analysis. The effect of metallisation can be seen in the UV-vis spectra in which the the free azo ligand and isolated metallised complex are superimposed on the same spectra (Figures 2.12.1-5).

Table 2.12: Changes in the UV-vis spectral data upon metallisation.

Dye name	Dye structure	λ_{max} shift	$W_{1/2}$ change	ε change
Pyridine **187 → 192**	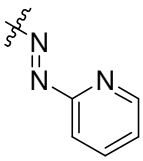	466 nm → 547 nm	86 nm → 88 nm	24400 → 27500
Pyridazine **188 → 193**	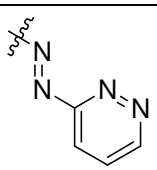	450 nm → 556 nm	115 nm → 95 nm	16200 → 19800
Phthalazine **189 → 194**	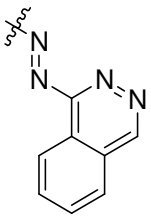	463 nm → 538 nm	151 nm → 117 nm	14800 → 12800
Isoquinoline **190 → 195**	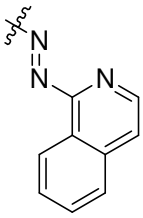	485 nm → 548 nm	109 nm → 103 nm	18600 → 27600
2-quinoline **191 → 196**	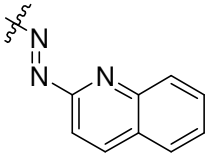	463 nm → 573 nm	96 nm → 89 nm	24200 → 31200

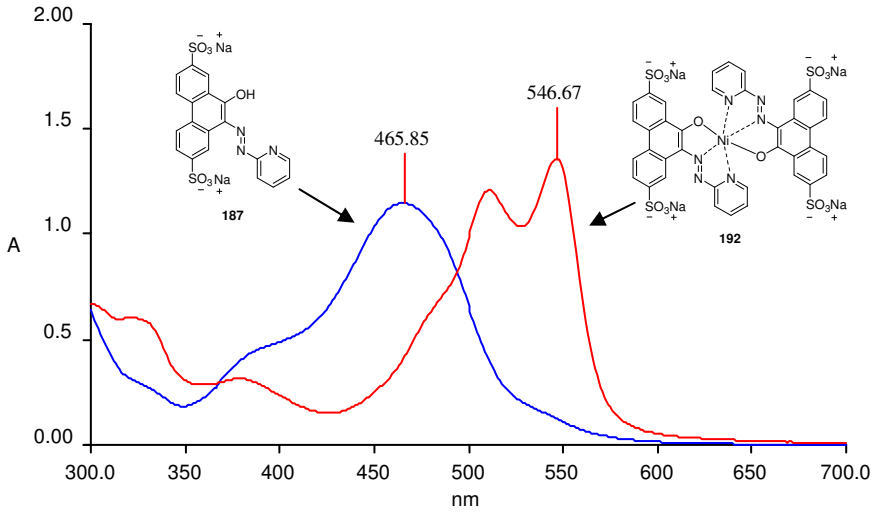

Figure 2.12.1: Metallisation of pyridine dye **187** → **192**.

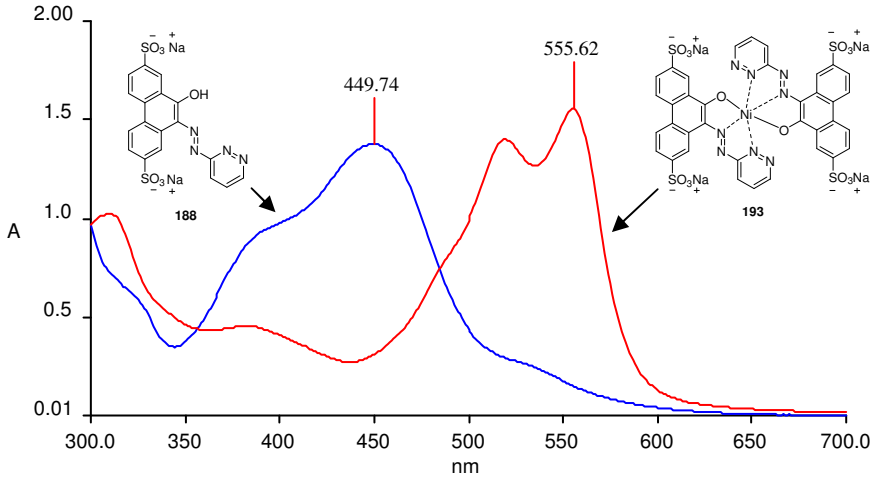

Figure 2.12.2: Metallisation of pyridazine dye **188** → **193**.

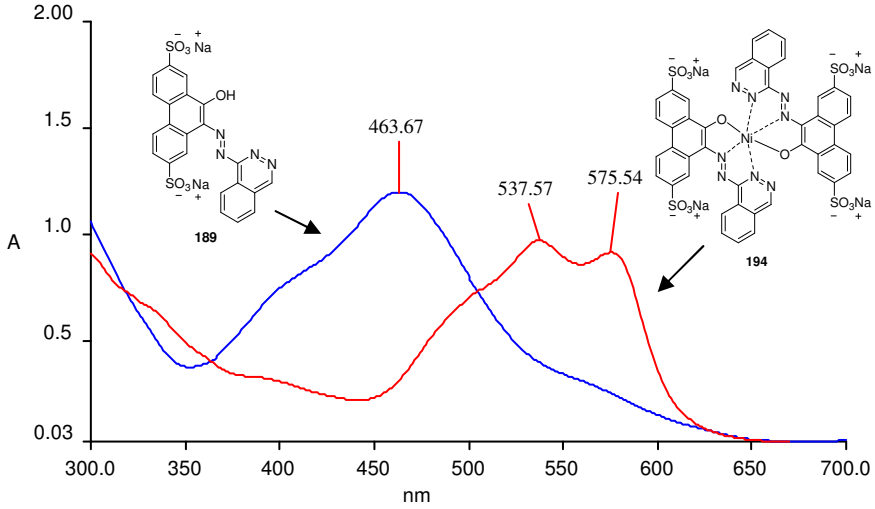

Figure 2.12.3: Metallisation of phthalazine dye **189** → **194**.

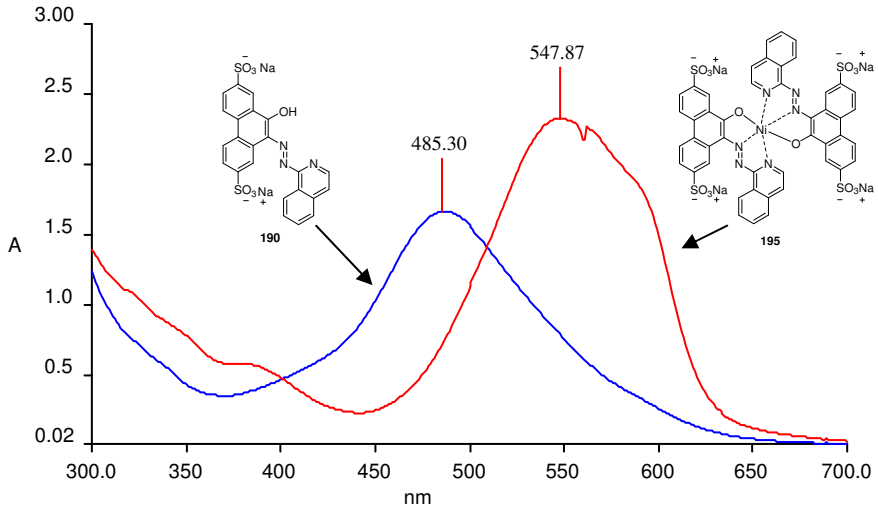

Figure 2.12.4: Metallisation of isoquinoline dye **190** → **195**.

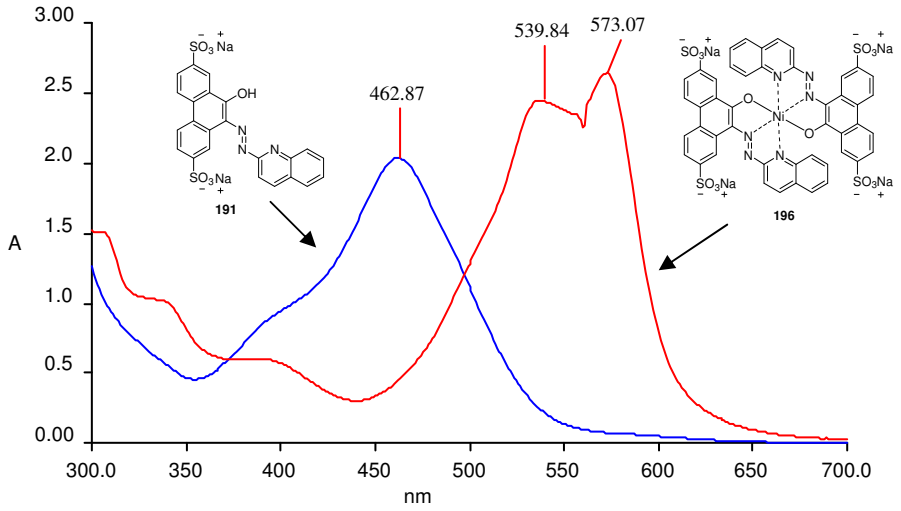

Figure 2.12.5: Metallisation of 2-quinoline dye **191** → **196**.

Changes in the UV-vis spectra can be seen upon metallisation of all of the above azo dyes **187** - **191** to give the 2:1 metal complex **192 – 196** as a bathochromic shift in λ_{max} which resulted in a colour change from red/orange to magenta. There is also a change in the extinction coefficient and the half width of the absorption peak.

The desired changes in the UV-vis spectra upon metallisation characteristic of an ideal magenta dye are a bathochromic shift in λ_{max} to 550 nm and an increase in the extinction coefficient (ε) which results in a more intense dye. Another desirable

UV-vis characteristic is a reduction in half width ($W_{1/2}$) of the absorption peak to below 100 nm with no secondary absorptions resulting in a brighter dye.

In the pyridine **192**, pyridazine **193** and isoquinoline **195** dyes, metallisation resulted in a bathochromic shift of λ_{max} to 547, 556 and 548 nm respectively which approached the ideal region for a magenta dye. However for the phthalazine dye **194** there is a bathochromic shift to 538 nm and also a significant absorption at λ = 576 nm indicating this dye may be too blue. This was also the case for the 2-quinoline dye **196** in which a bathachromic shift to λ_{max} = 573 nm was observed.

In the majority of dyes in table 2.12 an increase in the extinction coefficient was observed upon metallisation indicating a more intense dye. However, in the case of metallisation of the phthalazine dye **194** a slight reduction in the extinction coefficient was observed.

Finally in most of the dyes in table 2.12 there was little or a slight change in the half width ($W_{1/2}$) of the absorption peak. However in the case of the pyridazine dye **193** there was a large change from 115 nm to 95 nm resulting in a brighter dye. This was also the case for the phthalazine dye **194** in which the half width ($W_{1/2}$) reduced from 151 nm to 117 nm upon metallisation. However the half width of the metallised peak was not less than 100 nm typically associated with a bright dye (Figure 2.12.3).

In conclusion it was possible to prepare the metallised 2:1 nickel complexes of the pyridine, pyridazine, phthalazine, isoquinoline and 2-quinoline dyes **187 - 191** by treatment with half an equivalent of nickel acetate tetrahydrate. This metallisation was accompanied by a bathochromic shift of λ_{max} to afford magenta dyes **192 - 196** of increased intensity and brightness by comparison with the UV-vis spectral properties of the free ligands. Further testing is required to determine the suitability of these dyes as potential inkjet targets (Section 2.13).

2.12.2: Preparation of 1:1 Metallised Complexes

It is also possible to prepare the 1:1 metallised complexes by altering the stoichiometry of nickel acetate tetrahydrate to the azo ligand used during metallisation. The pyridine and pyridazine 1:1 metallised complexes **197** and **198** were prepared by the addition of one equivalent of nickel acetate tetrahydrate under similar conditions to those used earlier.

Firstly the pyridine azo **187** was metallised by addition of one equivalent of nickel acetate tetrahydrate with stirring in a basic aqueous solution to afford the 1:1 metallised complex (Scheme 2.12.2). The metallised product was recovered as in Section 2.12.1.

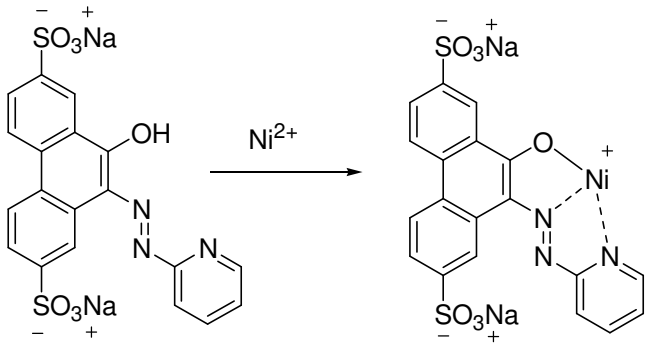

187 **197**

Scheme 2.12.2: Synthesis of pyridine dye 1:1 metallised complex **197**.

The metallisation progress could be monitored by UV-vis spectroscopy and was accompanied by a bathochromic shift in λ_{max} from 466 nm to 540 nm resulting in a colour change from red/orange to magenta (Figure 2.12.6). However further mass spectrometry analysis of the product indicated a mix of the 1:1 and 2:1 pyridine metallised complexes **197** and **192**. The main peaks in the negative electrospray mass spectrum corresponded to the 2:1 pyridine metallised complex **192** with $[M2H]^{2-}$ and $[MH]^{3-}$ at *m/z* = 486 and 324 respectively. There were also peaks corresponding to the 1:1 metallised complex **197** in lower intensity with $[MH]^{-}$ and $[M]^{2-}$ at *m/z* = 515 and 257 respectively. Also present were mass spectrum peaks corresponding to the free azo ligand **187**. Therefore from mass spectrometry and UV-vis analysis the dye appeared to be mainly in the 2:1 complex **192** and none of the required 1:1 nickel pyridine complex **197** could be isolated as a pure dye.

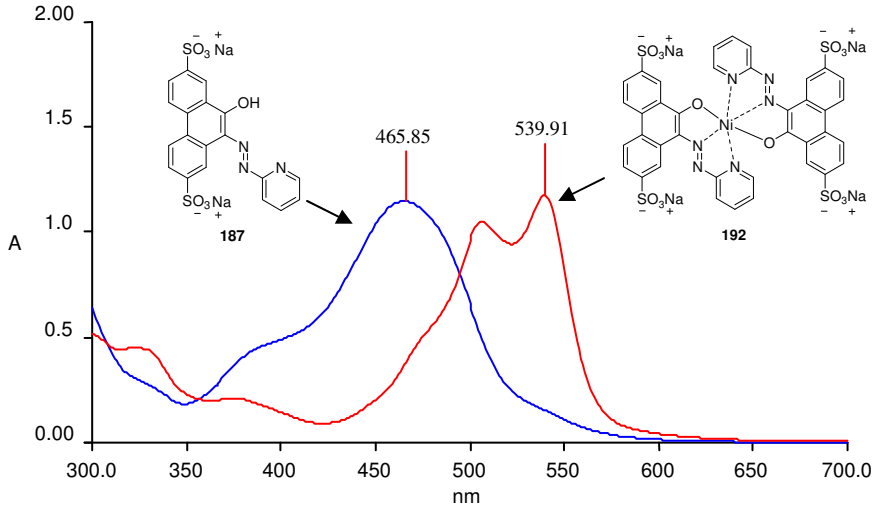

Figure 2.12.6: Metallisation of pyridine dye **187** to the 2:1 complex **192**.

The pyridazine azo **188** was also metallised by the addition of one equivalent of nickel acetate tetrahydrate with a corresponding colour change from orange to a magenta colour (Scheme 2.12.3).

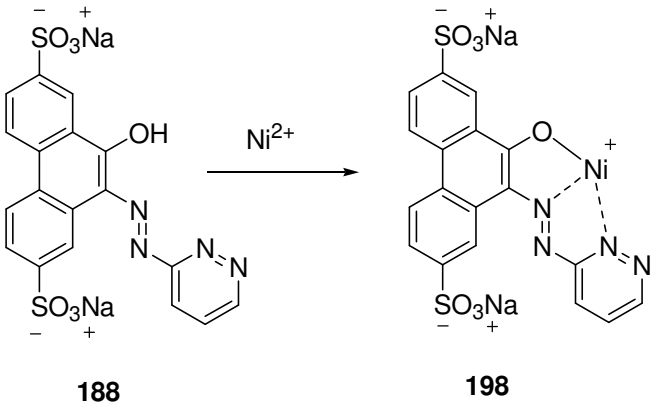

Scheme 2.12.2: Synthesis of 1:1 pyridazine dye **198**.

The metallisation progress could again be monitored by UV-vis spectroscopy and was accompanied by a bathochromic shift in λ_{max} from 450 nm to 489 nm (Figure 2.12.7). In this case the 1:1 complex **198** could be isolated and identified by its UV-vis spectral properties, however mass spectrometry did not reveal peaks corresponding to the metallised product. There was also a significant reduction in solubility of the dye.

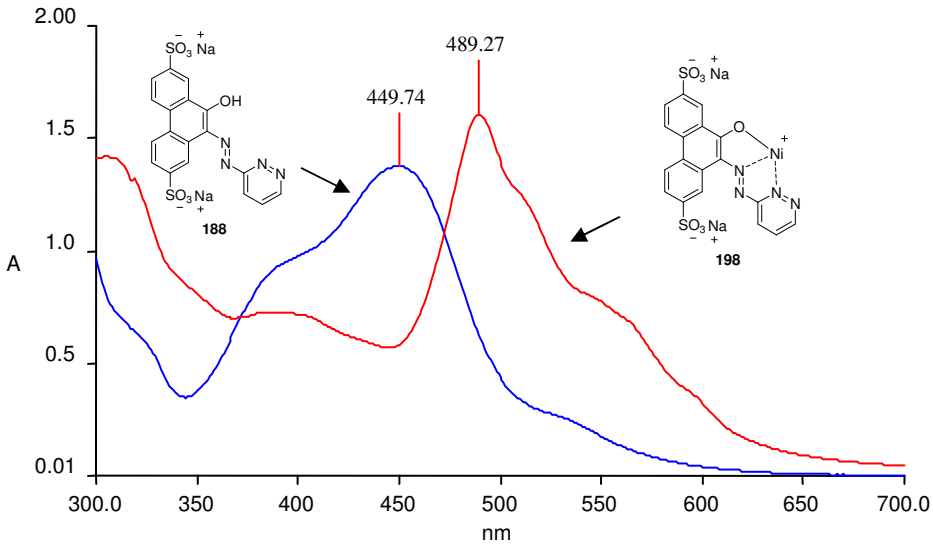

Figure 2.12.7: Metallisation of pyridazine dye **188** to the 1:1 complex **198**.

However over time in solution the UV-vis samples were also seen to equilibrate to the 2:1 complexed dye **193** with additional peaks at λ_{max} = 512 and 545 nm developing with a reduction in intensity of the peak at λ_{max} = 489 nm. After 24 h the solution appeared to contain mainly the 2:1 pyridazine metallised complex **193** by UV-vis analysis (Figure 2.12.8).

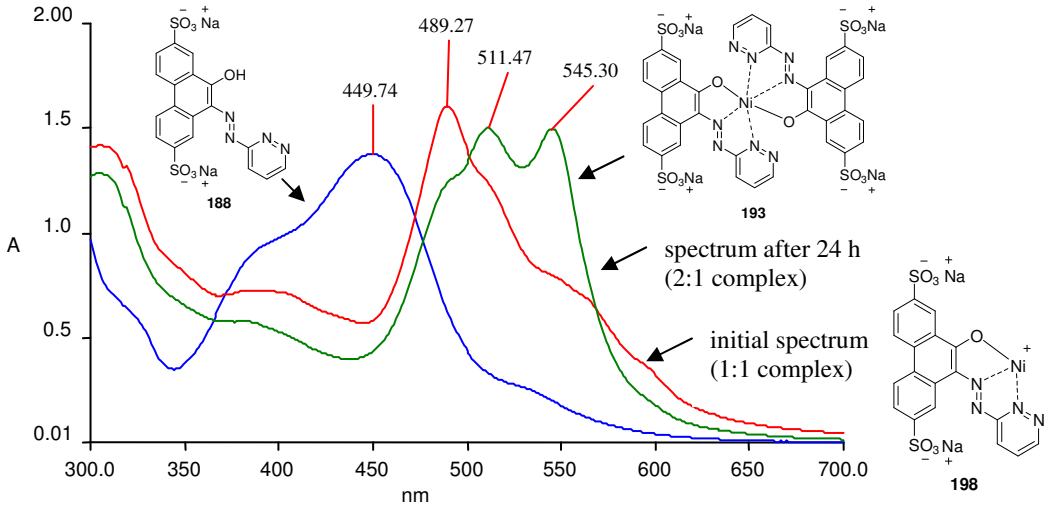

Figure 2.12.8: Pyridazine dye complex after 24 h in solution.

In conclusion there were significant problems with the stability and solubility of the 1:1 metal complexes of the pyridine and pyridazine dyes. Due to these problems these dyes were not pursued for testing and no attempts were made to prepare the 1:1 metal complexes of the phthalazine, isoquinoline and 2-quinoline dyes.

2.13: Dye Testing

The novel metallised pyridine **192**, pyridazine **193**, phthalazine **194**, isoquinoline **195** and 2-quinoline **196** magenta dyes were selected to be tested at Fujifilm, Blackley, due to their good UV-vis results (Appendix 2). The colour properties of these dyes were established and the fastness properties of the dyes on exposure to light and ozone were determined, which is the main problem encountered for magenta dyes.

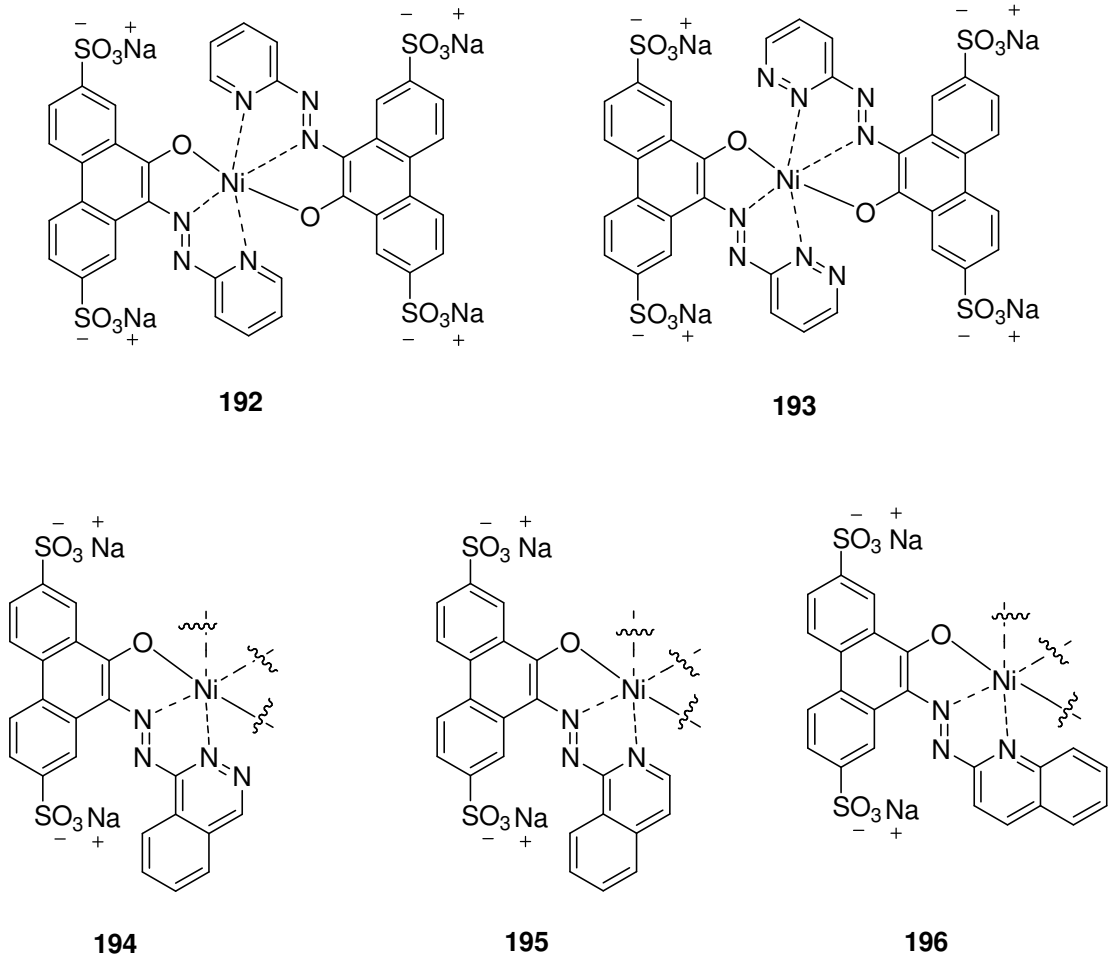

Figure 2.13.1: Structure of dyes tested as 2:1 complexed magenta dyes.

2.13.1: Formulation of the Generic Inks

Method

The dye (0.3 g, 3% w/v) was added to a 5:5:1 solution (9.7 cm^3) of 2-pyrrolidone, diethylene glycol and Surfynol 465. The weight of each dye used to make up the generic ink formulation was adjusted to account for the strength of the dye due to salt impurities during isolation which was calculated from elemental analysis. The pH of this suspension was adjusted to 8.5 using dilute sodium hydroxide solution (2 M) and then sonicated for 1 h. A dark coloured solution resulted similar to that observed after metallisation. The dyes were then filtered through an adapter (0.45 μm) fitted to the end of a syringe. However, these filtrations reduced the amount of the dyes in the inks slightly due to incomplete solubility.

Each of the 5 inks described above (5 cm^3) was injected *via* a syringe into the ink cartridge, and then loaded into a Canon i965 printer, from which all the prints were obtained on 3 different types of paper. Canon PR101 (microporous), SEC Crispia Photo (microporous) and HP Advanced Photo (microporous) or HP Premium Photo (swellable) papers were used. All the various fastness tests were performed on 3 of these papers, for each of the 5 inks. Dyes **192** and **193** were also printed onto a plain Xerox 4024 paper. However, generally fastness tests are not carried out on plain paper as there are large losses due to the way the ink binds to the surface.

2.13.2: Applications Testing

Colour Measurements

The colour properties of a dye in print may vary from those of the dye on its own, due to pH changes, paper properties *etc.*, and can be measured using a colorimeter.

There are various devices used to measure colour, such as a colorimeter or spectrophotometer, made by companies such as X-Rite or Gretag Macbeth. These are photoelectric devices that simply measure and compute how much of a known amount of light is reflected from an object as a function of wavelength. The amount of reflectance is measured and translated into ROD (Reflectance Optical density) values using Equation 2.[57]

Equation 2: $ROD = \log_{10} 1/R$, where R = reflectance

Light is shone through coloured filters and the appropriate colours, as described above, are removed by these filters. The filters remove light at specific wavelengths, and at these points, the reflectance, which is at a minimum (maximum absorbance), is measured, and reported as ROD values, using Equation 2. Black exhibits almost no reflectance.[14]

Measurements are taken, by simply holding the instrument directly over the prints, to measure the reflectance, which was converted to the reflectance optical density (ROD). A higher ROD value will appear as a denser colour on the paper and less white paper shown through. The L, a, b, C and h values were also calculated using this instrument with definitions described in Section 1.10.

The instrument was firstly calibrated, and the ROD values were then recorded for each dye on all 3 papers at 100% print strength (Table 2.13.1).

Table 2.13.1: ROD values of inks on various papers.

Dye	Xerox 4024	Canon PR101	SEC Crispia Photo	HP Premium Photo
192	1.12	1.93	1.91	1.90
193	1.14	2.11	2.20	2.13
				HP Advanced Photo
194	Failed to print on all substrates			
195	N/A	1.99	2.04	2.01
196	N/A	1.97	2.00	1.99

The ROD values were all quite high for dyes **192**, **193**, **195** and **196** printed on microporous and swellable papers with an ideal ROD value above 2.0 for magentas. However on plain paper the ROD values of dyes **192** and **193** dropped to 1.12 and 1.14 respectively due to the changes in the surface properties of the paper. An ROD value above 1.2 would be expected for a strong magenta dye on plain paper. Higher ROD values are obtained for the coated papers, where more of the ink is held at the surface, compared with a plain paper where there are voids for the ink to flow into.[58] The phthalazine dye **194** failed to print due to solubility problems and thus no further colour or fastness measurements could be taken.

Other measurements used to describe colour such as the L, a, b, C and h values could also be calculated using this instrument for the dyes printed on these papers (Table 2.13.2).

Table 2.13.2: L, a, b, C and h values on various papers.

Dye (paper)	L	a	b	C	h / º
192 (Xerox)	46	51	-6	52	354
192 (Canon)	39	72	-5	73	356
192 (SEC)	41	76	-7	76	355
192 (HP)	38	71	-6	71	355
193 (Xerox)	48	56	-8	57	352
193 (Canon)	43	77	-5	78	356
193 (SEC)	45	81	-4	81	357
193 (HP)	42	75	-5	76	356
195 (Canon)	21	53	-48	72	318
195 (SEC)	22	58	-55	80	317
195 (HP)	22	57	-54	78	317
196 (Canon)	25	58	-43	72	323
196 (SEC)	26	61	-48	78	322
196 (HP)	25	61	-48	77	322

The values of L, a, b, C and h can therefore be used to identify a suitable magenta dye however vary greatly depending on the paper used. Firstly the h value (hue) is measured as an angle with an ideal magenta h = 350º. These four magenta dyes gave values ranging from 317º to 357º with dyes **192** and **193** showing a good magenta colour. However dyes **195** and **196** had low h values on all papers indicating they were too blue, a trend also reflected in the high λ_{max} values.

The measure of lightness of these dyes could also be measured with the L value where a value of 0 was black and 100 white. A desirable L value for a magenta dye would be between 44 and 48. Dyes **192** and **193** showed promising L values of between 39 and 48 with dye **193** printed on Xerox and SEC papers showing best

lightness properties. However, dyes **195** and **196** showed extremely poor L values of 21 to 26 which were significantly darker or blacker than required.

A measure of the redness and greenness of the dyes was also taken from the a value with a positive value indicating red and a negative value green with an ideal a value above 80. Dyes **192** and **193** showed moderate results on Xerox paper with a values of 51 and 56 respectively indicating the dyes were too green. However, an a value of 60 is good for a plain paper. Moderate to good a values between 71 and 81 were obtained for these dyes on PR101, SEC and HP papers. However, analysis of dyes **195** and **196** gave very low a values on all papers of between 53 and 61.

The colour of these dyes on the substrates could also be expressed as a measure of the yellowness or blueness of the dye indicated by the b value with ideal values for magenta dyes between -5 and -10. Firstly analysis of dyes **192** and **193** on all papers showed good b values within the required range. However dyes **195** and **196** showed poor b values on all substrates which were very low between -43 and -55. This indicated these dyes were too blue.

Finally the brightness of the dye was measured and expressed in the C value which for magenta dyes was desired to be above 80. All dyes printed on the SEC substrate showed good C values above or slightly below 80. The remaining substrates showed moderate brightness levels with all dyes. Dyes **192** and **193** printed on Xerox paper also showed moderate brightness with C values of 52 and 57 respectively. C values of 60 are desired for a magenta dye on plain paper.

Overall analysis of dyes showed that dyes **192** and **193** gave the correct colour and were bright on the majority of substrates however dyes **195** and **196** appeared to be too blue.

Light and Ozone Fastness: Dyes 192 and 193

Small squares of each of the prints on all 3 microporous papers were cut out, mounted on cardboard and placed separate cabinets, one of which simulated exposure to light and the other to ozone. They were removed after 100 h and 24 h respectively. Colour measurements were then taken of the prints. A standard magenta control dye (BCI 7M) was printed alongside dyes **192** and **193** (See Appendix 2 for results)

The ozone test was an accelerated test lasting 24 hours at a constant ozone concentration of 1 ppm that simulated 100 days in an office. Light fastness tests lasted 100 hours at a relative humidity of 40%. The dyes fastness properties are easily and best seen from the ROD percentage loss column in the appendix, where the lower the value recorded, then the better the dye has performed. Upon fading, the L, a, b, C and h values change as the print becomes less dense. The fail time of the dye was established as the time in hours in the light and ozone machines at which the dye lost 25% of its initial ROD value. The light and ozone fastness fail times of dyes **192** and **193** were then plotted on a graph allowing comparison of the fastness of each dye on the substrates with some similar magenta dyes (S195310, 064, 197 and 352) prepared by Fujifilm Imaging Colorants (Graph 2.13.1). These results were also compared with the fastness properties of the control dye BCI 7M (Table 2.13.3).

Table 213.3: Light and Ozone Fastness Fail Times of Dyes **192** and **193**.

Dye (Paper)	Light Fastness Fail Time /h	Ozone Fastness Fail Time /h
192 (Canon)	247	129
193 (Canon)	235	46
BCI 7M (Canon)	293	258
192 (SEC)	209	129
193 (SEC)	322	12
BCI 7M (SEC)	142	273
192 (HP)	174	2607
193 (HP)	97	274
BCI 7M (HP)	167	1644

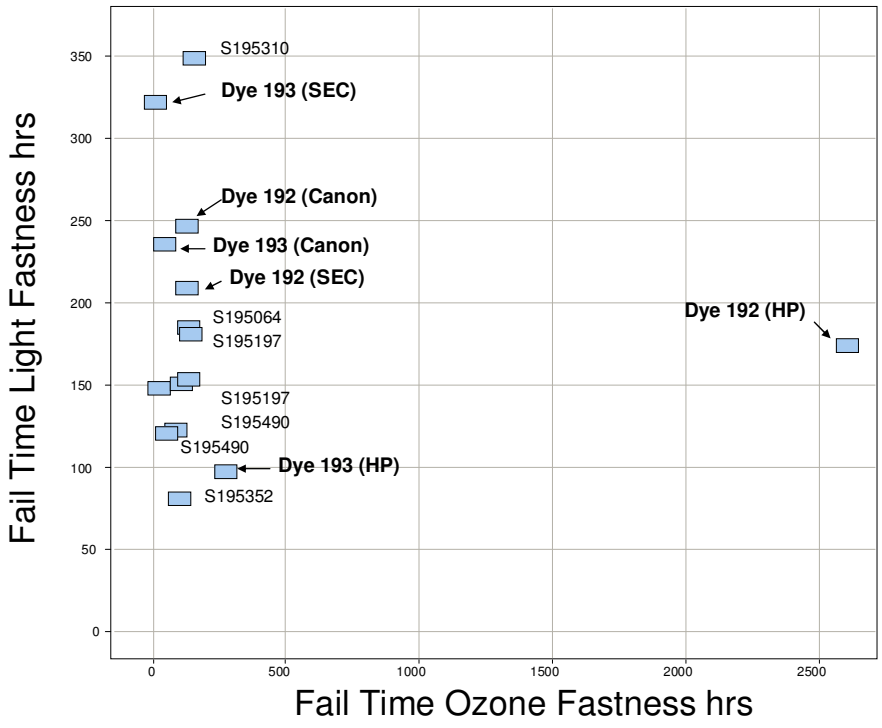

Graph 2.13.1: Generic ink testing results.

Analysis of these results show dyes **192** and **193** to have good fastness properties in comparison with similar magenta dyes (Graph 2.13.1). Dye **193** is the second best for light fastness when printed on a SEC substrate with a fail time of 322 h however, has low ozone fastness of 12 h. A good combination of light and ozone fastness is required which can be observed for dye **192** printed on the SEC substrate with light and ozone fastness of 209 h and 129 h respectively. For dyes **192** and **193** printed on the Canon substrate comparable light fastness is observed with the control dye however ozone fastness is poorer, particularly in the case of dye **193** where ozone fastness is only 46 h.

Finally the dyes printed on HP substrates show substantially different properties. Firstly dye **193** showed poor light and ozone fastness properties. However dye **192** showed impressive ozone fastness of 2607 h and good light fastness of 174 h.

Therefore overall in comparison with the control dye BCI 7M and similar magentas dyes, **192** and **193** showed impressive fastness properties when printed on some of the substrates although an improved mix of light and ozone fastness is

desired. As expected the addition of an extra heteroatom in the pyridazine dye **193** results in significant differences in the fastness properties when compared to dye **192** however the expected increases in fastness properties of dye **193** due to the electron deficient nature of the dye generally were not observed to a large extent.

Light and Ozone Fastness: Dyes 195 and 196

Due to a change in testing protocols at Fujifilm prior to the synthesis of dyes **195** and **196** these results could not be directly compared with the fastness properties of dyes **192** and **193**.

Small squares of each of the prints on all 3 microporous papers were cut out, mounted on cardboard and placed an instrument which simulated exposure to light and ozone. They were removed after 50 h, 100 h and 200 h for light fastness measurements and every 24 h for ozone fastness measurements. Colour measurements were then taken of the prints. A different standard magenta control dye (S196363) was also used (See Appendix 2 for results)

The ozone test was an accelerated test lasting 24 hours at a constant ozone concentration of 1 ppm that simulated 100 days in an office at 25% humidity. Light fastness tests were at a relative humidity of 40%. As with section 2.20.3, the fail times of the dyes were calculated on each substrate and compared with the standard magenta control dye S196363 (Table 2.13.4).

Table 2.13.4: Light and Ozone Fastness Fail Times of Dyes **195** and **196**.

Dye (Paper)	Light Fastness Fail Time /h	Ozone Fastness Fail Time /h
195 (Canon)	84	5
196 (Canon)	165	10
S196363 (Canon)	135	33
195 (SEC)	88	10
196 (SEC)	255	19
S196363 (SEC)	232	83
195 (HP)	112	14
196 (HP)	388	30
S196363 (HP)	400	102

Analysis of these results show dye **195** has relatively poor light and ozone fastness in comparison to that of the standard magenta dye S196363. Although dye **196** shows promising light fastness of 165 h, 255 h and 388 h on Canon, SEC and HP substrates respectively. However the ozone fastness results for dye **196** are not as promising and are significantly lower than those of the standard magenta control dye with fail times of 10 h, 19 h and 30 h on Canon, SEC and HP substrates respectively. Therefore dyes **195** and **196** did not show as promising a mix of light and ozone fastness properties as the case of dyes **192** and **193**.

2.13.3: Formulation of Specific Inks

In addition to the testing of Dyes **192** and **193** in a generic ink formulation, these dyes were also tested for colour and fastness properties in an ink formulation modelled on inks to be used with specific papers. Therefore three ink formulations were made up for each dye corresponding to "Canon", "SEC" and "HP" formulations.

The inks were then printed on the appropriate papers Canon PR101 (microporous), SEC Crispia Photo (microporous) or HP Advanced Photo (microporous). The colour and fastness properties of each dye were examined as in section 2.13.2 (See Appendix 3 for results).

The instrument was firstly calibrated, and the ROD values recorded for each dye on all 3 papers at 100% print strength (Table 2.13.5). The dyes **192** and **193** show good ROD values for the "Canon" ink formulation printed on Canon paper and slightly low ROD values for the "HP" formulation printed on the HP paper as they are below 2.0. However the ROD values for the "SEC" formulation on the appropriate paper were significantly lower indicating a very low density of colour on this substrate for dyes **192** and **193**.

Table 2.13.5: ROD values of inks on appropriate paper.

	Ink formulation / Paper Type		
Dye	"Canon" /PR101	"SEC"/Crispia Photo	"HP"/Advanced Photo
192	2.18	0.59	1.79
193	2.04	1.12	1.61

Other measurements used to describe colour such as the L, a, b, C and h values were also taken for the dyes printed on these papers (Table 2.13.6).

Table 2.13.6: L, a, b, C and h values on various papers.

Dye (formulation/paper)	L	a	b	C	h / º
192 (Canon)	42	74	8	74	6
192 (SEC)	72	51	-19	55	339
192 (HP)	49	80	-12	81	352
193 (Canon)	36	69	7	69	6
193 (SEC)	55	67	-21	70	342
193 (HP)	46	79	-23	82	344

The values in table 2.13.6 indicate dyes **192** and **193** give mostly good magentas on the appropriate substrates in most ink formulations. Dye **192** has good colour properties in the "Canon" and "HP" ink formulations. However, prints from the "SEC" formulation has a particularly low a value indicating a low redness of the dye and a low C value indicating a dull as opposed to bright dye.

Dye **193** also has some problems associated with the a values for the "Canon" and "SEC" formulations which indicates these are slightly less red than required. The b values of the "SEC" and "HP" formulations also indicate the dye is slightly more blue than required. However, for all formulations the brightness (C) and hue (h) are reasonable.

Overall there are some problems associated with the colour properties of these dyes when printed on the appropriate substrates. This was mainly in the case of the "SEC" formulation which could possibly be attributed to the low density of the dye due to the low ROD values (Table 2.13.5). The remaining "Canon" and "HP" formulations for dyes **192** and **193** give reasonable colour measurements for suitable magenta dyes.

Light and Ozone Fastness: Dyes 192 and 193 (Specific Formulation Testing)

In a similar manner to section 2.13.2 the light and ozone fastness of the specific formulations of dyes **192** and **193** on the appropriate substrate were measured. The "Canon" and "SEC" formulation prints were removed after 100 h and 24 h from the light and ozone instruments respectively. However the "HP" prints were exposed to high intensity light for 10 days which simulated 6 years exposure before being removed and colour measurements taken of the prints. As in section 2.13.3, all ink formulations of dyes **192** and **193** were printed alongside a standard magenta control dye which altered depending upon which formulation was being tested. The fail times of dyes **192** and **193** in these specific ink formulations were then calculated (Table 2.13.7). These results could also be put into graphical form and compared with similar magenta dyes for the "Canon" and "HP" formulations (Graphs 2.13.2 and 2.13.3).

Table 2.13.7: Light and Ozone Fastness Fail Times of Dyes 192 and 193.

Dye (Formulation/Paper)	Light Fastness Fail Time /h	Ozone Fastness Fail Time /h
192 (Canon)	252	33
193 (Canon)	247	128
BCI 7M (Canon)	170	219
192 (SEC)	396	13
193 (SEC)	757	93
SEC G700M (SEC)	78	48
192 (HP)	48	30
193 (HP)	28	225
BCI 7M (HP)	16	255

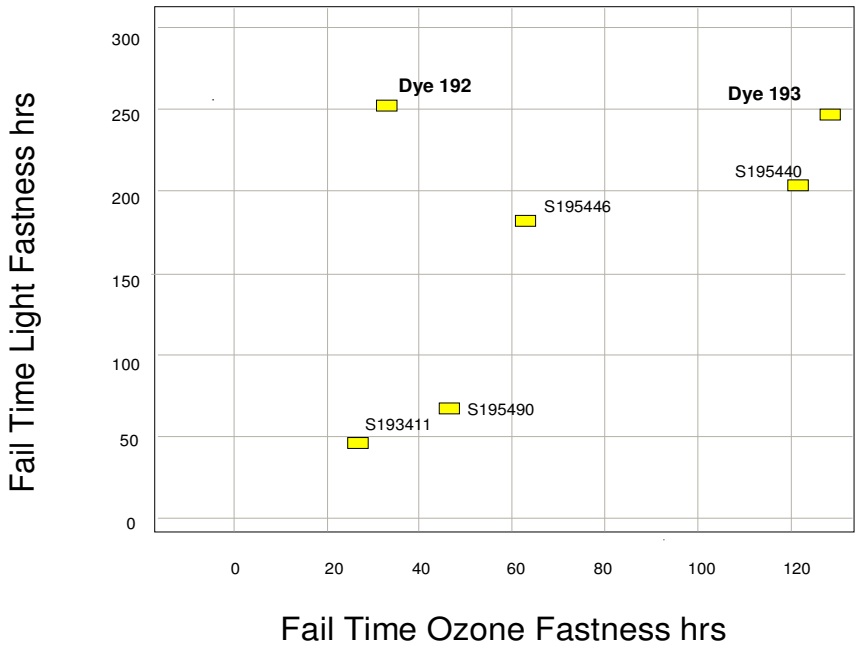

Graph 2.13.2: "Canon" formulation testing results.

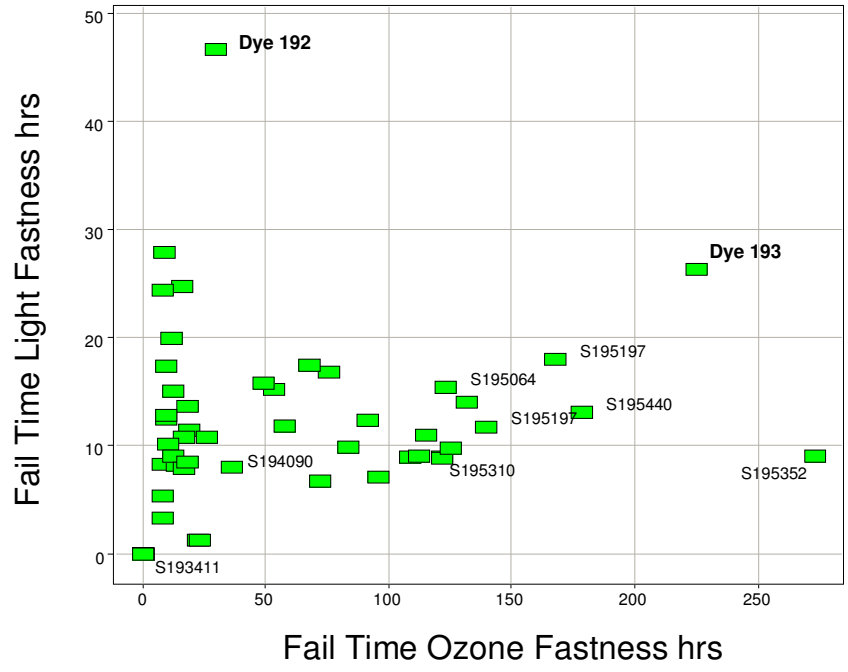

Graph 2.13.3: "HP" formulation testing results.

Analysis of these results show dyes **192** and **193** have good light fastness in comparison with the standard magenta control dyes. Dye **192** has particularly good

light fastness for all formulations although ozone fastness is lower than desired. However, dye **193** has good light fastness and improved ozone fastness when compared to dye **192** and the control magenta dyes. Dye **193** therefore gives the best mix of light and ozone fastness for magenta dyes of this type. This is particularly true for the "HP" formulation in which the dye giving the best light fastness, dye **192** has low ozone fastness and the dye giving the best ozone fastness (S195352) has low light fastness.

2.13.4: Dye Testing Conclusions

Some of the dyes analysed in this section have overall good properties required for potential magenta dyes with improved fastness. Firstly dyes **192** and **193** had good colour properties required for magenta dyes in the generic and specific ink formulations when printed onto a variety of substrates. However dye **194** failed to print due to solubility problems. In addition dyes **195** and **196** were shown to be too blue from the colour properties as shown by the low h values. The UV-vis curves also showed this, with their higher than ideal λ_{max} values.

The fastness and ozone properties of these dyes were also examined. Firstly dyes **192** and **193** showed good fastness properties in both the generic and specific ink formulations when printed on a variety of substrates and compared with similar magenta dyes previously prepared by Fujifilm. Dye **193** showed a particularly impressive balance of light and ozone fastness in the Canon and HP specific formulation inks.

However the fastness properties of dyes **195** and **196** were not as impressive and in addition to the poor colour properties indicated these were not as much use as potential magenta dyes.

2.14: Conclusions

Initial experimental synthetic routes phenanthrene based heterocyclic dyes were unsuccessful however, FVP of a biphenyl acid chloride **27** gave 4-methylfluoren-9-one **75** exclusively with no recovery of the required 9-phenanthrol **29**. Therefore a new route to fluorenones from biphenyl acid chlorides has been discovered.

Alternative routes towards the synthesis of 9-phenanthrol **29** *via* the FVP of biphenylacetic acid chloride **106** was successful in preparing the 9-phenanthrol **29** product in good yield. This method was then applied to heterocylic thiophene systems with some success to prepare naphtho[1,2-*b*]thiophen-4-ol **123** in good yield. However problems associated with self coupling in the Suzuki reaction of the 3-thiophene analogue were encountered. These problems were overcome using an alternative route by reaction of methyl (2-iodophenyl)acetate **114** with the 3-thiophene **124** and 2- and 3-furanboronic acids **128** and **129** to give the heterocyclic coupled products. FVP of these heterocyclic esters over tungsten trioxide afforded the 3-thiophene **126** and 2-furan **134** cyclised systems in low yields. This new route to heterocyclic phenanthrol systems avoided previous Suzuki reaction by-products due to self coupling and the use of unstable acid chlorides, however optimisation to increase yields and conversion is required.

It was then possible to couple 9-phenanthrol **29**, naphtho[1,2-*b*]thiophen-4-ol **123** and naphtho[2,1-*b*]thiophen-4-ol **126** with the diazonium salt of C. I. Acid Yellow 9 **136** to afford the corresponding azo compounds **137**, **138** and **139**. Initial UV analysis of these dyes showed little shift in the λ_{max} values of the absorption peaks due to the effects of the heteroatom upon the azo chromophore in comparison to the 9-phenanthrol azo dye. Scale up and testing of the effect of the heteroatom upon the fastness properties of these dyes is required.

New heterocyclic dyes could also be prepared from the condensation of heterocyclic hydrazines with 4,9-disulfophenanthrenequinone **171**. The pyridine **187**, pyridazine **188**, phthalazine **189**, isoquinoline **190** and 2-quinoline **191** disulfophenanthrene quinone dyes were prepared in good yields. These dyes were then metallised to afford the 2:1 nickel complexed magenta dyes which had increased fastness properties and were tested by Fujifilm by standard methods. This revealed that the pyridazine dye **193** has a particularly impressive balance of light and ozone fastness over similar magenta dyes.

3.0: Novel Routes to Heterocyclic Azo Compounds

3.1: Requirements of Synthetic Dyes

Dyes used in inkjet printing have to meet many requirements. The dye must display the same shade across a range of substrates, exhibit good light fastness, wet fastness and ozone fastness, high aqueous solubility to minimise crystallisation and nozzle blockage and high thermal stability. The ability of dyes to resist fading upon exposure to light and ozone is a major problem currently generating much research.

This key technical requirement of high light fastness has recently been achieved in metal-complexed dyes. Of the stable metal complexes required it is found that only meridional [5,5] complexes exhibit the required bright shades (Figure 3.1.1).

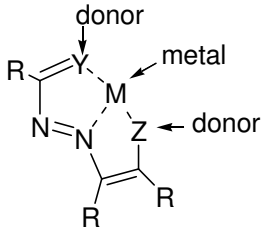

Figure 3.1.1: An example of a metallised complex (R = Ar).

Current research is focusing on increasing light and ozone fastness through the synthesis of electron deficient heterocyclic dyes (Section 1.15). These dyes are also expected to have increased resistance to photooxidation due to the electron deficient environment around the azo chromophore caused by the presence of the adjacent heterocycle. The suitability of these dyes to form a metallised complex is also of interest.

The theory is that the presence of an electron withdrawing atom (*eg*. nitrogen) within the heterocycle will enhance the push/pull mechanism resulting in the desired bathochromic shift. The presence of electron donating groups (D) on the corresponding aryl group could also enhance this mechanism (Figure 3.1.2).

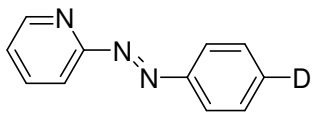

Figure 3.1.2: General structure of electron deficient azo dyes.

One of the main aims of this project is to develop novel routes to electron deficient heterocyclic azo compounds. However, standard azo coupling routes to several heterocyclic azo compounds are inapplicable due to pyridine-2-diazonium salts (and related heterocyclic diazonium salts) being unstable under aqueous conditions. The coupling of aryldiazonium salts to pyridines lacking electron donating groups cannot occur due to the deactivation of the 2-position of pyridine to electrophilic attack.

Another route to heterocyclic azo compounds involves the reaction of a hydrazine with a cyclic compound containing a good leaving group followed by oxidation. Several examples of this type of reaction have been reported involving the attack of halogen substituted pyridine systems by hydrazine derivatives to give heterocyclic azo compounds (Scheme 3.1.1).[59,60] However this does not appear to be a widely used route to azo compounds of this type.

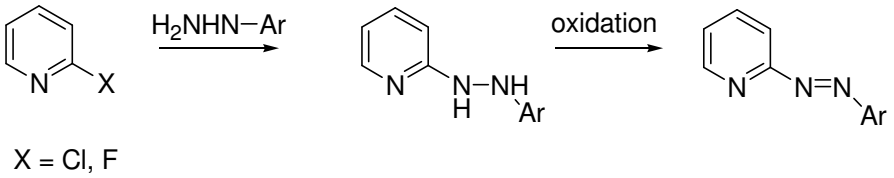

Scheme 3.1.1: Preparation of heterocyclic azo compounds.

Therefore, the aim of this section of the project is to study the scope of non-traditional condensation routes to heterocyclic azo compounds to overcome this problem.

3.2: The Mills Reaction

The Mills reaction has been known since the 19th century and involves the preparation of azo compounds by condensation of aromatic amines with nitroso compounds.[61] There are several examples of this reaction in the literature used to prepare a variety of azo compounds.

Baeyer first showed that by the action of nitrosobenzene **201** on aniline **202** in acetic acid, azobenzene **203** was formed.[62] This work was then continued by Mills to prepare a series of azo compounds by a similar method in good yield (Scheme 3.2.1).

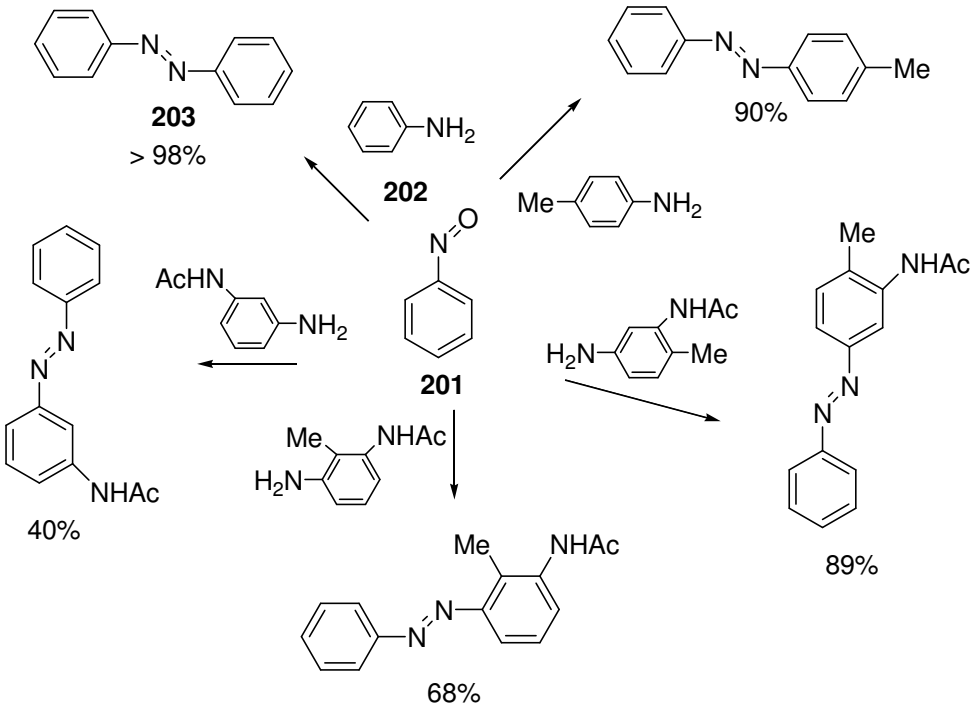

Scheme 3.2.1: Series of azo compounds prepared by Mills.[62]

This study showed the condensation of nitrosobenzene **201** with amines in glacial acetic acid was versatile under the conditions used. There are examples of various substituted amines and sterically hindered amines condensing with nitrosobenzene **201** with only slight reduction in yield of the azo product by comparison with azobenzene **203** itself. However, the reaction time and temperature were increased for more sterically hindered amines.

The mechanism of this condensation reaction has been studied in detail. Ueno and Akiyoshi carried out a kinetic study of the condensation of aniline **2** with a variety of substituted nitrosobenzenes (Scheme 3.2.2).[63] Conditions for this reaction were similar to those reported by Mills using glacial acetic acid. It was found that the rate of condensation of *p*-nitronitrosobenzene **204** with aniline **202** was twice that of nitrosobenzene **201**. Further investigation with *ortho* and *meta* substituted compounds revealed a reactivity series in which *p*- > *m*- > *o*-nitrosobenzene in terms of rate of condensation. The rate of condensation of *p*-chloronitrosobenzene **205** and aniline **202** was also found to be greater than that of nitrosobenzene **201**. However yields of the azo products of these reactions were not given.

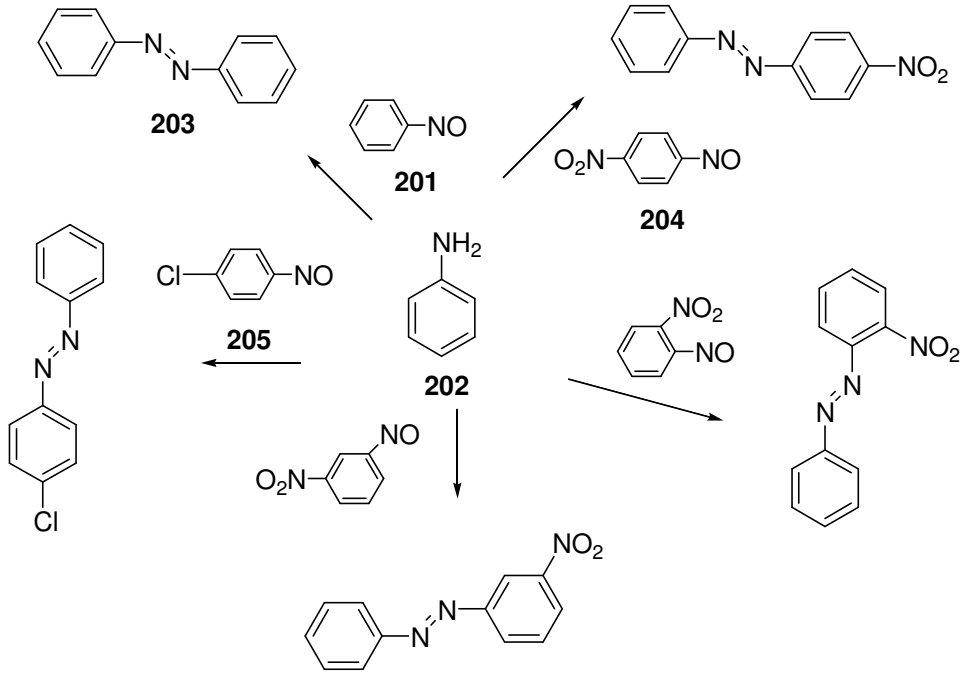

Scheme 3.2.2: Condensation of aniline with a variety of substituted nitrosobenzenes.[63]

Further investigation of the mechanism by Yunes and co-workers showed it to be subject to both hydronium ion and general acid catalysis with the rate determining step the attack of the nitroso group by the amino group (Scheme 3.2.3).[64, 65]

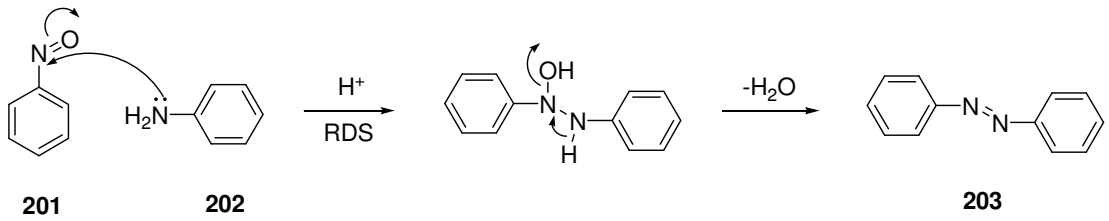

201 **202** **203**

Scheme 3.2.3: Condensation of aniline **202** and nitrosobenzene **201**.[64,65]

The rate determining step was confirmed by further investigation into the effect of various substituents around nitrosobenzene and aniline **202** upon the rate of condensation. The reaction rate increased in the presence of electron withdrawing substituents around the nitrosobenzene ring. This was due to increased electron withdrawal from the nitrogen resulting in a greater susceptibility to nucleophilic attack by aniline **202**. Likewise, the reaction rate increased due to the presence of electron donating substituents around the aniline ring due to electron donation to the amine group encouraging nucleophilic attack.

Overall this reaction has been the focus of several kinetic studies with the general conclusion that the rate of condensation is strongly dependent upon the electronic environment of the substituents around the nitrosobenzene and aniline rings. There is also evidence of steric hindrance causing a reduction in the rate of condensation due to *o*-substituents, however, this has not been studied in detail.

3.2.1: Heterocyclic Examples

The Mills reaction has been widely used in the literature however there are limited examples of this method being developed for the preparation of heterocyclic azo compounds.

One such example was reported by Campbell and co-workers in 1953 involving the condensation of nitrosobenzene **201** and substituted nitrosobenzenes **206** with 2-aminopyridine **207** in the presence of sodium hydroxide to give the corresponding azopyridines **208a,b** in a moderate yield (Scheme 3.2.4).[66]

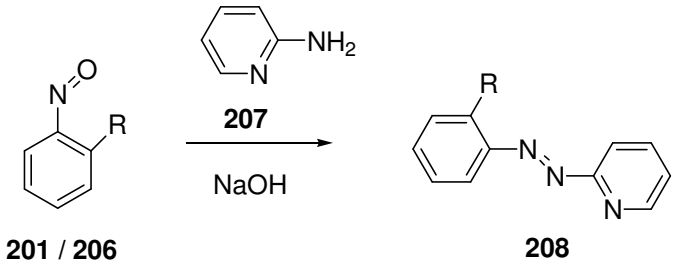

201 / 206 **208**

Scheme 3.2.4: Condensation of 2-aminopyridine **207** with nitrosobenzenes **201**,**206** to give azopyridines **208a:** R = H (82 %), **208b:** R = Cl (48 % yield).[66]

This reaction is unusual as a basic condensing agent was used and no reaction took place with the standard conditions of the Mills reaction using glacial acetic acid. The failure of 2-aminopyridine **207** to condense with nitrosobenzene **201** in an acid medium can be attributed to the addition of a proton to the ring nitrogen atom. This then results in a positive charge on the 2-amino nitrogen atom so that nucleophilic attack on the nitroso group is unrealistically slow (Scheme 3.2.5). Hence no condensation occurs in acid media.

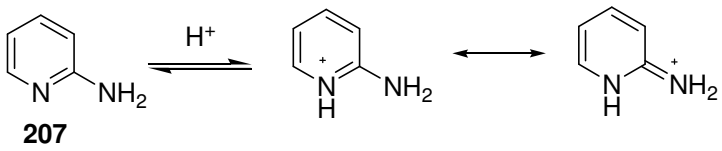

207

Scheme 3.2.5: Protonation of 2-aminopyridine **207**.

The use of a basic condensing agent deprotonated the amino group of 2-aminopyridine **207** to give the anion which could then attack the nitroso group. Subsequent protonation of the oxygen anion and dehydration afforded the pyridine-2-azo species **208** (Scheme 3.2.6).

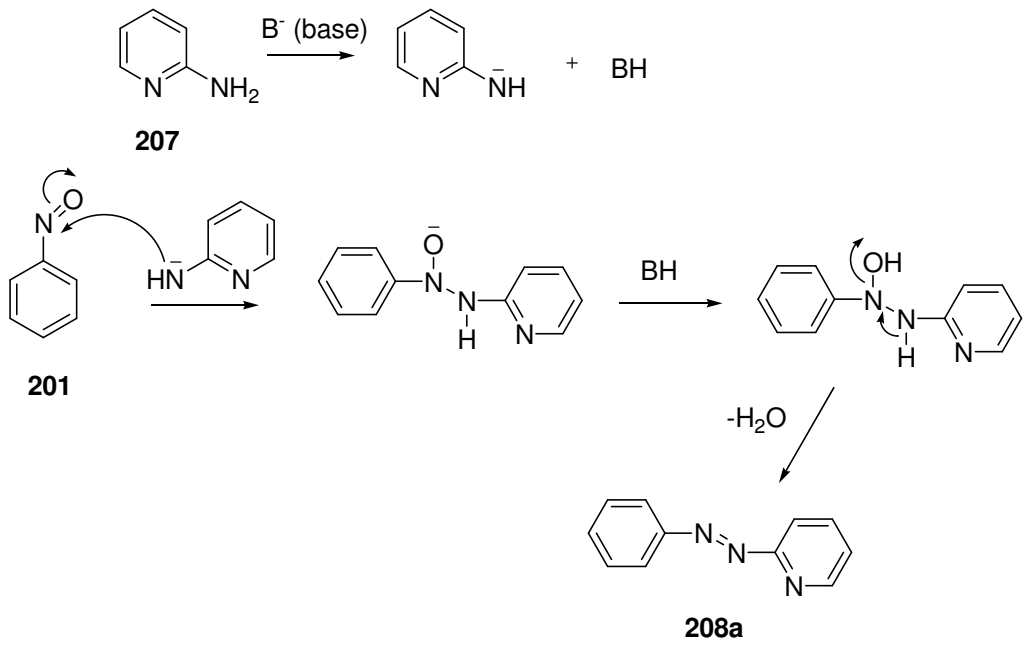

Scheme 3.2.6: Base induced condensation to pyridine-2-azo species **208**.

Research into this system was extended to include various substituted 2- and 3-aminopyridines to give the corresponding azopyridines in high yield. For example, 5-bromo-2-phenylazopyridine **209**, 3,5-bromo-2-phenylazopyridine **210** and 4-methyl-2-phenylazopyridine **211** could be prepared by treatment of nitrosobenzene **201** with the appropriate aminopyridine in the presence of sodium hydroxide solution (Scheme 3.2.7).

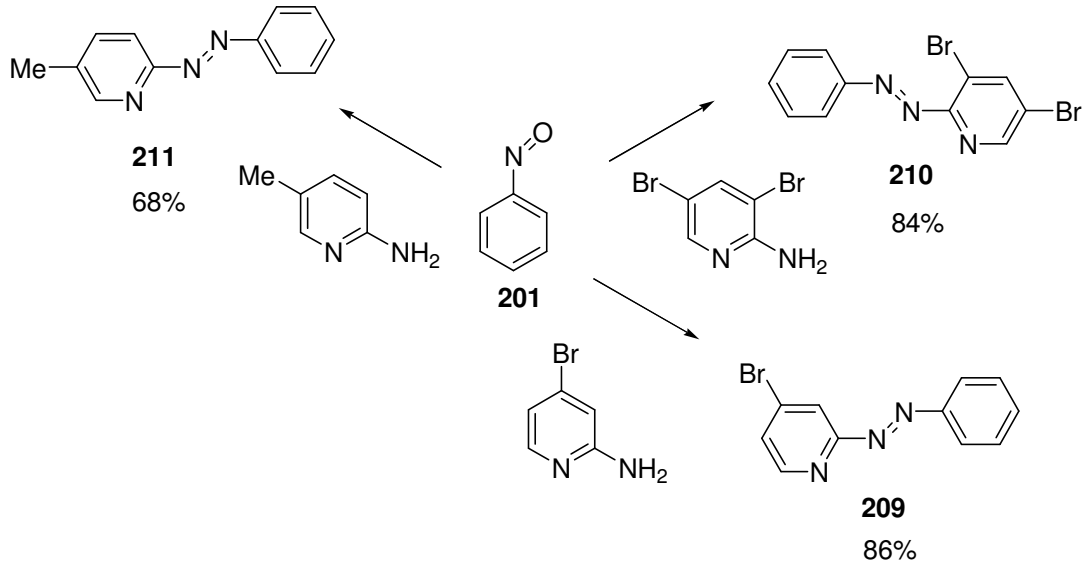

Scheme 3.2.7: Reaction of nitrosobenzene **201** with substituted 2-aminopyridines.[66]

3-(Phenylazo)pyridine **213** and 4-(phenylazo)pyridine **212** were also prepared by this method though the corresponding aminopyridines were inert in acid solution (Scheme 3.2.8).

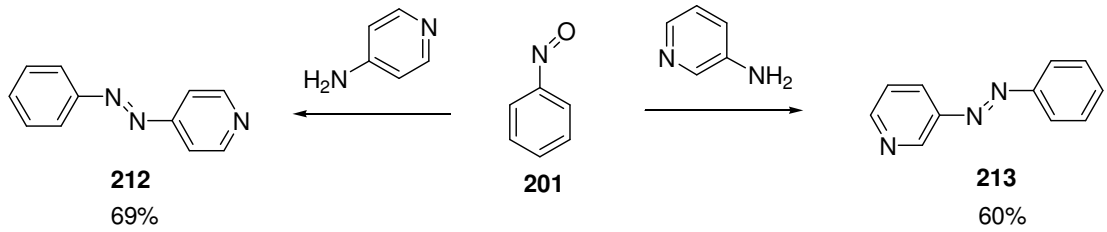

Scheme 3.2.8: Preparation of 3- and 4-(phenylazo)pyridines.[66]

Overall this method for the preparation of heterocylic azo compounds appeared to be versatile with only minor reductions in yield due to the presence of substituents around the phenyl and pyridine rings.

In subsequent reports the method devised by Campbell and co-workers appears to have been used as a standard preparative route to 2-(phenylazo)pyridine **208a** and other heterocyclic azo compounds with work being extended to some larger systems and with sodium metal used as an alternative to sodium hydroxide in some cases [67, 68, 69, 70, 71] This method appears to be an attractive route to heterocyclic azo compounds from heterocyclic amines.

3.2.2: Preparation of Azo Systems from Heterocyclic Nitroso Compounds

There have also been alternative methods for the preparation of heterocyclic azo compounds reported. One such method, reported by Taylor and co-workers, involved the preparation of 2-nitrosopyridine **215a** and 4-methyl-2-nitrosopyridine **215b** from the corresponding 2-aminopyridine **207** or 4-methyl-2-aminopyridine **207b** which could then condense with the aromatic amines **216a,b** to give the pyridine azo compounds **217a-d**.[72] This route to heterocyclic nitroso compounds involved the preparation of *S,S*-dimethylsulfilimine derivatives **214a,b** of the various aminopyridines from amino substituted heterocycles, dimethyl sulfide and *N*-chlorosuccinimide (NCS). This formed the sulfonium salt which was deprotonated with sodium methoxide to give the *S,S*-dimethylsulfilimines **214a,b**. Conversion to

the heterocyclic nitroso compounds **215a,b** then occurred by oxidation with *m*-chloroperbenzoic acid, subsequent deprotonation and loss of dimethylsufide.

The nitrosopyridines **215a,b** can then undergo subsequent condensation with *p*-substituted aromatic amines **216a,b** catalysed by trace amounts of glacial acetic acid in dichloromethane to give the corresponding azopyridines **217a-d** in a moderate to good yield (Scheme 3.2.9).

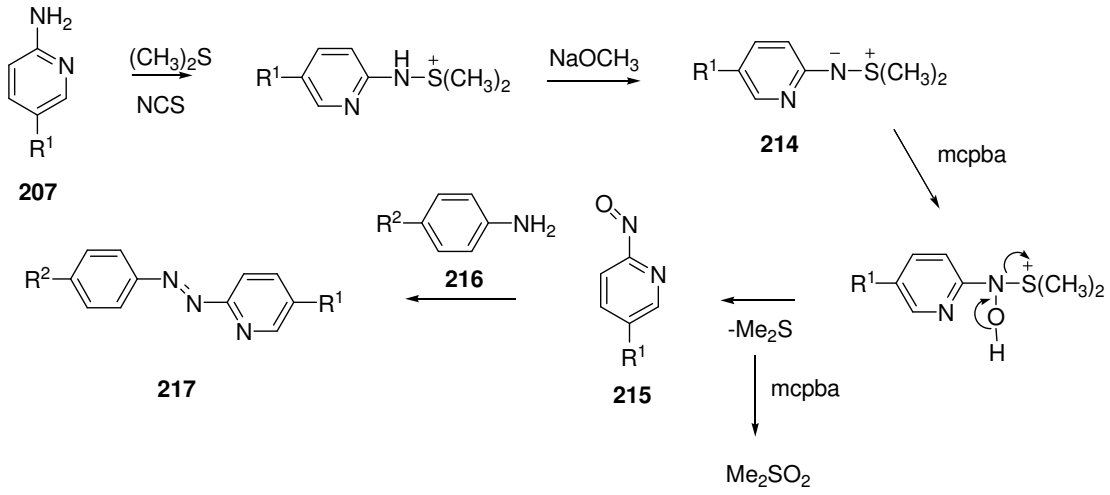

207a / 214 a / 215a: R^1 = H

207b / 214b / 215b: R^1 = Me

216a: R^2 = Cl

216b: R^2 = OMe

217a:	R^1 = H,	R^2 = Cl	50% yield
217b:	R^1 = H,	R^2 = OMe	70%
217c:	R^1 = Me,	R^2 = Cl	78%
217d:	R^1 = Me,	R^2 = OMe	83%

Scheme 3.2.9: Preparation of azopyridines **217a-d** from nitrosopyridines **215a,b**.[72]

There were also examples of azo derivatives of pyrimidine **218**, pyrazine **219, 220** and isoquinoline **221** heterocycles reported. Likewise, these were prepared *via* the dimethylsulfilimines from the appropriate amines and gave the corresponding azo compounds in moderate to good yields on treatment with aromatic amines (Scheme 3.2.10).

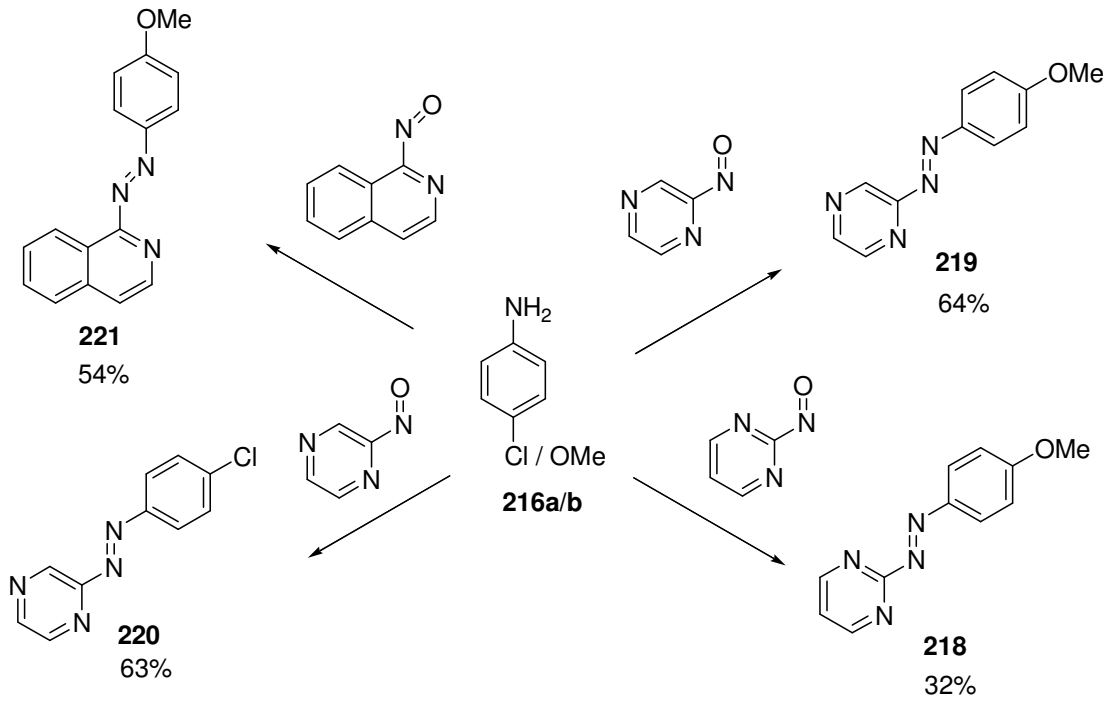

Scheme 3.2.10: Preparation of azopyrimidines, azopyrazines and azoisoquinolines.[72]

This reaction is an attractive route to unstable heterocyclic nitroso compounds with transformation of the primary amino groups *via* nitroso groups to azo dyes carried out sequentially in one vessel without the requirement for isolation of either the intermediate sulfilimine or the highly reactive and often unstable nitroso compound.

3.2.3: Heterocyclic Azo Systems from Nitroaryls Compounds

Alternate routes to azopyridine systems were reported by Okubo and co-workers.[73] These involved the condensation of iminodimagnesium reagents **223** derived from 2-amino-4-methylpyridine **222** with nitrobenzenes **224a-c** to give the corresponding azobenzenes **225a-c**. The first step in this process was the preparation of the iminodimagnesium reagent **223** from 4-methyl-2-aminopyridine **222** by treating with ethylmagnesium bromide in THF. This was then allowed to react with *p*-(Me, Cl, OMe) substituted nitrobenzenes **224a-c** to give the required azopyridine **225a-c** product and a variety of by-products **226**, **227** and **228** (Scheme 3.2.11, Table 3.2).

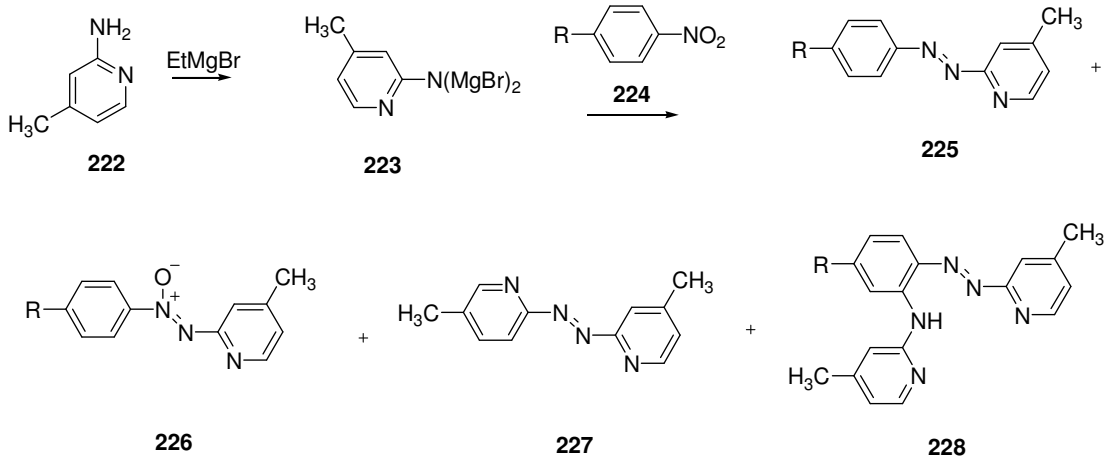

a: R = Me, **b**: R = Cl, **c**: R = OMe

Scheme 3.2.11: Reaction of iminodimagnesium reagent **223** with substituted nitrobenzenes **224a-c**.[73]

The azoxy by-product **226** was formed by attack at the nitro group and loss of the hydroxyl ion, the azo product **225** by deoxygenation of the azoxy and the symmetrical azo dimer **227** by oxidative dimerisation. There was also the presence of an *ortho* substituted by-product **228** although no mechanism of the formation of this by-product was proposed.

The yield distribution of these products appeared to be dependent upon the reaction time and the excess of iminodimagnesium reagent **223** relative to the nitrobenzene **224a-c** with some of these summarised in Table 3.2.

Table 3.2: Product distribution under varying reaction conditions

R	[**223**] / [**224**]	Reaction Time / h	Yield / % of **225**	Yield / % of **226**	Yield / % of **227**	Yield / % of **228**	Yield / % Recovery of **224**
Me	1.1	1.5	7	18	4	trace	71
Me	1.1	3.5	17	16	4	1	58
Me	2.5	1.5	31	16	7	2	39
Me	10.0	5.0	74	0	13	5	0
Cl	2.5	1.5	29	24	12	3	30
OMe	2.5	1.5	26	22	5	3	37

From these results it can be concluded that using an excess of the iminodimagnesium reagent **223** increases the yield of the azopyridine **225a** product in relation to the azoxypyridine **226a**. For a low yield of azoxypyridine **226a** prolonged heating and a large excess of iminodimagnesium reagent **223** is required so that the azoxypyridine **226a** completely consumed to yield the azopyridine **225a**. However there is an increased yield of the dimeric by-product **227a** and the *ortho*-substituted by-product **228a**. The unfavourable azoxy **226b,c**, dimeric **227b,c** and *ortho*-substituted by-products **228b,c** are also observed in the case when R = Cl and R = OMe although conditions of these reactions were not optimised to minimise yields of these by-products.

Although this reaction uses more stable and widely available nitrobenzene **224** derivatives rather than unstable nitroso reagents this route to azopyridines is unattractive due to the range of by-products observed. There is evidence that the yield of these by-products and in particular the azoxypyridine **226a-c** intermediate may be reduced with increased reaction time and excess of iminodimagnesium reagent **223** used, however further study into the optimisation and applicability of this reaction towards other heterocyclic azo compounds is required.

Another non-traditional route to heterocyclic azo compounds involves synthesis of azopyridines from the reaction of aromatic nitro compounds and aminopyridines. The first example of this was reported by Faessinger and Brown in 1951.[74] This involved the preparation of *para*-substituted phenylazopyridines **230** in

moderate yields from 2-aminopyridine **207** and the corresponding *para*-substituted nitrobenzene **229** in the presence of sodium metal in toluene solution (Scheme 3.2.12).

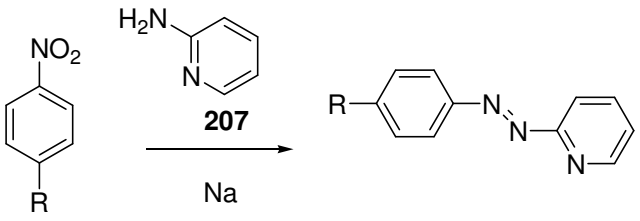

229 **230**

i): R = H	41% Yield	iii): R = Me	43%	v): R = NMe_2	35%
ii): R = Cl	45%	iv): R = OMe	55%		

Scheme 3.2.12: Preparation of phenylazopyridines by the Faessinger & Brown method.[74]

There are several reports of the preparation of 2-(phenylazo)pyridine **230i** using this method.[75, 76, 77] 2-(4-Methoxyphenyl)azopyridine **230iv** was also prepared by the same method but in a much reduced yield of 5%.[78] A variation of this method was also reported to prepare a guanidine derivative **232** from 2-(4-nitrophenyl)tetramethylguanidine **231.** However, no yield was given (Scheme 3.2.13).[79]

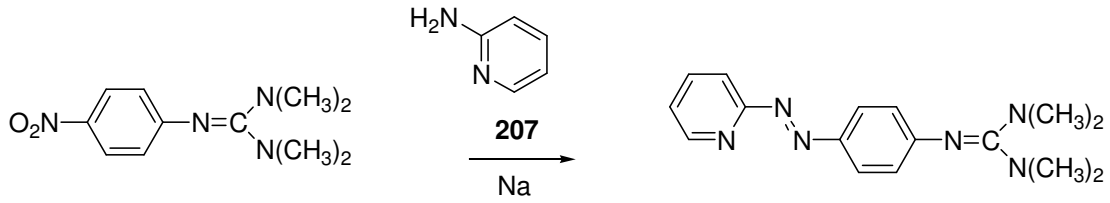

231 **232**

Scheme 3.2.13: Preparation of pyridine-2-azo-*p*-phenyltetramethylguanidine **32**.[79]

This method by Faessinger and Brown appears to have become the standard route used for the preparation of azopyridine compounds from the reaction of arylnitro compounds and aminopyridines, however, the mechanism has yet to be studied in detail. One possible mechanism involves nucleophilic attack of the nitro group **229** by the anion of the amine. The intermediate can then undergo loss of the

hydroxide ion to give the azoxy compound **233**, which is reduced under the reaction conditions to give the azo product **230** (Scheme 3.2.14).

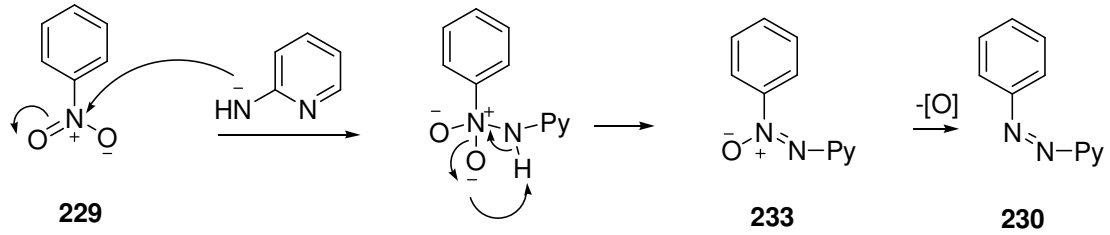

Scheme 3.2.14: Possible mechanism for azo coupling of nitro group to the amine.

There are examples of reaction of a nitro group with an amine under basic conditions to give an azoxy compound (Scheme 3.2.15). Angeli and Marchetti first reported the reaction of nitrobenzene **229** with aniline **202** in the presence of sodium to give azoxybenzene in 1906.[80] Further examples of the preparation of azoxy compounds from the reaction of a nitro group with an amine group in the presence of sodium or other strong bases were also reported. These include the reaction of α-naphthylamine **234** and 1-nitronaphthalene **236** with nitrobenzene **229** and aniline **202** respectively, which gave α-azoxynaphthalene **235a,b** in two isomeric forms (Scheme 3.2.15).[80] However, intermolecular reactions of this type using heterocyclic amino reagents have not been investigated in detail.

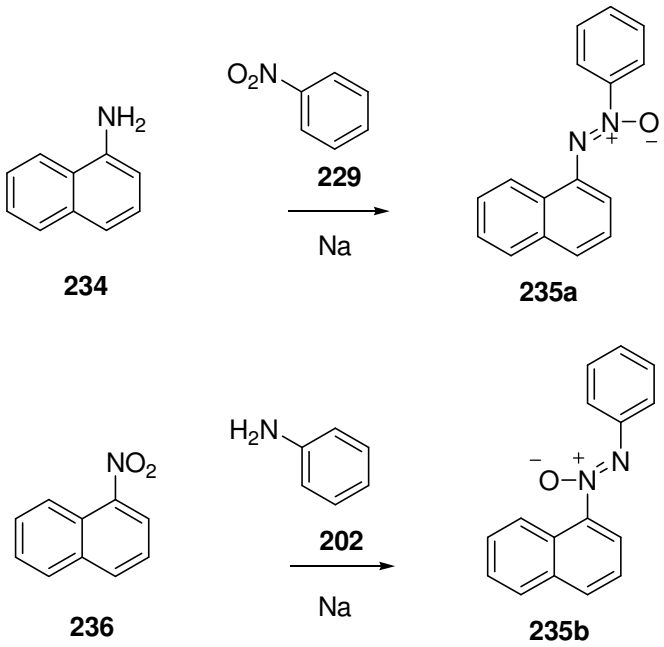

Scheme 3.2.15: Preparation of naphthalene examples of azoxy compounds.[80]

There are also intramolecular examples of the reaction of nitro and amino groups in the presence of a strong base to give heterocyclic *N*-oxides. These examples involve the warming of *o*-nitrophenylguanidines **237a,b** or *o*-nitrophenylureas **238** with aqueous alkali to yield 3-substituted benzo-1,2,4-triazine-*N*-oxides **239a-d** (Scheme 3.2.16).[81]

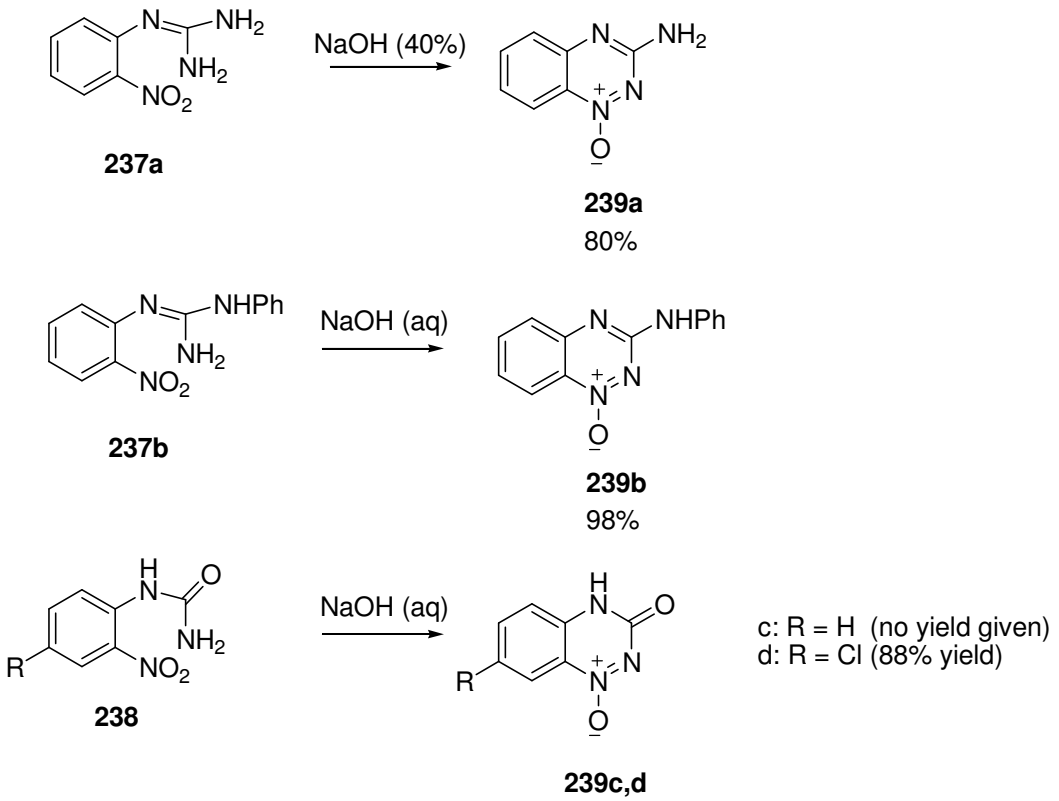

Scheme 3.2.16: Base catalysed cyclisation of *o*-nitrophenylguanidines **237a.b** and *o*-nitrophenylureas **238**.[81]

Various conditions for these reactions have been reported including the use of sodium hydroxide and potassium hydroxide although using aqueous sodium hydroxide appears to give the highest yields of the 3-substituted benzo-1,2,4-triazine-*N*-oxides and benzotriazinone *N*-oxides **239a-d**.[81, 82, 83]

Therefore the reaction of nitro groups with amines in the presence of base appears to be an attractive route the required aromatic azopyridine targets discussed in this study. A proposed alternative synthesis of heterocyclic azo compounds could be the reaction of nitroaryl rings with 2-aminopyridine **7** or other heterocyclic amines in the presence of sodium metal to give the required heterocyclic azo compounds.

This synthesis would avoid the problem of the limited availability and stability of nitroso compounds and would offer access to a variety of azo compounds.

3.2.4: Conclusions

In conclusion, there are four main routes to heterocyclic azo compounds reported in the literature. The most widely used and attractive route appears to be the condensation of nitrosobenzenes with aminoheterocycles and secondly the condensation of nitrosoheterocycles with aminobenzenes. Both of these occur *via* the Mills reaction in good yield with several examples of the robustness of this reaction also studied.[61]

There is also the reaction of iminodimagnesium reagents **223** with nitrobenzenes **224a-c** although there are few examples of this reported.[73] A further route to heterocyclic azo compounds reported which has not appeared to have undergone much recent investigation was the reaction of an amine with a nitro group in the presence of a strong base studied in some detail by Faessinger and Brown.[74]

3.3: Synthesis of Azo Systems from Nitroaryl Compounds

In the reaction of a nitroaryl compounds with 2-aminopyridine **207** to give azo compounds as proposed by Faessinger and Brown only five *para* substituted examples were reported (Scheme 3.2.12).[74]

The aim of this section is firstly to extend study of these reactions to include further substituted examples. No examples of the reaction of an *ortho* substituted aromatic nitro compounds with 2-aminopyridine **207** have been reported. There was also particular interest in the effect of *ortho* substituents with electron donating ability upon the formation and yields of the azo products due to the ability of these substituents to coordinate to a metal centre to give [5,5] metallised complexes.

Target azo compounds containing electron donating substitutents were of interest as the additional electron donating substituent would lead to enhanced conjugation between the aryl and pyridine rings increasing the bathochromic shift in the UV spectra. The application of this reaction to naphthalene and quinoline systems to obtain the corresponding azo compounds is also of interest.

Finally, another aim was investigation of the use of alternative reaction conditions such as the use of alternate bases and solvents to optimise yields.

3.3.1: Preparation of 2-(Phenylazo)pyridine

Firstly 2-(phenylazo)pyridine **230a** was prepared by the reaction of 2-aminopyridine **207** with nitrobenzene **229a** in the presence of sodium metal. This gave the azo product **230a** in an increased yield of 62% compared with the literature yield of 41% (Scheme 3.3.1).[74] This product was identified by ^{1}H and ^{13}C NMR spectra in addition to mass spectrometry. The IR spectrum of the product also showed a characteristic azo absorption peak at 1421 cm^{-1} in agreement with the literature.[84]

The preparation of 2-(phenylazo)pyridine **230a** was repeated with the use of THF as the reaction solvent which resulted in a slight reduction in the yield of the azo product **230a** (Table 3.3.1).

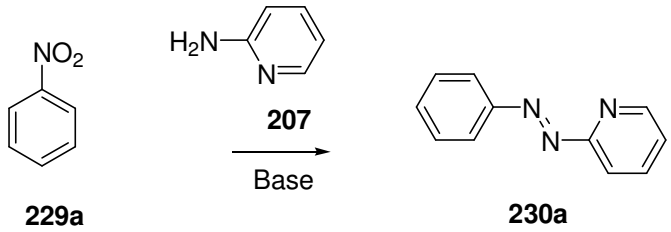

Scheme 3.3.1: Reaction of nitrobenzene **229a** and 2-aminopyridine **207**.

Table 3.3.1: Reaction yields

Base	Solvent	Azo yield 230a
Na	Toluene	63%
Na	THF	49%

A notable characteristic of the above reactions was that, following slow addition of sodium metal to the reaction mixture with stirring and gentle heating, the reaction mixture then suddenly turned black with gas evolution. The heat was then removed until gas evolution had subsided and was reapplied slowly with stirring until the black coloured reaction mixture was at reflux. Upon reaction completion, workup and purification of this black reaction mixture a surprisingly high yield of required azo compound **230a** was isolated.

The reaction of nitrobenzene **229a** and 2-aminopyridine **207** was then repeated with the use of sodium hydride the base. Sodium hydride has previously been used as a deprotonating agent in several literature reactions. These include the use of sodium hydride as a strong base in Claisen condensations (Scheme 3.3.2).[85, 86]

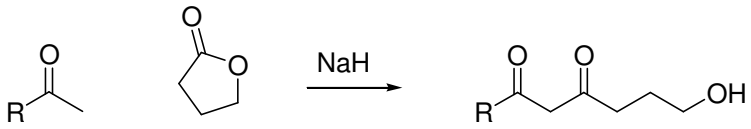

Scheme 3.3.2: Use of NaH in the Claisen condensation.[85]

Sodium hydride is a strong base but would result in less harsh reaction conditions than using metallic sodium and therefore may be expected to avoid decomposition of reagents or products. However, sodium hydride has more generally

been used as a base as opposed to as a reducing agent. Therefore the expected outcome of this experiment was to obtain the azoxy product **233** which could then undergo subsequent reduction to the required azo **230a** (Scheme 3.3.3). However, under these conditions the azo product **230a** was obtained directly with none of the expected azoxy **233** isolated (Table 3.3.2).

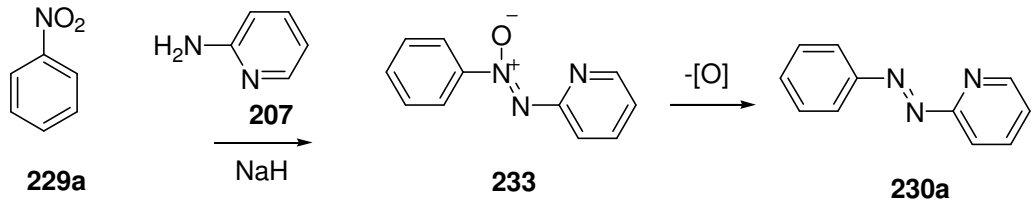

Scheme 3.3.3: Reaction of nitrobenzene **229c** and 2-aminopyridine **207**.

Table 3.3.2: Reaction Yields

Base	Solvent	Azo yield 230a
NaH	Toluene	40%
NaH	THF	24%

This was unexpected and it was unclear how the reduction step takes place under sodium hydride reaction conditions (Scheme 3.3.3). Azoxy compounds have previously been transformed to the azo product using several reducing agents such as triphenylphosphine, lithium aluminium hydride, sodium methoxide, potassium hydroxide and phosphorus trichloride.[86] However there have been no reports of the reduction of the azoxy group to an azo in the presence of sodium hydride. Therefore further investigation is required to determine how this occurs. The exposure of an authentic sample of the azoxy **233** to reaction conditions in the presence of sodium hydride could be carried out to investigate the mechanism further.

Overall, these results showed the literature conditions involving sodium metal and toluene appeared to afford the azo product **230a** in the highest yield (Table 3.3.1). There was the possibility of the use of sodium hydride and extension to other bases such as sodium hydroxide and potassium hydroxide which had been previously reported in the synthesis of azoxy compounds from the reaction of a nitroaryl compound and an amine. [81, 82, 83, 92]

3.3.2: Preparation of Substituted Azopyridines

Due to the successful preparation of 2-(phenylazo)pyridine **230a** by the reaction of nitrobenzene **229a** with 2-aminopyridine **230a** in the presence of both sodium and sodium hydride these routes to other heterocyclic azo compounds were investigated. The robustness of the Faessinger and Brown route to azo compounds was investigated by reaction of a variety of substituted nitroaryl compounds **229b-j**, nitronaphthalene **229k** and 8-nitroquinoline **229l** with 2-aminopyridine **207** with the aim of obtaining the corresponding heterocyclic azo compounds **230b-l** (Scheme 3.3.4). These reactions could be carried out in the presence of either sodium or sodium hydride.

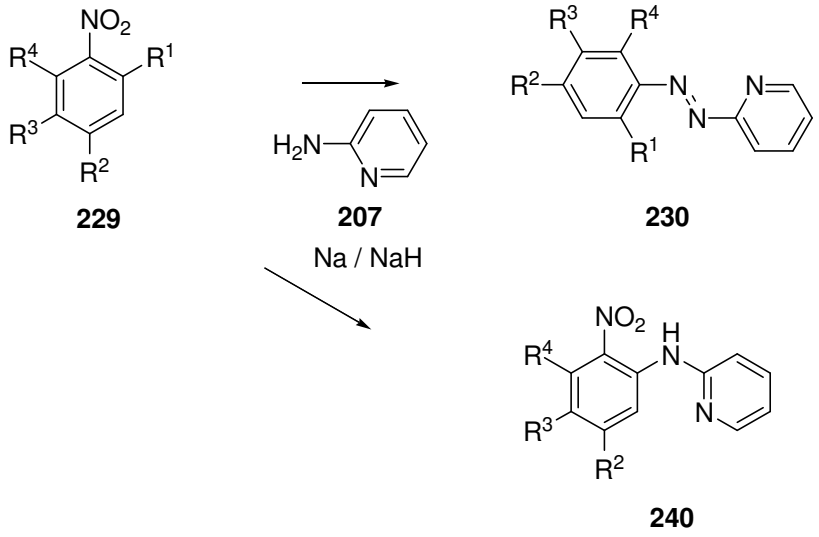

Scheme 3.3.4: Reaction of nitro compounds **229** with 2-aminopyridine **207**.

The results of these reactions showed two types of reaction products are possible (Scheme 3.3.4). Firstly reaction of 2-aminopyridine **207** can occur at the nitro group of the nitroaryl **229** to give the required azo product **230**. Secondly reaction could occur at the *ortho* position of the nitroaryl **229** relative to the nitro group resulting in nucleophilic displacement of the substituent and giving a nitro by-product **240**. In some cases a mixture of products was obtained. Evidence of this conclusion will be detailed in the remainder of the chapter. The reaction yields of isolated products purified by dry flash column chromatography were determined (Table 3.3.3).

Table 3.3.3: Product Yields (*Py = pyridine, Ph = phenyl)

Nitro starting material **229**								
	R^1	R^2	R^3	R^4	Azo **230** Yield	By-product **240** Yield	2-aminopyridine **207** Recovered	Base
b	H	Cl	H	H	9%	-	-	Na
c	OMe	H	H	H	1%	-	-	Na
c	OMe	H	H	H	28%	18%	49%	NaH
d	NHPy *	H	H	H	3%	-	-	Na
e	NHPh *	H	H	H	-	-	-	Na
f	OH	H	H	H	-	-	51%	NaH
g	OMe	OMe	H	H	-	10%	29%	NaH
h	OMe	$N(Et)_2$	H	H	-	41%	47%	NaH
i	OMe	$N(CH_2)_5$	H	H	-	30%	35%	NaH
j	O*i*Pr	$N(Et)_2$	H	H	-	17%	62%	NaH
k	H	H	CH=CH-CH=CH		-	-	-	Na
k	H	H	CH=CH-CH=CH		-	13%	-	NaH
l	H	H	N=CH-CH=CH		-	1%	-	NaH

3.3.3: Reaction of Substituted Nitro Compounds to Give Azo Products

The reaction of the nitro compound **229** with 2-aminopyridine **207** to afford the required azo compound **230** occurred in some cases. Firstly, *p*-chloronitrobenzene **229b** underwent a reaction with 2-aminopyridine **207** to give 2-(4-chlorophenylazo)pyridine **230b** in 9% unoptimised yield (Scheme 3.3.4). There was also an approximately equal amount of crude *p*-chloroaniline recovered as a by-product. However, no by-product involving the loss of chloride by nucleophilic displacement was obtained. The yield of azo product **230b** obtained in this reaction was significantly lower than the literature yield of 45% which may be due problems encountered during recovery and purification.[74]

In order to investigate the effect of *ortho* substituents upon this type of reaction 2-nitroanisole **229c** was heated with 2-aminopyridine **207** in the presence of

sodium metal. This gave 2-(2-methoxyphenylazo)pyridine **230c** but in only 1% yield (Scheme 3.3.5). Two other by-products were also isolated from the reaction mixture. Firstly 2-[2-(2-pyridylamino)phenylazo]pyridine **230d** was obtained in 13% yield as the main product and in addition to this 1-methoxyphenazine **241** was obtained in < 1% yield.

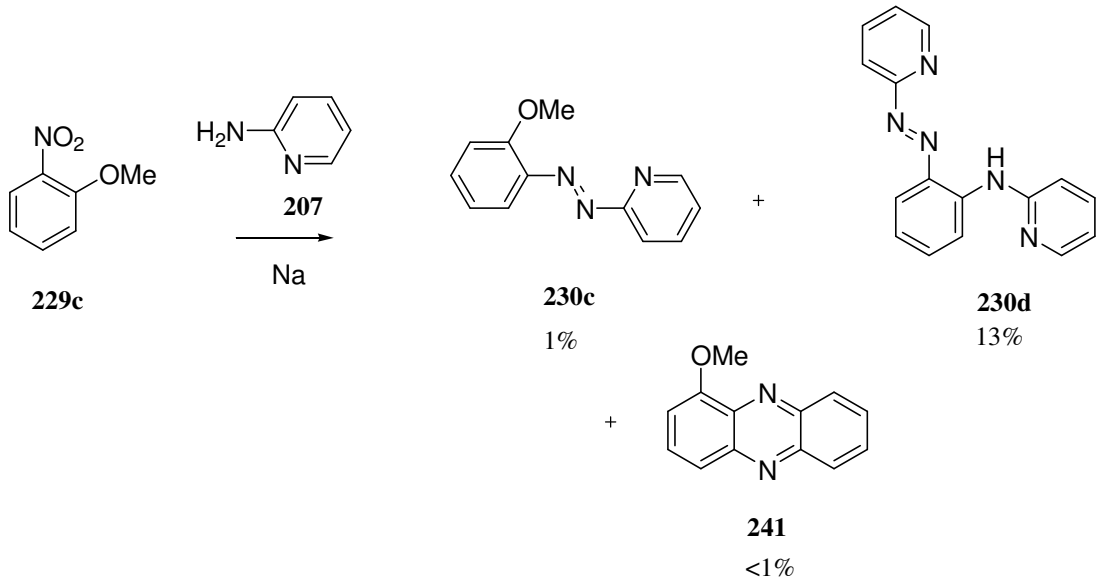

229c

230c
1%

230d
13%

241
<1%

Scheme 3.3.5: Reaction of 2-nitroanisole **229c** with 2-aminopyridine **207**.

The major product **230d** of this reaction was fully characterised by standard spectroscopic methods. Firstly the electron impact mass spectrum revealed a compound with a molecular ion peak of *m/z* = 275. Analysis of the ^{1}H NMR spectrum indicated twelve protons were present in the aromatic region which together with the multiplicity of the signals present indicated that there were two pyridine units and one benzene ring in the product. The ^{1}H NMR spectrum also showed an NH peak at δ = 10.62 and no sign of a methyl peak corresponding to an *ortho* methoxy substituent. Finally the IR spectrum contained an azo group absorption peak at 1423 cm^{-1}. Using this information 2-[(2-(2-pyridylamino)phenylazo]pyridine **230d** was proposed as the major product of the reaction and positively identified by 2D NMR spectroscopic methods.

In addition to spectral evidence for the formation of 2-[(2-(2-pyridylamino)phenylazo]pyridine **230d** a sample was prepared by the reaction of *N*-(2-nitrophenyl)pyridin-2-ylamine **229d** with 2-aminopyridine **207** in the presence of sodium metal. This gave the required azo product **230d** in 3% yield and the reduced amine **242** in 6% yield (Scheme 3.3.6).

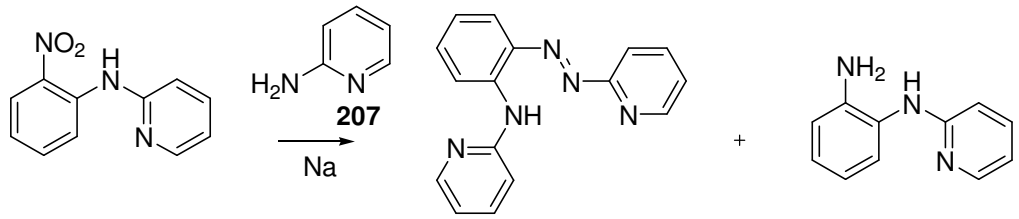

229d **230d** 3% **242** 6%

Scheme 3.3.6: Alternative synthesis of major by-product **230d**.

Two possible mechanisms are proposed for the formation of this azo by-product **230d**. The first mechanism involves nucleophilic attack on 2-nitroanisole **229c** by the 2-aminopyridine **207** anion at the *ortho* position relative the nitro group which displaces the methoxy group and gives (2-nitrophenyl)pyridin-2-ylamine **229d/240c**. This can then undergo reaction with a further molecule of the 2-aminopyridine **207** anion by the mechanism mentioned earlier to give 2-[2-(2-pyridylamino)phenylazo]pyridine **230d** (Scheme 3.3.7).

Secondly it is possible that the mechanism involves nucleophilic attack on the methoxy group of 2-(2-methoxyphenylazo)pyridine **230c** after formation of the azo compound (Scheme 3.3.7).

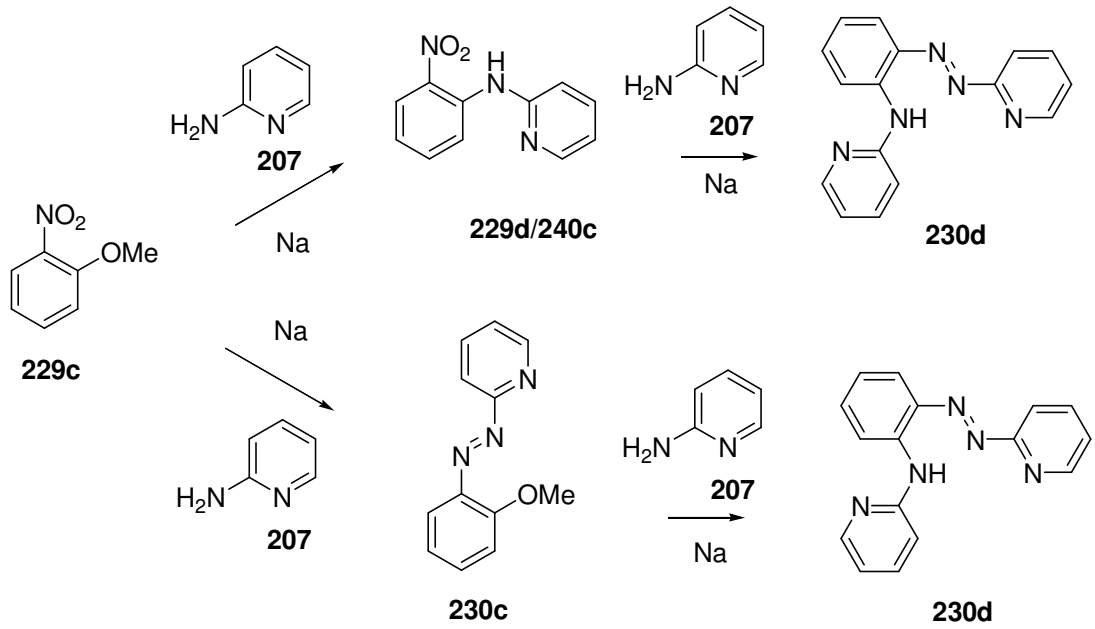

Scheme 3.3.7: Possible routes to the main by-product **230d**.

The observation that none of the reduced amine **242** was isolated from the reaction of 2-nitroanisole **229c** with 2-aminopyridine **207** indicates *N*-(2-nitrophenyl)pyridin-2-ylamine **229d/240c** is not an intermediate in the formation of 2-[(2-(2-pyridylamino)phenylazo]pyridine **230d** as proposed in scheme 3.3.7. This indicated that the formation of **230d** may proceed *via* the azo compound **230c**.

However if the methoxy group is indeed lost by nucleophilic attack of the azo **230c**, a similar reaction may be expected in the case of 2-(4-chlorophenylazo)pyridine **230b** as chlorine is a better leaving group than methoxy hence substituted easier to give 2-[(4-(pyridylamino)phenylazo]pyridine **243** which was not detected (Scheme 3.3.8).

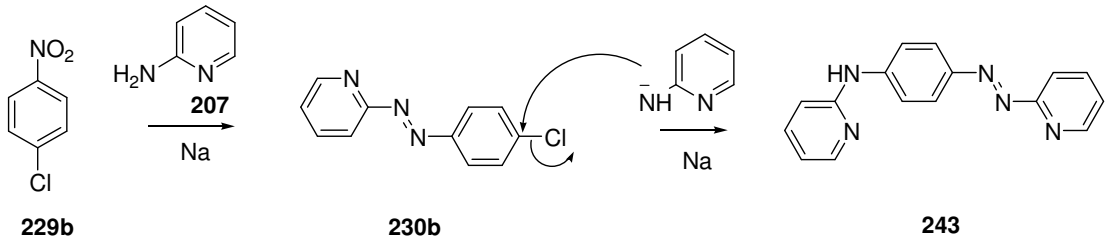

Scheme 3.3.8: Product expected by nucleophilic substitution of the chloro substituent.

A possible explanation for this observation is that the formation of 2-[(2-(2-pyridylamino)phenylazo]pyridine **230d** by nucleophilic substitution of the *ortho* methoxy group involves chelation of the sodium metal centre to the azo **230c** and the approaching 2-aminopyridine **207** (Scheme 3.3.9). Therefore formation of this intermediate metal complex **244** encourages nucleophilic substitution at the *ortho* position of **230c**. However in the case of 2-(4-chlorophenylazo)pyridine **230b** this coordination is not possible and therefore none of by-product **243** is isolated.

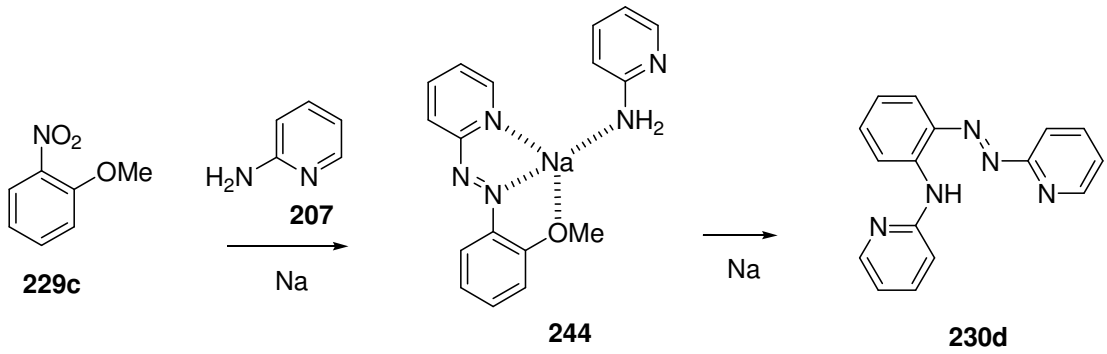

Scheme 3.3.9: Formation of **230d** by metal coordination.

A proposed mechanism for the formation of 1-methoxyphenazine **241** is that 2-nitroanisole **229c** is reduced to the amine by sodium metal. The corresponding anion then attacks the 3-position of 2-nitroanisole **229c**. Dehydration forms a nitroso compound which then undergoes ring closure with the adjacent ring to form a *N*-hydroxyphenazine ring structure. Subsequent loss of formaldehyde and water then affords 1-methoxyphenazine **241** (Scheme 3.3.10).

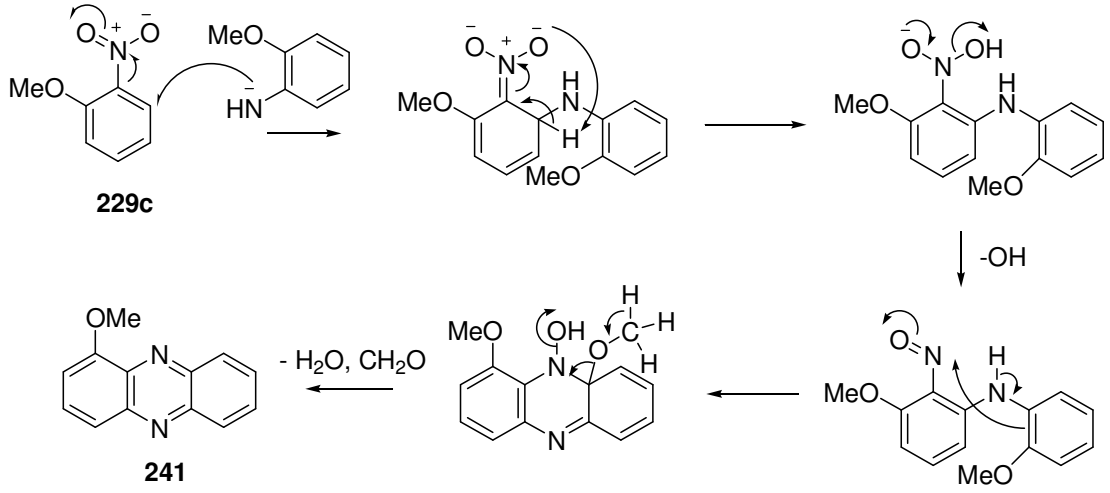

Scheme 3.3.10: Possible mechanism for the formation of 1-methoxyphenazine **241**.

A related cyclisation known as the Wohl-Aue reaction to give phenazine **245** has been known since the early 20th century and involves the vigorous heating of aniline **202** and nitrobenzene **229a** in the presence of a strong base (Scheme 3.3.11).[87]

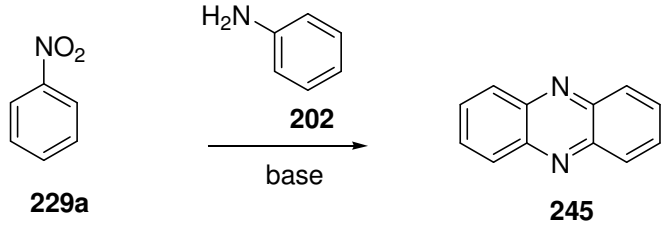

Scheme 3.3.11: Wohl-Aue reaction for synthesis of phenazine **245**.[87]

Previous examples describing the loss of methoxy groups in the Wohl-Aue reaction are known.[88] The preparation of 1-methoxyphenazine **241** in 4% yield in addition to 1,6-dimethoxyphenazine **247** in 10% yield has also been reported by the reaction of 2-nitroanisole **229c** with *o*-anisidine **246** in the presence of potassium hydroxide (Scheme 3.3.12).[88,89]

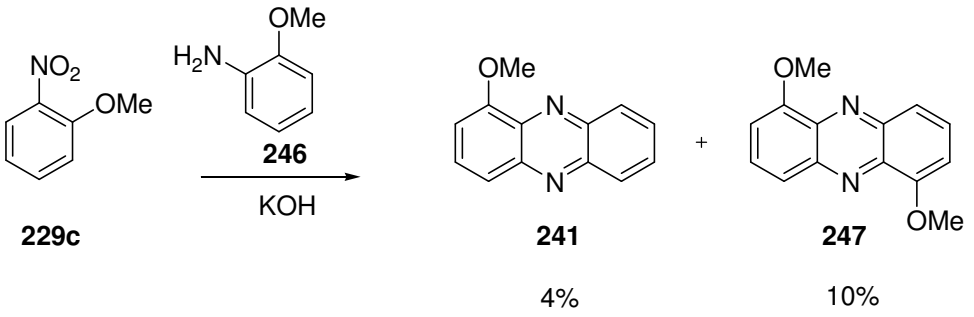

Scheme 3.3.12: Reaction of 2-nitroanisole **229c** and *o*-anisidine **246**.[88]

A further example of the Wohl-Aue reaction was observed in a subsequent experiment. In order to investigate the effect of the electronic nature of substituents *ortho* to the nitro group upon reaction with 2-aminopyridine **207** to give an azo compound, (2-nitrophenyl)phenylamine **229e** was heated with 2-aminopyridine **207** in the presence of sodium. This reaction did not yield any of the azo product **230e** however did give phenazine **245** in 13% yield and trace amounts of *N*-phenylbenzimidazole **248**. The mechanism for the formation of this by-product **248** is unknown, in particular the source of C(2) of the heterocyclic ring (Scheme 3.3.13).

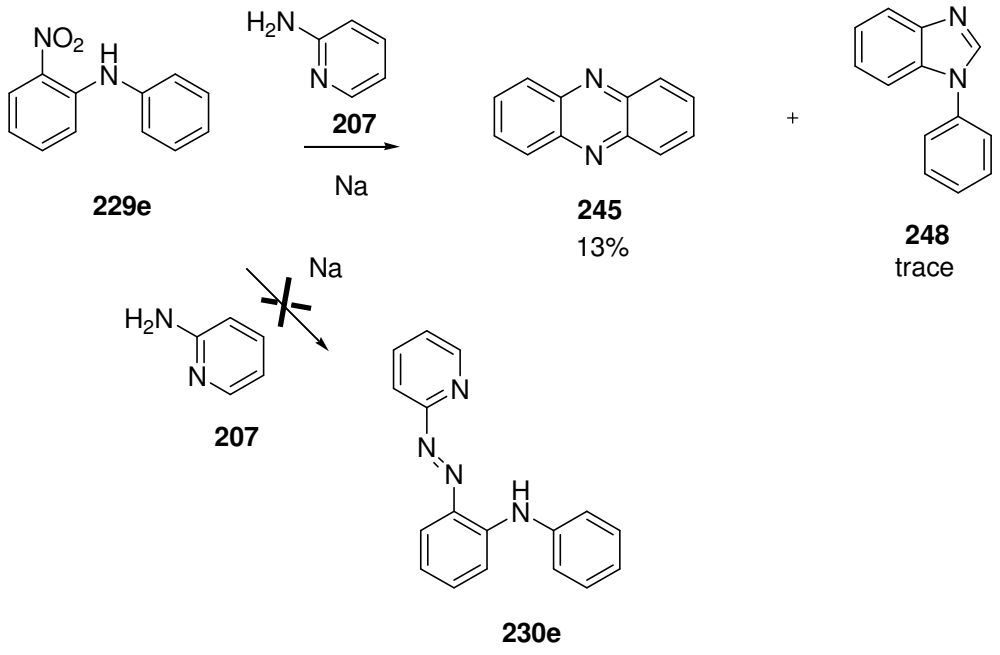

Scheme 3.3.13: Preparation of phenazine **245** by Wohl-Aue reaction.

This indicated that the electronic character of substituents *ortho* to the nitro group appeared to affect the ability of the nitro group to react with 2-aminopyridine **207** to give azo compounds. In the case of the reaction of *N*-(2-nitrophenyl)pyridin-2-ylamine **229d** with 2-aminopyridine **207** the azo product **230d** was obtained (Scheme 3.3.6). However treatment of (2-nitrophenyl)phenylamine **229e** with 2-aminopyridine **207** resulted in no reaction (3.3.13).

Therefore initial reactions indicate there are problems associated with the robustness of the Faessinger and Brown reaction to obtain azopyridine products.[74] Only the parent reaction of 2-aminopyridine **207** with nitrobenzene **229a** lead to high yields of the required azo product when sodium metal was used. Application of this route to the preparation of substituted 2-(phenylazo)pyridine systems resulted in low yields of the azo product and several unexpected by-products.

Reactions with other bases were then attempted. The absence of strongly reducing conditions may minimise the formation of some by-products and increase the yield of the azo product. Hence, as demonstrated earlier, sodium hydride could be used as an alternative to sodium metal (Section 3.3.2).

Firstly the reaction of 2-nitroanisole **229c** and 2-aminopyridine **207** was repeated with the use of sodium hydride as a base. This resulted in an increased 28% yield of the azo product **230c** in comparison with only trace amounts isolated under the previous reaction conditions. However, the *ortho* substituted by-product **240c** was also obtained in 18% yield (Table 3.3.3, Scheme 3.3.14). In addition 2-aminopyridine **207** was recovered in 49% crude yield. The by-product **240c** appeared to be formed due to nucleophilic attack at the *ortho* position of the nitro starting material **229c** with displacement of the methoxy group as opposed to attack at the nitro group to give the expected azo product **230c** (Scheme 3.3.14).

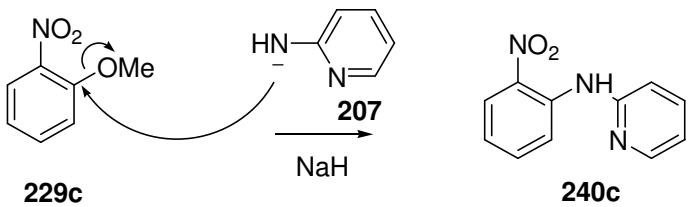

Scheme 3.3.14: Nucleophilic attack at the *ortho* position.

Therefore, it was concluded that under these conditions the reaction yield of 2-(2-methoxyphenylazo)pyridine **230c** can be increased by the use of sodium hydride. However there were reaction selectivity issues with a significant amount of by-product **240c** isolated due to nucleophilic substitution of the methoxy group. It is also worth noting that this by-product **240c** does not appear to undergo an additional reaction with 2-aminopyridine **207** to give 2-[(2-(pyridylamino)phenylazo]pyridine **230d** as previously observed under sodium metal conditions.

3.3.4: Reaction at the *Ortho* Position to give By-product

Additional substituted nitro compounds **229h-j** were then prepared by the treatment of the corresponding substituted nitrophenols **249h,i** with dimethyl sulfate or 2-bromopropane to afford the alkylated products in good yield (Scheme 3.3.15).

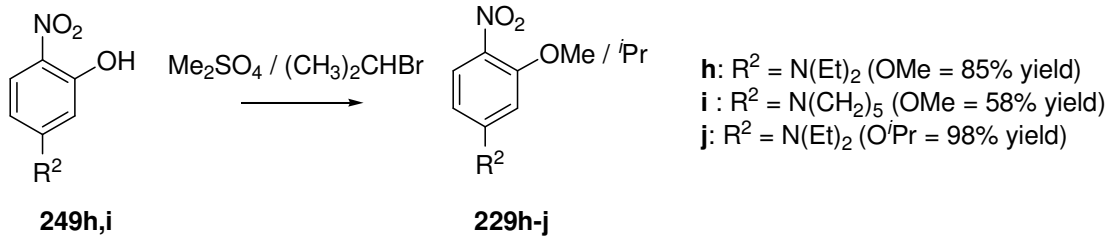

249h,i **229h-j**

Scheme 3.3.15: Alkylation of 6-nitro-3-(diethylamino)phenol **249h** and 2-nitro-5-piperidinophenol **249i**.

The reaction of these 2-nitroanisoles **229g-j** containing additional electron donating groups, with 2-aminopyridine **207** were then carried out (Scheme 3.3.4). The target azo compounds **230g-j** were of interest as the additional electron donating substituent would lead to enhanced conjugation and also the presence of additional electron donating groups would reduce the electrophilicity of the aryl ring of the nitro starting material and hence was predicted to decrease nucleophilic attack at the *ortho* position.

However, reaction of 1,3-dimethoxy-4-nitrobenzene **229g**, 2-methoxy-4-(diethylamino)nitrobenznene **229h** and 2-methoxy-4-piperidinonitrobenzene **229i** with 2-aminopyridine **207** only afforded the *ortho* substituted by-products **240g,h,i** in 10%, 41% and 30% yields respectively with no trace of the required azo product

230g,h,i (Table 3.3.3). These by-products were positively identified by characteristic ^{1}H NMR spectra containing NH signals at δ_H = 10.66, 10.90 and 10.86 in addition to the absence of methoxy peaks. Mass spectrometry evidence also confirmed the formation of the substituted by-products.

Likewise, reaction of diethyl-(3-isopropoxy-4-nitrophenyl)amine **229j** with 2-aminopyridine **207** did not afford the required azo product **230j** but as with the earlier methoxy examples afford only the *ortho* substitution by-product **240j** (Scheme 3.3.16). The reduced amine **250** was also recovered in 26% yield.

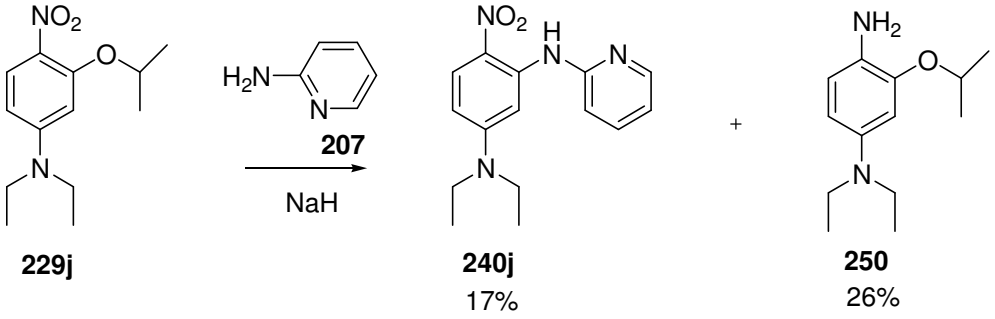

Scheme 3.3.16: Reaction of diethyl-(3-isopropoxy-4-nitrophenyl)amine **229j** and 2-aminopyridine **207**.

In all cases there was also a high yield of the 2-aminopyridine **207** starting material recovered (Table 3.3.3). Strangely it appears that even with these less electrophilic systems the favoured reaction site is the *ortho* position rather than the nitro group.

A possible explanation for the observed increase in the yield of the *ortho* substituted by-product **240** with the addition of electron donating groups at the 4-position of the substituted nitro compounds **229** may be due to conjugation around the aromatic ring. Electron donation from the substituent into the aromatic ring is *ortho*/*para* directing and thus electron density is conjugated to those positions. This results in an overall δ- effect at the *ortho* and *para* positions. However due to a lack of ability to conjugate at the *meta* position relative to the electron donating substituent a slightly δ_+ effect results (Figure 3.3.1). Hence nucleophilic attack at the

meta position relative to the electron donating substituent is now more favoured leading to increased yields of the observed by-product **240**.

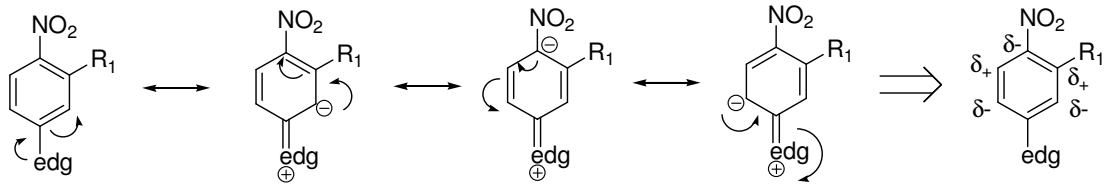

Figure 3.3.1: Electron donation.

The application of this reaction to target naphthalene and quinoline systems is also of particular interest. The naphthalene and quinoline systems did not contain substituents therefore it was expected this would avoid problems due to reaction at the *ortho* position of the nitro ring. However, the reaction of 1-nitronaphthalene **229k** with 2-aminopyridine **207** in the presence of sodium metal did not afford any isolated products with apparent decomposition reagents or products under these harsh conditions. 1-Nitronaphthalene **229k** and 8-nitroquinoline **229l** were then reacted with 2-aminopyridine **207** in the presence of sodium hydride with the aim of preparing target azo compounds **230k,l** (Scheme 3.3.17).

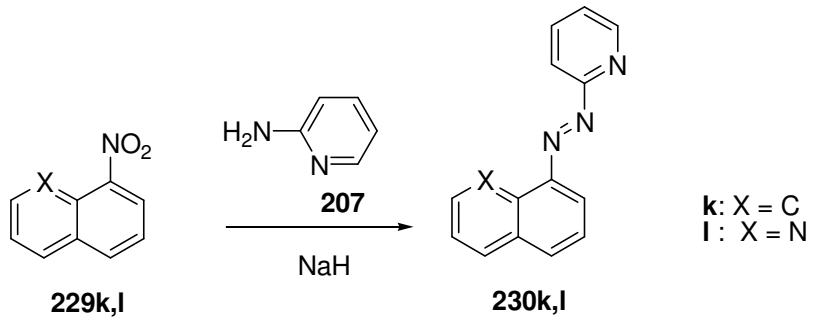

Scheme 3.3.17: Preparation of target azo compounds **230k,l**.

However upon reaction of 1-nitronaphthalene **229k** and 2-aminopyridine **207** analysis of the product by ^{1}H and ^{13}C NMR indicated it contained 10 aromatic CH signals rather than the 11 CH signals expected in the azo product **230k**. There was also a characteristic NH peak in the ^{1}H NMR spectrum at $\delta_H = 9.18$ which would not

be present in the expected product. Further analysis of the ^{13}C NMR spectra also indicated 5 quaternary signals as opposed to the 4 quaternary signals expected for the azo product **230k**. In addition to this electrospray mass spectrometry reveals a molecular ion peak at *m/z* = 265 rather than the expected molecular ion peak at *m/z* = 233. (2-Nitronaphthalen-2-yl)pyridin-2-yl amine **240k** was then proposed as the product in 13% yield.

The presence of this unexpected product **240k** was also supported by an X-ray crystal structure which confirmed substitution at the 2-position. Some notable characteristics of the crystal structure include observation that it is not planar, with the pyridine substituent extending at a torsion angle of 39º (Figure 3.3.2).

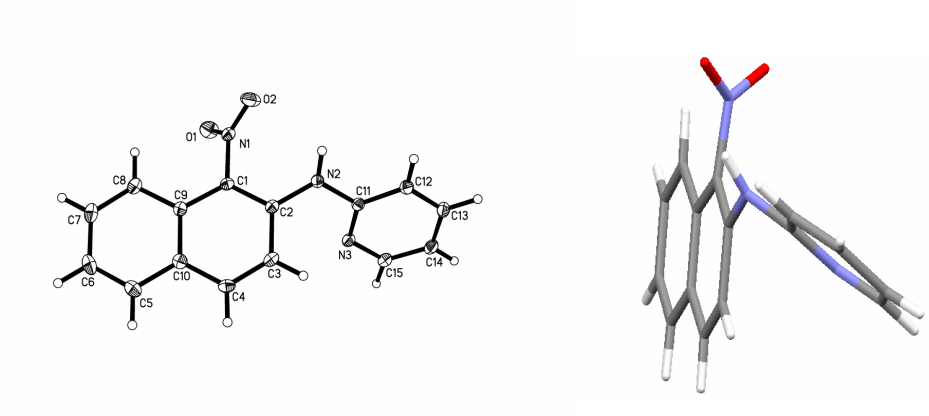

Figure 3.3.2: Crystal structure of (2-nitronaphthalen-2-yl)pyridin-2-yl amine **240k**.

Reaction of 8-nitroquinoline **229l** with 2-aminopyridine **207**, purification and isolation afforded two unknown products in low yield. Analysis by ^{1}H and ^{13}C NMR spectroscopy indicated these products were isomers each containing 9 CH and 5 quaternary carbon signals. Electrospray mass spectrometry confirmed molecular ion peaks of the unknown products at *m/z* = 266 rather than the expected molecular ion peak for the azo product **230l** at *m/z* = 234. The combination of these analytical data indicated a similar reaction had occurred as in the previous nitronaphthalene case with the unknown products being the 5- and 7-substituted nitroquinolines **240l** and **251l** (Scheme 3.3.18). However the low yields of this reaction remain unexplained with 98% of material unaccounted for. This was possibly due to decomposition of the starting materials or products under reaction conditions.

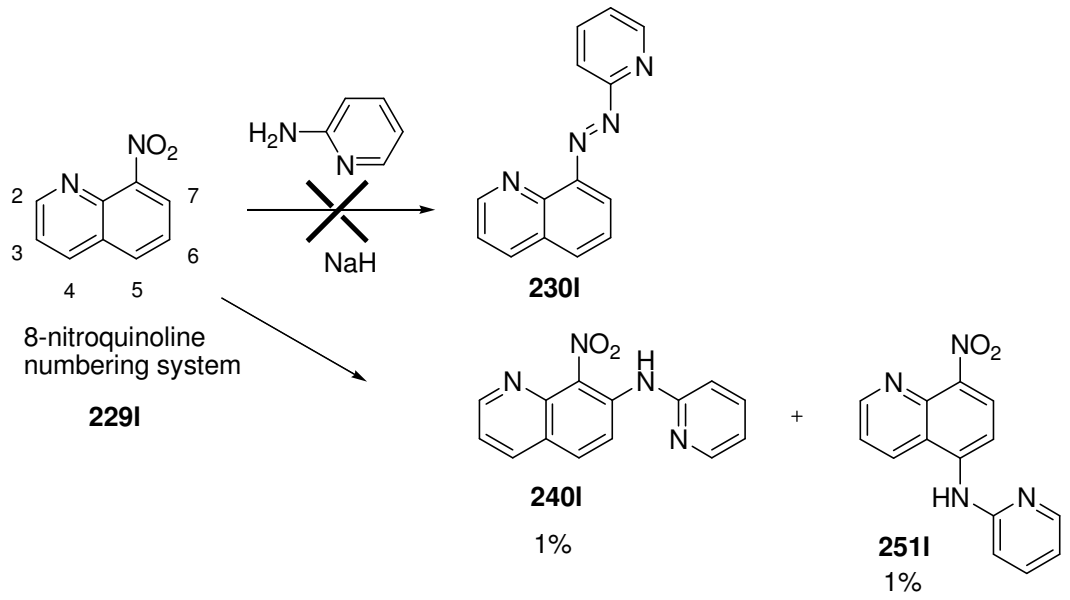

Scheme 3.3.18: Reaction of 8-nitroquinoline **229l** and 2-aminopyridine **207**.

The 5- and 7- substituted products **240l** and **251l** were distinguished by the use of 2D NMR spectroscopy. In particular the presence of NOESY interactions between the aromatic protons at the 4- and 5-positions indicated the position of the aminopyridine substituent at the 7-position characteristic of **240l** (Figure 3.3.4). These were not present in the NOESY spectrum of the **251l** indicating this contained the aminopyridine substituent at the 5-position.

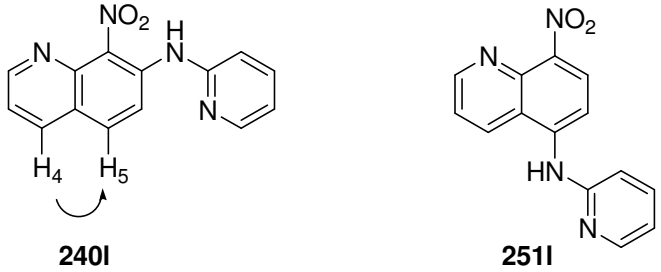

Figure 3.3.4: NOESY interactions between protons.

These results are strange as 1-nitronaphthalene **229k** and 8-nitroquinoline **229l** did not contain a good leaving group at the positions around the naphthalene or quinoline rings hence reaction at the nitro position would be expected to occur.

Therefore the mechanism of this reaction must proceed *via* the nucleophilic substitution of hydride which is uncommon.

It is also strange that the reaction site with 2-aminopyridine **207** is at the nitro group of nitrobenzene **229a** to give the azo product **230a** while the reaction site is at the 2-position of 1-nitronaphthalene **229k** to give the substituted by-product **240k**. This may be due to the steric effects of an additional ring in the nitro starting material.

Reaction of 2-aminopyridine **207** at the 5- and 7-positions of 8-nitroquinoline **229l** is possibly due to additional stabilisation of charges on the heteroatom of the adjacent ring as well as the nitro group (Scheme 3.3.19). This may explain attack at the 5- and 7-positions although the low yield remains unexplained.

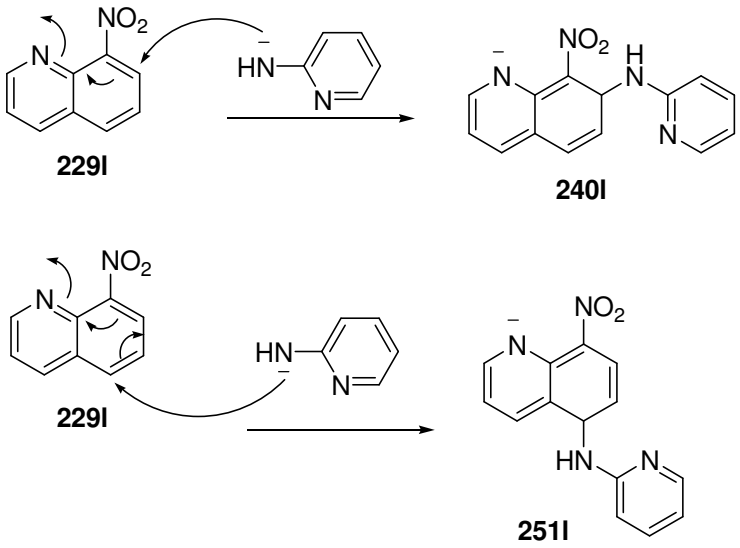

Scheme 3.3.19: Attack of 8-nitroquinoline **229l** by 2-aminopyridine **207**.

Literature Examples of the Formal Substitution of Hydride Anion

Although the nucleophilic substitution of hydride is uncommon reactions of this type have been reported. Firstly in the preparation of heterocyclic azo compounds from Grignard reagents reported by Okubo and co-workers (Section 3.2) by-products **228** were observed in low yields which appeared to involve the overall nucleophilic substitution of hydride (Scheme 3.2.11).[73]

Stern and co-workers also reported the nucleophilic substitution of hydride by the reaction of nitrobenzene **229a** and aniline **202** in the presence of tetramethylammonium hydroxide dihydrate.[90] This reaction gave 4-nitrodiphenylamine **252** in 80% yield and 4-nitrosodiphenylamine **253** in 15% yield. Azobenzene **203** and phenazine **245** were also obtained in 4% yields (Scheme 3.3.20).

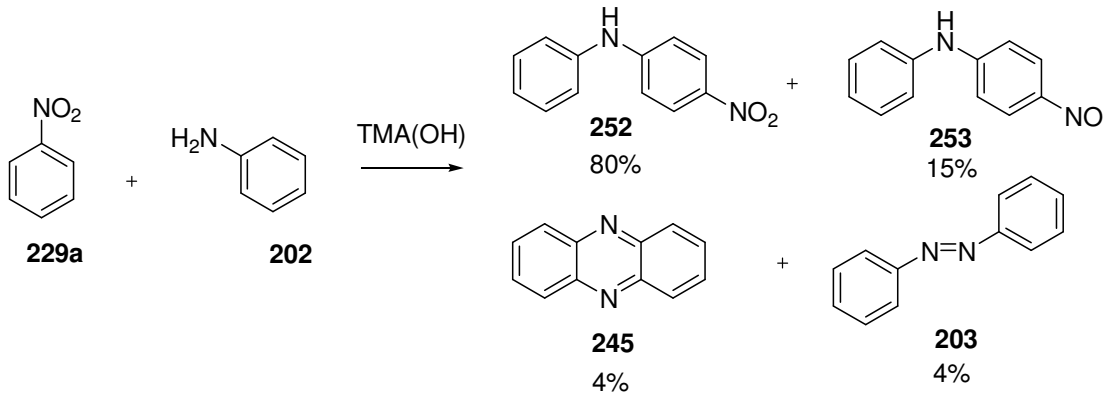

Scheme 3.3.20: Reaction of nitrobenzene **229a** and aniline **202** in TMA(OH) base.[90]

The authors proposed a mechanism involving the deprotonation of aniline **202** which generates the aniline ion which then attacks nitrobenzene **229a** at either the *ortho* or *para* positions. Firstly *para* attack of the amine lead to an anionic intermediate termed the σ^H–complex or adduct (Scheme 3.3.21). This can then undergo oxidation *via* an intra- or intermolecular process. Intermolecular oxidation with a molecule of free nitrobenzene **229a** functioning as the oxidant affords the *para* substituted nitro product **252**. This also liberates nitrosobenzene **201** which condenses to afford azobenzene **203**. However, intramolecular oxidation with the nitro group of the anionic intermediate functioning as the oxidant leads to the *para*

substituted nitroso product **253**. Secondly *ortho* attack of the amine leads to phenazine **245** *via* a similar intramolecular oxidation followed by ring closure.

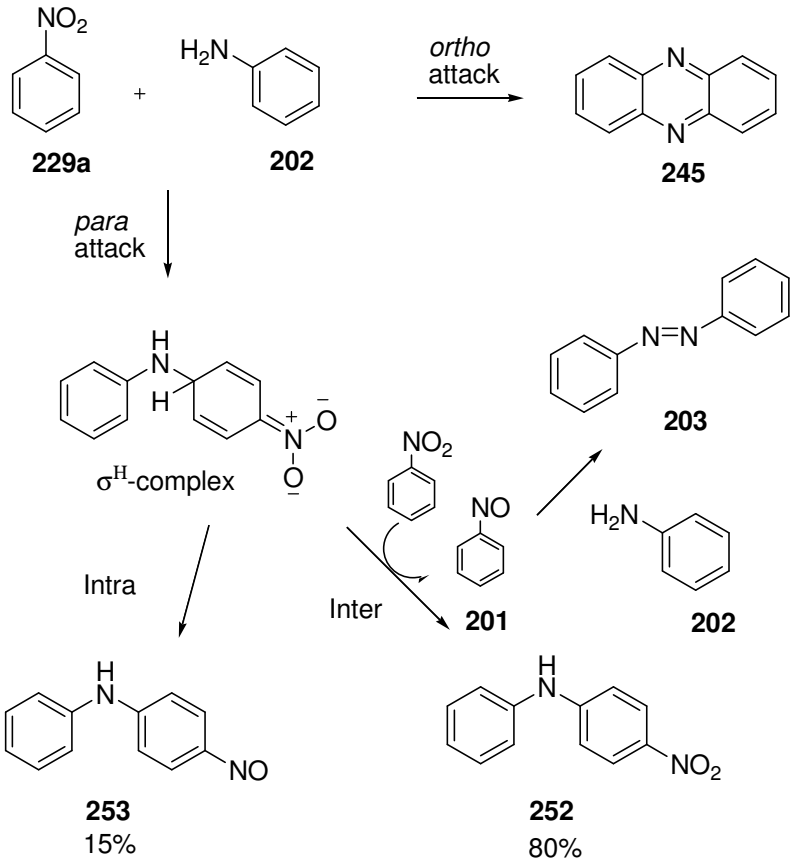

Scheme 3.3.21: Proposed mechanism of *ortho* and *para* attack.[90]

There have also been recent examples reported of the formal nucleophilic substitution of hydride by the reaction of substituted nitrobenzenes **229** with aniline **202** in the presence of an excess of *t*-BuOK.[91] This gave σ^H adducts which were then protonated with acetic acid and appeared to undergo an intramolecular redox process reducing the nitro group to the nitroso compounds (Scheme 3.3.22). A variety of substituted nitroso compounds **254** were prepared and isolated in good yields.

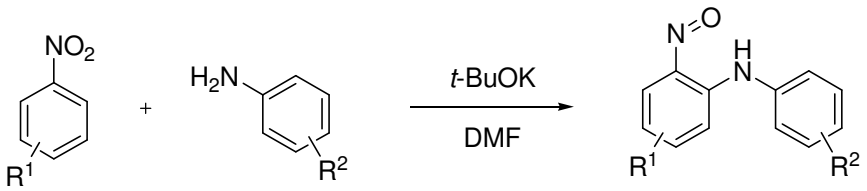

R^1 = *p*-OMe, *p*-Cl, *o*, *p*-diCl
R^2 = *p*-OEt, *p*-Me, *p*-Cl, *p*-Br, *o*, *p*-diCl

Scheme 3.3.22: Formation of substituted nitroso compounds **254**.[91]

Although there were no literature reports of the formal nucleophilic substitution of hydride from naphthalene or quinoline systems, reports of the nucleophilic substitution of hydride from the reaction of an arylnitro compound **229** with aniline **202** allowed a similar mechanism to be proposed. This would involve attack at the 2-position of 1-nitronaphthalene **229k** or 5- and 7-positions of 8-nitroquinoline **229l** to afford an anionic intermediate. Oxidation of the ionic intermediate by intermolecular means as proposed by Stern and co-workers could then lead to the observed substituted nitro products **240k,l** (Scheme 3.3.23).[90] Due to the lack of any nitroso substituted product it is unlikely that intramolecular oxidation of the anionic intermediate occurs.

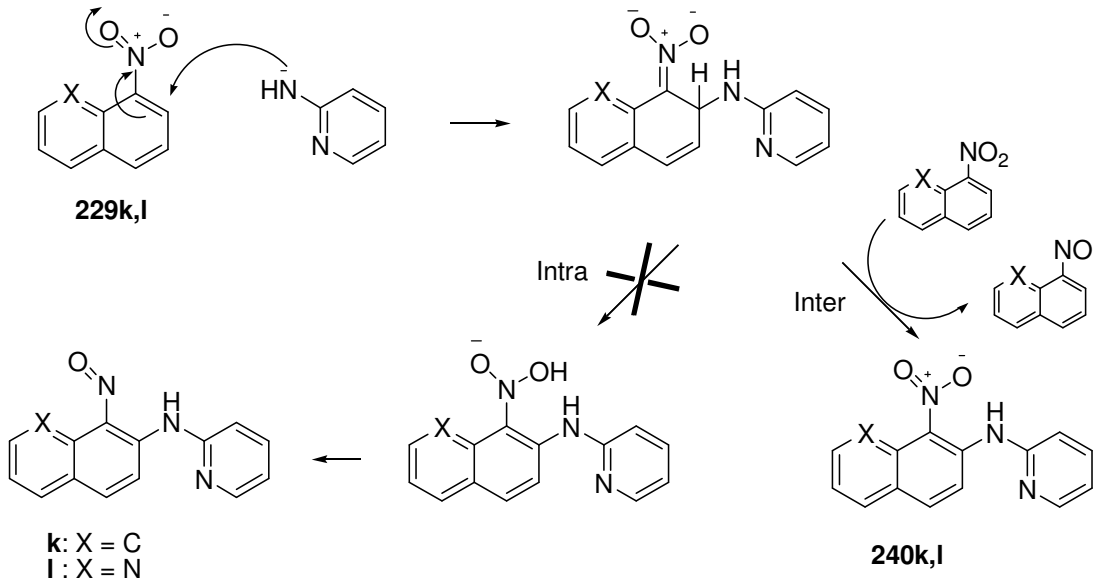

Scheme 3.3.23: Proposed mechanism for naphthalene and quinoline reactions.

At this stage this is only a proposed mechanism with further investigation required to determine the exact mechanism and account for the lack of material recovered from the reaction mixture.

3.4: Metallisation Targets

One of the overall aims was to prepare heterocyclic azo compounds with the correct donor set to coordinate to a metal centre to give a [5,5] metallised complex **255**. Therefore a target azo compound was 2-(2-hydroxyphenylazo)pyridine **230f** which could then coordinate to appropriate metals to give metallised complexes of interest. Hence the reaction of 2-nitrophenol **229f** with 2-aminopyridine **207** was examined in the presence of sodium hydride.

However, as expected this reaction failed with only starting materials recovered (Scheme 3.4.1). None of the required azo product **230f** was isolated. This is probably due to the effect of the anion of hydroxyl group reducing the electrophilicity of the nitro group and hence inhibiting reaction with 2-aminopyridine **207**.

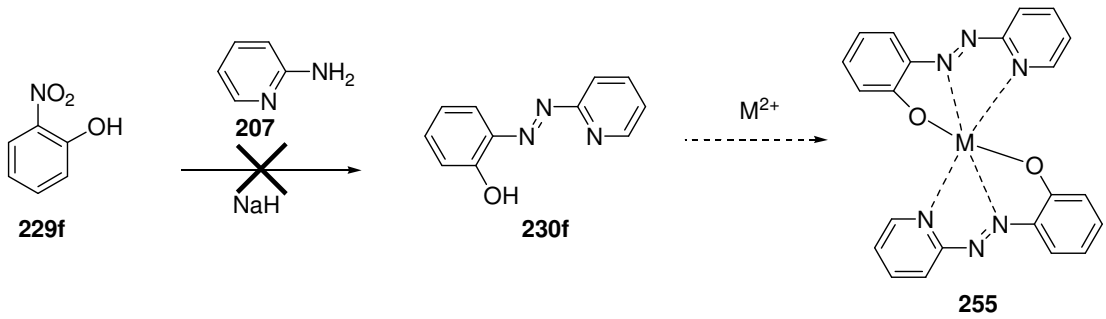

Scheme 3.4.1: Attempted reaction of 2-nitrophenol **229f** and 2-aminopyridine **207**.

3.5: Conclusions: Azo Compounds from Nitroaryl Compounds

The reaction of nitrobenzenes **229** with 2-aminopyridine **207** to form 2-(phenylazo)pyridines **230** appears to be an attractive route to azo compounds and would also be a particularly attractive route to heterocyclic azo compounds due to the increased availability of nitro over nitroso compounds which are required for another route to heterocyclic azo compounds (Section 3.6).

However, the extension of this route lead to major regioselective problems when applied to more complicated ring and substituted systems. In many cases this lead to reaction at the *ortho* position to give by-products as opposed to the required azo product. Overall three types of reaction products are possible.

Firstly reaction occurred at the nitro group to give the required azo product **230** in the case of the reaction of nitrobenzene **229a** and 2-nitroanisole **229c** with 2-aminopyridine **207** (Scheme 3.5.1). This was also the case for reaction with 4-chloronitrobenzene **229b** but in the presence of sodium metal as opposed to sodium hydride.

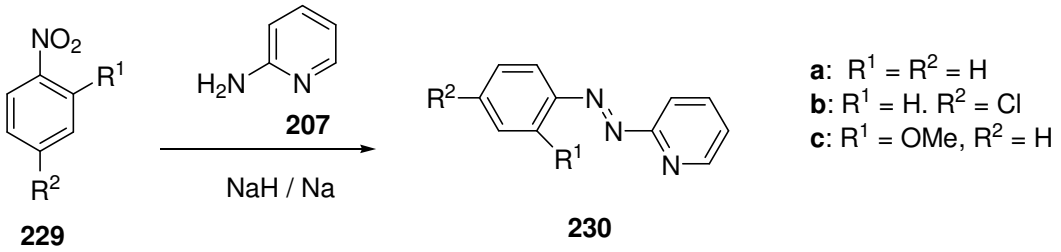

Scheme 3.5.1: Reaction at the nitro group to give azos.

Secondly, extension of this reaction to a variety of disubstituted nitroanisoles **229g-j** leads to isolation of predominantly the nucleophilic substitution by-product **240g-j** (Scheme 3.5.2). Substituents appeared to direct the reaction away from the nitro group.

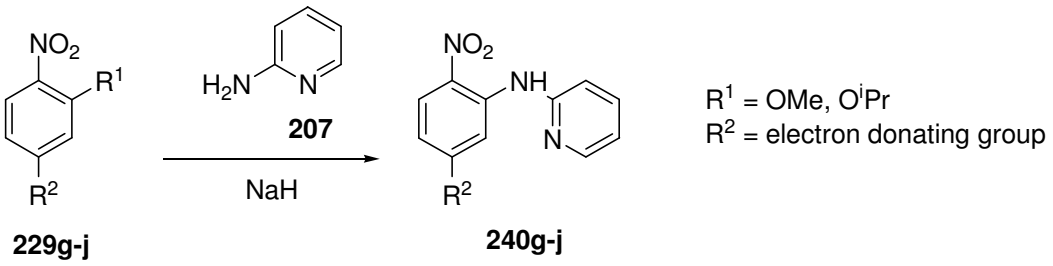

229g-j **240g-j**

Scheme 3.5.2: Nucleophilic substitution of *ortho* substituents.

Finally, application of these conditions to the 1-nitronaphthalene **229k** and 8-nitroquinoline **229l** systems also leads to a nucleophilic substitution by-product **240k,l** *via* the nucleophilic substitution of hydride although products are generally obtained in low yields (Scheme 3.5.3).

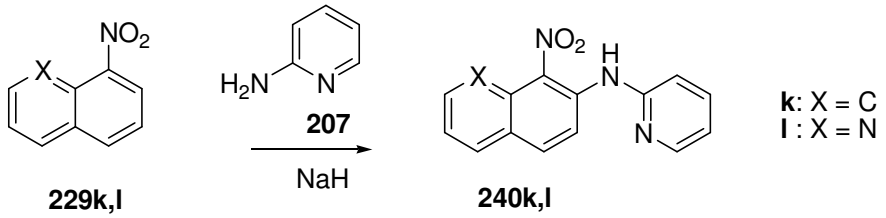

229k,l **240k,l**

Scheme 3.5.3: Nucleophilic substitution of hydrogen.

Therefore the extension of this potentially attractive route lead to major regioselective problems and does not appear to be a robust route to heterocyclic azo compounds.

A possible extension of this work may be the investigation of alternative bases such as NaOH or KOH which have previously been used for the reaction of a nitro group with an amine to give an azoxy product. [81, 82, 83, 92]

3.6: The Mills Reaction

Due to the problems encountered with the synthesis of heterocyclic azo compounds from the reaction of nitroaryl compounds with 2-aminopyridine **207**, the Mills reaction involving the condensation of an amine and a nitroso group was considered. This was also an attractive route to heterocyclic azo compounds due to reports of the synthesis of heterocyclic nitroso compounds from the corresponding amines. There have been several examples of the synthesis of heterocyclic azo compounds by this method (Section 3.2.2).[72] Therefore the aims of this section were to apply the Mills reaction to afford previously unobtainable heterocyclic azo compounds.

Firstly 2-nitrosopyridine **215** was prepared *via* the literature method by Taylor and co-workers explained in Section 3.2.2.[72] 2-Aminopyridine **207** was treated with dimethylsulfide to give the *S,S*-dimethylsulfilimine **214** followed by oxidation with *m*-chloroperbenzoic acid to give 2-nitrosopyridine **215** in good yield (Scheme 3.6.1). Gowenlock and Maidment later revealed that 2-nitrosopyridine **215** exists in a monomer-dimer equilibrium with the dimer **256** dominant at ambient temperatures.[93] However under the reaction conditions 2-nitrosopyridine **215** behaves as the monomer and hence is represented in this form throughout this chapter.

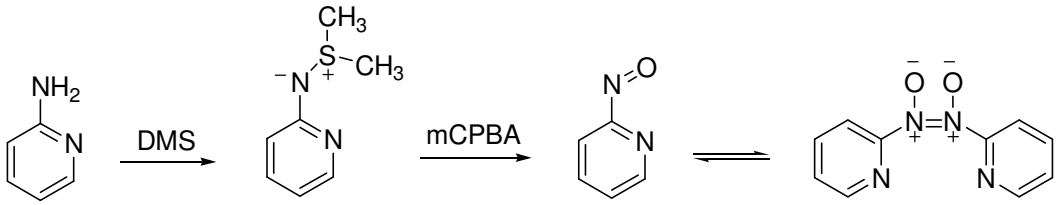

Scheme 3.6.1: Synthesis of 2-nitrosopyridine **215**.

3.6.1: Synthesis of Heterocyclic Azo Compounds under Acetic Acid Conditions

2-Nitrosopyridine **215** was condensed with several substituted amines **257** by stirring in DCM containing a few drops of acetic acid following conditions reported by Taylor to afford heterocyclic azo products **230b,c** in high yield (Scheme 3.6.2, Table 3.6.1). As in Section 3.3.1 there was particular interest in the preparation of azo compounds containing *ortho* substituents with the ability to coordinate to a metal centre to give [5,5] metallised complexes. Application of this reaction to naphthalene

and quinoline systems to obtain the corresponding azo compounds is also of interest.

This reaction was then applied to naphthalene target systems in which previous problems were encountered. 1-Naphthylamine **257k** and 8-aminoquinoline **247l** were treated with 2-nitrosopyridine **215** under dilute acetic acid conditions to afford the azo products **230k,l** in 31% and 51% yields respectively (Table 3.6.1).

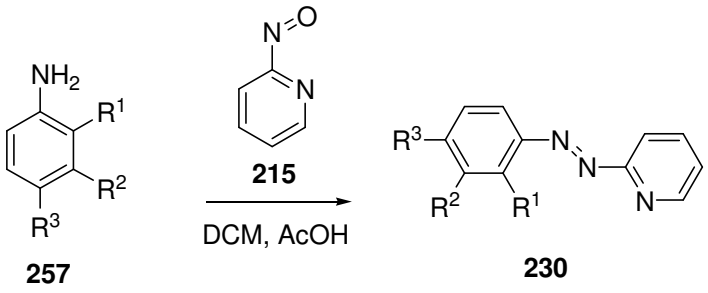

Scheme 3.6.2: Preparation heterocyclic azo compounds.

Table 3.6.1: Reaction of a variety amines with 2-nitrosopyridine.

	Amine starting material **257**			Azo **230** Yield	Azoxypyridine **258** Yield
	R^1	R^2	R^3		
b	H	H	Cl	98%	-
c	OMe	H	H	95%	-
f	OH	H	H	-	88%
k	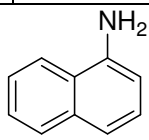			31%	-
l	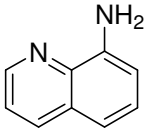			51%	-
m	H	OH	H	37%	-
n	H	H	OH	-	71%
o	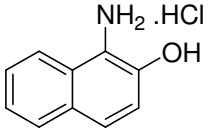			-	75%
p	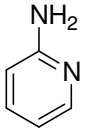			-	71%

Therefore it was possible to prepare several heterocyclic azo compounds in a high yield *via* the Mills reaction which were previously either unobtainable or only obtainable in reduced yields when prepared by alternate methods from nitro precursors.

Metal complexed azo compounds were also of interest. Therefore 2-aminophenol **257f**, 3-aminophenol **257m**, 4-aminophenol **257n** and 1-amino-2-naphthol hydrochloride **257o** were also treated with 2-nitrosopyridine **215** under acetic acid conditions. The reaction of 3-aminophenol **257m** and 2-nitrosopyridine **215** gave the azo product **230m** in a moderate 37% yield (Scheme 3.6.3, Table 3.6.1).

However the reaction of 2-aminophenol **257f** and 4-aminophenol **257n** with 2-nitrosopyridine **215** did not lead to the azo products **230f,n** but instead afforded a coloured product duller than expected for an azo compound which contained eight aromatic protons in the ^{1}H and ^{13}C NMR spectra as would be expected in the azo product. However further analysis revealed only two quaternary carbons in the ^{13}C spectrum rather than three in the expected azo product **230f**. Further, mass spectrometry showed a molecular ion peak (MH^+) at m/z = 201 rather than m/z = 199 in the case of the expected azo. Accurate mass revealed the product to be azoxypyridine **258** (Scheme 3.6.3).

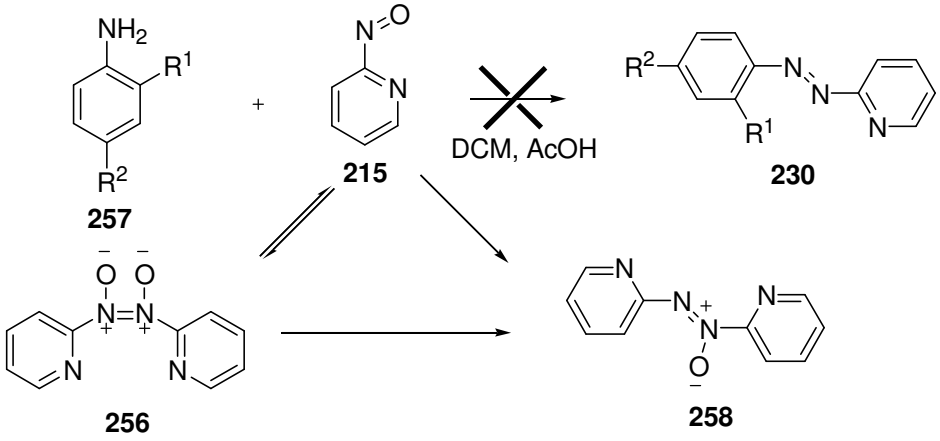

f : R^1 = OH, R^2 = H, 88% yield
n: R^1 = H, R^2 = OH, 71% yield

Scheme 3.6.3: Reaction of 2- and 4- aminophenol **257f,n** with 2-nitrosopyridine **215**.

The reaction of 1-amino-2-naphthol hydrochloride **257o** and 2-aminopyridine **257p** with 2-nitrosopyridine **215** in the presence of acetic acid also lead to formation of azoxypyridine **258** in 75% and 71% yield respectively and not the expected azo products **230o,p** (Scheme 3.6.4, Table 3.6.1).

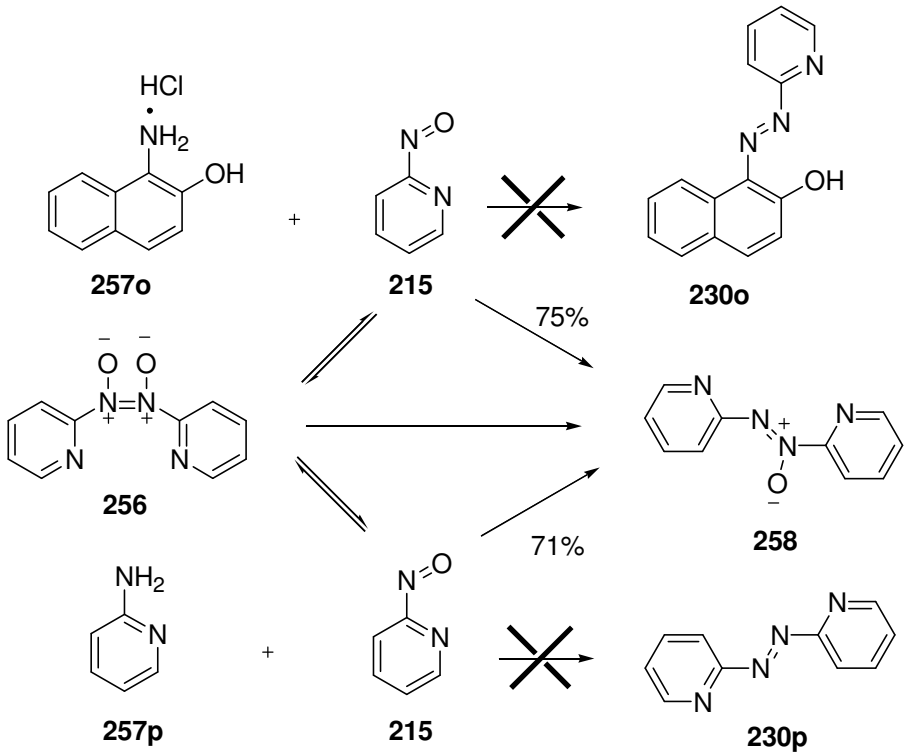

Scheme 3.6.4: Reaction of 1-amino-2-naphthol hydrochloride **257o** and 2-aminopyridine **257p** with 2-nitrosopyridine **215**.

It is strange that the reaction of 2-nitrosopyridine **215** with 3-aminophenol **257m** proceeds to the azo product **230m** while with 2-aminophenol **257f**, 4-aminophenol **257n**, 1-amino-2-naphthol hydrochloride **257o** and 2-aminopyridine **257p** only the reduced by-product **258** is obtained. This may be due to the possibility of these starting materials acting as reducing agents in the reaction mixture while 3-aminophenol **257m** was unable to.

Hence a proposed mechanism of reduction could involve formation of the quinonimine forms of 2-aminophenol **259**, 4-aminophenol **260** and 1-amino-2-naphthol **261** in the reduction process (Figure 3.6.1). This would be similar to known

reduction processes involving benzoquinone **262**.[94] However, 3-aminophenol **257m** could not behave in a similar manner.

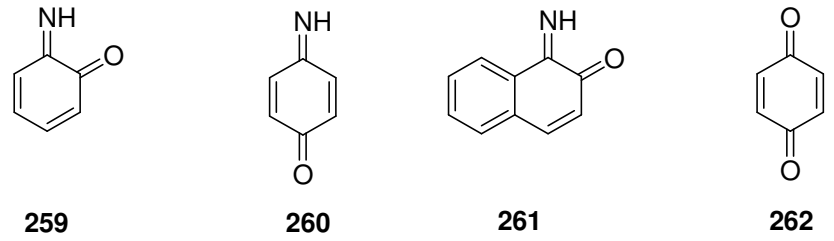

259 **260** **261** **262**

Figure 3.6.1: Reduction of 2-nitrosopyridine.

In an attempt to purify azoxypyridine **258** by Kugelrhor distillation at reduced pressure the ^{1}H and ^{13}C NMR spectra and mass spectrometry of the product confirmed transformation from azoxypyridine **258** to 1-(2-pyridyl)-2(1*H*)-pyridone **263** *via* the loss of nitrogen under these conditions (Scheme 3.6.5).

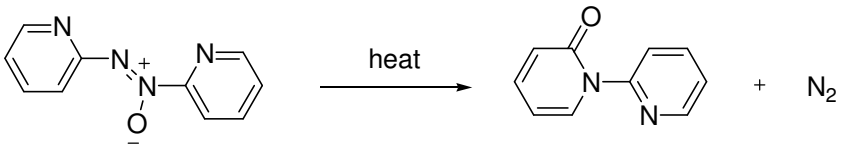

258 **263** 70%

Scheme 3.6.5: Distillation of azoxypyridine **258**.

A proposed mechanism for the behaviour of the dimeric form of 2-nitrosopyridine **215** under reaction conditions and subsequent transformation to 1-(2-pyridyl)-2(1*H*)-pyridone **263** upon distillation is shown in Scheme 3.6.6.

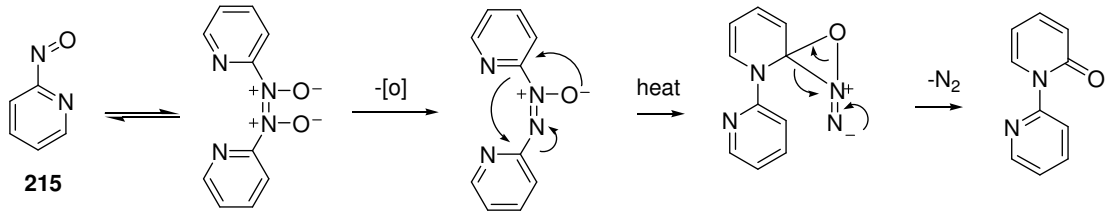

215 **256** **258** **263**

Scheme 3.6.6: Reduction of dimeric 2-nitrosopyridine.

Issues with the stability of 2-nitrosopyridine **215** were reported in a follow up paper by the original authors.[95] Taylor and co-workers reported the dimerisation of 2-nitrosopyridines **215** followed by rearrangement under reaction and work-up conditions to form 1-(2-pyridyl)-2(1*H*)-pyridone **263**. A mechanism was also proposed which proceeded *via* acid catalysed hydrolysis of the 2-nitrosopyridine dimer **256** (Scheme 3.6.7).

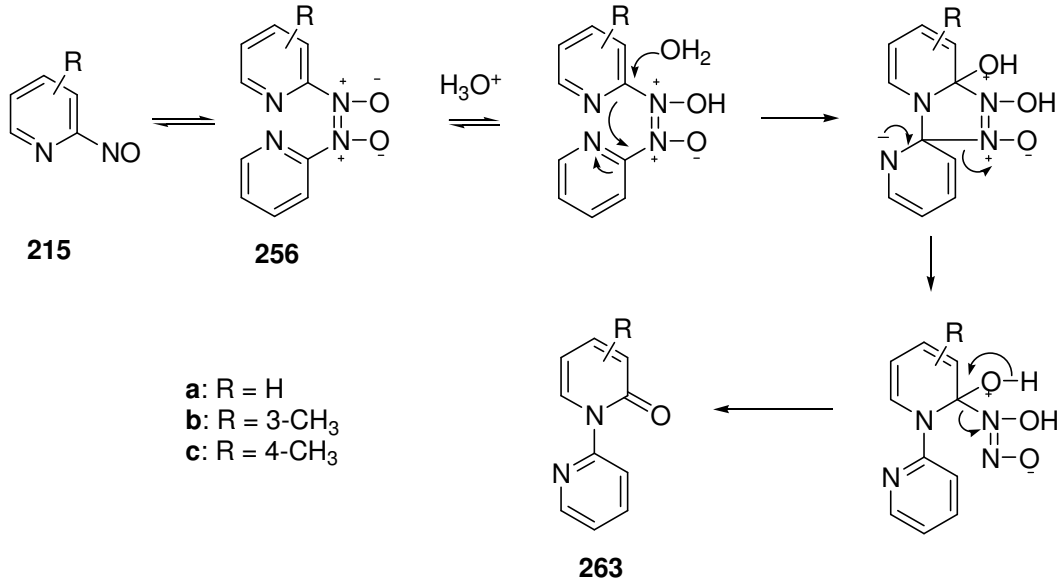

Scheme 3.6.7: Proposed mechanism of dimerisation and rearrangement.[95]

Hence an alternate route to azo systems which were of interest as potential metallisation targets was required which would avoid the problem of reduction of the nitrosopyridine dimer **256**.

3.6.2: Protected Hydroxyl Systems

Due to the problem of reduction of 2-nitrosopyridine **215** in the reaction with 2-aminophenol **257f** and 1-amino-2-naphthol hydrochloride **257o** protecting groups may be used to block the *ortho* hydroxy positions. Protection of the phenol group may minimise reduction of the starting material and encourage reaction with the amine similar to the reaction of *o*-anisidine **257a** and 2-nitrosopyridine **215** which proceeds in high yield.

Therefore the *tert*-butyldiphenyl silyl (TBDPS) and *tert*-butyldimethyl silyl (TBDMS) protected 2-aminophenol **264a,b** and 1-amino-2-naphthol **265a,b** derivatives were prepared by standard literature techniques.[96, 97] This afforded the protected aryl and naphthyl amines however in the case of the TBDPS protected cases excess *tert*-butyldiphenyl silyl hydroxide could not be removed and the product was taken to the next step in its crude form (Scheme 3.6.8).

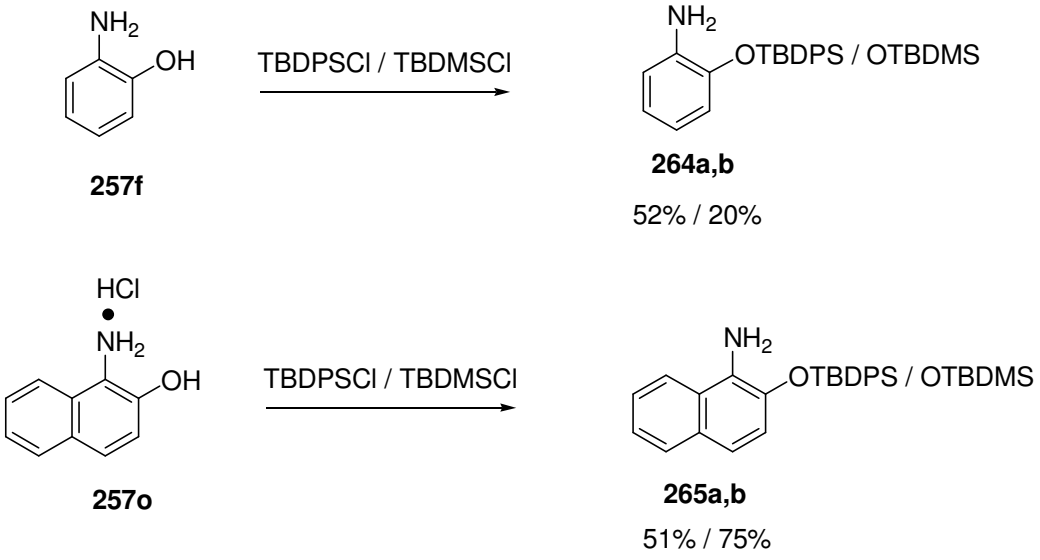

Scheme 3.6.8: Synthesis of protected amines.

In the case of the TBDPS protected cases **264a** and **265a** the strength of the crude material was estimated from the ratio of the integrals of the *tert*-butyl groups corresponding to the required product and TBDPSOH (*tert*-butyldimethylsilyl hydroxide) impurity in the ^{1}H NMR spectra. The strength of the aryl and naphthyl TBDPS protected crude products **264a** and **265a** was found to be 56% and 41% respectively.

Condensation of the TBDPS **264b** and TBDMS **265a,b** protected amines with 2-nitrosopyridine **215** to give the aryl and naphthyl azo compounds **266**, **267** and **268** was carried out under the standard conditions using DCM with a few drops of acetic acid as the solvent.[72]

However under these conditions no reaction with the amine occurred with only the protected amine starting material and azoxypyridine **258** due to reduction of the 2-nitrosopyridine dimer **256** obtained (Scheme 3.6.9).

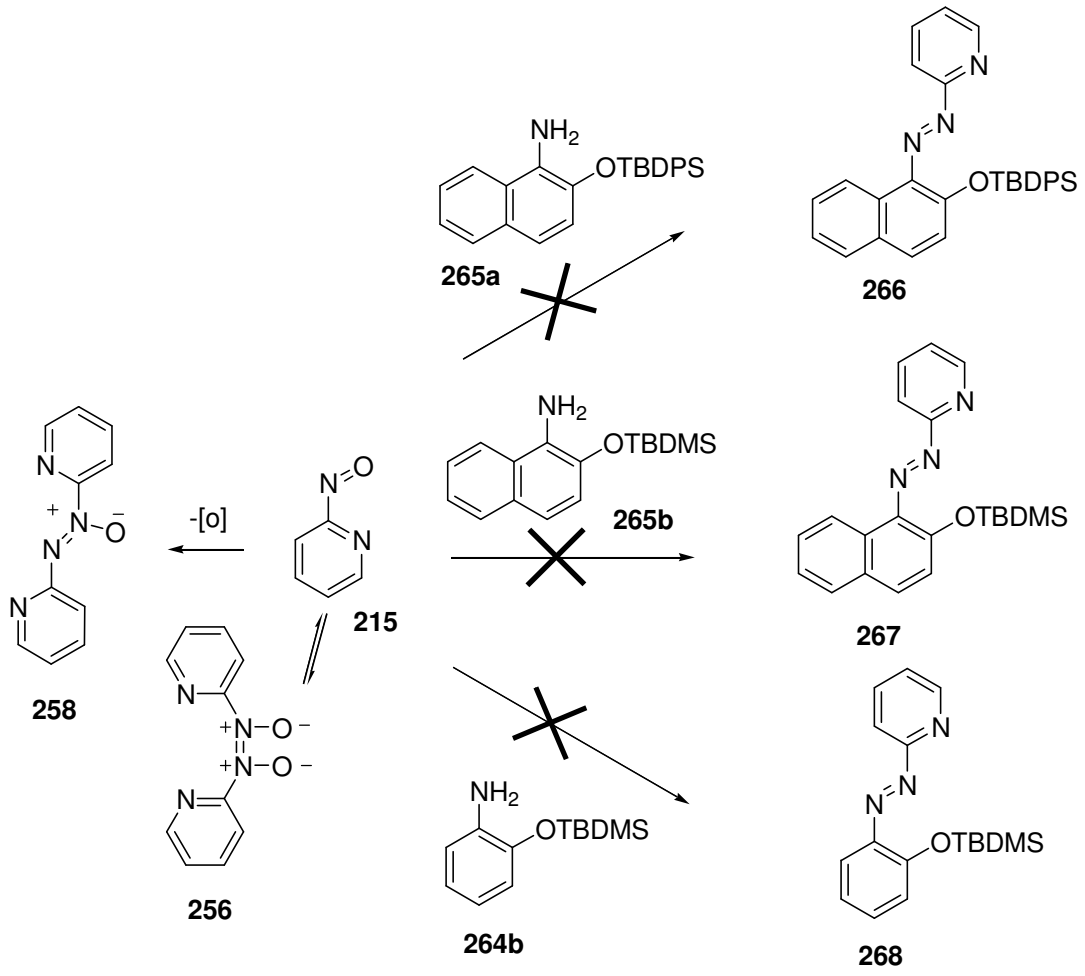

Scheme 3.6.9: Reaction of protected amines with 2-nitrosopyridine **215**.

Only in the case of the TBDPS protected aryl compound **264a** did condensation with 2-nitrosopyridine **215** occur and the required protected azo compound **269** was obtained in good yield (Scheme 3.6.10).

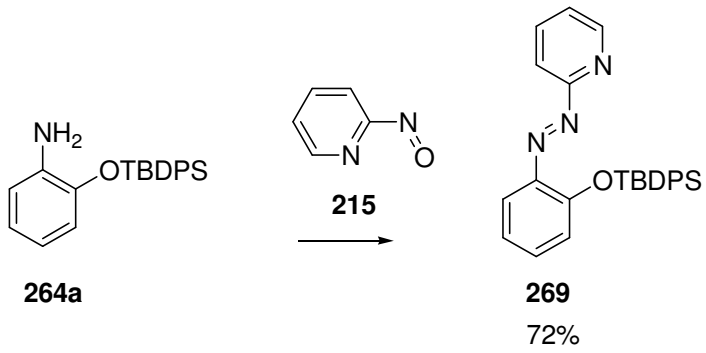

Scheme 3.6.10: Preparation of TBDPS protected azo compound **269**.

The OTBDPS azo **269** was de-protected by treating with tetrabutylammonium fluoride (TBAF) under standard conditions to afford 2-(2-hydroxyphenylazo)pyridine **230f** in good yield (Scheme 3.6.11).[98] The azo product was positively identified by ^{1}H and ^{13}C NMR spectroscopy including the characteristic broad singlet at δ_H = 12.89 corresponding to the hydrogen bonded phenol group.

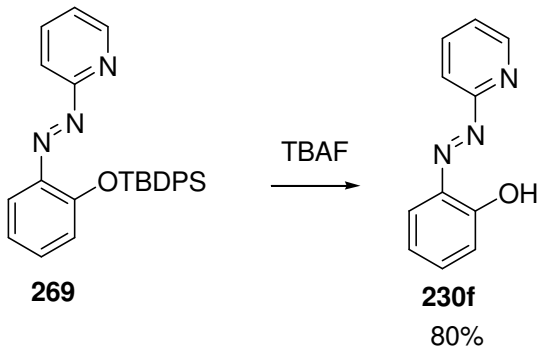

Scheme 3.6.11: De-protection of azo compound **269** with TBAF.

Therefore it did appear possible to prepare *ortho* hydroxy substituted azo compounds *via* a protecting group route. However, this was only successful in the case of the TBDPS protected aryl system **264a**. It is unclear why the alternate protected aryl system or protected naphthyl systems did not undergo condensation. Further study is required to determine if naphthyl systems can be prepared *via* the same method.

3.6.3: Application of Mills Reaction to Water Soluble Compounds

The applicability of this reaction for the preparation of heterocyclic azo compounds to aqueous conditions was of particular interest due to the requirement of the majority of current inkjet dyes to be water soluble.

Firstly the reaction of *o*-anisidine **257c** and 2-nitrosopyridine **215** was repeated in an aqueous ethanol solvent to establish the effect of these conditions upon the yield of the azo product **230c**. Under these conditions the azo product **230c** was obtained although in a reduced yield of 39% (Scheme 3.6.12).

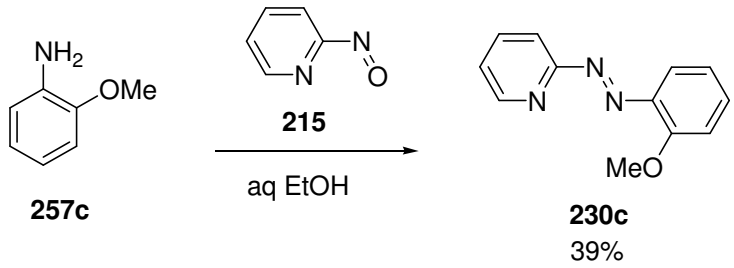

257c **230c** 39%

Scheme 3.6.12: Reaction of *o*-anisidine **257a** and 2-nitrosopyridine **215** in aqueous solvent.

A water soluble amine, 2-acetylamino-5-amino-benzenesulfonic acid **270** was then treated with 2-nitrosopyridine **215** in a 50% aqueous ethanol solvent containing two drops of acetic acid. The resulting azo product **271** was then obtained as an orange precipitate in a moderate yield (Scheme 3.6.13). This was identified by characteristic ^{1}H and ^{13}C NMR spectra including a NH signal at δ_H = 10.73 and methyl signal at 2.15. Therefore the application of the Mills reaction to aqueous conditions was successful.

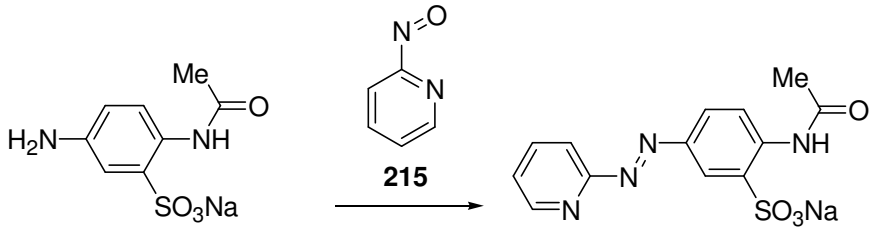

270 **271** 51%

Scheme 3.6.13: Reaction of 2-acetylamino-5-amino-benzenesulfonic acid **270** and 2-nitrosopyridine **215**.

3.6.4: Synthesis of Heterocyclic Azo Compounds under Basic Conditions

As explained in Section 3.2.1 there have been reports of the preparation of heterocyclic azo compounds under strongly basic conditions.[66] This method was then applied to several amines from the previous section in which preparation of the azo compounds under acid conditions had been problematic.

Firstly the reaction of 2-aminophenol **257f** and 2-nitrosopyidine **215** in a 50% sodium hydroxide solution afforded 2-(2-hydroxyphenylazo)pyridine **230f** in 33% yield (Scheme 3.6.14). This route to 2-(2-hydroxyphenylazo)pyridine **230f** was favoured over the previous route *via* the use of protecting groups due to the use of a one step synthesis rather than a three step synthesis (Section 3.6.2).

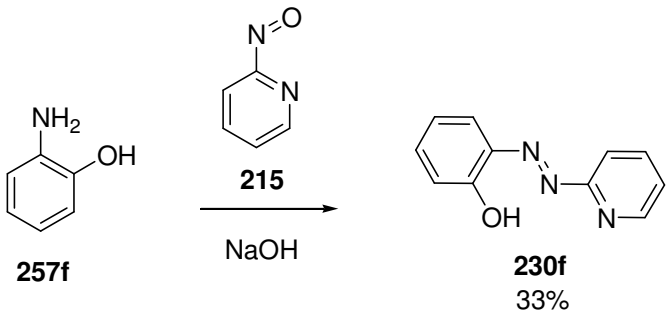

257f **230f** 33%

Scheme 3.6.14: Synthesis of 2-(2-hydroxyphenylazo)pyridine **230f**.

The reaction of 2-aminopyridine **257p** and 2-nitrosopyridine **215** was also carried out under these basic conditions to afford a crude product which contained 2-(2-pyridineazo)pyridine **230p**, 2-aminopyridine **257p** and azoxypyridine **258**. ^{1}H NMR analysis of the crude material and comparison of the integrals of specific peaks corresponding to each of these products allowed the composition of the crude material to be determined and the ratio of each product present measured (Scheme 3.6.15). Although further purification and calculation of isolated yields was not carried out.

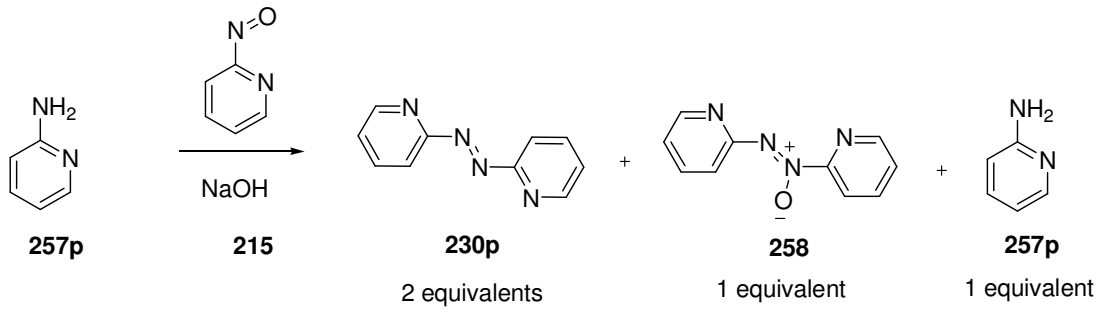

Scheme 3.6.15: Synthesis of 2-(2-pyridineazo)pyridine **230p**.

However treatment of 1-amino-2-naphthol hydrochloride **257o** with 2-nitrosopyridine **215** under basic conditions did not afford the required azo product **230o** and instead resulted in reduction of the 2-nitrosopyridine dimer **256** to yield azoxypyridine **258** (Scheme 3.6.16). This exposure of 2-nitrosopyridine **215** to reaction conditions in the absence of the amine also afforded azoxypyridine **258**.

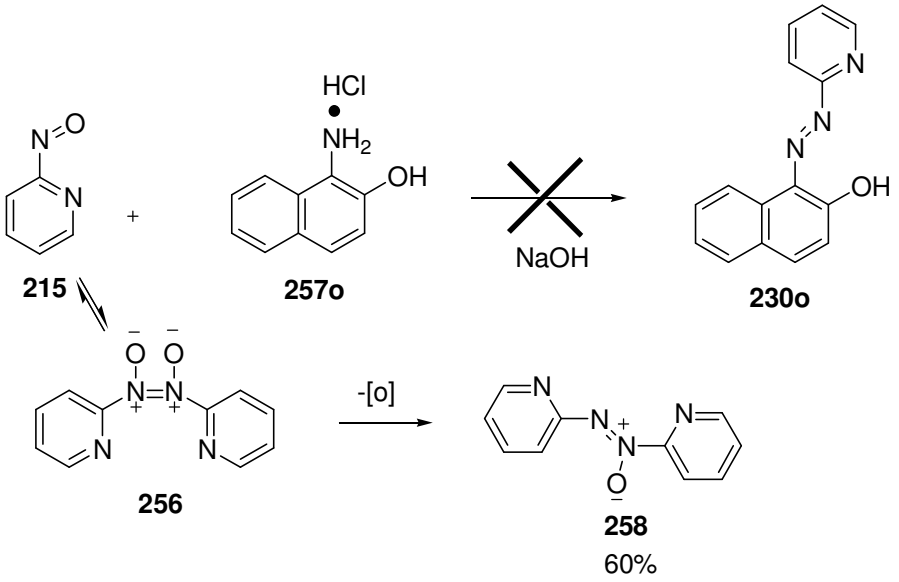

Scheme 3.6.16: Reaction of 1-amino-2-naphthol hydrochloride **257o** and 2-nitrosopyridine **215**.

An attempt was then made to couple the protected naphthylamine **265a** with 2-nitrosopyridine **215** under basic conditions. However this resulted in only 2-(2-pyridineazo)pyridine **230p** with none of the required azo product **266** obtained (Scheme 3.6.17). In this case 2-(2-pyridineazo)pyridine **230p** appeared to form as a result of reduction of the dimer of 2-nitrosopyridine **256**.

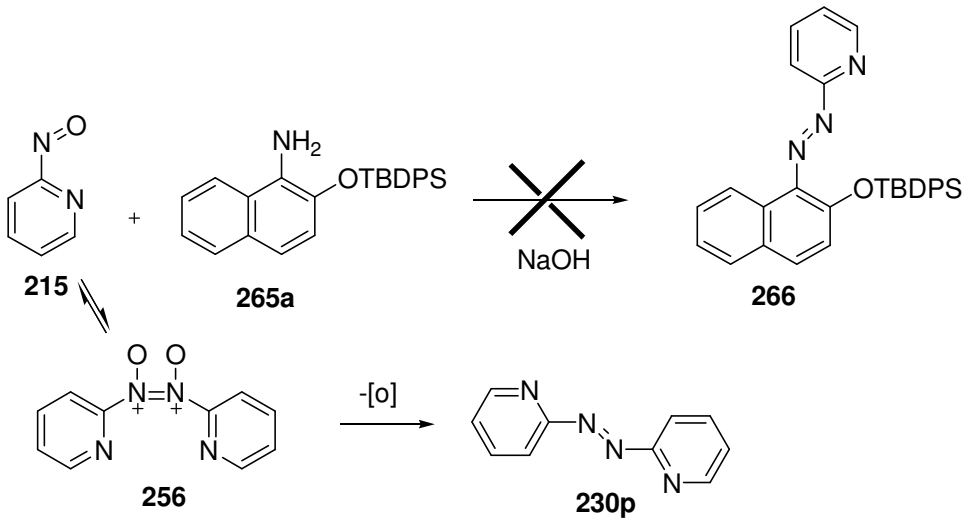

Scheme 3.6.17: Reaction of TBDPS protected aminonaphthol **265a** and 2-nitrosopyridine **215**.

Therefore under basic conditions 2-nitrosopyridine **215** could couple with 2-aminophenol **257f** to give the required azo product **230f**. However, azo yields under basic conditions were low with optimisation required. This eliminated the need for the use of protecting groups as was required under acidic coupling conditions. A single step reaction was preferred to the use of the acidic conditions method involving protecting groups.

However, the application of this reaction to naphthol systems failed to give the azo product with reduction of the 2-nitrosopyridine dimer **256** occurring to give azoxypyridine **258** and 2-(2-pyridineazo)pyridine **230p**. Hence further study is required into the limitations of this reaction type to give heterocyclic azo compounds.

3.7: Metallisation of Appropriate Dyes

As mentioned in Section 3.1 there is particular interest in [5,5] complexed azo systems which exhibit the required bright shades. Therefore there was the possibility to metallise some of the azopyridine systems to establish the effect of this metal centre upon dye properties. Methods of metallisation such as direct and oxidative metallisation have been reported.[99] In addition a de-alkylative metallisation involves the de-alkylation of a methoxy group to a hydroxyl. Examples include the de-alkylation of a naphthol azo dye **272** during metallisation with $CuSO_4$ which gave the [5,6] metallised complex **273** (Scheme 3.7.1).[99]

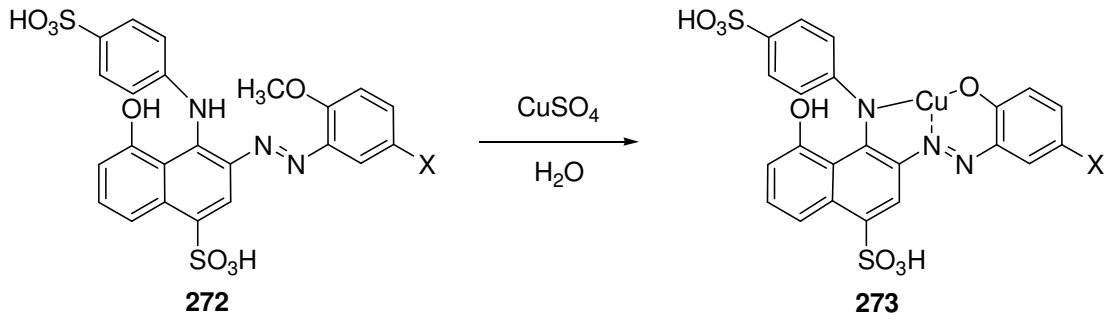

272 **273**

Scheme 3.7.1: De-alkylative metallisation with $CuSO_4$.[99]

The rate of the de-alkylation of copper complexes is also influenced by substituents *para* to the methoxy group with the rate of de-alkylation of **272** in the order of X = NO_2 > H > OMe > Me > Cl. Although the mechanism of this de-alkylation is unknown it is thought to include coordination of the methoxy group to the copper metal centre followed by the breaking of the O-CH_3 bond to afford methanol (Scheme 3.7.2).[100]

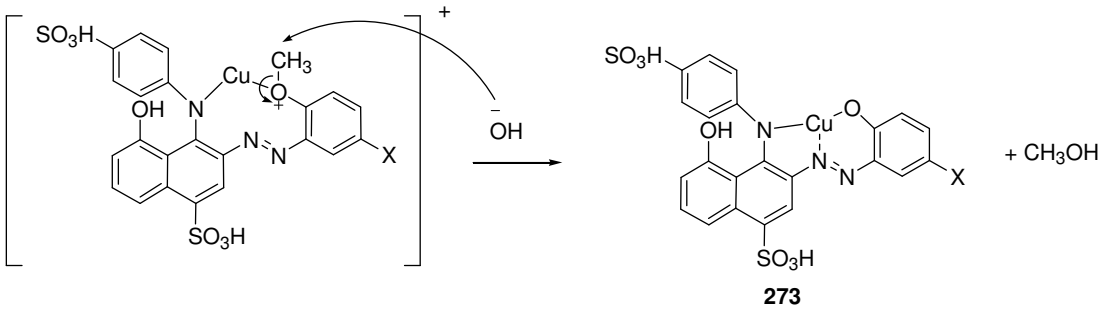

273

Scheme 3.7.2: Proposed mechanism of de-alkylation.[100]

Hence it is possible to de-alkylate a methoxy group during metallisation to afford the desired hydroxyl metallised complex, although this de-alkylative metallisation was only observed with copper and in the naphthalene series. No examples were found of de-alkylative metallisation with nickel, iron or aluminium.

2-(2-Methoxyphenylazo)pyridine **230c** was metallised with $CuSO_4$ with the aim of de-alkylation to afford the metallised dye **255** (Scheme 3.7.3). This would be a particularly attractive route to the metallised complex due to the high yielding synthetic route to 2-(2-methoxyphenylazo)pyridine **230c** and would avoid the problems associated with the use of protecting groups or low yields in the synthesis of 2-(2-hydroxyphenylazo)pyridine **230f** (Section 3.7). However, under the metallisation conditions used, the expected de-alkylated product was not formed and the metallised 2-(2-methoxyphenylazo)pyridine **230c** was recovered as its 2:1 complex **274** in 41% yield (Scheme 3.7.3).

The 2:1 metallised complex **274** which included two 2-(2-methoxyphenylazo)pyridine **230c** ligands coordinated around a copper metal centre and was positively identified by its mass spectrum showing a molecular ion peak M^+ at m/z = 489. The presence of a metallised complex **274** was also confirmed by a slight bathochromic shift in λ_{max} from 318 nm to 350 nm in the UV spectrum.

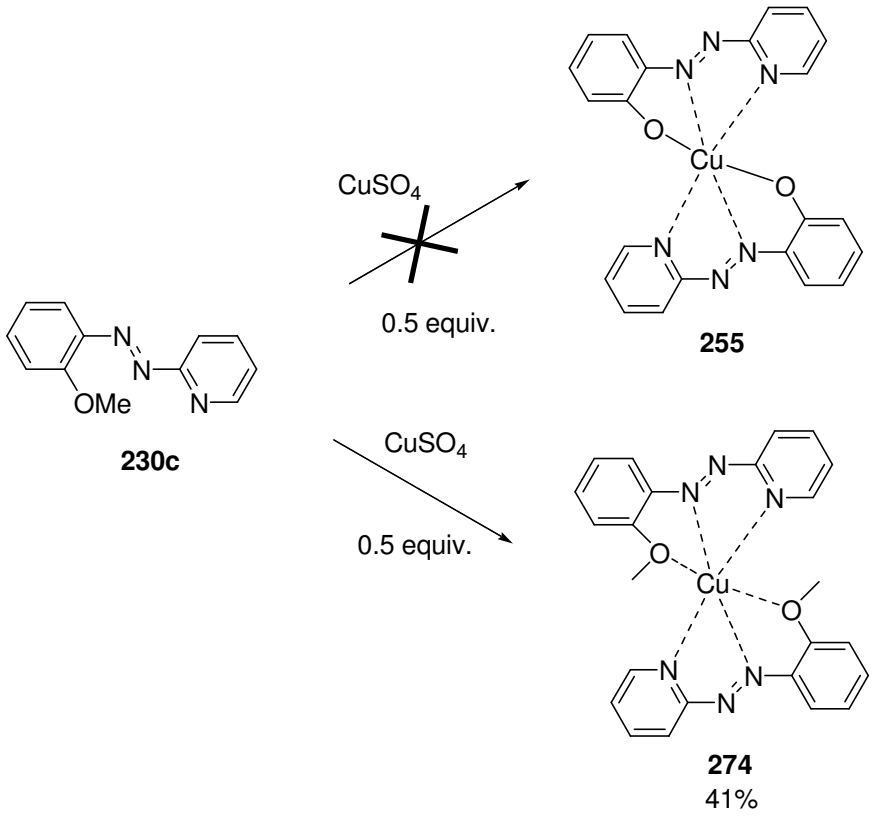

Scheme 3.7.3: Metallisation of 2-(2-methoxyphenylazo)pyridine **230c**.

An alternate route to the metallised pyridine azo compounds was by direct metallisation of 2-(2-hydroxyphenylazo)pyridine **230f** with nickel acetate tetrahydrate. This resulted in an immediate colour change of the reaction mixture from a red to magenta which was observed in the UV-vis spectum as a bathochromic shift in λ_{max} from 323 to 361 nm in the UV region of the spectrum and an additional peak in the visible region of the spectrum at 544 nm. The half width of this absorption peak in the metallised complex **255** was $W_{1/2}$ =114 nm which resulted in a moderate bright dye, although the half width was not below 100 nm typically required for suitably bright dyes (Figure 3.7.1).

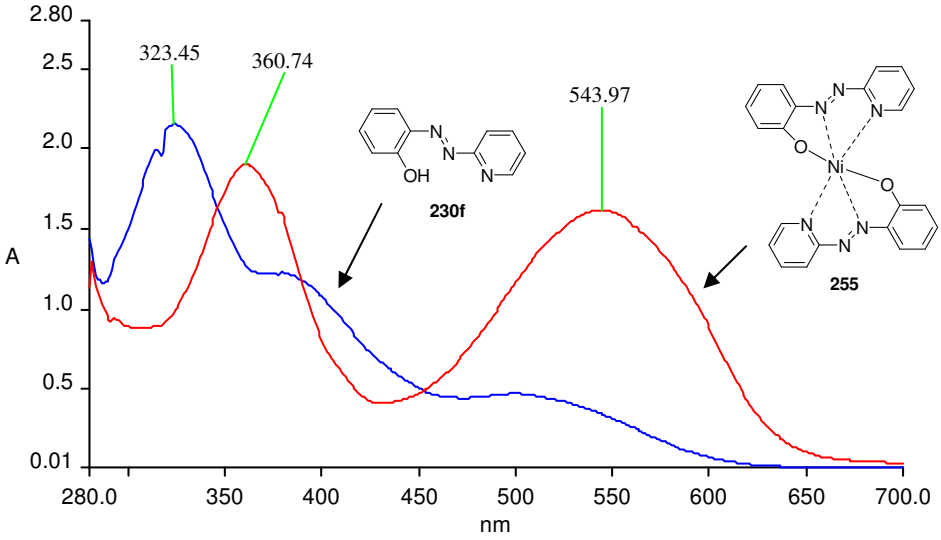

Figure 3.7.1: UV-vis spectra of the azo ligand **230c** (blue) and metallised complex **255** (red).

The metallised azo compound **255** was then isolated by extraction of the reaction mixture into DCM as the 2:1 Nickel complex in 64% yield (Scheme 3.7.4). This was positively identified by its mass spectrum showing a molecular ion peak (ESI) MH^+ at m/z = 455 corresponding to the 2:1 nickel metallised complex **255**.

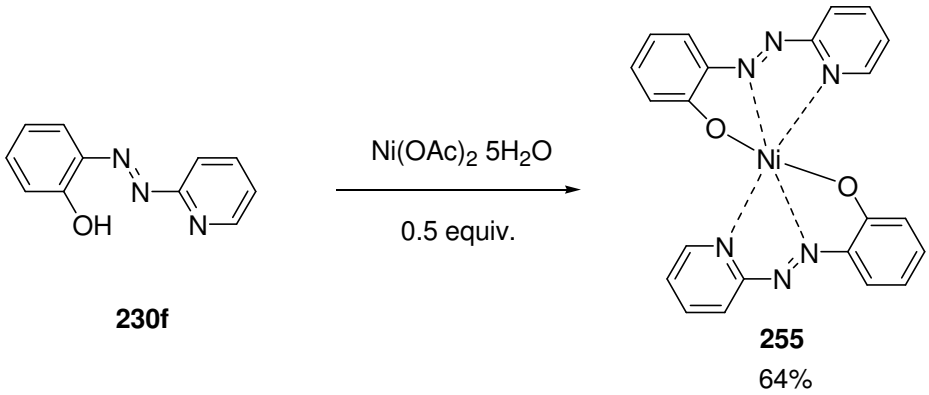

Scheme 3.7.4: Metallisation of 2-(2-hydroxyphenylazo)pyridine **230f**.

Therefore it was possible to form the required metallised complex **255** by direct metallisation methods as opposed to the preferred de-alkylative method. Further investigation is required into possible de-alkylative metallisation conditions that may afford the required metal complex.

3.8: Conclusions

The main aims of this section of the thesis were to develop new routes to heterocyclic azo compounds that could then be used to prepare electron deficient azo dyes.

Initially, the route to heterocyclic azo compounds by reaction of an arylnitro compound **229** with 2-aminopyridine **207** was studied and appeared to be an attractive and high yielding route to 2-(phenylazo)pyridine **230a**. However, application of this reaction to substituted and naphthalene systems failed. This afforded by-products due to nucleophilic substitution of groups such as methoxy and the relatively uncommon nucleophilic substitution of hydride with none of the required azo products recovered. Therefore it appeared that the reaction of an arylnitro compound and amine was not a robust and versatile route to heterocyclic azo compounds with alternative routes required.

An alternate route to heterocyclic azo compounds involved the use of the Mills reaction by the condensation of 2-nitrosopyridine **215** and an amine. 2-Nitrosopyridine **215** could be prepared in good yield from 2-aminopyridine **207** by a literature route.[72] Subsequent treatment of *o*-anisidine **257c**, *p*-chloroaniline **257b**, 3-aminophenol **257m**, 1-naphthylamine **257k** and 8-aminoquinoline **257l** with 2-nitrosopyridine **215** afforded the heterocyclic azo products in moderate to high yields. Another interesting result was that this reaction could also be extended to water soluble systems with the reaction of 2-acetylamino-5-amino-benzenesulfonic acid **270** and 2-nitrosopyridine **215** in an aqueous ethanol solvent affording the corresponding azo **271** product in moderate yield. However the treatment of 2-aminophenol **257f**, 4-aminophenol **257n** and aminonaphthol **257o** systems with 2-nitrosopyridine **215** afforded only azoxypyridine **258** as a result of dimerisation and subsequent reduction of the nitroso starting material.

2-Aminophenol **257f** could then be protected with TBDPSCl and the protected amine **264a** treated with 2-nitrosopyridine **207** to afford the azo compound **269** in good yield. This TBPDPS azo compound **269** could then be de-protected by treatment with TBAF to give 2-(2-hydroxyphenylazo)pyridine **230f** in good yield.

The reaction of nitroso compounds with amines under basic conditions was then applied to the reaction of 2-aminophenol **257f** with 2-nitrosopyridine **215** to

afford 2-(2-hydroxyphenylazo)pyridine **230f** without the need for protecting groups however in a lower yield of 33%.

In conclusion, the Mills reaction does appear to be the favoured route to heterocyclic azo compounds although several problems exist due to the dimerisation and reduction of 2-nitrosopyridine **215** under the reaction conditions. Further study is required to determine the optimum reaction conditions to minimise or eliminate this by-product and promote condensation with the amine to give the required heterocyclic azo compounds.

4.0: Azo Coupling Reactions of Chromotropic Acid

Most azo dyes are made on an industrial scale by a two stage reaction sequence which involves diazotisation and coupling. This involves the treatment of a primary amine with sodium nitrite under acidic conditions at relatively low temperatures to form a diazonium salt. This diazonium salt is relatively unstable and thus undergoes immediate reaction with an activated coupling component which may be a phenol or aromatic amine in the second stage of the reaction (Scheme 4.0.1).

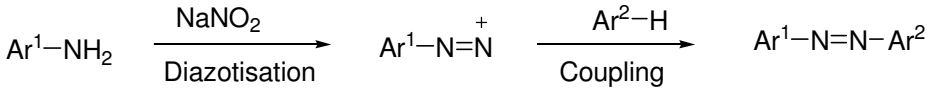

Scheme 4.0.1: Diazotisation and Coupling.

There is interest in dyes obtained by coupling of diazonium salts to chromotropic acid **301** (Figure 4.0.1). These dyes can be described as the 2-monoazo dyes **302** in which chromotropic acid has undergone a single azo coupling reaction at the 2-position of the naphthol ring or 2,7-bisazo dyes **303** in which a second azo coupling has also occurred at the 7-position of the naphthol ring (Figure 4.0.1). There is also interest arising from bisazo dyes derived from naphthol systems such as H acid and gamma acid (Section 1.20.2), Current targets include bisazo compounds of chromotropic acid **303** used in the development of improved black dyes for inkjet printing (Figure 4.0.1). Prints can be provided from these dye systems of attractive, neutral black shades which are particularly well suited for the inkjet printing of text and images. These images have good optical density, light fastness, wet fastness and ozone fastness.[101a,b] The compositions also have good storage stability and low tendency to block the fine nozzles.

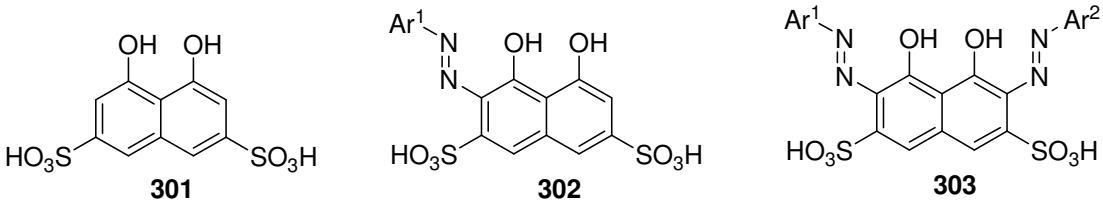

Figure 4.0.1: Chromotropic acid **301**, monoazo **302** and bisazo **303** dyes

However, in practice it has proved difficult to control the coupling process with respect to regiochemistry and multiple substitution (Scheme 4.0.2).[102] In many cases the second azo coupling reaction does not lead to the desired unsymmetrical 2,7-bisazo product **303** but instead *ipso* substitution occurs, in which the initial azo coupled group is displaced as its diazonium salt. *Ipso* substitution involves attack at the *ipso* position of the 2-monoazo compound **302** by a second diazonium salt resulting in an *ipso* substituted 2-monoazo compound **304**. There can then be subsequent azo coupling of this 2-monoazo compound **304** to give a symmetrical 2,7-bisazo compound **305** of the *ipso* substituted 2-monoazo compound **304**.

In addition to this there is also the possibility of further azo coupling of the diazonium salt ejected during *ipso* substitution with the 7-position of the *ipso* substituted monoazo compund **304** to give the required unsymmetrical 2,7-bisazo product **303**. Hence the yield of the unsymmetrical 2,7-bisazo product **303** may also be influenced by *ipso* substitution.

The symmetrical 2,7-bisazo compund **306** of the intial 2-monoazo compound **302** can also be present as a by-product in 2-monoazo coupling of the initial diazonium salt with chromotropic acid **301**. The yield of this by-product can also increase during the second azo coupling step due to the diazonium salt ejected during *ipso* substitution coupling with the 2-monoazo compound **302**. Hence, there can be several by-products of this bisazo coupling step but there is little understanding of the factors involved.

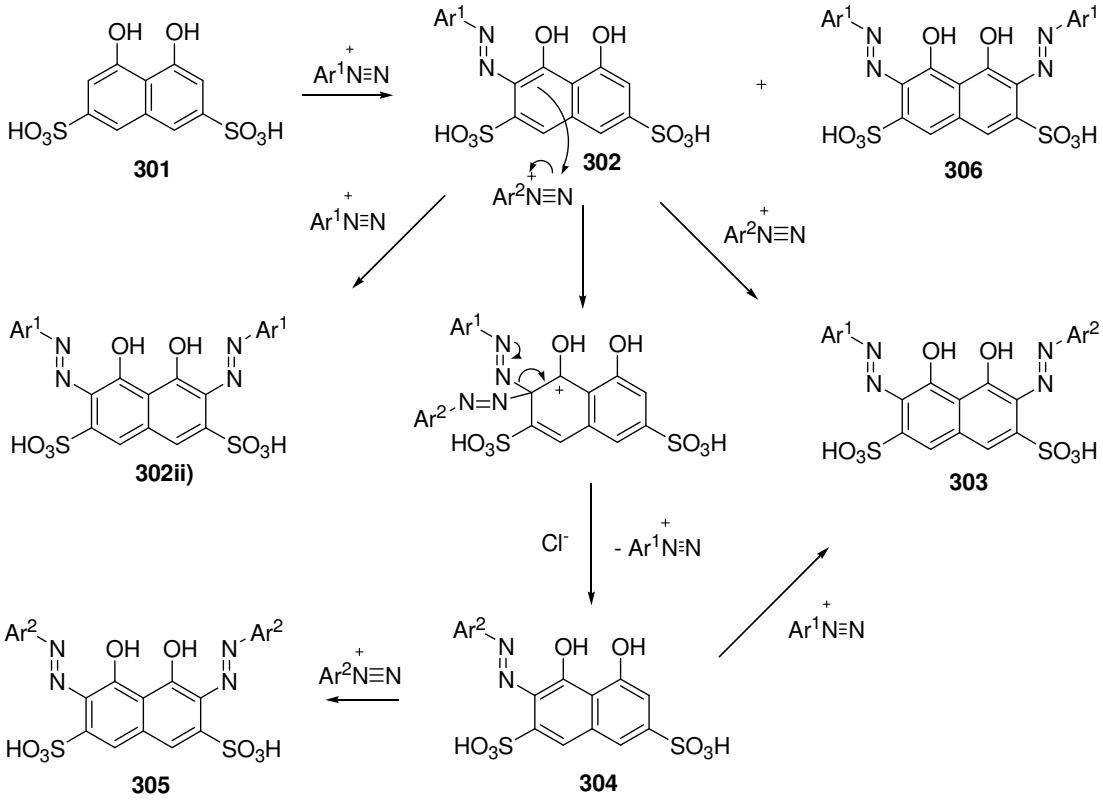

Scheme 4.0.2: Azo coupling of chromotropic acid **301**.

4.1: Azo / Hydrazone Tautomerism

The 2-monoazo compound **302** and 2,7-bisazo products **303** of azo coupling reactions may also be in either the azo **302 i)** or hydrazone **302 ii)** tautomeric form which can also affect the properties of the dye (Scheme 4.1.1).

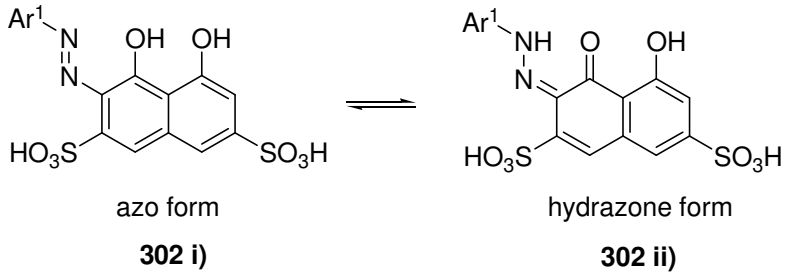

Scheme 4.1.1: Azo – hydrazone tautomerism.

A ^{13}C NMR study of several 2-monoazo compounds **302** and 2,7-bisazo compounds **303** by Fedorov and co-workers revealed that 2-monoazo **302** derivatives of chromotropic acid **301** are present in the hydrazone form **302 ii)** in D_2O and

DMSO at neutral pH at 300 K.[103] The main spectral feature of all the dyes confirming this was a quaternary carbon signal at δ_C = 179 – 192 corresponding to the carbonyl group rather than a signal at $\delta_C \approx 160$ corresponding to a hydroxyl substituted quaternary carbon.

Studies of three 2,7-bisazo **303** derivatives revealed both the azo groups to be in the azo form **303 i)** under these conditions.[104] The 2,7-bisazo **303** derivatives prepared contained a *para* substituted aromatic ring coupled to chromotropic acid **301** with substituents X = NO_2, SO_3Na, COOH. However, there are several factors which can affect the form of the product such as pH, solvent polarity and presence of *ortho* substituents which may be involved in hydrogen bonding.[105] Therefore it can be difficult to predict in which tautomeric form an azo compound will be present.

Throughout this chapter all 2-monoazo **302** and 2,7-bisazos copmounds **303** will be expressed in the azo form rather than the hydrazone form. This is common in the reporting of these compounds and also the major aims of this study do not include the establishment of the exact tautomeric form of these azo products.

4.2: Literature Examples

Many examples of azo compounds have been reported by standard diazonium salt azo coupling techniques involving electrophilic attack at a carbon position by a diazonium salt. However, a detailed study of electronic and steric effects upon azo coupling reactions of chromotropic acid **301** has not been carried out.

Although there have been many 2-monoazo **302** and 2,7-bisazo **303** compounds based on chromotropic acid **301** reported, the synthesis of these was rarely discussed. Some preparative routes to 2-monoazo compounds **302** reported recently involve standard azo coupling of diazonium salts to chromotropic acid **301**. McMinn and Kratochvil reported the preparation of the 2-monoazo compound **308** by coupling of the appropriate diazonium salt **307** with chromotropic acid **301**.[106] The crude product was then purified by column chromatography although no yield was given (Scheme 4.2.1).

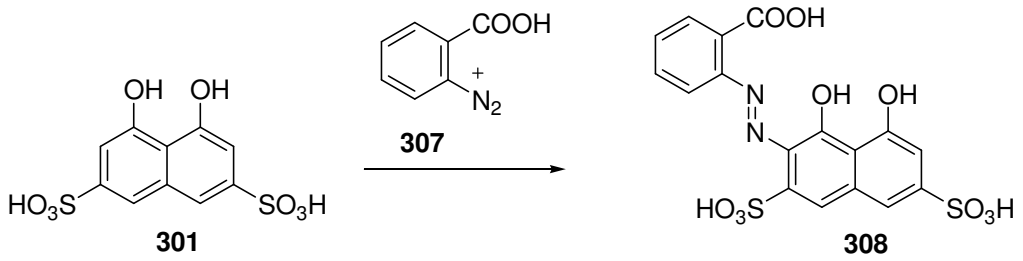

Scheme 4.2.1: Preparation of 2-monoazo derivative **308**.[106]

There have also been recent reports of the preparation of 2,7-bisazo derivatives of chromotropic acid **301** by Zhang and co-workers.[107] Firstly the arsenazo **309** was prepared by coupling of the appropriate diazonium salt to chromotropic acid **301**. This 2-monoazo compound **309** then underwent bisazo coupling with the diazonium salt of 2,6-dichloroaniline **310** to give the 2,7-bisazo compound **311** in 76% yield (Scheme 4.2.2).

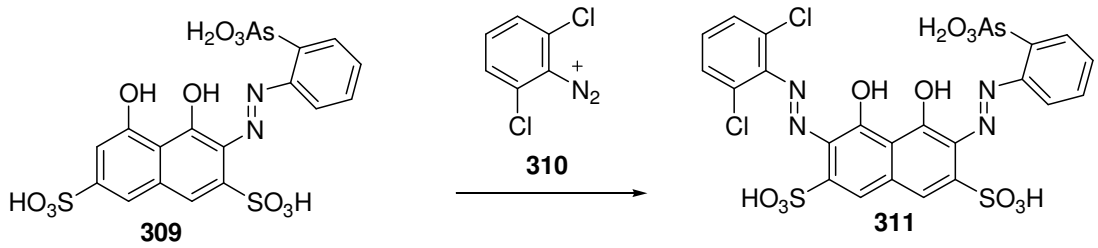

Scheme 4.2.2: Preparation of 2,7-bisazo derivative **311**.[107]

Recently there has been a more complete and extensive study of the chemistry of chromotropic acid **301** published in the development of new inkjet dyes by Fujifilm Imaging Colorants (formerly Avecia).[101a,b] A large number of bisazo coupled compounds with varying aryl substitutents and electronic properties were prepared by standard diazonium salt routes and tested for potential as inkjet printer dyes. Some of these are displayed in table 4.2.

Several heterocyclic examples were also prepared which could then be metallised in order to achieve increased light fastness. However, it was found that unmetallised dyes still showed suitable fastness properties. Such unmetallised dyes are cheaper and easier to prepare than the corresponding metallised dyes. They are also more environmentally friendly and less prone to nozzle blockage due to the absence of transition metals.[101a,b]

Table 4.2: Range of bisazo dyes prepared. [101a,b]

General bisazo dye structure	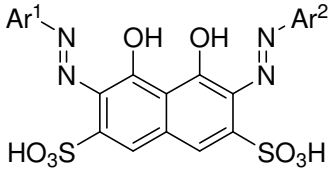	
	Ar^1	Ar^2
i	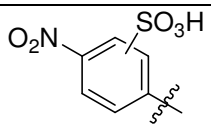	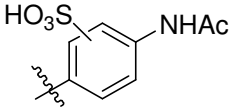
ii	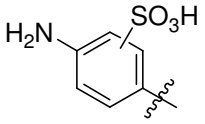	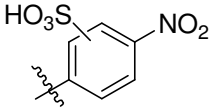
iii	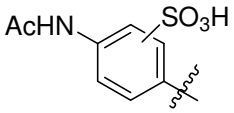	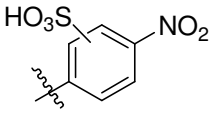
iv	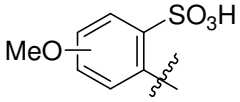	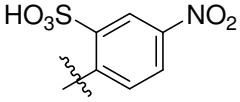
v	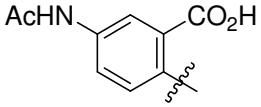	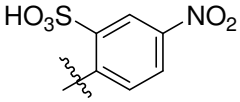
vi	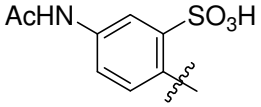	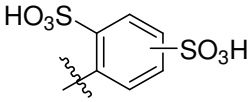
vii	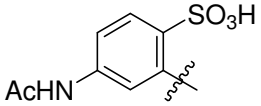	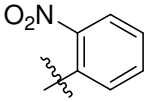
viii	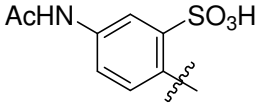	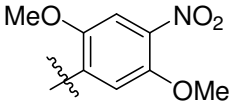
viiii	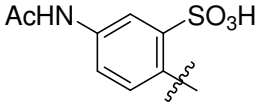	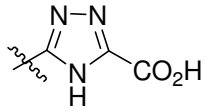
x	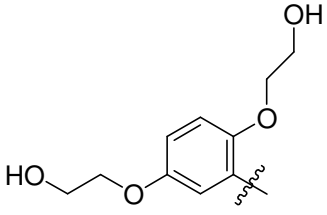	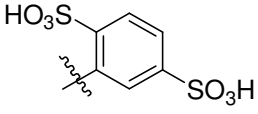

The optimisation of these reactions to minimise by-products as a result of *ipso* substitution is of particular interest and understanding the detailed chemistry behind bisazo coupling is now the focus of much research.

4.3: *Ipso* Substitution

Discussion of electrophilic attack or substitution at *ortho, meta* and *para* positions to a substituent is covered extensively in the literature. Although the possibility of electrophilic attack at the *ipso* (substituted) position is also known this has been largely ignored.[108] However, both recent and long standing investigations show that *ipso* electrophilic substitution can compete effectively with the unsubstituted positions in many aromatic substitution reactions and in some cases becomes the predominant or exclusive reaction. A range of electrophilic *ipso* substitutions has been reported, some of which are summarised below.

4.3.1: Electrophilic Aromatic Substitution

The term *ipso* substitution was first introduced by Perrin and Skinner to denote attack by a reagent at a substituted nuclear position during an investigation by the authors into directive factors associated with the nitration of anisole, *p*-iodo-, *p*-bromo- and *p*-chloroanisole **312**.[109] It was found that *ipso* attack was possible at iodine and bromine substituted sites with liberation of the halide to afford the *ipso* substituted product **313** (Scheme 4.3.1). However, no evidence of electrophilic *ipso* substitution at a chlorine substituent was obtained.

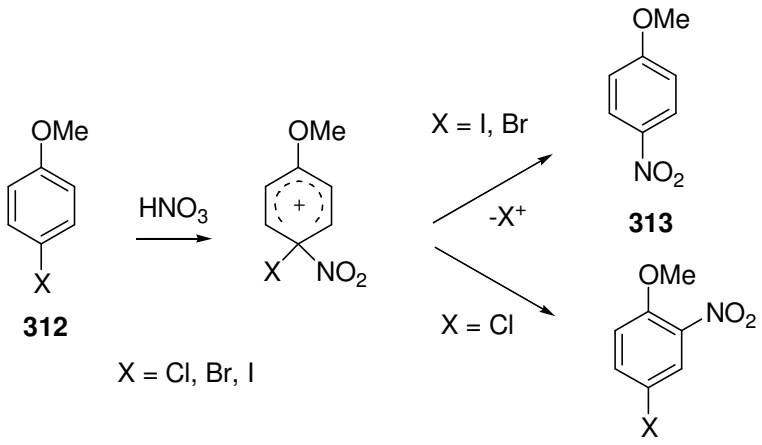

Scheme 4.3.1: Possible nitration products of *p*-haloanisoles.[109]

A later review on *ipso* attack in aromatic nitration described the various products of the attack of a substituted benzene derivative **314** by a nitronium ion (Scheme 4.3.2).[110] *Ipso* substitution in which X is displaced by a nitro group has been previously reported in cases where X = alkyl, acyl, -SiR_3, -SO_3H and -N_2Ar although was classed as an "anomalous nitration".[110]

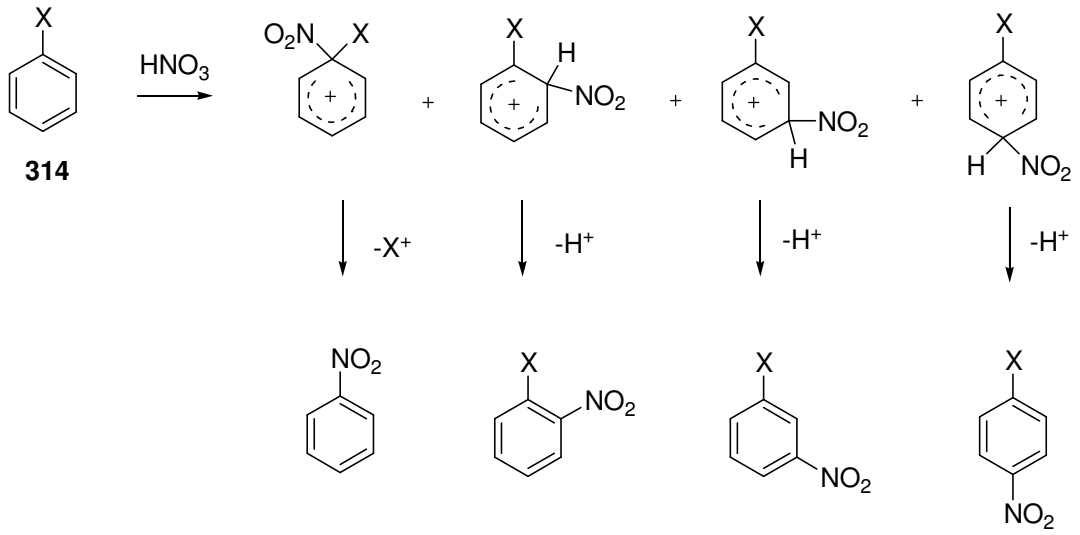

Scheme 4.3.2: Nitration products of substituted benzene derivatives.[110]

4.3.2: *Ipso* Substitution of Azo Groups

There have also been examples reported of the *ipso* attack of azo groups through electrophilic aromatic substitution. The replacement of an arylazo group of an azo dye by another diazo residue was first achieved by Nolting and Grandmougin in 1891.[111] They reported that the reaction of 4-benzeneazo-1-naphthol **315** and 4-diazobenzenesulfonic acid **316** did not lead to the expected 2-benzeneazo-4-*p*-sulfobenzeneazo-1-naphthol. Instead a mixture of 2,4-bis(*p*-sulfobenzeneazo)-1-naphthol **317** and 2,4-bis-benzeneazo-1-naphthol **318** were obtained (Scheme 4.3.3). This was as a result of *ipso* substitution at the 4-position of 4-benzeneazo-1-naphthol and azo coupling at the 2-position to afford **317**. Subsequent azo coupling of the ejected benzene diazonium salt with 4-benzeneazo-1-naphthol **315** at the 2-position afforded **318**.

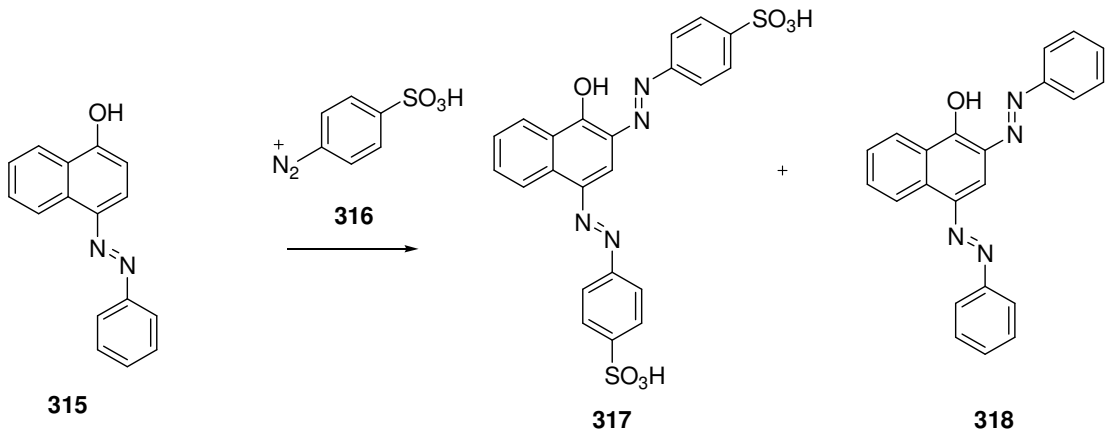

Scheme 4.3.3: Reaction of 2-benzeneazo-1-naphthol **315** and 4-diazobenzenesulfonic acid **316**.[111]

Filippytschew and Tschekalin also studied the substitution of an arylazo group by diazonium ions and found that the reaction occurs more easily as the reactivity of the incoming diazonium ion component increases.[112]

Similarly Lwoff observed that *p*-nitrobenzenediazonium ions or *o*-chloro-*p*-nitrobenzenediazonium ions **320** replace the *p*-sulfobenzeneazo group from 1-*p*-sulfobenzeneazo-2-naphthol **319** (Scheme 4.3.4).[113]

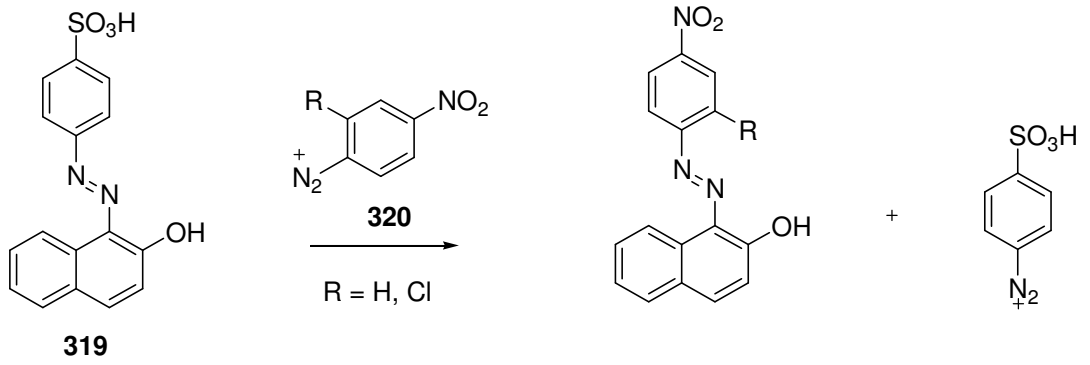

Scheme 4.3.4: *Ipso* substitution of sulfonic acid groups.[113]

In more recent work Lwoff's experiments were repeated using a ^{15}N labeled diazonium salt **321** which were reported to support the theory of a slow equilibrium set up between the diazonium ion, 1-(*p*-sulfobenzeneazo)-2-naphthol **319** and the metastable complex **322**, followed by rapid ejection of *p*-sulfobenzenediazonium salt

323 although no details of the experimental evidence were given in the review (Scheme 4.3.5).[114]

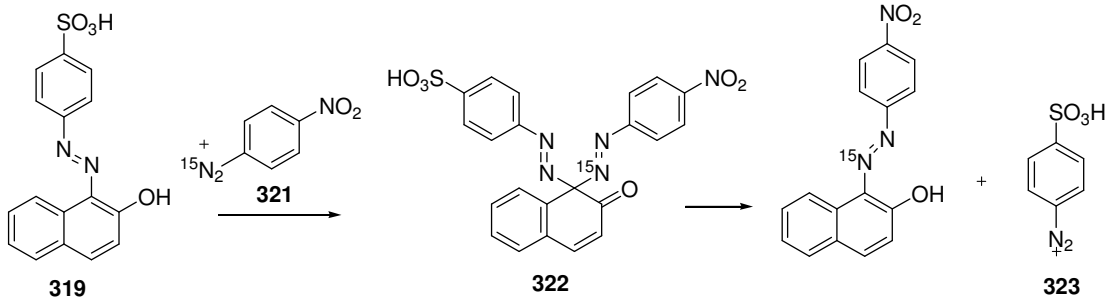

Scheme 4.3.5: Nitrogen labelling studies.[114]

That diazo exchange reactions of this type have been observed only rarely is rather surprising, as the diazo residue is a group readily eliminated as a diazonium ion.[115] The possibility of such *ipso* attack by a diazonium salt is a potential source of problems in the manufacture of azo dyes, since the replacement takes place under normal coupling conditions.

4.3.3: Conclusions

A variety of electrophilic *ipso* substitution reactions of a varying nature have now been reported in past and the recent literature. The significance of these reactions has increased due to *ipso* attack leading to the main product of the reaction in many cases.

Ipso substitution has become of particular interest in the synthesis of azo compounds due to the possibility of *ipso* attack of the monoazo dye during bisazo coupling by the second diazonium salt leading to ejection of the initial azo group as its diazonium salt.

4.4: Preparation of Electron Rich and Poor 2-Monoazo Derivatives

The aim of this section of this thesis was to investigate the extent of the influence of electronic effects upon monoazo coupling and in turn bisazo coupling. The reaction of electron rich and electron poor diazonium salts based upon a scale devised from the electron donating / withdrawing effects of the *p*-substituent of the diazonium salt were carried out. *p*-Substituted diazonium salts considered in this series were **324a,b,c,d,e,f,g**: X = OMe, OEt, Me, H, Cl, CN, NO_2 respectively. The reaction of *p*-substituted benzenediazonium salts **324a,c,e,g** with chromotropic acid **301** to give electron rich and poor monoazos **302a,c,e,g** was examined (Scheme 4.4.1).

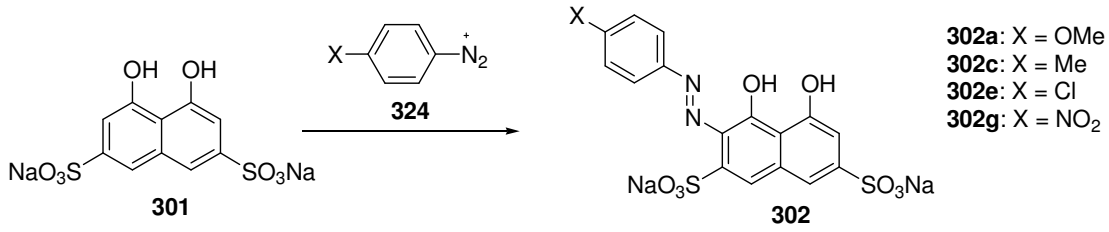

Scheme 4.4.1: Preparation monoazos **302a,c,e,g**: X = OMe, Me, Cl, NO_2.

Diazonium salt preparation and subsequent azo coupling were carried out under standard conditions using methods supplied by Fujifilm. This afforded the *p*-substituted monoPACAs (2-phenylazochromotropic acid) **302a,c,e,g** obtained as the disodium salt due to chromotropic acid **301** being prepared in this form and isolation techniques (see experimental section).

Throughout this chapter azo compounds are represented as the sodium salts (SO_3Na) although they can be detected in mass spectrometry in the free sulfonic acid form (SO_3H) due to electrospray ionisation conditions. Azo compounds of this type are commonly represented as the free sulfonic acid forms (SO_3H), however, they are present in solution as the disodium salts (SO_3Na) at normal pH.

Reaction progress was monitored by HPLC and appeared complete between 1 and 2 hours after addition dependent upon the strength of the diazonium salt. Diazonium salts containing electron withdrawing groups are more electrophilic and hence classed as “stronger” with increased reaction over diazonium salts containing electron donating substituents. Measurement of isolated yields was not a reliable

indication of organic content due to problems encountered in the recovery and purification of aqueous chemistry products. Therefore standard methods for calculating yields were not possible. Hence, yields were calculated using quantitative HPLC (QHPLC) (See experimental section).

The strength of organic content in the monoazo products was calculated by CHN analysis (see experimental section). This was used together with the % composition of the *p*-substituted monoPACAs **302** in the organic content by HPLC to calculate the strength of the *p*-substituted monoPACAs **302** in the isolated product after purification (Table 4.4.1). This was the standard method used for calculating organic strength of this type of water soluble azo compounds which contained salt impurities. Upon isolation, the products were positively identified by ^{1}H and ^{13}C NMR and electrospray mass spectrometry.

Table 4.4.1: QHPLC yields and strength of isolated *p*-substituted monoPACAs **302**

p-substituted mono PACA **302**	*p*-substituent	QHPLC yield	Organic content strength From CHN	*p*-substituted mono PACA **302** strength in organic content	Overall *p*-substituted mono PACA **302** strength in isolated product
a	OMe	97 %	93%	94%	87%
c	Me	85%	79%	99%	79%
e	Cl	69%	85%	92%	79%
g	NO_2	72%	99%	96%	96%

In addition to the required *p*-substituted monoPACAs **302a,c,e,g** the bisazo by-product *p*-substituted bisPACAs **306a,c,e,g** were also obtained in low yields (≈ 1% - 5%) (Scheme 4.4.2). The formation of these by-products **306a,c,e,g** could be reduced by controlled dropwise addition of the diazonium salt **324a,c,e,g**.

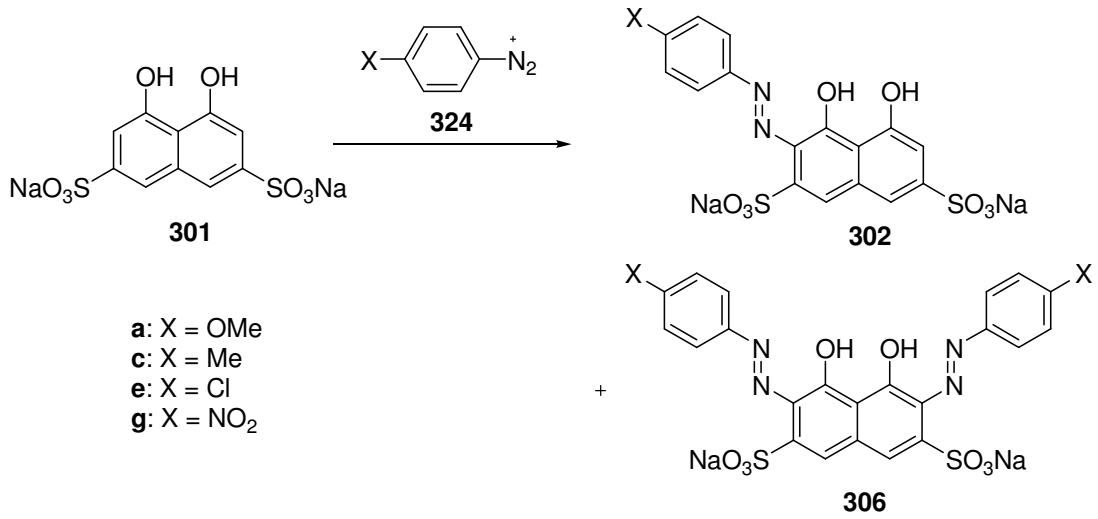

Scheme 4.4.2: Preparation of *p*-substituted monoPACAs **302a,c,e,g**.

Therefore it was possible to prepare *p*-substituted monoPACAs **302a,c,e,g** in high yield with little *p*-substituted bisPACAs **306a,c,e,g** obtained. Subsequent purification, isolation and analysis gave the strength of the required monoazo **302** products as the disodium salts for future use.

4.5: Tautomeric Forms of 2-Monoazo Derivatives

From analysis of the ^{13}C NMR spectra of *p*-methoxyPACA **302a** and *p*-nitroPACA **302g** it was clear that both of the products were in the hydrazone form in DMSO solvent used to record the spectra. This was shown by the signal corresponding to the quaternary carbon at the 1-position which had a chemical shift of $\delta \approx 180$ indicating a quaternary of a carbonyl group as opposed to $\delta \approx 160$ indicating a quaternary attached to a hydroxy group (Scheme 4.5.1). Hence the position of the equilibrium is far to the right in the case of these monoazos which agrees with the literature.[103, 104]

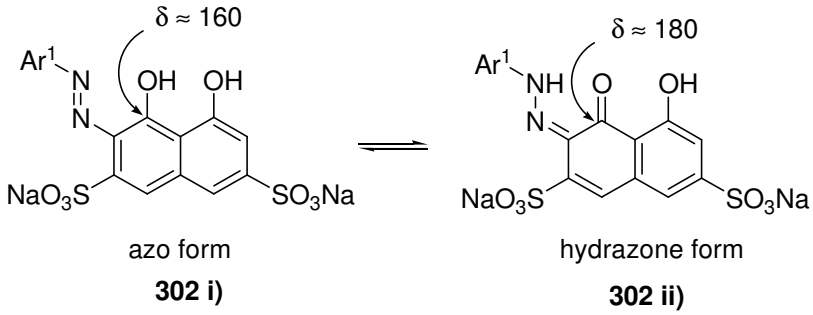

Scheme 4.5.1: Expected ^{13}C signals in each tautomeric form.

In the case of of *p*-methoxyPACA **302a** the C-1 signal was at δ = 179.00 confirming the hydrazone structure in DMSO and likewise in the case of *p*-nitroPACA **302g** the C-1 signal was at δ = 182.09 (Figure 4.5.1). However, initial attempts to determine the structural forms of these products under aqueous conditions in D_2O were unsuccessful due to poor solubility.

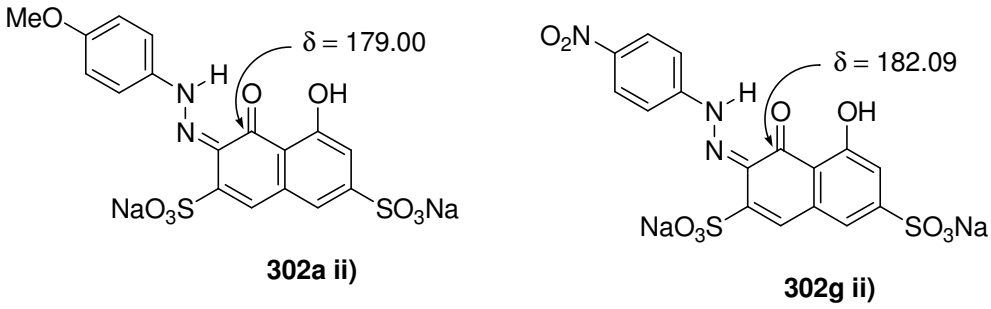

Figure 4.5.1: Tautomeric forms of *p*-methoxyPACA **302a** and *p*-nitroPACA **302g**.

4.6: Preparation of Bisazo Derivatives

The influence of electronic effects upon bisazo coupling was firstly considered. Extreme members **302a,g** of an electronic series were examined containing an electron donating substituent **302a** and an electron withdrawing substituent **302g**. Bisazo coupling of the monoPACAs **302a,g** with a diazonium salt was investigated to determine if the electronic nature of the monoazo electron donating and withdrawing groups affected the reactivity of the monoPACAs **302a,g** products obtained and yields.

As mentioned earlier the second azo coupling often does not lead to the desired unsymmetrical 2,7-bisPACA (phenylazochromotropic acid) product **303** with several by-products possible due to *ipso* substitution (Scheme 4.6.1). Possible by-products include the *ipso* substituted monoPACA **304**, the symmetrical *ipso* substituted bisPACA **305** and the symmetrical 2,7-bisPACA **306**. These abbreviations for reaction products and by-products will be used throughout this chapter.

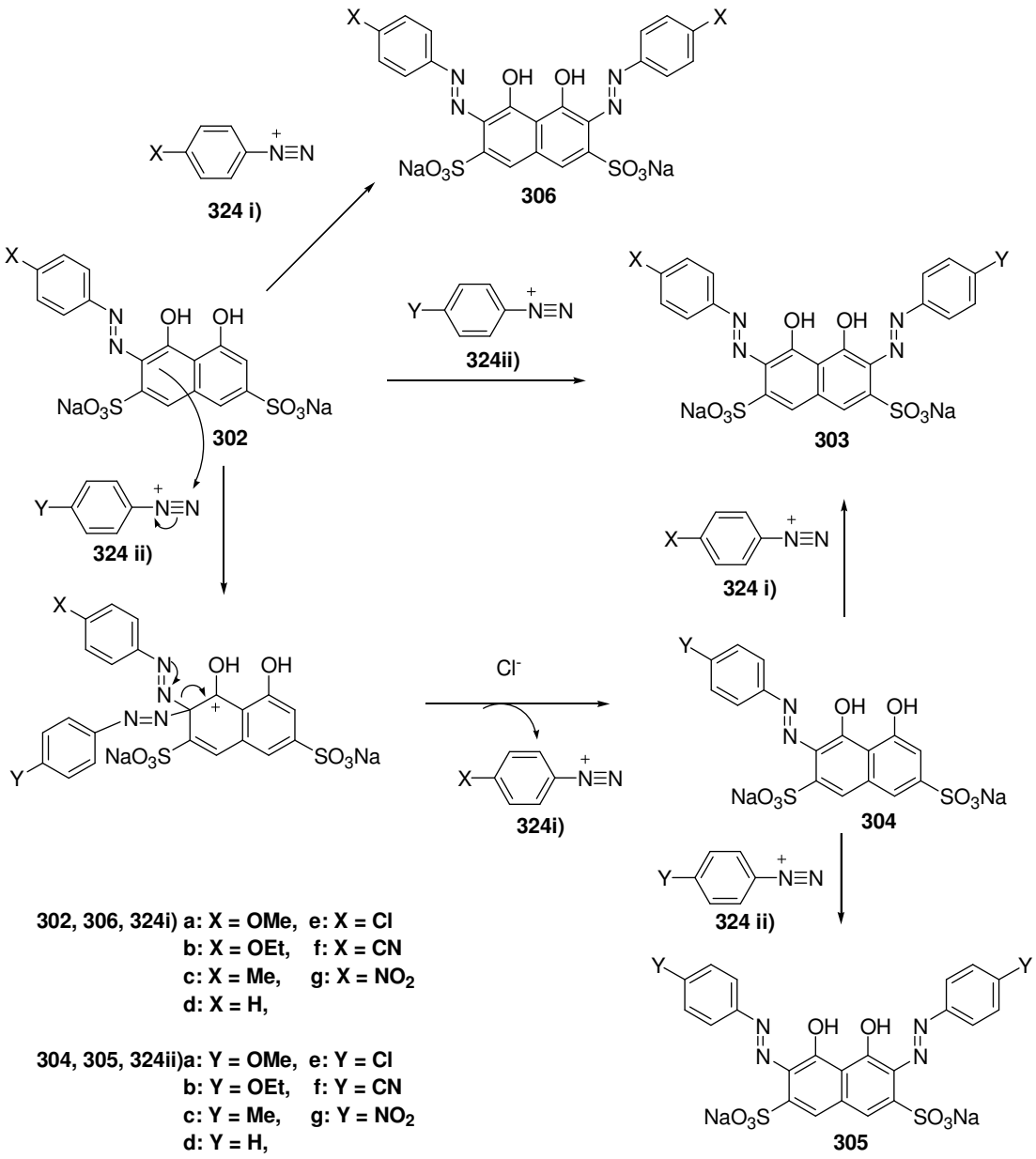

Scheme 4.6.1: Possible routes to the unsymmetrical 2,7-bisPACA **303** and by-products.

The compound numbering and assignment of the unsymmetrical 2,7-bisPACAs **303** products which is based on substitutents and used throughout the remainder of this chapter is represented in Table 4.6.

Table 4.6: Assignment unsymmetrical 2,7-bisPACAs **303** compound numbers.

	***p*-Substituent Y**							
***p*-Substituent X**		OMe	OEt	Me	H	Cl	CN	NO_2
	OMe	x	**303ab**	**303ac**	**303ad**	**303ae**	**303af**	**303ag**
	OEt	**303ba**	x	**303bc**	**303bd**	**303be**	**303bf**	**303bg**
	Me	**303ca**	**303cb**	x	**303cd**	**303ce**	**303cf**	**303cg**
	H	**303da**	**303db**	**303dc**	x	**303de**	**303df**	**303dg**
	Cl	**303ea**	**303eb**	**303ec**	**303ed**	x	**303ef**	**303eg**
	CN	**303fa**	**303fb**	**303bc**	**303fd**	**303fe**	x	**303fg**
	NO_2	**303ga**	**303gb**	**303gc**	**303gd**	**303ge**	**303gf**	x

4.6.1: Initial Bisazo Coupling Experiments

The reaction of *p*-nitroPACA **302g** with a less reactive *p*-methoxybenzenediazonium salt **324a** and the reaction of *p*-methoxyPACA **302a** with a very reactive *p*-nitrobenzenediazonium salt **324g** were carried out.

The procedures used for a typical reaction study is described. A freshly prepared slurry of the monoPACA **302a,g** was prepared but was not isolated prior to the second diazonium salt coupling. This was done to reduce loss of the product during filtration of the precipitate.

The diazonium salt **324a,g** (1 equivalent) was added slowly to the monoPACA **302a,g** reaction mixture at pH 6.0 – 7.0 over half an hour at a temperature of less than 5 ºC. In practice it proved difficult to ensure accurate pH control of these reaction mixtures as slurries. The reaction mixture was then stirred at a temperature of less than 5 ºC for a further four hours with the reaction progress monitored by HPLC. Although the lifetime of the diazonium salt **324a,g** is likely to be only a matter of hours the reaction mixture was stirred overnight at room temperature to ensure completion. Peaks in chromatograms of the reaction mixture were identified by LCMS and yields of reaction products calculated by Quantitative HPLC (QHPLC) (see experimental section).

After 48 hours there was no apparent reaction of *p*-nitroPACA **302g** with the diazonium salt **324a** under these reaction conditions at pH 6.0 – 7.0 and no presence of the expected *p*-nitro,*p*-methoxybisPACA **303ga**. Only the initial *p*-nitroPACA **302g** starting material was present (Scheme 4.6.2).

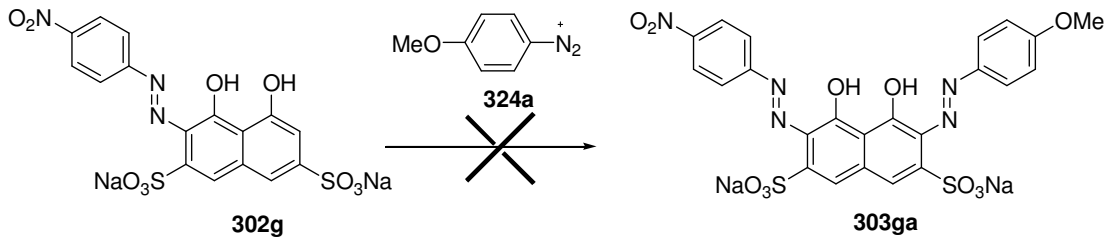

Scheme 4.6.2: Failed reaction of *p*-nitroPACA **302g** with *p*-methoxybenzene diazonium salt **324a**.

Upon treatment of a freshly prepared solution of *p*-methoxyPACA **302a** with the *p*-nitrobenzenediazonium salt **324g** under the same standard conditions, several products were detected by HPLC of the reaction mixture after an overnight reaction. These products were identified as the expected *p*-methoxy,*p*-nitrobisPACA product **303ag** in 34% yield, the *ipso* substituted *p*-nitroPACA by-product **304g** in 39% yield and finally *p*-nitrobisPACA **305g** in 12% yield (Scheme 4.6.3, Figure 4.6.1).

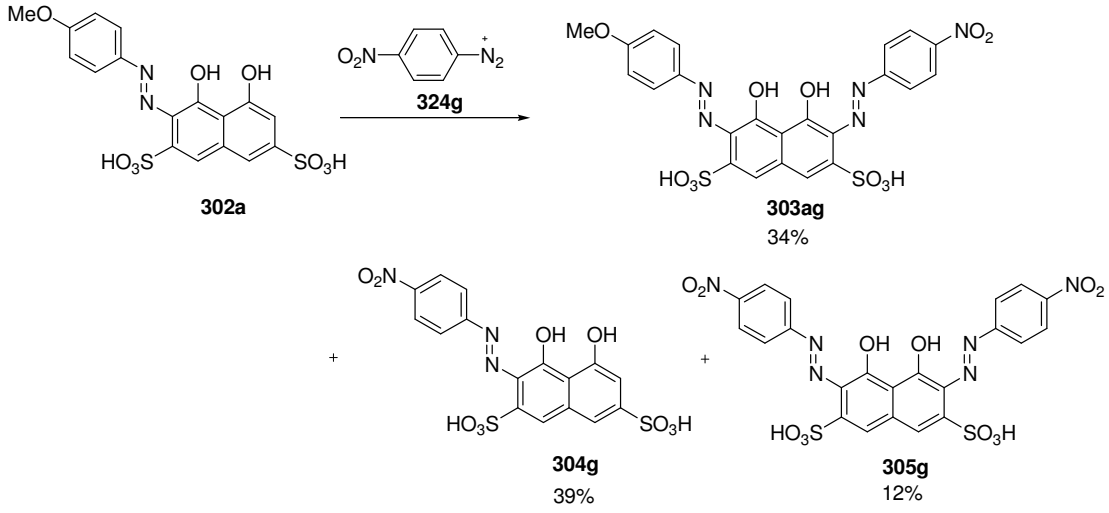

Scheme 4.6.3: Reaction *p*-methoxyPACA **302a** with *p*-nitrobenzenediazonium salt **324g**.

Peaks were assigned by LCMS.

- *p*-nitroPACA **304g**: ESI MS 468 $[MH]^-$ Req. 468
- *p*-nitrobisPACA **305g**: ESI MS 617 $[MH]^-$ Req. 617
- unsymmetrical 2,7-bisPACA **303ag**: ESI MS 602 $[MH]^-$ Req. 602
- Monoazo standard: used for QHPLC calculations.
- Bisazo standard: used for QHPLC calculations.

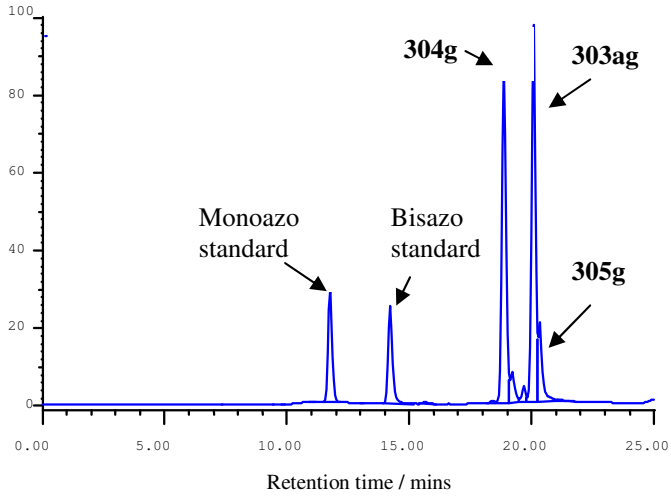

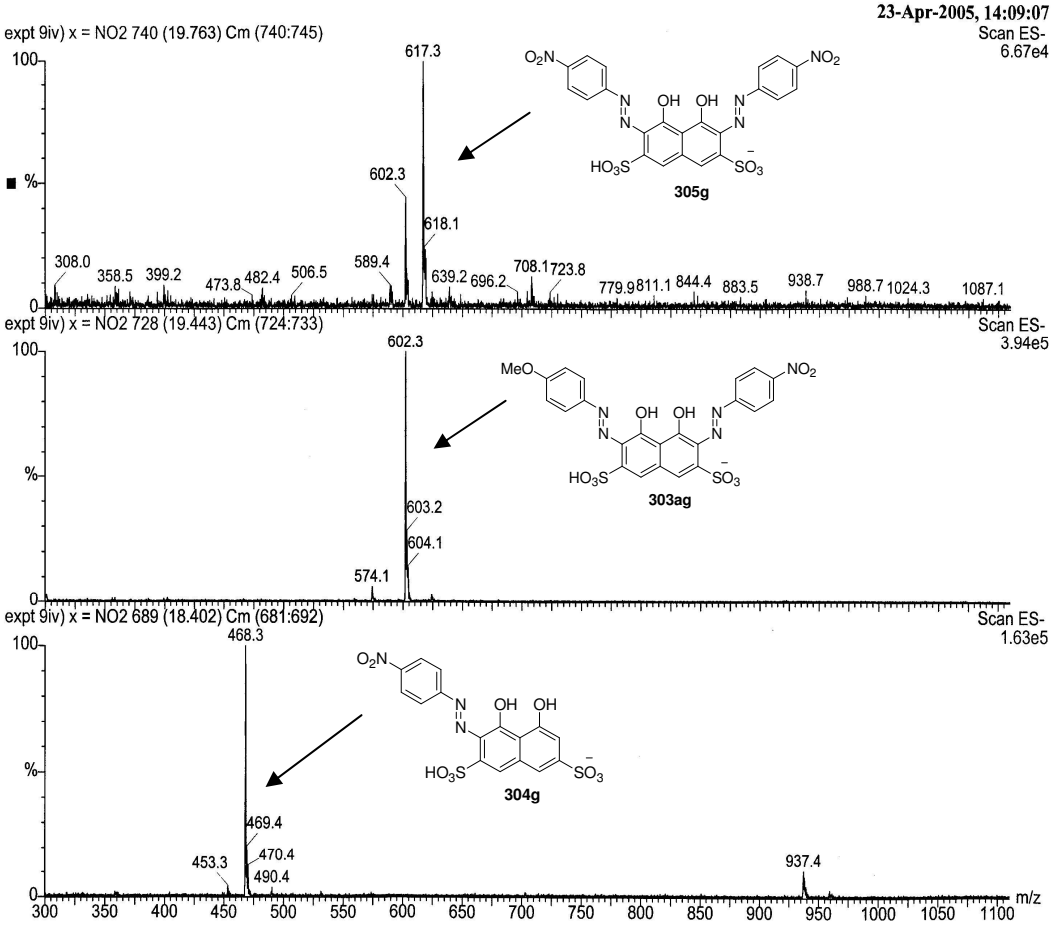

Figure 4.6.1: HPLC chromatogram and LCMS of reaction mixture.

The formation of these products and by-products can occur *via* several routes. Firstly the predominant product, *p*-nitroPACA **304g** can result from electrophilic attack of the *ipso* position of *p*-methoxyPACA **302a** by the *p*-nitrobenzenediazonium salt **324g**. The displacement of the *p*-methoxybenzene azo substituent as a diazonium **324a** salt to gives *p*-nitroPACA **304g** (Scheme 4.6.4). The *p*-nitroPACA **304g** can then undergo further azo coupling with the *p*-nitrobenzenediazonium salt **324g** in the reaction mixture to give the *p*-nitrobisPACA **305g** termed the *ipso* substituted bisPACA **305g** (Section 4.6.1).

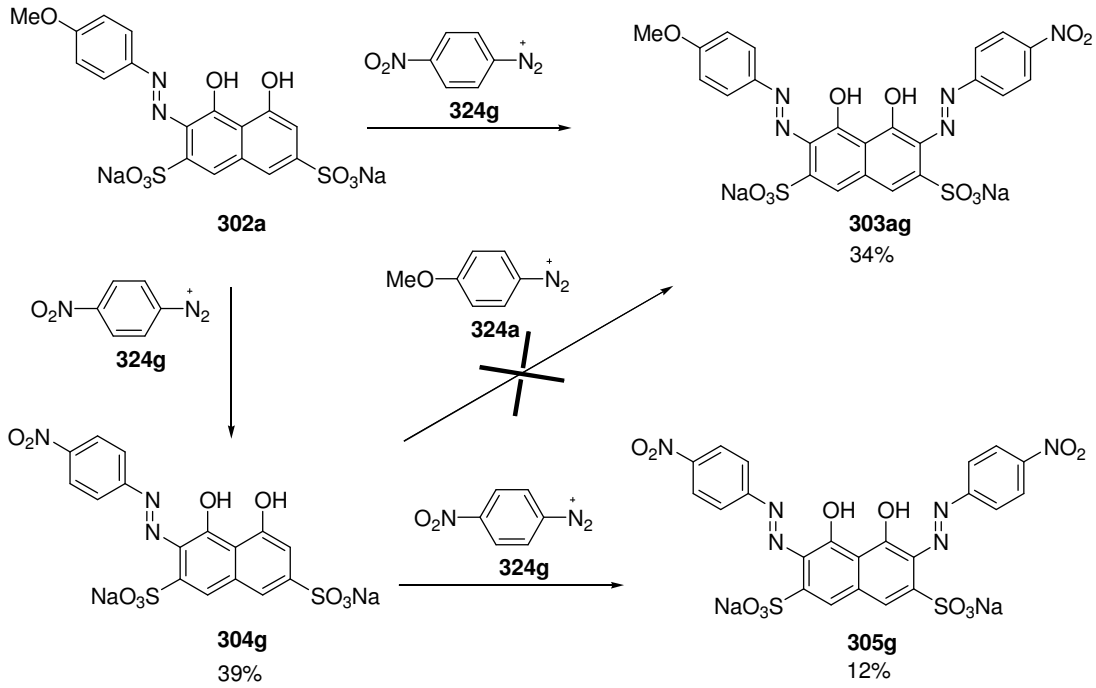

Scheme 4.6.4: Routes to products and by-products.

The required *p*-nitro,*p*-methoxybisPACA or unsymmetrical 2,7-bisPACA **303ag** can be formed by standard diazonium salt coupling of the *p*-nitrobenzenediazonium salt **324g** with *p*-methoxyPACA **302a** at the 7-position of the naphthol ring termed the bisazo coupling position. In principle the unsymmetrical 2,7-bisPACA **303ag** can also be formed by reaction of the *ipso* substituted monoPACA by-product *p*-nitroPACA **304g** with the displaced *p*-methoxybenzene diazonium salt **324a** assuming that the lifetime of the diazonium salt displaced during *ipso* substitution is suitably long to undergo a further reaction. However, in

this particular case this route can be eliminated since *p*-nitroPACA **304g** does not react with the *p*-methoxybenzenediazonium salt **324a** as was demonstrated earlier (Scheme 4.6.2).

The relative yields of the products of the reaction of *p*-methoxyPACA **302a** with the *p*-nitrobenzenediazonium salt **324g** indicate there is a higher yield of products as a result of attack at the *ipso* position than the bisazo coupling position (7-position) of *p*-methoxyPACA **302a**. This can be determined from an overall 51% yield of products **304g** and **305g** as a result of attack at the *ipso* position and a 34% yield of product **303ag** as a result of attack at the bisazo coupling position.

From these initial results it appears that *p*-methoxyPACA **302a** is much more reactive than *p*-nitroPACA **302g**. This may be due to electron withdrawal from the second azo coupling site by the *p*-nitro substituent due to conjugation which reduces its susceptibility to electrophilic attack by the second diazonium salt (Figure 4.6.2). In the hydrazone form the mechanism of electrophilic attack involves the lone pair on the nitrogen of the azo group which is withdrawn into the aryl system by the nitro substituent and hence reduces its availability for bisazo coupling. Hence no bisazo coupling reaction occurs. This may also explain the lack of *ipso* substitution in the case of *p*-nitroPACA **302g** due to withdrawal of electron density from the *ipso* position hence reducing its susceptibility to electrophilic attack by the second diazonium salt.

In the case of *p*-methoxyPACA **302a** electron donation from the *p*-methoxy group increases the availability of the nitrogen lone pair and may encourage electrophilic attack at both the *ipso* position and the bisazo coupling position by the second diazonium salt (Figure 4.6.2). Hence the reactivity of these positions is increased, correspondingly increasing the yields of the *ipso* substituted **304g** and unsymmetrical 2,7-bisPACA **303ag** products.

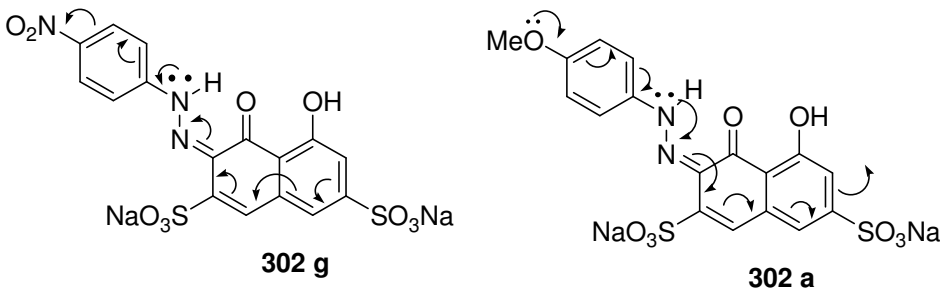

302 g **302 a**

Figure 4.6.2: Electron withdrawal from and donation to the naphthol ring.

This conclusion was supported by the ^{13}C NMR spectra of these monoazo compounds in DMSO. The chemical shift of the carbon at the bisazo coupling position in *p*-nitroPACA **302g** was δ = 113.20 compared with δ = 111.12 in the case of *p*-methoxyPACA **302a** (Figure 4.6.3).

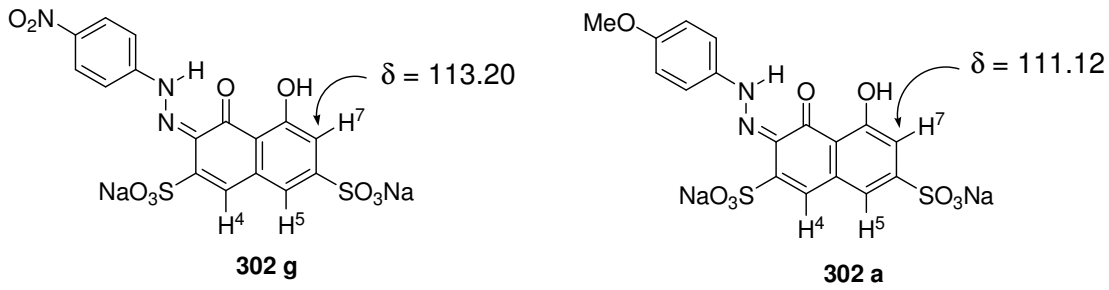

Figure 4.6.3: NMR data of *ipso* and bisazo coupling position.

Hence the bisazo coupling position in *p*-nitroPACA **302g** is more deshielded than in *p*-methoxyPACA **302a** suggesting that it is likely to be less susceptible to electrophilic attack and hence bisazo coupling, even though there are thirteen atoms between the substituents and the coupling site. The variation of ≈ 2 ppm in the chemical shift of this signal is comparable with the effect an acetoxy group would have upon the *para* position in a benzene ring.

The ^{1}H NMR signals of **302a,g** could be assigned by the observation of *meta* coupling between the two aromatic protons H-5 and H-7. A singlet was observed corresponding to the aromatic proton H-4. The two aromatic protons H-5 and H-7 could be assigned due to the observation of interactions in the NOESY spectrum between H-4 and H-5 due to the proximity of these adjacent protons. The HSQC spectrum was then used to assign C-4, C-5 and C-7 by the coupling of their proton and carbon signals. The remainder of signals in the ^{1}H and ^{13}C NMR spectra could be assigned by 2D NMR analysis.

However, this only tells us that this is the case with DMSO as a solvent. In order to determine if this is also the case in the aqueous reaction mixture ^{13}C NMR data in D_2O is required.

Another factor taken into consideration was the possible link between the reactivity of the diazonium salt used in the bisazo coupling step and the

corresponding products of the reaction due to the *p*-nitrobenzenediazonium salt **324g** being far more reactive than the *p*-methoxybenzenediazonium salt **324a**.

4.6.2: Reactvity of *p*-MethoxyPACA and *p*-NitroPACA

In order to determine if the reactivity of monoPACAs **302a,g** was affected by the electronic nature of the *para*-substituent or the strength of the diazonium salt used in bisazo coupling the reaction of *p*-methoxyPACA **302a** and *p*-nitroPACA **302g** towards a variety of *p*-substituted benzenediazonium salts **324a-g** was examined (Scheme 4.6.5). Reactions were carried out as described for a typical reaction study in section 4.6.1 and products identified by HPLC and LCMS analysis. Yields of the monoPACA **302**, unsymmetrical 2,7-bisPACA **303**, *ipso* substituted monoPACA **304**, *ipso* substituted bisPACA **305** and symmetrical bisPACA **306** were calculated by QHPLC as in section 4.6.1.

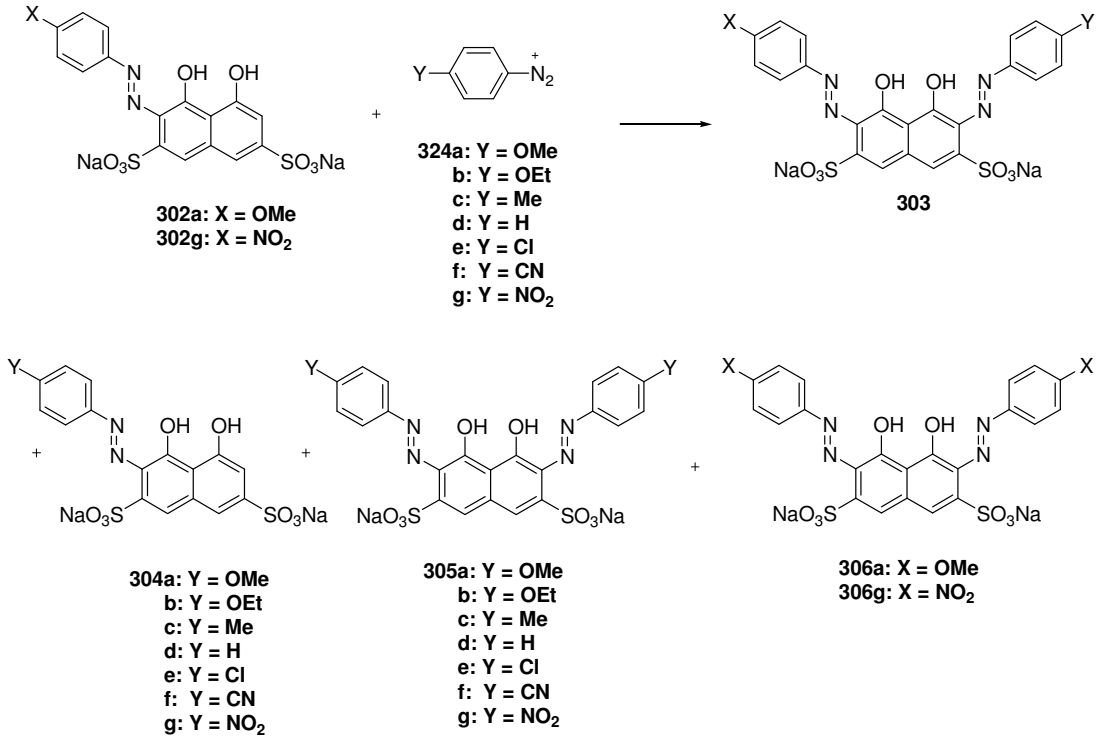

303: For substituent assignments see table 4.6.

Scheme 4.6.5: Reaction of *p*-methoxyPACA **302a** and *p*-nitroPACA **302g**.

The yields of the required unsymmetrical 2,7-bisPACAs **303** and each of the possible by-products from these reactions could then be plotted against the Hammett σ constant of the *p*-substituent of each of the diazonium salts **324** (Graphs 4.6.1 and 4.6.2). This gave a correlation between the electronic strength or reactivity of the diazonium salt based upon the *p*-substituent and the yield of each of the possible products. Hence, the reactivity of *p*-methoxyPACA **302a** and *p*-nitroPACA **302g** to a range of diazonium salts **324a-g** of differing strength could be shown.

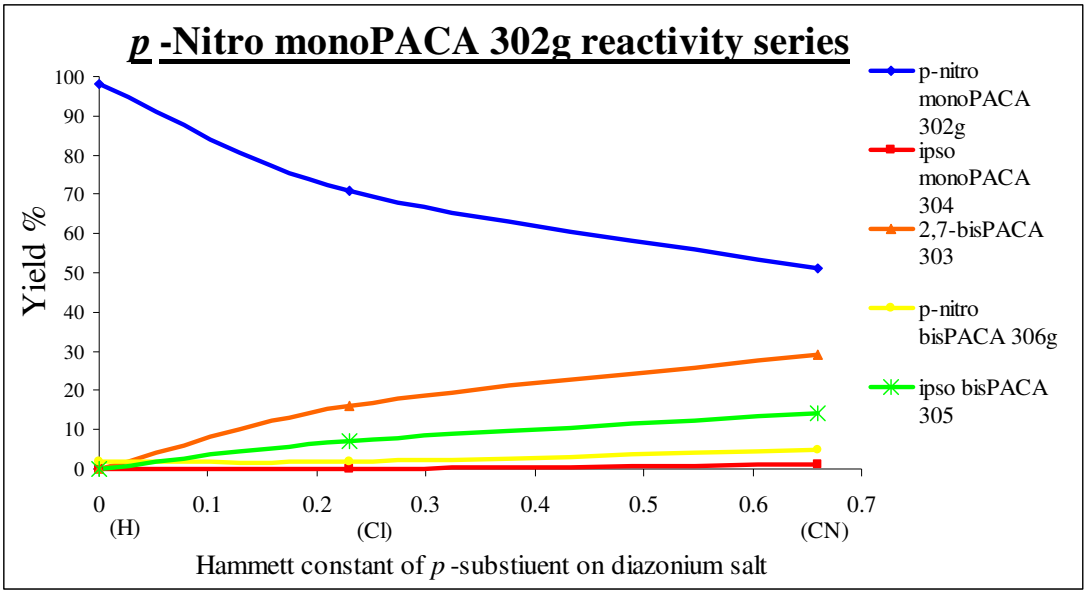

Graph 4.6.1: Reactivity of *p*-nitroPACA **302g** towards diazonium salts.

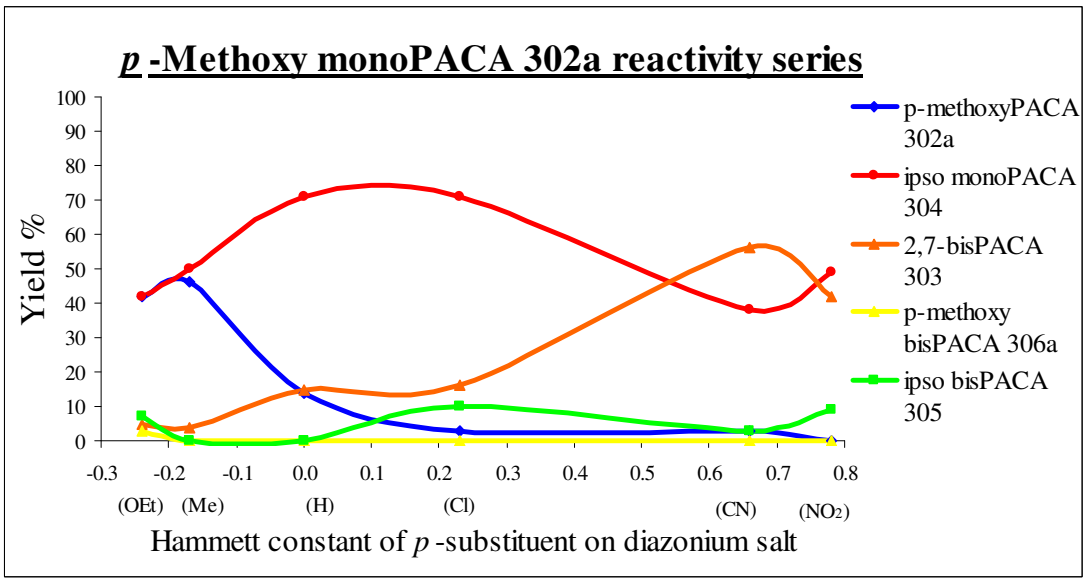

Graph 4.6.2: Reactivity of *p*-methoxyPACA **302a** towards diazonium salts.

From graph 4.6.1 it can be seen that there is no reaction of *p*-nitroPACA **302g** with the benzenediazonium salt **324d** resulting in only recovered starting material. Due to the absence of reaction in this case reaction of *p*-nitroPACA **302g** with the *p*-methylbenzene **324c**, *p*-ethoxybenzene **324b** and *p*-methoxybenzene **324a** diazonium salts were not carried out as no reaction was expected with these less reactive diazonium salts. From graph 4.6.2 it can be seen that there is reaction of *p*-methoxyPACA **302a** with all diazonium salts of the series.

Graphs 4.6.1 and 4.6.2 show that the yield the unsymmetrical 2,7-bisPACA **303** product increases with the strength of the diazonium salt **324** used in bisazo coupling. There is also a corresponding decrease in the yield of recovered monoPACA **302a,g** starting material with the strength of the diazonium salt used in bisazo coupling.

Reactions of *p*-nitroPACA **302g** with *p*-chlorobenzene- **324e** and *p*-cyanobenzene **324f** diazonium salts show that as the strength of the diazonium salt increases the yield of the unsymmetrical 2,7-bisPACA **303** also rises to a maximum of 21% in the case of the *p*-cyanobenzenediazonium salt **324f** and the yield of *p*-nitroPACA **302g** starting material recovered decreases from 72% to 38%.

In the case of the reaction of *p*-methoxyPACA **302a** with all diazonium salts of the series, the yield of the unsymmetrical 2,7-bisPACA **303** product also increases with the strength of the diazonium salt used in the bisazo coupling step. There is a large increase in the yield of the unsymmetrical 2,7-bisPACA **303** obtained in the case of reaction of *p*-methoxyPACA **302a** with the *p*-cyanobenzene- and *p*-nitrobenzenediazonium salts. This reaches a maximum of 44% in the case of the *p*-cyanobenzenediazonium salt **324f**. There is also a corresponding decrease in the yield of the *p*-methoxyPACA **302a** starting material recovered from 43% to 0% as the strength of the diazonium salt used in the bisazo coupling step increases.

In graphs 4.6.1 and 4.6.2 the yield of *ipso* substitution products does not appear to change significantly with the strength of the diazonium salt. In the reaction of *p*-nitroPACA **302g** with diazonium salts **324d-f** there was no significant *ipso* substitution by-products recovered. Only in the reaction of the *p*-cyanobenzene diazonium salt **324f** with *p*-nitroPACA **302g** was the *ipso* substitution bisPACA **305f** obtained in 11% yield.

However the reaction of *p*-methoxyPACA **302a** with a variety of diazonium salts **324b-g** resulted in a high yield of the *ipso* substitution monoPACA **304b-g** by-product. This appears to be the major product obtained in all reactions except in the case of the *p*-cyanobenzenediazonium salt **324f**. A maximum of 59% yield was achieved in the case of reaction with the benzenediazonium salt **324d**. This is unexpected and there appears to be no link to the yield of the *ipso* substitution monoPACA **304b-g** by-product recovered and the strength of the diazonium salt **324b-g** used during bisazo coupling. There also does not appear to be a pattern to the yield of the *ipso* substituted bisPACA **305b-g** and *p*-methoxybisPACA **306a** by-products and the strength of the diazonium salt **324b-g** which are only obtained in low yields.

A possible explanation for the high yield of *ipso* substituted monoPACA **304b-g** is that unlike the case of *p*-nitroPACA **302g** the *p*-methoxybenzene diazonium salt **324a** displaced during *ipso* substitution is a less reactive diazonium salt and hence further bisazo coupling to give the unsymmetrical 2,7-bisPACA **303** does not occur easily. Hence one route to the required unsymmetrical 2,7-bisPACA **303** product is unlikely with the *ipso* substituted monoPACA **304b-g** not undergoing further reaction (Scheme 4.6.6).

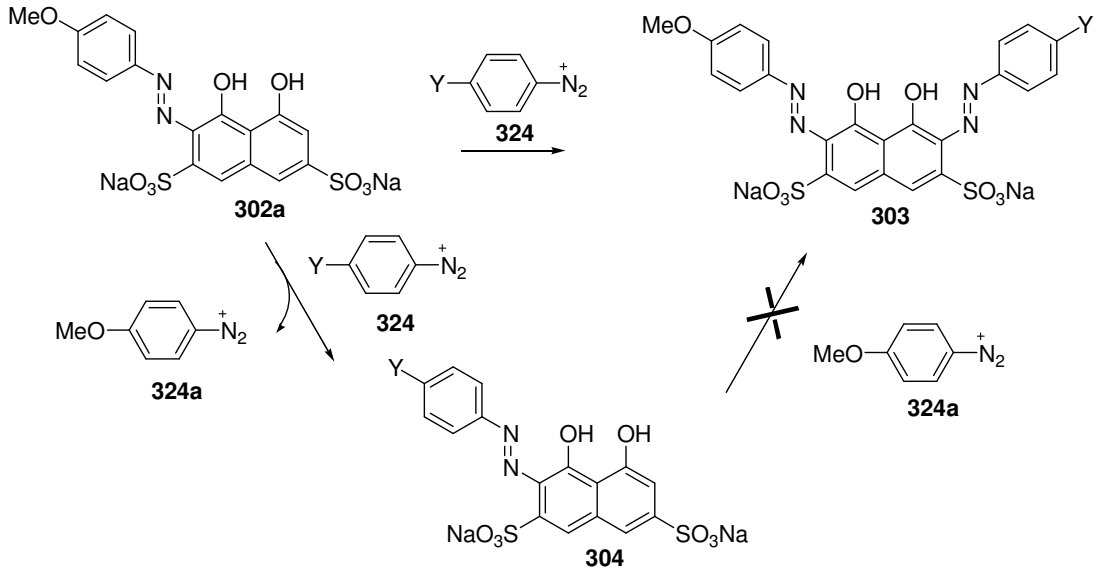

324, **304 b**: Y = OEt, **c**: Y = Me, **d**: Y = H, **e**: Y = Cl, **f**: Y = CN, **g**: Y = NO_2

Scheme 4.6.6: *Ipso* substitution followed by bisazo coupling to give unsymmetrical 2,7-bisPACA **303**.

Another observation from graph 4.6.2 is that in the case of reaction of *p*-ethoxybenzene- **324b** and *p*-methylbenzene **324c** diazonium salts with *p*-methoxyPACA there appears to be equal amounts of *p*-methoxyPACA **302a** and *ipso* substituted monoPACA **304b,c** present in the reaction mixture suggesting the species may be in equilibrium (Scheme 4.6.7). However further investigation is required in order to determine how fast the system comes to equilibrium.

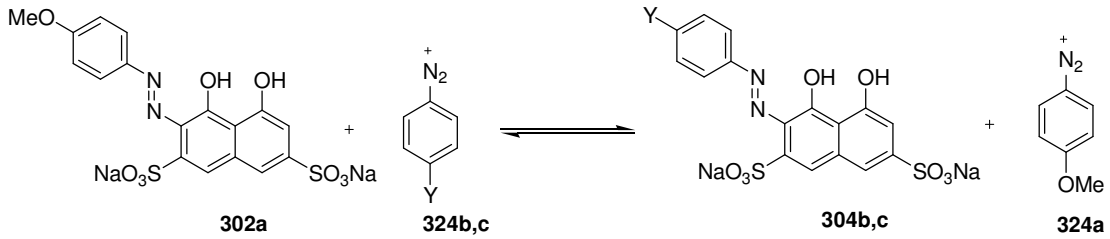

302a **324b,c** **304b,c** **324a**

Scheme 4.6.7: Possible equilibrium between *p*-methoxyPACA **302a** and *ipso* substituted monoPACA **304b**: Y = OEt, **c**: Y = Me.

The reaction of the monoPACAs **302a,g** can also be viewed in graphs 4.6.3 and 4.6.4 with yields adjusted to account for unreacted monoPACA **302** starting material. This then gives a representation of whether the reaction that does occur is at the bisazo coupling position to give the unsymmetrical 2,7-bisPACA **303** or at the *ipso* position to give the *ipso* substitution monoPACA **304** and *ipso* substituted bisPACA **305** by-products.

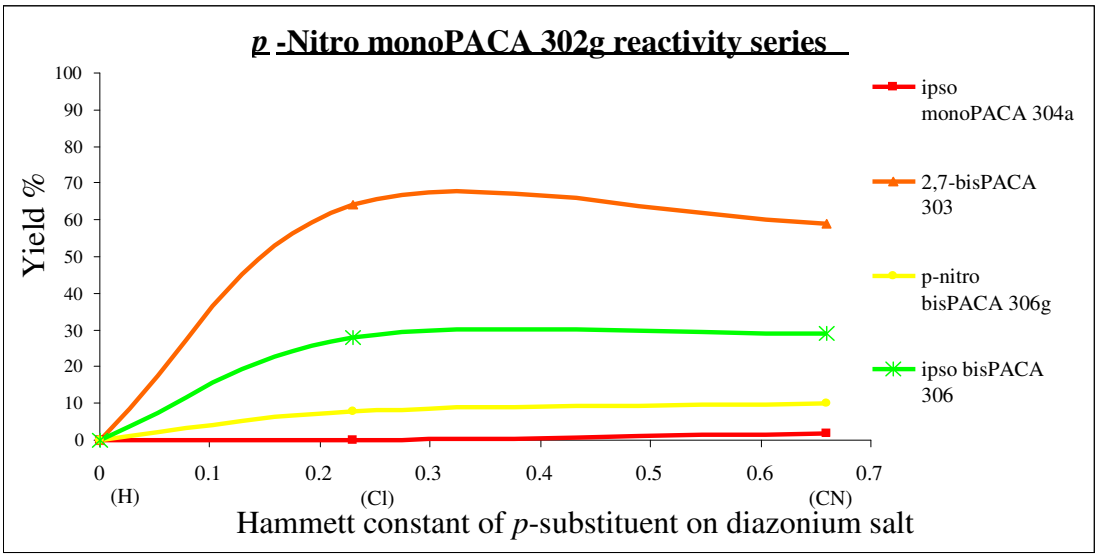

Graph 4.6.3: Reactivity of *p*-nitroPACA **302g** towards a variety of diazonium salts adjusted for recovery of starting material.

The above graph shows the major reaction site of *p*-nitroPACA **302g** is the bisazo coupling position to give the unsymmetrical 2,7-bisPACA **303** product. However, there does appear to be a high yield of *ipso* substituted bisPACA **305** by-product formed due to reaction at the *ipso* position and subsequent reaction of the resulting *ipso* substitution monoPACA **304** with another equivalent of diazonium salt.

Another observation is the lack of *ipso* substituted monoPACA **304d-f** in the reaction mixture which implies the *ipso* substituted monoPACA **304d-f** is particularly reactive and hence undergoes immediate coupling with the *p*-substituted benzenediazonium salt **324d-f** present to give the *ipso* substituted bisPACA **305d-f**. There is also the possibility that the reactive *ipso* substituted monoPACA **304d-f** undergoes subsequent bisazo coupling with the reactive *p*-nitrobenzenediazonium salt **324g** displaced during this process to give the unsymmetrical 2,7-bisPACA product **303**.

The reactivity of the *p*-methoxyPACA **302a** adjusted to account for recovered starting material showed that for diazonium salts containing electron donating substituents the main reaction site was at the *ipso* position to give the *ipso* substitution monoPACA **304** (Graph 4.6.4).

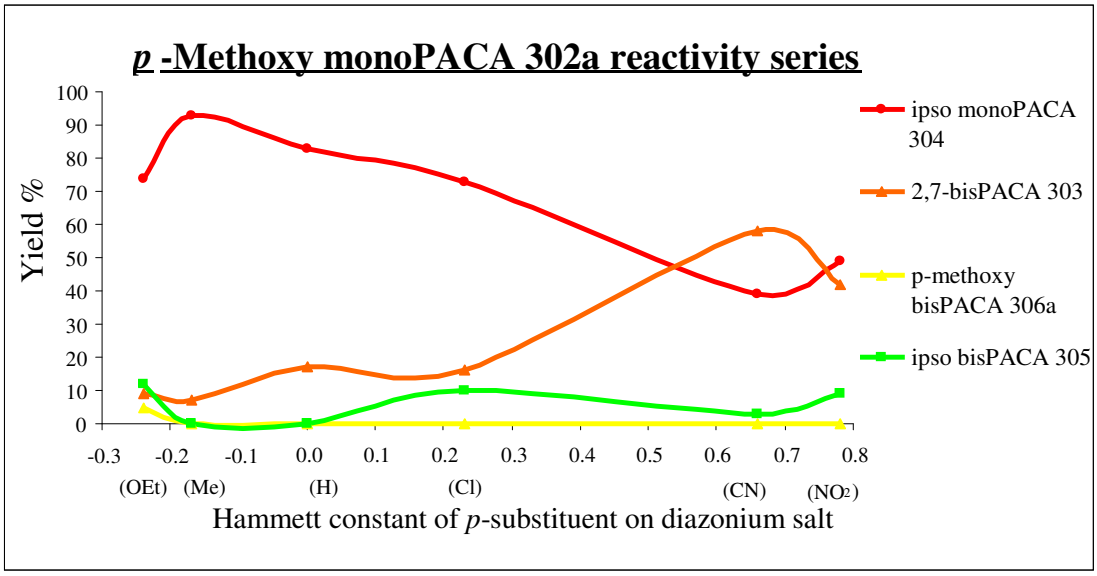

Graph 4.6.4: Reactivity of *p*-methoxyPACA **302a** towards a variety of diazonium salts adjusted for recovery of starting material.

However, as the strength of the diazonium salt increased reaction also occurred at the bisazo coupling position to afford the unsymmetrical 2,7-bisPACA **303** product. From these results it appeared that for the *p*-methoxyPACA **302a** the *ipso* position appeared more reactive and hence electron donating or weak diazonium salts only reacted at this position. However stronger electron withdrawing diazonium salts reacted at both the *ipso* and bisazo coupling positions resulting in similar yields of the unsymmetrical 2,7-bisPACA **303** and *ipso* substitution monoPACA **304**.

Overall, the reactivity of *p*-methoxyPACA **302a** and *p*-nitroPACA **302g** appears to be dependent upon the strength of the diazonium salt used for bis azo coupling **324** with the yield of the required unsymmetrical 2,7-bisPACA **303** product generally increasing with diazonium salt **324** strength. However, there does not appear to be a link between the yield of the *ipso* substitution monoPACA **304** and bisPACA **305** by-products obtained and the strength of the diazonium salt **324** used in bisazo coupling.

4.6.3: Effect of MonoPACA *p*-Substituents on *Ipso* Substitution

In order to understand the apparent deactivation of the bisazo coupling position by the electronic effect of the *p*-substituent of the monoPACA **302** and any possible effect upon *ipso* substitution the reactivity of a variety of monoPACAs **302a,c,e,g** towards single diazonium salts **324d,f** was examined. Reactions were carried out as described for a typical reaction study in section 4.6.1 and products identified by HPLC and LCMS analysis (Scheme 4.6.8). Yields were then calculated by QHPLC and plotted against the Hammett σ constant of the *p*-substituent of each of the monoPACAs **302** to give a correlation between the yields of products obtained and the electronic nature of the *p*-substituent of the monoPACA **302** (Graphs 4.6.5 and 4.6.6).

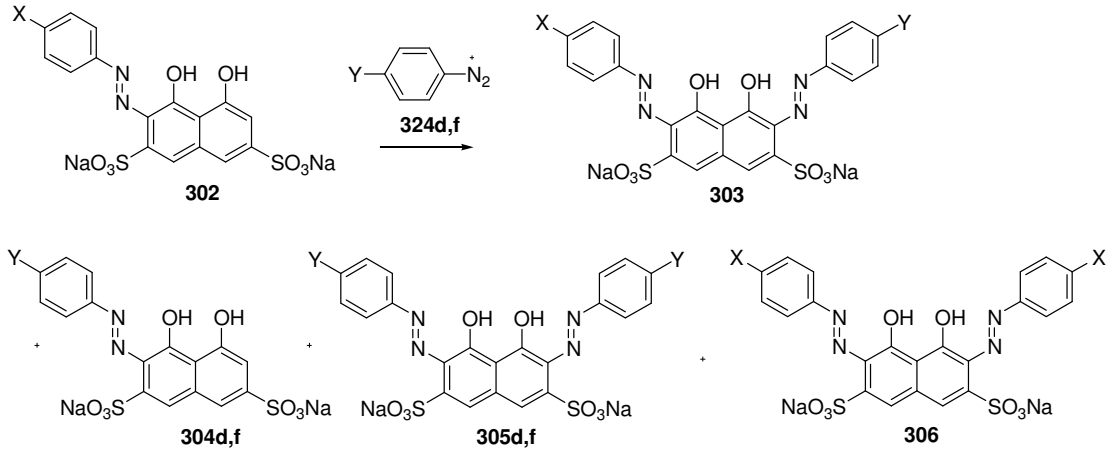

302, 306 a: X = OMe, **c**: X = Me, **e**: X = Cl, **g**: X = NO_2

324, 304, 305 d: Y = H, **f**: Y = CN

Scheme 4.6.8: Reaction of a variety of monoPACAs **302** with single diazonium salts **324d,f**.

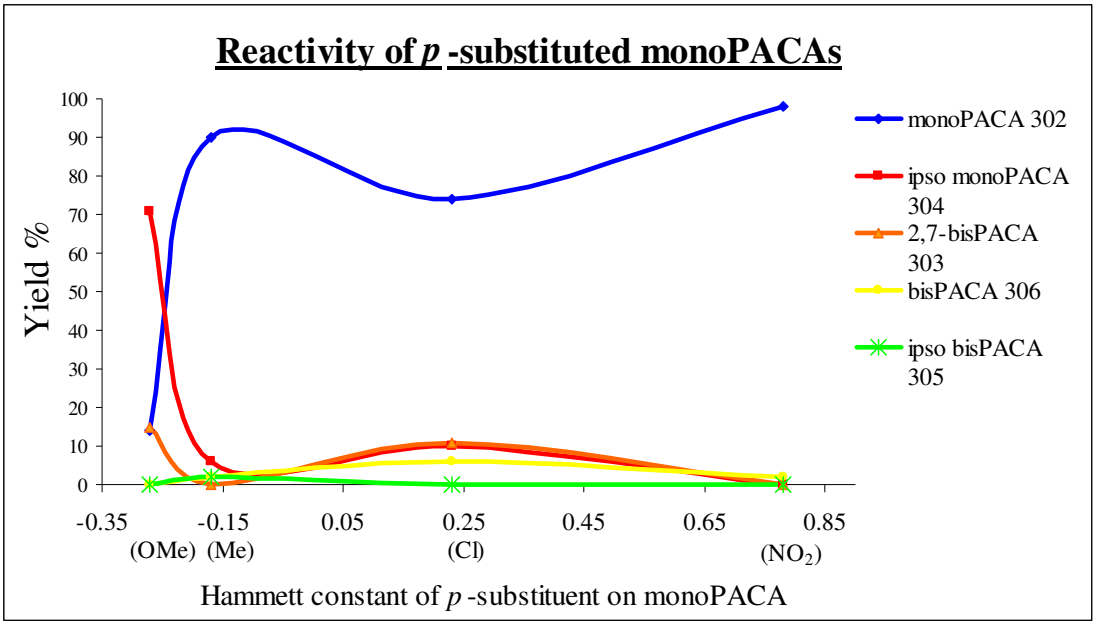

Graph 4.6.5: Reactivity of a variety of monoPACAs **302a,c,e,g** to benzenediazonium salt **324d**.

The results of this experiment show that as the electron withdrawing effect of the *p*-substituent of monoPACA **302** increases the yield of the monoPACA **302** starting material recovered after bisazo coupling also increases. This occurs rapidly upon transition from the *p*-methoxyPACA **302a** to *p*-methylPACA **302b** and then levels out. There is an opposite effect upon the yield of the *ipso* substitution monoPACA **304d** by-product, which decreases rapidly between the *p*-methoxyPACA **302a** and *p*-methylPACA **302b** monoazos and subsequently levels out. From these results there does not appear to be any obvious effect upon the yields of the unsymmetrical 2,7-bisPACA **303** product, *ipso* substituted bisPACA **305d** by-product and the bisPACA **306** by-product, all of which remain low throughout the series.

Another observation from graph 4.6.3 is that in the case of reaction of *p*-chloroPACA **302e** with the benzenediazonium salt **324d** there is a slight reduction in the yield of the starting material **302e** recovered in relation to the trend. This is accompanied by a slight increase in the yields of the *ipso* substituted monoPACA **304e** by-product and unsymmetrical 2,7-bisPACA **303ed** which could be attributed to the slight electron donating properties of the chloro substituent in addition to the electron withdrawing effects of the substituent.

In general these results do seem to indicate that the electronic nature of the *p*-substituent of the monoPACA **302** does effect the yield of the *ipso* substitution monoPACA **304** by-product and the monoPACA **302** starting material recovered. This suggests that the electronic nature affects electrophilic attack of the *ipso* position however in this case the transition from a high yield of the *ipso* substitution monoPACA **304** to a low yield is over such a small range no definite conclusions can be made.

In order to investigate these observations further the reaction of these *p*-substituted PACAs **302** with a stronger *p*-cyanobenzenediazonium salt **324f** was carried out under the same conditions as the benzenediazonium salt case (Scheme 4.6.8, Graph 4.6.6). This was expected to cause the transition from a high to low yield of *ipso* substituted monoPACA **304f** to occur over a greater Hammett σ constant range.

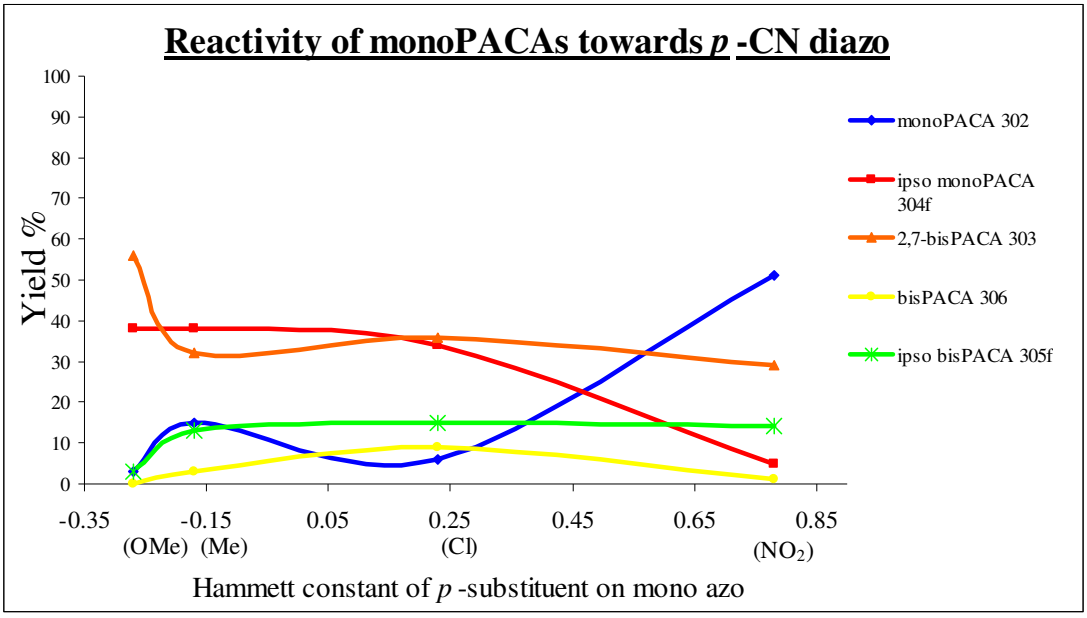

Graph 4.6.6: Reactivity of a variety of monoPACAs **302a,c,e,g** to *p*-cyanobenzene diazonium salt **324f**.

Similar trends in terms of yields were observed as in the previous benzenediazonium **324d** salt example (Graph 4.6.5). As the electron withdrawing effect of the *p*-substituent of the monoPACA **302** increases, the yield of the *p*-substituted PACA **302** starting material recovered after bisazo coupling also

increases. This is also accompanied by a reduction in the yield of *ipso* substituted monoPACA **304f**. However, this occurred over a larger range than was seen in graph 4.6.5 due to increased reactivity of the *p*-cyanobenzenediazonium salt **324f**.

Another effect of the increased reactivity of the *p*-cyanobenzenediazonium salt **324f** appeared to be an increased yield of the unsymmetrical 2,7-bisPACA **303** which remained between 29% and 56% throughout the series. There was also a higher yield of the *ipso* substituted bisPACA **305f** by-product and bisPACA **306** by-products throughout the series than in the benzenediazonium salt **324f** case. As in graph 4.6.5 there did not appear to be any effect of the electronic nature of the *p*-substitent of monoPACA **302** upon the yields of the unsymmetrical 2,7-bisPACA **303** product, bisPACA *ipso* by-product **305f** and the symmetrical 2,7-bisPACA **306** by-product which remained relatively constant throughout.

Yields can also be adjusted to account for recovered monoPACA **302** starting material (Graph 4.6.7). This shows that reaction at the bisazo coupling position to give the unsymmetrical 2,7-bisPACA **303** remained relatively constant with the electronic nature of the *p*-substituent on the monoPACA **302**. Comparison with graph 4.6.6 showed the same trend of reduction of reaction at the *ipso* position with increased electron withdrawing ability of the *p*-substituent of the monoPACA **302**.

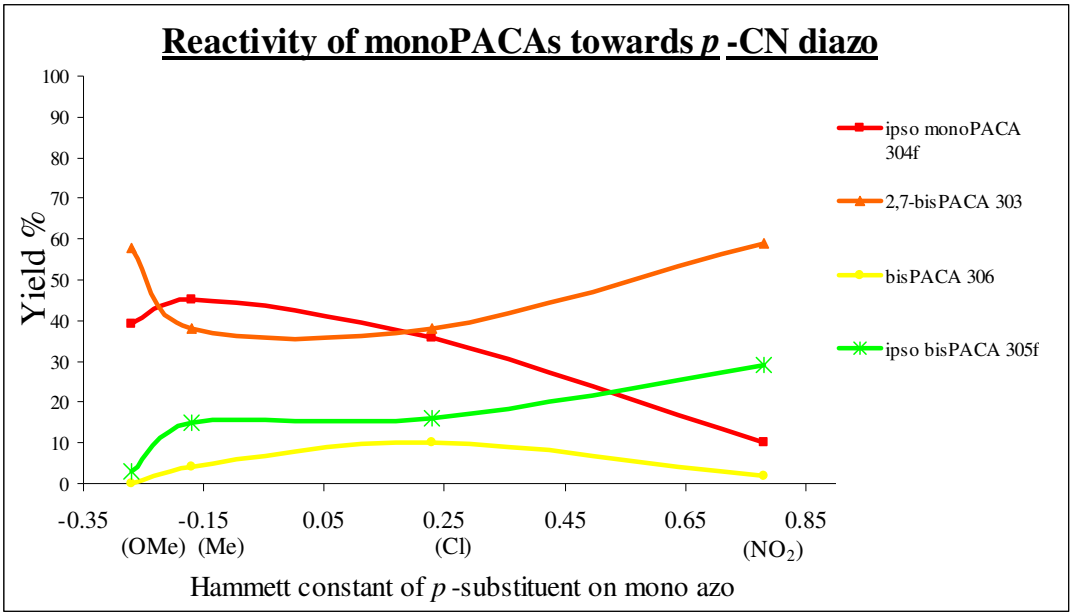

Graph 4.6.7: Reactivity of a variety of monoPACAs **302a,c,e,g** to *p*-cyanobenzene diazonium salt **324f** adjusted for recovery of starting material.

Therefore these results also indicated that the electronic nature of the *p*-substituent of PACA **302** did affect the yield of the *ipso* substituted monoPACA **304** by-product obtained and the *p*-substituted monoPACA **302** starting material recovered. The extent of attack at the *ipso* position appears to increase with increasing electron donating ability of the *p*-substituent in the monoPACA **302**. However, the strength of the diazonium salt used also greatly influenced the yields of the *ipso* substitution monoPACA **304** and unsymmetrical 2,7-bisPACA **303** with the increased strength of the *p*-cyanobenzenediazonium salt **324f** over the benzenediazonium salt **324d** reflected in the low yields of monoPACA **302** recovered in that case.

4.6.4: Stability of Diazonium Salts

Another important factor in considering the chemistry of these reactions was the lifetime of the diazonium salts under reaction conditions. A possible reason for incomplete reaction and recovery of the monoPACA **302** starting material may be due to decomposition of the diazonium salt before it has sufficient time to react. Therefore, the stability of the *p*-cyanobenzenediazonium salt **324f** under bisazo coupling reaction conditions was studied.

Firstly a solution of the *p*-cyanobenzenediazonium salt **324f** was prepared and conditions of the solution altered to mimic bisazo coupling reaction conditions with the pH raised to pH 6.0. Aliquots of the diazonium salt solution were then taken at certain time intervals and added to solutions of *p*-methoxyPACA **302a**. The reaction mixtures were stirred overnight and the yields of product calculated by QHPLC. The product distribution at each time interval after exposure of the diazonium salt to reaction conditions could then be plotted (Graph 4.6.8).

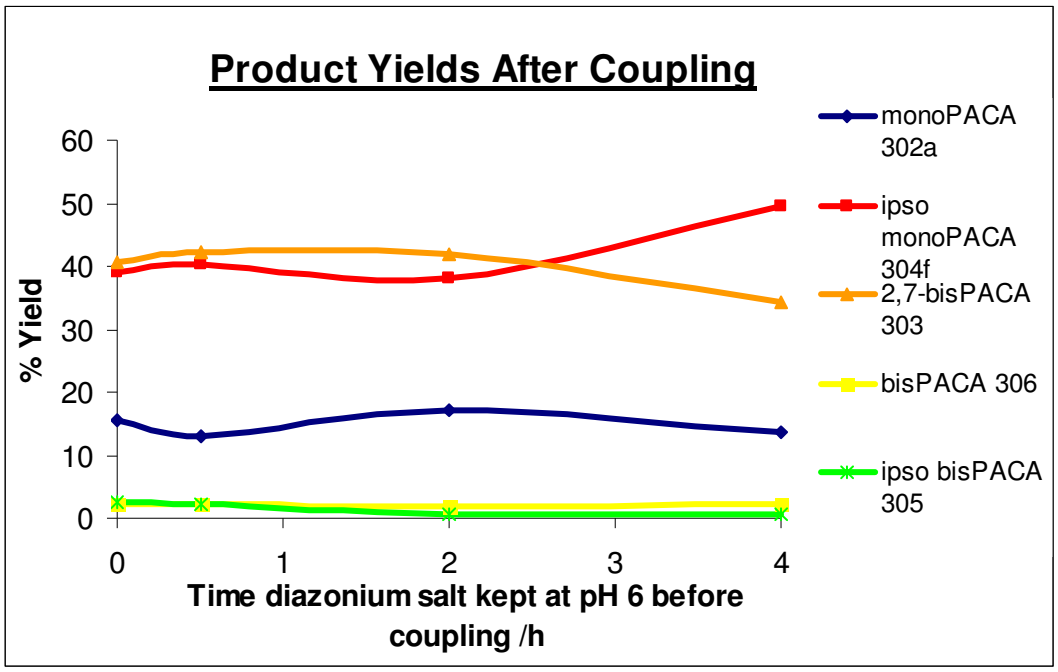

Graph 4.6.8: Product yields after exposure of the *p*-cyanobenzenediazonium salt **324f** to reaction conditons.

From the above graph it can be seen that even after exposure of the diazonium salt to reaction conditions at pH 6.0 for 4 hours, reaction with *p*-methoxyPACA **302a** still occurs and results in a high yield of the unsymmetrical 2,7-bisPACA **303af** and *ipso* substituted monoPACA **304f**. Therefore the diazonium salt **324f** was stable under reaction conditions for a number of hours as it gave a similar product distribution to the aliquot of diazonium salt solution removed and coupled immediately. In conclusion decomposition of the diazonium salt under reaction conditions did not appear to be a major factor influencing product distribution.

4.6.5: Initial Conclusions

Preliminary reactions suggests that the electronic nature of the monoPACA **302** and *p*-substituted diazonium salts **324** used during bisazo coupling does affect the yield of the unsymmetrical 2,7-bisPACA **303** product and possible by-products due to *ipso* substitution.

Firstly, graphs 4.6.1 and 4.6.2 indicate that the yield of the required unsymmetrical 2,7-bisPACA **303** increases with increasing strength of the diazonium salt **324** used in the bisazo coupling step. However, there does not appear to be any effect of the strength of the diazonium salt **324** used upon the yields of *ipso* substitution by-products **304** and **305** which remain constant throughout. Graphs 4.6.1 and 4.6.2 also show a clear difference in the reactivity of *p*-methoxyPACA **302a** and *p*-nitroPACA **302g** with electron donating and withdrawing effects of the *para* substituent influencing this reactivity.

Analysis of the reactivity of a variety of *p*-substituted monoPACAs **302** towards single diazonium salts **324d,f** (Graphs 4.6.5 and 4.6.6) indicated the yield of the *ipso* substituted monoPACA **304** increases with the electron donating ability of the *p*-substituent of the monoPACA **302** starting material. However, there did not appear to be any major effect of the electron donating ability of the *p*-substituent of the monoPACA **302** starting material upon the yield of the unsymmetrical 2,7-bisPACA **303**.

Therefore initial conclusions suggest the electronic nature of both the monoPACA **302** and diazonium salt **324** used greatly effect the bisazo coupling reaction.

4.7: Reactivity of Isolated MonoPACAs

In section 4.6 freshly prepared solutions of the monoPACAs **302** were used for the subsequent bisazo coupling without isolation or purification of the monoPACA **302** starting material. However, it would be useful to establish any differences in the product distribution of the reaction if isolation and purification of the monoPACA **302** prior to the bisazo coupling step was carried out.

Therefore a sample of *p*-methoxyPACA **302a** prepared in section 4.4 which had been isolated and the strength accurately determined was treated with the *p*-cyanobenzenediazonium salt **324f** (Scheme 4.7.1).

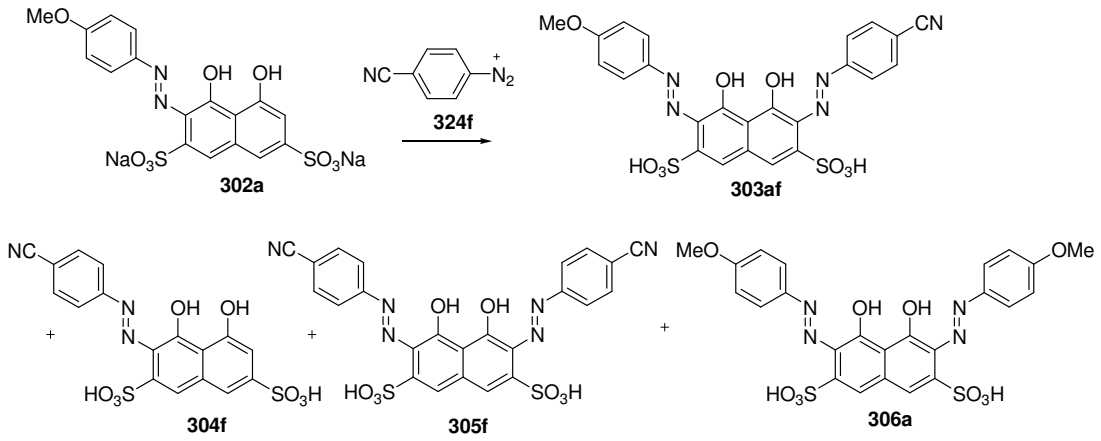

Scheme 4.7.1: Reaction of *p*-methoxyPACA **302a** (isolated) and *p*-cyanobenzene diazonium salt **324f**.

The product yields were then determined by QHPLC and compared with the same reaction in section 4.6 without the use of an isolated *p*-methoxyPACA **302a** (Table 4.7).

Table 4.7: QHPLC yields of reaction products

monoPACA	Yield / % **302a**	Yield / % **306a**	Yield / % **304f**	Yield / % **305f**	Yield / % **303af**
In-situ	3	0	38	3	56
Isolated	19	2	27	2	51

Therefore from these results it appears that the isolated *p*-methoxyPACA **302a** is less reactive than the monoPACA **302a** solution prepared *in situ*. There is a 19% recovery of *p*-methoxyPACA **302a** starting material in the isolated case in comparison with only a 3% recovery of the *p*-methoxyPACA **302a** starting material in the *in situ* experiment. There is also a decrease in the yield of the *ipso* substituted monoPACA **304f** by-product in the isolated starting material case in comparison to the *in situ* experiment from 38% to 27%. However there was little change in the yields of the required unsymmetrical 2,7-bisPACA **303af** which remained at 56% and 51% differences in which could be attributed to experimental error.

The conclusion from this experiment is that the use of an isolated monoPACA **302** starting material rather than to a monoPACA **302** solution prepared without isolation for subsequent bisazo coupling results in decreased reactivity of the monoazo starting material. This is accompanied by increased recovery of the monoPACA **302** starting material and a reduction in the yield of the *ipso* substitution monoPACA **304** by-product. Therefore the use of a monoazo solution generated *in situ* for the subsequent bisazo coupling step is favoured for maximum reactivity.

4.8: Dilute Buffered Conditions

In section 4.6 reactions were also carried out in a slurry rather than in complete solution which lead to poor pH control and reaction mixing. This may have also lead to inaccuracies in sampling of the mixtures for QHPLC due to poor mixing. To increase accuracy, conditions were altered to repeat the previous reactions in a more dilute buffer solution on a smaller scale using isolated monoPACA **302** starting materials of known strength (Section 4.4). This allowed monitoring of the reaction in complete solution and at an accurate pH as opposed to in a slurry on a larger scale as was the case in section 4.6.3.

4.8.1: Reactivity of *p*-MethoxyPACA Under Dilute Buffered Conditions

The reactivity of the isolated *p*-methoxyPACA **302a** towards a variety of diazonium salts **324b-g** was repeated as in section 4.6.2 but using a reduced scale (1.75 mmol) and a dilute buffer solution (pH 6.0) to establish if similar trends as in Graph 4.6.2 were observed (Scheme 4.8.1).

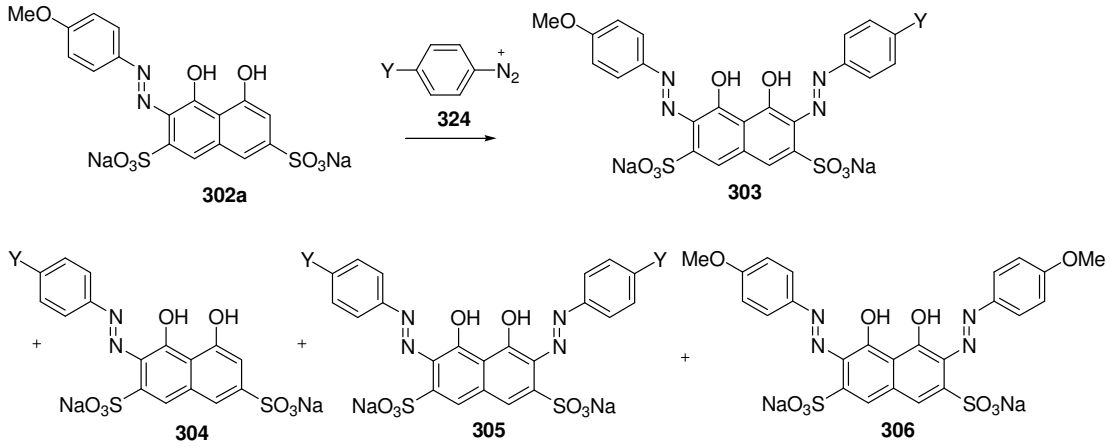

324, 303, 304, 305 b: Y = OEt, **c**: Y = Me, **d**: Y = H,

e: Y = Cl, **f**: Y = CN, **g**: Y = NO_2

Scheme 4.8.1: Reaction of *p*-methoxyPACA **302a** with a variety of diazonium salts.

As earlier, yields of the unsymmetrical 2,7-bisPACAs **303** and of each of the possible by-products from these reactions could then be plotted against the Hammett σ constant of the *p*-substituent of each of the diazonium salts **324** (Graph 4.8.1).

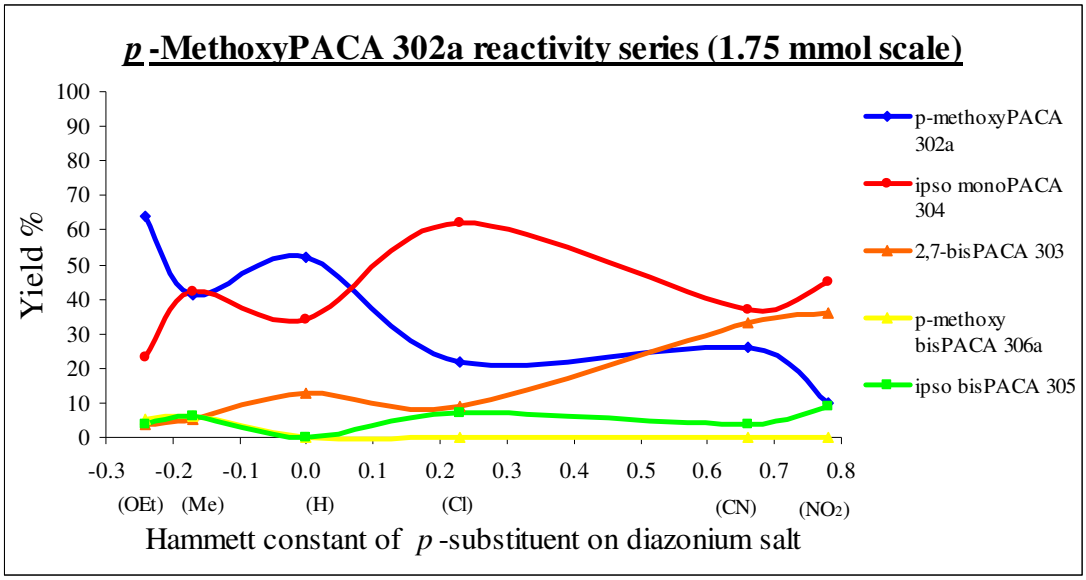

Graph 4.8.1: Reaction of *p*-methoxyPACA **302a** with a variety of diazonium salts.

When the results of the above graph were compared to graph 4.6.2 similar trends in the yields of products were observed. Firstly the yield of the unsymmetrical 2,7-bisPACA **303** seemed to increase with the strength of the diazonium salt used in the bisazo coupling step to a maximum of 36% yield in the case of reaction of *p*-methoxyPACA **302a** with the *p*-nitrobenzenediazonium salt **324g**. This was accompanied by a reduction in the yield of the *p*-methoxyPACA **302a** starting material recovered along the same axis.

Again there did not appear to be any link between the yield of the *ipso* substituted monoPACA **304** by-product and the strength of the diazonium salt **324** used in the bisazo coupling step. However, differences were observed in regard to the reaction of *p*-methoxyPACA **302a** with *p*-ethoxybenzenediazonium salt **324b**. The yield of the *ipso* substituted monoPACA **304b** by-product fell in the buffered experiments to 23% from 42% in the case of the earlier experiment in section 4.6.3. There was also an increase in recovery of the *p*-methoxyPACA **302a** starting

material from 42% in the case of the reaction in section 4.6.3 to 64% in the buffered solution case.

Other small differences between the yields of products in graphs 4.6.2 and 4.8.1 were observed, although they were within experimental error and still agreed with previously observed trends. However, it was unclear why a large discrepancy existed in the *p*-ethoxybenzenediazonium salt **324b** case.

The reactivity of *p*-methoxyPACA **302a** could also be plotted with yields adjusted to account for recovery of the starting materials (Graph 4.8.2). Comparison with graph 4.6.4 showed similar trends with reactivity at the *ipso* position dominant with weaker electron donating substituted diazonium salts and increased reaction at the bisazo coupling position with increased strength of the diazonium salts. Therefore this supported the initial conclusion that the *ipso* position of *p*-methoxyPACA **302a** was more reactive than the bisazo coupling position.

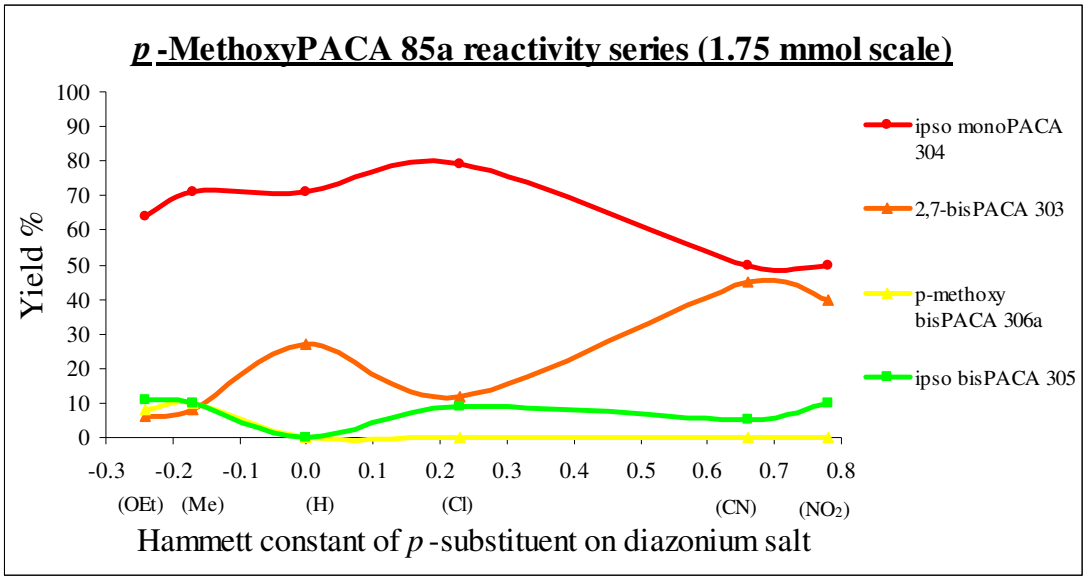

Graph 4.8.2: Reaction of *p*-methoxyPACA **302a** with a variety of diazonium salts with yields adjusted accounting for recovered starting material.

4.8.2: Reactivity of Variety of MonoPACAs Under Dilute Buffered Conditions

In order to confirm the trends observed in section 4.6.4 a variety of isolated monoPACAs **302** of known strength were treated with the *p*-cyanobenzenediazonium salt under dilute buffered conditions (pH 6.0) (Scheme 4.8.2). Yields were calculated by QHPLC and plotted as in section 4.6.4 (Graph 4.8.3).

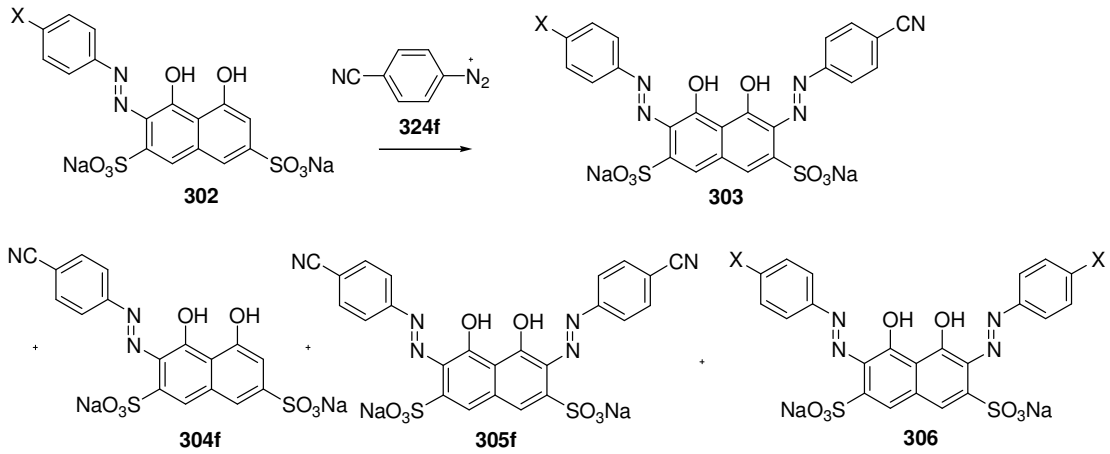

Scheme 4.8.2: Reactivity of a variety of monoPACAs **302a,c,e,g** to *p*-cyanobenzenediazonium salt **324d**.

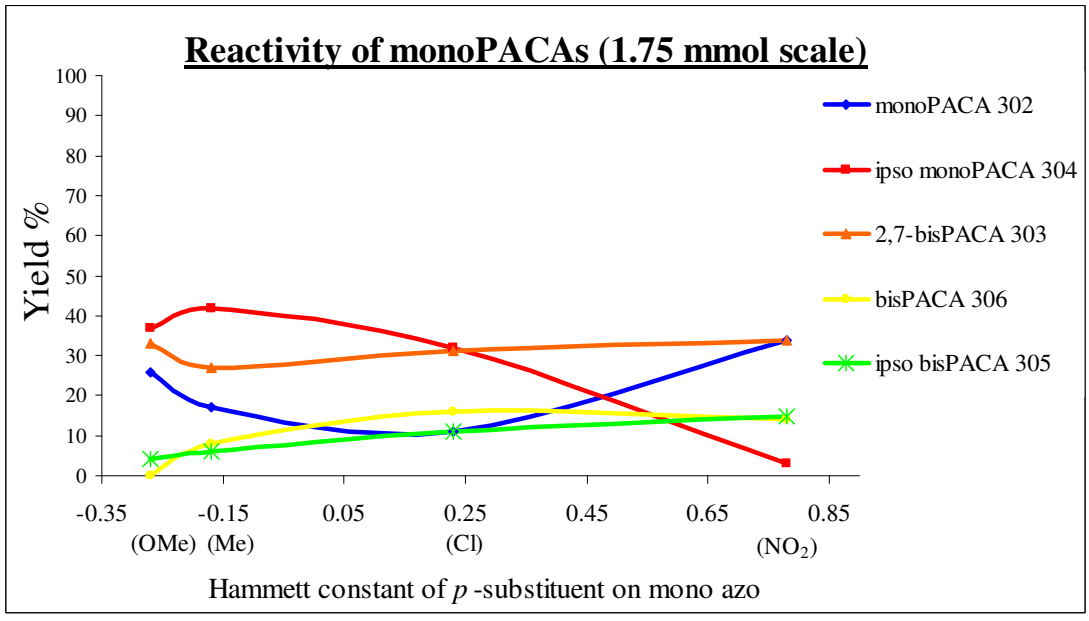

Graph 4.8.3: Reactivity of a variety isolated monoPACAs **302** towards *p*-cyanobenzenediazonium salt **324f**.

Similar trends were observed when a comparison of graphs 4.6.6 and 4.8.3 were made. Firstly the yield of the *ipso* substituted monoPACA **304f** by-product decreased with the electron withdrawing ability of the *p*-substituent of the monoPACA **302** starting material. There also seemed to be a general increase in the yield of the recovered starting material monoPACA **302** along the same axis. However this was not to the same extent as in graph 4.6.6 in which the yield of monoPACA **302** recovered varied from 3% to 51%. Although in the buffered solution experiment using an isolated monoPACA **302** this only varied from 26% to 34% with a dip to 11% in the case of reaction of *p*-chloroPACA **302e**.

This experiment did however support the initial conclusion from section 4.6.4 that the yield of the *ipso* substituted monoPACA **304f** by-product did increase with the electron donating ability of the *p*-substituent in the monoPACA **302** starting material.

The reactivity of these monoPACAs **302** towards the *p*-cyanobenzenediazonium salt **324d** could also be shown with yields adjusted to account for recovered starting material (Graph 4.8.4). This graph showed similar trends to graph 4.6.7 with reduction of reaction at the *ipso* position with increased electron withdrawing ability of the *p*-substituent of the monoPACA **302**.

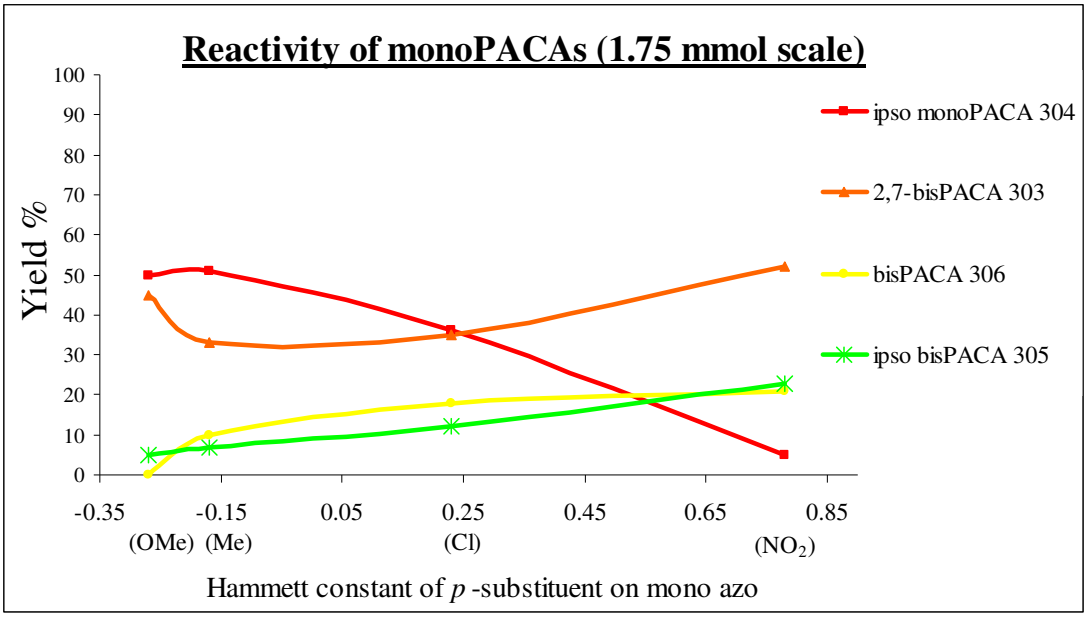

Graph 4.8.4: Reactivity of isolated monoPACAs **302** towards *p*-cyanobenzene diazonium salt with yields adjusted accounting for recovered starting material.

Therefore dilute buffered conditions confirmed the initial conclusions reached about the effect of the electronic nature of the *para*-substituent upon the reaction yields of the unsymmetrical 2,7-bisPACA **303** product and by-products with the same trends observed in the graphs in section 4.8 as in section 4.6. In addition, the electronic effect of the *para*-substituent of the diazonium salt **324** used in bisazo coupling upon reaction yields of products and by-products was confirmed.

The use of dilute buffered conditions was therefore preferred for a more accurate investigation of the effect of other factors such as pH and additives upon bisazo coupling.

4.9: Effect of pH upon Bisazo Coupling

In order to study the effect of the pH upon bisazo coupling and product distribution a single reaction was selected and bisazo coupling carried out in several different pH buffered solutions.

The reaction of the *p*-methoxyPACA **302a** with *p*-ethoxybenzenediazonium salt **324b** was selected firstly due to the increased reactivity of the monoPACA **302a** and also because previous experiments showed this reaction gave a moderate yield of the *ipso* substitution monoPACA **304b** by-product at pH 7.0. Therefore the effect factors such as pH have upon *ipso* substitution could be studied and also upon the yield of the unsymmetrical 2,7-bisPACA **303**. The aim would be to identify conditions under which attack at the *ipso* position is minimised leading to increased attack at the bisazo coupling position to maximise yields of the unsymmetrical 2,7-bisPACA **303**. This was also a particularly suitable experiment as the electronic nature of the methoxy and ethoxy groups were similar which minimised any electronic influence upon the product distribution. *p*-MethoxyPACA **302a**, as the isolated monoazo was then treated with *p*-ethoxybenzenediazonium salt **324b** in a variety of dilute pH buffered solutions (pH 5 – 11) (Scheme 4.9.1).

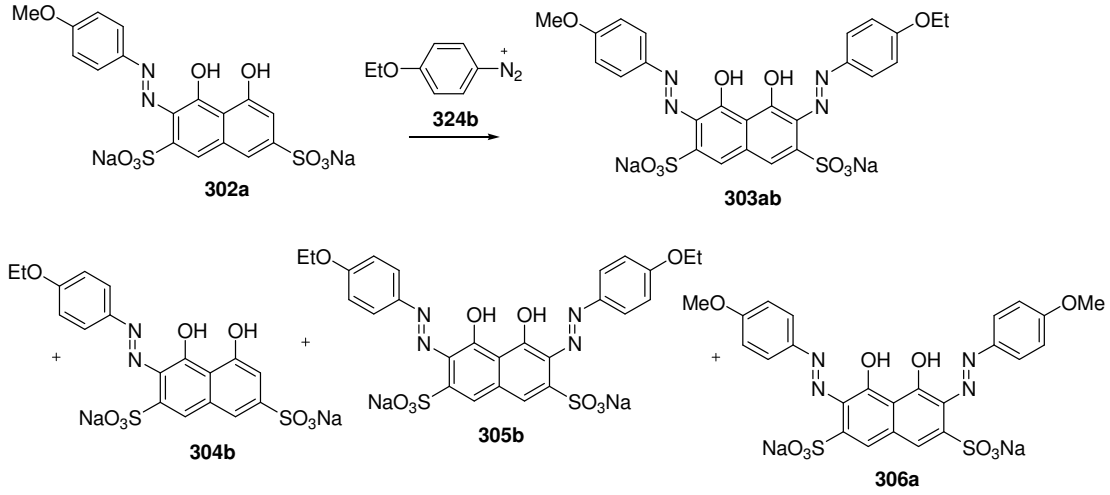

Scheme 4.9.1: Reaction of *p*-methoxyPACA **302a** and *p*-ethoxybenzenediazonium salt **324b**.

The yields of the required unsymmetrical 2,7-bisPACA **303ab** and other by-products were then calculated by QHPLC and plotted against the pH of the reaction mixture (Graph 4.9.1).

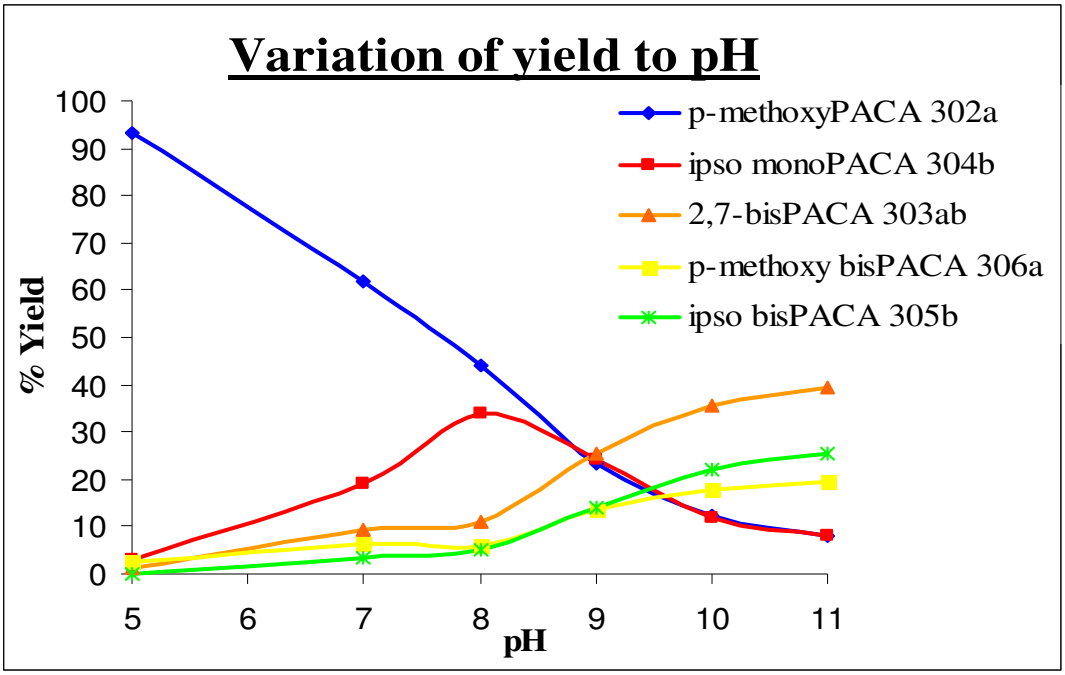

Graph 4.9.1: Reaction yields at varying pH.

Graph 4.9.1 shows that as the pH of the reaction mixture increases, the yield of the *p*-methoxyPACA **302a** starting material decreases. This is accompanied by an increase in the yield of the unsymmetrical 2,7-bisPACA **303ab** with increasing pH. This pattern is presumably explained by the increased availability of the phenoxide anion in the *p*-methoxyPACA **302a** at higher pH which allows coupling to occur more easily at the bisazo coupling position (Scheme 4.9.2).

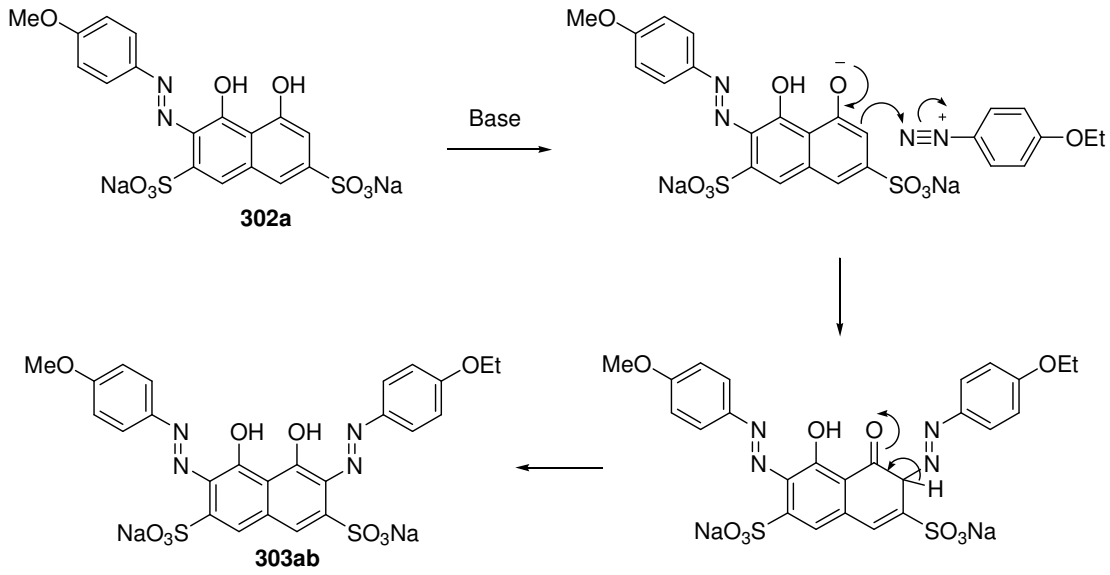

Scheme 4.9.2: Bisazo coupling at higher pH.

The yields of *ipso* substitution by-products also appear to be affected by the pH of the bisazo coupling. The yield of the *ipso* substituted monoPACA **304b** increases with pH to a maximum of 34% at pH = 8 where the yield then falls to 8% at pH = 11. However this reduction in the *ipso* substituted monoPACA **304b** yield is accompanied by an increase in the yield of *ipso* substituted bisPACA **305b** by-product due to increased attack of the bisazo coupling position of **304b** at higher pH by a second equivalent of *p*-ethoxybenzenediazonium salt **324b** (Scheme 4.9.3).

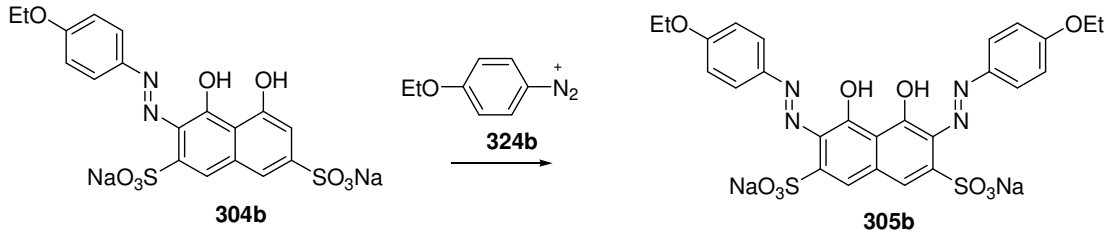

Scheme 4.9.3: Attack of the bisazo coupling position of *p*-ethoxyPACA **304b**.

It appears a higher pH is required for attack at the bisazo coupling position to lead to bisPACA products **303ab**, **305b** and **306a** than the *ipso* position leading to *p*-ethoxyPACA **304b** (Scheme 4.9.1). As in scheme 4.9.2 increased reactivity at the

bisazo coupling position at higher pH can be explained by increased availability of the phenoxide anion.

There was also a notable increase in the yield of the bisPACA by-product **306a** from 2% at pH 5.0 to 19% at pH 11. This by-product is formed as a result of coupling of the ejected *p*-methoxybenzenediazonium salt **324a** with the *p*-methoxyPACA **302a** starting material which now has a more activated bisazo coupling position at a higher pH (Scheme 4.9.4).

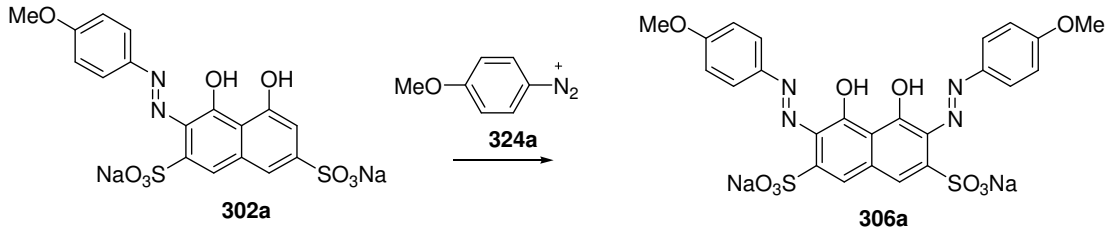

Scheme 4.9.4: Attack of the bisazo coupling position of *p*-methoxyPACA **302a**.

Therefore in conclusion, the pH of the bisazo coupling reaction greatly affects reactivity at the *ipso* and bisazo coupling position of the monoPACA **302** starting material. In general reactivity of the monoPACA **302** appears to increase with increasing pH of the reaction mixture with reactivity at the *ipso* position favoured at a pH < 8. At pH > 8 reaction at the bisazo coupling position dominates and general reactivity of the monoPACA **302** increases. However, although the yield of the *ipso* substituted monoPACA **304b** by-product decreases at higher pH, the yield of the *ipso* substituted bisPACA **305b** and **306a** by-products increase. Therefore the yield of the required unsymmetrical 2,7-bisPACA **303ab** increases with pH although *ipso* substitution by-products are still obtained in high yield.

4.10: Effect of NMP upon Bisazo Coupling

The effect of additives upon reaction yields was also of interest. Several co-solvents have been examined with the aim of increasing the yield of the required unsymmetrical 2,7-bisPACA **303**. It was found that for similar reactions the addition of up to a 15% weight of *N*-methylpyrrolidine (NMP) to the reaction mixture resulted in an increased yield of the unsymmetrical 2,7-bisPACA **303**.[102]

To examine the effect of additives such as NMP upon bisazo coupling the reaction of *p*-methoxyPACA **302a** with *p*-ethoxybenzenediazonium salt **324b** was studied under different conditions (Scheme 4.9.1). The reaction was repeated at pH 9.0 with differing percentage weights of NMP and reaction yields calculated by QHPLC. Product yields at differing percentage weights of NMP were then plotted (Graph 4.10.1).

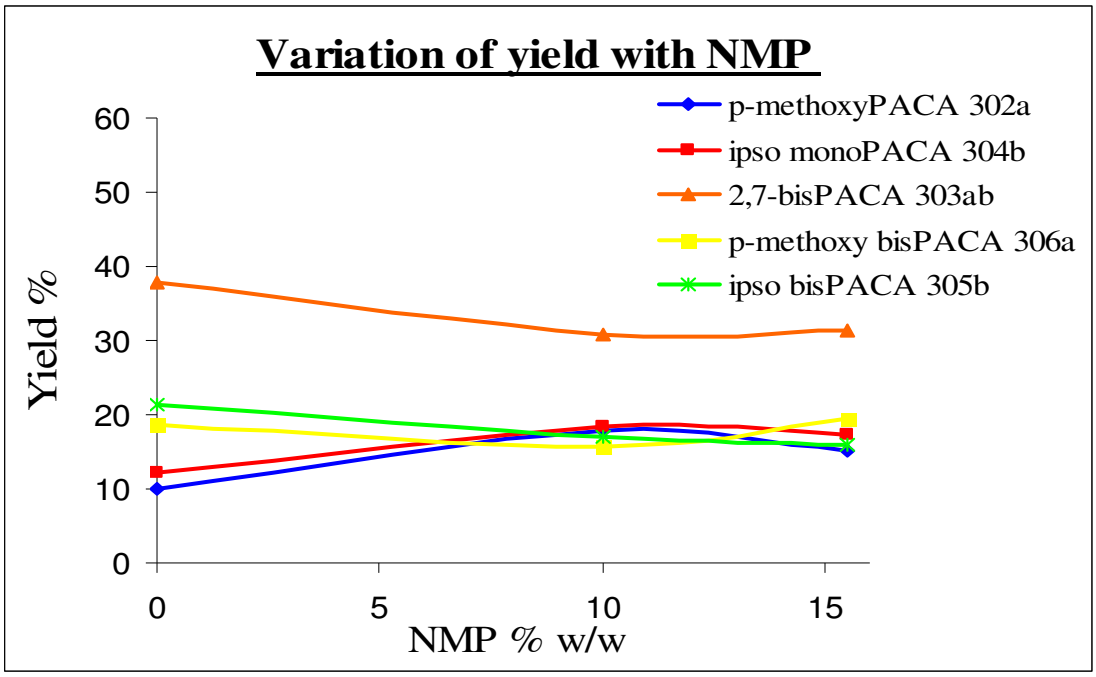

Graph 4.10.1: Reaction yields at varying % NMP.

The results showed little change in the product distribution with variation in percentage weight of NMP therefore in conclusion NMP did not have a significant effect upon this reaction at pH 9. Further investigation into the effect of NMP and other additives upon bisazo coupling under differing reaction conditions is required.

The progress of this reaction could also be tracked by sampling the reaction mixture at time intervals and quenching with 3-methylpyrazolone **325** solution which coupled to any remaining diazonium salt **324** to afford a coupled pyrazolone species **326** and hence stopped any further reaction occurring (Scheme 4.10.1). The composition of the reaction mixture samples were then determined by HPLC and the progress of the reactions with 0% and 15% weight of NMP shown in Graphs 4.10.2 and 4.10.3.

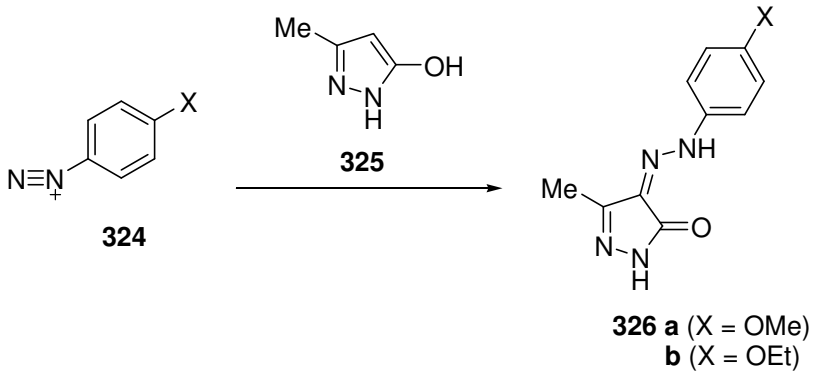

Scheme 4.10.1: Quenching of samples with pyrazolone solution (X = OMe, OEt).

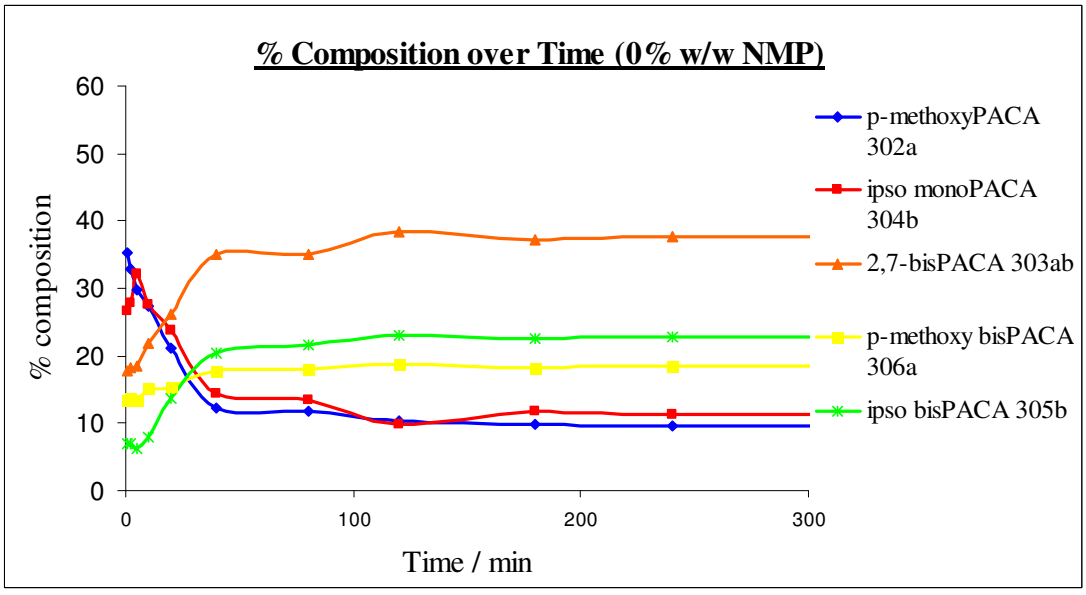

Graph 4.10.2: % Composition over time at 0% NMP.

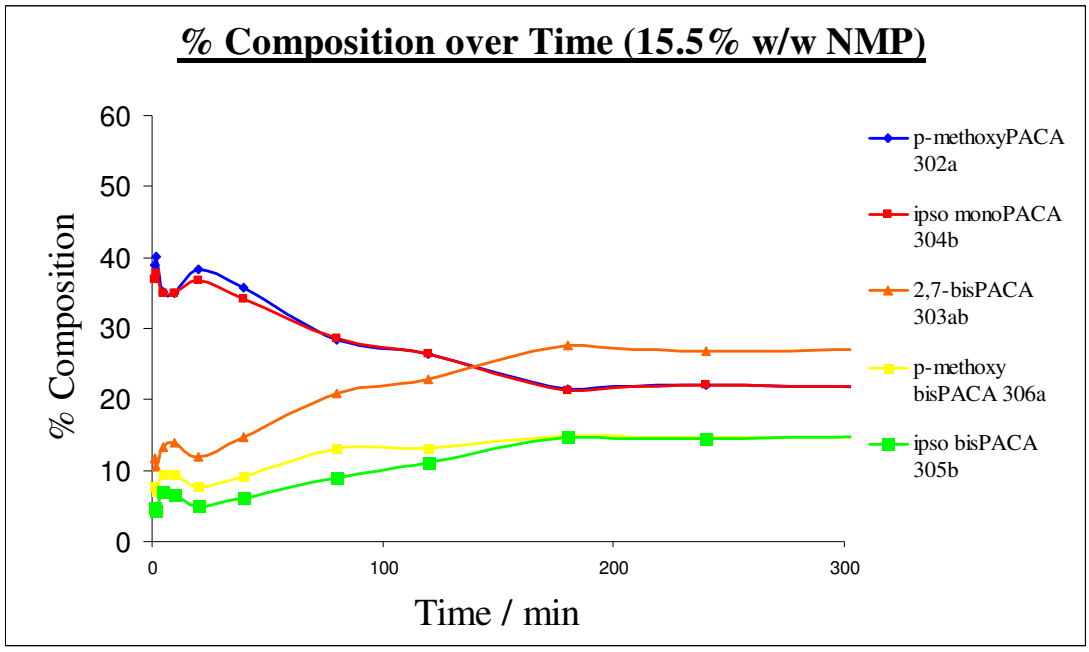

Graph 4.10.3: % Composition over time at 15% NMP.

Firstly by analysis of Graphs 4.10.2 and 4.10.3 it can be seen that *ipso* substitution appears to occur immediately upon addition of the *p*-ethoxybenzene diazonium salt **324b** resulting in an initial 1:1 mixture of the *p*-methoxyPACA **302a** starting material and the *ipso* substituted monoPACA **304b**. The rate at which the bisazo products then form differs depending on the percentage of NMP present in the reaction mixture.

In the case where 0% NMP is present the yield of the unsymmetrical 2,7-bisPACA **303ab**, and bisazo by-products **305b** and **306a** increases over 1-2 h to a maximum of 38% yield of **303ab**. The increase in yield of the bisazo by-products **305b** and **306a** also occurs over the same time period.

However, in the example where 15.5% NMP is present in the reaction mixture the rate of bisazo coupling appears slower. Maximum bisazo yields of **303ab**, **305b** and **306a** do not occur until the reaction has been underway for 3 h with notable differences in the rate of increase in yields observed by comparison of Graphs 4.10.2 and 4.10.3.

Therefore this experiment has demonstrated that the rate of *ipso* substitution is extremely fast and occurs immediately upon treatment of the *p*-methoxyPACA **302a** with *p*-ethoxybenzenediazonium salt **324b**. The rate of bisazo coupling appears slower and also appears to be greatly reduced in the presence of NMP. It is possible the increased dilution caused by the addition of NMP to the reaction mixture reduces the rate of reaction. However the overall yield of reaction products does not differ significantly with variation in the percentage of NMP as an additive in the reaction mixture still resulting in similar yields of the unsymmetrical 2,7-bisPACA product **303ab** and by-products **304b**, **305b** and **306a** obtained upon reaction completion.

4.11: Steric Effects

Another factor thought to affect the yield of the unsymmetrical 2,7-bisPACA **303** and by-products due to *ipso* substitution is the possibility of steric and other interactions between the substituents around the aryl ring and approaching diazonium salts. Therefore it would be useful to determine if monoPACAs **302** with substituents at the *ortho* position rather than the *para* position were less susceptible to *ipso* substitution due to steric crowding at this position. Hence the reaction of a *p*-methoxyPACA **302a** and *o*-methoxyPACA **302h** with *p*-cyanobenzenediazonium salt **324f** was carried out in dilute buffer solutions at pH 6 and the yields of the reaction products calculated by QHPLC (Scheme 4.11.1, Table 4.11.1).

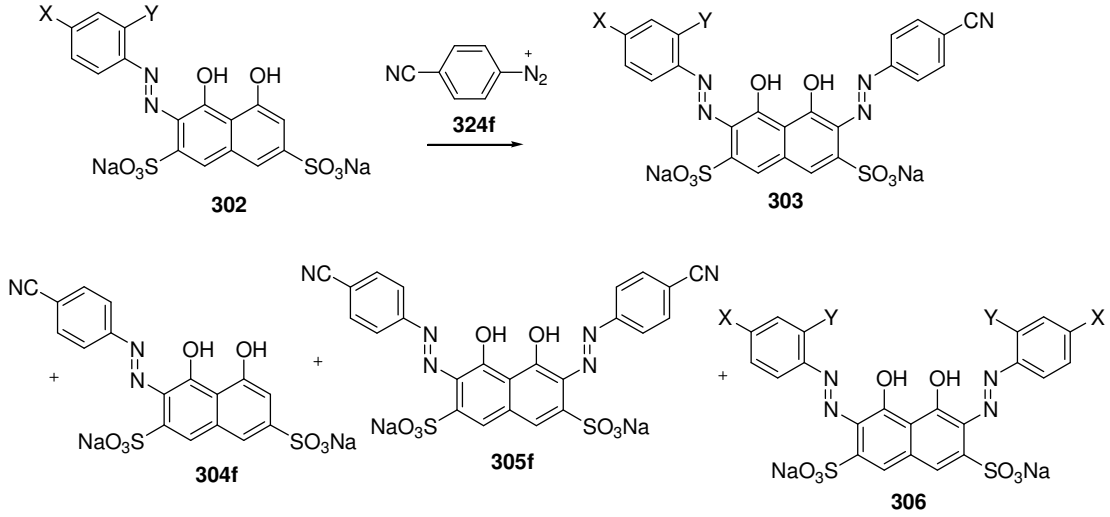

Scheme 4.11.1: Reaction of *p*-methoxyPACA **302a** and *o*-methoxyPACA **302h** with *p*-cyanobenzenediazonium salt **324f**. a) X = OMe, Y = H, b) X = H, Y = OMe.

Table 4.11.1: QHPLC yields (%) of products in reaction mixtures

monoPACA	methoxy PACA **302**	methoxybis PACA **306**	*ipso* mono PACA **304**	*ipso* bis PACA **305**	2,7-bis PACA **303**
1) **302a** *p*—methoxyPACA	26	0	37	4	32
2) **302h** *o*--methoxyPACA	74	0	5	0	21

The results showed a significant decrease in the yield of the *ipso* substitution by-products **304** and **305** in the case of the *o*-methoxyPACA **302h** compared with the *p*-methoxyPACA **302a**. The yield of the *ipso* substitution monoPACA **304** decreased from 37% in the *p*-methoxyPACA **302a** case to 5% in the case of reaction of the diazonium salt with *o*-methoxyPACA **302h**. This is possibly due to additional steric crowding around the azo group due to the *ortho* methoxy substituent which hinders attack at the *ipso* position.

There was however no significant increase in attack at the bisazo coupling position of the *o*-methoxyPACA **302h** resulting in an increased yield of the required unsymmetrical 2,7-bisPACA **303** as was desired by the blocking of the *ipso* position. The yield of the unsymmetrical 2,7-bisPACA **303** decreased slightly from 32% in the case of the reaction of **302a** to 21% in the case of **302h**.

There was also an increase in the recovery of monoPACA **302** starting material from 26% in the *p*-methoxyPACA **302a** example to 74% in the *o*-methoxyPACA **302h** case. This indicated a large difference in reactivity due to the presence of an *ortho* substituent around the aryl ring which may hinder attack at the *ipso* position and therefore increase recovery of the starting material **302**.

In conclusion, there appeared to be a significant decrease in *ipso* substitution due to the presence of an *ortho* substituent around the aryl ring of the monoPACA which may possibly be due to steric crowding at this position. However, although the presence of an *ortho* substituent did minimise attack at the *ipso* position there was not the expected corresponding increase in attack at the bisazo coupling position to increase yields of the required unsymmetrical 2,7-bisPACA product **303**. Alteration of other factors, such as the pH of the reaction would also be required to increase the reactivity of the starting material and encourage attack at the bisazo position.

4.12: Position of Sulfonic Acid Groups

Several potential chromotropic acid based dyes reported in section 4.2 contain additional sulfonic acid groups on the aryl ring of the monoPACA which results in increased solubility of the dye. Also of interest was the effect of the position of these additional sulfonic acid groups upon *ipso* substitution and the yield of the required unsymmetrical 2,7-bisPACA **303**.

Hence two monoPACAs **302i,j** were prepared as in section 4.4 with an additional sulfonic acid group at the *ortho*-position monoPACA **302i** or the *meta*-position monoPACA **302j**. These monoPACAs were then treated with a *p*-cyanobenzenediazonium salt **324f** in dilute buffer at pH 6 and the reaction yields calculated by QHPLC (Scheme 4.12.1, Table 4.12.1).

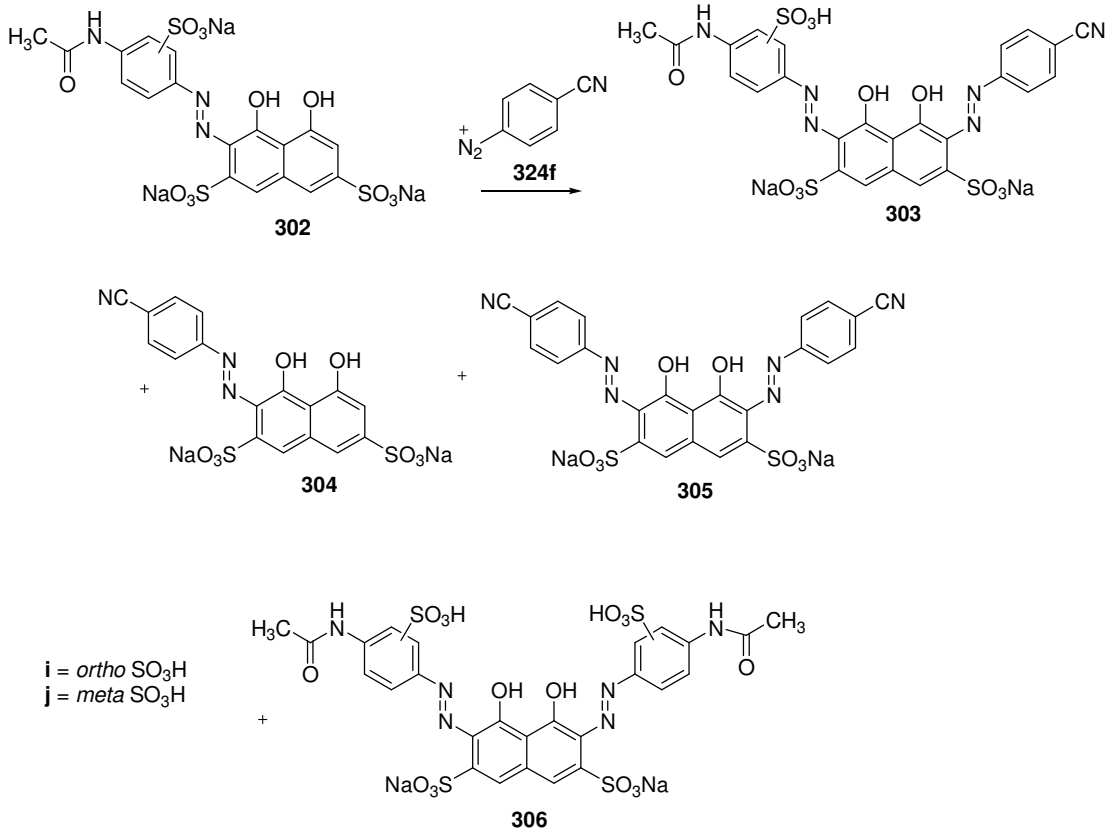

Scheme 4.12.1: Reaction of *ortho* substituted PACA **302i** and *meta* substituted PACA **302j** with *p*-cyanobenzenediazonium salt **324f**.

Table 4.12.1: QHPLC yields (%) of products in reaction mixtures

monoPACA	mono PACA **302**	Bis PACA **306**	*ipso* mono PACA **304**	*ipso* bis PACA **305**	2,7-bis PACA **303**
1) **302i** ***(ortho)***	18	0	4	11	67
2) **302j** ***(meta)***	24	4	17	24	31

There was a notable difference between the reaction yields depending upon the position of the sulfonic acid group in the monoPACA **302i,j**. Firstly the yield of the *ipso* substituted monoPACA **304** decreased from 17% in the case of the *meta* sulfonic acid monoPACA **302j** to 4% in the case of the *ortho* sulfonic acid monoPACA **302i**. There was also a decrease in the yield of the *ipso* substituted bisPACA **305** by-product from 24% in the *meta* sulfonic acid monoPACA **302j** case to 11% for the reaction of **302i**.

Secondly the presence of a sulfonic acid group at the *ortho* position of the monoPACA **302i** rather than the *meta* position **302j** appeared to result in a significant increase in the yield of the required unsymmetrical 2,7-bisPACA **303i,j**. The yield of this product **303i,j** increased from 31% in the case of the *meta* sulfonic acid monoPACA **302j** to 67% when the *ortho* sulfonic acid monoPACA **302i** underwent the same reaction.

Therefore in conclusion the position of additional sulfonic acid groups around the aryl rings of monoPACAs **302i,j** appeared to have a significant effect upon attack at the *ipso* position and the yield of the required unsymmetrical 2,7-bisPACA **303i,j**. As with section 4.11 the reduction in *ipso* substitution in the case when an *ortho* substituent was thought to be due to steric crowding resulting in decreased access and attack at the *ipso* position. This reduced attack at the *ipso* position also appeared to result in increased attack at the bisazo coupling position of the monoPACA **302** to give an increased yield of the required unsymmetrical 2,7-bisPACA **303**.

4.13: Conclusions

In conclusion, several factors have been identified which affect the process of bisazo coupling of chromotropic acid **301** and products recovered. Initial reactions probing the reactivity of an electron deficient and electron rich monoPACA **302a,g** revealed reaction at the *ipso* position was a major issue and gave a high yield of the *ipso* substituted monoPACA **304** in many cases. A more detailed study of the electronic nature of the monoPACA **302** starting material indicated reactivity at the *ipso* position was greatly reduced by the presence of electron withdrawing groups around the azo coupled phenyl ring.

Further study of the effect of the electronic nature of the diazonium salt upon bisazo coupling revealed that the yield of the required unsymmetrical 2,7-bisPACA **303** product increased with the strength of the diazonium salt used in bisazo coupling. However this did not have any significant effect upon attack at the *ipso* position. Therefore the electronic nature of the monoPACA **302** starting material and the diazonium salt **324** used in bisazo coupling greatly affected the products obtained.

Another factor such as the reaction pH was also investigated for a specific example. This revealed that attack at the bisazo coupling position increases with pH to afford a higher yield of the required unsymmetrical 2,7-bisPACA **303** product. At lower pH (5.0 – 8.0) attack at the *ipso* position dominated leading to increased yields of the *ipso* substitution monoPACA **304** by-product. It was also found that the reactivity of the monoPACA **302** starting material increased with pH.

The influence of steric effects upon bisazo coupling was also investigated with the presence of an *ortho* methoxy substitutent on the monoPACA **302** rather than a *para* methoxy group resulting in a reduction in attack at the *ipso* position. However, this did not lead to an increase in attack at the bisazo coupling position and hence an increase in the yield of the required unsymmetrical 2,7-bisPACA **303**.

Finally the effect of the position of sulfonic acid groups around the aryl ring of the monoPACA **302** upon bisazo coupling was also studied with sulfonic acid substituents in the *ortho* and *meta* positions. Reaction of the monoPACAs **302i,j** revealed an increased yield of the required unsymmetrical 2,7-bisPACA **303** in the case where *ortho* sulfonic acid groups were present and also a reduction in attack at

the *ipso* position. Hence the reaction appeared to be directed towards the required bisazo coupling position.

Therefore by analysis of all results in this chapter the structural features of the reactants and reaction conditions required to minimise attack at the *ipso* position of the monoPACA **302** and hence maximise attack at the bisazo coupling site leading to increased yields of the required unsymmetrical 2,7-bisPACA **303** can be predicted. Firstly reaction of a monoPACA **302** containing electron withdrawing groups around the aryl ring with a diazonium salt **324** with electron withdrawing groups would minimise attack at the *ipso* position and maximise attack at the bisazo coupling position (Scheme 4.13.1).

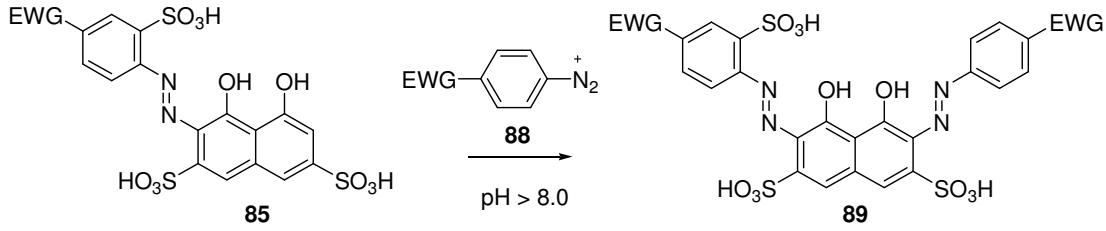

Scheme 4.13.1: Idealised reaction features for bisazo coupling.

Another structural feature which was shown to minimise attack at the *ipso* position and increase attack at the bisazo coupling position was the presence of a sulfonic acid group at the *ortho* position of the monoPACA **302**.

Finally, carrying out the bisazo coupling reaction at a pH greater than 8.0 would minimise attack at the *ipso* position and favour attack at the bisazo coupling site leading to increased yields of the required unsymmetrical 2,7-bisPACA **303** product.

5.0: Conclusions

The aims of this work defined in the introduction of the thesis have been achieved. Heterocyclic azo compounds could be prepared from the development of a new FVP route to 9-phenanthrol **29** and related heterocyclic phenanthrol systems. This FVP route to phenanthrols can be developed further with the use of several other heterocyclic and substituted boronic acids to prepare more unusual systems. The coupling of these phenanthrols with appropriate diazonium salts can then be used to afford azo compounds of interest as potential inkjet dyes.

New heterocyclic dyes could also be prepared from the condensation of heterocyclic hydrazines with 4,9-disulfophenanthrenequinone **171**. Metallisation then afforded the 2:1 nickel complexed magenta dyes which had increased fastness properties.

Investigation of non traditional routes to heterocyclic azo compounds revealed that the Mills reaction, involving the condensation of a heterocyclic nitroso compound with an amine, gave the highest yields of azo product. This route to heterocyclic azo compounds could also be applied to several substituted amines to prepare pyrid-2-yl azo systems. However, further investigation of the reduction of 2-nitrosopyridine **215** under reaction conditions is required.

The investigation of the bisazo coupling reactions of chromotropic acid **301** revealed *ipso* substitution under reaction conditions was a major problem. Detailed study of the reaction conditions revealed the yield of these by-products could be minimised by carrying out reactions at a pH > 8.0. Studies also indicated the electronic nature of the monoPACAs **302** and the diazonium salt used in bisazo coupling affected the level of *ipso* substitution. Electron deficient monoPACAs **302** underwent less reaction at the *ipso* position, which lowered the yield of by-products. The use of more reactive or electron deficient diazonium salts in bisazo coupling resulted in increased yields of the required unsymmetrical 2,7-bisPACA **303** product. The main conclusion is that these factors should be taken into consideration when optimising similar industrial scale reactions.

6.0: Experimental

6.1: Abbreviations

δ_C	chemical shift of carbon
δ_H	chemical shift of hydrogen
m/*z*	mass to charge ratio
T	temperature
mp	melting point
bp	boiling point
NMR	Nuclear Magnetic Resonance
IR	Infrared Spectroscopy
HPLC	High performance liquid chromatography
LCMS	Liqiud chromatography mass spectrometry
QHPLC	Quantitative high performance liquid chromatography
ν_{max}	Maximum vibrational frequency
FVP	Flash Vacuum Pyrolysis
T_f	furnace temperature
T_I	inlet temperature
P	pressure
t	time of pyrolysis
s	singlet
d	doublet
dd	doublet of doublets
ddd	doublet of doublet of doublets
t	triplet
td	triplet of doublets
dt	doublet of triplets
m	multiplet
quat	quaternary carbon
^3J	coupling constant for protons 3 bonds apart in Hertz
^4J	coupling constant for protons 4 bonds apart in Hertz

^{5}J	coupling constant for protons 5 bonds apart in Hertz
DMSO	dimethylsulfoxide
DCM	dichloromethane
DMF	dimethylformamide
NMP	*N*-methylpyrrolidine
EtOAc	ethyl acetate
Et_2O	diethyl ether
Monoazo standard	3-(4-Acetylamino-2-sulfophenylazo)-4,5-dihydroxynaphthalene-2,7-disulfonic acid
Bisazo standard	3-(4-Acetylamino-2-sulfophenylazo)-4,5-dihydroxy-6-(4-nitro-2-sulfophenylazo)-naphthalene-2,7-disulfonic acid
monoPACA	mono(Phenylazochromotropic acid)
bisPACA	bis(Phenylazochromotropic acid)
mmol	millimoles
w/w	weight to weight
NaOAc	sodium acetate
TBAF	Tetrabutylammonium fluoride
TBDPSCl	*Tert*butyldiphenylsilyl chloride
TBDMSCl	*Tert*butyldimethylsilyl chloride
TBDPSOH	*Tert*butyldimethylsilyl hydroxide
Tris Base	Tris(hydroxymethyl)aminomethane
C. I. Acid Yellow 9	2-Amino-5-(4-sulfophenylazo)-benzenesulfonic acid

6.2: Instrumental and General Techniques

Nuclear Magnetic Resonance Spectroscopy

^{1}H NMR spectroscopy was recorded on a Varian Gemini 200 spectrometer, Bruker ARX250 spectrometer operated by Mr J. Millar and Bruker DPX360 spectrometer. ^{1}H NMR spectra quoted were recorded on Bruker ARX250 spectrometer unless otherwise stated.

^{13}C NMR spectroscopy was performed on a Bruker DPX360 (90 MHz) and Bruker ARX250 (63 MHz). ^{13}C NMR spectra were recorded on Bruker ARX250 spectrometer unless otherwise stated.

Spectra were recorded in [^{2}H] chloroform by the author, unless otherwise stated. Chemical shifts (δ_H and δ_C) are quoted in ppm relative to tetramethylsilane and all coupling constants are given in Hertz (Hz).

Infrared Spectroscopy

All infrared spectroscopy measurements were taken on a JASCO FT/IR-460 Plus Fourier Transform Infrared spectrometer. Samples were dissolved in CH_2Cl_2 and the solvent allowed to evaporate to give a film of the sample over the silica plates which was then analysed.

Melting Points

All melting points were determined using Gallenkamp Capillary Tube Melting Point apparatus and are uncorrected.

Boiling Points

All boiling points were determined using Kugelrohr apparatus with a standard Hg thermometer.

Chromatography

Thin Layered Chromatography experiments were performed on MERCK TLC aluminium sheets coated with Silica gel 60 F_{254}.

HPLC

HPLC were carried out on a Gilson instrument with an Agilent 1100 series degasser and a Genesis C18 reverse phase column. The solvent system used was acetonitrile and water with a varying gradient.

QHPLC

Measurement of isolated yields of dyes was not a reliable indication of organic content due to problems encountered in the recovery and purification of aqueous chemistry products giving variable salt content. Therefore standard methods for calculating yields were not possible. Hence yields were calculated using quantitative HPLC.

QHPLC was carried out using monoazo and bisazo standards supplied by Fujifilm which had similar UV response to the mono and bisazo species detected in the reaction mixtures. The monoazo and bisazo standards used are listed in the abbreviations.

A sample of the reaction mixture was weighed out (≈ 0.5 g) using an open ended syringe and deposited in a volumetric flask (25 cm^3). A sample of monoazo standard (of known % composition) and bisazo standard (of known % composition) which were supplied by Fujifilm were also added (0.005 g) and the volumetric flask made up to the mark with water. A sample of this (0.02 cm^3) was then run on the HPLC.

By comparison of the ratios of the monoazo product peaks to the monoazo standard peak the number of moles of the monoazo products in the injection can be calculated. Therefore the number of moles in the overall reaction mixture by comparison of the weight of the sample taken to the weight of the reaction mixture could be calculated. Hence a yield of each of these products can be calculated.

Likewise by comparison of the ratios of the bisazo product peaks to the bisazo standard peak the yield of each of these products can be calculated.

This gives us the yields of each of the products in the reaction mixture without isolation and purification of the products. However this technique does assume all monoazo products have an equal response to UV light at 254 nm and all bisazo products have an equal response.

Yields were expressed as a percentage of the overall number of moles of products in the reaction mixture. Hence addition of all the component yields equalled 100%.

Recovery of Water Soluble Azo Compounds by "Salting out of solution"

Water soluble dyes containing sulfonic acid groups were isolated from solution by the addition of a minimal percentage weight of sodium chloride (≈ 10% w/w) to the reaction mixture until when spotted onto filter paper most of the colour was out of solution and the liquid outspread was pale. This process known as "salting out of solution" resulted in the dye precipitating out of solution and being recovered by filtration. The recovered paste was dried in an oven overnight to give the resulting azo dye containing significant salt impurities. The majority of these could be removed by dialysis through visking tubing which allows molecules of low molecular weight such as salts to pass through while retaining higher molecular weight compounds such as the azo products. Evaporation of the dialysis solution then afforded the largely desalinated azo product. This procedure is used in industry as a standard method of recovering water soluble azo compounds from aqueous reaction mixtures.

Calculation of Organic Content Strength by CHN Analysis

Measurement of isolated yields of water soluble azo compounds containing sulfonic acid groups was not a reliable indication of organic content due to salt impurities remaining from the recovery and purification techniques. Therefore standard methods for calculating yields were not possible.

The standard method used for the calculation of the organic strength of aqueous dyes is by the use of CHN analysis. An estimate of the organic strength of the product quoted based on the percentage of carbon and nitrogen in the sample over the expected percentage of each element could then be made from CHN analysis. The remainder of the dye consists of salt impurities and water due to isolation techniques of salting out of solution and the hydroscopic nature of azo compounds containing sulfonic acid groups. Therefore the strength of these water soluble azo compounds could be calculated and yields adjusted to account for the strength of the product recovered.

LCMS

LCMS was carried out using a Waters 2795 separations module, Waters 486 tunable absorbance detector and Micromass platform mass spectrometer. The same solvent system and column were used as in HPLC.

Electrospray mass spectrometry was a common method for the identification of water soluble azo compounds containing sulfonic acid groups ($SO_3^-Na^+$) in which the negative molecular ions such as $[M]^{2-}$ could be observed. In this case M represented the weight of the azo compound with the sulfonic acid groups in the absence of the sodium cation (SO_3^-). The molecular ions could also more commonly be detected as the single negative ions $[MH]^-$ and $[MNa]^-$ with single cations of H^+ or Na^+ around one of the sulfonic acid groups.

Mass Spectrometry

Mass spectrometry data obtained by electron impact were recorded on a Kratos Profile instrument for nominal masses and a Kratos MS 50TC instrument for accurate masses operated by Mr A. Taylor.

Chemical Analysis

All CHN chemical analysis was performed on a Perkin Elmer 240 CHN Elemental Analyser operated by Mrs S. Djurdjevic or on a Carlo Erba CHNS analyser operated by Mrs Sylvia Williamson.

Solvents

All solvents used in the experimental section were of laboratory grade and were used as supplied. Dried solvents were sodium dried.

FVP

Flash Vacuum Pyrolysis (FVP) involves a process where the reactants are converted into products by heat alone.

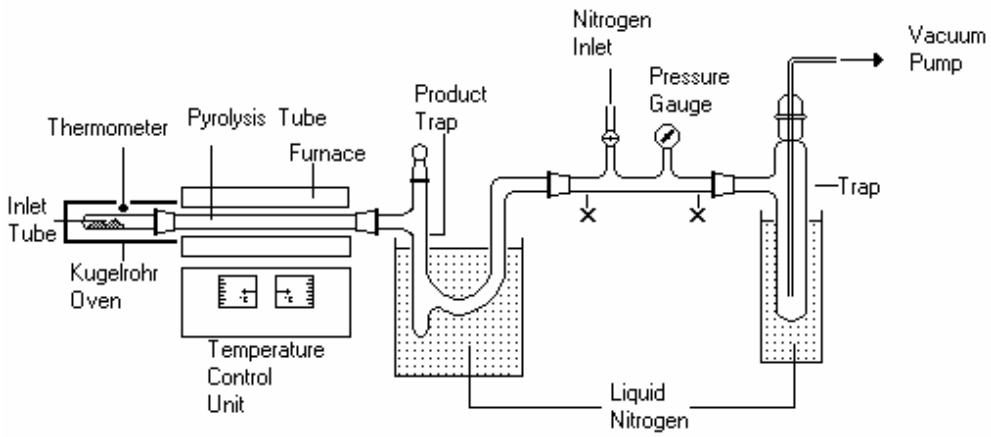

Figure 6.1: FVP apparatus.

The reactant molecules are decomposed in the vapour phase, under vacuum, by a very short exposure to high temperature. The system was evacuated and the vacuum maintained by an Edwards Model ED100 high capacity oil pump for pressures of 1×10^{-2} Torr or an oil diffusion pump for pressures of 1×10^{-6} Torr. The pyrolysis inlet tube was heated to sublime the reactant using a metal Kugelrohr oven at temperatures up to 100 ºC. The volatile reactant in the gas phase was then drawn through a silica tube (30 × 2.5 cm) heated by a Carbolite electronically controlled laboratory tube furnace Model No MTF 12/38/250 in the range of 200-1000 ºC. The product mixture

condensed on the surface of the U-tube trap immersed in liquid N_2. The system was allowed to come to atmospheric pressure under N_2. The trap was then allowed to come to room temperature, washed in deuteriated chloroform or another suitable solvent and the product mixture analysed immediately by ^{1}H NMR spectroscopy.

Standard pyrolysis parameters used throughout in this section are furnace temperature T_f, inlet temperature T_i, pressure P and time of pyrolysis t.

Buffer Solutions

Buffer solutions of fixed ionic strength were prepared as follows.

pH 5.0: NaOH (1 mol dm^{-3}) (25 cm^3) + acetic acid (1 mol dm^{-3}) (36.5 cm^3)
pH 6.0: NaH_2PO_4 (0.5 mol dm^{-3}) (35.5 cm^3) + Na_2HPO_4 (0.5 mol dm^{-3}) (4.9 cm^3)
pH 7.0: NaH_2PO_4 (0.5 mol dm^{-3}) (9.8 cm^3) + Na_2HPO_4 (0.5 mol dm^{-3}) (13.4 cm^3)
pH 8.0: HCl (1 mol dm^{-3}) (25 cm^3) + Tris Base (1 mol dm^{-3}) (42.3 cm^3)
pH 9.0: $NaHCO_3$ (1 mol dm^{-3}) (19.2 cm^3) + Na_2CO_3 (1 mol dm^{-3}) (2.0 cm^3)
pH 10.0: $NaHCO_3$ (1 mol dm^{-3}) (6.2 cm^3) + Na_2CO_3 (1 mol dm^{-3}) (6.3 cm^3)
pH 11.0: $NaHCO_3$ (1 mol dm^{-3}) (0.2 cm^3) + Na_2CO_3 (1 mol dm^{-3}) (3.2 cm^3)

All solutions were made up to 250 cm^3 with water.

pH Measurements

All pH measurements were carried out using a Hanna instruments Checker Pocket-Sized pH meter.

6.3: Novel Routes to Heterocyclic Phenanthrol Azo Compounds

6.3.1: Routes to Phenanthrol Systems

2-Methylbiphenyl-2-carboxylic acid 74

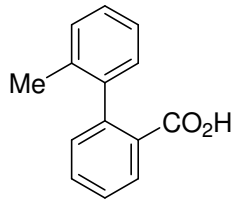

o-Tolylboronic acid **72** (1.502 g, 11.05 mmol), *o*-iodobenzoic acid **73** (2.745 g, 11.06 mmol), K_2CO_3 (9.182 g, 66.43 mmol) and tetrakis(triphenylphosphine)palladium (0.279 g, 0.24 mmol) were added to a mixture of dioxane (56 cm^3) and water (19 cm^3). The mixture was heated under reflux for 4 h under N_2. The reaction mixture was cooled to room temperature and diluted with ether (150 cm^3) and filtered through a silica plug (1 cm^3). The solvent was then removed under reduced pressure, the residue taken up in chloroform (100 cm^3) and the solution washed with HCl (3 × 20 cm^3). The solution was filtered to remove any KCl, the organic layer separated and recovered. The solvent was then removed under reduced pressure to give an orange oil which was purified by dry flash column chromatography (1:1, EtOAc : hexane) to give 2-methylbiphenyl-2-carboxylic acid **74** as a white solid (0.586 g, 25%), mp 96 – 101 ºC [lit.,[116] 104 – 105 ºC]; ν_{max} (CH_2Cl_2) 3018 (OH), 1694 (C=O) cm^{-1}; δ_H ($CDCl_3$) 7.94 (1H, dd, ^3J 7.8, ^4J 1.3, ArH), 7.46 (1H, td, ^3J 7.5, ^4J 1.5, ArH), 7.32 (1H, td, ^3J 7.6, ^4J 1.4, ArH), 7.09 – 7.16 (4H, m, ArH), 6.97 (1H, dd, ^3J 6.8, ^4J 1.3, ArH) and 1.97 (3H, s, CH_3); δ_C ($CDCl_3$) 172.52 (quat), 143.47 (quat), 141.13 (quat), 135.23 (quat), 132.31 (CH), 131.21 (CH), 130.75 (CH), 129.47 (CH), 129.01 (quat), 128.40 (CH), 127.23 (CH), 127.13 (CH), 125.21 (CH) and 19.99 (CH_3); *m/z* 212 (M^+, 80%), 197 (25), 195 (27), 194 (60), 167 (34), 166 (66), 165 (100) and 152 (20).

2-Methylbiphenyl-2-carbonyl chloride 27

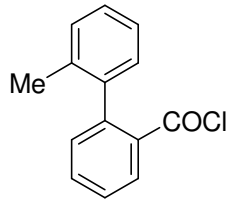

Thionyl chloride (0.841 g, 7.07 mmol) was carefully added to 2-methylbiphenyl-2-carboxylic acid **74** (0.304 g, 1.43 mmol) and the solution stirred at room temperature for 2 h. The solution was then heated under reflux for 20 min and heated without a condenser for a further 10 mins. On cooling excess thionyl

chloride was removed under water pump vacuum to leave the acid chloride **27** as a dark yellow / brown liquid (0.321 g, 97%), ν_{max} (CH_2Cl_2) 1772 (C=O) cm^{-1}; δ_H ($CDCl_3$) 8.04 (1H, d, ^3J 7.8, ArH), 7.51 (1H, t, ^3J 7.2, ArH), 7.38 (1H, t, ^3J 7.6, ArH), 7.07 – 7.17 (4H, m, ArH), 6.96 (1H, d, ^3J 7.1, ArH) and 1.97 (3H, s, CH_3); δ_C ($CDCl_3$) 166.81 (quat), 142.95 (quat), 139.54 (quat), 135.13 (quat), 133.56 (quat), 133.42 (CH), 131.90 (CH), 131.20 (CH), 129.76 (CH), 128.51 (CH), 127.82 (CH), 127.51 (CH), 125.54 (CH) and 19.84 (CH_3).

A boiling point and mass spectrum of the acid chloride were not recorded due to the instability of the product.

4-Methylfluoren-9-one 75

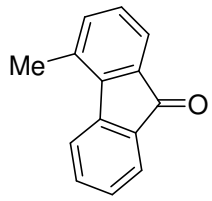

2-Methylbiphenyl-2-carbonyl chloride **27** (0.269 g, 1.17 mmol) was subjected to FVP (T_f 900 ºC, T_i 50 ºC, P 3 x 10^{-2} Torr, t 1 h) to give a dark yellow pyrolysate which was purified by dry flash column chromatography (3:1, EtOAc : hexane) to give 4-methylfluoren-9-one **75** as a yellow solid (0.226 g, 58%), mp 81 - 86 ºC [lit.,[117] 88 – 89 ºC]; ν_{max} (CH_2Cl_2) 1710 (C=O) cm^{-1}; δ_H ($CDCl_3$) 7.70 (1H, ddd, ^3J 7.3, ^4J 1.3, ^5J 0.7, ArH), 7.63 (1H, d, ^3J 7.6, ArH), 7.48 – 7.59 (2H, m, ArH), 7.18 – 7.34 (3H, m, ArH) and 2.60 (3H, s, CH_3); δ_C ($CDCl_3$) 194.17 (quat), 145.16 (quat), 142.01 (quat), 137.30 (CH), 134.54 (CH), 134.36 (quat), 134.30 (quat), 133.53 (quat), 128.65 (CH), 128.27 (CH), 124.10 (CH), 123.26 (CH), 121.80 and 20.11 (CH_3); *m/z* 194 (M^+, 100%), 193 (12), 180 (17), 166 (20), 165 (74), 164 (12), 163 (11) and 82 (8).

Biphenyl-2-yl acetic acid 105

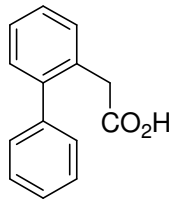

2-Bromophenylacetic acid **103** (2.421 g, 11.26 mmol), phenylboronic acid **104** (2.748 g, 22.54 mmol), K_2CO_3 (9.421 g, 68.17 mmol) and $Pd(PPh_3)_4$ (0.339 g, 0.29 mmol) were added to a mixture of dioxane (50 cm^3) and water (20 cm^3). The mixture was heated under reflux for 18 h under N_2. The reaction mixture was cooled to room temperature, filtered through celite and the filtrates concentrated under reduced pressure to a volume of 50 cm^3. The remaining mixture was extracted with chloroform (4 × 100 cm^3), the combined organic extracts washed with water (3 × 50 cm^3) and dried ($MgSO_4$). The

solvent was then removed to give a brown oil (0.794 g) which was identified as the self coupled boronic acid, biphenyl.

The remaining aqueous layer was then concentrated under reduced pressure to afford a dark aqueous layer (20 cm^3) which was diluted with 2M HCl (1000 cm^3). The acidic aqueous solution was then extracted with chloroform (6 × 250 cm^3), the combined organic extracts washed with 2M HCl (2 × 100 cm^3), dried ($MgSO_4$) and the solvent removed under reduced pressure to afford an off white solid (1.886 g). This was then recrystallised from light petroleum (b.p. 60 – 80 ºC) with the removal of a black oily insoluble impurity to afford the biphenyl acetic acid **105** as an off white crystalline solid (1.662 g, 70%), mp 112 – 114 ºC [lit.,[118] 114 – 115 ºC]; ν_{max} (CH_2Cl_2) 1711 (C=O) cm^{-1}; δ_H ($CDCl_3$) 7.35 – 7.47 (9H, m, ArH), and 3.70 (2H, s, CH_2); δ_C ($CDCl_3$) 178.55 (quat), 142.54 (quat), 140.82 (quat), 135.59 (CH), 130.94 (quat), 130.33 (CH), 130.21 (CH), 129.15 (CH), 128.22 (CH), 127.94 (CH), 127.53 (CH), 127.35 (CH), 127.20 (CH) and 38.49 (CH_2); *m/z* 212 (M^+, 14%), 171 (32), 169 (33), 167 (22), 135 (100), 91 (35), 90 (30) and 89 (23).

Biphenyl-2-yl acetyl chloride 106

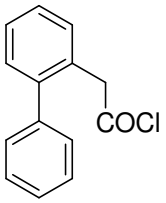

Biphenyl-2-yl acetic acid **105** (1.005 g, 4.73 mmol) was stirred in anhydrous DCM (10 cm^3) containing 1 drop of anhydrous DMF. Oxalyl chloride (0.913 g, 7.19 mmol) was then added and the reaction mixture heated to reflux for 3 h under nitrogen. Ether (10 cm^3) was then added to the cooled reaction mixture and the precipitate was filtered. The filtrates were then concentrated under reduced pressure to afford the acid chloride **106** as a light yellow oily solid (1.055 g, 99%), bp 115 – 120 ºC (0.5 Torr); [lit.,[124] 130 - 132 °C (0.4 Torr)]; (Found: M^+ 230.0499. $C_{14}H_{11}{}^{35}ClO$ requires *M* 230.0493); ν_{max} (CH_2Cl_2) 1798 (C=O) cm^{-1}; δ_H ($CDCl_3$) 7.15 – 7.40 (9H, m, ArH) and 4.05 (2H, s, CH_2); δ_C ($CDCl_3$) 172.31 (quat), 142.70 (quat), 140.35 (quat), 135.63 (CH), 130.42 (CH), 129.45 (quat), 128.93 (2 × CH), 128.49 (2 × CH), 128.23 (CH), 127.85 (CH), 127.58 (CH) and 50.96 (CH_2); *m/z* 232 (M^+ 8%), 230 (M^+, 25%), 168 (15), 167 (100), 166 (41), 165 (76), 164 (15) and 152 (22).

9-Phenanthrol 29

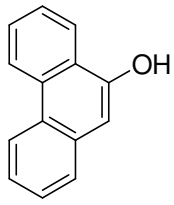

Biphenyl-2-yl acetyl chloride **106** (0.164 g, 0.71 mmol) was subjected to FVP (T_f 850 ºC, T_i 50 – 100 ºC, P 3 x 10^{-2} Torr, t 1.5 h) to give an off white solid. This solid was recrystallised from light petroleum (bp 60 – 80 ºC) to afford 9-phenanthrol **29** as an red / brown solid (0.115 g, 84%), mp 133 - 139 °C [lit.,[119] 139 - 140 °C]; ν_{max} (CH_2Cl_2) 3434 (OH) cm^{-1}; δ_H ($CDCl_3$) 8.59 – 8.79 (2H, m, ArH), 8.32 (1H, m, ArH), 7.60 – 7.75 (3H, m, ArH), 7.46 – 7.58 (2H, m, ArH) and 7.02 (1H, s, CH); δ_C ($CDCl_3$) 149.72 (quat), 132.76 (quat), 132.64 (quat), 131.50 (quat), 127.12 (CH), 126.86 (CH), 126.68 (CH), 126.33 (CH), 125.68 (quat), 124.12 (CH), 122.64 (CH), 122.54 (CH), 122.41 (CH) and 106.00 (CH).

2-(Phenylthio)benzoic acid 85

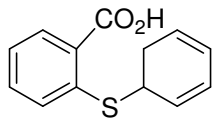

Anthranilic acid (5.007 g, 36.51 mmol) was added to a mixture of HCl conc. (10 cm^3) and water (25 cm^3) and the mixture stirred until the amine dissolved. The solution was then cooled to < 5 ºC and $NaNO_2$ (2.532 g, 36.70 mmol) in water (12 cm^3) was added dropwise keeping the temperature < 5 ºC. The reaction mixture was stirred for a further 1 h at < 5 ºC.

A mixture of thiophenol **84** (4.264 g, 38.70 mmol), NaOH (0.788 g, 20.00 mmol) and water (38 cm^3) was heated to 45 – 50 ºC on a water bath and the diazonium salt prepared above added dropwise. The alkaline solution became orange / red and nitrogen was evolved. The mixture was warmed on a water bath for 1 h, or until all the nitrogen had evolved, the mixture cooled, acidified and the precipitated acid filtered off. The acid precipitate was then dissolved in Na_2CO_3 solution (2.000 g in 100 cm^3) and the phenyldisulphide precipitate filtered off. The solution was then re-acidified and the solid obtained separated by filtration, washed with water (2 × 25 cm^3) and then light petroleum (2 × 25 cm^3) to remove excess thiophenol. The solid was then dried by filtration and under vacuum to give the crude product as an orange / red solid. This was then recrystallised from aq. ethanol (50%) to give 2-(phenylthio)benzoic acid **85** as a light orange solid (1.936 g, 24%), mp 163 – 166 ºC [lit.,[120] 166 – 168 ºC]; ν_{max} (CH_2Cl_2) 1682 (C=O) cm^{-1}; δ_H ($CDCl_3$) 9.05 (1H, br s,

1H), 8.07 (1H, dd, ^3J 7.8, ^4J 1.3, ArH), 7.49 – 7.55 (2H, m, ArH), 7.35 – 7.41 (3H, m, ArH), 7.22 (1H, m, ArH), 7.09 (1H, dd, ^3J 7.8, ^4J 1.3) and 6.75 (1H, dd, ^3J 8.2, ^4J 1.0); δ_C ($CDCl_3$) 172.22 (quat), 145.04 (quat), 136.25 (2 × CH), 133.56 (CH), 132.54 (CH), 132.48 (quat), 130.23 (2 × CH), 129.90 (CH), 127.57 (CH), 125.69 (quat) and 124.66 (CH).

2-(Phenylthio)benzoyl chloride 86[39]

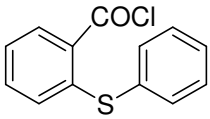

To a stirred solution of pyridine (0.22 cm^3, 2.73 mmol) and 2-(phenylthio)benzoic acid **85** (1.170 g, 5.08 mmol) in anhydrous ether (20 cm^3) was added thionyl chloride (1.1 cm^3, 15.1 mmol) slowly, the mixture was stirred at room temperature and under nitrogen for 1 h. The reaction mixture was then filtered to remove pyridinium chloride as an off white solid. The filtrates were then concentrated under reduced pressure to afford 2-(phenylthio)benzoyl chloride **86** as a pale yellow oil (1.213 g, 92%), bp 116-118 °C (9.0×10^{-1} Torr); ν_{max} (CH_2Cl_2) 1676 (C=O) cm^{-1}; δ_H ($CDCl_3$) 8.22 (1H, dd, ^3J 8.0, ^4J 1.6, ArH), 7.29 - 7.52 (5H, m, ArH), 7.08 - 7.28 (2H, m, ArH) and 6.72 (1H, dd, ^3J 7.7, ^4J 1.0, ArH); δ_C ($CDCl_3$)166.31 (quat), 145.72 (quat), 135.67 (2CH), 134.81 (CH), 134.09 (CH), 130.95 (quat), 129.90 (2CH), 129.62 (CH), 128.87 (quat), 127.12 (CH) and 124.46 (CH); *m/z* 250 (M^+ 19), 248 (M^+, 51%), 214 (22), 213 (100), 184 (54), 106 (11), 69 (11) and 51 (14).

Thioxanthen-9-one 87[39]

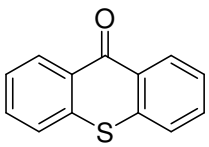

2-(Phenylthio)benzoyl chloride **86** (0.035 g, 0.13 mmol) was subjected to FVP (T_f 900 ºC, T_i 100 – 110 ºC, P 3 x 10^{-2} Torr, t 1 h) to give thioxanthone **87** as a yellow solid (0.027 g, 91%), mp 210 - 220 °C [lit.,[121] 218-220 °C]; ν_{max} (CH_2Cl_2) 1641 (C=O) cm^{-1}; δ_H ($CDCl_3$) 8.55 - 8.65 (2H, m, ArH), 7.40 - 7.70 (6H, m, ArH); δ_C ($CDCl_3$) 178.93 (quat), 136.43 (2 quat), 132.11 (2CH), 129.61 (2CH), 129.06 (2 quat), 126.13 (2CH) and 125.82 (2CH); *m/z* 212 (M^+, 31%), 184 (18), 170 (62), 114 (64), 70 (45), 69 (40), 48 (35) and 41 (100).

2-Phenoxybenzoyl chloride 89

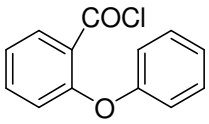

To a stirred solution of pyridine (0.22 cm^3, 2.73 mmol) and 2-phenoxybenzoic acid **88** (1.003 g, 4.68 mmol) in anhydrous ether (20 cm^3) was added thionyl chloride (1.1 cm^3, 15.1 mmol) slowly, the mixture was stirred at room temperature and under nitrogen for 2 h. The reaction mixture was then filtered to remove pyridinium chloride as an off white solid. The filtrates were then concentrated under reduced pressure to afforded the crude acid chloride **89** an off white crystalline solid (1.078 g, 99%), mp 39 – 40 °C [lit.,[122] 39 - 40 °C]; (Found: M^+ 232.0290. $C_{13}H_9{}^{35}ClO_2$ requires *M* 232.0286); ν_{max} (CH_2Cl_2) 1773 (C=O) cm^{-1}; δ_H ($CDCl_3$) 8.14 (1H, dd, ^3J 8.4, ^4J 2.1, ArH), 7.53 (1H, ddd, ^3J 8.4, ^3J 7.4, ^4J 1.8, ArH), 7.37 – 7.43 (2H, m, ArH), 7.15 – 7.27 (2H, m, ArH), 7.01 – 7.07 (2H, m, ArH) and 6.92 (1H, dd, ^3J 8.4, ^4J 1.1, ArH); δ_C ($CDCl_3$) 163.95 (quat), 157.27 (quat), 155.81 (quat), 135.72 (CH), 133.94 (CH), 130.00 (2 × CH), 124.86 (quat), 124.42 (CH), 122.86 (CH), 119.51 (2 × CH) and 118.97 (CH); *m/z* 234 (M^+, 3%), 232 (M^+, 8%), 198 (12), 197 (100), 168 (9), 141 (6), 139 (7) and115 (6).

Xanthen-9-one 90

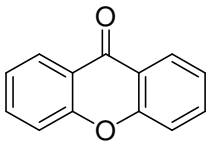

2-Phenoxybenzoyl chloride **89** (0.106 g, 0.49 mmol) was subjected to FVP (T_f 900 ºC, T_i 50 – 100 ºC, *P* 3 x 10^{-2} Torr, *t* 0.5 h) to give a light yellow solid which was recrystallised from ethanol to afford xanthen-9-one **90** as an off white crystalline solid (0.084 g, 87%), mp 173 - 175 °C [lit.,[123] 175 °C]; ν_{max} (CH_2Cl_2) 1651 (C=O) cm^{-1}; δ_H ($CDCl_3$) 8.21 (2H, d, ^3J 8.0, ArH), 7.58 (2H, t, ^3J 7.0, ArH), 7.34 (2H, d, ^3J 8.4, ArH) and 7.24 (2H, t, ^3J 7.3, ArH); δ_C ($CDCl_3$) 177.02 (quat), 156.00 (2 × quat), 134.67 (2 × CH), 126.56 (2 × CH), 123.77 (2 × quat), 121.69 (2 × quat) and 117.84 (2 × CH).

(4-Cyanobiphenyl-2-yl) acetic acid 109

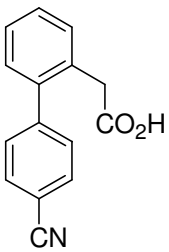

2-Iodophenylacetic acid **107** (1.015 g, 3.87 mmol), K_2CO_3 (3.292 g, 23.82 mmol) and $Pd(PPh_3)_4$ (0.150 g, 0.13 mmol) were added to a mixture of dioxane (20 cm^3) and water (8 cm^3). 4-Cyanophenylboronic acid **108** (0.569 g, 3.87 mmol) was then added slowly with stirring. The mixture was heated under reflux for 4 h

under N_2 after which time a further equivalent of 4-cyanophenylboronic acid **108** (0.574 g, 3.91 mmol) was added and the reaction mixture heated at reflux for a further 18 h under N_2. The reaction mixture was cooled to room temperature, filtered through celite and the filtrates concentrated under reduced pressure to a volume of 20 cm^3 which was diluted with 2M HCl (150 cm^3). The acidic aqueous solution was then extracted with chloroform (3 × 75 cm^3), the combined organic extracts washed with 2M HCl (2 × 100 cm^3), dried ($MgSO_4$) and the solvent removed under reduced pressure to afford an off white solid (1.352 g). The crude solid was then purified by dry flash column chromatography (0% - 50%, EtOAc : Hexane) to afford (4-cyanobiphenyl-2-yl) acetic acid **109** as an off white solid (0.289 g, 32%), mp 165 – 168 ºC; (Found: M^+ 237.07898. $C_{15}H_{11}NO_2$ requires *M* 237.07898); ν_{max} (CH_2Cl_2) 1643 (C=O) cm^{-1}; δ_H ($[^2H]_6$DMSO) 7.93 (2H, d, ^3J 8.4 ArH), 7.53 (2H, d, ^3J 8.5, ArH), 7.34 – 7.44 (3H, m, ArH), 7.27 (1H, m, ArH) and 3.55 (2H, s, CH_2); δ_C ($[^2H]_6$DMSO) 173.51 (quat), 146.67 (quat), 141.20 (quat), 133.38 (quat), 133.20 (2 × CH), 132.03 (CH), 130.97 (2 × CH), 130.51 (CH), 129.19 (CH), 128.13 (CH), 119.76 (quat), 111.05 (quat) and 39.38 (CH_2); *m/z* 237 (M^+, 58%), 204 (63), 192 (93), 191 (43), 190 (68), 136 (36), 91 (100) and 41 (20).

(4-Cyanobiphenyl-2-yl) acetyl chloride 111

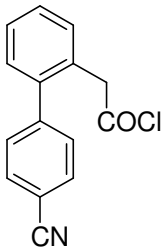

(4-Cyanobiphenyl-2-yl) acetic acid **109** (0.251g, 1.06 mmol) was stirred in anhydrous DCM (2 cm^3) containing 1 drop of anhydrous DMF. Oxalyl chloride (0.412 g, 3.25 mmol) was then added and the reaction mixture heated to reflux for 6 h under nitrogen. The solution was then concentrated under reduced pressure to afford the acid chloride **111** as a light yellow oil (0.271 g, >99%), bp 95 – 100 ºC (0.5 Torr); (Found: M^+ 255.0450. $C_{15}H_{10}{}^{35}ClNO$ requires *M* 255.0451); ν_{max} (CH_2Cl_2) 1796 (C=O) cm^{-1}; δ_H ($CDCl_3$) 7.68 – 7.63 (2H, m, ArH), 7.39 – 7.26 (4H, *m*, ArH), 7.15 – 7.22 (2H, *m*, ArH) and 4.01 (2H, s, CH_2); δ_C ($CDCl_3$) 171.88 (quat), 145.07 (quat), 140.69 (quat), 132.26 (2 × CH), 130.81 (CH), 129.98 (CH), 129.75 (2 × CH), 129.04 (quat), 128.82 (CH), 128.52 (CH), 118.48 (quat), 111.62 (quat) and 50.72 (CH_2); *m/z* 257 (M^+ 6%), 255 (M^+, 17%), 193 (15), 192 (100), 191 (30), 190 (51), 165 (24) and 91 (24).

FVP of (4-cyanobiphenyl-2-yl) acetyl chloride 111

(4-Cyanobiphenyl-2-yl) acetyl chloride **111** (0.267 g, 1.04 mmol) was subjected to FVP (T_f 850 ºC, T_i 50 – 100 ºC, P 3 x 10^{-2} Torr, t 3.0 h) to give an off white solid. The crude product was then purified by dry flash column chromatography (0% - 20%, EtOAc : Hexane) although the required product was not obtained. It is possible much of the acid chloride precursor hydrolysed to the acid prior to FVP.

6.3.2: Heterocyclic Phenanthrol Analogues

2-(Thiophen-2-yl)phenylacetic acid 121

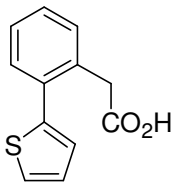

2-Iodophenylacetic acid **107** (1.002 g, 3.83 mmol), K_2CO_3 (3.286 g, 23.77 mmol) and $Pd(PPh_3)_4$ (0.149 g, 0.13 mmol) were added to a mixture of dioxane (20 cm^3) and water (8 cm^3). 2-Thiopheneboronic acid **120** (0.490 g, 3.83 mmol) was then added slowly with stirring. The mixture was heated under reflux for 4 h under N_2 after which time a further equivalent of 2-thiopheneboronic acid (0.490 g, 3.83 mmol) was added and the reaction mixture heated at reflux for a further 18 h under N_2. The reaction mixture was cooled to room temperature, filtered through celite and the filtrates concentrated under reduced pressure to a volume of 20 cm^3 which was diluted with 2M HCl (250 cm^3). The acidic aqueous solution was then extracted with chloroform (3 × 100 cm^3), the combined organic extracts washed with 2M HCl (2 × 100 cm^3), dried ($MgSO_4$) and the solvent removed under reduced pressure to afford a light brown oil (1.011 g). The crude solid was then purified by dry flash column chromatography (0% - 50%, EtOAc : hexane) to afford 2-(thiophen-2-yl)phenylacetic acid **121** as a light brown solid (0.757 g, 91%), mp 79 – 84 ºC; (Found: M^+ 218.0392. $C_{12}H_{10}O_2S$ requires M 218.0396); ν_{max} (CH_2Cl_2) 1707 (C=O) cm^{-1}; ($CDCl_3$) 11.82 (1H, br s, OH), 7.33 - 7.51 (5H, m, ArH), 7.10 - 7.15 (2H, m, ArH) and 3.83 (2H, s, CH_2); δ_C ($CDCl_3$) 178.44 (quat), 141.63 (quat), 134.79 (quat), 131.90 (quat), 131.22 (CH), 130.77 (CH), 128.18 (CH), 127.43 (CH), 127.23 (CH), 127.03 (CH), 125.81 (CH) and 38.85 (CH_2); m/z 218 (M^+, 100 %), 174 (14), 173 (98), 172 (30), 171 (29), 135 (13), 129 (24) and 128 (17).

2-(Thiophen-2-yl)phenylacetyl chloride 122

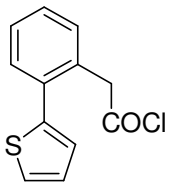

(2-Thiophen-2-ylphenyl) acetic acid **121** (0.715 g, 3.28 mmol) was stirred in anhydrous DCM (5 cm^3) containing 2 drops of anhydrous DMF. Oxalyl chloride (1.295 g, 10.20 mmol) was then added and the reaction mixture heated to reflux for 6 h under nitrogen. The reaction mixture was then concentrated under reduced pressure to afford the acid chloride **122** as a yellow oily solid (0.824 g, 98%), bp 85 – 90 ºC (0.5 Torr); (Found: M^+ 236.0060. $C_{12}H_9{}^{35}ClOS$ requires *M* 236.0057); ν_{max} (CH_2Cl_2) 1796 (C=O) cm^{-1}; δ_H ($CDCl_3$) 7.30 – 7.49 (5H, m, ArH), 7.12 (1H, dd, ^3J 5.2, ^3J 3.4, ArH), 7.01 (1H, dd, ^3J 3.6, ^4J 1.3, ArH) and 4.29 (2H, s, CH_2); δ_C ($CDCl_3$) 172.19 (quat), 141.06 (quat), 134.99 (quat), 131.54 (CH), 130.83 (CH), 130.53 (quat), 128.55 (CH), 128.30 (CH), 127.41 (CH), 127.07 (CH), 126.22 (CH) and 51.24 (CH_2); *m/z* 238 (M^+ 16%), 236 (M^+, 43%), 217 (20), 200 (19), 173 (100), 172 (27), 171 (39) and 129 (18).

Naphtho[1,2-*b*]thiophen-4-ol 123

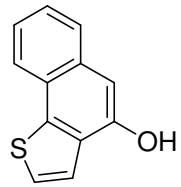

2-(Thiophen-2-yl)phenylacetyl chloride **122** (0.769 g, 3.25 mmol) was subjected to FVP (T_f 850 ºC, T_i 150 – 250 ºC, *P* 3 x 10^{-2} Torr, *t* 6.0 h) to give an orange brown solid (0.594 g). This crude solid was purified mp by dry flash column chromatography (0% - 20%, EtOAc : hexane) to afford naphtho[1,2-*b*]thiophene-4-ol **123** as a red/brown solid (0.395 g, 61%) mp 120 - 124 °C; (Found: M^+ 200.0297. $C_{12}H_8OS$ requires *M* 200.0294); ν_{max} (CH_2Cl_2) 3304 (OH) cm^{-1}; δ_H ($CDCl_3$) 7.93 (1H, m, ArH), 7.57 (1H, m, ArH), 7.49 (1H, d, ^3J 5.4 ArH), 7.26 – 7.36 (3H, m, ArH), 6.80 (1H, s, ArH) and 5.49 (1H, br s, OH); δ_C ($CDCl_3$) 149.02 (quat), 139.56 (quat), 132.22 (quat), 130.17 (quat), 127.05 (CH), 126.04 (CH), 125.00 (quat), 124.74 (CH), 124.15 (CH), 123.45 (CH), 121.21 (CH) and 105.47 (CH); *m/z* 200 (M^+, 100%), 172 (16), 171 (43), 129 (13), 101 (21), 100 (15), 59 (25) and 58 (23).

Reaction of 2-iodophenylacetic acid 107 and 3-thiopheneboronic acid 124

2-Iodophenylacetic acid **107** (1.026 g, 3.92 mmol), K_2CO_3 (3.299 g, 23.87 mmol) and $Pd(PPh_3)_4$ (0.138 g, 0.12 mmol) were added to a mixture of dioxane (20 cm^3) and water (8 cm^3). 3-Thiopheneboronic acid **124** (0.502 g, 3.92 mmol) was then

added slowly with stirring. The mixture was heated under reflux for 18 h under N_2. The reaction mixture was cooled to room temperature, filtered through celite and the filtrates concentrated under reduced pressure to a volume of 20 cm^3 which was diluted with 2M HCl (250 cm^3). The acidic aqueous solution was then extracted with chloroform (3 × 100 cm^3), the combined organic extracts washed with 2M HCl (2 × 100 cm^3), dried ($MgSO_4$) and the solvent removed under reduced pressure to afford a light brown oil (1.271 g). Analysis of the crude product by NMR revealed only (2'-carboxymethylbiphenyl-2-yl)acetic acid **110** and 2-iodophenyl acetic acid **107** starting material. None of the required carboxylic acid was obtained.

6.3.3: Preparation of Methyl Esters

General Method

The carboxylic acid (5.0 mmol) was stirred in DMF (7.5 cm^3) and K_2CO_3 (5.0 mmol) added. Iodomethane (5.0 mmol) was then added dropwise and the reaction mixture stirred for 18 h at room temperature. The reaction mixture was then diluted with water (7.5 cm^3) and extracted with EtOAc (3 × 25 cm^3). The combined extracts were washed with water (3 × 20 cm^3), dried ($MgSO_4$) and the solvent removed under reduced pressure to afford the methyl ester.

Methyl biphenyl-2-ylacetate 113

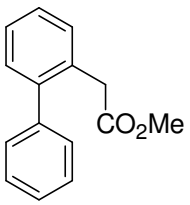

The above general method with biphenyl-2-yl acetic acid **105** (0.154 g, 0.73 mmol), DMF (1 cm^3), K_2CO_3 (0.106 g, 0.73 mmol) and iodomethane (0.239 g, 1.68 mmol) afforded methyl biphenyl-2-ylacetate **113** as a yellow oily solid (0.163 g, 99%), bp 94 - 101 °C (0.5 Torr); (Found: M^+ 226.0997. $C_{15}H_{14}O_2$ requires *M* 226.0988); ν_{max} (CH_2Cl_2) 1738 (C=O) cm^{-1}; δ_H ($CDCl_3$) 7.21 – 7.38 (9H, m, ArH), 3.58 (3H, s, CH_3) and 3.56 (2H, s, CH_2); δ_C ($CDCl_3$) 172.29 (quat), 142.42 (quat), 141.02 (quat), 135.57 (CH), 131.70 (quat), 130.23 (CH), 130.14 (CH), 129.15 (2 × CH), 128.13 (2 × CH), 127.50 (CH), 127.11 (CH), 51.85 (CH_3) and 38.70 (CH_2); *m/z* 226 (M^+, 53%), 194 (7), 168 (13), 167 (100), 166 (38), 165 (65), 164(4) and 152 (13).

Methyl (2-iodophenyl)acetate 114

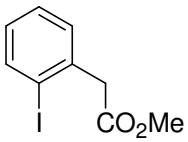

The above general method with 2-iodophenylacetic acid **107** (0.794 g, 5.74 mmol), K_2CO_3 (1.492 g, 5.69 mmol) and iodomethane (1.822 g, 5.69 mmol) in DMF (7.5 cm^3) was used to afford methyl (2-iodophenyl)acetate **114** as an orange oily solid (1.463 g, 93%), bp 84 - 88 °C (0.5 Torr), [lit.,[125] 105 -106 °C (2.0 Torr)]; ν_{max} (CH_2Cl_2) 1739 (C=O) cm^{-1}; δ_H ($CDCl_3$) 7.91 (1H, d, ^3J 8.5, ArH), 7.36 (2H, m, ArH), 7.03 (1H, ddd, ^3J 7.9, ^3J 6.5, ^4J 2.6 ArH), 3.88 (2H, s, CH_2) and 3.79 (3H, s, CH_2); δ_C ($CDCl_3$) 170.83 (quat), 139.44 (CH), 137.64 (quat), 130.55 (CH), 128.83 (CH), 128.37 (CH), 100.92 (quat), 52.11 (CH_3) and 46.07 (CH_2).

6.3.4: Preparation of Suzuki Coupled Methyl Esters

Methyl 2-(thiophen-3-yl)phenylacetate 127

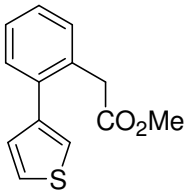

Methyl (2-iodophenyl)acetate **114** (0.300 g, 1.09 mmol), K_2CO_3 (0.921 g, 6.66 mmol) and $Pd(PPh_3)_4$ (0.039 g, 0.33 mmol) were stirred in dioxane (5 cm^3) and water (2 cm^3). 3-Thiopheneboronic acid **124** (0.139 g, 1.09 mmol) was then added with stirring and the mixture heated to reflux for 18 h under N_2. The reaction was then filtered through celite and the filtrates concentrated under reduced pressure to afford a brown residue. This was taken up in 2M HCl (100 cm^3) and the acid solution extracted with chloroform (3 × 75 cm^3). The combined extracts were washed with 2M HCl (2 × 50 cm^3), dried ($MgSO_4$) and the solvent removed to afford an orange oil (0.271 g). The crude oil was then purified by dry flash column chromatography (0% - 50%, EtOAc : hexane) to afford methyl 2-(thiophen-3-yl)phenylacetate **127** as an orange oil (0.255 g, 99%), bp 105 - 108 °C (0.5 Torr); (Found: M^+ 232.0558. $C_{13}H_{12}O_2S$ requires *M* 232.0558); ν_{max} (CH_2Cl_2) 1735 (C=O) cm^{-1}; δ_H ($CDCl_3$) 7.11 – 7.27 (5H, m, ArH), 7.15 (1H, dd, ^3J 3.2, ^4J 1.3, ArH), 7.02 (1H, dd, ^3J 4.9, ^4J 1.4, ArH), 3.56 (2H, s, CH_2) and 3.54 (3H, s, CH_3); δ_C ($CDCl_3$) 172.17 (quat), 141.14 (quat), 137.10 (quat), 132.04 (quat), 130.33 (CH), 130.13 (CH), 128.88 (CH), 127.52 (CH), 127.09 (CH), 125.27 (CH), 123.03 (CH), 51.84 (CH_3) and 38.78 (CH_2); *m/z* 232 (M^+, 83%), 217 (23), 199 (44), 173 (93), 172 (96), 171 (96), 166 (100) and 129 (38).

2-(Furan-2-yl)phenylacetic acid 132

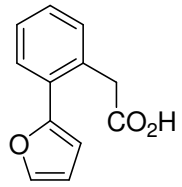

Methyl (2-iodophenyl)acetate **114** (0.300 g, 1.09 mmol), K_2CO_3 (0.921 g, 6.66 mmol) and $Pd(PPh_3)_4$ (0.039 g, 0.33 mmol) were stirred in dioxane (5 cm^3) and water (2 cm^3). 2-Furanboronic acid **128** (0.139 g, 1.09 mmol) was then added with stirring and the mixture heated to reflux for 18 h under N_2. The reaction mixture was worked up as in the 3-thophene example to afford an off white solid identified as 2-(furan-2-yl)phenylacetic acid **132** (0.199 g, 90%), mp 118 - 121 °C; (Found: M^+ 202.0630. $C_{12}H_{10}O_3$ requires *M* 202.0628); ν_{max} (CH_2Cl_2) 1713 (C=O) cm^{-1}; δ_H ($CDCl_3$) 7.54 (1H, d, ^3J 6.5, ArH), 7.41 (1H, d, ^4J 1.1, ArH), 7.18 - 7.30 (3H, m, ArH), 6.50 (1H, d, ^3J 3.3, ArH), 6.40 (1H, dd, ^3J 3.1, ^4J 1.8, ArH) and 3.82 (2H, s, CH_2); δ_C ($CDCl_3$) 178.25 (quat), 153.64 (quat), 142.76 (CH), 132.19 (CH), 131.18 (quat), 130.56 (quat), 128.49 (CH), 128.38 (CH), 128.09 (CH), 111.79 (CH), 108.76 (CH) and 40.21 (CH_2); *m/z* 202 (M^+, 71%), 185 (24), 184 (83), 135 (93), 129 (45), 128 (76), 127 (33) and 41 (100).

No significant quantities of the methyl ester product **130** were obtained.

2-(Furan-3-yl)phenylacetic acid 133

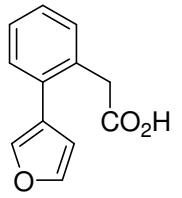

Methyl (2-iodophenyl)acetate **114** (0.233 g, 0.84 mmol), K_2CO_3 (0.753 g, 5.45 mmol) and $Pd(PPh_3)_4$ (0.040 g, 0.33 mmol) were stirred in dioxane (5 cm^3) and water (2 cm^3). 3-Furanboronic acid **129** (0.096 g, 0.86 mmol) was then added with stirring and the mixture heated to reflux for 18 h under N_2. The reaction mixture was worked up as above to afford an off white solid (0.143 g) identified as 2-(furan-3-yl)phenylacetic acid **133** and 2-iodophenylacetic acid **107** in a 75 : 25 ratio. Further separation of these two components failed. The overall weight of 2-(furan-3-yl)phenylacetic acid **133** in the crude product was 0.104 g, (61%), (Found: M^+ 202.0630. $C_{12}H_{10}O_3$ requires *M* 202.0628); ν_{max} (CH_2Cl_2) 1707 (C=O) cm^{-1}; δ_H ($CDCl_3$) 7.77 (1H, t, ^4J 1.3, ArH), 7.71 (1H, t, ^4J 1.6, ArH), 7.50 - 7.61 (4H, m, ArH), 6.77 (1H, dd, ^3J 1.7, ^4J 0.8, ArH) and 3.96 (2H, s, CH_2); δ_C ($CDCl_3$) 178.24 (quat), 142.85 (CH), 140.10 (CH), 133.08 (quat), 131.44 (quat), 130.63 (CH), 130.13

(CH), 127.55 (CH), 127.50 (CH), 124.66 (quat), 111.68 (CH) and 38.87 (CH_2); *m/z* 202 (M^+, 66%), 184 (67), 157 (67), 156 (52), 135 (90), 129 (81), 128 (76) and 127 (100).

No significant quantities of the methyl ester product **131** were obtained.

Methyl 2-(furan-2-yl)phenylacetate130

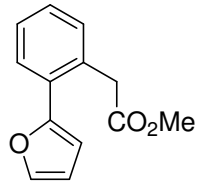

The general method for the preparation of methyl esters was carried out with 2-(furan-2-yl)phenylacetic acid **132** (0.052 g, 0.25 mmol), K_2CO_3 (0.040 g, 0.29 mmol) and iodomethane (0.070 g, 0.49 mmol) in DMF (1.0 cm^3) to afford methyl 2-(furan-2-yl)phenylacetate **130** as an orange oil (0.049 g, 91%), bp 108 - 115 °C (0.5 Torr); (Found: M^+ 216.0786. $C_{13}H_{12}O_3$ requires *M* 216.0786); ν_{max} (CH_2Cl_2) 1735 (C=O) cm^{-1}; δ_H ($CDCl_3$) 7.54 (1H, m, ArH), 7.41 (1H, dd, ^3J 1.8, ^4J 0.8, ArH), 7.16 – 7.28 (3H, m, ArH), 6.49 (1H, dd, ^3J 3.4, ^4J 0.8, ArH), 6.40 (1H, dd, ^3J 3.4, ^4J 1.8, ArH), 3.79 (2H, s, CH_2) and 3.59 (3H, s, CH_3); δ_C ($CDCl_3$) 172.10 (quat), 153.25 (quat), 142.18 (CH), 131.55 (CH), 130.87 (quat), 130.68 (quat), 128.03 (CH), 127.88 (CH), 127.38 (CH), 111.32 (CH), 108.27 (CH), 51.96 (CH_3) and 39.90 (CH_2); *m/z* 216 (M^+, 100%), 157 (16), 149 (12), 129 (21), 128 (22), 127 (10), 102 (2) and 90 (5).

Methyl 2-(furan-3-yl)phenylacetate 131

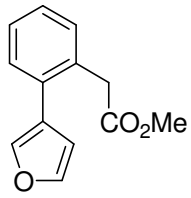

The general method for the preparation of methyl esters was carried out with the crude 2-(furan-3-yl)phenylacetic acid **133** (0.074 g, 73% strength, 0.25 mmol), K_2CO_3 (0.043 g, 0.31 mmol) and MeI (0.071 g, 0.50 mmol) in DMF (1.0 cm^3) to afford methyl 2-(furan-3-yl)phenylacetate **131** as a brown oil (0.087 g). However analysis indicated the product also contained approximately 25% composition of methyl 2-iodophenylacetate **114** which could not be separated and thus was carried onto the next step. Therefore the overall yield of methyl 2-(furan-3-yl)phenylacetate **131** in the crude product was 0.065 g (99%), bp 100 - 105 °C (0.5 Torr); (Found: M^+ 216.0790. $C_{13}H_{12}O_3$ requires *M* 216.0781); ν_{max} (CH_2Cl_2) 1737 (C=O) cm^{-1}; δ_H ($CDCl_3$) 7.45 (1H, dd, ^3J 1.6, ^4J 0.9, ArH), 7.39 (1H, t, ^3J 1.6, ArH), 7.17 – 7.29 (4H,

m, ArH), 6.45 (1H, dd, ^3J 2.7, ^4J 0.9, ArH), 3.62 (2H, s, CH_2) and 3.59 (3H, s, CH_3); δ_C ($CDCl_3$) 172.18 (quat), 142.76 (CH), 140.07 (CH), 132.94 (quat), 132.11 (quat), 130.53 (CH), 130.04 (CH), 127.50 (CH), 127.27 (CH), 124.78 (quat), 111.69 (CH), 52.07 (CH_3) and 38.98 (CH_2); *m/z* 216 (M^+, 100%), 184 (10), 157 (48), 156 (39), 149 (95), 129 (72), 128 (95) and 91 (47).

6.3.5: FVP of Esters over Tungsten Trioxide

The general method for the FVP of substrates over a tungsten trioxide catalyst involved firstly heating the catalyst packed in a furnce tube between two glass wool plugs to 600 ºC for 0.5 h. This activated the catalyst upon which point it would turn an orange colour from the original yellow colour at room temperature. The substrate was then pyrolysed over the catalyst at reduced pressure taking extra care to open taps to bring the system to a reduced pressure slowly to avoid dislodging the catalyst packing. The pyrolysate was then collected in the U-tube immersed in liquid N_2.

9-Phenanthrol 29

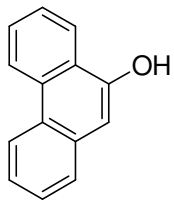

Biphenyl-2-yl acetic acid methyl ester **113** (0.123 g, 0.54 mmol) was subjected to FVP (T_f 600 ºC, T_i 140 ºC, P 3 x 10^{-2} Torr, t 1.0 h) over tungsten trioxide (10 g) packed in the furnace tube to give a light orange-white solid (0.071 g). Analysis of this crude pyrolysate by NMR revealed it to be a 2 : 3 mix of 9-Phenanthrol **29** : ester starting material **113**.

Naphtho[2,1-*b*]thiophen-4-ol 126

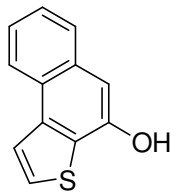

Methyl 2-(thiophen-3-yl)phenylacetate **127** (0.242 g, 1.0 mmol) was subjected to FVP (T_f 600 ºC, T_i 150 ºC, P 3 x 10^{-2} Torr, t 2.0 h) over tungsten trioxide (10 g) packed in the furnace tube to give brown oil (0.133 g). The crude oil was then purified by dry flash column chromatography (0% - 50%, EtOAc : Hexane) to afford unreacted starting material **127** (0.057 g, 24% recovery) and naphtho[2,1-*b*]thiophen-4-ol **126** as a brown solid (0.017 g, 8%), mp = 141 - 145 ºC; (Found: M^+ 200.0289. $C_{12}H_8OS$ requires M 200.0296); ν_{max} (CH_2Cl_2) 3505 (OH) cm^{-1}; δ_H (360 MHz, $CDCl_3$) 8.26 (1H, m, ArH), 7.98 (1H, d, ^3J 5.3, ArH), 7.77 (1H, m, ArH), 7.62 (1H, d, ^3J 5.3, ArH), 7.47 (2H, m,

ArH), 7.02 (1H, s, ArH) and 5.76 (1H, br s, OH); δ_C (90 MHz, $CDCl_3$) 148.58 (quat), 138.36 (quat), 133.02 (quat), 129.00 (quat), 126.86 (CH), 126.39 (CH), 125.73 (CH), 125.48 (quat), 124.02 (CH), 123.60 (CH), 122.44 (CH) and 105.27 (CH); *m/z* 200 (M^+, 100%), 172 (14), 171 (73), 127 (7), 86 (6), 85 (12), 43 (7) and 41 (31).

Naphtho[1,2-*b*]furan-4-ol 134

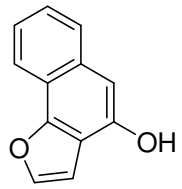

Methyl 2-(furan-2-yl)phenylacetate **130** (0.045 g, 0.18 mmol) was subjected to FVP (T_f 600 ºC, T_i 0 - 250 ºC, P 3 x 10^{-2} Torr, t 4.0 h) over tungsten trioxide (10 g) packed in the furnace tube to give a brown oil (0.032 g). The crude oil was then purified by dry flash column chromatography (0% - 50%, EtOAc : Hexane) to afford naphtho[1,2-*b*]furan-4-ol **134** as a brown solid (0.007 g, 20%), (Found: M^+ 184.0524. $C_{12}H_8O_2$ requires *M* 184.0519); δ_H (360 MHz, $CDCl_3$) 7.63 (1H, d, ^3J 7.2, ArH), 7.30 (4H, m, ArH), 6.54 (1H, d, ^3J 3.3, ArH) and 6.19 (1H, d, ^3J 3.3, ArH); δ_C (90 MHz, $CDCl_3$) 165.00 (quat), 152.78 (quat), 144.99 (quat), 124.56 (CH), 123.73 (quat), 123.31 (quat), 120.64 (CH), 120.46 (CH), 120.29 (CH), 101.77 (CH), 99.16 (CH) and 96.67 (CH); *m/z* 184 (M^+, 100%), 155 (6), 128 (17), 127 (8), 92 (4), 77 (4), 64 (4) and 40 (20).

FVP of methyl 2-(furan-3-yl)phenylacetate 131

Methyl 2-(furan-3-yl)phenylacetate **131** (0.071 g, 0.25 mmol) was subjected to FVP (T_f 600 ºC, T_i 50 - 250 ºC, P 3 x 10^{-2} Torr, t 3.0 h) over tungsten trioxide (10 g) packed in the furnace tube to give a brown oil (0.023 g). The crude oil was then purified by dry flash column chromatography (0% - 50%, EtOAc : Hexane) to afford a brown residue (0.009 g).

NMR and mass spec analysis did not indicate the presence of any cyclised product **135** or the starting material.

6.3.6: Attempted Acid Chloride Route to Naphtho[1,2-*b*]furan-4-ol and Naphtho[2,1-*b*]furan-4-ol

Treatment of 2-(furan-2-yl)phenylacetic acid 132 with oxalyl chloride

2-(Furan-2-yl)phenylacetic acid **132** (0.077 g, 0.38 mmol) was stirred in anhydrous DCM (1 cm^3) containing 1 drops of anhydrous DMF. Oxalyl chloride (0.253 g, 1.99 mmol) was then added and the reaction mixture heated to reflux for 6 h under N_2. The reaction mixture was then concentrated under reduced pressure to afford a dark yellow oil (0.133 g).

NMR analysis of the crude product could not confirm the presence of the acid chloride **130** and full purification and characterisation was not possible due to stability problems.

FVP of Crude 2-(furan-2-yl)phenylacetyl chloride 130

The possible crude 2-(furan-2-yl)phenylacetyl chloride **130** (0.109 g) was subjected to FVP (T_f 850 ºC, T_i 50 - 250 ºC, P 3 x 10^{-2} Torr, t 1.5 h) to afford a brown oil (0.029 g) and a black solid residue (0.072 g) in the inlet tube. No identifiable product was found in the crude pyrolysate.

Treatment of 2-(furan-3-yl)phenylacetic acid 133 with oxalyl chloride

2-(Furan-3-yl)phenylacetic acid **133** (0.068 g, 0.25 mmol) was stirred in anhydrous DCM (1 cm^3) containing 1 drops of anhydrous DMF. Oxalyl chloride (0.200 g, 1.57 mmol) was then added and the reaction mixture heated to reflux for 6 h under N_2. The reaction mixture was then concentrated under reduced pressure to afford dark yellow oil (0.165 g).

NMR analysis of the crude product could not confirm the presence of the acid chloride **131** and full purification and characterisation was not possible due to stability problems.

FVP of Crude 2-(furan-3-yl)phenylacetyl chloride 131

The possible crude 2-(furan-3-yl)phenylacetyl chloride **131** (0.109 g) was subjected to FVP (T_f 850 ºC, T_i 50 - 250 ºC, P 3 x 10^{-2} Torr, t 3.0 h) to afford a brown oil

(0.056 g) and a black solid residue (0.031 g) in the inlet tube. No identifiable product was found in the crude purolysate.

6.3.7: Coupling with C. I. Acid Yellow 9 Diazonium Salt

General Method

A general method for the preparation the C. I. Acid Yellow 9 diazonium salt and coupling with the phenanthrol systems was used. 2-Amino-5-(4-sulfophenylazo)-benzenesulfonic acid **136** (C. I. Acid yellow 9, 1.31 mmol) was stirred in HCl (conc., 2 cm^3) and water (2 cm^3) and cooled to < 5 ºC. Sodium nitrite (1.77 mmol) was then added slowly ensuring the temperature did not exceed 5 ºC The reaction mixture was stirred for a further 1 h at < 5ºC.

9-Phenanthrol **29** or the heterocyclic phenanthrol system (1.31 mmol) was stirred in 10% NaOH (2 cm^3) and cooled to < 5 ºC. The diazonium salt solution was then added dropwise with stirring at < 5 ºC during which time the colour changed from a light red to magenta colour. The reaction mixture was stirred at T < 5 ºC for 4 h and overnight at room temperature.

The product was then obtained by the addition of NaCl (5 % w/w) to the reaction mixture until the precipitate was out of solution followed by filtration under reduced pressure. The resulting paste was then redissolved in water (20 cm^3) and the precipitate drowned out of solution with acetone (1.5 L), recovered by filtration and dried to afford the azo product as a solid.

2-(10-Hydroxyphenanthren-9-ylazo)-5-(4-sulfophenylazo) benzenesulfonic acid disodium salt 137

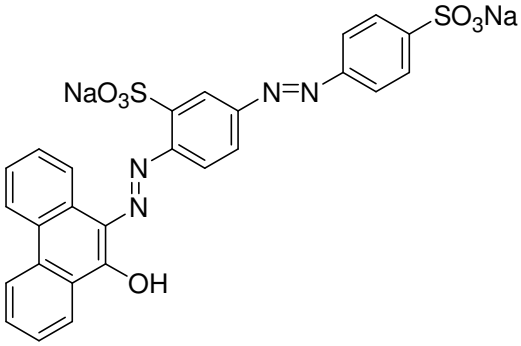

The above general method was applied for the preparation of the C. I. Acid Yellow 9 diazonium salt solution. This was coupled to 9-phenanthrol **29** (0.253 g, 1.31 mmol) and purified as above to afford the azo **137** as a magenta solid (0.614 g, 77%), mp >

330 ºC (Found: C, 10.2; H, 0.6; N, 1.6. $C_{26}H_{16}N_4Na_2O_7S_2.41NaCl.H_2O$ requires C, 10.3; H, 0.6; N, 1.9%); δ_H (360 MHz, $[^2H]_6$DMSO) 8.49 (2H, t, ^3J 7.6, ArH), 8.40 (2H, m, ArH), 8.31 (1H, d, ^3J 8.60, ArH), 8.28 (1H, d, ^4J 2.3, ArH), 8.08 (1H, dd, ^3J 8.7, ^4J 2.0, ArH), 7.80 – 7.90 (5H, m, ArH), 7.62 (1H, t, ^3J 7.3, ArH) and 7.52 – 7.57 (2H, m, ArH); δ_C (90 MHz, $[^2H]_6$DMSO) 178.22 (quat), 151.81 (quat), 150.21 (quat), 147.27 (quat), 141.76 (quat), 135.57 (quat), 135.52 (quat), 134.25 (quat), 131.68 (CH), 130.12 (quat), 129.66 (quat), 128.85 (CH), 128.03 (CH), 127.86 (CH), 127.77 (CH), 127.44 (quat), 126.69 (2 × CH), 126.48 (CH), 123.72 (CH), 123.61 (CH), 123.14 (CH), 122.02 (2 × CH), 120.67 (CH) and 116.58 (CH); *m/z* (ESI): 583.3 $[MNa]^-$ $C_{26}H_{16}N_4NaO_7S_2$ requires 583.0; λ_{max} 499 nm (ε 53000 dm^{-3} mol^{-1} cm^{-1}), $W_{1/2}$ 78 nm.

The strength of the product was estimated to be 20% by CHN due to salt impurities, which gave an overall reaction yield of 15%.

2-(4-Hydroxynaphtho[1,2-*b*]thiophen-5-ylazo)-5-(4-sulfophenylazo) benzenesulfonic acid disodium salt 138

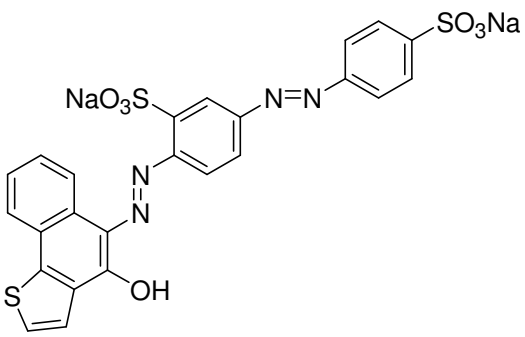

The general method was used with naphtho[1,2-*b*]thiophen-4-ol **123** (0.250 g, 1.25 mmol), 10% NaOH (2 cm^3), C. I. Acid Yellow 9 (0.500 g, 1.25 mmol), HCl conc. (2 cm^3), water (2 cm^3) and sodium nitrite (0.129 g, 1.87 mmol) to afford the crude 4-hydroxynaphtho[1,2-*b*]thiophen-5-yl azo **138** as a red precipitate (0.563 g). Purification as with the preparation of **137** afforded the azo **138** as a red solid (0.303 g, 40%), mp > 330 ºC (Found: C, 32.5; H, 2.0; N, 5.6. $C_{24}H_{14}N_4Na_2O_7S_3.4NaCl.3H_2O$ requires C, 32.0; H, 2.2; N, 6.2 %); δ_H (360 MHz, $[^2H]_6$DMSO) 8.41 (1H, d, ^3J 7.6, ArH), 8.29 – 8.32 (2H, m, ArH), 8.08 (1H, dd, ^3J 8.7, ^4J 1.9, ArH), 7.69 – 7.92 (7H, m, ArH) and 7.43 – 7.58 (2H, m, ArH); δ_C (90 MHz, $[^2H]_6$DMSO) 174.34 (quat), 152.25 (quat), 150.67 (quat), 149.49 (quat), 147.85 (quat), 142.00 (quat), 132.28 (quat), 136.15 (quat), 131.34 (quat), 130.74 (quat), 129.11 (CH), 128.27 (CH), 127.13 (2 × CH), 126.86 (CH), 126.81 (CH),

126.22 (CH), 125.66 (quat), 124.48 (CH), 123.64 (CH), 122.46 (2 × CH), 121.06 (CH) and 117.08 (CH); *m/z* (ESI): 589.2 $[MNa]^-$ $C_{24}H_{14}N_4NaO_7S_3$ requires 589.0; λ_{max} 490 nm (ε 31000 dm^{-3} mol^{-1} cm^{-1}), $W_{1/2}$ 108 nm.

The strength of the product was estimated to be 73% by CHN due to salt impurities, which gave an overall reaction yield of 29%.

2-(4-Hydroxynaphtho[2,1-*b*]thiophen-5-ylazo)-5-(4-sulfophenylazo) benzenesulfonic acid disodium salt 139

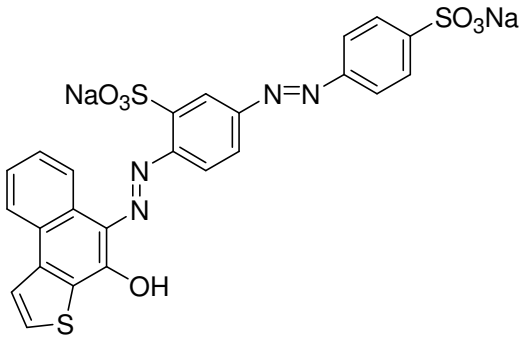

The general method was used with naphtho[2,1-*b*]thiophen-4-ol **126** (0.013 g, 0.07 mmol), 10% NaOH (0.1 cm^3), C. I. Acid yellow 9 (0.027 g, 0.07 mmol), HCl conc. (0.1 cm^3), water (0.1 cm^3) and sodium nitrite (0.043 g, 0.62 mmol) to afford the crude 4-hydroxynaphtho[2,1-*b*]thiophen-5-ylazo **139** as a red paste. Purification as with the preparation of **137** afforded the azo **139** as a red solid (0.020 g, 49%), mp > 330 ºC (Found: C, 25.3; H, 1.7; N, 4.2. $C_{24}H_{14}N_4Na_2O_7S_3.8NaCl.4H_2O$ requires C, 25.0; H, 1.9; N, 4.8 %); δ_H (360 MHz, $[^2H]_6$DMSO) 8.47 (1H, d, ^3J 7.2, ArH), 8.28 – 8.32 (3H, m, ArH), 8.15 (1H, d, ^3J 7.3, ArH), 8.07 – 8.09 (2H, m, ArH), 7.88 (2H, d, ^3J 7.45, ArH), 7.80 (2H, d, ^3J 7.31, ArH) and 7.50 – 7.58 (2H, m, ArH); δ_C (90 MHz, $[^2H]_6$DMSO) 174.40 (quat), 153.33 (quat), 151.94 (quat), 148.95 (quat), 146.91 (quat), 143.17 (quat), 138.70 (CH), 137.44 (quat), 136.52 (quat), 133.62 (quat), 131.65 (quat), 130.02 (CH), 129.16 (CH), 128.23 (2 × CH), 127.95 (quat), 127.73 (CH), 126.55 (CH), 126.36 (CH), 124.84 (CH), 123.58 (2 × CH), 122.19 (CH) and 118.20 (CH); *m/z* (ESI): 589.2 $[MNa]^-$ $C_{24}H_{14}N_4NaO_7S_3$ requires 589.0; λ_{max} 503 nm (ε = 21800 dm^{-3} mol^{-1} cm^{-1}), $W_{1/2}$ > 200 nm.

The strength of the product was estimated to be 58% by CHN due to salt impurities, which gave an overall reaction yield of 28%.

6.4: 4,9-Disulfophenanthrenoquinone Based Dyes

6.4.1: Hydrazino Precursors

4,5-Dichloro-*2H*-pyridazin-3-one 177

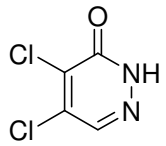

Hydrazine monohydrate (3.150 g, 63 mmol) and water (30 cm^3) were added to concentrated HCl (10 cm^3) and the solution heated to boiling with stirring. A solution of mucochloric acid **176** (10.002 g, 59 mmol) in water (20 cm^3) was then added slowly with continued stirring. The heating of the reaction mixture was then discontinued due to the exothermiciy of the reaction and the mixture was stirred for a futher 15 min. The precipitate formed was then filtered off and dried under reduced pressure to yield 4,5-dichloro-*2H*-pyridazin-3-one **177** as a beige solid (9.366 g, 96%), mp 198 – 200 ºC [lit.,[126] 200 – 202 ºC]; δ_H ($[^2H]_6$DMSO) 13.70 (1H, br s, NH) and 8.10 (1H, s, ArH); δ_C ($[^2H]_6$DMSO) 156.86 (quat), 136.65 (quat), 136.55 (CH) and 133.27 (quat).

Pyridazin-3-one 173

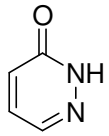

4,5-Dichloro-*2H*-pyridazin-3-one **177** (6.035 g, 37 mmol) and ammonium hydroxide (3.940 g, 39 mmol) were dissolved in ethanol (40 cm^3) and palladium charcoal (10%, 0.154 g) added. The reaction mixture was then stirred at 35 ºC for 9 h in a Parr 4842 hydrogenation apparatus at high pressure (20 bar). The reaction mixture was then filtered through a celite pad to remove the heterogeneous catalyst and the solvent removed under reduced pressure to afford the crude hydrogenated product. This off-white solid was then recrystallised from xylene with the removal of an insoluble impurity to afford pyridazin-3-one **173** as light yellow crystals (3.146 g, 90%), mp 100 – 102 ºC [lit.,[126] 101 – 102 ºC]; δ_H ($[^2H]_6$DMSO) 12.66 (1H, br s, NH), 7.85 (1H, dd, ^3J 3.8, ^4J 1.6, ArH), 7.27 (1H, dd, ^3J 9.7, ^3J 3.8, ArH) and 7.01 (1H, dd, ^3J 9.7, ^4J 1.6, ArH); δ_C ($[^2H]_6$DMSO) 162.57 (quat), 137.16 (CH), 132.61 (CH) and 130.11 (CH).

3-Chloropyridazine 174[53]

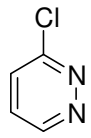

Pyridazin-3-one **173** (5.01 g, 52 mmol) was added slowly to phosphorus oxychloride (45 cm^3). After the reaction had moderated, additional phosphorus oxychloride (40 cm^3) was added and the reaction mixture heated to 75 ºC with continuous stirring for 1 h. Excess reagent was then removed under water pump pressure to afford an orange oil which was added dropwise with stirring to cold saturated sodium bicarbonate solution (85 cm^3) over 0.5 h. The pH was then adjusted to pH 6 –7 with sodium bicarbonate as required. The solution was extracted with DCM (3 × 100 cm^3) the combined organic extracts washed with water (2 × 50 cm^3) and dried ($MgSO_4$). The solvent was then removed under reduced pressure to afford 3-chloropyridazine **174** as a brown oily solid (5.85 g, 98%), bp 68 - 70 ºC (3.5 Torr); δ_H ($CDCl_3$) 9.07 (1H, dd, ^3J 4.3, ^4J 1.8, ArH) and 7.44 – 7.54 (2H, m, ArH); δ_C ($CDCl_3$) 157.02 (quat), 150.22 (CH), 128.50 (CH) and 128.25 (CH); *m/z* 116 (M^+ 86%), 114 (M^+, 100%), 88 (51), 86 (81), 60 (50), 52 (60), 51 (94) and 50 (59).
Although 3-chloropyridazine was known, no analytical data has been reported.

3-Hydrazinopyridazine dihydrochloride 175

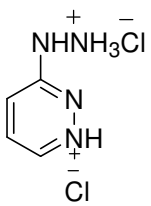

3-Chloropyridazine **174** (5.65 g, 49 mmol) was stirred in hydrazine hydrate (80%, 10 cm^3) and the reaction mixture heated to 75 ºC with stirring for 6 h. The reaction mixture was then cooled to < 5 ºC and HCl (37%, 40 cm^3) added dropwise with stirring. The resulting hydrazine hydrochloride salt precipitate was then removed by filtration and the filtrates concentrated under reduced pressure to afford the crude 3-hydrazinopyridazine dihydrochloride **175** as a light orange solid (10.75 g, > 100%). The crude product was then slurried in ethanol (500 cm^3) at 80 ºC for 1 h and the solution filtered to afford the 3-hydrazinopyridazine dihydrochloride as a light orange solid (5.12 g, 71%), mp > 330 ºC (Found: C, 22.7; H, 4.4; N, 28.5. $C_4H_6N_4.2HCl.H_2O$ requires C, 23.9; H, 5.0; N, 27.9 %); δ_H ($[^2H]_6$DMSO) 8.80 (1H, dd, ^3J 4.5, ^4J 1.2, ArH), 7.88 (1H, dd, ^3J 9.3, ^3J 4.6, ArH) and 7.68 (1H, dd, ^3J 9.3, ^4J 1.3, ArH); δ_C 156.15 (quat), 143.29 (CH), 131.76 (CH) and 121.08 (CH); *m/z* (ESI): 111 MH^+ $C_4H_6N_4$ requires 111. The product was considered to be present as the dihydrochloride salt due to

CHN analysis. The strength of the product was estimated to be 72% by CHN due to HCl and water impurities, which gave an overall reaction yield of 51%.

1-Hydrazinoisoquinoline 180

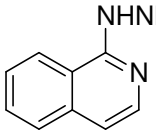

1-Chloroisoquinoline **179** (4.196 g, 26 mmol) was dissolved in a mixture of hydrazine hydrate 80% (20 cm^3, 411.51 mmol) and absolute ethanol (40 cm^3) and the reaction mixture heated at reflux for 2 h. The reaction mixture was then left to cool and stand at room temperature overnight during which time a yellow precipitate formed. This precipitate was filtered and recrystallised from ethyl acetate to afford 1-hydrazinoisoquinoline **180** as light yellow crystals (4.060 g, 99%), mp 175 – 178 ºC [lit.,[56] 179 ºC] (Found: M^+ 159.0786. $C_9H_9N_3$ requires *M* 159.0791); δ_H ([^{2}H]$_6$DMSO) 8.21 (1H, d, ^3J 8.3, ArH), 7.90 (1H, d, ^3J 5.9, ArH), 7.71 (1H, dd, ^3J 8.1, ^4J 1.1, ArH), 7.62 (1H, m, ArH), 7.47 (1H, ddd, ^3J 8.3, ^3J 6.9, ^4J 1.6, ArH) and 6.91 (1H, d, ^3J 5.9, ArH); δ_C 157.46 (quat), 141.53 (CH), 137.22 (quat), 130.76 (CH), 127.36 (CH), 126.64 (CH), 123.63 (CH), 118.36 (quat) and 110.88 (CH); *m/z* 159 (M^+, 53%), 145 (11), 130 (13), 129 (100), 128 (19), 115 (11), 102 (22) and 51 (12).

2-Hydrazinoquinoline 182

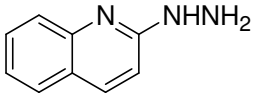

2-Chloroquinoline **181** (4.002 g, 24.46 mmol) was dissolved in a mixture of hydrazine hydrate 80% (20 cm^3, 411.51 mmol) and absolute ethanol (40 cm^3) and the reaction mixture heated at reflux for 2 h. The reaction mixture was then left to cool and stand at room temperature overnight during which time a light yellow precipitate formed. This precipitate was then filtered and recrystallised from ethyl acetate to afford 2-hydrazinoquinoline **182** as light yellow crystals (2.884 g, 74%), mp 139 – 143 ºC [lit.,[127] 142 - 143 ºC] (Found: M^+ 159.0787. $C_9H_9N_3$ requires *M* 159.0791); δ_H ($CDCl_3$) 7.85 (1H, d, ^3J 8.9, ArH), 7.75 (1H, m, ArH), 7.54 – 7.67 (2H, m, ArH), 7.28 (1H, ddd, ^3J 8.0, ^3J 6.9, ^4J 1.2, ArH) and 6.78 (1H, d, ^3J 8.9, ArH); δ_C 158.85 (quat), 147.33 (quat), 137.39 (CH), 129.69 (CH), 127.54 (CH), 126.21 (CH), 124.17 (quat), 122.79 (CH), and 110.62 (CH); *m/z* 159 (M^+, 77%), 130 (16), 129 (100), 128 (19), 115 (9), 102 (19), 89 (11) and 77 (15).

6.4.2: Synthesis of New Heterocyclic Azo Compounds

9-Hydroxy-10-(pyridazin-3-ylazo)phenanthrene-2,7-disulfonic acid disodium salt 188

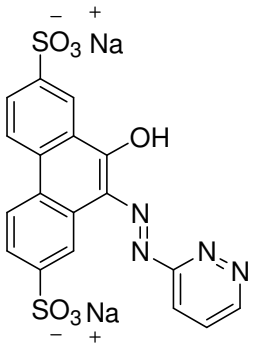

4,9-Disulfophenanthroquinone **171** (3.05 g, 84% strength, 7.0 mmol) was added to HCl (2 M, 90 cm^3) with stirring until all the quinone had dissolved. 3-Hydrazinopyridazine dihydrochloride **175** (1.93 g, 72% strength, 9.5 mmol) was added and the reaction mixture was heated to 75 ºC with continued stirring for 16 h until only one major peak was present by HPLC. The reaction mixture was cooled to room temperature and salt added (5% w/v) with stirring until an orange product precipitated. The reaction mixture was filtered and the precipitate dried under suction to afford an orange paste. The paste was dissolved in water (500 cm^3) and the pH adjusted to pH 7 using 2M NaOH as required. The solution was then filtered, dialysed and dried to afford 9-hydroxy-10-(pyridazin-3-ylazo)phenanthrene-2,7-disulfonic acid disodium salt **188** as a dark orange/red solid (2.299 g, 70%), mp > 330 ºC (Found: C, 37.6; H, 3.4; N, 9.8. $C_{18}H_{10}N_4Na_2O_7S_2.4H_2O$ requires C, 37.5; H, 3.2; N, 9.7%); δ_H ([^{2}H]$_6$DMSO) 9.01 (1H, d, ^3J 4.2, ArH), 8.62 (2H, dd, ^3J 9.1, ^4J 1.4 ArH), 8.50 (1H, d, ^3J 8.6, ArH), 8.41 (1H, d, ^3J 8.7, ArH), 8.17 – 8.05 (2H, m, ArH), 7.95 (1H, dd, ^3J 9.1, ^3J 4.6, ArH) and 7.81 (1H, dd, ^3J 8.3, ^4J 1.3, ArH); δ_C ([^{2}H]$_6$DMSO) 180.51 (quat), 158.08 (quat), 148.94 (CH), 148.26 (quat), 147.68 (quat), 135.78 (quat), 132.07 (CH), 131.08 (quat), 130.59 (quat), 130.32 (CH), 129.55 (quat), 127.79 (quat), 125.98 (CH), 125.00 (CH), 124.22 (CH), 124.12 (CH), 120.51 (CH) and 115.14 (CH); *m/z* (ESI): 461 MH^+ $C_{18}H_{13}N_4O_7S_2$ requires 461; *m/z* (ESI): 459.4 $[MH]^-$ $C_{18}H_{11}N_4O_7S_2$ requires 459.0; λ_{max} 450 nm (ε 16200 dm^{-3} mol^{-1} cm^{-1}), $W_{1/2}$ 115 nm.

The strength of the product was estimated to be 88% by CHN due to water impurities, which gave an overall reaction yield of 62%.

The above method was used as the general method in subsequent coupling reactions of this type.

9-Hydroxy-10-(pyridin-2-ylazo)phenanthrene-2,7-disulfonic acid disodium salt 187

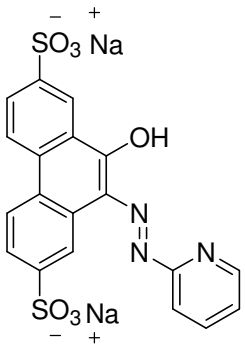

The above general method with 4,9-disulfophenanthroquinone **171** (5.01 g, 84% strength, 11.4 mmol), HCl (2 M, 160 cm^3) and 2-hydrazinopyridine **184** (1.29 g, 11.5 mmol) at 65 ºC with continued stirring for 16 h afforded 9-hydroxy-10-(pyridin-2-ylazo)phenanthrene-2,7-disulfonic acid disodium salt **187** as a light orange solid (6.95 g, >100%), mp > 330 ºC (Found: C, 29.2; H, 2.8; N, 5.2. $C_{19}H_{11}N_3Na_2O_7S_2.3NaCl.6H_2O$ requires C, 29.0; H, 3.0; N, 5.3%); δ_H ($[^2H]_6$DMSO) 8.65 (1H, d, ^4J 1.8, ArH), 8.54 – 8.50 (2H, m, ArH), 8.44 (1H, d, ^3J 8.6, ArH), 8.34 (1H, d, ^3J 8.6, ArH), 8.29 (1H, ddd, ^3J 8.7, ^3J 7.4, ^4J 1.7, ArH), 8.04 (1H, dd, ^3J 8.3, ^4J 2.0, ArH), 7.96 (1H, d, ^3J 8.5, ArH), 7.79 (1H, dd, ^3J 8.4, ^4J 1.8, ArH) and 7.42 (1H, td, ^3J 6.5, ^4J 1.0, ArH); δ_C ($[^2H]_6$DMSO) 180.47 (quat), 152.41 (quat), 148.35 (quat), 147.85 (quat), 144.16 (CH), 142.99 (CH), 135.66 (quat), 132.08 (CH), 131.82 (quat), 130.43 (quat), 129.47 (quat), 128.12 (quat), 126.27 (CH), 124.91 (CH), 124.21 (CH), 124.15 (CH), 120.90 (CH), 120.18 (CH), and 111.27 (CH); ***m/z*** (ESI): 460 MH^+ $C_{19}H_{14}N_3O_7S_2$ requires 460; *m/z* (ESI): 458.2 $[MH]^-$ $C_{19}H_{12}N_3O_7S_2$ requires 458.5; λ_{max} 466 nm (ε 24441 dm^{-3} mol^{-1} cm^{-1}), $W_{1/2}$ 86 nm.

The strength of the product was estimated to be 63% by CHN due to salt impurities, which gave an overall reaction yield of 77%.

9-Hydroxy-10-(phenylazo)phenanthrene-2,7-disulfonic acid disodium salt 186

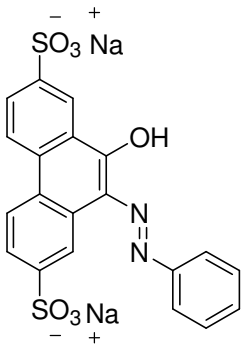

The above general method with 4,9-disulfophenanthroquinone **171** (1.025 g, 2.8 mmol), HCl (2 M, 29 cm^3) and phenylhydrazine **183** (0.303 g, 2.8 mmol) at 65 ºC with continued stirring for 3 h afforded 9-hydroxy-10-(phenylazo)phenanthrene-2,7-disulfonic acid disodium salt **186** as a dark red powder (0.748 g, 59%), mp > 330 ºC; δ_H ($[^2H]_6$DMSO) 8.70 (2H, dd, ^3J 4.6, ^4J 1.7, ArH), 8.57 (1H, d, ^3J 8.6, ArH), 8.47 (1H, d, ^3J 8.6, ArH), 8.08 (1H, dd, ^3J 8.3, ^4J 1.8, ArH), 7.81 – 7.72

(3H, m, ArH), 7.55 (2H, t, ^3J 7.7, ArH), and 7.27 (1H, t, ^3J 7.2, ArH); δ_C ([^{2}H]$_6$DMSO) 177.95 (quat), 147.89 (quat), 147.33 (quat), 142.15 (quat), 135.37 (quat), 131.41 (quat), 131.10 (CH), 129.99 (2 × CH), 129.12 (quat), 128.17 (quat), 126.61 (quat), 125.88 (CH), 124.53 (CH), 123.99 (CH), 123.38 (CH), 119.48 (CH), 116.61 (2 × CH) and 114.46 (CH); *m/z* (ESI): 457.3 $[MH]^-$ $C_{20}H_{13}N_2O_7S_2$ requires 457.5; λ_{max} 483 nm (ε 15200 dm^{-3} mol^{-1} cm^{-1}), $W_{1/2}$ 82 nm.

The strength of the product was estimated to be 89% by CHN due to salt and water impurities, which gave an overall reaction yield of 53%.

9-Hydroxy-10-(phthalazin-1-ylazo)phenanthrene-2,7-disulfonic acid disodium salt 189

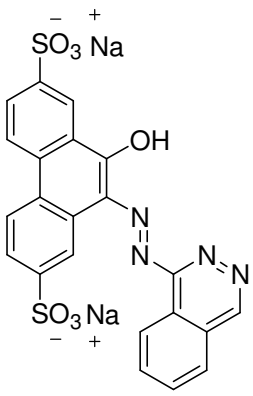

The general method with 4,9-disulfophenanthroquinone **171** (1.044 g, 84% strength, 2.4 mmol), HCl (2 M, 35 cm^3) and 1-hydrazinophthalazine hydrochloride **185** (0.473 g, 2.4 mmol) at 75 ºC with continued stirring for 2 h afforded 9-hydroxy-10-(phthalazin-1-ylazo)phenanthrene-2,7-disulfonic acid disodium salt **189** as a dark red solid (1.140 g, 86%), mp > 330 ºC; (Found: C, 44.7; H, 2.5; N, 9.8. $C_{22}H_{12}N_4Na_2O_7S_2.2H_2O$ requires C, 44.8; H, 2.7; N, 9.5%); δ_H (360 MHz, [^{2}H]$_6$DMSO) 8.86 – 8.97 (2H, m, ArH), 8.64 (1H, m, ArH), 8.51 (1H, d, ^3J 8.2, ArH), 8.43 (1H, d, ^3J 8.4, ArH), 8.04 – 8.29 (5H, m, ArH) and 7.81 (1H, dd, ^3J 8.4, ^4J 1.2, ArH); δ_C (90 MHz, [^{2}H]$_6$DMSO) 181.08 (quat), 151.32 (quat), 151.02 (quat), 148.51 (2 × quat), 147.91 (2 × quat), 135.68 (quat), 133.37 (2 × CH), 132.91 (quat), 131.82 (CH), 131.80 (CH), 127.98 (2 × quat), 127.24 (CH), 125.95 (CH), 124.85 (CH), 124.00 (3 × CH) and 123.91 (CH); *m/z* (ESI): 508.7 $[MH]^-$ $C_{22}H_{13}N_4O_7S_2$ requires 509.0; λ_{max} 463 nm (ε 14800 dm^{-3} mol^{-1} cm^{-1}), $W_{1/2}$ 151nm.

The strength of the product was estimated to be 90% by CHN due to water impurities, which gave an overall reaction yield of 78%.

9-Hydroxy-10-(isoquinolin-1-ylazo)phenanthrene-2,7-disulfonic acid disodium salt 190

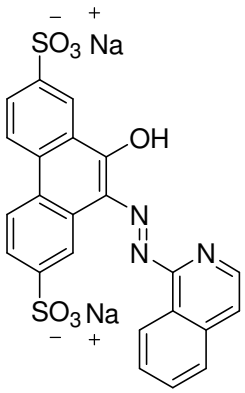

The above general method with 4,9-disulfophenanthroquinone **171** (5.040 g, 84% strength, 11.5 mmol), HCl (2 M, 160 cm^3) and 1-hydrazinoisoquinoline **180** (1.846 g, 11.6 mmol) at 75 ºC with continued stirring for 20 h afforded 9-hydroxy-10-(isoquinolin-1-ylazo)phenanthrene-2,7-disulfonic acid disodium salt **190** as a dark red solid (5.717 g, 89%), mp > 330 ºC; (Found: C, 45.4; H, 2.8; N, 6.6. $C_{23}H_{13}N_3Na_2O_7S_2.3H_2O$ requires C, 45.5; H, 3.1; N, 6.9%); δ_H ([^{2}H]$_6$DMSO) 8.82 (1H, s, ArH), 8.71 (1H, d, , ^4J 1.9, ArH), 8.53 – 8.60 (2H, m, ArH), 8.46 (1H, d, ^3J 3.3, ArH), 8.44 (1H, d, ^3J 3.3, ArH), 8.05 – 8.10 (2H, m, ArH), 7.86 – 7.90 (2H, m, ArH), 7.81 (1H, dd, ^3J 8.4, ^4J 1.7, ArH) and 7.70 (1H, d, ^3J 5.9, ArH); δ_C (90 MHz, [^{2}H]$_6$DMSO) 179.89 (quat), 161.55 (quat), 149.42 (quat), 148.47 (quat), 147.73 (quat), 146.87 (quat), 141.43 (CH), 137.52 (quat), 135.55 (quat), 135.27 (quat), 131.69 (CH), 131.49 (quat), 130.99 (CH), 128.52 (CH), 127.54 (CH), 127.25 (quat), 125.41 (CH), 124.87 (CH), 123.96 (CH), 123.77 (CH), 122.26 (CH), 120.56 (CH) and 118.09 (CH); *m/z* (ESI): 507.7 $[MH]^-$ $C_{23}H_{14}N_3O_7S_2$ requires 508.0; λ_{max} 485 nm (ε 18600 dm^{-3} mol^{-1} cm^{-1}), $W_{1/2}$ 109 nm.

The strength of the product was estimated to be 87% by CHN due to water impurities, which gave an overall reaction yield of 78%.

9-Hydroxy-10-(quinolin-2-ylazo)phenanthrene-2,7-disulfonic acid disodium salt 191

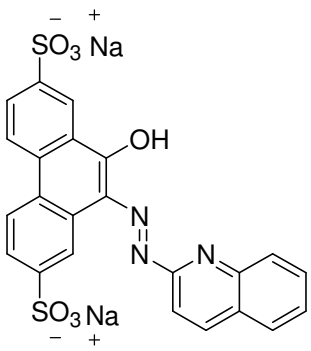

The above general method with 4,9-disulfophenanthroquinone **171** (5.035 g, 84% strength, 11.5 mmol), HCl (2 M, 160 cm^3) and 2-hydrazinoquinoline **182** (1.831 g, 11.5 mmol) at 75 ºC with continued stirring for 20 h afforded 9-hydroxy-10-(quinolin-2-ylazo)phenanthrene-2,7-disulfonic acid disodium salt **191** as a dark red solid (5.569 g, 88%), mp > 330 ºC; (Found: C, 48.6; H, 2.4; N,

7.2. $C_{23}H_{13}N_3Na_2O_7S_2.H_2O$ requires C, 48.3; H, 2.7; N, 7.4%); δ_H (360 MHz, $[^2H]_6$DMSO) 8.68 (1H, d, ^4J 1.6, ArH), 8.59 – 8.62 (2H, m, ArH), 8.50 (1H, d, ^3J 8.6, ArH), 8.41 (1H, d, ^3J 8.6, ArH), 7.93 – 8.08 (4H, m, ArH), 7.73 – 7.80 (2H, m, ArH) and 7.53 (1H, t, ^3J 7.2, ArH); δ_C (90 MHz, $[^2H]_6$DMSO) 179.88 (quat), 153.63 (quat), 148.40 (quat), 147.72 (quat), 146.50 (quat), 139.67 (CH), 135.48 (quat), 131.64 (CH), 130.68 (quat), 130.66 (CH), 129.64 (quat), 129.55 (quat), 128.11 (CH), 127.35 (quat), 127.27 (CH), 126.15 (quat), 125.52 (CH), 125.42 (CH), 124.75 (CH), 123.88 (CH), 123.82 (CH), 120.06 (CH) and 109.08 (CH); *m/z* (ESI): 253.5 $[M]^{2-}$ $C_{23}H_{13}N_3O_7S_2$ requires 253.5; λ_{max} 463 nm (ε 24200 dm^{-3} mol^{-1} cm^{-1}), $W_{1/2}$ 96 nm.

The strength of the product was estimated to be 96% by CHN due to water impurities, which gave an overall reaction yield of 84%.

6.4.3: Metallisation of Dyes

1:1 Ni Complexes

9-Hydroxy-10-(pyridazin-3-ylazo)phenanthrene-2,7-disulfonic acid disodium salt: 1:1 Ni Complex 198

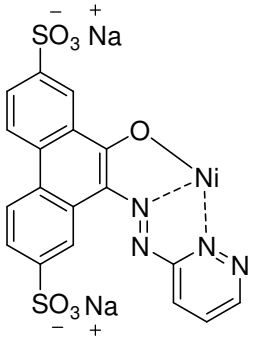

9-hydroxy-10-(pyridazin-3-ylazo)phenanthrene-2,7-disulfonic acid disodium salt **188** (2.009 g, 88% strength, 3.51 mmol) was stirred in water (100 cm^3) and the pH adjusted to pH 8 – 9 with the addition of NaOH solution (2 M) as required. Nickel acetate tetrahydrate solution (0.5 M, 7 cm^3, 3.5 mmol) was then added causing the reaction mixture to change from orange to a deep magenta colour. The pH of the reaction mixture was maintained at pH 8 – 9 and the reaction progress monitored by TLC and UV-vis spectroscopy. After 16 h the reaction appeared incomplete by UV-vis spectroscopy hence a further equivalent of nickel acetate solution 0.5 M (7 cm^3, 3.5 mmol) was added and the reaction mixture stirred for a further 16 h at 60 ºC. The reaction mixture was then cooled to room temperature and salt (10% w/v) added slowly with stirring until a magenta solid precipitated. The reaction mixture was filtered and the precipitate dried under suction to afford a magenta paste, which was dissolved in water (500

cm^3). The pH of the solution was then adjusted to pH 7 using NaOH (2 M) as required, filtered, dialysed and dried to afford the 9-hydroxy-10-(pyridazin-3-ylazo)phenanthrene-2,7-disulfonic acid disodium salt 1:1 complex **198** as a magenta solid (2.525 g, > 100%), mp > 330 ºC (Found: C, 26.8; H, 2.9; N, 6.7. $C_{18}H_9N_4NiNa_2O_7S_2.2NaCl.7H_2O$ requires C, 26.9; H, 2.9; N, 7.0%); λ_{max} 489 nm (ε = 12800 dm^{-3} mol^{-1} cm^{-1}), $W_{1/2}$ 97 nm.

The strength of the product was estimated to be 71% by CHN due to salt impurities, which gave an overall reaction yield of 90%.

However, over 24 hours in solution the 1:1 complex was found to equilibrate to a mixture of mainly the 2:1 complex and the 1:1 complex by UV-vis spectroscopy. Hence no further testing was carried out on this dye.

9-Hydroxy-10-(pyridin-2-ylazo)phenanthrene-2,7-disulfonic acid disodium salt: 1:1 Ni Complex 197

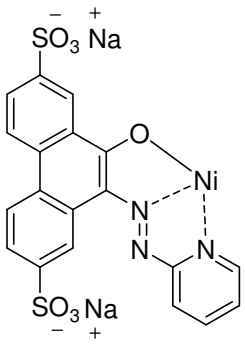

9-Hydroxy-10-(pyridin-2-ylazo)phenanthrene-2,7-disulfonic acid disodium salt **187** (3.002 g, 63% strength, 3.8 mmol) was stirred in water (100 cm^3) and the pH adjusted to pH 8 – 9 with the addition of NaOH solution (2 M) as required. Nickel acetate tetrahydrate solution (0.5M, 7.55 cm^3, 3.8 mmol) was then added causing the reaction mixture to change from orange to a deep magenta colour. The pH was maintained at pH 8 – 9 and the reaction progress monitored by TLC and UV-vis spectroscopy. After 0.5 h the reaction appeared incomplete by UV-vis spectroscopy. Hence, a further equivalent of nickel acetate solution (0.5 M, 7 cm^3, 3.5 mmol) was added and the reaction mixture stirred for a further 16 h at 60 ºC. The reaction mixture was then cooled to room temperature and salt (10% w/v) added slowly with stirring until a magenta solid precipitated. The reaction mixture was then filtered and the precipitate dried under suction to afford a magenta paste, which was dissolved in water (500 cm^3). The pH of the solution was then adjusted to pH 7 using NaOH (2 M) as required, filtered, dialysed and dried to afford the 9-hydroxy-10-(pyridin-2-ylazo)phenanthrene-2,7-disulfonic acid disodium salt 1:1 complex **197** (1.974 g, > 100%), mp > 330 ºC

(Found: C, 30.0; H, 2.9 N, 5.3. $C_{19}H_{10}N_3NiNa_2O_7S_2$ requires C, 40.7; H, 1.8; N, 7.5%); *m/z* (ESI): 515 $[MH]^-$ $C_{19}H_{11}N_3NiO_7S_2$ requires 515.

Analysis of the product by TLC and UV-vis spectroscopy and CHN indicated it consisted of mainly the 2:1 complex and trace amounts if the required 1:1 complex.

2:1 Ni Complexes

General Metallisation Method

The 9-hydroxy-10-(azo)phenanthrene-2,7-disulfonic acid disodium salt ligand (3.5 mmol) was stirred in water (100 cm^3) and the pH adjusted to pH 8 – 9 with the addition of NaOH solution (2 M) as required. Nickel acetate tetrahydrate solution (0.5 M, 3.5 cm^3, 1.9 mmol) was then added causing the reaction mixture to turn from an orange to a deep magenta colour. The pH was maintained at pH 8 – 9 and the reaction progress monitored by TLC and UV-vis spectroscopy. After 1 h the reaction appeared complete however was stirred at room temperature overnight to ensure completion. Salt (35% w/v) was then added slowly with stirring until a magenta solid precipitated. The reaction mixture was then filtered and the precipitate dried under suction to afford a magenta paste, which was dissolved in water (500 cm^3). The pH of the solution was then adjusted to pH 7 using NaOH (2 M) as required, filtered, dialysed and dried to afford the 9-hydroxy-10-(azo)phenanthrene-2,7-disulfonic acid disodium salt metallised 2:1 complexed dye as a magenta solid

9-Hydroxy-10-(pyridazin-3-ylazo)phenanthrene-2,7-disulfonic acid disodium salt: 2:1 Ni complex 193

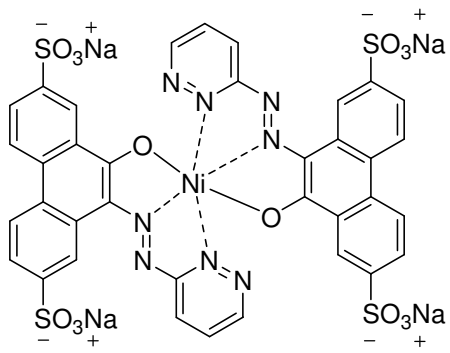

The general metallisation method was used with 9-hydroxy-10-(pyridazin-3-ylazo)phenanthrene-2,7-disulfonic acid disodium salt **188** (2.003 g, 87% strength, 3.5 mmol), water (100 cm^3) and nickel acetate tetrahydrate solution (0.5 M, 3.77 cm^3, 1.9 mmol) to afford 9-hydroxy-10-(pyridazin-3-ylazo)phenanthrene-2,7-disulfonic acid disodium salt metallised 2:1 complexed dye **193** as a magenta solid (2.105 g, >100%), mp > 330 ºC (Found: C, 31.2; H, 3.2; N, 7.8. $C_{36}H_{18}N_8NiNa_4O_{14}S_4.2NaCl.12H_2O$ requires C, 30.9; H, 3.0; N, 8.0%); λ_{max} 556 nm (ε 19800 dm^{-3} mol^{-1} cm^{-1}), $W_{1/2}$ 95 nm.

The strength of the product was estimated to be 77% by CHN due to salt and water impurities, which gave an overall reaction yield of 87%.

9-Hydroxy-10-(pyridin-2-ylazo)phenanthrene-2,7-disulfonic acid disodium salt: 2:1 Ni complex 192

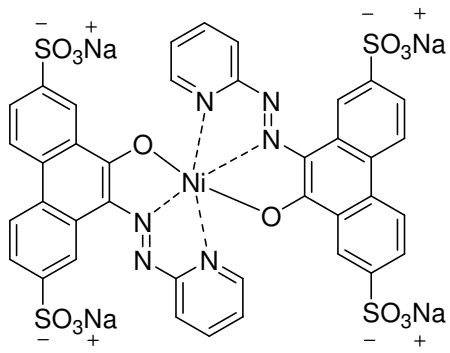

The general metallisation method was used with 9-hydroxy-10-(pyridin-2-ylazo)phenanthrene-2,7-disulfonic acid disodium salt **187** (3.005 g, 63% strength, 3.8 mmol), water (100 cm^3) and nickel acetate tetrahydrate solution (0.5 M, 3.77 cm^3, 1.9 mmol) to afford 9-hydroxy-10-(pyridin-2-ylazo)phenanthrene-2,7-disulfonic acid disodium salt 2:1 complex **192** as a magenta solid (1.993 g, 99%), mp > 330 ºC (Found: C, 29.2; H, 2.7; N, 5.3. $C_{38}H_{20}N_6NiNa_4O_{14}S_4.5NaCl.12H_2O$ requires C, 29.0; H, 2.8; N, 5.4%); *m/z* (ESI): 486 $[M2H]^{2-}$ $C_{38}H_{22}N_6Ni\ O_{14}S_4$ requires 486; λ_{max} 547 nm (ε 27500), $W_{1/2}$ 88 nm.

The strength of the product was estimated to be 68% by CHN due to salt impurities, which gave an overall reaction yield of 67%.

9-Hydroxy-10-(phthalazin-1-ylazo)phenanthrene-2,7-disulfonic acid disodium salt: 2:1 Ni Complex 194

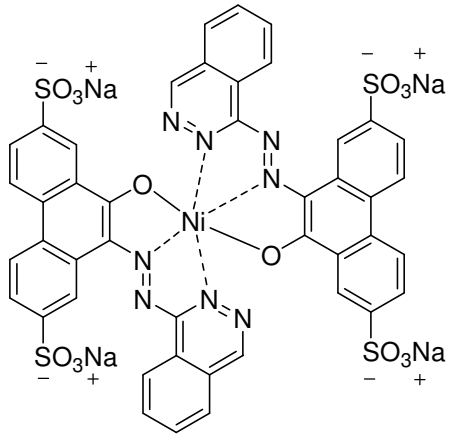

The general metallisation method was used with 9-hydroxy-10-(phthalazin-1-ylazo)phenanthrene-2,7-disulfonic acid disodium salt **189** (3.022 g, 90% strength, 4.9 mmol), water (150 cm^3) and nickel acetate tetrahydrate (0.619 g, 2.5 mmol) to afford 9-hydroxy-10-(phthalazin-1-ylazo)phenanthrene-2,7-disulfonic acid disodium salt 2:1 complexed dye **194** as a magenta solid (3.288 g, >100%), mp > 330 ºC (Found: C, 37.6; H, 1.8; N, 7.7. $C_{44}H_{22}N_8Na_4NiO_{14}S_4.3NaCl.3H_2O$ requires C, 37.9; H, 2.0; N, 8.0%); *m/z* (ESI): 365.1 $[MNa]^{3-}$ $C_{44}H_{22}N_8NaNiO_{14}S_4$ requires 365.0; λ_{max} 538 nm (ε 12800 dm^{-3} mol^{-1} cm^{-1}) $W_{1/2}$ 117 nm.

The strength of the product was estimated to be 77% by CHN due to salt and water impurities, which gave an overall reaction yield of 87%.

9-Hydroxy-10-(isoquinolin-1-ylazo)phenanthrene-2,7-disulfonic acid disodium salt: 2:1 Complex 195

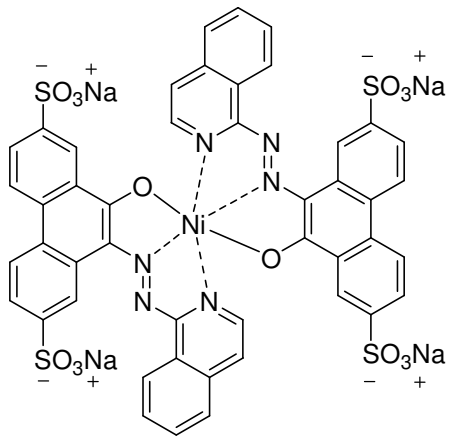

The general metallisation method was used with 9-hydroxy-10-(isoquinolin-1-ylazo)phenanthrene-2,7-disulfonic acid disodium salt **190** (3.006 g, 87% strength, 4.7 mmol), water (150 cm^3) and nickel acetate tetrahydrate (0.588 g, 2.4 mmol) to afford 9-hydroxy-10-(isoquinolin-1-ylazo)phenanthrene-2,7-disulfonic acid disodium salt 2:1 complexed dye **195** as a magenta solid (2.830 g, >100%), mp > 330 ºC (Found: C, 36.5; H, 1.9; N, 5.2. $C_{46}H_{24}N_6Na_4NiO_{14}S_4.5NaCl.4H_2O$ requires C, 36.2; H, 2.1; N, 5.5%); *m/z* (ESI): 558.1 $[M2Na]^{2-}$ $C_{46}H_{24}N_6Na_2NiO_{14}S_4$ requires 558.0; λ_{max} 548 nm (ε 27600 dm^{-3} mol^{-1} cm^{-1}); $W_{1/2}$ 103 nm.

The strength of the product was estimated to be 77% by CHN due to salt and water impurities, which gave an overall reaction yield of 87%.

9-Hydroxy-10-(quinolin-2-ylazo)phenanthrene-2,7-disulfonic acid disodium salt: 2:1 Complex 196

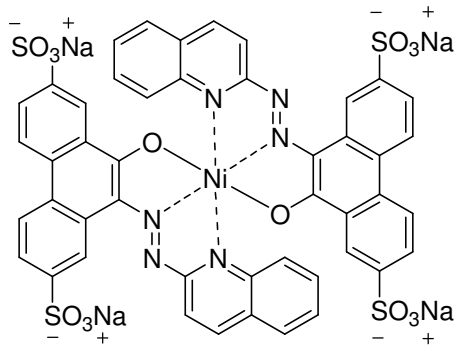

The above general metallisation method was used with 9-hydroxy-10-(quinolin-2-ylazo)phenanthrene-2,7-disulfonic acid disodium salt **191** (3.002 g, 96% strength, 5.2 mmol), water (150 cm^3) and nickel acetate tetrahydrate (0.648 g, 2.6 mmol) to afford 9-hydroxy-10-(quinolin-2-ylazo)phenanthrene-2,7-disulfonic acid disodium salt 2:1 complexed dye **196** as a magenta solid (2.633 g, 87%), mp > 330 ºC (Found: C, 41.3; H, 2.6; N, 6.4. $C_{46}H_{24}N_6Na_4NiO_{14}S_4.NaCl.6H_2O$ requires C, 41.5; H, 2.7; N, 6.3%); *m/z* (ESI): 558.3 $[M2Na]^{2-}$ $C_{46}H_{24}N_6Na_2NiO_{14}S_4$ requires 558.0; λ_{max} 573 nm (ε 31200 dm^{-3} mol^{-1} cm^{-1}), $W_{1/2}$ 89 nm.

The strength of the product was estimated to be 77% by CHN due to salt and water impurities, which gave an overall reaction yield of 87%.

6.5: Novel Routes to Heterocyclic Azo Compounds

6.5.1: Azo Compounds by Reaction of Nitroaryl Compounds with Amines

General Method: Reaction of a Nitro Compound with an Amine in Presence of Na Metal

To a solution of the arylnitro compound **229** (50 mmol) and 2-aminopyridine **207** (50 mmol) in HPLC grade toluene (75 cm^3) was added clean sodium (100 mmol) with vigorous stirring under N_2. The mixture was carefully warmed until reaction occurred and the heat then removed until activity had subsided. The reaction mixture was then heated under reflux for 3 h with continued stirring. The resulting mixture was then filtered hot and extracted with HCl (17%, 2 × 15 cm^3). The acid solution was then diluted to 150 cm^3 with ice water and filtered. The solution was then made basic with cold NaOH (20%) and the basic solution extracted with hexane (4 × 50 cm^3). The combined extracts were washed with water (3 × 25 cm^3) and dried (Na_2SO_4). The solvent was then removed under reduced pressure to afford the product.

2-(Phenylazo)pyridine 230a

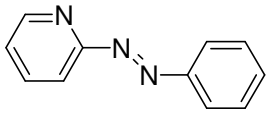

The above general method was used with nitrobenzene **229a** (6.252 g, 50.79 mmol), 2-aminopyridine **207** (4.702 g, 49.96 mmol), HPLC grade toluene (75 cm^3) and clean sodium (2.326 g, 101.11 mmol) to afford 2-(phenylazo)pyridine **230a** as a dark red liquid (5.692 g, 62%), bp 136 – 140 ºC (0.24 Torr) [lit.,[74] mp 33 – 34 ºC]; (Found: M^+ 183.0792. $C_{11}H_9N_3$ requires *M* 183.0797); υ_{max} 1421 (N=N) cm^{-1}; δ_H ($CDCl_3$) 8.60 (1H, d, ^3J 3.7, ArH), 7.90 – 7.97 (2H, m, ArH), 7.66 – 7.78 (2H, m, ArH), 7.36 - 7.43 (3H, m, ArH) and 7.24 (1H, m, ArH); δ_C ($CDCl_3$) 162.46 (quat), 152.01 (quat), 149.16 (CH), 137.99 (CH), 131.82 (CH), 128.80 (2 × CH), 124.91 (CH), 123.20 (2 × CH) and 114.69 (CH); *m/z* 183 (M^+, 1%), 155 (94), 154 (77), 105 (60), 78 (91), 77 (100), 52 (51) and 51 (88).

2-(4-Chlorophenylazo)pyridine 230b

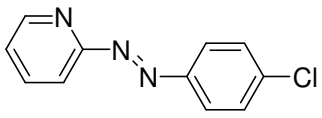

The general method was used with *p*-chloronitrobenzene **229b** (3.175 g, 20.15 mmol), 2-aminopyridine **207** (1.903 g, 20.22 mmol), HPLC grade toluene (30 cm^3) and clean sodium (0.963 g, 41.85 mmol) to give a red solid which was purified by dry flash column chromatography (3:1, EtOAc : Hexane) to afford 2-(4-chlorophenylazo)pyridine **230b** as a orange solid (0.380 g, 9%), mp 116 – 120 ºC [lit.,[74] 115 - 118 ºC]; δ_H ($CDCl_3$) 8.73 (1H, d, ^3J 4.7, ArH), 7.99 (2H, d, ^3J 8.7, ArH), 7.80 – 7.9. (2H, m, ArH), 7.50 (2H, d, ^3J 8.7, ArH) and 7.40 (1H, ddd, ^3J 7.0, ^3J 4.7, ^4J 1.1, ArH); δ_C ($CDCl_3$) 162.54 (quat), 150.65 (quat), 149.55 (CH), 138.34 (CH), 138.17 (quat), 129.40 (2 × CH), 125.40 (CH), 124.75 (2 × CH) and 115.83 (CH); *m/z* 220 (M^+, 13%), 218 (M^+, 38%), 191 (79), 189 (96), 155 (82), 154 (83), 113 (84) and 111 (100).

Reaction of 2-nitroanisole 229c and 2-aminopyridine 207

The general method was used with 2-nitroanisole **229c** (0.428 g, 2.80 mmol), 2-aminopyridine **207** (0.270 g, 2.87 mmol), HPLC grade toluene (5 cm^3) and clean sodium (0.139 g, 6.03 mmol) to give a dark red oily solid (0.083 g) which was purified by dry flash column chromatography (Et_2O). The following products were isolated and identified.

a) 2-[2-(2-Pyridylamino)phenylazo]pyridine 230d

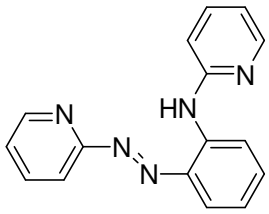

2-[2-(2-Pyridylamino)phenylazo]pyridine **230d** was isolated as a red solid (0.051 g, 13%), mp 87 – 90 ºC [lit.,[128] 90 ºC]; ν_{max} (CH_2Cl_2) 2445 (NH) and 1423 (N=N) cm^{-1}; (Found: M^+ 275.1172. $C_{16}H_{13}N_5$ requires *M* 275.1171); δ_H (360 MHz, $CDCl_3$) 10.62 (1H, brs, NH), 8.73 (1H, ddd, ^3J 4.8, ^4J 1.8, ^5J 0.8, ArH), 8.65 (1H, dd, ^3J 8.6, ^4J 1.2, ArH), 8.34 (1H, ddd, ^3J 5.0, ^4J 1.8, ^5J 0.8, ArH), 8.01 (1H, dd, ^3J 8.1, ^4J 1.6, ArH), 7.90 (1H, ddd, ^3J 9.2, ^3J 7.3, ^4J 1.9, ArH), 7.79 (1H, dt, ^3J 8.0, ^4J 2.0, ^5J 1.0, ArH), 7.59 (1H, ddd, ^3J 9.2, ^3J 7.3, ^4J 2.0, ArH), 7.47 (1H, ddd, ^3J 8.6, ^3J 7.1, ^4J 1.6, ArH), 7.39 (1H, ddd, ^3J 7.3, ^3J 4.8, ^4J 1.2, ArH), 6.98 – 7.06 (2H, m, ArH) and 6.86 (1H, ddd, ^3J 7.2, ^3J 4.98, ^4J 0.9, ArH); δ_C (90

MHz, $CDCl_3$) 162.85 (quat), 154.42 (quat), 149.35 (CH), 147.84 (CH), 138.33 (quat), 138.19 (CH), 137.98 (quat), 137.45 (CH), 133.84 (CH), 126.74 (CH), 124.62 (CH), 120.06 (CH), 118.00 (CH), 116.43 (CH), 114.12 (CH) and 112.84 (CH); *m/z* 275 (M^+, 12%), 246 (28), 185 (47), 184 (30), 170 (37), 169 (100), 168 (47) and 149 (47).

b) 2-(2-Methoxyphenylazo)pyridine 230c

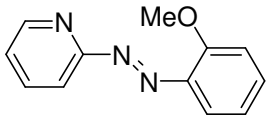

2-(2-Methoxyphenylazo)pyridine **230c** was isolated as a dark brown solid (0.005 g, 1%), (Found: M^+ 213.0904. $C_{12}H_{11}N_3O$ requires *M* 213.0902); δ_H (360 MHz, $CDCl_3$) 8.71 (1H, ddd, ^3J 4.8, ^4J 2.7, ^5J 0.8, ArH), 7.79 – 7.89 (3H, m, ArH), 7.49 (1H, ddd, ^3J 9.0, ^3J 7.3, ^4J 1.7, ArH), 7.37 (1H, ddd, ^3J 7.3, ^3J 4.8, ^4J 1.2, ArH), 7.11 (1H, dd, ^3J 8.4, ^4J 1.1, ArH), 7.02 (1H, ddd, ^3J 8.4, ^3J 7.3, ^4J 1.2, ArH) and 4.03 (3H, s, CH_3); δ_C (90 MHz, $CDCl_3$) 161.41 (quat), 157.77 (quat), 149.37 (CH), 138.13 (CH), 135.60 (quat) 133.81 (CH), 124.80 (CH), 120.58 (CH), 117.01 (CH), 114.80 (CH), 112.60 (CH) and 56.13 (CH_3); *m/z* 213 (M^+, 1%), 185 (21), 184 (75), 183 (20), 169 (82), 168 (100), 155 (28) and 92 (58).

c) 1-Methoxyphenazine 241

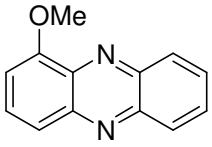

1-Methoxyphenazine **241** was also isolated as a orange solid (0.002 g, < 1%), δ_H (360 MHz, acetone d_6) 8.28 (1H, m, ArH), 8.22 (1H, m, ArH), 7.90 – 7.97 (2H, m, ArH), 7.85 (1H, m, ArH), 7.79 (1H, dd, ^3J 8.9, ^4J 1.3, ArH), 7.25 (1H, dd, ^3J 7.3, ^4J 1.0, ArH) and 4.13 (3H, s, CH_3); δ_C (90 MHz, $CDCl_3$) 183.10 (quat), 161.42 (quat), 135.61 (quat), 130.75 (CH), 130.44 (CH), 130.14 (CH), 130.08 (CH), 129.25 (CH), 127.00 (quat), 121.38 (CH), 106.36 (CH), 101.20 (quat) and 56.41 (CH_3); *m/z* 210 (M^+, 70%), 181 (100), 180 (43), 179 (27), 167 (16), 149 (20), 41 (16) and 39 (20).

The above ^1H NMR spectrum agrees with the literature.[131]

2-[2-(2-Pyridylamino)phenylazo]pyridine 230d (Alternative preparation)

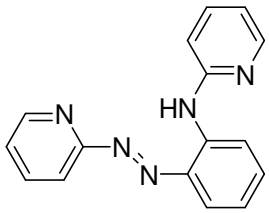

The earlier general method was used with (2-nitrophenyl)pyridin-2-ylamine **229d** (0.314 g, 1.46 mmol), 2-aminopyridine **207** (0.1405 g, 1.49 mmol), HPLC grade toluene (5 cm^3) and clean sodium (0.088 g, 3.80 mmol) to give a dark orange solid which was purified by dry flash column chromatography (Et_2O) to afford the following products.

a) 2-[2-(pyridylamino)phenylazo]pyridine **230d** was obtained as a red solid (0.011 g, 3%). The ^1H and ^{13}C NMR spectra agreed with earlier analytical data.

b) *N*-Pyridin-2-ylbenzene-1,2-diamine 242

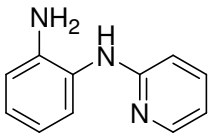

N-Pyridin-2-ylbenzene-1,2-diamine **242** was also recovered from the column as a dark brown oily solid (0.016 g, 6%), mp 131 - 135 ºC [lit.,[129] 134 - 137 ºC]; δ_H (360 MHz, $CDCl_3$) 8.14 (1H, dd, ^3J 5.1, ^4J 1.0, ArH), 7.43 (1H, ddd, ^3J 9.1, ^3J 7.2, ^4J 1.9, ArH), 7.18 (1H, dd, ^3J 7.8, ^4J 1.4, ArH), 7.08 (1H, ddd, ^3J 8.0, ^3J 7.4, ^4J 1.5, ArH), 6.82 (1H, dd, ^3J 8.0, ^4J 1.3, ArH), 6.77 (1H, ddd, ^3J 15.1, ^3J 7.7, ^4J 1.4, ArH), 6.68 (1H, ddd, ^3J 7.2, ^3J 5.0, ^4J 0.9, ArH), 6.42 (1H, d, ^3J 8.4, ArH) and 3.59 (2H, brs, NH_2); δ_C (90 MHz, $CDCl_3$) 157.63 (quat), 148.06 (CH), 143.01 (quat), 137.95 (CH), 127.19 (CH), 127.02 (CH), 125.68 (quat), 118.93 (CH), 116.20 (CH), 114.34 (CH) and 107.28 (CH); *m/z* 185 (M^+, 83%), 184 (59), 170 (48), 169 (100), 80 (25), 78 (40), 65 (20) and 52 (22).

Reaction of (2-nitrophenyl)phenylamine 229e with 2-aminopyridine 207

The earlier general method was used with (2-nitrophenyl)phenylamine **229e** (1.002 g, 4.68 mmol), 2-aminopyridine **207** (0.442 g, 4.69 mmol), HPLC grade toluene (15 cm^3) and clean sodium (0.228 g, 9.91 mmol) to afford a dark brown oil which was purified by dry flash column chromatography (EtOAc) to give none of the desired 2-[2-(phenylamino)phenyl]azopyridine product. Instead two by-products were also recovered from this reaction:

a) Phenazine 245

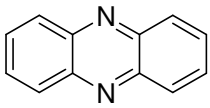

The main product recovered from this reaction was phenazine **245** as an off white crystalline solid (0.105 g,13%), mp 173 – 175 ºC [lit.,[130] 176 – 177 ºC]; δ_H ($CDCl_3$) 8.17 (4H, dd, ^3J 6.8, ^4J 3.4, ArH) and 7.75 (4H, dd, ^3J 6.8, ^4J 3.4, ArH); δ_C ($CDCl_3$) 143.16 (4 × quat), 130.17 (4 × CH) and 129.36 (4 × CH).

b) *N*-Phenylbenzimidazole 248

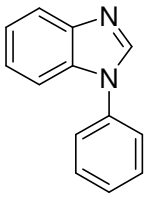

A by-product also recovered as a red solid was identified as *N*-phenylbenzimidazole **248** (0.008 g, 1%), δ_H (360 MHz, Acetone d_6) 8.36 (1H, brs, CH), 7.77 (1H, m, ArH), 7.66 – 7.71 (3H, m, ArH), 7.61 – 7.64 (2H, m, ArH) 7.53 (1H, m, ArH) and 7.31 – 7.34 (2H, m, ArH); δ_C (90 MHz, $CDCl_3$) 143.92 (quat), 142.20 (CH), 136.24 (quat), 133.61 (quat), 129.94 (2 × CH), 127.93 (CH), 123.95 (2 × CH), 123.59 (CH), 122.69 (CH), 120.48 (CH) and 110.35 (CH); *m/z* 194 (M^+, 100%), 193 (36), 168 (10), 167 (15), 166 (17), 77 (26), 66 (14) and 51 (19).

The above ^1H and ^{13}C NMR sepectrum agrees with the literature.[132]

6.5.2: Azo Compounds by Reaction of Nitroaryl Compounds with Amines (alternative conditions)

2-Methoxy-4-(diethylamino)nitrobenzene 229h

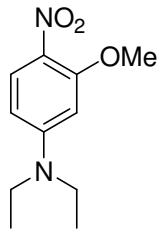

6-Nitro-3-(diethylamino)phenol **249h** (10.001 g, 47.57 mmol) was dissolved in NaOH (20%, 50 cm^3) by stirring at reflux for 30 min. The reaction mixture was then cooled to 60 ºC and dimethyl sulfate (24 cm^3, 140.00 mmol) added dropwise over 30 min, heated to 75 ºC and the pH of the reaction mixture maintained at pH 12 – 14 with the addition of NaOH (20%) as required. The reaction progress was monitored by TLC over 4 h. A further portion of dimethyl sulfate (48 cm^3, 280.00 mmol) was then added, the pH maintained with NaOH (20%) as required and the reaction mixture stirred at 95 ºC for a further 16 h. The reaction mixture was then cooled to room temperature and the brown precipitate filtered (7.790 g). The filtrates were extracted

with ether (3 × 150 cm^3), dried ($MgSO_4$) and the solvent removed to afford a yellow crystalline solid (2.202 g). The initial brown precipitate and the yellow crystalline solid were then combined and recrystallised from hexane to afford 2-methoxy-4-(diethylamino)nitrobenzene **229h** as a yellow solid (9.114 g, 85%), mp 76 - 78 ºC (Found: C, 58.6; H, 7.1; N, 12.4. $C_{11}H_{16}N_2O_3$ requires C, 58.9; H, 7.2; N, 12.5%); δ_H ($CDCl_3$) 7.98 (1H, d, ^3J 9.5, ArH), 6.18 (1H, dd, ^3J 9.5, ^4J 2.6, ArH), 6.04 (1H, d, ^4J 2.5, ArH), 3.91 (3H, s, CH_3), 3.42 (4H, q, ^3J 7.0, 2 × CH_2) and 1.21 (6H, t, ^3J 7.0, CH_2); δ_C ($CDCl_3$) 156.92 (quat), 153.01 (quat), 129.28 (CH), 127.13 (quat), 103.14 (CH), 93.66 (CH), 55.95 (CH_3), 44.84 (2 × CH_2) and 12.32 (2 × CH_3); *m/z* (ESI): 225 $[MH]^+$.

2-Methoxy-4-(1-piperidino)nitrobenzene 229i

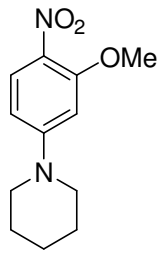

2-Nitro-5-(1-piperidino)phenol **249i** (4.967 g, 22.35 mmol) was dissolved in NaOH (20%, 100 cm^3) by stirring at reflux for 30 min. The reaction mixture was then cooled to 80 ºC and dimethyl sulfate (26 cm^3, 270.00 mmol) added dropwise over 30 min, heated to 95 ºC with stirring and the pH maintained at pH 12 – 14 with the addition of NaOH (20%) as required. The reaction progress was monitored by TLC over 4 h. A further portion of dimethyl sulfate (13 cm^3, 135.00 mmol) was then added and the reaction mixture stirred at 95 ºC for a further 16 h. The reaction mixture was then cooled to room temperature and the crude methylated product recovered by filtration as an orange precipitate (3.004 g). The filtrates were the extracted with DCM (3 × 200 cm^3), the combined extracts washed with water (1 × 100 cm^3) and dried ($MgSO_4$). The solvent was then removed to afford an orange oil which was purified by dry flash column chromatography (1:3, EtOAc : Hexane) to afford the crude methylated product (0.780 g). This product was then combined with the previously recovered orange precipitate (3.004 g) and recrystallised from hexane to afford 2-methoxy-4-(1-piperidino)nitrobenzene **229i** as dark yellow crystals (3.065 g, 58%), mp 85 - 88 ºC (Found: C, 60.9; H, 6.9; N, 11.7. $C_{12}H_{16}N_2O_3$ requires C, 61.0; H, 6.8; N, 11.9%); δ_H ($CDCl_3$) 7.93 (1H, d, ^3J 9.4, ArH), 6.34 (1H, dd, ^3J 9.5, ^4J 2.6, ArH), 6.24 (1H, d, ^4J 2.5, ArH), 3.90 (3H, s, CH_3), 3.37 (4H, s, 2 × CH_2) and 1.64 (6H, s, 3 × CH_2); δ_C ($CDCl_3$) 156.50 (quat), 155.58 (quat), 128.80 (CH), 128.16

(quat), 105.15 (CH), 96.24 (CH), 55.97 (CH_3), 48.22 (2 × CH_2), 25.14 (2 × CH_2) and 24.01 (CH_2); *m/z* (ESI): 237 $[MH]^+$.

The phenol starting material **249i** (0.370 g, 7%) was also recovered from the DCM extract by dry flash column chromatography.

4-Nitro-3-isopropoxy-*N,N*-diethylaniline 229j

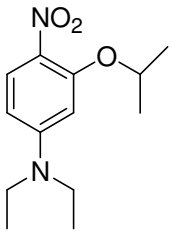

6-Nitro-3-(diethylamino)phenol **249h** (3.018 g, 14.35 mmol), K_2CO_3 (3.030 g, 21.92 mmol) and 2-bromopropane (4.511 g, 36.68 mmol) were stirred in dry *N,N*-dimethylformamide (50 cm^3) under N_2 for 23 h. By TLC the reaction still appeared incomplete hence a further equivalent of 2-bromopropane (4.511 g, 36.68 mmol) was added and the reaction mixture stirred for a further 4 h at 60 ºC under N_2. The reaction mixture was diluted with water (200 cm^3) and extracted with DCM (4 × 100 cm^3). The combined extracts were then washed with water (2 × 200 cm^3), dried ($MgSO_4$) and the solvent removed to afford 4-nitro-3-isopropoxy-*N,N*-diethylaniline **229j** as a dark yellow oil (3.537 g, 98%), bp 115 - 118 ºC (1.0 Torr); (Found: M^+ 252.1469. $C_{13}H_{20}N_2O_3$ requires *M* 252.1468); δ_H ($CDCl_3$) 7.91 (1H, d, ^3J 9.4, ArH), 6.16 (1H, dd, ^3J 9.5, ^4J 2.6, ArH), 6.05 (1H, d, ^3J 2.6, ArH), 4.56 (1H, sept, ^3J 6.1, CH), 3.36 (4H, q, ^3J 7.1, 2 × CH_2), 1.36 (6H, d, ^3J 6.0, 2 × CH_3) and 1.17 (6H, t, ^3J 7.1, 2 × CH_3); δ_C ($CDCl_3$) 155.04 (quat), 152.54 (quat), 128.93 (CH), 128.52 (quat), 103.45 (CH), 97.57 (CH), 72.41 (CH), 44.72 (2 × CH_2), 21.80 (2 × CH_3) and 12.33 (2 × CH_3); *m/z* 252 (M^+, 28%), 237 (12), 210 (5), 205 (9), 195 (100), 167 (7), 149 (6), and 69 (8).

General Method: Reaction of a Nitro Compound with an Amine in Presence of NaH

To a solution of the nitroaryl compound **229** (50 mmol) and 2-aminopyridine **207** (50 mmol) in HPLC grade toluene (75 cm^3) was added clean sodium hydride (100 mmol) with vigorous stirring under N_2. The mixture was carefully warmed until reaction occurred and the heat then removed until activity had subsided. The reaction mixture was then heated under reflux for 3 h with continued stirring. The resulting mixture was then filtered hot and the celite washed with toluene (500 cm^3). The organic layer

was then extracted with HCl (17%, 2 × 15 cm^3). The acid solution was then diluted to 150 cm^3 with ice water and filtered. The solution was then made basic with cold NaOH (20 %) and the basic solution extracted with hexane (4 × 200 cm^3). The combined extracts were washed with water (3 × 100 cm^3) and dried ($MgSO_4$). The solvent was removed under reduced pressure to afford the product **230**.

2-(Phenylazo)pyridine 230a

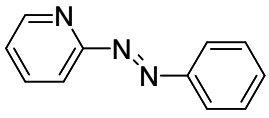

The general method was used with nitrobenzene **229a** (6.191 g, 50.29 mmol), 2-aminopyridine **207** (4.745 g, 50.40 mmol), HPLC grade toluene (75 cm^3) and clean sodium hydride (2.467 g, 102.79 mmol) to give 2-(phenylazo)pyridine **230a** as a dark red / orange liquid (3.733 g, 40%), spectra as earlier.

2-(2-Methoxyphenylazo)pyridine 230c

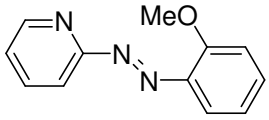

The general method was used with 2-nitroanisole **229c** (5.002 g, 32.66 mmol), 2-aminopyridine **207** (3.074 g, 32.66 mmol), HPLC grade toluene (50 cm^3) and clean sodium hydride (1.573 g, 65.54 mmol) with to give a reaction mixture which was then filtered hot and the celite washed several times with toluene. The organic layer was then extracted with HCl (17%, 5 × 100 cm^3). The solution was then filtered, made basic with cold NaOH (20 %) and the basic solution extracted by a continuous extraction method with DCM (5 × 100 cm^3). The combined extracts were then washed with water (3 × 50 cm^3) and dried ($MgSO_4$). The solvent was then removed under reduced pressure to give a dark red oily solid which was purified by dry flash column chromatography (Et_2O). The following products were isolated and identified.

a) 2-(2-Methoxyphenylazo)pyridine 230c

2-(2-Methoxyphenylazo)pyridine **230c** was isolated as a dark red solid (1.952 g, 28%), mp 83 – 86 ºC; *m/z* (ESI): 214.0 MH^+; ^1H NMR spectrum as earlier.

b) (2-Nitrophenyl)pyridin-2-yl amine 240c

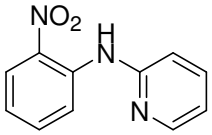

(2-Nitrophenyl)pyridin-2-yl amine **240c** was isolated as a red solid (1.229 g, 18%), mp 64 – 68 ºC [lit.,[133] 67 - 68 ºC]; δ_H ($CDCl_3$) 10.14 (1H, br s, NH), 8.74 (1H, dd, ^3J 8.7, ^4J 1.2, ArH), 8.34 (1H, dd, ^3J 5.6, ^4J 1.9, ArH), 8.21 (1H, dd, ^3J 8.5, ^4J 1.6, ArH), 7.62 (1H, ddd, ^3J 8.2, ^3J 7.4, ^4J 2.0, ArH), 7.55 (1H, ddd, ^3J 8.6, ^3J 7.0, ^4J 1.6, ArH) and 6.90 – 6.97 (3H, m, ArH); δ_C ($CDCl_3$) 153.51 (quat), 147.85 (CH), 138.87 (quat), 137.98 (CH), 135.61 (CH), 134.70 (quat), 126.14 (CH), 119.61 (CH), 119.58 (CH), 117.78 (CH) and 113.73 (CH).

1-Nitro-2-(pyridin-2-ylamino)naphthalene 240k

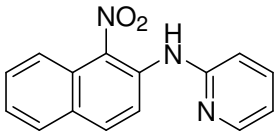

The general method was used with 1-nitronaphthalene **229k** (1.740 g, 10.00 mmol), 2-aminopyridine **207** (0.948 g, 10.07 mmol), HPLC grade toluene (15 cm^3) and clean sodium hydride (0.482 g, 20.06 mmol) to give a dark yellow residue which was purified by dry flash column chromatography (25% - 50%, Et_2O : Hexane) to afford 1-nitro-2-(pyridin-2-ylamino)naphthalene **240k** as light yellow crystals (0.335 g, 13%), mp 172 – 175 ºC (from acetone); δ_H (360 MHz, $CDCl_3$) 9.18 (1H, br s, NH), 8.22 – 8.34 (3H, m, ArH), 7.89 (1H, d, ^3J 9.3, ArH), 7.78 (1H, d, ^3J 8.5, ArH), 7.57 – 7.67 (2H, m, ArH), 7.44 (1H, ddd, ^3J 8.0, ^3J 6.9, ^4J 1.0, ArH) and 6.94 – 6.99 (2H, m, ArH); δ_C (90 MHz, $CDCl_3$) 153.38 (quat), 148.21 (CH), 138.20 (CH), 136.18 (quat), 134.06 (CH), 133.42 (quat), 129.36 (CH), 128.85 (quat), 128.21 (CH), 126.80 (quat), 125.23 (CH), 122.25 (CH), 119.35 (CH), 119.06 (CH), and 113.00 (CH); *m/z* 265 (M^+, 6%), 220 (27), 219 (100), 218 (33), 146 (10), 140 (14), 127 (11) and 115 (11).

None of the required azo product **230k** was obtained.

a) 8-Nitro-7-(pyridin-2-ylamino)quinoline 240l

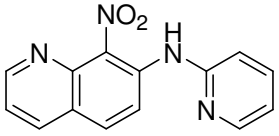

The general method was used with 8-nitroquinoline **229l** (1.761 g, 10.11 mmol), 2-aminopyridine **207** (0.951 g, 10.11 mmol), HPLC grade toluene (15 cm^3) and clean sodium hydride (0.488 g, 20.34 mmol) give a dark yellow residue which was purified by dry

flash column chromatography (25% - 50%, Et_2O : Hexane) to afford 8-nitro-7-(pyridin-2-ylamino)quinoline **240l** as an orange solid (0.036 g, 1%), mp 155 – 159 ºC; δ_H ($CDCl_3$) 8.94 (1H, dd, ^3J 4.4, ^4J 1.7, ArH), 8.45 (1H, d, ^3J 9.3, ArH), 8.31 (1H, dd, ^4J 1.9, ^4J 0.8, ArH), 8.10 (1H, dd, ^3J 8.2, ^4J 1.7, ArH), 7.84 (1H, d, ^3J 9.3, ArH), 7.65 (1H, ddd, ^3J 8.3, ^3J 7.4, ^4J 1.9, ArH), 7.37 (1H, dd, ^3J 8.2, ^3J 4.3, ArH) and 6.90 - 7.00 (2H, m, ArH); δ_C ($CDCl_3$) 153.17 (quat), 152.17 (CH), 148.10 (CH), 141.66 (quat), 138.31 (CH), 136.05 (quat), 135.60 (CH), 131.24 (CH), 123.49 (2 × quat), 120.58 (CH), 120.42 (CH), 118.08 (CH) and 112.55 (CH); *m*/*z* (ESI): 266.8 $[MH]^+$.

b) 8-Nitro-5-(pyridin-2-ylamino)quinoline 251l

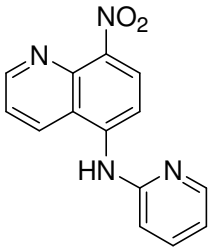

8-Nitro-5-(pyridin-2-ylamino)quinoline **251l** was also recovered as an orange solid (0.022 g, 1%), mp 168 – 175 ºC; δ_H (360 MHz, $CDCl_3$) 9.06 (1H, dd, ^3J 4.2, ^4J 1.5, ArH), 8.44 (1H, dd, ^3J 8.7, ^4J 1.5, ArH), 8.26 (1H, m, ArH), 8.14 (1H, d, ^3J 8.5, ArH), 7.87 (1H, d, ^3J 8.5, ArH), 7.62 (1H, ddd, ^3J 8.4, ^3J 7.4, ^4J 1.9, ArH), 7.50 (1H, dd, ^3J 8.7, ^3J 4.2, ArH), 7.05 (1H, dd, ^3J 8.3, ^4J 0.6, ArH) and 6.92 (1H, dd, ^3J 7.3, ^3J 5.0, ArH); δ_C (90 MHz, $CDCl_3$) 154.64 (quat), 152.52 (CH), 148.53 (CH), 142.32 (quat), 141.22 (2 × quat), 141.09 (quat), 138.34 (CH), 130.23 (CH), 126.37 (CH), 121.75 (CH), 117.42 (CH), 113.06 (CH) and 110.67 (CH); *m*/*z* (ESI): 266.8 $[MH]^+$.

None of the required azo product **230l** was obtained.

Reaction of 2-nitrophenol 229f and 2-aminopyridine 207

The general method was used with 2-nitrophenol **229f** (4.180 g, 30.05 mmol), 2-aminopyridine **207** (2.820 g, 29.96 mmol), HPLC grade toluene (45 cm^3) and clean sodium hydride (1.485 g, 61.70 mmol) afford a dark brown solid identified as impure 2-aminopyridine **207** (1.425 g, 51%).

Removal of the solvent from the remaining toluene layer also afforded 2-nitrophenol **229f** (3.410 g, 81%).

None of the azo product **230f** was recovered from the reaction mixture.

Reaction of 1,3-dimethoxy-4-nitrobenzene 229g and 2-aminopyridine 207

The general method was used with 1,3-dimethoxy-4-nitrobenzene **229g** (4.526 g, 24.70 mmol), 2-aminopyridine **207** (2.325 g, 24.70 mmol), HPLC grade toluene (45 cm^3) and clean sodium hydride (1.200 g, 50.00 mmol) to afford a dark brown oily solid (2.001 g) which was purified by dry flash column chromatography (1:3, EtOAC: Hexane). The following product was isolated and identified.

(5-Methoxy-2-nitrophenyl)pyridin-2-yl-amine 240g

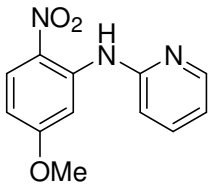

(5-Methoxy-2-nitrophenyl)pyridin-2-yl-amine **240g** was isolated as a yellow solid (0.590 g, 10%), mp 113 – 115 ºC; (Found: M^+ 245.0797. $C_{12}H_{11}N_3O_3$ requires *M* 245.0795); δ_H ($CDCl_3$) 10.66 (1H, br s, NH), 8.61 (1H, d, ^3J 2.7, ArH), 8.36 (1H, m, ArH), 8.23 (1H, d, ^3J 9.39, ArH), 7.65 (1H, ddd, ^3J 9.8, ^3J 7.3, ^4J 2.0, ArH), 6.93 – 6.99 (2H, m, ArH), 6.50 (1H, dd, ^3J 9.5, ^4J 2.7, ArH) and 3.92 (3H, s, CH_3); δ_C ($CDCl_3$) 165.70 (quat), 153.79 (quat), 147.73 (CH), 141.59 (quat), 137.96 (CH), 128.48 (CH), 128.33 (quat), 117.72 (CH), 114.23 (CH), 108.08 (CH), 101.53 (CH), and 55.86 (CH_3); *m/z* (ESI): 246 $[MH]^+$; *m/z* 245 (M^+, 31%), 200 (37), 199 (100), 2184 (66), 156 (51), 155 (54), 82 (60) and 23 (11).

Reaction of 2-methoxy-4-(diethylamino)nitrobenzene 229h and 2-aminopyridine 207

The general method was used with 2-methoxy-4-(diethylamino)nitrobenzene **229h** (1.003 g, 4.47 mmol), 2-aminopyridine **207** (0.424 g, 4.50 mmol), anhydrous toluene (10 cm^3) and clean sodium hydride (0.248 g, 10.30 mmol) to afford a dark yellow solid (0.560 g) which was purified by dry flash column chromatography (1:3, EtOAc : Hexane) to give the following isolated products.

a) 4-Nitro-3-(pyridin-2-yl-amino)-*N*,*N*-diethylaniline 240h

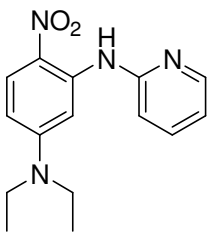

4-Nitro-3-(pyridin-2-yl-amino)-*N*,*N*-diethylaniline **240h** was isolated as an orange solid (0.520 g, 41%), mp 92 - 95 ºC; (Found: M^+ 286.1420. $C_{15}H_{28}N_4O_2$ requires *M* 286.1420); δ_H ($CDCl_3$) 10.90 (1H, br s, NH), 8.31 (1H, d, ^3J 2.9, ArH), 8.28 (1H,

m, ArH), 8.10 (1H, d, ^3J 9.8, ArH), 7.56 (1H, ddd, ^3J 8.2, ^3J 7.3, ^4J 2.0, ArH), 6.83 – 6.90 (2H, m, ArH), 6.21 (1H, dd, ^3J 9.9, ^4J 2.9, ArH), 3.43 (4H, q, ^3J 7.2, 2 × CH_2) and 1.23 (6H, t, ^3J 7.0, 2 × CH_3); δ_C ($CDCl_3$) 154.23 (quat), 153.38 (quat), 147.36 (CH), 141.49 (quat), 137.45 (CH), 128.89 (CH), 123.94 (quat), 116.82 (CH), 113.92 (CH), 101.77 (CH), 97.51 (CH), 45.08 (2 × CH_2) and 12.47 (2 × CH_2); *m/z* (ESI): 287 $[MH]^+$; *m/z* 286 (M^+, 11%), 240 (98), 224 (55), 210 (31), 209 (100), 168 (18), 162 (34) and 82 (24).

None of the required azo product **230h** was obtained. However, 2-methoxy-4-(diethylamino)nitrobenzene (0.635 g) was recovered from evaporation of the remaining toluene layer. The remaining aqueous layer was also extracted with DCM to afford impure 2-aminopyridine **207** (0.200 g).

Reaction of 2-methoxy-4-(1-piperidino)nitrobenzene 229i and 2-aminopyridine 207

The general method was used with 2-methoxy-4-(1-piperidino)nitrobenzene **229i** (1.006 g, 4.26 mmol), 2-aminopyridine **207** (0.399 g, 4.24 mmol), HPLC grade toluene (10 cm^3) and clean sodium hydride (0.203 g, 8.46 mmol) to give a brown oily solid (0.890 g) which was purified by dry flash column chromatography (1:3, EtOAc : Hexane) to afford the following product.

a) 4-Nitro-3-(pyridin-2-yl-amino)-piperidin-1-ylbenzene 240i

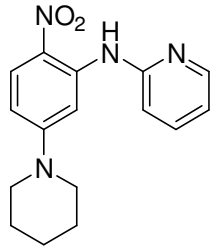

4-Nitro-3-(pyridin-2-yl-amino)-piperidin-1-ylbenzene **240i** was obtained as a dark red solid (0.390 g, 30%), mp 100 - 105 ºC (Found: C, 64.5; H, 6.1; N, 19.0. $C_{16}H_{18}N_4O_2$ requires C, 64.4; H, 6.1; N, 18.8%); δ_H ($CDCl_3$) 10.86 (1H, br s, NH), 8.41 (1H, d, ^4J 2.7, ArH), 8.31 (1H, d, ^4J 3.8, ArH), 8.10 (1H, d, ^3J 9.8, ArH), 7.58 (1H, ddd, ^3J 9.0, ^3J 7.9, ^4J 1.9, ArH), 6.89 (2H, m, ArH), 6.37 (1H, dd, ^3J 9.8, ^4J 2.7, ArH), 3.45 (4H, s, 2 × CH_2) and 1.66 (6H, s, 3 × CH_2); δ_C ($CDCl_3$) 155.56 (quat), 154.16 (quat), 147.52 (CH), 141.58 (quat), 137.55 (CH), 128.67 (CH), 124.55 (quat), 116.96 (CH), 114.02 (CH), 106.30 (CH), 99.24 (CH), 48.11 (2 × CH_2), 25.34 (2 × CH_2) and 24.24 (CH_2); *m/z* (ESI): 299 $[MH]^+$.

Impure 2-aminopyridine **207** (0.140g) was also recovered as a brown oily solid.

None of the required azo product **230i** was isolated.

Reaction of 4-nitro-3-isopropoxy-*N,N*-diethylaniline 229j and 2-aminopyridine 207

The general method was used with 4-nitro-3-isopropoxy-*N,N*-diethylaniline **229j** (1.104 g, 4.38 mmol), 2-aminopyridine **207** (0.416 g, 4.42 mmol), HPLC grade toluene (10 cm^3) and clean sodium hydride (0.213 g, 8.85 mmol) to afford a brown / yellow oil (1.106 g) which was purified by dry flash column chromatography (1:3, EtOAc : Hexane) to give the following products.

a) 4-Nitro-3-(pyridin-2-yl-amino)-*N,N*-diethylaniline 240h

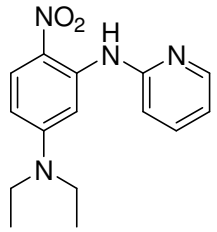

4-Nitro-3-(pyridin-2-yl-amino)-*N,N*-diethylaniline **240h** was isolated as an orange solid (0.216 g, 17%), ^1H and ^{13}C NMR spectra as earlier.

b) 4-Amino-3-isopropoxy-*N,N*-diethylaniline 250

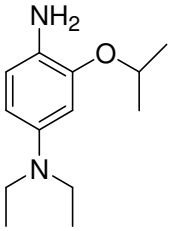

4-Amino-3-isopropoxy-*N,N*-diethylaniline **250** was obtained as red oil (0.251 g, 26%), bp 120 - 125 ºC (1.0 Torr); (Found: M^+ 222.1725. $C_{13}H_{22}N_2O$ requires *M* 222.1727); δ_H ($CDCl_3$) 6.65 (1H, d, ^3J 8.4, ArH), 6.39 (1H, d, ^4J 2.5, ArH), 6.30 (1H, dd, ^3J 8.4, ^4J 2.6 ArH), 4.49 (1H, sept, ^3J 6.1, CH), 3.33 (2H, br s, NH_2), 3.18 (4H, q, ^3J 7.1, 2 × CH_2), 1.35 (6H, d, ^3J 6.1, 2 × CH_3) and 1.08 (6H, t, ^3J 7.0, 2 × CH_3); δ_C ($CDCl_3$) 146.20 (quat), 141.98 (quat), 128.94 (quat), 116.35 (CH), 108.88 (CH), 104.07 (CH), 70.63 (CH), 45.85 (2 × CH_2), 22.20 (2 × CH_3) and 12.36 (2 × CH_3); *m/z* 222 (M^+, 55%), 207 (13), 180 (34), 179 (12), 165 (100), 151 (28), 136 (14), and 41 (42).

Impure 2-aminopyridine **207** (0.259 g) and 4-nitro-3-isopropoxy-*N,N*-diethylaniline **229j** (0.458 g) were also recovered as brown oily solids. None of the required azo product was isolated.

6.5.3: TBDPSCl / TBDMSCl Protection of Hydroxy Groups

General Method

The aminophenol (25 mmol) and imidazole (60 mmol) were stirred in anhydrous DMF (20 cm^3). TBDPSCl or TBDMSCl (35 mmol) was then added dropwise and the reaction mixture stirred at room temperature under N_2 for 16 h. The reaction mixture was then quenched by the addition of water (100 cm^3) and extracted with EtOAc (3 × 200 cm^3). The combined extracts were washed with water (1000 cm^3), dried ($MgSO_4$) and the solvent removed to afford the crude product.

TBDPS Protection

2-(*tert*-Butyldiphenylsilanyloxy)phenylamine 264a

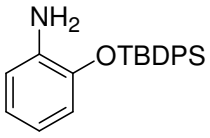

The general method was used with 2-aminophenol **257f** (2.665 g, 24.42 mmol), imidazole (3.992 g, 58.62 mmol), anhydrous DMF (20 cm^3) and TBDPSCl (10.024 g, 36.47 mmol) to afford the crude product as a yellow oil (13.094 g). The crude product was then purified by dry flash column chromatography (1:1, EtOAc : Hexane) to afford 2-(*tert*-butyldiphenylsilanyloxy)phenylamine **264a** as a yellow oil (7.951 g, 56% strength) containing a 44% TBDPSOH impurity by NMR. The overall yield of the protected amine in the crude product was (4.417 g, 52%), bp 120 – 124 ºC (2.0 Torr); (Found: M^+ 347.1698. $C_{22}H_{25}NOSi$ requires *M* 347.1705); δ_H ($CDCl_3$) 7.84 – 7.89 (4H, m, ArH), 7.42 – 7.50 (6H, m, ArH), 6.75 – 6.83 (2H, m, ArH), 6.39 – 6.54 (2H, m, ArH), 4.01 (2H, br s, NH_2) and 1.25 (9H, s, 3 × CH_3); δ_C ($CDCl_3$) 142.75 (quat), 137.24 (quat), 135.25 (4 × CH), 132.46 (2 × quat), 129.82 (2 × CH), 127.70 (4 × CH), 121.52 (CH), 118.43 (CH), 118.14 (CH), 115.57 (CH), 26.58 (3 × CH_3) and 19.32 (quat); *m*/*z* FAB 348 ($[MH]^+$, 37%) and 347 (M^+ 94).

2-(*tert*-Butyldiphenylsilanyloxy)naphthalen-1-ylamine 265a

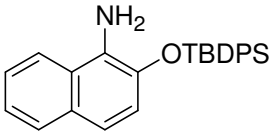

The general method was used with 1-amino-2-naphthol hydrochloride **257o** (0.196 g, 1.00 mmol), imidazole (0.173 g, 2.54 mmol), anhydrous DMF (1 cm^3) and TBDPSCl (0.468 g, 1.70 mmol) to afford the crude product as a red oil (0.618 g). The crude product was then purified by dry flash column chromatography (1:1, EtOAc : Hexane) to afford

2-(*tert*-butyldiphenylsilanyloxy)naphthalen-1-ylamine **265a** as a yellow oil (0.500 g, 41% strength) containing a 59% TBDPSOH impurity by NMR. The overall yield of the protected amine in the crude product was (0.204 g, 51%), bp 141 – 144 ºC (2.0 Torr); (Found: M^+ 397.1863. $C_{26}H_{27}NOSi$ requires *M* 397.1862); δ_H ($CDCl_3$) 7.87 – 7.98 (5H, m, ArH), 7.77 (1H, d, ^3J 8.2, ArH), 7.39 – 7.59 (8H, m, ArH), 7.08 (1H, d, ^3J 8.8, ArH), 6.91 (1H, d, ^3J 8.8, ArH), 4.50 (2H, br s, NH_2) and 1.35 (9H, s, 3 × CH_3); δ_C ($CDCl_3$) 138.50 (quat), 135.32 (4 × CH), 135.26 (quat), 132.66 (2 × quat), 129.96 (2 × CH), 129.41 (quat), 128.25 (quat), 127.85 (4 × CH), 124.87 (CH), 124.51 (CH), 123.47 (CH), 120.38 (CH), 119.78 (CH), 118.25 (CH), 26.70 (3 × CH_3) and 19.46 (quat); *m/z* FAB 397 (M^+, 12%).

TBDMS Protection

2-(*tert*-Butyldimethylsilanyloxy)phenylamine 264b

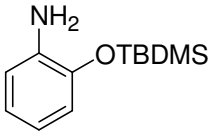

The earlier general method was used with 2-aminophenol **257f** (0.112 g, 1.02 mmol), imidazole (0.107 g, 1.58 mmol), anhydrous DMF (1 cm^3) and TBDMSCl (0.154 g, 1.02 mmol) to afford the crude product as a yellow oil (0.186 g). The crude product was then purified by dry flash column chromatography (1:1, EtOAc : Hexane) to afford 2-(*tert*-butyldimethylsilanyloxy)phenylamine **264b** as an orange oil (0.046 g, 20%), bp 108 – 110 ºC (2.0 Torr); (Found: M^+ 223.1379. $C_{12}H_{21}NOSi$ requires *M* 223.1387); δ_H ($CDCl_3$) 6.60 – 6.84 (4H, m, ArH), 1.04 (9H, s, 3 × CH_3) and 0.26 (6H, s, 2 × CH_3); δ_C ($CDCl_3$) 142.90 (quat), 138.13 (quat), 121.80 (CH), 118.47 (CH), 118.37 (CH), 115.62 (CH), 25.83 (3 × CH_3), 18.23 (quat) and -4.25 (2 × CH_3); *m/z* 223 (M^+, 15%), 208 (2), 167 (12), 166 (100), 150 (26), 148 (6), 135 (8) and 75 (8).

2-(*tert*-Butyldimethylsilanyloxy)naphthalen-1-ylamine 265b

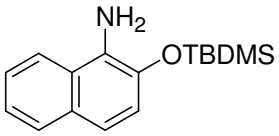

1-Amino-2-naphthol hydrochloride **257o** (0.197 g, 1.01 mmol) and imidazole (0.107 g, 1.60 mmol) were stirred in anhydrous DMF (1 cm^3) and TBDMSCl (0.163 g, 1.08 mmol) added dropwise with stirring under N_2. The reaction mixture was stirred at room temperature for 96 h after which time a further equivalent TBDMSCl (0.175 g, 1.16 mmol) was added and stirred for a further 6 h. The reaction worked up as in the general method to afford the crude product as a brown oil (0.255 g). The crude

product was then purified by dry flash column chromatography (1:1, EtOAc : hexane) to afford 2-(*tert*-butyldimethylsilanyloxy)naphthalen-1-ylamine **265b** as a red oil (0.207 g, 75%), bp 120 – 125 ºC (2.0 Torr); (Found: M^+ 273.1550. $C_{16}H_{23}NOSi$ requires *M* 273.1549); δ_H ($CDCl_3$) 7.66 - 7.75 (2H, m, ArH), 7.42 (1H, ddd, ^3J 8.3, ^3J 6.8, ^4J 1.3, ArH), 7.33 (1H, ddd, ^3J 8.1, ^3J 6.8, ^4J 1.3, ArH), 7.23 (1H, d, ^3J 8.7, ArH), 7.07 (1H, d, ^3J 8.7, ArH), 1.07 (9H, s, 3 × CH_3) and 0.28 (6H, s, 2 × CH_3); δ_C ($CDCl_3$) 138.30 (quat), 131.04 (quat), 129.76 (quat), 128.33 (CH), 124.90 (CH), 124.59 (quat), 123.58 (CH), 120.40 (CH), 120.21 (CH), 118.39 (CH), 25.88 (3 × CH_3), 18.30 (quat) and - 4.03 (2 × CH_3); *m/z* 273 (M^+, 1%), 272 (29), 216 (36), 215 (19), 185 (16), 77 (100), 62 (29) and 41 (27).

6.5.4: Mills Reaction Route to Azo Pyridines

S,S-Dimethyl-*N*-(2-pyridyl)sulfilimine 214[72]

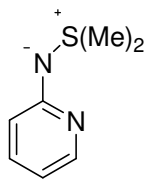

To a solution of 2-aminopyridine **207** (9.405 g, 99.92 mmol) and dimethylsulfide (8.0 cm^3, 110.00 mmol) in DCM (100 cm^3) was added dropwise over 1 h, *N*-chlorosuccinamide (13.301 g, 99.61 mmol) in DCM (250 cm^3). During this time the temperature of the reaction mixture was maintained at – 20 ºC. After addition was complete the reaction mixture was stirred for 1 h at – 20 ºC and a further 1 h at room temperature.

A solution of sodium methoxide in methanol [from sodium (4.05 g) in methanol (25 cm^3)] was then added and the mixture stirred for 10 min. Water (150 cm^3) was then added and stirring continued for a further 4 h. The organic layer was then separated and the aqueous layer extracted with DCM (3 × 100 cm^3). The combined organic extracts were washed with water (2 × 100 cm^3), dried ($MgSO_4$) and concentrated under reduced pressure to afford *S,S*-dimethyl-*N*-(2-pyridyl)sulfilimine **214** as a light orange oil (11.430 g, 74%), δ_H ($CDCl_3$) 7.93 (1H, ddd, ^3J 5.2, ^4J 1.9, ^4J 0.9, ArH), 7.26 (1H, ddd, ^3J 8.6, ^3J 7.0 , ^4J 2.0, ArH), 6.61 (1H, dt, ^3J 8.6, ^4J 1.0, ArH), 6.41 (1H, ddd, ^3J 6.9, ^3J 5.2 , ^4J 1.0, ArH) and 2.65 (6H, s, 2 × CH_3); δ_C ($CDCl_3$) 165.28 (quat), 146.91 (CH), 136.57 (CH), 113.97 (CH), 111.27 (CH) and 33.61 (2 × CH_3).

The sulfilimine was not characterised further to avoid possible decomposition of the product. This compound has been previously reported but has not been characterised.[72]

2-Nitrosopyridine 215

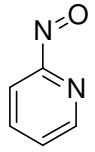

A solution of *m*-chloroperbenzoic acid (29.328 g, 70% strength) in anhydrous DCM (500 cm^3) was cooled to 0 ºC. A solution of the sulfilimine **214** (11.430 g) in anhydrous DCM (100 cm^3) was then added and the mixture stirred for 1.5 hr at 0 – 5 ºC. Dimethylsulfide (4 cm^3, 55.00 mmol) was then added and stirring continued for 0.5 h. The reaction mixture was then added to sodium carbonate solution (sat, 500 cm^3) with stirring and the solution allowed to settle. The green organic layer was separated, washed with water (2 × 100 cm^3), dried ($MgSO_4$) and concentrated under reduced pressure to afford the crude 2-nitrosopyridine **215** as a tan coloured solid (7.747 g). The crude product was

recrystallised from ethanol to afford yellow crystals (5.052 g, 63%), mp 111 - 115 ºC [lit.,[72] 120 - 122 ºC]; (Found: M^+ 108.0324. $C_5H_4N_2O$ requires *M* 108.0324); δ_H ($CDCl_3$) 7.99 (1H, dd, ^3J 4.8, ^4J 1.0, ArH), 7.90 (1H, dd, ^3J 7.5, ^4J 1.7, ArH), 7.81 (1H, d, ^3J 8.1, ArH) and 7.29 (1H, ddd, ^3J 7.2, ^3J 4.8, ^4J 1.0, ArH); δ_C ($CDCl_3$) 155.53 (quat), 146.91 (CH), 139.33 (CH), 125.55 (CH) and 118.62 (CH); *m/z* 108 (M^+, 70%), 94 (16), 79 (35), 78 (50), 76 (9), 52 (42), 51 (100), and 50 (25).

Mills Reaction:

General Method

A solution of 2-nitrosopyridine **215** (2.00 mmol), an aromatic amine **257** (2.00 mmol) in DCM (35 cm^3) containing 2 drops of glacial acetic acid was stirred at room temperature for 18 h. The reaction mixture was then evaporated to dryness under reduced pressure and the residue purified by dry flash column chromotagraphy (2.5:1, chloroform : hexane) to afford the azo product **230**.

2-(4-Chlorophenylazo)pyridine 230b

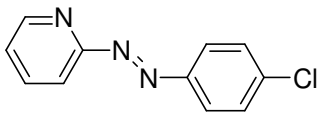

The general method was applied with 2-nitrosopyridine **215** (0.216 g, 2.00 mmol), *p*-chloroaniline **257b** (0.503 g, 3.96 mmol) in DCM (35 cm^3) containing 2 drops of glacial acetic to afford 2-(4-chlorophenylazo)pyridine **230b** as an orange solid (0.441 g , > 98%). The NMR spectra agreed with the earlier preparation of 2-(4-chlorophenylazo)pyridine **230b**.

2-(2-Methoxyphenylazo)pyridine 230c

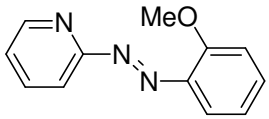

The general method was applied with 2-nitrosopyridine **215** (0.109 g, 1.01 mmol), *o*-anisidine **257c** (0.251 g, 2.04 mmol) in DCM (17 cm^3) containing 2 drops of glacial acetic acid to afford 2-(2-methoxyphenylazo)pyridine **230c** as an red solid (0.206 g , 95%). The NMR spectra agreed with the earlier preparation of 2-(2-methoxyphenylazo)pyridine **230c**.

Reaction of 2-Nitrosopyridine 215 and 2-Aminophenol 257f

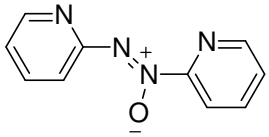

The general method was applied with 2-nitrosopyridine **215** (0.434 g, 4.01 mmol), 2-aminophenol **257f** (0.438 g, 4.01 mmol) in DCM (70 cm^3) containing 2 drops of glacial acetic acid to afford a dark red oil identified as azoxypyridine **258** (0.354 g, 88%), bp 96 – 98 ºC (1.0 Torr); (Found: MH^+ 201.0776. $C_{10}H_9N_4O$ requires *M* 201.0772); δ_H ($CDCl_3$) 8.64 (1H, ddd, ^3J 4.8, ^4J 1.8, ^4J 0.8, ArH), 8.60 (1H, ddd, ^3J 4.7, ^4J 1.8, ^4J 0.8, ArH), 8.31 (1H, dt, ^3J 8.2, ^4J 0.8, ArH), 8.31 (1H, dt, ^3J 8.2, ^4J 0.9, ArH), 7.91 (1H, ddd, ^3J 8.2, ^3J 7.5, ^4J 1.8, ArH), 7.81 (1H, ddd, ^3J 8.2, ^3J 7.5, ^4J 1.9, ArH), 7.51 (1H, ddd, ^3J 7.4, ^3J 4.7, ^4J 0.9, ArH) and 7.24 (1H, ddd, ^3J 7.5, ^3J 4.8, ^4J 1.0, ArH); δ_C ($CDCl_3$) 156.96 (quat), 156.02 (quat), 149.35 (CH), 148.48 (CH), 139.12 (CH), 137.80 (CH), 127.14 (CH), 123.69 (CH), 118.40 (CH) and 117.50 (CH); *m*/*z* (FAB) 201 (MH^+, 100%), 185 (30), 170 (93), 149 (94), 147 (94), 136 (40), 107 (30) and 95 (86).

None of the azo compound **230f** was obtained.

1-(2-Pyridyl)-2-pyridone 263

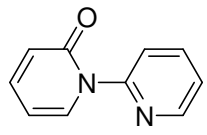

Attempted distillation the crude azoxypyridine **258** (0.306 g, 1.53 mmol) afforded 1-(2-pyridyl)-2-pyridone **263** as a red oily solid (0.214 g, 70%), bp 112 – 118 ºC (1.0 Torr) [lit.,[95] 127 – 128 ºC (1.0 Torr)]; δ_H ($CDCl_3$) 8.52 (1H, ddd, ^3J 4.9, ^4J 2.0, ^4J 0.9, ArH), 7.76 – 7.94 (3H, m ArH), 7.35 (1H, ddd, ^3J 9.3, ^3J 6.5, ^4J 2.0, ArH) 7.28 (1H, ddd, ^3J 7.3, ^3J 4.9, ^4J 1.1, ArH), 6.61 (1H, ddd, ^3J 9.3, ^4J 1.7, ^4J 0.7, ArH) and 6.26 (1H, ddd, ^3J 7.1, ^3J 6.5, ^4J 1.4, ArH); δ_C ($CDCl_3$) 162.08 (quat), 151.75 (quat), 148.79 (CH), 140.10 (CH), 137.61 (CH), 135.97 (CH), 123.05 (CH), 121.94 (CH), 121.34 (CH) and 106.17 (CH); *m*/*z* 172 (M^+, 32%), 171 (100), 144 (14), 143 (19), 118 (12), 117 (10), 79 (14) and 78 (19).

Reaction of 2-Nitrosopyridine 215 and 1-Amino-2-naphthol hydrochloride 257o

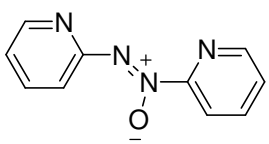

A solution of 2-nitrosopyridine **215** (0.108 g, 1.00 mmol), 1-amino-2-naphthol hydrochloride **257o** (0.218 g, 90% strength, 1.00 mmol) in DCM (70 cm^3) containing 2 drops of glacial

acetic acid and *N,N*-diisopropylethylamine (0.129 g, 1.00 mmol) was stirred at room temperature for 18 h. The reaction mixture was then concentrated under reduced pressure to afford a dark red oil which was taken up in 2M HCl (50 cm^3). The acidic solution was then made basic with NaOH (sat) and the basic solution extracted with DCM (3 × 100 cm^3). The combined extracts were washed with water (3 × 50 cm^3), dried ($MgSO_4$) and the solvent removed under reduced pressure to afford a brown oil (0.255 g). The crude product was then purified by dry flash column chromatography (1:2, EtOAc : Hexane) to afford a red brown oil identified as azoxypyridine **258** (0.075 g, 75%). The NMR spectra agreed with the previous preparation of azoxypyridine **258**.

2-(3-hydroxyphenylazo)pyridine 230m

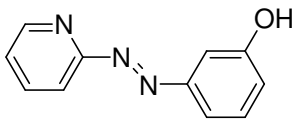

The general method was applied with 2-nitrosopyridine **215** (0.051 g, 0.47 mmol), *m*-aminophenol **257m** (0.051 g, 0.47 mmol) in DCM (8 cm^3) containing 2 drops of glacial acetic acid to afford 2-(3-hydroxyphenylazo)pyridine **230m** as an orange solid (0.035 g, 37%), mp 145 ºC; (Found: M^+ 199.0741. $C_{11}H_9N_3O$ requires *M* 199.0740); δ_H (acetone d_6) 8.72 (1H, ddd, ^3J 4.7, ^4J 1.8, ^4J 0.8, ArH), 8.02 (1H, ddd, ^3J 8.0, ^3J 7.4, ^4J 1.8, ArH), 7.73 (1H, dt, ^3J 8.1, ^4J 0.9, ArH), 7.42 – 7.56 (4H, m, ArH) and 7.10 (1H, ddd, ^3J 8.1, ^3J 2.3, ^4J 1.2, ArH); δ_C (acetone d_6) 165.42 (quat), 160.20 (quat), 155.65 (quat), 151.22 (CH), 140.33 (CH), 132.03 (CH), 127.27 (CH), 121.30 (CH), 118.18 (CH), 114.74 (CH) and 109.87 (CH); *m/z* 199 (M^+, 1%), 172 (13), 171 (100), 170 (12), 142 (10), 109 (77), 93 (78) and 44 (39); λ_{max} 319 nm (ε = 12812 dm^{-3} mol^{-1} cm^{-1}), $W_{1/2}$ > 200 nm.

Reaction of 2-Nitrosopyridine 215 and 4-Aminophenol 257n

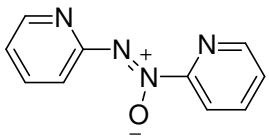

The general method was applied to 2-nitrosopyridine **215** (0.050 g, 0.46 mmol) and 4-aminophenol **257n** (0.050 g, 0.46 mmol) in DCM (8 cm^3) containing 2 drops of glacial acetic acid to afford a dark red solid (0.088 g). The crude product was then purified by dry flash column chromatography (1:2, EtOAc : hexane) to afford a brown solid identified as azoxypyridine **258** (0.065 g, 71%). The NMR spectra agreed with the previous preparation of azoxypyridine **258**. None of the azo product **230n** was obtained.

2-(1-Naphthylazo)pyridine 230k

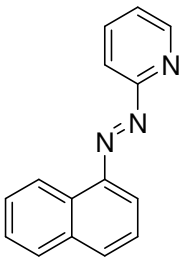

A solution of 2-nitrosopyridine **215** (0.056 g, 0.52 mmol), 1-naphthylamine **257k** (0.074 g, 0.51 mmol) in DCM (8 cm^3) containing 2 drops of glacial acetic acid was stirred at reflux for 16 h. The reaction mixture was then concentrated under reduced pressure to afford a dark red oil (0.188 g). The crude product was then purified by dry flash column chromatography (1:2, EtOAc : hexane) to give 2-(1-naphthylazo)pyridine **230k** as a dark red solid (0.037 g, 31%), mp 110 – 112 ºC; (Found: M^+ 233.0952. $C_{15}H_{11}N_3$ requires *M* 233.0953); δ_H ($CDCl_3$) 8.95 (1H, ddd, ^3J 8.3, ^4J 1.7, ^4J 0.9, ArH), 8.79 (1H,dt, ^3J 4.8, ^4J 1.4, ArH), 8.01 – 8.06 (2H, m, ArH), 7.92 – 7.96 (3H, m, ArH), 7.56 – 7.70 (3H, m, ArH) and 7.43 (1H, td, ^3J 4.8, ^3J 3.4, ArH); ($CDCl_3$) 163.60 (quat), 149.54 (CH), 147.34 (quat), 138.24 (CH), 134.28 (quat), 132.67 (CH), 131.56 (quat), 128.00 (CH), 127.17 (CH), 126.55 (CH), 125.57 (CH), 125.18 (CH), 123.33 (CH), 113.45 (CH) and 112.74 (CH); *m/z* FAB 233 (M^+, 45%).

2-(8-Quinolinylazo)pyridine 230l

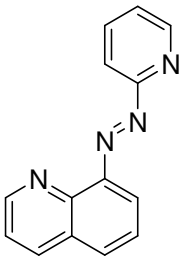

A solution of 2-nitrosopyridine **215** (0.056 g, 0.52 mmol) and 8-aminoquinoline **257l** (0.072 g, 0.50 mmol) in DCM (8 cm^3) containing 2 drops of glacial acetic acid was stirred at reflux for 16 h. The reaction mixture was then concentrated under reduced pressure to afford a dark red oil (0.203 g). The crude product was then purified by dry flash column chromatography (1:2, EtOAc : hexane) to give 2-(8-quinolinylazo)pyridine **230l** as a dark red solid (0.039 g, 34%), (Found: MH^+ 235.0984. $C_{14}H_{11}N_4$ requires *M* 235.0984); δ_H ($CDCl_3$) 9.14 (1H, dd, ^3J 4.2, ^4J 1.7, ArH), 8.75 (1H, d, ^3J 4.7, ArH), 8.25 (1H, dd, ^3J 8.3, ^4J 1.8, ArH), 7.87 – 8.10 (4H, m, ArH), 7.64 (1H, dd, ^3J 8.1, ^3J 7.6, ArH), 7.52 (1H, dd, ^3J 8.3, ^3J 4.2, ArH) and 7.41 (1H, ddd, ^3J 7.2, ^3J 4.8, ^4J 1.4 ArH); ($CDCl_3$) 163.26 (quat), 151.53 (CH), 149.39 (CH), 148.44 (quat), 144.63 (quat), 138.38 (CH), 136.29 (CH), 132.07 (CH), 129.08 (quat), 126.42 (CH), 125.41 (CH), 121.83 (CH), 116.31 (CH) and 114.97 (CH); *m/z* FAB 235 ($[MH]^+$, 32%) and 234 (M^+, 100); λ_{max} 324 nm (ε 24324 dm^{-3} mol^{-1} cm^{-1}), $W_{1/2}$ > 200 nm.

Reaction of 2-Nitrosopyridine 215 and 2-Aminopyridine 257p

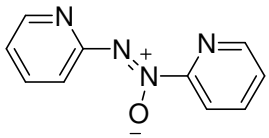

The general method was applied to 2-nitrosopyridine **215** (0.058 g, 0.54 mmol) and 2-aminopyridine **257p** (0.051 g, 0.54 mmol) in DCM (8 cm^3) containing 2 drops of glacial acetic acid. After 18 h at room temperature only starting materials remained by TLC hence the reaction mixture was heated at reflux for a further 24 h. The solvent was then removed to afford a dark red oil (0.146 g). The crude product was purified by dry flash column chromatography (1:2, EtOAc : hexane) to afford a brown solid identified as azoxypyridine **258** (0.052 g). The yield was 96% based on the reduction of the 2-nitrosopyridine dimer. The NMR spectra agreed with the previous preparation of azoxypyridine **258**.

None of the azo product **230p** was obtained.

Mill's Reaction with Protected Phenol / Naphthol Systems

[2-(*tert*-Butyldiphenylsilanyloxy)phenyl]pyridin-2-yldiazene 269

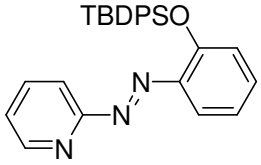

The general method was applied to 2-nitrosopyridine **215** (0.0284 g, 0.26 mmol) and 2-(*tert*-butyldiphenylsilanyloxy)phenylamine **264a** (0.286 g, 28% strength, 0.23 mmol) in DCM (4 cm^3) containing 2 drops of glacial acetic acid to afford an orange oil (0.329 g). The crude product was then purified by dry flash column chromatography (1:1, EtOAc : hexane) to give the protected azo compound **269** as an orange oil (0.072 g, 72%), bp 105 - 109 ºC (1.0 Torr); (Found: MH^+ 438.2002. $C_{27}H_{28}N_3OSi$ requires *M* 438.2002); δ_H ($CDCl_3$) 8.58 (1H, ddd, ^3J 4.8, ^4J 1.9, ^4J 0.9, ArH), 7.70 (1H, ddd, ^3J 8.0, ^4J 1.8, ^4J 0.5, ArH), 7.61 – 7.65 (4H, m, ArH), 7.50 (1H, ddd, ^3J 8.1, ^3J 7.4, ^4J 1.9, ArH), 7.14 – 7.32 (8H, m, ArH), 7.07 (1H, dt, ^3J 8.1, ^4J 1.0, ArH), 6.82 – 6.90 (2H, m, ArH) and 1.04 (9H, s, 3 $\times CH_3$); δ_C ($CDCl_3$) 163.55 (quat), 155.02 (quat), 148.99 (CH), 143.13 (quat), 137.71 (CH), 135.23 (4 × CH), 133.44 (CH), 132.60 (2 × quat), 129.80 (2 × CH), 127.62 (4 × CH), 124.58 (CH), 121.73 (CH), 121.407 (CH), 117.05 (CH), 111.50 (CH), 26.46 (3 × CH_3) and 19.95 (quat); *m*/*z* FAB 438 (MH^+, 22%).

Reaction of 2-Nitrosopyridine 215 and

2-(*tert*-butyldimethylsilanyloxy)phenylamine 264b

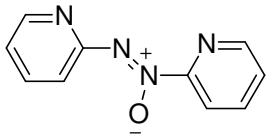

The general method was applied to 2-nitrosopyridine **215** (0.013 g, 0.12 mmol) and 2-(*tert*-butyldimethylsilanyloxy)phenylamine **264b** (0.025 g, 0.11 mmol) in DCM (2 cm^3) containing 2 drops of glacial acetic acid to afford an orange oil (0.022 g) identified by NMR spectra as azoxypyridine **258** and the protected amine starting material **264b**. None of the azo product **268** was obtained.

Reaction of 2-Nitrosopyridine 215 and

2-(*tert*-butyldiphenylsilanyloxy)naphthalen-1-ylamine 265a

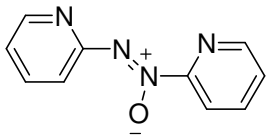

The general method was applied to 2-nitrosopyridine **215** (0.0284 g, 0.26 mmol) and 2-(*tert*-butyldiphenylsilanyloxy)naphthalen-1-ylamine **265a** (0.168 g, 41% strength, 0.25 mmol) in DCM (4 cm^3) containing 2 drops of glacial acetic acid to afford a dark red oil (0.195 g). The crude product was then purified by dry flash column chromatography (1:1, EtOAc : Hexane) to afford a brown solid identified by NMR spectra as azoxypyridine **258** (0.025 g,. The yield was 96% based on the reduction of the 2-nitrosopyridine dimer.

The protected amine starting material **265a** was also recovered. None of the azo product **266** was obtained.

Reaction of 2-Nitrosopyridine 215 and

2-(*tert*-butyldimethylsilanyloxy)naphthalen-1-ylamine 265b

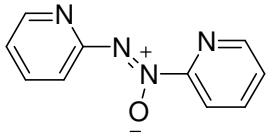

The general method was applied to 2-nitrosopyridine **215** (0.046 g, 0.42 mmol) and 2-(*tert*-butyldimethylsilanyloxy)naphthalen-1-ylamine **265b** (0.113 g, 0.41 mmol) in DCM (4 cm^3) containing 2 drops of glacial acetic acid to afford a dark red oil (0.123 g). The crude product was then purified by dry flash column chromatography (1:1, EtOAc : hexane) to afford a brown oil identified by NMR spectra as azoxypyridine **258** (0.046 g, 100%). The protected amine starting material **265b** was also recovered. None of the azo product **267** was obtained.

2-(2-Hydroxyphenylazo)pyridine 230f

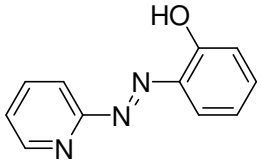

[2-(*tert*-Butyldiphenylsilanyloxy)phenyl]pyridin-2-yldiazene **269** (2.940 g, 6.72 mmol) was stirred in THF (50 cm^3) and TBAF (1.0 M in THF, 20 cm^3, 20.0 mmol) added dropwise with stirring. The reaction mixture immediately turned a dark red / magenta colour and was stirred for 0.5 h. Water (50 cm^3) was then added and the reaction mixture extracted with EtOAc (3 × 100 cm^3). The combined extracts were washed with water (3 × 100 cm^3), dried ($MgSO_4$) and the solvent removed under reduced pressure to afford a red oil. The crude product was then purified by dry flash column chromatography (1:1, EtOAc : Hexane) to afford 2-(2-hydroxyphenylazo)pyridine **230f** as a red solid (1.452 g, 99%), mp 118 - 120 ºC; (Found: M^+ 199.0746. $C_{11}H_9N_3O$ requires *M* 199.0740); δ_H ($CDCl_3$) 12.89 (1H, br s, OH), 8.69 (1H, ddd, ^3J 4.8, ^4J 1.8, ^4J 0.9, ArH), 8.00 (1H, ddd, ^3J 7.6, ^4J 1.8, ^4J 0.7, ArH), 7.78 – 7.91 (2H, m, ArH), 7.34 – 7.41 (2H, m, ArH) and 7.02 – 7.09 (2H, m, ArH); ($CDCl_3$) 161.07 (quat), 153.32 (quat), 149.59 (CH), 138.34 (CH), 137.54 (quat), 134.56 (CH), 133.94 (CH), 125.12 (CH), 120.00 (CH), 118.51 (CH) and 114.92 (CH); *m/z* 199 (M^+, 12%), 171 (85), 170 (99), 121 (40), 93 (100), 78 (35), 65 (46) and 41 (57); λ_{max} 324 nm (ε = 18386 dm^{-3} mol^{-1} cm^{-1}), $W_{1/2}$ 70 nm.

2-Acetylamino-5-(pyridin-2-ylazo)benzenesulfonic acid 271

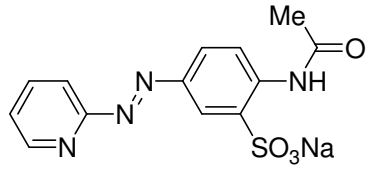

2-Acetylamino-5-aminobenzenesulfonic acid **270** (4.263 g, 18.52 mmol) and 2-nitrosopyridine **215** (2.002 g, 18.52 mmol) were stirred in 50% aqueous ethanol (150 cm^3) containing 2 drops of acetic acid for 18 h at room temperature. The product was then recovered by the addition of NaCl (1% w/w) to the reaction mixture until the solid precipitated, followed by filtration under reduced pressure. The resulting paste was dried to afford the azo compound **271** as an orange solid (3.040 g, 51%), mp > 330 ºC (Found: C, 45.7; H, 3.1; N, 16.2. $C_{13}H_{11}N_4NaO_4S$ requires C, 45.6; H, 3.2; N, 16.4%); δ_H ($[^2H]_6$DMSO) 10.73 (1H, br s, NH), 8.82 (1H, d, ^3J 4.8, ArH), 8.62 (1H, d, ^3J 8.8, ArH), 8.32 – 8.38 (2H, m, ArH), 8.06 (1H, dd, ^3J 8.8, ^4J 2.3, ArH), 8.00 (1H, d, ^3J 8.1, ArH), 7.81 (1H, dd, ^3J 7.8, ^3J 7.8, ArH) and 2.15 (3H, s, CH_3); δ_C ($[^2H]_6$DMSO) 168.32 (quat), 159.21(quat), 146.30 (CH), 146.04 (quat), 142.74 (CH), 139.84 (quat), 135.88 (quat),

127.59 (CH), 126.51 (CH), 120.62 (CH), 119.78 (CH), 114.93 (CH) and 25.05 (CH_3); *m/z* (ESI): 318.8 M^- $C_{13}H_{11}N_4O_4S$ requires 319.0; λ_{max} 343 nm (ε = 25124 dm^3 mol^{-1} cm^{-1}), $W_{1/2}$ 70 nm.

6.5.5: Mills Reaction under Basic Conditions (NaOH)

General Method

The amine **257** (0.5 mmol) was stirred in NaOH (50%, aq, 5 cm^3) and toluene (0.5 cm^3). 2-Nitrosopyridine **215** (0.5 mmol) was then added and the reaction mixture heated to 80 ºC with stirring for 18 h. The reaction mixture was then allowed to cool and extracted with EtOAc (3 × 25 cm^3). The combined extracts were washed with water (2 × 25 cm^3), dried ($MgSO_4$) and the solvent removed under reduced pressure. The crude product was then purified by dry flash column chromatography (1:1, EtOAc : hexane) to afford the azo **230** product.

2-(2-Hydroxyphenylazo)pyridine 230f

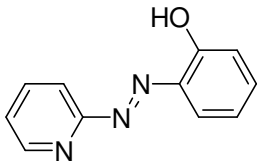

The general method was used with 2-aminophenol **257f** (0.051 g, 0.46 mmol), NaOH (50%, aq, 5 cm^3), toluene (0.5 cm^3) and 2-nitrosopyridine **215** (0.053 g, 0.49 mmol) to afford 2-(2-hydroxyphenylazo)pyridine **230f** as a red solid (0.030 g, 33%). The NMR spectra agreed with the previous preparation of 2-(2-hydroxyphenylazo)pyridine **230f**.

2-(2-Pyridineazo)pyridine 230p

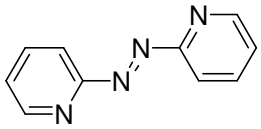

The general method was used with 2-aminopyridine **257p** (0.053 g, 0.56 mmol), NaOH (50%, aq, 1 cm^3), toluene (0.5 cm^3) and 2-nitrosopyridine **215** (0.061 g, 0.56 mmol) to afford an orange/red oil (0.080 g). NMR analysis of the crude product revealed it to be a 2:1:1 mixture of 2-(2-pyridineazo)pyridine **230p**: 2-aminopyridine **257p**: azoxypyridine **258**. Analytical data corresponding to 2-(2-pyridineazo)pyridine **230p** was selected, δ_H ($CDCl_3$) 8.69 (2H, ddd, ^3J 4.8, ^4J 1.5, ^4J 0.8, ArH), 7.84 – 7.92 (4H, m, ArH) and 7.37 (2H, ddd, ^3J 6.4, ^3J 4.7, ^4J 1.5, ArH); ($CDCl_3$) 162.38 (quat), 149.37 (2 × CH), 138.30 (2 × CH), 125.93 (2 × CH) and 115.13 (2 × CH); *m/z* (ESI): 185.2 $[MH]^+$.

Reaction of 1-Amino-2-naphthol Hydrochloride and 2-Nitrosopyridine

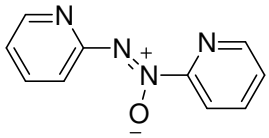

The general method was used with 1-amino-2-naphthol hydrochloride **257o** (0.098 g, 0.50 mmol), NaOH (50%, aq, 1 cm^3), toluene (1 cm^3) and 2-nitrosopyridine **215** (0.054 g, 0.50 mmol) to afford azoxypyridine **258** as a red solid (0.030 g, 60%). NMR agrees with earlier. None of the azo product **230o** was obtained.

Reaction of 2-(*tert*-Butyl-diphenylsilanyloxy)-naphthalen-1-ylamine 265a and 2-Nitrosopyridine 215

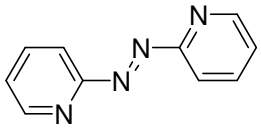

The general method was used with 2-(*tert*-butyldiphenylsilanyloxy)naphthalen-1-ylamine **265a** (0.181 g, 50% strength, 0.23 mmol), NaOH (50%, aq, 1 cm^3), toluene (0.5 cm^3) and 2-nitrosopyridine **215** (0.026 g, 0.24 mmol) to afford a red oil (0.1758 g). NMR analysis revealed the product to be a mixture of 2-(2-pyridineazo)pyridine **230p** and TBDPSOH. NMR agreed with earlier data for 2-(2-pyridineazo)pyridine. None of the azo product **266** was obtained.

Azoxypyridine 258

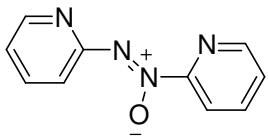

2-Nitrosopyridine **215** (0.050 g, 0.46 mmol) in NaOH (50%, aq, 1 cm^3) and toluene (0.5 cm^3) was heated to 80 ºC with stirring for 18 h. The reaction mixture was worked up as before to afford a red oil (0.031 g, 67%) identified by NMR spectra as azoxypyridine **258**.

6.5.6: Metallisation of Pyridine Azo Dyes

2-(2-Methoxyphenylazo)pyridine : Cu 2:1 Complex 274

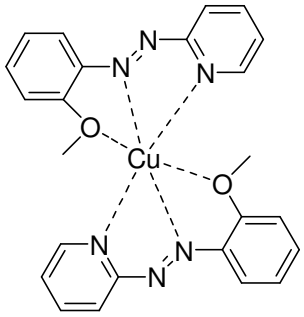

2-(2-Methoxyphenylazo)pyridine **230c** (0.485 g, 2.28 mmol) was stirred in water : NMP (2:1, 7.5 cm^3) until all the solids were in solution. The pH of the solution was then adjusted to pH 9 – 10 with the addition of 2M NaOH solution as required. $CuSO_4.5H_2O$ (0.580 g, 2.28 mmol) was then added and the pH maintained at pH 9 – 10 with stirring at 80 ºC for 20 h. The progress of the reaction was monitored by TLC. The reaction appeared incomplete after 20 h hence a further equivalent of $CuSO_4.5H_2O$ (0.600 g, 2.40 mmol) was added. Heating of the reaction at 80 ºC was continued with stirring for a further 48 h. The reaction mixture was then filtered to remove a green precipitate (1.30 g) and the filtrates concentrated under reduced pressure to afford a dark green oil which was extracted with DCM (6 × 100 cm^3). The combined organic extracts were washed with water (4 × 100 cm^3), dried ($MgSO_4$) and the solvent removed under reduced pressure to afford a dark green oily solid identified by mass spectroscopy as the 2-(2-methoxyphenylazo)pyridine : Cu 2:1 Complex **274** (0.230 g, 41%), *m/z* (ESI): 489 M^+ $C_{24}H_{22}N_6CuO_2$ requires 489; λ_{max} 350 nm, $W_{1/2}$ >200 nm.

2-(2-Hydroxyphenylazo)pyridine: Ni 2:1 Complex 255

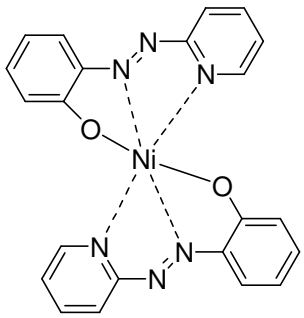

2-(2-Hydroxyphenylazo)pyridine **230c** (1.287 g, 6.46 mmol) was stirred in water (50 cm^3) and NMP (30 cm^3) added to aid solubility. The reaction mixture was heated to 70 ºC with stirring and $Ni(OAc)_2.5H_2O$ (0.804 g, 3.23 mmol) added causing the reaction mixture to turn from a red to magenta colour. The pH of the reaction mixture was then adjusted to pH 9.0 by addition of sat. NaOH solution as required and stirring continued for 0.5 h. The reaction mixture was then cooled and extracted with DCM (5 × 200 cm^3). The combined extracts were washed with water (3 × 200 cm^3), dried ($MgSO_4$) and the solvent removed to afford the metallised species **255** as a magenta solid (0.934 g, 64%), mp >330 ºC (Found: C, 58.6; H, 3.9; N, 18.3. $C_{22}H_{16}N_6NiO_2$ requires C, 58.1; H, 3.5; N, 18.5%); *m/z* (ESI): 455.1 MH^+; λ_{max} 549 nm (ε 17473 dm^{-3} mol^{-1} cm^{-1}), $W_{1/2}$ 114 nm.

6.6: Bisazo Coupling Reactions of Chromotropic Acid

6.6.1: Monoazo Coupling Reactions

General Method for Preparation of MonoPACAs

Aromatic amine diazotization

The aromatic amine (16 mmol) was stirred in water (15 cm^3). To this was added HCl (conc., 5 cm^3) and the temperature (T) reduced to < 5 ºC. The solution was stirred for 1 h to ensure thorough dispersion. Sodium nitrite (16 mmol) was then added over 30 min ensuring T < 5 ºC and a positive nitrite test (starch iodide papers) upon completion of addition. The reaction mixture was then stirred for a further 1 h maintaining a positive nitrite test and T < 5 ºC. Extra sodium nitrite was then added as required. Urea was then added as required to destroy excess nitrite. NaOAc (1.062 g, 12.95 mmol) was added just before addition to the chromotropic acid solution.

Chromotropic Acid dissolution

Chromotropic acid **301** (7.0 g @ 71.13%, 15.5 mmol) was dissolved in water (25 cm^3), Na_2CO_3 (14 mmol) added with continued stirring and the solution was cooled to < 5 ºC.

Azo coupling

The diazonium salt **324** solution was then added to the chromotropic acid **301** solution dropwise over 30 min with constant stirring. The pH was maintained at pH 6.0 – 7.0 by addition of NaOH (47%) as required. The reaction mixture was stirred at T < 5 ºC for 4 h and overnight at room temperature. The reaction progress was monitored by HPLC and peaks identified by LCMS. The yield of the reaction of the monoPACA **302** was then calculated using QHPLC.

Product recovery

NaCl was then added as required (10-12% w/w) to the reaction mixture until, when spotted onto filter paper, most of the coloured product had precipitated and the liquid outspread was pale. The reaction mixture was then filtered and the resulting paste dried in an oven overnight to give the monoPACA **302** in the disodium salt form as a

dark blue/purple solid. The crude product was then purified by dissolving in water (100 cm^3) and drowning out with acetone (1000 cm^3). The monoPACA precipitate was then filtered and the process repeated twice more to afford the purified monoPACA **302** as a dark blue/purple solid.

4,5-Dihydroxy-3-(4-methoxyphenylazo)naphthalene-2,7-disulfonic acid 302a

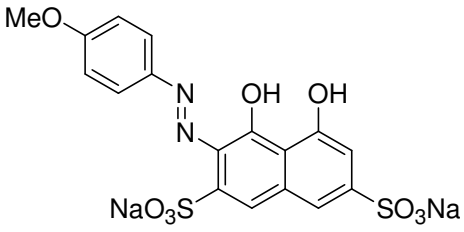

The general method was applied with *p*-anisidine (1.993 g, 16.18 mmol) water (15 cm^3), HCl (conc., 5 cm^3), sodium nitrite (1.160 g, 16.82 mmol), NaOAc 1.062 g, 12.95 mmol) to prepare the diazonium salt **324g**. As in the general method, this was added to chromotropic acid **301** (7.044 g @ 71.13%, 15.64 mmol), in water (25 cm^3) and Na_2CO_3 (1.461 g, 13.81 mmol). The yield of the reaction was then calculated using QHPLC to give 4,5-dihydroxy-3-(4-methoxyphenylazo)naphthalene-2,7-disulfonic acid **302a** (7.177 g, 97%). Product recovery and purification as in the general method gave the *p*-methoxyPACA **302a** in the disodium salt form as a dark blue/purple solid (4.440 g, 60%), mp > 330 ºC; (Found: C, 37.8; H, 2.5; N, 5.1. $C_{17}H_{12}N_2Na_2O_9S_2.0.5NaCl.0.5H_2O$ requires C, 38.1; H, 2.4; N, 5.2%); δ_H (360 MHz, $[^2H]_6$DMSO) 7.84 (2H, d, *J* 9.0, ArH), 7.48 (1H, s, ArH), 7.38 (1H, d, ^4J 1.0, ArH), 7.06 (2H, d, ^3J 9.1, ArH), 7.05 (1H, d, ^4J 1.0, ArH) and 3.83 (3H, s, CH_3); δ_C (90 MHz, $[^2H]_6$DMSO) 179.00 (quat), 162.41 (quat), 158.65 (quat), 154.34 (quat), 143.75 (quat), 136.71 (quat), 135.75 (quat), 127.26 (quat), 119.93 (CH), 119.68 (2 × CH), 116.53 (CH), 115.80 (quat), 115.11 (2 × CH), 111.12 (CH) and 55.73 (CH_3); *m/z* (ESI): 474.8 $[MNa]^-$ $C_{17}H_{12}N_2NaO_9S_2$ requires 475.4.

Large Scale

The above general method was applied on a large scale to afford *p*-methoxyPACA **302a** (200 g) which had been purified by dialysis. The % composition monoazo in the organic content by HPLC was calculated to be 94%. CHN gave the organic and sodium content to be 93% hence an overall strength of the *p*-methoxyPACA **302a** as the sodium salt was calculated to be 87%.

4,5-Dihydroxy-3-(4-nitrophenylazo)naphthalene-2,7-disulfonic acid 302g

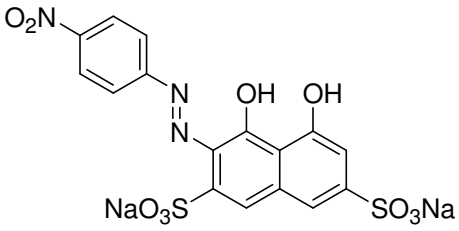

The general method was applied with *p*-nitroaniline (2.232 g, 16.16 mmol), water (15 cm^3), HCl (conc., 5 cm^3), sodium nitrite (1.127 g, 16.33 mmol), NaOAc (1.081 g, 13.17 mmol) to prepare the diazonium salt **324g**. As in the general method, this was added to chromotropic acid **301** (7.040 g @ 71.13%, 15.63 mmol), in water (25 cm^3) and Na_2CO_3 (1.433 g, 13.52 mmol). The yield of the reaction was then calculated using QHPLC to give 4,5-dihydroxy-3-(4-nitrophenylazo)naphthalene-2,7-disulfonic acid **302g** (5.293 g, 72%). Product recovery and purification as in the general method gave the *p*-nitroPACA **302g** in the disodium salt form as a dark blue/purple solid (4.295 g, 58%), mp > 330 ºC; (Found: C, 36.9; H, 2.3; N, 8.7. $C_{16}H_9N_3Na_2O_{10}S_2$ requires C, 37.4; H, 1.8; N, 8.2%); δ_H (360 MHz, $[^2H]_6$DMSO) 8.23 (2H, d, *J* 9.2, ArH), 7.94 (2H, d, *J* 9.2, ArH), 7.58 (1H, s, ArH), 7.43 (1H, d, ^4J 1.3, ArH) and 7.15 (1H, d, ^4J 1.3, ArH); δ_C (90 MHz, $[^2H]_6$DMSO) 182.09 (quat), 163.32 (quat), 155.17 (quat), 148.03 (quat), 144.19 (quat), 142.91 (quat), 136.81 (quat), 129.85 (quat), 125.69 (2 × CH), 123.79 (CH), 117.87 (2 × CH), 117.78 (CH), 115.68 (quat) and 113.20 (CH); *m/z* (ESI): 489.7 $[MNa]^-$.

The strength of the monoazo was estimated to be 96% by CHN and HPLC analysis.

4,5-Dihydroxy-3-(4-methylphenylazo)naphthalene-2,7-disulfonic acid 302c

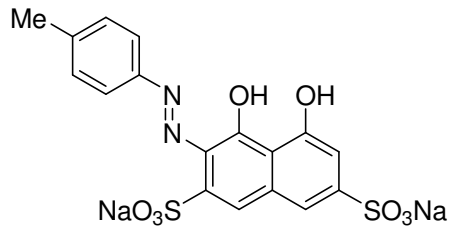

The general method was applied with *p*-toluidine (1.740 g, 16.24 mmol), water (15 cm^3), HCl (conc., 5 cm^3), sodium nitrite (1.140 g, 16.52 mmol), NaOAc (1.014 g, 12.36 mmol) to prepare the diazonium salt **324c**. As in the general method, this was added to chromotropic acid **301** (7.131 g @ 71.13%, 15.84 mmol), in water (25 cm^3) and Na_2CO_3 (1.4327, 13.46 mmol). The yield of the reaction was then calculated using QHPLC to give 4,5-dihydroxy-3-(4-methylphenylazo)naphthalene-2,7-disulfonic acid **302c** (5.871 g, 85%). Product recovery and purification as in the general method gave the *p*-methylPACA **302c** in

the disodium salt form as a dark blue/purple solid (3.037 g, 40%), mp > 330 ºC; (Found: C, 34.6; H, 3.6; N, 4.5. $C_{17}H_{12}N_2Na_2O_8S_2.4.5H_2O.0.5NaCl$ requires C, 34.5; H, 3.6; N, 4.7%); δ_H ($[^2H]_6$DMSO) 7.74 (2H, d, ^3J 8.2, ArH), 7.51 (1H, s, ArH), 7.41 (1H, s, ArH), 7.28 (2H, d, ^3J 8.2, ArH), 7.09 (1H, s, ArH) and 2.32 (3H, s, CH_3); δ_C ($[^2H]_6$DMSO) 179.39 (quat), 162.46 (quat), 154.20 (quat), 143.42 (quat), 139.82 (quat), 136.58 (quat), 136.51 (quat), 130.07 (2 × CH), 127.48 (quat), 120.42 (CH), 117.88 (2 × CH), 116.53 (CH), 115.74 (quat), 111.33 (CH) and 20.80 (CH_3); *m/z* (ESI): 458.6 $[MNa]^-$.

The strength of *p*-methylPACA **302c** was estimated to be 79% by CHN and HPLC analysis.

4,5-Dihydroxy-3-(4-chlorophenylazo)naphthalene-2,7-disulfonic acid 302e

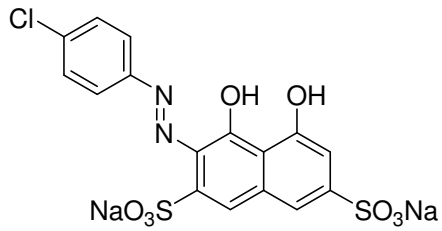

The general method was applied with *p*-chloroaniline (2.075 g, 16.27 mmol), water (15 cm^3), HCl (conc., 5 cm^3), sodium nitrite (1.157 g, 16.77 mmol), NaOAc (1.014 g, 12.36 mmol) to prepare the diazonium salt **324e**. As in the general method, this was added to chromotropic acid **301** (7.049 g @ 71.13%, 15.65 mmol), in water (25 cm^3) and Na_2CO_3 (1.429 g, 13.48 mmol). The yield of the reaction was then calculated using QHPLC to give 4,5-dihydroxy-3-(4-chlorophenylazo)naphthalene-2,7-disulfonic acid **302e** (4.946 g, 69%). Product recovery and purification as in the general method gave the *p*-chloroPACA **302e** in the disodium salt form as a dark blue/purple solid (5.658 g, 72%), mp > 330 ºC; (Found: C, 32.7; H, 2.7; N, 4.7. $C_{16}H_9ClN_2Na_2O_8S_2.3H_2O.0.5NaCl$ requires C, 32.8; H, 2.6; N, 4.8%); δ_H ($[^2H]_6$DMSO) 7.85 (2H, d, ^3J 8.9, ArH), 7.50 – 7.54 (3H, m, ArH), 7.38 (1H, d, ^4J 0.9, ArH) and 7.09 (1H, d, ^4J 1.0, ArH); δ_C ($[^2H]_6$DMSO) 180.45 (quat), 162.57 (2 × quat), 154.83 (quat), 143.39 (quat), 136.59 (quat), 130.13 (quat), 129.39 (2 × CH), 127.96 (quat), 121.13 (CH), 119.20 (2 × CH), 116.73 (CH), 115.35 (quat) and 111.73 (CH), *m/z* (ESI): 478.7 $[MNa]^-$.

The strength of *p*-chloroPACA **302e** was estimated to be 79% by CHN and HPLC analysis.

3-(4-Acetylamino-3-sulfophenylazo)-4,5-dihydroxynaphthalene-2,7-disulfonic acid 302j

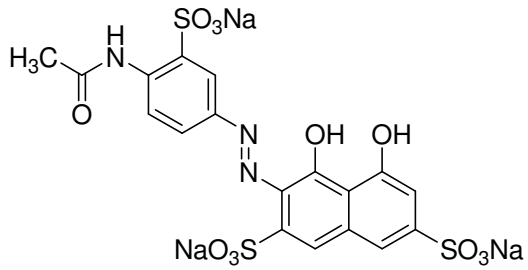

The earlier general method was applied with 2-acetylamino-5-aminobenzenesulfonic acid **270** (3.739 g, 16.24 mmol), water (15 cm^3), HCl (conc.,5 cm^3), sodium nitrite (1.198 g, 17.36 mmol), NaOAc (1.024 g, 12.48 mmol) to prepare the diazonium salt **324j**. As in the general method, this was added to chromotropic acid **301** (7.047 g @ 71.13%, 15.65 mmol), in water (25 cm^3) and Na_2CO_3 (1.437, 13.56 mmol). The yield of the reaction was then calculated using QHPLC to give 3-(4-acetylamino-3-sulfo-phenylazo)-4,5-dihydroxy-naphthalene-2,7-disulfonic acid **302j** (7.518 g, 86%). Product recovery and purification as in the general method gave the monoPACA **302j** in the disodium salt form as a dark blue/purple solid (8.095 g, 82%), mp > 330 ºC; (Found: C, 31.5; H, 2.7; N, 5.9. $C_{18}H_{12}N_3Na_3O_{12}S_3.3H_2O$ requires C, 31.7; H, 2.7; N, 6.2%); δ_H ($[^2H]_6$DMSO) 10.33 (1H, s, NH), 8.41 (1H, d, ^3J 9.0, ArH), 8.06 (1H, d, ^4J 2.3, ArH), 7.90 (1H, dd, ^3J 8.9, ^4J 2.3, ArH), 7.54 (1H, s, ArH), 7.43 (1H, s, ArH), 7.11 (1H, s, ArH) and 2.12 (3H, s, CH_3); δ_C ($[^2H]_6$DMSO) 179.57 (2 × quat), 167.90 (quat), 162.43 (quat), 154.26 (quat), 143.13 (quat), 136.46 (quat), 135.90 (quat), 133.76 (quat), 127.66 (quat), 121.08 (CH), 120.69 (CH), 118.67 (CH), 116.96 (CH), 116.67 (CH), 115.66 (quat), 111.52 (CH) and 24.98 (CH_3); *m*/*z* (ESI): 603.7 $[MNa]^-$.

The strength of the monoazo **302j** was estimated to be 88% by CHN and HPLC analysis.

4,5-Dihydroxy-3-(2-methoxyphenylazo)naphthalene-2,7-disulfonic acid 302h

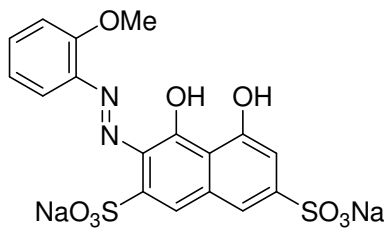

The earlier general method was applied with *o*-anisidine (1.994 g, 16.19 mmol), water (15 cm^3), HCl (conc., 5 cm^3), sodium nitrite (1.185 g, 17.17 mmol), NaOAc (1.026 g, 12.50 mmol) to prepare the diazonium salt **324h**. As in the general method, this was added to chromotropic acid **301** (7.049 g @ 71.13%, 15.65 mmol), in water (25

cm^3) and Na_2CO_3 (1.434 g, 13.53 mmol). The yield of the reaction was then calculated using QHPLC to give 4,5-dihydroxy-3-(2-methoxyphenylazo)naphthalene-2,7-disulfonic acid **302h** (6.078 g, 85%). Product recovery and purification as in the general method gave the *o*-methoxyPACA **302h** in the disodium salt form as a dark blue/purple solid (3.986 g, 72%), mp > 330 ºC; (Found: C, 38.3; H, 3.0; N, 5.0. $C_{17}H_{16}N_2Na_2O_{11}S_2.2H_2O$ requires C, 38.2; H, 3.0; N, 5.2%); δ_H ($[^2H]_6$DMSO) 8.02 (1H, d, ^3J 7.8, ArH), 7.53 (1H, s, ArH), 7.41 (1H, s, ArH), 7.21 – 7.29 (2H, m, ArH), 7.10 – 7.14 (2H, m, ArH) and 4.02 (3H, s, CH_3); δ_C ($[^2H]_6$DMSO) 179.80 (quat), 162.39 (quat), 154.54 (quat), 148.59 (quat), 143.39 (quat), 136.50 (quat), 130.48 (quat), 128.41 (quat), 127.48 (CH), 121.61 (CH), 120.69 (CH), 116.60 (2 × CH), 115.49 (quat), 111.98 (CH), 111.44 (CH) and 56.37 (CH_3); *m*/*z* (ESI): 474.8 $[MNa]^-$.

The strength of *o*-methoxyPACA **302h** was estimated to be 89% by CHN and HPLC analysis.

6.6.2: Bisazo Coupling Reactions

a) Electronic Effects of the Diazonium Salt

302 X = **a**:OMe, **g**: NO_2

324 Y = **a**: OMe, **b**: OEt, **c**:Me, **d**: H, **e**: Cl, **f**: CN, **g**: NO_2

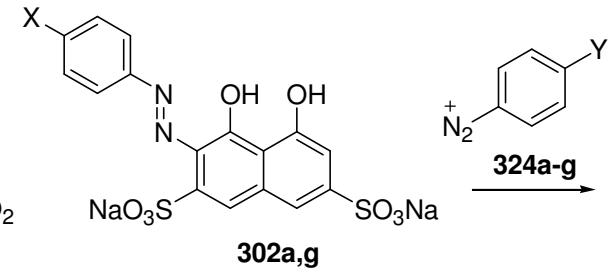

302a,g

Reactivity of the *p*-nitroPACA **302g** and *p*-methoxyPACA **302a** towards a number of *p*-substituted benzenediazonium salts **324a-g** with varying electron donating strength / electron withdrawing strength of the *p*-substituent was examined (*p*-substituents: OMe, OEt, Me, H, Cl, CN, NO_2). Products and by-products in this and subsequent bisazo coupling reaction mixtures were identified by LCMS and the yields calculated using QHPLC.

Standard Preparative Route

MonoPACA preparation

MonoPACAs **302a,g** were prepared on a 15.61 mmol scale as described in the earlier general method with a fresh monoPACAs **302** prepared for each bisazo coupling reaction. MonoPACAs **302** were not isolated from the solution prior to addition of subsequent diazonium salt.

Preparation of bisazo diazonium salt

The appropriate *p*-substituted amine (16.01 mmol) was used to prepare the diazonium salt as in the general method.

Bisazo coupling

To the monoPACA **302** reaction mixture was added NMP (15.5% w/w). The reaction mixture was then cooled to < 5 ºC and the *p*-substituted diazonium salt **324** solution added dropwise over 30 min with constant stirring. The pH was maintained at pH 6.0

– 7.0 by addition of NaOH (2M) as required. The reaction mixture was stirred at T < 5 ºC for 4 h and overnight at room temperature to allow completion of reaction.

i) *p*-NitroPACA 302g Reactivity

Table 6.6.1: QHPLC yields (%) of products in reaction mixtures

p-substituent	*p*-nitroPACA **302g**	*p*-nitrobisPACA **306g**	*ipso* monoPACA **304**	*ipso* bisPACA **305**	unsymmetrical 2,7-bisPACA **303**
d: H	98	2	0	0	0
e: Cl	71	5	0	7	16
f: CN	51	5	1	14	29

The remainder of the series was not carried out due to the absence of reaction with benzenediazonium salt hence further reaction would not be expected with less reactive diazonium salts with electron donating substitents

ii) *p*-MethoxyPACA 302a Reactivity

Table 6.6.2: QHPLC yields (%) of products in reaction mixtures

p-substituent	*p*-methoxyPACA **302a**	*p*-methoxybisPACA **306a**	*ipso* monoPACA **304**	*ipso* bisPACA **305**	unsymmetrical 2,7-bisPACA **303**
b: OEt	42	3	42	7	5
c: Me	46	0	50	0	4
d: H	14	0	71	0	15
e: Cl	3	0	71	10	16
f: CN	3	0	38	3	56
g: NO_2	0	0	49	9	42

b) Electronic Effects of MonoPACA *para*-Substituent

302 X = **a**: OMe, **c**: Me,
e: Cl, **g**: NO_2

324 Y = **d**: H, **f**: CN

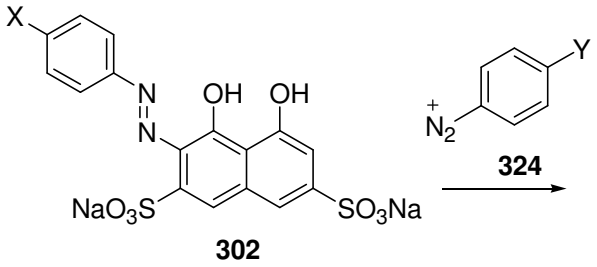

302

Reactivity of a series of monoPACAs **302 a,c,e,g** to the benzene and *p*-cyanobenzene diazonium salts **324d,f** was examined to assess the electronic effect of the *p*-substituent upon the yields of products. A series of monoPACAs were prepared with *p*-substituent altered (*p*-substituents: OMe, Me, Cl, NO_2). Fresh samples of the monoPACAs were prepared for each experiment.

Standard Preparative Route

MonoPACA preparation

MonoPACAs **302a,c,e,g** were prepared on a 15.61 mmol scale as described earlier with a fresh monoazo prepared for each bisazo coupling. The monoPACAs **302** were not isolated from the solution prior to addition of subsequent benzenediazonium salt **324d** or *p*-cyanobenzenediazonium salt **324f** during bisazo coupling.

Bisazo coupling

The monoPACAs **302** which was cooled to < 5 ºC and NMP (15.5% w/w) added. The reaction mixture was then treated with the benzenediazonium salt **324d** (Table 6.6.3) or *p*-cyanobenzenediazonium salt **324f** (Table 6.6.4) dropwise over 30 min with constant stirring. The pH was maintained at pH 6.0 – 7.0 by addition of NaOH (2M) as required. The reaction mixture was stirred at T < 5 ºC for 4 h and overnight at room temperature.

Table 6.6.3: i) Benzenediazonium salt expt QHPLC yields (%) of products in reaction mixtures

p-substituent	*p*-substituted monoPACA **302**	*p*-substituted bisPACA **306**	*ipso* monoPACA **304d**	*ipso* bisPACA **305d**	unsymmetrical 2,7-bisPACA **303**
a: OMe	14	0	71	0	15
c: Me	90	2	6	2	0
e: Cl	74	6	10	0	11
g: NO_2	98	2	0	0	0

Table 6.6.4: ii) *p*-Cyanobenzenediazonium salt expt QHPLC yields (%) of products in reaction mixtures

p-substituent	*p*-substituted monoPACA **302**	*p*-substituted bisPACA **306**	*ipso* monoPACA **304f**	*ipso* bisPACA **305f**	unsymmetrical 2,7-bisPACA **303**
a: OMe	3	0	38	3	56
c: Me	15	3	38	13	32
e: Cl	6	9	34	15	36
g: NO_2	51	1	5	14	29

c) Reactivity of Isolated MonoPACA rather than *In-situ* MonoPACA

The reactivity of an isolated *p*-methoxyPACA **302a** towards a diazonium salt was then compared with the reaction of the same monoazo prepared *in-situ*.

Monoazo preparation

The *p*-methoxyPACA **302a** (8.766 g, strength 89%, 15.28 mmol) was stirred in a water (25 cm^3) and Na_2CO_3 (1.377 g, 12.99 mmol) and NMP (6.644 g, 15.5% w/w) added. The reaction mixture was then cooled to < 5 ºC.

Preparation diazonium salt

The *p*-cyanodiazonium **324f** was prepared as described in the earlier general method from 4-aminobenzonitrile (15.66 mmol), water (15 cm^3), HCl conc. (5 cm^3) and sodium nitrite (15.66 mmol). NaOAc (11.90 mmol) was added just before addition to the *p*-methoxyPACA **302a** reaction mixture.

Bisazo coupling

The *p*-cyanodiazonium salt **324f** solution was cooled to < 5 ºC and added to the *p*-methoxyPACA **302a** reaction mixture dropwise over 30 min with constant stirring. The pH was maintained at pH 6.0 – 7.0 by addition of NaOH (2M) and HCl (2M) as required.

Results from previous experiments were used for the *p*-methoxyPACA **302a** prepared *in-situ*.

Table 6.6.5: QHPLC yields (%) of products in reaction mixtures

monoazo	*p*-methoxyPACA **302a**	*p*-methoxybisPACA **306a**	*ipso* monoPACA **304**	*ipso* bisPACA **305**	unsymmetrical 2,7-bisPACA **303**
In-situ	3	0	38	3	56
Isolated	19	2	27	2	51

d) Electronic Effects of the Diazonium Salt (Accurately Buffered pH Solutions)

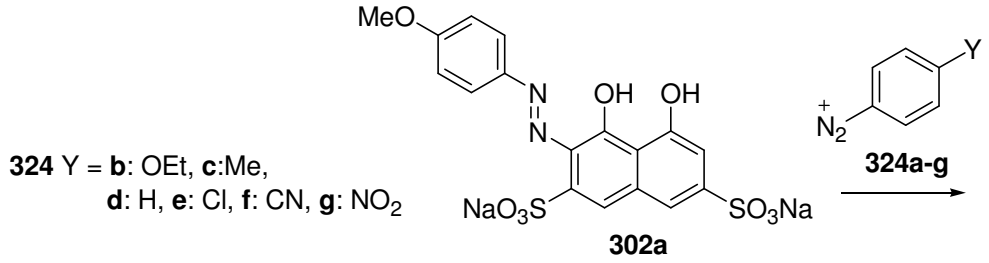

The reactivity of *p*-methoxyPACA **302a** towards a number of *p*-substituted benzenediazonium salts **324b-g** was repeated on a smaller scale with all reagents in complete solution. The pH was controlled with accurately buffered solutions.

MonoPACA preparation

The *p*-methoxyPACA **302a** (1.0 g, strength 87%, 1.75 mmol) was stirred in a buffer solution (10 cm^3, pH 6.0) until all solids were in solution and NMP (1.65 g, 15.5% w/w) was added.

Preparation of diazonium salt

The diazonium salt **324** of the appropriate *p*-substituted amine (1.80 mmol) was prepared as described in the earlier general method with water (2.4 cm^3), HCl (conc., 0.8 cm^3) and sodium nitrite (2.00 mmol). NaOAc (1.51 mmol) was added just before addition to the monoazo reaction mixture.

Bisazo coupling

The *p*-substituted diazonium salt **324** solution was cooled to < 5 ºC and added to the monoPACA **302a** reaction mixture dropwise over 10 min with constant stirring. The pH was maintained at pH 6.0 by addition of NaOH (2M) and HCl (2M) as required. The reaction mixture was stirred at < 5 ºC for 4 h and overnight at room temperature.

Table 6.6.6: QHPLC yields (%) of products in reaction mixtures

p-substituent	*p*-methoxy PACA **302a**	*p*-methoxybis PACA **306a**	*Ipso* monoPACA **304**	*ipso* bisPACA **305**	unsymmetrical 2,7-bisPACA **303**
b: OEt	64	5	23	4	4
c: Me	41	6	42	6	5
d: H	52	0	34	0	13
e: Cl	22	0	62	7	9
f: CN	26	0	37	4	33
g: NO_2	10	0	45	9	36

e) Electronic Effects of MonoPACA *para*-Substituent on Bisazo Coupling (Accurately Buffered pH Solutions)

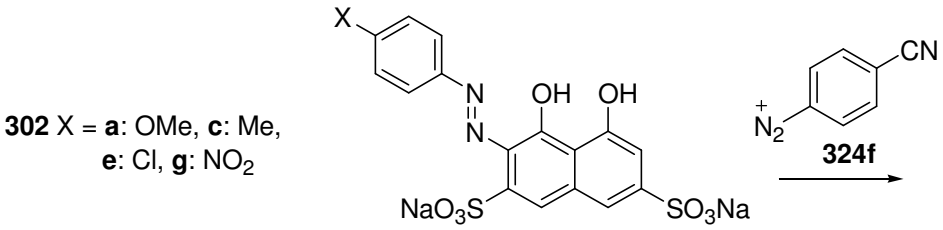

Reactivity of a series of monoPACAs **302a,c,e,g** to the *p*-cyanobenzenediazonium salt **324f** was repeated on a smaller scale with all reagents in complete solution. The pH was controlled with accurately buffered solutions.

Monoazo preparation

The monoPACAs **302a,c,e,g** (1.0 g, 1.75 mmol) were stirred in a buffer solution (10 cm^3, pH 6.0) until all the solids were in solution and NMP (1.65 g, 15.5% w/w) added (Table 6.6.7).

Table 6.6.7: Weight and strength of monoPACAs used

MonoPACA	Weight	Strength %	mmol
a: OMe	1.012 g	86.86	1.76
c: Me	1.075 g	78.62	1.75
e: Cl	1.118 g	78.76	1.75
g: NO_2	0.933 g	96.27	1.75

Bisazo coupling

The monoPACA **302a,c,e,g** reaction mixture was cooled to < 5 ºC and treated with the *p*-cyanobenzenediazonium salt **324f** dropwise over 10 min with constant stirring. The pH was maintained at pH 6.0 by addition of NaOH (2M) and HCl (2M) as required. The reaction mixture was stirred at < 5 ºC for 4 h and overnight at room temperature.

Table 6.6.8: ii) *p*-Cyanobenzenediazonium salt **324f** expt QHPLC yields (%) of products in reaction mixtures

p-substituent	*p*-substituted monoPACA **302**	*p*-substituted bisPACA **306**	*ipso* monoPACA **304f**	*ipso* bisPACA **305f**	unsymmetrical 2,7-bisPACA **303**
a: OMe	26	0	37	4	33
c: Me	17	8	42	6	27
e: Cl	11	16	32	11	31
g: NO_2	34	14	3	15	34

f) Effect of pH upon Bisazo Coupling

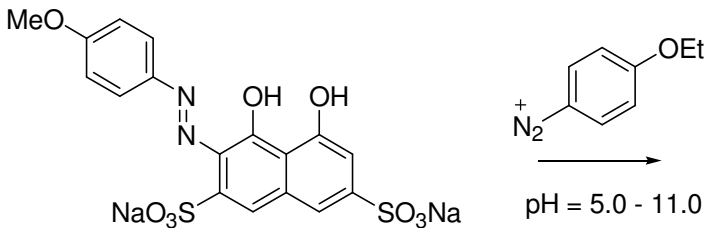

The reactivity of *p*-methoxyPACA **302a** towards a *p*-ethoxybenzenediazonium salt **324b** was studied at pH range 5.0 – 11.0.

Monoazo preparation

The *p*-methoxyPACA **302a** (1.0 g, strength 87%, 1.75 mmol) was stirred in an appropriate buffer solution (10 cm^3) until all the solids had dissolved and NMP (1.65 g, 15.5% w/w) was added.

Preparation of diazonium salt

The *p*-ethoxybenzenediazonium salt **324b** was prepared as described in the earlier general method from *p*-phenetidine (1.80 mmol), water (2.4 cm^3), HCl conc. (0.8 cm^3) and sodium nitrite (2.00 mmol). NaOAc (1.51 mmol) was added just before addition to the *p*-methoxyPACA **302a** reaction mixture.

Bisazo coupling

The *p*-methoxyPACA **302a** reaction mixture was cooled to < 5 ºC and treated with the *p*-ethoxybenzenediazonium salt **324b** reaction mixture dropwise over 10 min with constant stirring. The pH was maintained by addition of NaOH (2M) and HCl (2M) as required. The reaction mixture was stirred at T < 5 ºC for 4 h and overnight at room temperature.

Table 6.6.9: QHPLC yields (%) of products in reaction mixtures

pH	*p*-methoxy PACA **302a**	*p*-methoxybis PACA **306a**	*ipso* monoPACA **304**	*ipso* bisPACA **305**	unsymmetrical 2,7-bisPACA **303**
5.0	93	2	3	1	1
7.0	62	6	19	3	10
8.0	44	6	34	5	11
9.0	23	13	24	14	25
10.0	12	18	12	22	36
11.0	8	19	8	25	39

g) Effect of NMP % upon Bisazo Coupling

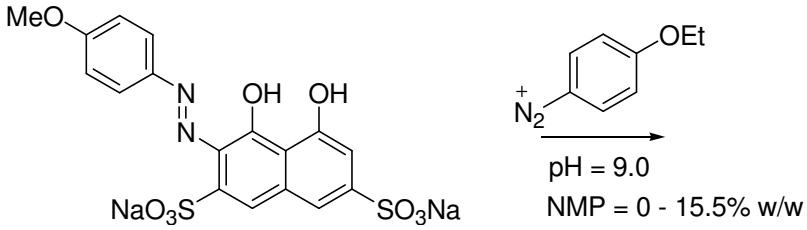

The reactivity of *p*-methoxyPACA **302a** towards a *p*-ethoxybenzenediazonium salt **324b** was studied at a range of NMP % w/w.

Monoazo preparation

The *p*-methoxyPACA **302a** (1.0 g, strength 87%, 1.75 mmol) was stirred in a buffer solution (10 cm^3, pH 9.0) until all the solids had dissolved and NMP (0%, 10% or 15.5% w/w) was added as appropriate.

Preparation of diazonium salt

The *p*-ethoxybenzenediazonium salt **324b** was prepared as described earlier from *p*-phenetidine (1.80 mmol), water (2.4 cm^3), HCl (conc., 0.8 cm^3) and sodium nitrite

(2.00 mmol). NaOAc (1.51 mmol) was added just before addition to the monoPACA reaction mixture.

Bisazo coupling

The *p*-methoxyPACA **302a** reaction mixture was cooled to < 5 ºC and treated with the *p*-ethoxybenzenediazonium salt **324b** reaction mixture dropwise over 10 min with constant stirring. The pH was maintained at pH 9.0 by addition of NaOH (2M) and HCl (2M) as required. The reaction mixture was stirred at < 5 ºC for 4 h and overnight at room temperature.

Table 6.6.10: QHPLC yields (%) of products in reaction mixtures

NMP % w/w	*p*-methoxy PACA **302a**	*p*-methoxybis PACA **306a**	*ipso* monoPACA **304**	*ipso* bisPACA **305**	unsymmetrical 2,7-bisPACA **303**
0	10	19	12	21	38
10	18	16	19	17	31
15.5	16	20	17	16	31

h) Steric Effects

i) *Ortho / para* Methoxy Substituents

302a: X = OMe, Y = H
302h: X = H, Y = OMe

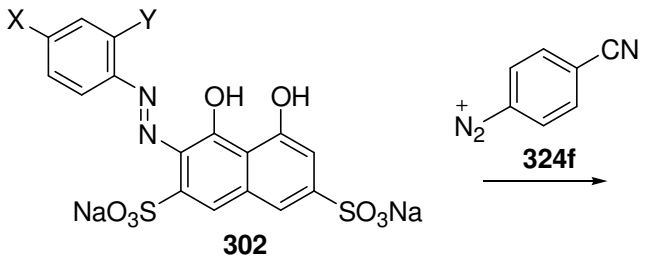

302 **324f**

The reactivity of *o*-methoxyPACA **302h** and *p*-methoxyPACA **302a** were compared by reaction with a single diazonium salt.

Monoazo preparation

The *o*-methoxyPACA **302h** (1.0 g, strength 89%, 1.75 mmol) was stirred in a buffer solution (pH 6.0, 10 cm^3) until all the solids had dissolved and NMP (1.65 g, 15.5% w/w) was added.

Preparation of bisazo diazonium salt

The *p*-cyanobenzenediazonium salt **324f** was prepared as described earlier from 4-aminobenzonitrile (1.80 mmol), water (2.4 cm^3), HCl conc. (0.8 cm^3) and sodium nitrite (2.00 mmol). NaOAc (1.51 mmol) was added just before addition to the monoazo reaction mixture.

Bisazo coupling

The diazonium salt **324f** solution was then added dropwise over 10 min with constant stirring to the monoPACA **302h** reaction mixture which was cooled to < 5 ºC. The pH was maintained at pH 6.0 by addition of NaOH (2M) and HCl (2M) as required.

Table 6.6.11: QHPLC yields (%) of products in reaction mixtures

monoPACA	methoxy PACA **302**	methoxy bisPACA **306**	*ipso* monoPACA **304**	*ipso* bisPACA **305**	unsymmetrical 2,7-bisPACA **303**
a: *p*-methoxyPACA	26	0	37	4	32
h: *o*-methoxyPACA	74	0	5	0	21

ii) *Ortho* / *meta* Sulfonic Acid Substituents

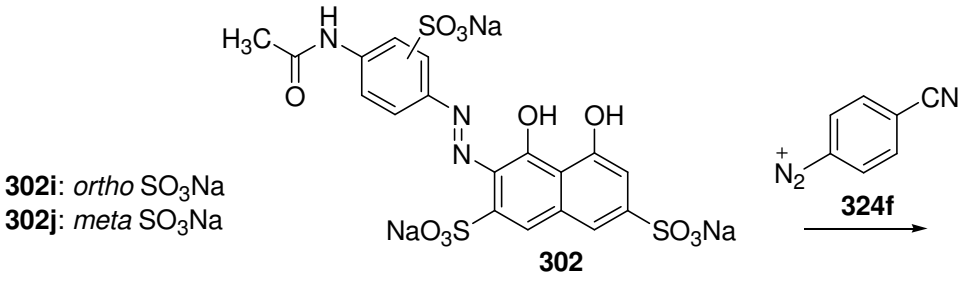

The reactivity of an *ortho* sulfonic acid substituted monoPACA **302i** and a *meta* sulfonic acid substituted monoPACA **302j** were compared by reaction with a single diazonium salt **324f**.

Monoazo preparation

The monoPACA **302i** (1.322 g, strength 74%, 1.75 mmol) was stirred in a buffer solution (pH 6.0, 10 cm^3) until all solids had dissolved and NMP (1.65 g, 15.5% w/w) was added.

Preparation of bisazo diazonium salt

The *p*-cyanobenzenediazonium salt **324f** was prepared as described in the previous section (Section 6.6.2 h i).

Bisazo coupling

The *p*-substituted diazonium salt **324f** solution was then added dropwise over 10 min with constant stirring to the monoazo reaction mixture which was cooled to < 5 ºC. The pH was maintained at pH 6.0 by addition of NaOH (2M) and HCl (2M) as required.

This experiment was then repeated with the monoPACA **302j** (1.249 g, strength 88%, 1.75 mmol).

Table 6.6.12: QHPLC yields (%) of products in reaction mixtures

monoPACA	monoPACA **302**	bisPACA **306**	*ipso* monoPACA **304**	*ipso* bisPACA **305**	unsymmetrical 2,7-bisPACA **303**
monoPACA **302i**	18	0	4	11	67
monoPACA **302j**	24	4	17	24	31

In calculating the QHPLC yields of these products due to the usual internal standard (Mono186) being a possible reaction product the methoxyPACA **302a** (87% strength) was used as an alternative monoazo internal standard.

i) Stability of Diazonium Salts under Bisazo Coupling Reaction Conditions

The stability of the *p*-cyanobenzenediazonium salt **324f** under bisazo coupling conditions was studied.

Preparation of the *p*-cyanobenzenediazonium salt **324f**

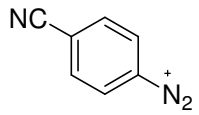

The earlier general method for the preparation of diazonium salts was applied with *p*-aminobenzonitrile (0.417 g, 3.53 mmol), water (3.25 cm^3), HCl conc. (1.25 cm^3) and sodium nitrite (0.259 g, 3.75 mmol). The pH of the diazonium salt solution was then adjusted to 6.0 by the addition of an acetic acid/sodium acetate buffer solution (5 cm^3) and NMP (10%w/w) added. The pH was further adjusted by additions of NaOH (2M) as required and the temperature maintained at < 5 ºC with the use of an ice bath.

Bisazo coupling

Weighted portions of the diazonium salt solution **324f** were then added to samples of the isolated *p*-methoxyPACA **302a** (0.5 g, 0.88 mmol) in buffer solution (pH 6.0, 10 cm^3) at certain time intervals after preparation of the diazonium salt (T = 0, 0.5 h, 2 h, 4 h) The temperature was maintained at < 5 ºC and pH maintained at 6.0 by addition of NaOH (2 M) as required. The reaction mixtures were then stirred for 4 h at < 5 ºC and overnight at room temperature.

Table 6.6.13: QHPLC yields (%) of products in reaction mixtures

Time after preparation of diazo (h)	monoPACA **302**	bisPACA **306**	*ipso* monoPACA **304**	*ipso* bisPACA **305**	unsymmetrical 2,7-bisPACA **303**
0	16	2	39	3	41
0.5	13	2	40	2	42
2.0	17	2	38	1	42
4.0	14	2	50	1	34

j) Stability of Diazonium Salts under Bisazo Coupling Reaction Conditions Pyrazolone Method

4-[(4-Methoxyphenyl)hydrazono]-5-methyl-2,4-dihydropyrazol-3-one 326a

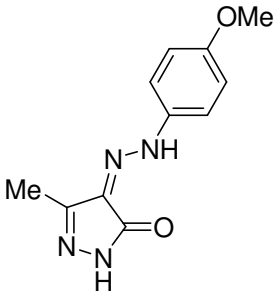

p-Anisidine (1.009 g, 8.19 mmol) was stirred in water (7 cm^3) and conc. HCl (2.5 cm^3). The reaction mixture was cooled to 0 ºC and sodium nitrite (0.593 g, 8.59 mmol) added slowly ensuring the temperature did not rise above 5 ºC. The reaction mixture was then stirred at < 5 ºC for 1 h and quenched with 3-methylpyrazolone **325** solution (50 cm^3, 0.306 mmol dm^{-3}, 15.29 mmol). An orange precipitate formed which was filtered and dried to afford the coupled pyrazolone **326a** as an orange solid (1.901 g, > 99%), δ_H ($[^2H]_6$DMSO) 11.16 (1H, s, NH), 7.47 (2H, d, ^3J 9.1, ArH), 6.94 (2H, ^3J 9.1, ArH), 3.75 (3H, s, CH_3) and 2.14 (3H, s, CH_3); δ_C ($[^2H]_6$DMSO) 159.48 (quat), 156.95 (2 × quat), 146.22 (quat), 125.45 (quat), 118.26 (2 × CH), 114.37 (2 × CH), 55.25 (CH_3) and 12.12 (CH_3).

4-[(4-Ethoxyphenyl)hydrazono]-5-methyl-2,4-dihydropyrazol-3-one 326b

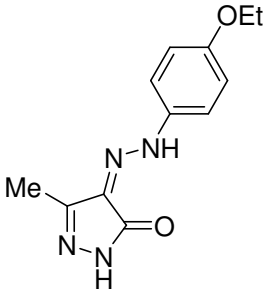

The above method was also applied to *p*-phenetidene (1.133 g, 8.26 mmol), water (7 cm^3), conc. HCl (2.5 cm^3), sodium nitrite (0.601 g, 8.71 mmol) and 3-methylpyrazolone **325** solution (50 cm^3, 0.306 mmol dm^{-3}, 15.29 mmol) to afford an orange precipitate (2.691 g). Problems with the solubility of the *p*-ethoxyphenyl coupled pyrazolone **326b** prevnted full characterisation although the HPLC retention time required for the future experiment was obtained.

k) The Effect of NMP upon Bisazo Coupling and Progress of Reaction

The stability of diazonium salts under the reaction conditions and progress of reactions could then be obtained by sampling reaction mixtures (≈ 0.2 g, 0.02 mmol) at time intervals and quenching with pyrazolone solution (1 cm^3, 0.31 mmol). HPLC analysis of the resulting quenched solutions showed the reaction products and any remaining diazonium salt as a pyrazolone species and gave the progress of the reaction with time (Tables 6.6.14, 6.6.15 and 6.6.16).

However, problems with the solubility of the pyrazolone species in comparison to the sulfonic acid products meant no accurate comparison could be made between these species to give a quantitative measure of the yield of each diazonium salt remaining in the reaction mixture.

1) 15.5% w/w NMP

Table 6.6.14: QHPLC yields (%) of products in reaction mixtures

Time (mins)	monoPACA **302**	bisPACA **306**	*ipso* monoPACA **304**	*ipso* bisPACA **305**	unsymmetrical 2,7-bisPACA **303**
1	39	8	37	5	12
2	40	7	38	4	11
5	35	10	35	7	13
10	35	10	35	6	14
20	38	8	37	5	12
40	36	9	34	6	15
80	28	13	29	9	21
120	27	13	26	11	23
180	21	15	21	15	28
240	22	15	22	15	27
1200	17	16	19	19	30

2) 10.0% w/w NMP

Table 6.6.14: QHPLC yields (%) of products in reaction mixtures

Time (mins)	monoPACA **302**	bisPACA **306**	*ipso* monoPACA **304**	*ipso* bisPACA **305**	unsymmetrical 2,7-bisPACA **303**
1	60	4	28	2	6
2	54	5	31	4	7
5	50	5	34	4	7
10	45	5	38	5	7
20	44	5	41	3	7
40	42	5	41	4	8
80	35	8	36	8	12
120	34	8	35	8	15
180	32	10	31	10	17
240	25	13	24	13	25
1200	18	16	19	17	31

3) 0% w/w NMP

Table 6.6.16: QHPLC yields (%) of products in reaction mixtures

Time (mins)	monoPACA **302**	bisPACA **306**	*ipso* monoPACA **304**	*ipso* bisPACA **305**	unsymmetrical 2,7-bisPACA **303**
1	35	13	27	7	18
2	33	14	28	7	18
5	30	14	32	6	18
10	27	15	28	8	22
20	21	15	24	14	26
40	12	18	14	20	35
80	12	18	13	22	35
120	10	19	10	23	38
180	10	18	12	23	37
240	10	18	11	23	38
1200	10	18	12	23	38

7.0: Appendices

Appendix 1: Crystal Data

Crystal Structure of 240k

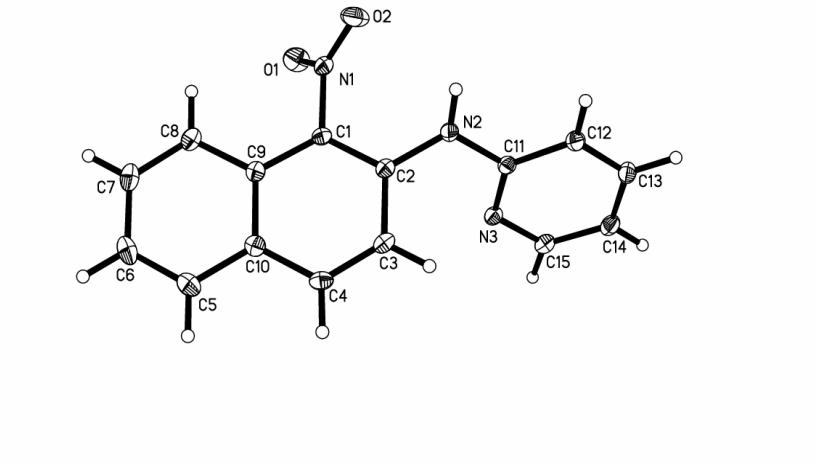

A: CRYSTAL DATA

Empirical formula	C15 H11 N3 O2
Formula weight	265.27
Wavelength	0.71073 A
Temperature	150 K
Crystal system	Orthorhombic
Space group	P b c a
Unit cell dimensions	a = 15.4664(7) A alpha = 90 deg.
	b = 7.8752(3) A beta = 90 deg.
	c = 20.1933(9) A gamma = 90 deg.
Volume	2459.56(18) A^3
Number of reflections for cell	3844 (2 < theta < 26 deg.)
Z	8
Density (calculated)	1.433 Mg/m^3
Absorption coefficient	0.099 mm^{-1}
F(000)	1104

B. DATA COLLECTION

Crystal description	yellow block
Crystal size	0.44 x 0.15 x 0.14 mm
Instrument	Bruker SMART Apex CCD
The ta range for data collection	2.017 to 30.551 deg.
Index ranges	-21<=h<=22, -11<=k<=11, -26<=l<=27
Reflections collected	24460
Independent reflections	3676 [R(int) = 0.023]
Scan type	\f & \w scans
Absorption correction	Semi-empirical from equivalents (Tmin= 0.67, Tmax=0.99)

C. SOLUTION AND REFINEMENT.

Solution	direct (SHELXS 86 (Sheldrick, 1986))
Refinement type	Full-matrix least-squares on F^2
Program used for refinement	CRYSTALS
Hydrogen atom placement	geom
Hydrogen atom treatment	constr
Data	3676
Parameters	181
Goodness-of-fit on F^2	0.7366
Conventional R [F>4sigma(F)]	R1 = 0.0395 [2036 data]
Rw	0.0911
Final maximum delta/sigma	0.000307
Weighting scheme	Sheldrick Weights
Largest diff. peak and hole	0.28 and -0.17 e.A^-3

Table 7.1: Atomic coordinates (x 10^4) and equivalent isotropic displacement parameters (A^2 x 10^3) for **240k**. U(eq) is defined as one third of the trace of the orthogonalized Uij tensor.

	x	y	z	U (eq.)
O(1)	4617(1)	7309(1)	864(1)	41
O(2)	4320(1)	9970(1)	974(1)	41
N(1)	4155(1)	8554(1)	761(1)	26
N(2)	2550(1)	9716(1)	1258(1)	24
N(3)	1572(1)	7842(1)	1732(1)	23
C(1)	3364(1)	8308(2)	379(1)	21
C(2)	2592(1)	8841(1)	656(1)	21
C(3)	1823(1)	8457(2)	306(1)	25
C(4)	1844(1)	7627(2)	-280(1)	26
C(5)	2655(1)	6271(2)	-1190(1)	32
C(6)	3421(1)	5773(2)	-1463(1)	35
C(7)	4200(1)	6113(2)	-1137(1)	33
C(8)	4207(1)	6947(2)	-544(1)	28
C(9)	3423(1)	7457(2)	-240(1)	22
C(10)	2633(1)	7112(2)	-573(1)	24
C(11)	1908(1)	9409(2)	1722(1)	22
C(12)	1661(1)	10664(2)	2175(1)	27
C(13)	1053(1)	10263(2)	2646(1)	29
C(14)	691(1)	8650(2)	2657(1)	29
C(15)	966(1)	7506(2)	2190(1)	26

Table 7.2: Bond lengths [A] and angles [deg] for hm0504.

O(1)-N(1)	1.2305(13)
O(2)-N(1)	1.2214(13)
N(1)-C(1)	1.4596(15)
N(2)-C(2)	1.3983(15)

N(2)-C(11)	1.3875(15)
N(2)-H(2)	0.851
N(3)-C(11)	1.3385(15)
N(3)-C(15)	1.3432(15)
C(1)-C(2)	1.3832(16)
C(1)-C(9)	1.4219(17)
C(2)-C(3)	1.4168(17)
C(3)-C(4)	1.3516(19)
C(3)-H(3)	0.947
C(4)-C(10)	1.4161(17)
C(4)-H(4)	0.935
C(5)-C(6)	1.3634(19)
C(5)-C(10)	1.4114(18)
C(5)-H(5)	0.944
C(6)-C(7)	1.398(2)
C(6)-H(6)	0.941
C(7)-C(8)	1.3650(19)
C(7)-H(7)	0.943
C(8)-C(9)	1.4180(17)
C(8)-H(8)	0.945
C(9)-C(10)	1.4206(17)
C(11)-C(12)	1.4002(17)
C(12)-C(13)	1.3747(18)
C(12)-H(12)	0.950
C(13)-C(14)	1.3881(19)
C(13)-H(13)	0.972
C(14)-C(15)	1.3721(18)
C(14)-H(14)	0.944
C(15)-H(15)	0.976
O(1)-N(1)-O(2)	123.16(11)

O(1)-N(1)-C(1)	118.01(10)
O(2)-N(1)-C(1)	118.81(10)
C(2)-N(2)-C(11)	122.30(10)
C(2)-N(2)-H(2)	120.4
C(11)-N(2)-H(2)	116.7
C(11)-N(3)-C(15)	117.55(11)
N(1)-C(1)-C(2)	118.03(11)
N(1)-C(1)-C(9)	118.32(10)
C(2)-C(1)-C(9)	123.57(10)
N(2)-C(2)-C(1)	122.70(11)
N(2)-C(2)-C(3)	119.98(11)
C(1)-C(2)-C(3)	117.32(11)
C(2)-C(3)-C(4)	121.30(11)
C(2)-C(3)-H(3)	116.8
C(4)-C(3)-H(3)	121.9
C(3)-C(4)-C(10)	121.68(11)
C(3)-C(4)-H(4)	118.4
C(10)-C(4)-H(4)	120.0
C(6)-C(5)-C(10)	120.87(13)
C(6)-C(5)-H(5)	120.5
C(10)-C(5)-H(5)	118.6
C(5)-C(6)-C(7)	120.17(13)
C(5)-C(6)-H(6)	120.8
C(7)-C(6)-H(6)	119.0
C(6)-C(7)-C(8)	120.81(13)
C(6)-C(7)-H(7)	119.7
C(8)-C(7)-H(7)	119.4
C(7)-C(8)-C(9)	120.58(13)
C(7)-C(8)-H(8)	120.4
C(9)-C(8)-H(8)	119.0

C(1)-C(9)-C(8)	124.67(11)
C(1)-C(9)-C(10)	116.87(10)
C(8)-C(9)-C(10)	118.46(12)
C(9)-C(10)-C(4)	119.22(11)
C(9)-C(10)-C(5)	119.09(12)
C(4)-C(10)-C(5)	121.69(12)
N(2)-C(11)-N(3)	116.66(11)
N(2)-C(11)-C(12)	120.92(11)
N(3)-C(11)-C(12)	122.35(11)
C(11)-C(12)-C(13)	118.47(12)
C(11)-C(12)-H(12)	120.2
C(13)-C(12)-H(12)	121.4
C(12)-C(13)-C(14)	119.81(12)
C(12)-C(13)-H(13)	120.2
C(14)-C(13)-H(13)	120.0
C(13)-C(14)-C(15)	117.68(12)
C(13)-C(14)-H(14)	121.2
C(15)-C(14)-H(14)	121.1
C(14)-C(15)-N(3)	124.11(12)
C(14)-C(15)-H(15)	120.6
N(3)-C(15)-H(15)	115.2

Table 7.3: Anisotropic displacement parameters (A^2 x 10^3). The anisotropic displacement factor exponent: $-2\ pi^2\ [h^2\ a^{*2}\ U11 + ... + 2\ h\ k\ a^*\ b^*\ U12\ ]$

	U11	U22	U33	U23	U13	U12
O(1)	33(1)	39(1)	50(1)	-2(1)	-13(1)	12(1)
O(2)	32(1)	33(1)	59(1)	-12(1)	-11(1)	-3(1)
N(1)	19(1)	31(1)	28(1)	-2(1)	1(1)	1(1)
N(2)	23(1)	22(1)	28(1)	-4(1)	5(1)	-4(1)
N(3)	20(1)	23(1)	27(1)	1(1)	2(1)	1(1)

C(1)	18(1)	21(1)	24(1)	2(1)	-2(1)	0(1)
C(2)	21(1)	18(1)	24(1)	3(1)	1(1)	0(1)
C(3)	18(1)	26(1)	30(1)	4(1)	1(1)	0(1)
C(4)	22(1)	27(1)	29(1)	4(1)	-6(1)	-2(1)
C(5)	39(1)	30(1)	26(1)	-1(1)	-5(1)	-2(1)
C(6)	53(1)	31(1)	22(1)	-2(1)	4(1)	2(1)
C(7)	39(1)	28(1)	30(1)	3(1)	12(1)	4(1)
C(8)	26(1)	29(1)	29(1)	4(1)	5(1)	1(1)
C(9)	24(1)	20(1)	22(1)	4(1)	1(1)	1(1)
C(10)	27(1)	23(1)	23(1)	3(1)	-1(1)	0(1)
C(11)	18(1)	22(1)	24(1)	-1(1)	-1(1)	2(1)
C(12)	24(1)	23(1)	33(1)	-4(1)	1(1)	1(1)
C(13)	25(1)	36(1)	27(1)	-6(1)	1(1)	5(1)
C(14)	22(1)	39(1)	25(1)	3(1)	3(1)	1(1)
C(15)	22(1)	28(1)	29(1)	4(1)	1(1)	0(1)

Table 7.4: Hydrogen coordinates (x 10^4) and isotropic displacement parameters (A^2 x 10^3) for **67d**.

	x	y	z	U(eq)
H(2)	2874	10573	1326	31
H(3)	1296	8822	499	29
H(4)	1320	7395	-492	30
H(5)	2130	6080	-1415	37
H(6)	3435	5196	-1871	41
H(7)	4726	5742	-1323	38
H(8)	4736	7201	-332	32
H(12)	1919	11759	2158	32
H(13)	865	11114	2964	35
H(14)	280	8342	2981	35
H(15)	737	6351	2182	28

Appendix 2: Dye Testing Results

COLOUR MEASUREMENTS GRETAG MACBETH - NO FILTER (U)
ILLUMINANT - D50

PROTOCOL PATENT II (CANON i965)

Table 7.5: Dye Testing Results for Dyes 192 and 193 (Generic Protocols)

Dye	SUBSTRATE	TEST	DEPTH %	ROD	L	A	B	C	H	DE	% ROD LOSS	FAIL TIME
BCI 7M Control	XEROX 4024	INITIAL	100	1.09	48	61	-22	65	340			
BCI 7M Control	XEROX 4024	INITIAL	70	1.01	51	61	-24	65	338			
BCI 7M Control	HP PREMIUM PLUS MKII	INITIAL	100	2.08	37	86	-34	92	339			
BCI 7M Control	HP PREMIUM PLUS MKII	INITIAL	70	1.54	43	81	-36	89	336			
BCI 7M Control	HP PREMIUM PLUS MKII	LF/NG//100H	70	1.23	48	68	-24	72	341	**19**	**20**	**167**
BCI 7M Control	HP PREMIUM PLUS MKII	LF/NG//200H	70	1.12	51	63	-18	66	344	**27**	**27**	**167**
BCI 7M Control	HP PREMIUM PLUS MKII	OF/1PPM/40C/24H	70	1.53	43	81	-36	89	336	**1**	**1**	**1644**
BCI 7M Control	HP PREMIUM PLUS MKII	OF/1PPM/40C/48H	70	1.52	44	81	-35	88	337	**2**	**1**	**1644**
BCI 7M Control	HP PREMIUM PLUS MKII	OF/1PPM/40C/72H	70	1.52	43	81	-36	88	336	**1**	**1**	**1644**
BCI 7M Control	HP PREMIUM PLUS MKII	OF/1PPM/40C/96H	70	1.52	44	81	-35	88	336	**1**	**1**	**1644**
BCI 7M Control	HP PREMIUM PLUS MKII	OF/5PPM/25C/24H	70	1.53	43	81	-36	89	336	**0**	**1**	**1076**
BCI 7M Control	HP PREMIUM PLUS MKII	OF/5PPM/25C/48H	70	1.52	44	81	-35	88	337	**2**	**1**	**1076**
BCI 7M Control	HP PREMIUM PLUS MKII	OF/5PPM/25C/72H	70	1.53	43	81	-35	88	336	**1**	**1**	**1076**
BCI 7M Control	HP PREMIUM PLUS MKII	OF/5PPM/25C/96H	70	1.53	43	81	-35	88	336	**1**	**1**	**1076**
BCI 7M Control	SEC CRISPIA PHOTO	INITIAL	100	1.86	42	88	-32	94	340			
BCI 7M Control	SEC CRISPIA PHOTO	INITIAL	70	1.48	48	85	-38	93	336			
BCI 7M Control	SEC CRISPIA PHOTO	LF/NG//100H	70	1.24	52	76	-26	80	341	**16**	**16**	**142**
BCI 7M Control	SEC CRISPIA PHOTO	LF/NG//200H	70	0.95	59	64	-18	67	344	**31**	**36**	**142**
BCI 7M Control	SEC CRISPIA PHOTO	OF/1PPM/40C/24H	70	1.46	48	85	-36	92	337	**2**	**1**	**273**
BCI 7M Control	SEC CRISPIA PHOTO	OF/1PPM/40C/48H	70	1.42	50	83	-34	90	338	**5**	**4**	**273**
BCI 7M Control	SEC CRISPIA PHOTO	OF/1PPM/40C/72H	70	1.38	50	82	-33	88	338	**6**	**7**	**273**
BCI 7M Control	SEC CRISPIA PHOTO	OF/1PPM/40C/96H	70	1.34	50	80	-32	86	338	**9**	**9**	**273**
BCI 7M Control	SEC CRISPIA PHOTO	OF/5PPM/25C/24H	70	1.39	49	81	-33	88	338	**6**	**6**	**97**
BCI 7M Control	SEC CRISPIA PHOTO	OF/5PPM/25C/48H	70	1.28	52	78	-28	83	340	**14**	**14**	**97**
BCI 7M Control	SEC CRISPIA PHOTO	OF/5PPM/25C/72H	70	1.19	53	74	-26	79	341	**17**	**20**	**97**
BCI 7M Control	SEC CRISPIA PHOTO	OF/5PPM/25C/96H	70	1.12	54	72	-23	75	342	**21**	**24**	**97**
BCI 7M Control	PR101	INITIAL	100	1.83	41	86	-31	92	340			
BCI 7M Control	PR101	INITIAL	70	1.53	46	85	-36	92	337			
BCI 7M Control	PR101	LF/NG//100H	70	1.40	49	78	-25	82	342	**13**	**9**	**293**
BCI 7M Control	PR101	LF/NG//200H	70	1.25	52	73	-22	77	343	**19**	**18**	**293**
BCI 7M Control	PR101	LF/NG//300H	70	1.14	54	69	-20	72	344	**24**	**25**	**293**
BCI 7M Control	PR101	OF/1PPM/40C/24H	70	1.52	46	84	-34	90	338	**2**	**1**	**258**
BCI 7M Control	PR101	OF/1PPM/40C/48H	70	1.48	47	82	-30	88	340	**6**	**3**	**258**
BCI 7M Control	PR101	OF/1PPM/40C/72H	70	1.43	48	80	-29	85	340	**9**	**7**	**258**
BCI 7M Control	PR101	OF/1PPM/40C/96H	70	1.38	49	79	-27	83	341	**11**	**10**	**258**
BCI 7M Control	PR101	OF/5PPM/25C/24H	70	1.34	49	77	-25	81	342	**14**	**12**	**59**

BCI 7M Control	PR101	OF/5PPM/25C/48H	70	1.20	52	73	-20	75	345	**21**	**22**	**59**
BCI 7M Control	PR101	OF/5PPM/25C/72H	70	1.09	54	68	-17	70	346	**26**	**29**	**59**
Pyridazine Dye **193**	XEROX 4024	INITIAL	100	1.14	48	56	-8	57	352			
Pyridazine Dye **193**	XEROX 4024	INITIAL	70	1.10	51	59	-9	60	351			
Pyridazine Dye **193**	HP PREMIUM PLUS	INITIAL	100	2.13	42	75	-5	76	356			
Pyridazine Dye **193**	HP PREMIUM PLUS	INITIAL	70	1.64	47	75	-12	76	351			
Pyridazine Dye **193**	HP PREMIUM PLUS	LF/NG//100H	70	1.22	51	67	-12	68	350	**9**	**26**	**97**
Pyridazine Dye **193**	HP PREMIUM PLUS	OF/1PPM/40C/24H	70	1.54	48	74	-12	75	351	**1**	**6**	**274**
Pyridazine Dye **193**	HP PREMIUM PLUS	OF/1PPM/40C/48H	70	1.54	49	74	-12	75	351	**2**	**6**	**274**
Pyridazine Dye **193**	HP PREMIUM PLUS	OF/1PPM/40C/72H	70	1.54	48	74	-13	75	350	**1**	**6**	**274**
Pyridazine Dye **193**	HP PREMIUM PLUS	OF/1PPM/40C/96H	70	1.54	48	74	-13	75	350	**2**	**6**	**274**
Pyridazine Dye **193**	HP PREMIUM PLUS	OF/5PPM/25C/24H	70	1.51	49	74	-13	75	350	**2**	**8**	**211**
Pyridazine Dye **193**	HP PREMIUM PLUS	OF/5PPM/25C/48H	70	1.51	49	74	-12	75	351	**2**	**8**	**211**
Pyridazine Dye **193**	HP PREMIUM PLUS	OF/5PPM/25C/72H	70	1.50	49	74	-13	75	350	**2**	**9**	**211**
Pyridazine Dye **193**	HP PREMIUM PLUS	OF/5PPM/25C/96H	70	1.50	49	74	-13	75	350	**2**	**9**	**211**
Pyridazine Dye **193**	SEC CRISPIA PHOTO	INITIAL	100	2.20	45	81	-4	81	357			
Pyridazine Dye **193**	SEC CRISPIA PHOTO	INITIAL	70	1.84	50	83	-14	84	350			
Pyridazine Dye **193**	SEC CRISPIA PHOTO	LF/NG//100H	70	1.67	52	81	-15	83	349	**2**	**9**	**322**
Pyridazine Dye **193**	SEC CRISPIA PHOTO	LF/NG//200H	70	1.56	53	80	-15	81	349	**4**	**15**	**322**
Pyridazine Dye **193**	SEC CRISPIA PHOTO	LF/NG//300H	70	1.40	55	78	-15	79	349	**7**	**24**	**322**
Pyridazine Dye **193**	SEC CRISPIA PHOTO	OF/1PPM/40C/24H	70	1.03	61	71	-20	74	344	**17**	**44**	**12**
Pyridazine Dye **193**	SEC CRISPIA PHOTO	OF/5PPM/25C/24H	70	0.54	74	46	-13	48	344	**44**	**71**	**6**
Pyridazine Dye **193**	PR101	INITIAL	100	2.11	43	77	-5	78	356			
Pyridazine Dye **193**	PR101	INITIAL	70	1.79	48	80	-14	81	350			
Pyridazine Dye **193**	PR101	LF/NG//100H	70	1.51	51	77	-14	78	350	**4**	**16**	**235**
Pyridazine Dye **193**	PR101	LF/NG//200H	70	1.39	54	76	-14	77	349	**7**	**22**	**235**
Pyridazine Dye **193**	PR101	LF/NG//300H	70	1.26	56	74	-16	76	348	**10**	**30**	**235**
Pyridazine Dye **193**	PR101	OF/1PPM/40C/24H	70	1.56	51	78	-15	79	349	**4**	**13**	**46**
Pyridazine Dye **193**	PR101	OF/1PPM/40C/48H	70	1.32	55	75	-16	77	348	**9**	**26**	**46**
Pyridazine Dye **193**	PR101	OF/1PPM/40C/72H	70	0.88	63	63	-17	65	345	**23**	**51**	**46**
Pyridine Dye **192**	PR101	OF/5PPM/25C/24H	70	0.53	73	42	-10	44	347	**45**	**70**	**6**
Pyridine Dye **192**	XEROX 4024	INITIAL	100	1.12	46	51	-6	52	354			
Pyridine Dye **192**	XEROX 4024	INITIAL	70	1.06	49	53	-7	54	352			
Pyridine Dye **192**	HP PREMIUM PLUS	INITIAL	100	1.90	38	71	-6	71	355			
Pyridine Dye **192**	HP PREMIUM PLUS	INITIAL	70	1.51	44	68	-12	69	350			
Pyridine Dye **192**	HP PREMIUM PLUS	LF/NG//100H	70	1.20	47	61	-14	63	347	**8**	**21**	**174**
Pyridine Dye **192**	HP PREMIUM PLUS	LF/NG//200H	70	1.11	50	60	-15	62	345	**11**	**26**	**174**
Pyridine Dye **192**	HP PREMIUM PLUS	OF/1PPM/40C/24H	70	1.50	43	69	-12	70	350	**1**	**1**	**2607**
Pyridine Dye **192**	HP PREMIUM PLUS	OF/1PPM/40C/48H	70	1.50	44	69	-12	70	350	**1**	**1**	**2607**
Pyridine Dye **192**	HP PREMIUM PLUS	OF/1PPM/40C/72H	70	1.50	43	69	-12	70	350	**1**	**1**	**2607**
Pyridine Dye **192**	HP PREMIUM PLUS	OF/1PPM/40C/96H	70	1.50	44	69	-12	70	350	**1**	**1**	**2607**

Pyridine Dye **192**	HP PREMIUM PLUS	OF/5PPM/25C/24H	70	1.50	43	69	-12	70	350	**1**	**1**	**2607**
Pyridine Dye **192**	HP PREMIUM PLUS	OF/5PPM/25C/48H	70	1.50	44	69	-12	70	350	**1**	**1**	**2607**
Pyridine Dye **192**	HP PREMIUM PLUS	OF/5PPM/25C/72H	70	1.50	43	69	-12	70	350	**1**	**1**	**2607**
Pyridine Dye **192**	HP PREMIUM PLUS	OF/5PPM/25C/96H	70	1.50	44	69	-12	70	350	**1**	**1**	**2607**
Pyridine Dye **192**	SEC CRISPIA PHOTO	INITIAL	100	1.91	41	76	-7	76	355			
Pyridine Dye **192**	SEC CRISPIA PHOTO	INITIAL	70	1.54	47	75	-15	77	349			
Pyridine Dye **192**	SEC CRISPIA PHOTO	LF/NG//100H	70	1.42	49	75	-16	77	348	**3**	**8**	**209**
Pyridine Dye **192**	SEC CRISPIA PHOTO	LF/NG//200H	70	1.18	53	70	-15	72	348	**8**	**23**	**209**
Pyridine Dye **192**	SEC CRISPIA PHOTO	LF/NG//300H	70	0.92	59	61	-12	63	349	**19**	**40**	**209**
Pyridine Dye **192**	SEC CRISPIA PHOTO	OF/1PPM/40C/24H	70	1.48	47	74	-16	76	348	**1**	**4**	**129**
Pyridine Dye **192**	SEC CRISPIA PHOTO	OF/1PPM/40C/48H	70	1.39	49	73	-16	75	348	**3**	**10**	**129**
Pyridine Dye **192**	SEC CRISPIA PHOTO	OF/1PPM/40C/72H	70	1.32	50	72	-16	74	347	**5**	**14**	**129**
Pyridine Dye **192**	SEC CRISPIA PHOTO	OF/1PPM/40C/96H	70	1.24	51	70	-16	72	347	**7**	**19**	**129**
Pyridine Dye **192**	SEC CRISPIA PHOTO	OF/5PPM/25C/24H	70	1.32	50	72	-16	74	347	**5**	**14**	**49**
Pyridine Dye **192**	SEC CRISPIA PHOTO	OF/5PPM/25C/48H	70	1.16	53	68	-16	70	347	**10**	**25**	**49**
Pyridine Dye **192**	SEC CRISPIA PHOTO	OF/5PPM/25C/72H	70	1.05	55	65	-16	67	346	**14**	**32**	**49**
Pyridine Dye **192**	PR101	INITIAL	100	1.93	39	72	-5	73	356			
Pyridine Dye **192**	PR101	INITIAL	70	1.57	44	72	-12	73	351			
Pyridine Dye **192**	PR101	LF/NG//100H	70	1.41	48	74	-19	76	345	**8**	**10**	**247**
Pyridine Dye **192**	PR101	LF/NG//200H	70	1.25	51	72	-20	74	344	**11**	**20**	**247**
Pyridine Dye **192**	PR101	LF/NG//300H	70	1.10	54	68	-20	71	343	**14**	**30**	**247**
Pyridine Dye **192**	PR101	OF/1PPM/40C/24H	70	1.53	45	72	-14	73	349	**2**	**3**	**129**
Pyridine Dye **192**	PR101	OF/1PPM/40C/48H	70	1.46	46	72	-14	73	349	**3**	**7**	**129**
Pyridine Dye **192**	PR101	OF/1PPM/40C/72H	70	1.36	48	70	-15	72	348	**5**	**13**	**129**
Pyridine Dye **192**	PR101	OF/1PPM/40C/96H	70	1.26	49	68	-15	70	347	**8**	**20**	**129**
Pyridine Dye **192**	PR101	OF/5PPM/25C/24H	70	1.10	53	64	-13	65	348	**13**	**30**	**19**

Table 7.6: Dye Testing Results for Dyes 194, 195 and 196 (Generic Protocols)

Dye	SUBSTRATE	TEST	DEPTH %	ROD	L	A	B	C	H	DE	% ROD LOSS	FAIL TIME
S196363	HP ADVANCED PHOTO	INITIAL	100	2.09	48	82	9	83	7			
S196363	HP ADVANCED PHOTO	INITIAL	90	1.9	50	82	2	82	1			
S196363	HP ADVANCED PHOTO	INITIAL	80	1.7	52	80	-4	81	357			
S196363	HP ADVANCED PHOTO	INITIAL	70	1.45	55	78	-8	78	354			
S196363	HP ADVANCED PHOTO	INITIAL	60	1.19	58	73	-11	74	352			
S196363	HP ADVANCED PHOTO	INITIAL	50	0.94	63	65	-13	66	349			
S196363	HP ADVANCED PHOTO	INITIAL	40	0.72	68	55	-13	57	347			
S196363	HP ADVANCED PHOTO	INITIAL	30	0.51	74	42	-12	44	345			
S196363	HP ADVANCED PHOTO	INITIAL	20	0.34	81	29	-10	30	341			
S196363	HP ADVANCED PHOTO	INITIAL	10	0.2	87	16	-7	17	336			
S196363	HP ADVANCED PHOTO	LF/ATLAS/NG/0H	50	0.92	63	64	-13	66	349			400
S196363	HP ADVANCED PHOTO	LF/ATLAS/NG/50H	50	0.87	64	62	-13	63	349	3	5	400
S196363	HP ADVANCED PHOTO	LF/ATLAS/NG/100H	50	0.82	66	61	-11	62	349	4	11	400
S196363	HP ADVANCED PHOTO	LF/ATLAS/NG/200H	50	0.77	67	58	-11	59	349	8	16	400
S196363	HP ADVANCED PHOTO	LF/ATLAS/NG/400H	50	0.69	69	54	-11	55	349	12	25	400
S196363	HP ADVANCED PHOTO	LF/HPUV/NG/0Y	50	0.92	63	64	-13	66	349			16
S196363	HP ADVANCED PHOTO	LF/HPUV/NG/6Y	50	0.83	66	61	-11	62	350	4	10	16
S196363	HP ADVANCED PHOTO	LF/HPUV/NG/12Y	50	0.74	67	56	-11	57	348	10	20	16
S196363	HP ADVANCED PHOTO	LF/HPUV/NG/18Y	50									16
S196363	HP ADVANCED PHOTO	LF/HPUV/NG/24Y	50									16
S196363	HP ADVANCED PHOTO	OF/5PPM/25C/0H	50	0.93	63	65	-13	66	349			102
S196363	HP ADVANCED PHOTO	OF/5PPM/25C/24H	50	0.85	65	61	-13	63	348	4	9	102
S196363	HP ADVANCED PHOTO	OF/5PPM/25C/48H	50	0.79	66	59	-12	60	348	7	15	102
S196363	HP ADVANCED PHOTO	OF/5PPM/25C/72H	50	0.78	67	59	-11	60	349	7	16	102
S196363	PR101	INITIAL	100	2.04	47	82	9	83	6			
S196363	PR101	INITIAL	90	1.88	49	82	2	82	2			
S196363	PR101	INITIAL	80	1.7	51	81	-3	81	358			
S196363	PR101	INITIAL	70	1.47	54	79	-7	79	355			

S196363	PR101	INITIAL	60	1.22	57	74	-10	75	353			
S196363	PR101	INITIAL	50	0.99	61	67	-12	68	350			
S196363	PR101	INITIAL	40	0.77	66	58	-13	60	348			
S196363	PR101	INITIAL	30	0.56	73	47	-12	48	345			
S196363	PR101	INITIAL	20	0.37	79	33	-11	35	342			
S196363	PR101	INITIAL	10	0.21	87	18	-7	20	338			
S196363	PR101	LF/ATLAS/NG/0H	50	0.99	61	68	-13	69	350			135
S196363	PR101	LF/ATLAS/NG/50H	50	0.88	64	62	-9	63	352	7	11	135
S196363	PR101	LF/ATLAS/NG/100H	50	0.79	67	60	-7	60	353	11	20	135
S196363	PR101	LF/ATLAS/NG/200H	50	0.66	71	52	-7	53	352	19	33	135
S196363	PR101	OF/5PPM/25C/0H	50	0.99	61	67	-12	69	350			33
S196363	PR101	OF/5PPM/25C/24H	50	0.78	66	58	-10	59	350	11	21	33
S196363	PR101	OF/5PPM/25C/48H	50	0.68	69	53	-9	54	350	17	31	33
S196363	SEC CRISPIA PHOTO	INITIAL	100	2.11	48	84	8	85	5			
S196363	SEC CRISPIA PHOTO	INITIAL	90	1.91	51	84	0	84	360			
S196363	SEC CRISPIA PHOTO	INITIAL	80	1.68	53	83	-6	83	356			
S196363	SEC CRISPIA PHOTO	INITIAL	70	1.46	56	81	-10	81	353			
S196363	SEC CRISPIA PHOTO	INITIAL	60	1.2	59	76	-13	77	350			
S196363	SEC CRISPIA PHOTO	INITIAL	50	0.93	63	68	-15	69	347			
S196363	SEC CRISPIA PHOTO	INITIAL	40	0.72	69	58	-16	60	345			
S196363	SEC CRISPIA PHOTO	INITIAL	30	0.5	75	45	-15	48	342			
S196363	SEC CRISPIA PHOTO	INITIAL	20	0.33	82	32	-13	34	338			
S196363	SEC CRISPIA PHOTO	INITIAL	10	0.18	89	18	-10	21	332			
S196363	SEC CRISPIA PHOTO	LF/ATLAS/NG/0H	50	0.93	63	68	-16	69	347			232
S196363	SEC CRISPIA PHOTO	LF/ATLAS/NG/50H	50	0.86	66	64	-10	64	351	7	8	232
S196363	SEC CRISPIA PHOTO	LF/ATLAS/NG/100H	50	0.81	68	63	-8	63	352	10	13	232
S196363	SEC CRISPIA PHOTO	LF/ATLAS/NG/200H	50	0.72	69	57	-9	58	351	13	23	232
S196363	SEC CRISPIA PHOTO	LF/ATLAS/NG/400H	50	0.59	73	51	-9	51	350	21	37	232
S196363	SEC CRISPIA PHOTO	OF/5PPM/25C/0H	50	0.94	63	68	-15	70	347			83
S196363	SEC CRISPIA PHOTO	OF/5PPM/25C/24H	50	0.84	66	64	-14	65	348	5	11	83
S196363	SEC CRISPIA PHOTO	OF/5PPM/25C/48H	50	0.77	68	61	-13	62	348	9	18	83
S196363	SEC CRISPIA PHOTO	OF/5PPM/25C/72H	50	0.76	69	61	-12	63	349	9	19	83
isoquinoline **195**	HP ADVANCED PHOTO	INITIAL	100	2.01	22	57	-54	78	317			
isoquinoline **195**	HP ADVANCED PHOTO	INITIAL	90	1.84	25	57	-57	81	315			
isoquinoline **195**	HP ADVANCED PHOTO	INITIAL	80	1.56	30	55	-59	81	313			
isoquinoline **195**	HP ADVANCED PHOTO	INITIAL	70	1.34	34	51	-59	79	311			
isoquinoline **195**	HP ADVANCED PHOTO	INITIAL	60	1.1	40	44	-56	72	308			
isoquinoline **195**	HP ADVANCED PHOTO	INITIAL	50	0.85	48	35	-50	62	305			
isoquinoline **195**	HP ADVANCED PHOTO	INITIAL	40	0.67	56	28	-44	52	302			
isoquinoline **195**	HP ADVANCED PHOTO	INITIAL	30	0.51	64	21	-36	42	300			
isoquinoline **195**	HP ADVANCED PHOTO	INITIAL	20	0.37	72	15	-28	31	298			
isoquinoline **195**	HP ADVANCED	INITIAL	10	0.19	84	6	-15	16	292			

	PHOTO											
isoquinoline **195**	HP ADVANCED PHOTO	LF/ATLAS/NG/0H	50	0.84	49	35	-50	61	305			112
isoquinoline **195**	HP ADVANCED PHOTO	LF/ATLAS/NG/50H	50	0.77	51	32	-46	57	305	5	8	112
isoquinoline **195**	HP ADVANCED PHOTO	LF/ATLAS/NG/100H	50	0.66	57	29	-39	49	307	15	21	112
isoquinoline **195**	HP ADVANCED PHOTO	LF/ATLAS/NG/200H	50	0.45	69	20	-27	34	307	34	46	112
isoquinoline **195**	HP ADVANCED PHOTO	LF/HPUV/NG/0Y	50	0.84	49	35	-50	61	305			11
isoquinoline **195**	HP ADVANCED PHOTO	LF/HPUV/NG/6Y	50	0.72	54	31	-43	53	305	9	14	11
isoquinoline **195**	HP ADVANCED PHOTO	LF/HPUV/NG/12Y	50	0.61	59	25	-38	46	303	18	27	11
isoquinoline **195**	HP ADVANCED PHOTO	OF/5PPM/25C/0H	50	0.84	48	35	-50	61	305			14
isoquinoline **195**	HP ADVANCED PHOTO	OF/5PPM/25C/24H	50	0.52	70	30	-10	32	343	46	38	14
isoquinoline **195**	PR101	INITIAL	100	1.99	21	53	-48	72	318			
isoquinoline **195**	PR101	INITIAL	90	1.84	24	54	-52	75	316			
isoquinoline **195**	PR101	INITIAL	80	1.6	28	54	-55	77	314			
isoquinoline **195**	PR101	INITIAL	70	1.38	33	50	-55	75	312			
isoquinoline **195**	PR101	INITIAL	60	1.14	39	44	-53	69	310			
isoquinoline **195**	PR101	INITIAL	50	0.91	46	37	-49	61	307			
isoquinoline **195**	PR101	INITIAL	40	0.72	53	29	-44	53	304			
isoquinoline **195**	PR101	INITIAL	30	0.55	62	22	-37	44	301			
isoquinoline **195**	PR101	INITIAL	20	0.4	70	16	-30	34	299			
isoquinoline **195**	PR101	INITIAL	10	0.2	84	7	-16	18	293			
isoquinoline **195**	PR101	LF/ATLAS/NG/0H	50	0.9	46	37	-50	62	306			84
isoquinoline **195**	PR101	LF/ATLAS/NG/50H	50	0.81	50	34	-43	55	308	8	10	84
isoquinoline **195**	PR101	LF/ATLAS/NG/100H	50	0.62	60	28	-33	43	310	23	31	84
isoquinoline **195**	PR101	OF/5PPM/25C/0H	50	0.91	46	37	-50	62	307			5
isoquinoline **195**	PR101	OF/5PPM/25C/24H	50	0.25	84	17	-3	17	349	64	73	5
isoquinoline **195**	SEC CRISPIA PHOTO	INITIAL	100	2.04	22	58	-55	80	317			
isoquinoline **195**	SEC CRISPIA PHOTO	INITIAL	90	1.85	25	59	-58	83	315			
isoquinoline **195**	SEC CRISPIA PHOTO	INITIAL	80	1.56	30	57	-61	83	313			
isoquinoline **195**	SEC CRISPIA PHOTO	INITIAL	70	1.34	34	53	-62	81	311			
isoquinoline **195**	SEC CRISPIA PHOTO	INITIAL	60	1.09	40	46	-59	75	308			
isoquinoline **195**	SEC CRISPIA PHOTO	INITIAL	50	0.84	49	37	-53	65	305			
isoquinoline **195**	SEC CRISPIA PHOTO	INITIAL	40	0.66	56	29	-47	56	302			
isoquinoline **195**	SEC CRISPIA PHOTO	INITIAL	30	0.49	65	22	-40	45	299			
isoquinoline **195**	SEC CRISPIA PHOTO	INITIAL	20	0.35	74	16	-31	35	297			
isoquinoline **195**	SEC CRISPIA PHOTO	INITIAL	10	0.17	86	7	-18	19	292			
isoquinoline **195**	SEC CRISPIA PHOTO	LF/ATLAS/NG/0H	50	0.83	49	36	-53	64	304			88
isoquinoline	SEC CRISPIA	LF/ATLAS/NG/50H	50	0.74	53	32	-45	55	306	10	11	88

195	PHOTO											
isoquinoline **195**	SEC CRISPIA PHOTO	LF/ATLAS/NG/100H	50	0.59	61	28	-33	44	310	24	29	88
isoquinoline **195**	SEC CRISPIA PHOTO	OF/5PPM/25C/0H	50	0.85	49	37	-54	65	305			10
isoquinoline **195**	SEC CRISPIA PHOTO	OF/5PPM/25C/24H	50	0.44	75	30	-6	31	349	55	48	10
2-quinoline **196**	HP ADVANCED PHOTO	INITIAL	100	1.99	25	61	-48	77	322			
2-quinoline **196**	HP ADVANCED PHOTO	INITIAL	90	1.74	29	61	-51	80	320			
2-quinoline **196**	HP ADVANCED PHOTO	INITIAL	80	1.53	33	60	-53	80	318			
2-quinoline **196**	HP ADVANCED PHOTO	INITIAL	70	1.33	37	57	-54	78	317			
2-quinoline **196**	HP ADVANCED PHOTO	INITIAL	60	1.09	43	51	-51	72	315			
2-quinoline **196**	HP ADVANCED PHOTO	INITIAL	50	0.89	49	43	-48	64	312			
2-quinoline **196**	HP ADVANCED PHOTO	INITIAL	40	0.69	56	35	-42	54	310			
2-quinoline **196**	HP ADVANCED PHOTO	INITIAL	30	0.5	66	25	-33	42	307			
2-quinoline **196**	HP ADVANCED PHOTO	INITIAL	20	0.34	75	16	-25	29	303			
2-quinoline **196**	HP ADVANCED PHOTO	INITIAL	10	0.19	85	8	-15	16	298			
2-quinoline **196**	HP ADVANCED PHOTO	LF/ATLAS/NG/0H	50	0.86	50	42	-47	63	312			388
2-quinoline **196**	HP ADVANCED PHOTO	LF/ATLAS/NG/50H	50	0.83	51	41	-46	61	312	2	3	388
2-quinoline **196**	HP ADVANCED PHOTO	LF/ATLAS/NG/100H	50	0.79	53	40	-45	60	312	4	8	388
2-quinoline **196**	HP ADVANCED PHOTO	LF/ATLAS/NG/200H	50	0.73	55	37	-43	57	311	8	15	388
2-quinoline **196**	HP ADVANCED PHOTO	LF/ATLAS/NG/400H	50	0.64	59	33	-39	51	311	15	26	388
2-quinoline **196**	HP ADVANCED PHOTO	LF/HPUV/NG/0Y	50	0.87	49	42	-47	63	312			23
2-quinoline **196**	HP ADVANCED PHOTO	LF/HPUV/NG/6Y	50	0.81	52	41	-44	60	312	4	7	23
2-quinoline **196**	HP ADVANCED PHOTO	LF/HPUV/NG/12Y	50	0.75	54	37	-42	56	311	9	14	23
2-quinoline **196**	HP ADVANCED PHOTO	LF/HPUV/NG/18Y	50									23
2-quinoline **196**	HP ADVANCED PHOTO	LF/HPUV/NG/24Y	50									23
2-quinoline **196**	HP ADVANCED PHOTO	OF/5PPM/25C/0H	50	0.87	49	42	-47	63	312			30
2-quinoline **196**	HP ADVANCED PHOTO	OF/5PPM/25C/24H	50	0.68	57	34	-39	52	311	14	22	30
2-quinoline **196**	HP ADVANCED PHOTO	OF/5PPM/25C/48H	50	0.57	62	29	-34	45	311	22	34	30
2-quinoline **196**	PR101	INITIAL	100	1.97	25	58	-43	72	323			
2-quinoline **196**	PR101	INITIAL	90	1.76	29	59	-47	75	321			
2-quinoline	PR101	INITIAL	80	1.56	32	58	-49	76	320			

196												
2-quinoline **196**	PR101	INITIAL	70	1.34	36	55	-50	74	318			
2-quinoline **196**	PR101	INITIAL	60	1.12	42	50	-48	69	316			
2-quinoline **196**	PR101	INITIAL	50	0.92	47	43	-46	63	313			
2-quinoline **196**	PR101	INITIAL	40	0.74	54	36	-42	55	311			
2-quinoline **196**	PR101	INITIAL	30	0.54	63	26	-34	43	308			
2-quinoline **196**	PR101	INITIAL	20	0.36	73	17	-26	32	304			
2-quinoline **196**	PR101	INITIAL	10	0.2	84	9	-16	18	299			
2-quinoline **196**	PR101	LF/ATLAS/NG/0H	50	0.92	48	43	-46	63	313			165
2-quinoline **196**	PR101	LF/ATLAS/NG/50H	50	0.85	50	40	-42	58	313	6	8	165
2-quinoline **196**	PR101	LF/ATLAS/NG/100H	50	0.77	54	38	-40	56	314	10	16	165
2-quinoline **196**	PR101	LF/ATLAS/NG/200H	50	0.65	59	33	-37	50	312	18	29	165
2-quinoline **196**	PR101	OF/5PPM/25C/0H	50	0.93	47	44	-46	63	313			10
2-quinoline **196**	PR101	OF/5PPM/25C/24H	50	0.48	67	26	-28	38	312	32	48	10
2-quinoline **196**	SEC CRISPIA PHOTO	INITIAL	100	2	26	61	-48	78	322			
2-quinoline **196**	SEC CRISPIA PHOTO	INITIAL	90	1.75	30	62	-53	82	320			
2-quinoline **196**	SEC CRISPIA PHOTO	INITIAL	80	1.53	33	61	-55	82	318			
2-quinoline **196**	SEC CRISPIA PHOTO	INITIAL	70	1.32	38	58	-55	80	316			
2-quinoline **196**	SEC CRISPIA PHOTO	INITIAL	60	1.08	43	51	-54	74	314			
2-quinoline **196**	SEC CRISPIA PHOTO	INITIAL	50	0.87	50	44	-50	67	311			
2-quinoline **196**	SEC CRISPIA PHOTO	INITIAL	40	0.68	57	36	-45	57	309			
2-quinoline **196**	SEC CRISPIA PHOTO	INITIAL	30	0.48	67	26	-37	45	305			
2-quinoline **196**	SEC CRISPIA PHOTO	INITIAL	20	0.31	76	16	-28	32	301			
2-quinoline **196**	SEC CRISPIA PHOTO	INITIAL	10	0.17	86	9	-18	20	296			
2-quinoline **196**	SEC CRISPIA PHOTO	LF/ATLAS/NG/0H	50	0.86	50	43	-50	66	311			255
2-quinoline **196**	SEC CRISPIA PHOTO	LF/ATLAS/NG/50H	50	0.83	51	42	-46	62	313	5	3	255
2-quinoline **196**	SEC CRISPIA PHOTO	LF/ATLAS/NG/100H	50	0.78	53	41	-44	60	313	7	9	255
2-quinoline **196**	SEC CRISPIA PHOTO	LF/ATLAS/NG/200H	50	0.7	57	38	-40	55	313	13	19	255
2-quinoline **196**	SEC CRISPIA PHOTO	LF/ATLAS/NG/400H	50	0.52	65	30	-33	44	312	27	40	255
2-quinoline **196**	SEC CRISPIA PHOTO	OF/5PPM/25C/0H	50	0.87	50	44	-50	67	311			19
2-quinoline **196**	SEC CRISPIA PHOTO	OF/5PPM/25C/24H	50	0.61	61	34	-39	51	311	19	30	19
phthalazine **194**	SEC CRISPIA PHOTO	INITIAL	0	0	0	0	0	0	0	0	0	0

Table 7.7: Dye Testing Results for Dyes 192 and 193 ("Canon" Protocols)

Dye	SUBSTRATE	TEST	DEPTH %	ROD	L	A	B	C	H	DE	% ROD LOSS	FAIL TIME
BCI 7M Control	PR101	INITIAL	100	1.79	42	82	-24	86	344			
BCI 7M Control	PR101	INITIAL	50	1.37	50	79	-32	85	338			
BCI 7M Control	PR101	LF/NG//50H	50	1.24	52	73	-24	77	342	**10**	**9**	**170**
BCI 7M Control	PR101	LF/NG//100H	50	1.15	54	69	-22	73	343	**15**	**16**	**170**
BCI 7M Control	PR101	LF/NG//200H	50	0.98	58	63	-18	66	344	**23**	**28**	**170**
BCI 7M Control	PR101	OF/1PPM/40C/24H	50	1.34	51	78	-30	83	339	**2**	**2**	**219**
BCI 7M Control	PR101	OF/1PPM/40C/48H	50	1.29	51	76	-28	81	340	**5**	**6**	**219**
BCI 7M Control	PR101	OF/1PPM/40C/72H	50	1.25	52	75	-26	79	341	**8**	**9**	**219**
BCI 7M Control	PR101	OF/1PPM/40C/96H	50	1.21	53	73	-25	77	341	**10**	**12**	**219**
Pyridazine Dye **193**	PR101	INITIAL	100	2.04	36	69	7	69	6			
Pyridazine Dye **193**	PR101	INITIAL	50	1.60	46	73	-8	73	354			
Pyridazine Dye **193**	PR101	LF/NG//50H	50	1.48	48	73	-13	74	350	**6**	**8**	**247**
Pyridazine Dye **193**	PR101	LF/NG//100H	50	1.42	49	72	-14	74	349	**8**	**11**	**247**
Pyridazine Dye **193**	PR101	LF/NG//200H	50	1.27	52	71	-16	73	347	**11**	**21**	**247**
Pyridazine Dye **193**	PR101	OF/1PPM/40C/24H	50	1.53	47	72	-10	73	352	**3**	**4**	**128**
Pyridazine Dye **193**	PR101	OF/1PPM/40C/48H	50	1.46	48	72	-11	73	351	**4**	**9**	**128**
Pyridazine Dye **193**	PR101	OF/1PPM/40C/72H	50	1.36	50	70	-12	71	350	**6**	**15**	**128**
Pyridazine Dye **193**	PR101	OF/1PPM/40C/96H	50	1.29	51	69	-12	70	350	**8**	**19**	**128**
Pyridine Dye **192**	PR101	INITIAL	100	2.18	42	74	8	74	6			
Pyridine Dye **192**	PR101	INITIAL	50	1.93	48	78	-5	78	356			
Pyridine Dye **192**	PR101	LF/NG//50H	50	1.73	50	77	-7	77	355	**3**	**10**	**252**
Pyridine Dye **192**	PR101	LF/NG//100H	50	1.67	51	77	-7	77	355	**3**	**13**	**252**
Pyridine Dye **192**	PR101	LF/NG//200H	50	1.58	52	76	-8	77	354	**5**	**18**	**252**
Pyridine Dye **192**	PR101	OF/1PPM/40C/24H	50	1.64	52	77	-10	78	353	**6**	**15**	**33**
Pyridine Dye **192**	PR101	OF/1PPM/40C/48H	50	1.17	59	71	-14	72	349	**15**	**39**	**33**

Table 7.8: Dye Testing Results for Dyes 192 and 193 ("SEC" Protocols)

Dye	SUBSTRATE	TEST	DEPTH %	ROD	L	A	B	C	H	DE	% ROD LOSS	FAIL TIME
SEC G700M	XEROX 4024	INITIAL	100	1.01	55	61	-9	61	351			
SEC G700M	SEC CRISPIA PHOTO	INITIAL	100	1.43	54	81	-20	83	346			
SEC G700M	SEC CRISPIA PHOTO	LF/UG//100H	100	0.99	61	67	-12	68	350	**18**	**31**	**78**
SEC G700M	SEC CRISPIA PHOTO	LF/UG//200H	100	0.76	67	56	-9	57	351	**30**	**47**	**78**
SEC G700M	SEC CRISPIA PHOTO	OF/1PPM/40C/24H	100	1.24	57	76	-12	77	351	**10**	**13**	**48**
SEC G700M	SEC CRISPIA PHOTO	INITIAL	70	0.98	61	69	-23	73	342			
SEC G700M	SEC CRISPIA PHOTO	LF/UG//100H	70	0.68	69	53	-13	55	347	**21**	**31**	**79**
SEC G700M	SEC CRISPIA PHOTO	LF/UG//200H	70	0.49	76	41	-8	41	349	**36**	**50**	**79**
SEC G700M	SEC CRISPIA PHOTO	OF/1PPM/40C/24H	70	0.86	64	64	-16	66	346	**10**	**12**	**84**
SEC G700M	SEC CRISPIA PHOTO	OF/1PPM/40C/48H	70	0.80	66	60	-14	62	347	**14**	**18**	**84**
SEC G700M	SEC CRISPIA PHOTO	OF/1PPM/40C/72H	70	0.75	67	58	-12	59	348	**17**	**23**	**84**
SEC G700M	SEC CRISPIA PHOTO	OF/1PPM/40C/96H	70	0.72	68	56	-11	57	348	**19**	**27**	**84**
Pyridazine Dye **193**	XEROX 4024	INITIAL	100	1.06	49	50	-10	51	349			
Pyridazine Dye **193**	SEC CRISPIA PHOTO	INITIAL	100	1.12	55	67	-21	70	342			
Pyridazine Dye **193**	SEC CRISPIA PHOTO	LF/UG//100H	100	1.07	56	66	-20	69	343	**2**	**4**	**757**
Pyridazine Dye **193**	SEC CRISPIA PHOTO	LF/UG//200H	100	1.04	57	65	-20	68	343	**3**	**7**	**757**
Pyridazine Dye **193**	SEC CRISPIA PHOTO	OF/1PPM/40C/24H	100	1.04	57	65	-20	68	343	**3**	**7**	**93**
Pyridazine Dye **193**	SEC CRISPIA PHOTO	INITIAL	70	0.76	64	54	-22	59	338			
Pyridazine Dye **193**	SEC CRISPIA PHOTO	LF/UG//100H	70	0.74	65	53	-20	57	339	**2**	**3**	**379**
Pyridazine Dye **193**	SEC CRISPIA PHOTO	LF/UG//200H	70	0.70	67	52	-20	55	339	**4**	**8**	**379**
Pyridazine Dye **193**	SEC CRISPIA PHOTO	LF/UG//300H	70	0.65	68	49	-18	52	340	**8**	**14**	**379**
Pyridazine Dye **193**	SEC CRISPIA PHOTO	LF/UG//400H	70	0.55	72	43	-15	45	341	**16**	**28**	**379**
Pyridazine Dye **193**	SEC CRISPIA PHOTO	OF/1PPM/40C/24H	70	0.72	66	53	-20	57	339	**3**	**5**	**134**
Pyridazine Dye **193**	SEC CRISPIA PHOTO	OF/1PPM/40C/48H	70	0.68	67	51	-20	55	339	**5**	**11**	**134**
Pyridazine Dye **193**	SEC CRISPIA PHOTO	OF/1PPM/40C/72H	70	0.65	68	49	-19	53	339	**7**	**14**	**134**
Pyridazine Dye **193**	SEC CRISPIA PHOTO	OF/1PPM/40C/96H	70	0.62	70	48	-18	51	339	**10**	**18**	**134**
Pyridine Dye **192**	XEROX 4024	INITIAL	100	1.06	52	55	-5	55	355			
Pyridine Dye **192**	SEC CRISPIA PHOTO	INITIAL	100	0.59	72	51	-19	55	339			
Pyridine Dye **192**	SEC CRISPIA PHOTO	LF/UG//100H	100	0.56	73	49	-17	52	341	**3**	**5**	**396**
Pyridine Dye **192**	SEC CRISPIA PHOTO	LF/UG//200H	100	0.51	75	46	-16	49	341	**7**	**14**	**396**
Pyridine Dye **192**	SEC CRISPIA PHOTO	OF/1PPM/40C/24H	100	0.34	82	33	-14	36	338	**21**	**42**	**13**
Pyridine Dye **192**	SEC CRISPIA PHOTO	INITIAL	70	0.49	75	44	-18	48	338			
Pyridine Dye **192**	SEC CRISPIA PHOTO	LF/UG//100H	70	0.46	77	42	-16	45	339	**4**	**6**	**363**
Pyridine Dye **192**	SEC CRISPIA PHOTO	LF/UG//200H	70	0.43	78	40	-15	43	340	**6**	**12**	**363**
Pyridine Dye **192**	SEC CRISPIA PHOTO	LF/UG//300H	70	0.40	79	37	-13	39	341	**10**	**18**	**363**
Pyridine Dye **192**	SEC CRISPIA PHOTO	LF/UG//400H	70	0.35	81	32	-10	34	343	**16**	**29**	**363**
Pyridine Dye **192**	SEC CRISPIA PHOTO	OF/1PPM/40C/24H	70	0.29	84	30	-13	32	336	**18**	**41**	**13**

Table 7.9: Dye Testing Results for Dyes 192 and 193 ("HP" Protocols)

Dye	SUBSTRATE	TEST	DEPTH %	ROD	L	A	B	C	H	DE	% ROD LOSS	FAIL TIME
HP FUJI CONTROL	HP PRINTING PAPER	INITIAL	100	1.05	53	63	-5	63	355			
HP FUJI CONTROL	HP ADVANCED PHOTO	INITIAL	100	1.54	51	80	-11	81	352			
HP FUJI CONTROL	HP ADVANCED PHOTO	INITIAL	50	0.49	74	41	-14	44	342			
HP FUJI CONTROL	HP ADVANCED PHOTO	LF/NG//6Y	50	0.44	76	38	-11	39	344	**5**	**10**	**20**
HP FUJI CONTROL	HP ADVANCED PHOTO	LF/NG//12Y	50	0.41	78	35	-10	36	344	**8**	**16**	**20**
HP FUJI CONTROL	HP ADVANCED PHOTO	LF/NG//18Y	50	0.38	79	32	-9	33	345	**12**	**22**	**20**
HP FUJI CONTROL	HP ADVANCED PHOTO	OF/1PPM/40C/24H	50	0.47	75	40	-13	42	342	**2**	**4**	**255**
HP FUJI CONTROL	HP ADVANCED PHOTO	OF/1PPM/40C/48H	50	0.46	75	39	-13	41	342	**3**	**6**	**255**
HP FUJI CONTROL	HP ADVANCED PHOTO	OF/1PPM/40C/72H	50	0.45	76	38	-13	40	342	**4**	**8**	**255**
HP FUJI CONTROL	HP ADVANCED PHOTO	OF/1PPM/40C/96H	50	0.44	76	38	-12	40	342	**4**	**10**	**255**
PyridazineDye **193**	HP PRINTING PAPER	INITIAL	100	1.09	48	55	-15	57	345			
Pyridazine Dye **193**	HP ADVANCED PHOTO	INITIAL	100	1.61	46	79	-23	82	344			
Pyridazine Dye **193**	HP ADVANCED PHOTO	INITIAL	50	0.50	72	41	-19	45	335			
Pyridazine Dye **193**	HP ADVANCED PHOTO	LF/NG//6Y	50	0.47	74	38	-17	42	335	**3**	**6**	**26**
Pyridazine Dye **193**	HP ADVANCED PHOTO	LF/NG//12Y	50	0.44	75	36	-17	40	335	**6**	**12**	**26**
Pyridazine Dye **193**	HP ADVANCED PHOTO	LF/NG//18Y	50	0.41	76	34	-15	37	336	**9**	**18**	**26**
Pyridazine Dye **193**	HP ADVANCED PHOTO	OF/1PPM/40C/24H	50	0.48	73	39	-19	44	334	**2**	**4**	**225**
Pyridazine Dye **193**	HP ADVANCED PHOTO	OF/1PPM/40C/48H	50	0.47	73	38	-19	43	334	**3**	**6**	**225**
Pyridazine Dye **193**	HP ADVANCED PHOTO	OF/1PPM/40C/72H	50	0.46	74	37	-18	42	334	**4**	**8**	**225**
PyridazineDye **193**	HP ADVANCED PHOTO	OF/1PPM/40C/96H	50	0.44	75	36	-18	41	334	**5**	**12**	**225**
Pyridine Dye **192**	HP PRINTING PAPER	INITIAL	100	1.15	49	59	-9	60	351			
Pyridine Dye **192**	HP ADVANCED PHOTO	INITIAL	100	1.79	49	80	-12	81	352			
Pyridine Dye **192**	HP ADVANCED PHOTO	INITIAL	50	0.57	72	48	-17	50	340			
Pyridine Dye **192**	HP ADVANCED PHOTO	LF/NG//6Y	50	0.55	72	46	-16	48	341	**2**	**4**	**47**
Pyridine Dye **192**	HP ADVANCED PHOTO	LF/NG//12Y	50	0.53	73	45	-16	47	341	**3**	**7**	**47**
Pyridine Dye **192**	HP ADVANCED PHOTO	LF/NG//18Y	50	0.51	74	43	-15	46	341	**5**	**11**	**47**
Pyridine Dye **192**	HP ADVANCED PHOTO	OF/1PPM/40C/24H	50	0.46	76	40	-15	43	339	**9**	**19**	**30**
Pyridine Dye **192**	HP ADVANCED PHOTO	OF/1PPM/40C/48H	50	0.34	80	30	-13	33	337	**20**	**40**	**30**

8.0: References

1. P. Gregory, *Proceedings of the Royal Microscopical Society*, 2001, 36.
2. P. Gregory, *Chemistry in Britain*, 2000, **36**, 39.
3. R. W. Kenyon, *Chemistry and Technology of Printing and Imaging Systems*, Chapter 5, p 113, Blackie, Glasgow, 1996.
4. H. P. Lue, *J. Imaging Science and Technology*, 1998, **42**, 49.
5. R. N. Mills, proc, IS&T's NIP 12: *International Congress on Digital Printing Technologies*, l996, 262.
6. P. Gregory, *High Technology Applications of Organic Colorants*, Chapter 9, p 175, New York and London: Plenum, 1991.
7. R. W. Kenyon, *Chemistry and Technology of Printing and Imaging Systems*, p 158, Blackie, Glasgow, 1996.
8. P. F. Gordon and P. Gregory, *Organic Chemistry in Colour*, Springer-Verlag, Heidelberg, 1987.
9. R. L. M. Allen, *Studies in Modern Chemistry*, *Colour Chemistry*, Chapter 1, p 1-3 and 11, Chapter 2, p 14-20, Chapter 3, p 21, Nelson, London, 1971.
10. J. March, *Advanced Organic Chemistry*, 4th Edition, p 139, Wiley-Interscience, New York, 1992.
11. S. F. Pond, *Inkjet Technology*, Torrey Pines Research, California, 2000.
12. X- Rite Inc., *The Colour Guide and Glossary,* USA, 1998.
13. X- Rite Inc., *A Guide to Understanding Colour Communication*, 2000.
14. Gretag Macbeth, *Fundamentals of Colour and Appearance,* 1998.
15. D. J. Palmer, 4th International Congress on Advances in Non-impact Printing Technologies, "*Development of Ink/Media for Paintjet Printers"*, p 127, California, 1988.
16. S. Kishimoto, S. Kitahara, O. Manabe and H. Hiyama, *J. Org. Chem.*, 1978, **43**, 3882.
17. R. M. Christie, *Colour Chemistry*, Chapter 2, *The Physical and Chemical Basis of Colour*, RSC, Cambridge, 2001.
18. Z. Cspregi, P. Aranyosi, I. Ruznak, L. Toke, J. Frankl, A. Vig, *Dyes and Pigments*, 1998, **37**, 1.

19. W. Bauer, IS & T's NIP 12: *International Conference on Digital Printing Technologies*, "*Magenta Dyes for Ink-Jet Applications"* p 60, 1998.
20. H. Oda, *Dyes and Pigments*, 2001, **48**, 151.
21. F. Beffa and G. Back, *Rev. Prog. Coloration*, "Metal-Complex Dyes for Wool and Nylon", 1984, **14**, 33.
22. K. Boyle, PhD Thesis, The University of Edinburgh, Edinburgh, UK, 2007.
23. K. Carr, *Dyes For Ink-Jet Printing*, Colorants for Non-textile Applications, The Royal Society of Chemistry, Cambridge, 2001.
24. P. Schiess and M. Heitzmann, *Angew. Chem. Int. Ed. Engl.*, 1977, **89**, 485.
25. P. Schiess, P. V. Brave, F. E. Dussy, A. Pfiffner, *Org. Synth.,* 1995, **72**, 116.
26. C. H. Chou, C. C. Wu, W. K. Chen, *Tetrahedron Lett.*, 1995, **36**, 5065.
27. B. L. Chenard, C. Slapak, D. K. Anderson, J. S. Swenton, *J. Chem. Soc. Chem. Comm.*, 1981, 179.
28. M. Karpf, *Angew. Chem. Int. Ed. Engl*., 1986, **25**, 414.
29. P.C. Miller, P. P. Gaspar, *J. Org. Chem.*, 1991, **25**, 414.
30. F. McMillan, PhD Thesis, The University of Edinburgh, Edinburgh, UK, 2007.
31. R. F. C. Brown, F. W. Eastwood, K. J. Harrington, G. L. McMullen, *Aust. J. Chem.*, 1974, **27**, 2393.
32. G. G. Qiao, W. Meutermans, M. W. Wong, M. Träubel and C. Wentrup, *J. Am. Chem. Soc.*, 1996, **118**, 3852.
33. C. D. Hurd, *The Pyrolysis of Carbon Compounds*, The Chemical Catalogue Company Inc., New York, 1929.
34. R. F. Stevenson and W. H. Schuller, *Can. J. Chem.*, 1973, **51**, 3237.
35. T. Hattori, T. Suzuki, N. Hayashizaka, N. Koike, S. Miyano, *Bull. Chem. Soc. Jpn.,* 1993, **66**, 10, 3034.
36. S. Karady, N. L. Abramson, U. Dolling, A. W. Douglas, G. J. McManemin, B. Marcune, *J. Am. Chem. Soc.*, 1995, **117**, 5425.
37. K. Takegoshi, F. Terano, A. Saika, *J. Chem. Phys.*, 1984, **80**, 1089.
38. H. McNab, M. E. Murray, *J. Chem. Soc. Perkin Trans. 1,* 1989, 583.
39. K. X. Huang, *Unpublished work*, The University of Edinburgh, Edinburgh, UK, 2006.
40. W. S. Weedon, H. W. Doughty, *Am. Chem. J.,* 1905, **33**, 393.

41. W. Kimerse, *Angew. Chem. Int. Ed. Engl*., 1965, **4**, 1.
42. S. L. Saha, *Bioorg. Med. Chem.,* 2002, **10**, 2779.
43. H. McNab, R. Tyas, *unpublished work*, The University of Edinburgh, Edinburgh, UK, 2007.
44. H. E. Fierz-Davis, L. Blangey, H. Streiff, *Helv. Chim. Acta*, 1946, **29**, 1718.
45. E. Hecker, *Chem. Ber*., 1959, **92**, 3198.
46. M. Mure, S. X. Wang, J. P. Klinman, *J. Am. Chem. Soc.*, 2003, **125**, 6113.
47. N. A. Kassab, S. O. Abd Allah, S. A. Elbahai, *Z. Nat. Tel. Anorg. Chem. Org. Chem.,* 1978, **33**, 75.
48. A. Crabtree, B. Parton, *UK. Patent Appl.*, 1979, GB2032448A.
49. D. D. Chapman, *US. Patent Appl.*, 1990, US4892584.
50. A. V. Ivanshchenko, B. E. Krasitelei, S. V. Krikunova, R. V. Poponova, *Khim. Geterotsikl. Soedinenii*, 1980, **12**, 1682.
51. I. Singh, A. K. Sharma, S. K. Yadav, D. Singh, D. S. Han, *Asian J. Chem*, 2003, **15**, 185.
52. P. Coad, R. A. Coad, *J. Org. Chem*., 1963, **28**, 1919.
53. R. C. Evans, F. Y. Wiselogle, *J. Am. Chem. Soc*., 1945, **67**, 60.
54. D. Libermann, A. Rouaix, *Bull. Soc. Chim. Fr*., 1959, 1793.
55. G. B. Barlin, C. Y. Yap, *Aust. J. Chem.*, 1977, **30**, 2319.
56. F. H. Case, A. A. Schilt, *J. Chem. Eng. Data*., 1986, **31**, 503.
57. X-Rite Inc., *A Guide to Understanding Colour Communications*, 2000.
58. D. Benstead, PhD Thesis, The University of Edinburgh, Edinburgh, UK, 2007.
59. K. Kobrakov, V. Korolev, I. Rybina, V. Kelarev, *Khim. Geterotsikl. Soedinenii*, 2000, **36**, 931.
60. E. Kucharska, J. Hanuza, M. Maczka, Z. Talik, *Vib. Spec.*, 2005, **39**, 1.
61. C. Mills, *J. Chem. Soc*., 1895, **67**, 925.
62. A. Bayer, *Ber. Dtsch. Chem. Ges*., 1874, **7**, 1638.
63. K. Ueno, *J. Am. Chem. Soc.*, 1954, **76**, 3670.
64. R. Yunes, *J. Chem. Soc. Perkin Trans. 2*, 1972, 696.
65. R. Yunes, *J. Am. Chem. Soc.*, 1973, **97**, 368.
66. N. Campbell, A.W. Henderson, D. Taylor, *J. Chem. Soc.*, 1953, 1281.
67. J. S. Morley, *J. Chem. Soc.*, 1959, 2280.

68. R. Krause, K. Krause, *Inorg. Chem.*, 1980, **19**, 2600.
69. M. N. Ackermann, W. G. Fairbrother, N. S. Amin, C. J. Deodene, C. M. Lamborg, P. T. Martin, *J. Organomet. Chem.*, 1996, **523**, 145.
70. K. Cheon, R. A. Cox, S. Keum, E. Buncel, *J. Chem. Soc., Perkin Trans. 2*, 1998, **5**, 1231.
71. T. Lu, T. K. Misra, P. Lin, F. Liao, C. Chung, *Polyhedron*, 2003, **22**, 535.
72. E. C. Taylor, C. Tseng, J. B. Rampal, *J. Org. Chem.*, 1982, **47**, 552.
73. M. Okubo, C. Sugimori, M. Tokisada, T. Tsutsumi, *Bull. Chem. Soc. Jpn.*, 1986, **59**, 1644.
74. R. W. Faessinger, E. V. Brown, *J. Am. Chem. Soc.*, 1951, **73**, 4608.
75. A. K. Deb, S. Choudhury, S. Goswami, *Polyhedron*, 1990, **9**, 2251.
76. T. S. Basu Baul, A. Lycka, *Polyhedron*, 1992, **11**, 2423.
77. M. K. Stern, F. D. Hileman, J. K. Bashkin, *J. Am. Chem. Soc.*, 1992, **114**, 9237.
78. E. Buncel, S. R. Keum, *Tetrahedron*, 1983, **39**, 1091.
79. K. T. Leffek, A. Jarczewski, *Can. J. Chem.*, 1991, **69**, 1238.
80. A. Angeli, L. Marchetti, *Atti. accad. Lincei.*, 1906, **15**, 480. (cited in H. E. Bigelow, *Chem. Rev.,* 1931, **9**, 117).
81. J. C. Mason, G. Tennant, *J. Chem. Soc. B.*, 1970, 911.
82. F. Arndt, B. Rosenau, *Chem. Ber.*, 1917, **50**, 1248.
83. F. J. Wolf, A. M. Wilson, J. K. Pfister, M. Toshler, *J. Am. Chem. Soc.*, 1954, **76**, 4611.
84. P.S. Rao, G. A. Thakur, G. K. Lahiri, *Ind. J. Chem. Sect. A.*., 1996, **35**, 946.
85. J. Clayden, N. Greeves, P. Wothers, S. Warren, *Organic Chemistry*, Oxford University Press*,* 945, 2001.
86. J. March, *Advanced Organic Chemistry*, p1106*.*
87. A. Whol, W. Aue, *Ber. Dtsch. Chem. Ges.*, 1901, **34**, 2442.
88. M. Tracy, E. M. Acton, *J. Org. Chem.*, 1984, **49**, 5116.
89. I. Yosioka, H. Otomasu, *Chem. Pharm. Bull.*, 1953, **1**, 67.
90. M. K. Stern, F. D. Hileman, J. K. Bashkin, *J. Am. Chem. Soc.*, 1992, **114**, 9237.
91. Z. Wrobel, A. Kwast, *Synlett.*, 2007, 1525.
92. Merz, Coray, *Ber. Dtsch. Chem. Ges*., 1871, **4**, 982. (cited in H. E. Bigelow, *Chem. Rev.,* 1931, **9**, 117).

93. B. D. Gowenlock, M. J. Maidment, *J. Chem. Soc., Perkin Trans. 2*, 2000, 2280.
94. R. McDonald, J. M. Richmond, *J. Chem. Soc., Chem. Commun.,* 1973, 605.
95. E. C. Taylor, K. A. Harrison, J. B. Rampal, *J. Org. Chem.*, 1986, **51**, 101.
96. R. A. Freitag, J, A, Mercer-Smith, D. G. Whitten, *J. Am. Chem. Soc*., 1981, **103**, 1226.
97. T. Suzuki, E. Sato, K. Unno, *J. Chem. Soc., Perkin. Trans. 1*, 1986, 2263.
98. J. Otera, Y. Niibo, H. Nozaki, *Tetrahedron. Lett*., 1992, **33**, 3655.
99. D. Crossley, *Unpublished work*, Avecia, 2001.
100. P. Gregory, *Unpublished work*, ICI, 1971.
101. a) A. Dickinson, N. J. Thompson, P. Wight, P. Gregory, P. J. Double, R. Bradbury, *Int. Patent, Appl*., 2003, WO 03/104332 A1.
b) R. Bradbury, A. Dickinson, P. J. Double, P. Gregory, M. S. Hadjisoteriou, P. Thomas, A. H. Popat, N. J. Thompson, P. Wight, *Int. Patent. Appl.*, 2003, WO 03/106572 A1.
102. A. Dickinson, H. Bell, D. Coutts, *Unpublished work*, Avecia, 2004.
103. L. A. Fedorov, *Russ. Chem. Rev.*, 1988, **57**, 941.
104. L. A. Fedorov, M. S. Zhukov, T. V. Petrova, S. B. Savvin, *Zhur. Anal. Khim.*, 1984, **39**, 10, 1754.
105. D. Atkinson, *Unpublished work*, Avecia, 2004.
106. D. G. McMinn, B. Kratochivl, *Can. J. Chem.*, 1977, **55**, 3909.
107. H. Zhang, J. Zhang, H. Wang, X. Li, *Anal. Chim. Acta.*, 1999, **380**, 101.
108. J. G. Traynham, *J. Chem. Educ*., 1983, **60**, 937.
109. C. L. Perrin, G. A. Skinner, *J. Am. Chem. Soc*., 1971, **93**, 3389.
110. S. R. Hartshorn, *Chem. Soc. Rev.*, 1974, **3**, 167.
111. E. Nolting, E. Grandmougin, *Ber. Dtsch. Chem. Ges.*, 1891, **24**, 1601.
112. S. F. Filippytschew, M. A. Tschekalin, *Anal. Prom.,* 1935, **5**, 76.
113. A. Lwoff, *Ber. Dtsch. Chem. Ges*., 1908, **41**, 1096.
114. A. Lwoff, *Anal. Prom.*, 1935, **5**, 76.
115. W. Voegtill, H. Muhr, P. Lauger, *Helv. Chim. Acta*, 1954, **37**, 1627.
116. D. Davies, C. Waring, *J. Chem. Soc.*, 1967, 1639.
117. B. R. T. Keene, P. Tissington, *J. Chem. Soc.*, 1965, 3032.
118. P. J. Bunyan, D. H. Hey, *J. Chem. Soc.,* 1962, 1360.

119. Y. Lin, L. C. Chen, *Tetrahedron*, 1998, **9**, 63.
120. B. Bonnet, D. Soullez, S. Girault, L. Landry, D. E. Valerie, C. Sergheraert, *Bioorg. Med. Chem*., 2000, **8**, 95.
121. M. Hori, T. Kataoka, H. Shimizu, S. Ohno, *J. Org. Chem.,* 1980, **45**, 2468.
122. D. F. DeTar, A. Hlynsky, *J. Am. Chem. Soc.,* 1955, **77**, 4411.
123. T. Vilsmas, *J. Chem. Soc.,* 1963. 612.
124. W. Walter, K. Wohlers, *Justus Liebigs Ann. Chem.,* 1971, **752**, 115.
125. U. Kobayashi, *J. Chem. Soc.,* 1957, 638.
126. P. Coad, R. A. Coad, *J. Org. Chem*., 1963, **28**, 1919.
127. R. C. Khulbe, Y. K. Bhoon, R. P. Singh, *J. Ind. Chem. Soc*., 1981, **58**, 840.
128. K. L. Kamar, S. Das, C. Hung, A. Castineiras, M. D. Kuz'min, C. Rillo, J. Bartolome, S. Goswami, *Inorg. Chem.*, 2003, **42**, 5367.
129. L. Stephenson, W. K. Warburton, *J. Chem. Soc.*, 1970, 1355.
130. D. R. Brimage, R. S. Davidson, P. R. Steiner, *J. Chem., Soc. Perkin Trans. 1*, 1973, 526.
131. A. Romer, *Org. Magn. Reson*., 1982, **19**, 66.
132. L. A. Crawford, PhD Thesis, The University of Edinburgh, Edinburgh, UK, 2002.
133. S. I. Wharton, PhD Thesis, The University of Edinburgh, Edinburgh, UK, 2005.